Book of Proceedings of the 24th Symposium on Theory and Practice of Shuipbuilding, In Memoriam of prof. Leopold Sorta

Matulja, Tin; Turk, Anton; Legović, Dunja; Hadjina, Marko; Degiuli, Nastia; Blagojević, Branko; Kos, Serđo; Vukelić, Goran

24th Symposium on the Theory and Practice of Shipbuilding
(in memoriam prof. Leopold Sorta)

with International participation

15.10.-16.10.2020. – online event
in the organization of the University of Rijeka - Faculty of Engineering

Proceedings

University of Rijeka
FACULTY OF ENGINEERING

Book of Proceedings of the 24th Symposium on Theory and Practice of Shuipbuilding, In Memoriam of prof. Leopold Sorta

Editor in Chief: Tin Matulja, RITEH

Editorial Board	**Organizing Committee**
Tin Matulja, RITEH – chairman	Marko Hadjina, RITEH – chairman
Anton Turk, RITEH – member	Boris Ljubenkov, FESB – vice-chairman
Dunja Legović, RITEH – member	Anton Turk, RITEH – vice-chairman
Marko Hadjina, RITEH – member	Dunja Legović, RITEH – cashier
Nastia Degiuli, FSB – member	Tin Matulja, RITEH – secretary
Branko Blagojević, FESB – member	Ozren Bukovac, RITEH – member
Serđo Kos, PFRI – member	Davor Bolf, RITEH – member
Goran Vukelić, PFRI – member	Joško Parunov, FSB - member

ORGANIZED BY

University of Rijeka
FACULTY OF ENGINEERING

IN COOPERATION WITH

University of Zagreb	University of Split
Faculty of Mechanical Engineering and Naval Architecture	Faculty of Electrical Engineering, Mechanical Engineering and Naval Architecture

SUPPORTERD BY

Hrvatska akademija znanosti i umjetnosti
Croatian Academy of Sciences and Arts

SPONSORS

MAIN:

IHC Engineering Croatia d.o.o.
Milutina Barača 7
51000 Rijeka
T +385 51 372 384
info.iec@royalihc.com

GOLDEN:

Lloyd's Register
Radmile Matejčić 10
51000 Rijeka
T +385 51 336 608
https://www.lr.org

SILVER:

TSI d.o.o.
Slavka Tomašića 5,
51000 Rijeka
T +385 51 734 225
infotsi@tsi.hr

SILVER:

METAL SHARK CROATIA
Tometići 1/D
51215, Kastav
T +385 51 627 850
sales@metalsharkboats.com

SCIENTIFIC COMMITTEE

Albert Zamarin	Marko Valčić
Anton Turk	Ozren Bukovac
Boris Ljubenkov	Rene Prenc
Dunja Legović	Roko Dejhalla
Duško Pavletić	Tin Matulja
Jasna Prpić Oršić	Tomislav Mrakovčić
Marko Hadjina	

INVITED LECTURES

Milovan Perić	Prediction of Flow and Cavitation Around Propeller
Carlo Rsso	Polar Code – An Overview
Marko Pirija	PC6 SFIC – Ice class Hull design principles

Table of Contents

PREDICTION OF CAVITATING FLOW AROUND PROPELLER

PRORAČUN STRUJANJA I KAVITACIJE OKO PROPELERA

Milovan Perić

Institute of ship Technology, Ocean Engineering and Transport Systems, University of Duisburg-Essen,
Bismarckstraße 69, 47057 Duisburg, Germany
milovan.peric@uni-due.de

Abstract

The emphasis of this paper is on challenges in simulation of cavitating flow around propeller. First the sources of various errors are highlighted: the accuracy of geometry, grid quality and fineness, turbulence modeling and cavitation modeling. The interaction between errors from different sources is also discussed. The importance of turbulence in the flow upstream of propeller and the difficulty of accounting for it is described next. Special attention is paid to the prediction of tip-vortex cavitation and to scale effects. Results from simulations are compared to experimental data from SVA Potsdam, except for the full-scale analysis of flow around hull, propeller and rudder, for which no experimental data is available.

Key words: simulation; flow; propeller; cavitation;

1. Introduction

In ship hydrodynamics, one of the most important tasks is to determine the hull resistance and to choose an appropriate propeller whose thrust matches the resistance at a minimum of required power. However, propeller performance can be impaired by cavitation, among other factors. Cavitation not only adversely affects the performance of propeller – it also leads to vibration, noise and erosion and could even cause structural damage. It is therefore important to be able to predict whether cavitation takes place at a particular operating point and what kind of cavitation it is, in order to be able to take mitigating measures.

In the past, propellers were designed using potential flow theory and then tested in towing tanks or cavitation tunnels. Often propellers are tested under open-water conditions, i.e. propeller is rotating at a constant rotation rate in a uniform stream. Similarly, the resistance is often determined for a bare hull and calm water, i.e., without propeller, rudder, and the superstructure, and without waves and wind effects. Besides, experiments usually take a long time to perform and are costly. Using experiments to optimize the ship as a system operating under realistic conditions is obviously not a perfect approach.

On the other hand, computational methods based on Navier-Stokes equations (known under the acronym CFD for „Computational Fluid Dynamics") have experienced a tremendous development over the past 40 years. Several commercial and public software packages have nowadays features specifically designed to simulate ship performance. The computational method can, in principle, consider all the relevant factors affecting the ship performance: the complete geometry without simplification (i.e., hull, rotating propeller, moving rudder, any other appendages like energy-saving devices, superstructure exposed to wind, etc.), turbulent water flow with incoming waves and possible wave-breaking, wind flow around superstructure, cavitation on propeller and rudder etc. However, one has to bear in mind that numerical methods produce only *approximate solutions* which are always containing errors from different sources.

Iteration errors (due to the fact that we solve discretized governing equations iteratively and have to stop iterations at some stage) are relatively easy to control by monitoring residuals. When residuals are

reduced by ca. 4 orders of magnitude, we can expect that variable values are not changing on the three most significant digits, which is usually enough; that corresponds to iteration errors being of the order of 0.1% or smaller.

Discretization errors depend on the choice of approximations used in different discretization steps (approximation of surface, volume and time integrals; interpolation of solution to locations other than computational points; approximation of gradients, etc.), and on the properties of the computational grid. For given selections, discretization errors can only be reduced by refining the grid, i.e. reducing the grid spacing. However, the comparison of results from a series of systematically refined grids may be deceiving if the original grid design is improper to resolve all the relevant flow features; an example will be shown in Sect. 5.

Modeling errors are usually the largest and most difficult to estimate. There are many possible sources of such errors, the major ones being:

- Turbulence model;

- Cavitation model;

- Geometry of the solution domain not being the same as in reality;

- Boundary conditions not corresponding to reality;

- Incorrect fluid properties, etc.

The first three causes of modeling errors will be discussed in more detail in the following sections.

What makes the assessment of accuracy of numerical simulations difficult is the fact that errors from different sources interact with each other: they may partially cancel out or augment, depending on their sign and magnitude. In order to minimize such effects, it is important to ensure that iteration errors are at least an order of magnitude lower than discretization errors, and that discretization errors are at least an order of magnitude lower than modeling errors.

In the following section the aspect of accuracy of the solution domain geometry are discussed. This is followed by a section devoted to the effects of turbulence modeling approach. Section 4 is devoted to incipient cavitation and Sect. 5 to the prediction of tip-vortex cavitation. In Sect. 6 scale effects are discussed, followed by concluding remarks.

2. Accuracy of Geometry

In numerical simulations of fluid flow, the geometry of solution domain is taken from a CAD-model. In a CAD-model of a propeller, all blades are identical and the circumferential distance between them is the same. However, the geometry of a manufactured propeller used in model tests or on the real vessel usually differ from CAD-model. One reason are manufacturing tolerances (e.g. casting process, followed by the final surface preparation and polishing). Especially for model-scale propellers, whose diameter is typically between 0.2 and 0.25 m, it is difficult to achieve the blade shape specified in the CAD-model. International Towing Tank Conference (ITTC) specifies in its guidelines that a model-scale propeller for tests should be manufactured with 0.1 mm tolerance (0.05 mm for the leading end trailing edges).

In order to assess the differences between a manufactured propeller and the CAD-model, SVA Potsdam performed detailed measurements of the built geometry of two samples of their Potsdam Propeller Test Case (PPTC). Figure 1 shows the deviations of pressure and suction side from CAD-model for all five blades. While the deviations are clearly within the ITTC recommendations, it is also obvious that each blade is different. For example, blade 5 is almost identical to CAD-geometry on suction side, but

around 0.05 mm off on pressure side. The same is true for blade 4, only the pressure side is perfect and the suction side is up to 0.1 mm off.
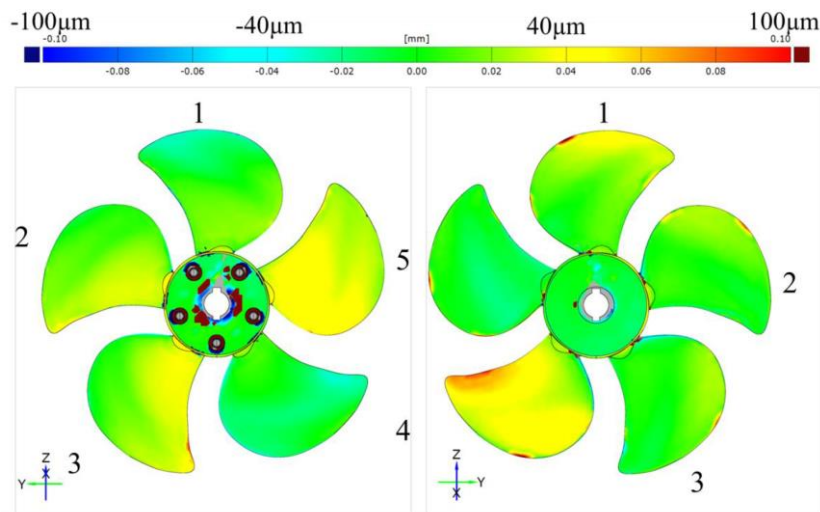
Figure 1 *Deviation of the manufactured geometry from CAD model, Potsdam Propeller Test Case [1].*

While the optical scanning of suction and pressure side of propeller blades is relatively easy, measuring the shape of leading and trailing edges is very difficult. SVA Potsdam is since 2016 able to make such measurements and performed a detailed assessment of leading edge geometry for two versions of the PPTC-propeller (controllable pitch and fixed pitch) along the contour of constant radius $r = 0.7R$, where R is the propeller diameter. Figure 2 shows the contours of two manufactured propellers together with the contour taken from the CAD-model. The CAD-model geometry exhibits a pronounced „nose" at the leading edge, with a very small radius of curvature, followed with short sections on both sides which are almost straight lines at the end of which larger radii of curvature connect these lines to the blade contour on pressure and suction sides. Both manufactured profiles have a smoothly varying curvature of leading edge, which is significantly different from CAD-shape (although being within the tolerance specified by ITTC). Both the stagnation line (along which the flow splits to suction and pressure side streams) and the possible tendency to flow separation and cavitation may be significantly influenced by the difference between CAD-shape and manufactured shape.

Figure 2 also includes a plot of grid and pressure distribution from a simulation of flow around PPTC. In this simulation the thickness of the first cell next to wall was 0.005 mm in order to achieve the dimensionless distance of the first computational point from wall of the order of $y^+ = 1$. This is required when the grid is supposed to resolve the viscous sublayer (e.g., when using low-Re wall treatment in RANS-computations or when using LES approach to turbulence modeling; see Sect. 3). By comparing the two plots in Fig. 2 it is obvious that several near-wall prism layers in the computational grid fall within the difference between CAD-profile and manufactured profile. Also, the blade is thicker in both manufactured models than in CAD-model; in the middle of the blade part shown in Fig. 2, the thickness difference is about 9%.

Unfortunately, there is no full CAD-model of the manufactured geometry, which could be used to generate the grid for a simulation of the flow in a domain bounded by the built geometry. Only by comparing solutions obtained using CAD geometry and built geometry would it be possible to reliably assess the significance of the observed discrepancy between manufactured propellers and the CAD-model. Until such data becomes available we can only speculate about the effects of the leading edge shape on

simulation results and the magnitude of the modeling error resulting from geometry differences. It would also be important to assess the effects of the difference between blades, but this too requires a CAD-model of the built geometry. We hope that such data will become available in near future.
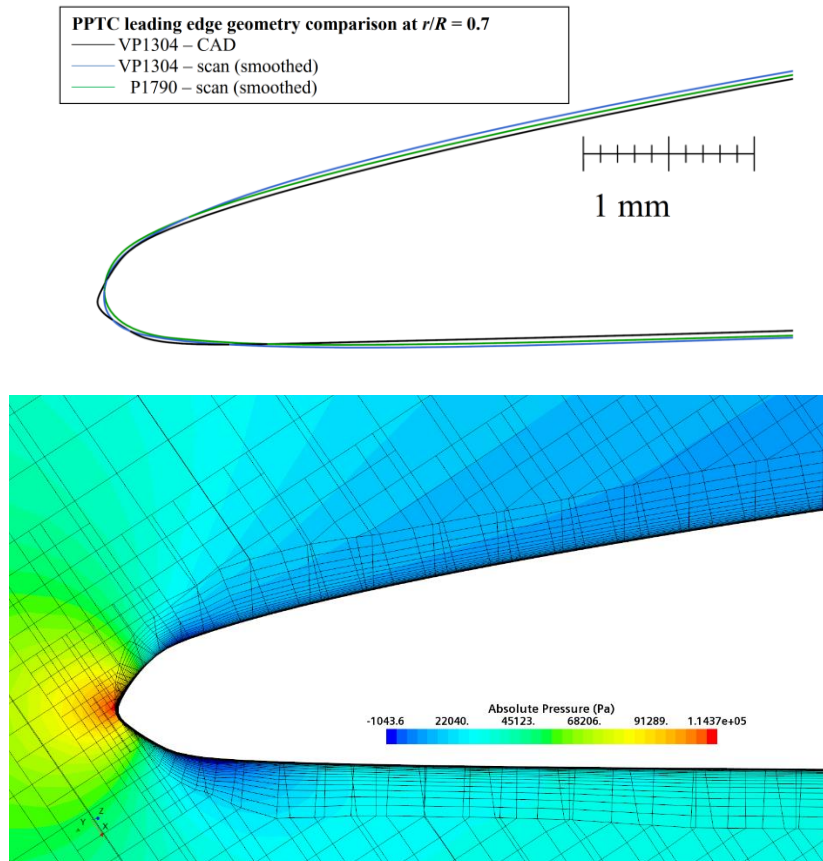
Figure 2 *Deviation of the two manufactured blade profiles at r/R = 0.7 from CAD (upper [1]) and the numerical grid with pressure distribution around the CAD-profile (lower).*

Even when we have the correct geometry as input, the generated grid may not produce an accurate representation of the CAD-geometry. Especially when the CAD-model contains parts with very small curvature radius, it is easy to falsify the geometry if the grid is not locally sufficiently refined. An example is presented in Fig. 3, showing a longitudinal cut through the polyhedral grid around the PPTC-propeller and a surface view of the leading edge for two grids. In one grid the leading edge zone is locally refined so that the curvature of the leading edge is relatively accurately represented (minimum cell size 0.011 mm), while in the other grid no special measures were taken to refine the grid where curvature is high (minimum cell size 0.176 mm); further away from leading edge, the two grids have cells of a similar size.

As can be seen in Fig. 3, the coarse grid representation of the leading edge geometry is far from the CAD-geometry; the curvature is not resolved and the leading edge is very rough. Obviously, the two grids represent two different geometries of propeller blade leading edge. Thus, when we compare solutions from these two grids, we see the difference which is not only due to different cell size in critical zones, but also due to different shapes of leading edge. Simulations were performed for a single blade with periodic conditions in circumferential direction. The coarse grid had 930,649 cells and the fine grid had 3,309,770 cells.
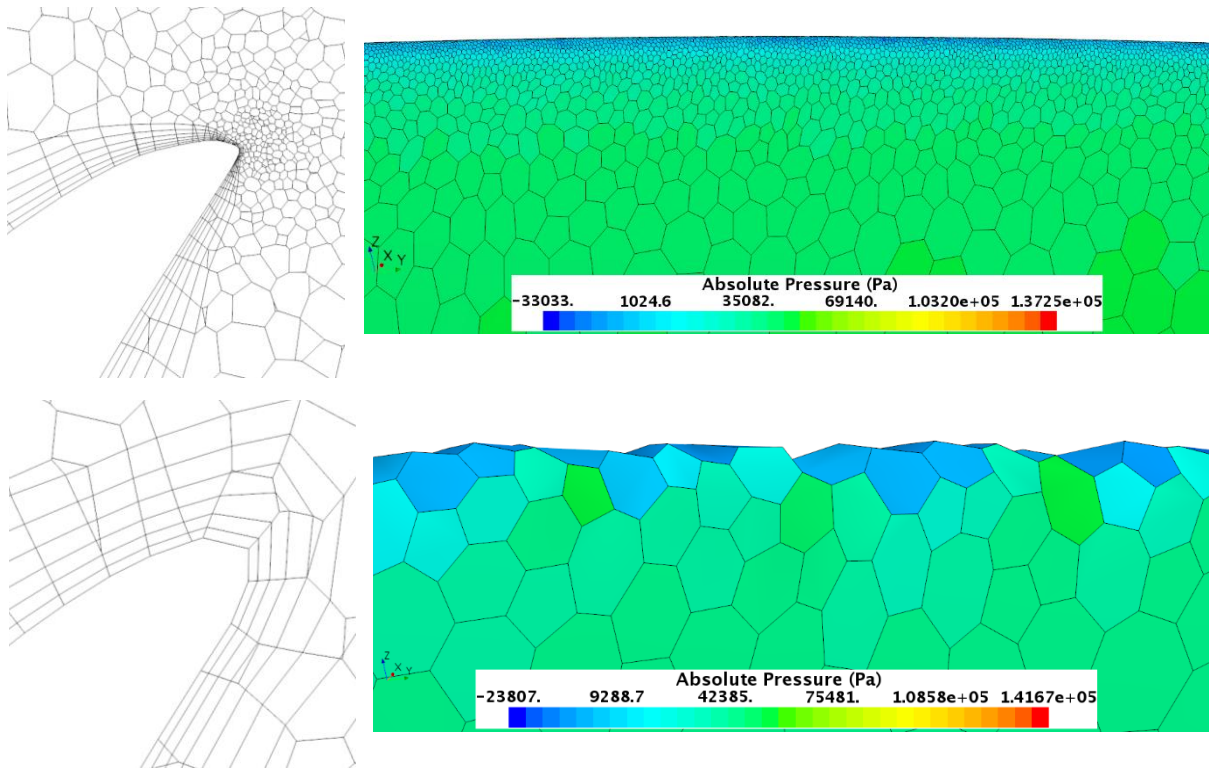
Figure 3 *Representation of leading edge geometry by the computational grid, in a longitudinal section through propeller blade (left) and in a view onto blade from suction side (right), from a fine grid (upper) and coarse grid (lower).*

With the view of different leading edge resolution one would expect a significant difference in solutions obtained with the two grids depicted in Fig. 3. The blunt and rough form of leading edge from the coarse grid suggests that the solution should be significantly in error. However, the comparison of thrust and torque computed on the two grids leads to a surprise: the results do not differ much! Table 1 presents the thrust and torque computed on the two grids and the measured values [2].

Table 1 Comparison of results from two grids with experimental data of SVA Potsdam [2]

	Experiment	Coarse grid	Fine grid
Thrust	181.74 N	183.4 N (+0.91%)	182.95 N (+0.67%)
Torque	11.796 Nm	12.13 Nm (+2.83%)	12.06 Nm (+2.24%)

As can be seen from Table 1, the difference between solutions obtained on the two grids is much smaller than the difference between either solution and experimental data. One may ask: how is that possible? The answer lies in partial cancellation of errors. Due to the randomness of leading edge „roughness" because of too coarse grid, the local errors along leading edge vary in amplitude and sign, and when the forces are integrated over the whole blade, positive and negative errors partially cancel out. However, one cannot expect that such partial cancellation will happen for every operating point or for every propeller; for reliable solutions, one needs to design the grid such that important geometry features are adequately resolved.

3. Accounting for Turbulence

The flow around ship and propeller is always turbulent. Because we cannot afford to resolve all turbulent fluctuations in space and time, we cannot use pure Navier-Stokes equations to simulate such flows. When computing the flow around ship hull (with or without propeller), we have to use Reynolds-averaged Navier-Stokes (RANS) equations instead. These equations are obtained by splitting the variable values into a sum of a mean and a fluctuating component, and by averaging the equations as well, either over a sufficiently long time or a sufficiently large ensemble of realizations. Unsteadiness may be present in the case of ensemble-averaging, like vortex shedding behind bluff bodies, if it happens on a time scale significantly longer than the time scale of turbulence. The averaging leads to the appearance of additional unknowns in the equations – the so called *Reynolds stresses*. These involve products of velocity fluctuations (variance and co-variance) and have to be obtained by using an appropriate turbulence model. The most widely used models (eddy-viscosity type models) require solution of two additional equations – one for velocity scale and one for length scale of turbulence. From these two quantities one can compute the so called *turbulent viscosity*, and the effect of turbulence on the mean flow is accounted for by adding the turbulent viscosity (which may vary by several orders of magnitude within the solution domain) to the fluid viscosity. For more details on RANS-based simulation approaches, see books on this subject and references therein [4], [5], [7].

For propeller alone (open-water or cavitation tunnel arrangement), one can afford to use large-eddy simulation (LES), in which larger scales from turbulence spectrum are resolved and the smaller scales – which are more universal – are modeled. In this case one usually does not solve additional equations, but needs to use finer grids and smaller time steps than when RANS-approach is used. The modeling of subgrid-scale turbulence (i.e., the part of turbulence spectrum which cannot be resolved by the computational grid) is usually achieved using algebraic models, like the one from Smagorinsky [6].
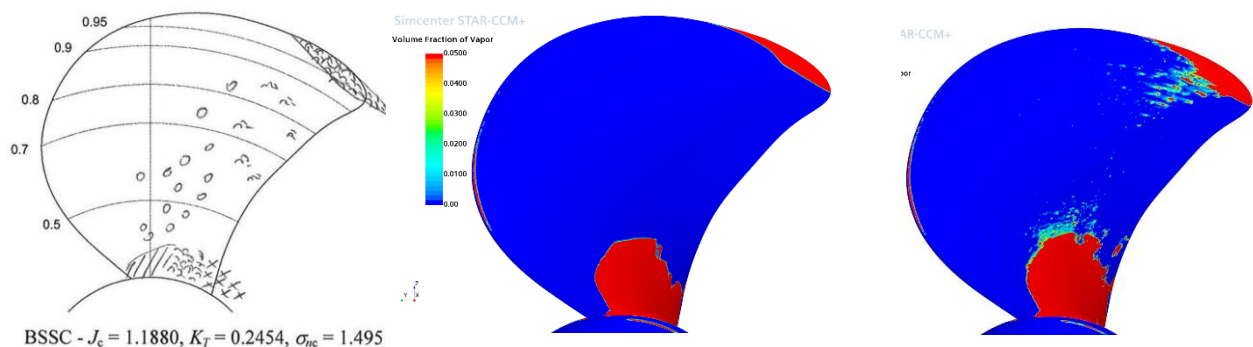
Figure 4 *Cavitation on blade suction side: observation in experiment [3] (left), RANS-solution (middle) and an instantaneous picture from LES-solution (right).*

Certain flow phenomena cannot be captured well when RANS-approach is used. An example is the begin of suction-side cavitation on propeller blades, see Fig. 4. Experimental observations at SVA Potsdam show that, under particular conditions, cavitation bubbles appear on the downstream half of the suction side, as shown in the sketch in Fig. 4. RANS simulation does not produce such cavitation even when a very fine grid is used (here a grid with 29 million cells for a single blade with periodic conditions in circumferential direction was used). With LES-approach on the same grid, cavitation bubbles do appear in the zone indicated by experimental observations. Because the same grid and the same cavitation model is used in both RANS and LES simulations, the difference is obviously due to the turbulence modeling approach.
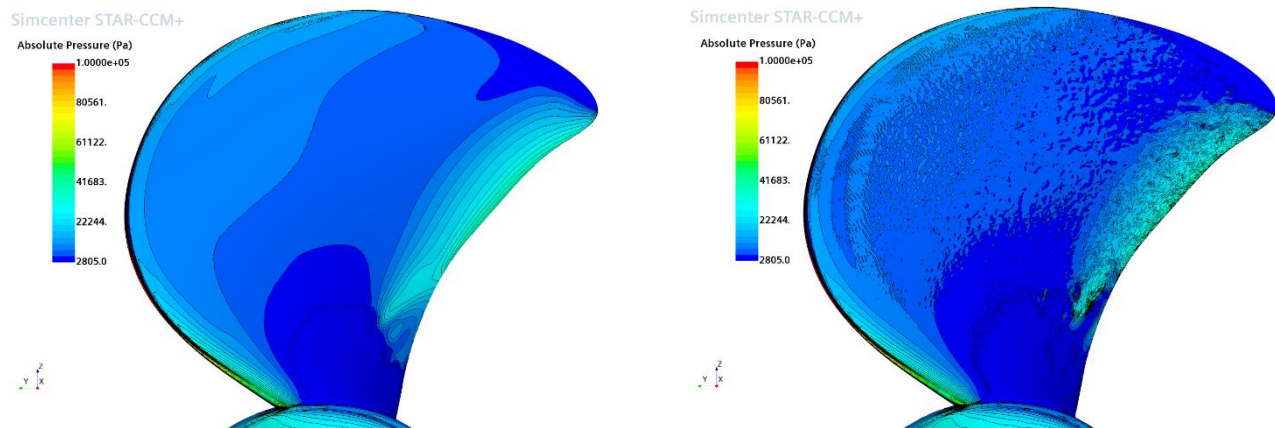
Figure 5 *Distribution of instantaneous pressure on the suction side of propeller blade from RANS-solution (left) and from LES-solution (right), for conditions from Fig. 4.*

Figure 5 explains why RANS-approach leads to no cavitation on suction side: the mean pressure resulting from solving the RANS-equations is below saturation level only in the zones where the tip-vortex cavitation and blade-root cavitation were visible in Fig. 4; over the rest of suction side blade surface, the pressure is above saturation level (see Fig. 5 left) and the cavitation does not happen. Even though the RANS-simulation was performed in unsteady mode (here the SST k-ω model was used [8]), the solution was practically steady, except at the edges of the tip-vortex and blade-root cavitation zones.

In the LES-simulation, turbulent fluctuations of velocity and pressure are resolved up to the grid scale. This is clearly seen in Fig. 5 (right), which shows that pressure not only fluctuates over the blade surface, but that locally low pressure zones are present where the mean pressure from RANS-simulation is higher. These small low-pressure zones are created when the fluctuating (fluttering) boundary layer tends to move away from wall. In an animation one can see how the local low-pressure zones appear, move over some distance and then disappear. The same happens to vapor bubbles: they are created when the pressure falls below saturation pressure, and they move until the pressure rises again above saturation level, leading to bubble collapse. Therefore, this kind of bubbly cavitation can only be predicted by turbulence modeling approaches which resolve velocity and pressure fluctuations; RANS-methods do not fall into this category. We will see in Sect. 5 that RANS-methods also significantly under-predict tip-vortex cavitation, due to the fact that high turbulent viscosity is computed where velocity gradients are high. This is the case with vortex core, and the too high turbulent viscosity leads to smearing of velocity peaks, which then results in a higher pressure in vortex core and too early stop of cavitation. Thus, LES-type approaches are also better suited for tip-vortex cavitation.

Figure 6 shows pressure distribution in a longitudinal section through the blade and propeller hub, computed on the same grid using RANS and LES approach to turbulence simulation. The main features are similar, but there are also important differences:

- LES-solution shows turbulent fluctuations behind hub and near blade wall, where the contours from RANS-simulation are smooth;
- Pressure in the core of tip vortex is much lower in the LES than in RANS-simulation;
- The low-pressure zone on pressure side near blade root is larger in the LES than in the RANS-solution.

These differences are important under the conditions leading to hub and tip-vortex cavitation.

When studying the flow around propeller mounted on a vessel, the velocity field approaching propeller is highly inhomogeneous. A propeller blade encounters during its 360° rotation different velocity (both in magnitude and direction) field and different turbulence levels. In order to accurately predict cavitation and especially hydro-acoustics, it is important to account for the effects of turbulence in the incoming flow on the flow around propeller blades. Unfortunately, LES of flow around the whole hull and all appendages is not possible in practical applications, not even at model scale. However, one could do embedded LES of flow around propeller, provided that turbulent fluctuations in the upstream flow are reconstructed from RANS-solution. Such simulations are just emerging [9,10] and more applications of this kind are expected in future.
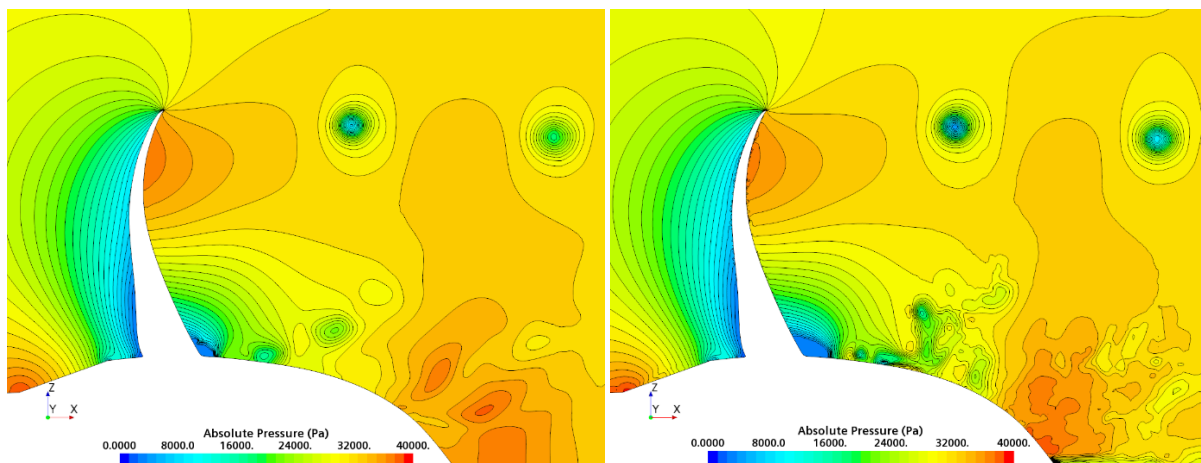
Figure 6 *Distribution of instantaneous pressure in the longitudinal section through propeller blade from RANS-solution (left) and from LES-solution (right), for conditions from Fig. 4.*

4. Incipient Cavitation

It is often important to determine under which conditions cavitation begins. If cavitation has to be avoided (e.g., in an optimization study in which one of the objectives is to find a design without cavitation), it is not necessary to use two-phase flow analysis with a particular cavitation model. From a single-phase analysis, one can recognize whether cavitation will be taking place or not by examining pressure distribution in the solution domain. If pressure locally falls below saturation level, then cavitation will be taking place. However, it may be difficult to determine whether cavitation is significant or not: if pressure is only slightly below saturation level in a very small volume, that may not be affecting the flow and the propeller performance to an extent which could be critical. Criteria to determine the cavitation inception are also not unique in experiments: usually, an engineer observing the flow needs to decide when to classify the flow as being affected by incipient cavitation.
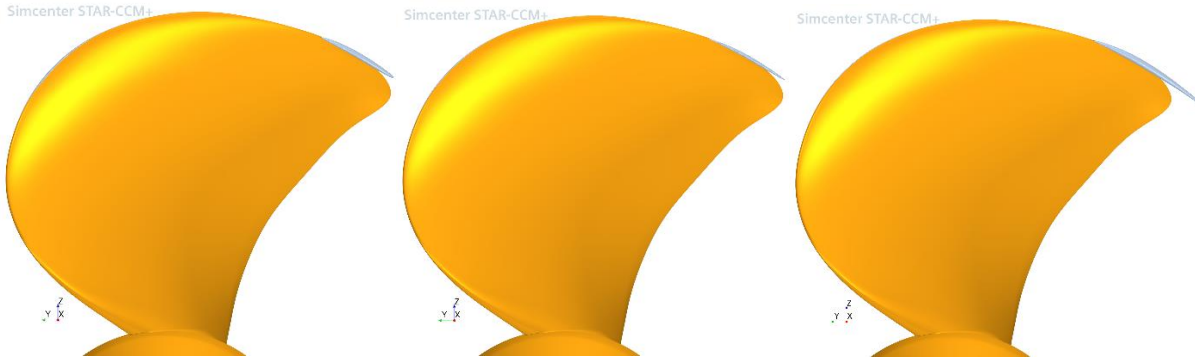
Figure 7 *Simulation of incipient cavitation around propeller: iso-surface of 5% vapor volume fraction (left) and iso-surface of saturation pressure (middle) from a two-phase computation using cavitation model, and iso-surface of saturation pressure from a single-phase computation without cavitation model (right).*

Figure 7 shows iso-surfaces of saturation pressure (2873 Pa absolute) from a two-phase simulation of flow around propeller using Schnerr-Sauer cavitation model [11] and from a single-phase flow without a cavitation model, compared with iso-surface of 5% vapor volume fraction from the two-phase simulation. When cavitation is not modeled, the zone of low pressure is larger than in the case of two-phase flow, and also somewhat larger than the zone in which vapor volume fraction is larger than 5%. Also, in the case of single-phase flow, the minimum value of absolute pressure is significantly lower than in the case of two-phase flow: -23902 Pa compared with 2732 Pa (141 Pa below saturation pressure), see Fig. 8.
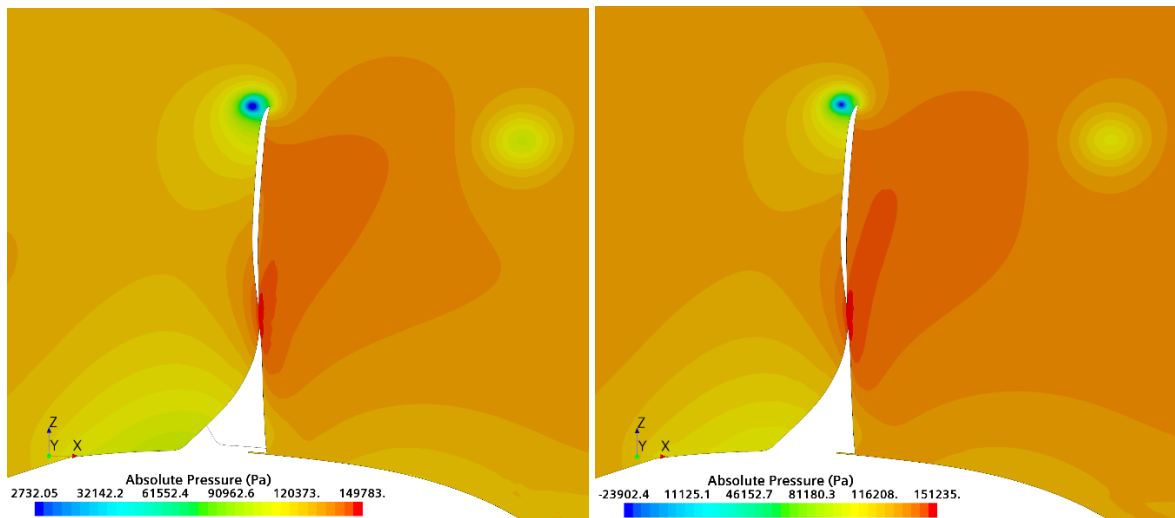
Figure 8 *Pressure distribution in a section through propeller blade orthogonal to the iso-surfaces from Fig. 7, from a two-phase simulation (left) and from a single-phase simulation (right).*

Table 2 Comparison of solutions from a two-phase and a single-phase simulation of flow around propeller with incipient tip-vortex cavitation with experimental data of SVA Potsdam (Case No. 3, page 2.9) [2]

Flow	Thrust (Exp.)	Thrust (Simulation)	Torque (Exp.)	Torque (Simulation)
Two-phase	218.28 N	216.50 N (-0.82%)	13.544 Nm	13.834 Nm (+2.14%)
Single-phase		216.05 N (-1.07%)		13.820 Nm (+2.04%)

In spite of the differences in details between solutions from single-phase and two-phase simulations of flow with incipient cavitation, the integral quantities of engineering interest do not differ much, as can be seen from Table 2. The thrust from single-phase simulation is only 0.25% lower than from two-phase simulation, while the difference in torque is only 0.1%.

In many cases cavitation occurs at more than one place in the flow (e.g., blade leading edge, blade root, tip vortex, hub vortex). When that is the case, one has to use two-phase simulation to predict the propeller performance, because cavitation does not start at the same time at all locations. Single-phase prediction is only useful when the very first cavitation zone is just appearing.

Note that negative absolute pressure in the liquid phase may occur even when cavitation model is active in a two-phase flow simulation. Inside vortices and recirculation zones, where the residence time of vapor bubbles is long enough, pressure remains close to saturation pressure. However, in some flow zones, where flow acceleration is very high and the residence time very short, pressure in liquid my become very low, leading to very high bubble growth rates. An example is shown in the next section.

5. Tip-Vortex Cavitation

Prediction of tip-vortex cavitation has always been a great challenge. It was long believed that cavitation models used in CFD (like the Schnerr-Sauer model [11] used here) are not capable of predicting this type of cavitation. This view was supported by the fact that the usual grid-dependence studies suggested that no significant changes in solution would happen with further refinement, because thrust and torque were well converged while tip-vortex cavitation was limited to a small zone near blade tip, see Fig. 9.
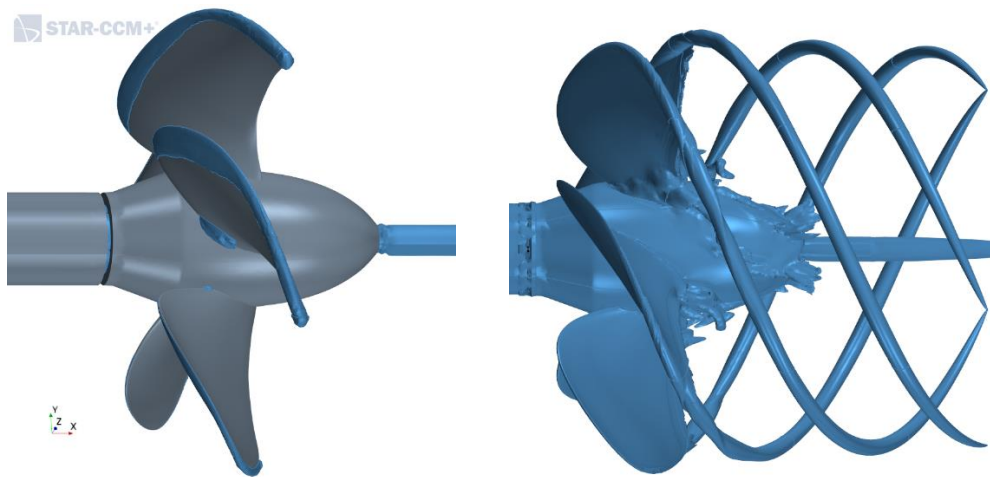
Figure 9 *Iso-surfaces of 5% vapor volume fraction (left) and of vorticity magnitude (right); computation using Reynolds-averaged Navier-Stokes equations, a version of k-ε turbulence model and cavitation model from [11].*

The location of tip vortex can be visualized by creating an iso-surface of vorticity, as shown in Fig. 9. By locally refining the grid within vorticity iso-surface to a sufficiently low level, one can better resolve extremely high gradients of velocity and pressure across tip vortex. A section through a such locally refined grid (4.73 million cells in total for a solution domain consisting of a single blade, with periodic conditions in circumferential direction) is shown in Fig. 10. The cell size within tip vortex was 0.234 mm (D/1068, where D is the propeller diameter, here 250 mm). The grid is also refined within hub vortex zone. The flow is from left to right; the setup parameters correspond to Case No. 5 on Page 2.13 in the report by SVA Potsdam [2]. One finer grid was also created by reducing the cell size everywhere in all directions by a factor of 1.5, leading to a total number of cells around 17 million.
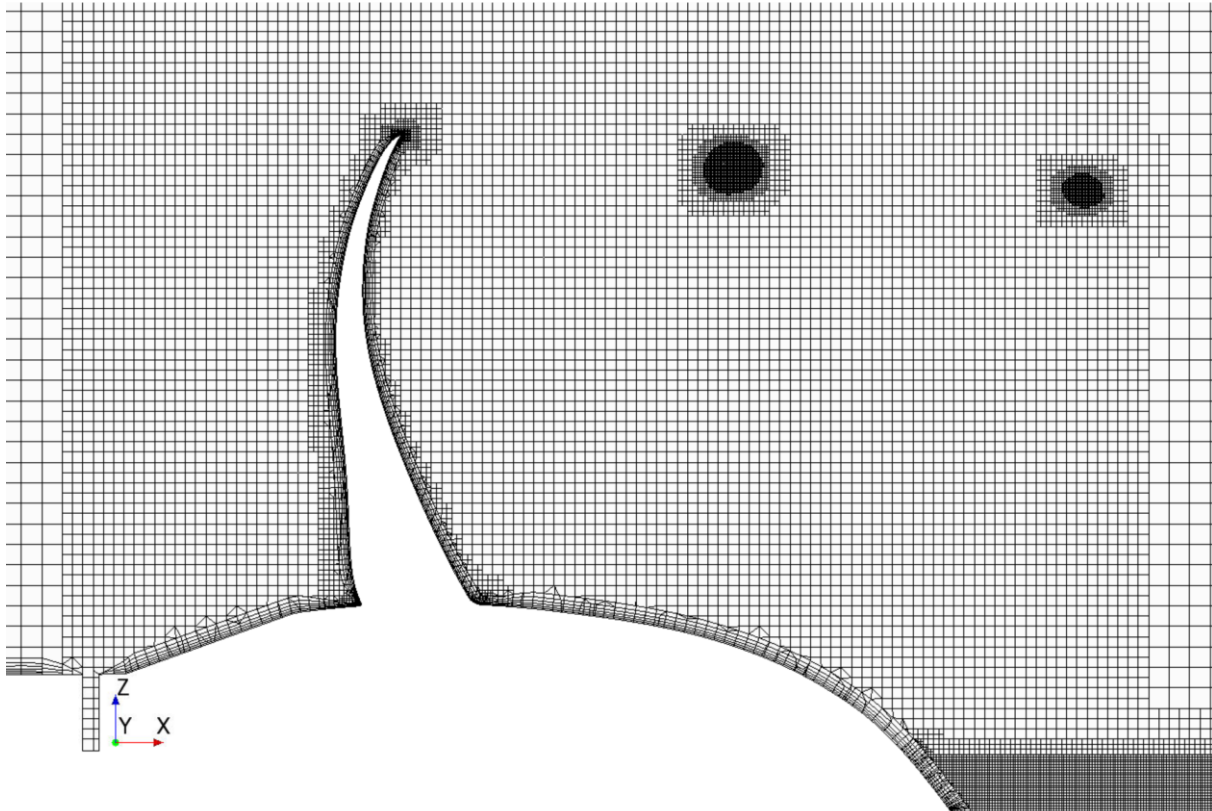
Figure 10 *A longitudinal section through the computational grid, showing local refinement within the tip vortex zone, as indicated by the vorticity iso-surface from Fig. 9.*

Simulation using locally refined grid and Reynolds-averaged Navier-Stokes (RANS) equations and a version of k-ε turbulence model [4] together with the Schnerr-Sauer cavitation model [11] shows an improvement compared to the result obtained without local grid refinement, cf. Fig. 9 and 11. The improvement is moderate even when the finest grid with 17 million cells for a single blade is used, as shown in Fig. 11: the tip-vortex cavitation ends too soon, even though the grid was refined to a much longer distance. The thrust is relatively well predicted – 1.8% smaller than in experiment. However, the thrust was almost equally well predicted already on the grid without local refinement in tip vortex zone.

The finest grid is so fine, that even LES-approach to turbulence modeling can be used. The WALE model was used to account for the unresolved part of turbulence [12], but the grid near wall was not fine enough to fully resolve the viscous sublayer of the boundary layer on propeller blades. However, the focus here was to capture the tip-vortex cavitation, and for this the wall treatment is not essential.
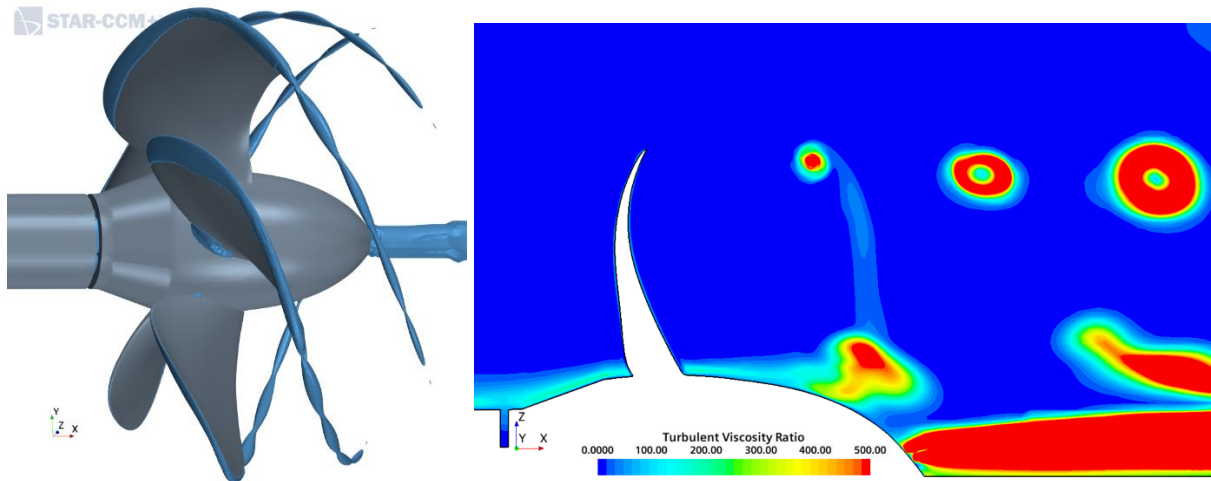
Figure 11 *Iso-surfaces of 5% vapor volume fraction (left) and contours of turbulent viscosity ratio (right) from a RANS-computation of flow around propeller using the finest grid with 17 million cells for a single blade.*

As can be seen from Fig. 12, with LES-approach to modeling the effects of turbulence, the tip-vortex cavitation is very well captured: the picture of iso-surface of the vapor volume fraction 0.05 looks very similar to the photograph of tip-vortex cavitation taken in experiment [2]. This shows that turbulence model plays a more important role for tip-vortex cavitation than cavitation model; the simple Schnerr-Sauer cavitation model [11] produces a pretty good solution when applied together with LES.
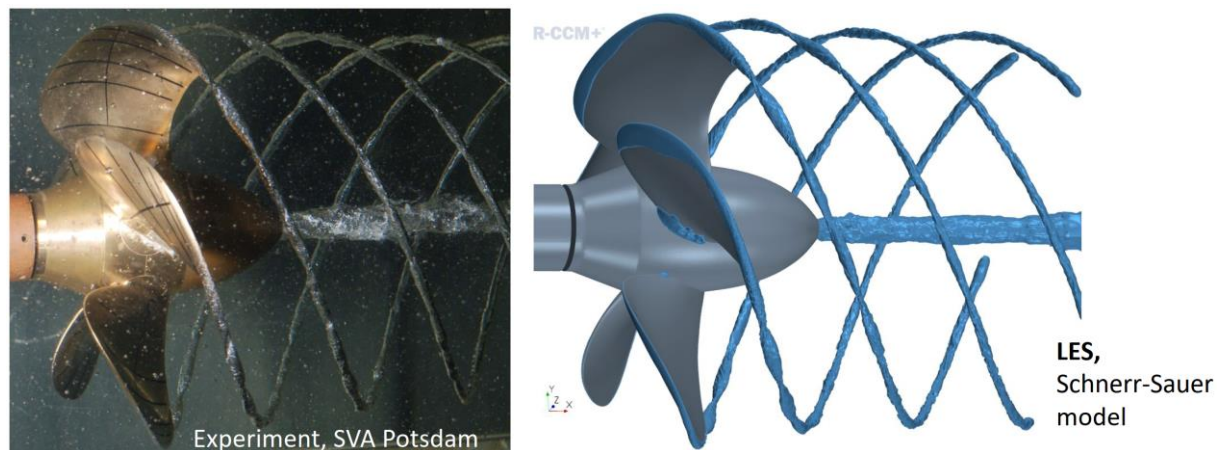
Figure 12 *Photograph of tip-vortex cavitation in experiment (left) and iso-surfaces of 5% vapor volume fraction (right) from LES-computation of flow around propeller using the finest grid with 17 million cells for a single blade.*

The thrust obtained from LES-simulation is 4% too high; this is most probably due to insufficiently fine grid near walls. The DES-approach (Detached-Eddy Simulation) uses RANS-approach near wall, for which the current grid was adequate, and LES in zones away from wall. This sounds like a good choice for the flow around propeller blade. Indeed, the results obtained with IDDES (Improved Delayed DES, [13]) produces the best solution: tip-vortex cavitation extends as long as the grid is fine enough, like in LES, but the thrust is now only 1.5% below measured value, which is as good as in RANS-solutions – but with an adequate resolution of tip-vortex cavitation, see Fig. 13.
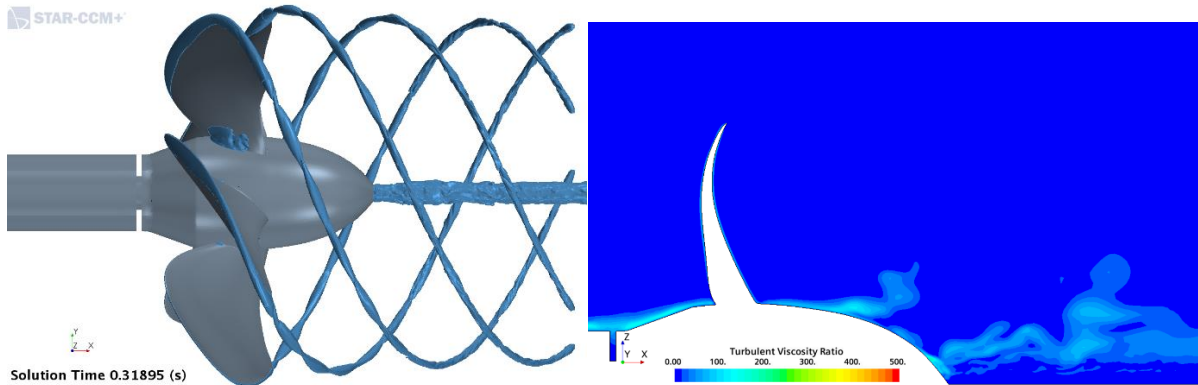
Figure 13 *Iso-surfaces of 5% vapor volume fraction (left) and contours of turbulent viscosity ratio (right) from a DES-computation of flow around propeller using the finest grid with 17 million cells for a single blade.*

The question is now: why is the turbulence model so important for capturing tip-vortex cavitation? The answer comes from a comparison of turbulent viscosity ratios (the ratio of turbulent viscosity over fluid viscosity) for RANS and DES simulations presented in Figs. 11 and 13. While in DES and LES simulations turbulent viscosity in the tip vortex zone is very small, every RANS-model produces there high turbulent viscosity. This high turbulent viscosity leads to smearing of velocity gradients, and that in turn leads to an increase in pressure. Once the pressure in tip-vortex zone becomes higher than saturation level, cavitation stops.
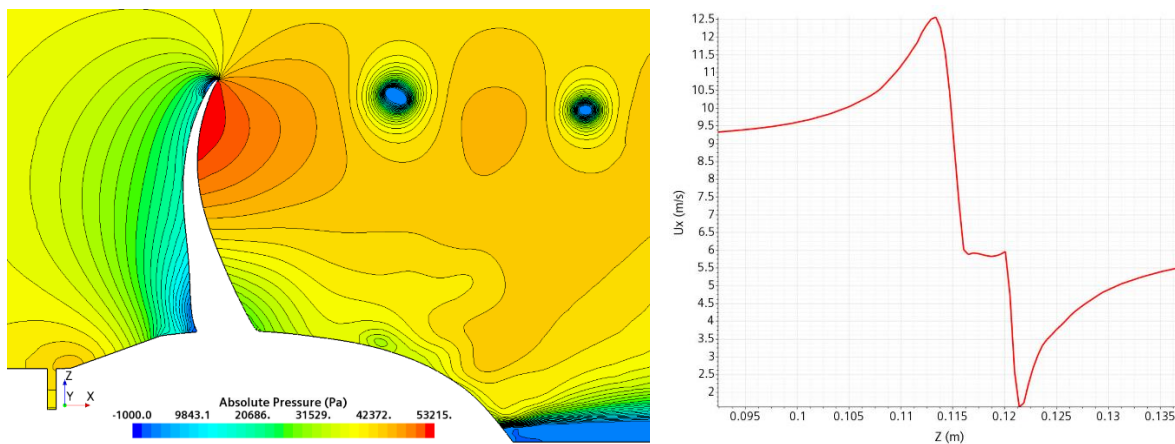
Figure 14 *Contours of absolute pressure in a longitudinal section through propeller blade and hub (left) and the profile of streamwise velocity component in radial direction across tip vortex (right) from a DES-computation of flow around propeller using the finest grid with 17 million cells for a single blade.*

The pressure inside tip vortex cavitation zone is nearly constant and slightly below saturation pressure, as can be seen from Fig. 14. However, outside cavitation zone pressure increases very rapidly, as can be seen from dens pressure contours around the vortex core. The streamwise velocity component is also almost constant inside tip vortex, as shown in Fig. 14, but the gradients with which the velocity decreases on one side and increases on the other side of vortex core are extremely high. Thus, for a

23

successful resolution of tip-vortex cavitation one needs a fine grid to resolve the extreme pressure and velocity gradients around tip vortex core, and a turbulence model which does not generate high turbulent viscosity in this zone, in spite of high velocity gradients. The cavitation model seems to play a less important role.

Figure 14 also shows that in a small zone within hub vortex and close to blade tip, the absolute pressure is below -1000 Pa (the minimum pressure at the suction side near leading edge is actually much lower). As discussed in Sect. 4, this is due to the fact that (i) pure liquid can sustain tensile stresses (i.e., negative pressure) to a relatively high degree, and (ii) the bubble growth rate is finite. Thus, where fluid velocity is very high and the residence times of bubbles within low-pressure zone are short, absolute pressure in liquid can become negative. Some cavitation models cannot account for this behavior, which is sometimes even advertised as a quality feature of the model. However, it is well known that cavitation strongly depends on liquid purity; if all solid particles and dissolved non-condensable gases were removed from water, it would not cavitate until pressure drops to a very low level (the lowest measured pressure in water – before cavitation started – known to the author was around -280 bar [14]).

6. Scale Effects

Scale effects play an important role in ship hydrodynamics: it is practically impossible to match both Froude and Reynolds numbers in an experiment at model scale and in full scale. The same is true for studies of cavitating flow around propeller: the model-scale propeller used in experiments is ca. 40 times smaller than the full-scale propeller, and it rotates much faster. For this reason, cavitation is present on propeller blade during its full rotation in model scale, while at full scale, cavitation is present only during ca. 1/3ʳᵈ of rotation, see Fig. 15. The pressure increases by 1 bar from top to bottom of propeller in full scale (propeller diameter 10 m). As Fig. 15 shows, the similarity between the flows in model and full scale is limited, making an extrapolation from results obtained in model scale to full scale rather difficult.
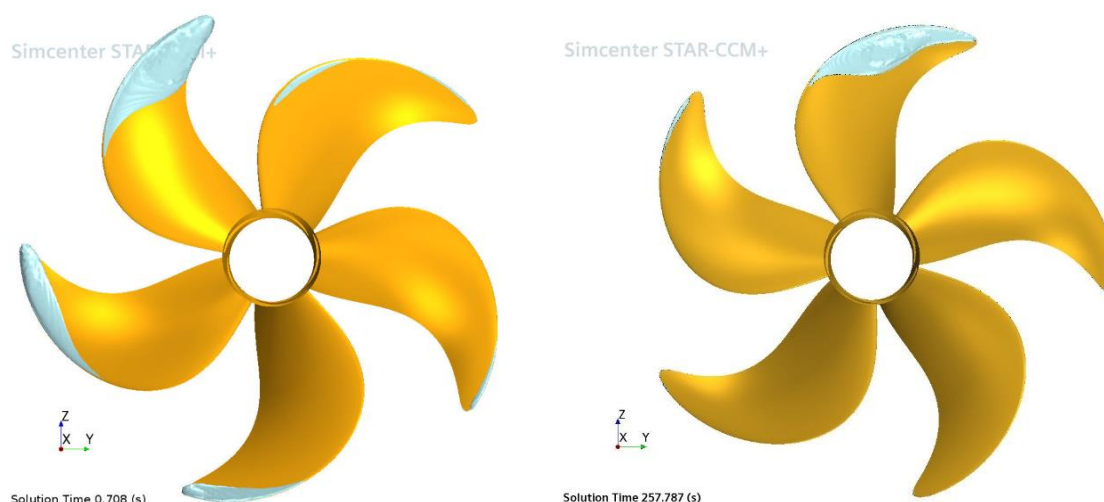
Figure 15 *Iso-surfaces of 5% vapor volume fraction on propeller blades: model scale (left) and full scale (right).*

Another problem with cavitation studies in model scale is that experiments are usually performed in a cavitation tunnel of a relatively small cross-section and without free surface. Thus, the flow around propeller is different from what it would be if the free surface was present and the blockage effects were negligible. The reflection of pressure waves from cavitation tunnel walls is also problematic, especially if pressure fluctuations on propeller blades, rudder and hull above propeller are studied.

Performing simulation at full scale is hardly any more difficult than at model scale: one only needs to reduce the thickness of the near-wall cells compared to the grid that would be suitable for a simulation at model scale, in order to ensure that the same number of cells is present within the logarithmic range of the boundary layer. The far-field boundary conditions are easy to impose, and the effects of free surface waves – both incoming and ship-induced – and ship motion in waves can easily be taken into account.

The problem is that full-scale data is scarce and the confidence in full-scale simulation is still limited. Although the quality of CFD-predictions has been verified in numerous comparisons between simulation and experimental data, the suspicion is still large, even though nothing is suggesting that the accuracy of CFD-solutions could be lower at full than at model scale. We hope that more data from full-scale measurements will become available in near future, and that full-scale analysis will become a commonplace.

7. Conclusions

In ship hydrodynamics, one of the most important tasks is to determine the hull resistance and to choose an appropriate propeller whose thrust matches the resistance at a minimum of required power. The workshop organized by Lloyds Register in 2016 demonstrated that full-scale simulation of self-propulsion can be reliably conducted with state-of-the-art CFD-software [13].

Cavitation on propeller can be predicted with a satisfactory accuracy using common cavitation models (like Schnerr-Sauer model [11]), provided that the grid is locally refined within appropriate zones (leading edge, tip vortex, hub vortex). Capturing tip-vortex cavitation requires also a turbulence model which does not produce excessive turbulent viscosity.

An accurate representation of propeller geometry by the computational grid is also important. Especially the insufficient resolution of the leading-edge curvature can falsify the geometry and affect the splitting of the flow to the pressure and suction sides of propeller blades. Simulation can be used to study the effects of manufacturing tolerances (shape of blades and the deviation of built geometry compared to the CAD-model).

REFERENCES

[1]   https://www.sva-potsdam.de/wp-content/uploads/2020/11/PPTC-update_on_cavitation-VP1304vsP1790-1-1.pdf

[2]   SVA Report No. 3753, page 2.13, Case No. 5 (https://www.sva-potsdam.de/wp-content/uploads/2016/03/SVA-report-3753.pdf)

[3]   SVA Report No. 3753, page 2.9, Case No. 40 (https://www.sva-potsdam.de/wp-content/uploads/2016/03/SVA-report-3753.pdf)

[4]   Durbin, P. A., & Pettersson Reif, B. A. (2011). *Statistical theory and modeling for turbulent flows* (2nd ed.). Chichester, England: Wiley.

[5]   Pope, S. B. (2000). *Turbulent flows*. Cambridge: Cambridge Univ. Press.

[6]   Smagorinsky, J. (1963). General circulation experiments with the primitive equations. Part I: The basic experiment. *Monthly Weather Rev*., **91**, 99-164.

[7]   Wilcox, D. C. (2006). *Turbulence modeling for CFD* (3rd ed.). La Cañada, CA: DCW Industries, Inc.

[8]   Menter, F. R. (1994). Two-equation eddy-viscosity turbulence models for engineering applications. *AIAA J*., **32**, 1598-1605.

[9]   De Laage de Meux, B., Audebert, B., Manceau, R., Perrin, R. 2015. Anisotropic linear forcing for synthetic turbulence generation in large eddy simulation and hybrid RANS/LES modeling. *Physics of Fluids,* **27** (3), 035115.

[10]   Skillen, A., Revell, A., Craft, T. 2016. Accuracy and efficiency improvements in synthetic eddy methods. *Int. J. Heat and Fluid Flow*, **62**, 386-394.

[11]   Schnerr, G. H., Sauer, J. (2001). Physical and numerical modeling of unsteady cavitation dynamics. In *Fourth international conference on multiphase flow*. New Orleans, USA.

[12]   Nicoud, F. and Ducros, F., 1999. Subgrid-Scale Stress Modelling Based on the Square of the Velocity Gradient Tensor. *Flow, Turbulence and Combustion*, **62**, 183-200.

[13]   Spalart, P.R., Deck, S., Shur, M.L., Squires, K.D., Strelets. M. and Travin, A. 2006. A new version of detached eddy simulation, resistant to ambiguous grid densities. *Theor. Comput. Fluid Dynamics*, **20**, 181-195.

[14]   *Cavitation in control valves*. Technical Information, Samson AG, www.samson.de.

[15]   D. Ponkratov (Ed.), Proceedings: 2016 Workshop on Ship Scale Hydrodynamic Computer Simulations, Lloyd's Register, Southampton, United Kingdom (2017)

PC6 SFIC – Ice class Hull design principles

Marijan, Ferenčić; Darko, Burlović; Marko, Pirija

IHC Engineering Croatia d.o.o., Milutina Baraća 7, 51000 Rijeka
m.ferencic@royalihc.com ; d.burlovic@royalihc.com ; m.pirija@royalihc.com

Abstract

Recently there has been a major interest for exploration cruises in the polar regions. A number of vessels are under construction or already built, mainly as exploration yachts to offer cruises in the Antarctic or Artic regions. These vessels, especially their hull construction, need to be designed to withstand first or multi-year ice loading. This area is rather new in aspect of best practices and rules and regulations offered from major classification societies, especially for sailing in stern first mode.

This article brings an insight into the hull structure design and calculation principles in accordance with PC6 and stern first ice class (SFIC) notations of Lloyd's register of shipping rules for navigation in Artic or Antarctic first-year ice conditions. The ice pressure zone determination, ice pressure calculation, basic scantlings determination, FEA primary elements verification and buckling analysis methodology is presented.

Key words: *Exploration Yacht; PC6 Polar Class; Stern First Ice Class (SFIC); Engineering; Finite Element Analysis; Buckling Analysis*

Sažetak

U posljednje vrijeme povećana je potražnja za istraživačko-turistička krstarenja u polarnim vodama. Popriličan broj brodova, većinom klase istraživačkih jahti, je izgrađen ili u izgradnji sa svrhom krstarenja u područja Antarktika ili Arktika. Ovi brodovi, posebno u aspektu konstrukcije trupa, moraju biti projektirani da zadovolje kriterija naprezanja uzrokovane opterećenjem od jednogodišnjeg ili višegodišnjeg leda. Ovo područje je relativno novo sa aspekta iskustvenih podataka, kao i pravila vodećih brodarskih klasifikacijskih društava. Osobito se to odnosi na lomljenje leda krmom.

Ovaj članak obuhvaća principe projektiranja konstrukcije trupa i proračunske metode u skladu s klasom PC6 i dodatnom notacijom SFIC, ledolomac krmom, prema „Lloyd's register of shipping" pravilima za navigaciju arktičkim i antartičkim vodama i jednogodišnjim ledom. Prezentirani su određivanje osnovne podjele broda na zone opterećenja od leda, proračun ulaznih opterećenja leda, proračun osnovnih elemenata strukture, verifikacija primarnih elemenata brodske strukture pomoću MKE, te metodologija proračuna izvijanja brodske strukture.

Ključne riječi: *Istraživačka jahta; PC6 polarna klasa; SFIC Ledolomac Krmom dodatna klasna notacija; MKE; Proračun Izvijanja*

List of Abbreviations and Symbols

Abbreviation	Designation	Chapter
FE	Finite element	6
IACS	International Association of Classification Societies	2
LIWL	Lower ice waterline	
PC	Polar class	4
PI	Associated plate induced failure	6
SFIC	Stern First Ice Class	2
SI	Stiffener induced failure	6
SP	Stiffened panel	6
UIWL	Upper ice waterline	
UP	Unstiffened panel	6
WMO	World Meteorological Organization	2

Symbol	Designation	Chapter
t_{net}	Net plate thickness	5
t_s	Corrosion and abrasion allowance	5
s	Frame spacing	5
AF	Hull area factor	5
K_i	Peak pressure factor	5
P_a	Average patch pressure	5
σ_y	Minimum upper yields stress of material	5
b	Height of design load patch	5
l	Distance between frame supports	5
l_L	Length of loaded portion of span	5
a	Effective span of longitudinal frame	5
h_w	Web height of framing member	5
t_{wn}	Net web thickness of framing member	5
t_{pn}	Net thickness of shell plate in way of framing member	5
b_f	Flange width of framing member	5
b_o	Flange outstand of framing member	5
t_{fn}	Net thickness of the flange of the framing member	5
As	Net sectional area	6
b	Width of plate panel	6
b_{eff}	Effective width of attached plating of stiffeners	6
β_p	Plate slenderness parameter	6
h_w	Height of local web frame	6
I	Moment of inertia	6
K	Buckling factor	6
l_{eff}	Effective length of the stiffener	6
λ	Reference degree of slenderness	6
P	Lateral pressure	6
s	Stiffener spacing	6

8. Introduction

Ice classes have been independently evolving during the past century according different operational needs and organized ways of navigation. First a short overview is given of different sets of rules used according to Ice Class Rules Description and Comparison [Ref. 3]

One of the first set of rules evolved were the Finish-Sweedish rules (1AS in 1965). These are present in major classification societies for years now, and have been revised several times (1979, 2008). These are issued by the Swedish Transport Agency and Finish transport and Communications agency (TRAFICOM) and offer a rule set [Ref. 4] and guidelines for application of the rules [Ref. 5]. First ASPPR (Arctic Shipping Polution Prevention) rules were developed in 1972, revised in 1989 (1995). IACS Polar Rules were developed 1992-2000. Russian Register were revised in 1995 and 2008. In 2012 ABS fully adopted IACS Polar Rules. The IMO Polar Code entered into force 1st of January 2017.
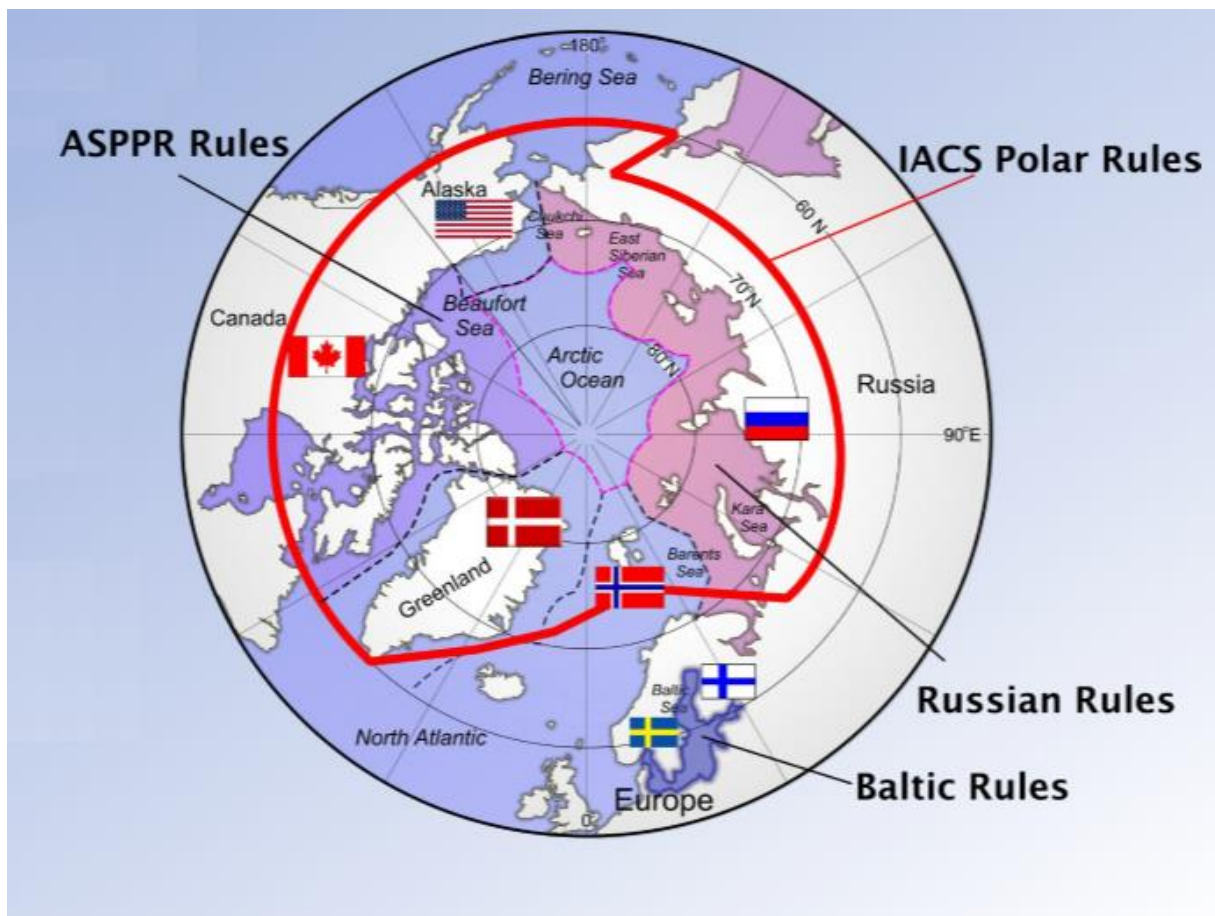
Figure 1 *Overview of Independent Ice Rules Areas in the Arctic and Sub-Arctic Regions*
Slika 1 *Pregled različitih pravila za navigaciju u arktičkom i sub-arktičkom području*

Each rule set is unique, with it's own approach to ice loads and strength assessment and areas of ice strenghtening. The ice loading approach for each is shown in Figure 2, while the overview of ice loading areas is given in Figure 3. Overview of polar classes in presented in Table 2.
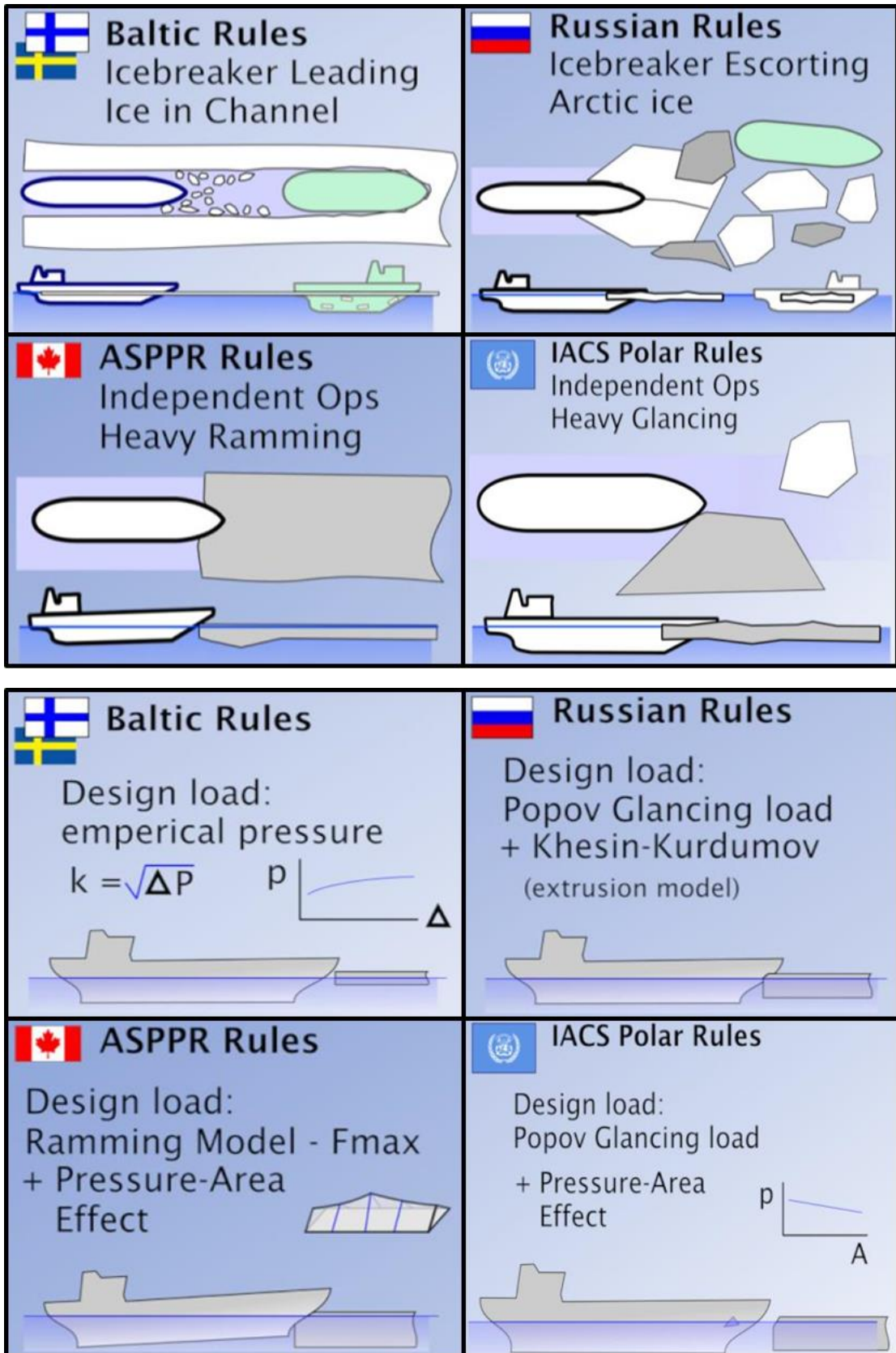
Figure 2 *Overview of Ice loading approach*
Slika 2 *Pregled različitih pristupa opterećenjima uzrokovanih ledom*
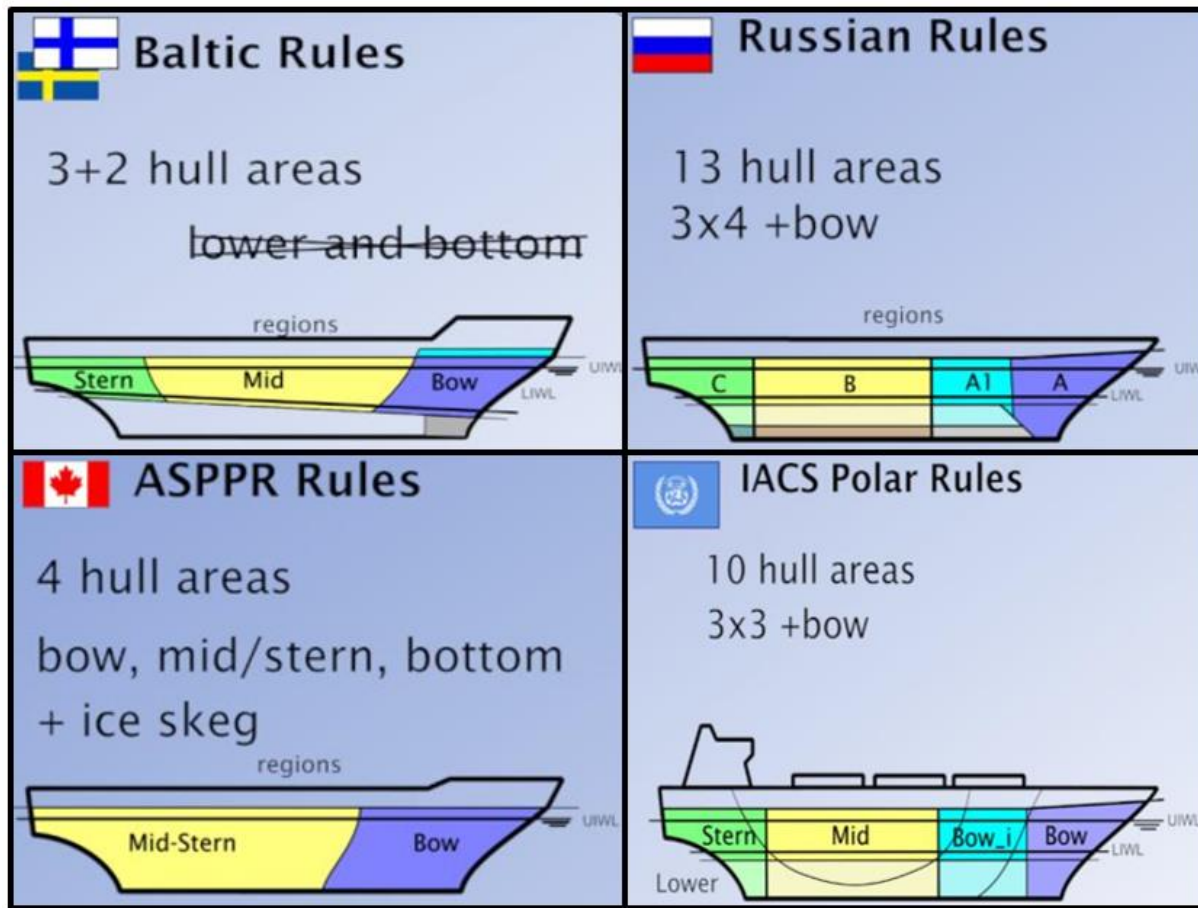
Figure 3 *Overview of Ice loading areas for Different Rules*
Slika 3 *Pregled različitih definicija zona pod opterećenjem uzrokovanog ledom*

Table 2 *Polar Classes*
Tablica 1 *Polarne klase*

		RRS	IACS	
		Arc9[i]	PC1	
			PCS	
		Arc8[e]	PC3	Year-Round Navigation in Arctic Waters
		Arc7	PC4	
		Arc6	PC5	
	1 AS	Arc5	PC6	Summer Navigation in Arctic Waters
Winter Navigation in Sub-Arctic Waters	1 A	Arc4	PC7	
	1 B	Ice3	**Notes:**	
	1 C	Ice2	i – independent operation allowed in all Russian sea areas in all winters	
		Ice1		
	TRAFI	RRS	e – icebreaker escorted operation allowed in all Russian sea areas in all winters	

It is evident that different approaches were also developed with regard to the environment and preferred operation in ice infested waters. One of the most widely used for a variety of vessels, Baltic, Finish-Swedish Rules were developed for brash ice loadings in ice channels and the loadings and ice reinforcement is mostly present in the waterline areas. The IACS Polar Code is meant to provide a uniform approach for Polar Navigation.

9. Polar Class Overview According Lloyds Register of Shipping

This study investigates the structural design and calculation of an exploration yacht with the requirement for summer/autumn operation in medium first-year ice which may include old ice inclusions, which corresponds to an Ice Class PC 6 according to Lloyds Rules and regulations [Ref. 1]. The vessel has an additional notation of SFIC – Stern First Ice Class (Provisional Rules for the Classification of Stern First Ice Class Ships).

Table 3 *Polar class description [Ref 1.]*
Tablica 2 *Opis polarne klase [Ref 1.]*

Polar class	Ice description (WMO Sea Ice Nomenclature)
Ice Class PC 1	Year-round operation in all Polar waters
Ice Class PC 2	Year-round operation in moderate multi-year ice conditions
Ice Class PC 3	Year-round operation in second-year ice which may include multi-year ice inclusions
Ice Class PC 4	Year-round operation in thick first-year ice which may include old ice inclusions
Ice Class PC 5	Year-round operation in medium first-year ice which may include old ice inclusions
Ice Class PC 6	Summer/autumn operation in medium first-year ice which may include old ice inclusions
Ice Class PC 7	Summer/autumn operation in thin first-year ice which may include old ice inclusions

While the Lloyds Rules and regulations [Ref. 1] for the first-year ice conditions prescribe Finnish-Swedish Ice Class Rules, for the multi-year ice conditions (old ice inclusions) the IACS Polar Ship Rules become applicable (see Table 3). The ice conditions according to WMO definition are described in Table 4.

Table 4 *WMO definition of ice conditions*
Tablica 3 *WMO definicija polarnih uvjeta*

Ice conditions		Ice thickness range
Old ice	Multi-year	> 2.5 m
	Second-year	< 2.5 m
	Thick first-year	< 1.2 m
	Medium first-year	0.7 – 1.2 m
First-year ice	Thin first-year, second stage	0.5 – 0.7 m
	Thin first-year, first stage	0.3 – 0.5 m
	Grey-white	0.15 – 0.3 m

Grey		0.1 – 0.15 m
Nilas		< 0.1 m

The basis for the calculation of hull strengthening for navigation in ice conditions is the determination of hull ice regions and calculating the corresponding design ice loads (the calculation is is described in more detail in Chapter 11). According to [Ref. 1], the hull of all polar class ships is divided into specified areas, as presented in Figure 4. Each hull area needs to withstand the different magnitude of the loads that are expected to act upon them. In the longitudinal direction, four regions exist:

a) bow (B),
b) bow intermediate (BI),
c) midbody (M), and
d) stern (S).

The bow intermediate, midbody and stern regions are further divided in the vertical direction into three regions:

a) bottom (b),
b) lower (l), and
c) icebelt (i).
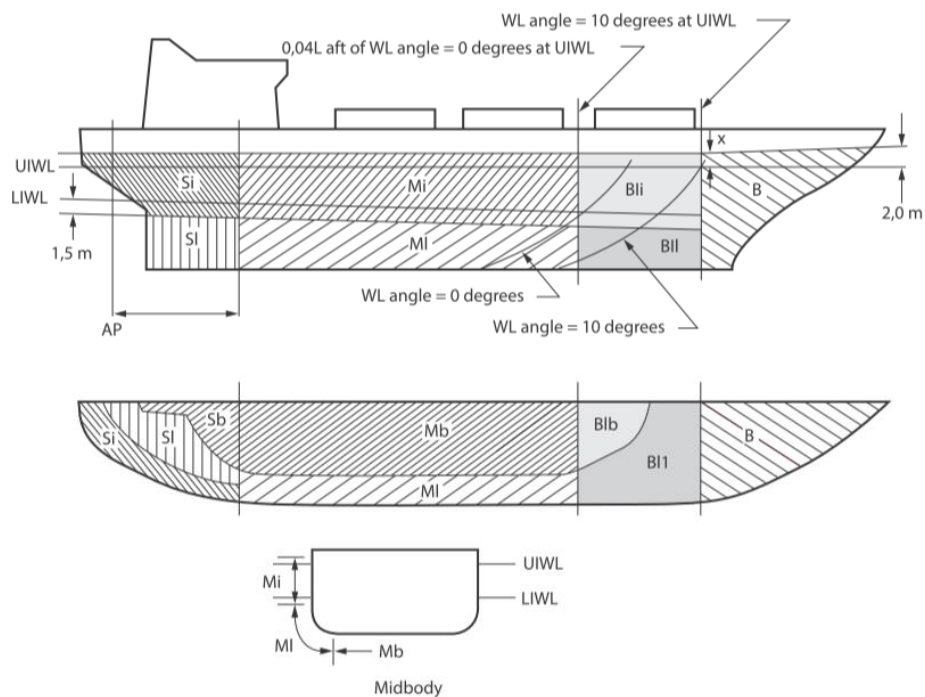
Figure 4 *Extent of hull areas for polar class ships (LR/ IACS Polar Ship Rules)*
Slika 4 *Prikaz definiranih područja trupa za brodove polarne klase (LR/ IACS Polar Ship Rules)*

The upper ice waterline (UIWL) is defined by the maximum draughts fore, amidships and aft, while the lower ice waterline (LIWL) is defined by the minimum draughts fore, amidships and aft. This exploration yacht is equipped with podded propulsion units or azimuthing thrusters and designed for stern first operations in ice going conditions (see Figure 5), resulting in a design that consists of two sets of UIWL and LIWL. Hull area definition for stern first mode is described in Figure 6.
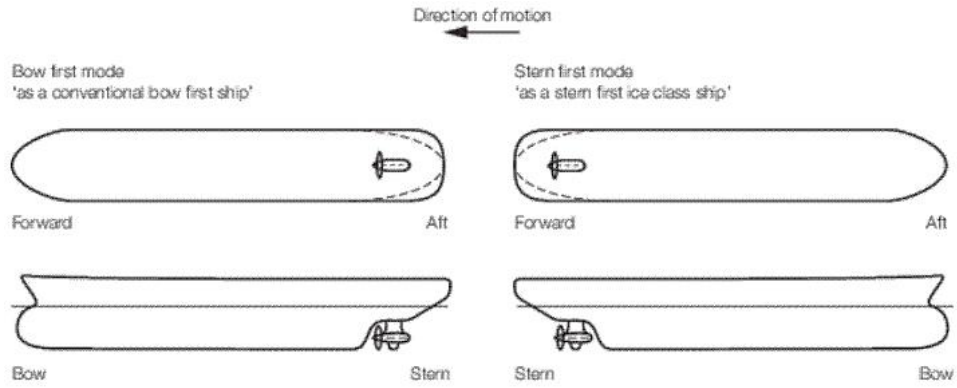
Figure 5 *Direction of motion*
Slika 5 *Smjer gibanja*
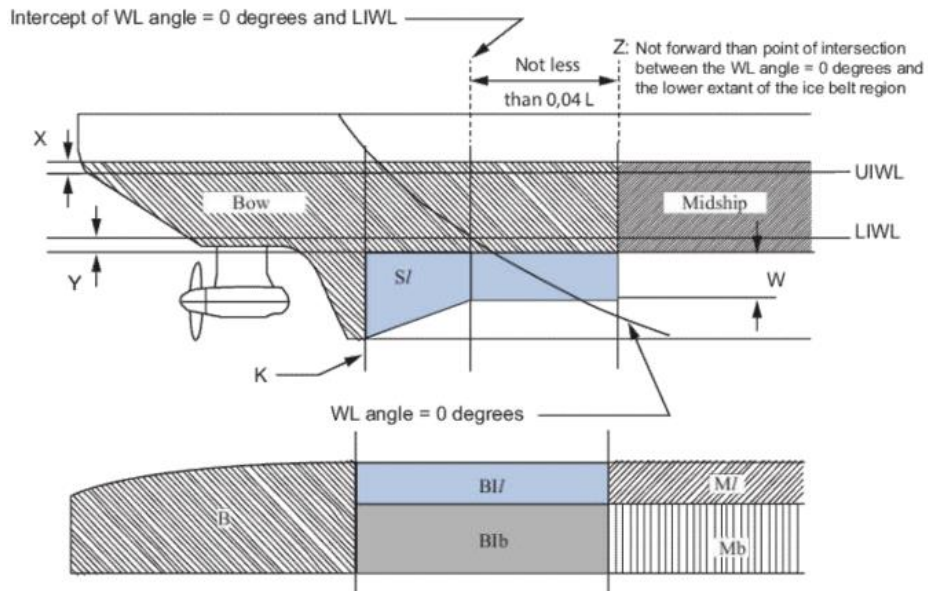
Figure 6 *Stern hull areas*
Slika 6 *Prikaz definiranih područja krme*

10. Case Study

The case study of this article is a polar expedition yacht with the following particulars, as seen in Table 5:

Table 5 *Main particulars*
Tablica 4 *Glavne značajke*

Length Overall, Loa	120.00 m
Length between Perpendiculars, L_{pp}	100.00 m
Length (Scantling), L	104.00 m
Breadth (moulded), B	19.00 m
Depth (moulded), D	10.00 m
Draft (Design), Td	7.00 m

Block coefficient, Cb	0.6
Service speed (Design Draft)	Abt. 16.0 kn
Gross tonnage	Abt. 8000 ton

The yacht's general arrangement can be seen in Figure 7.
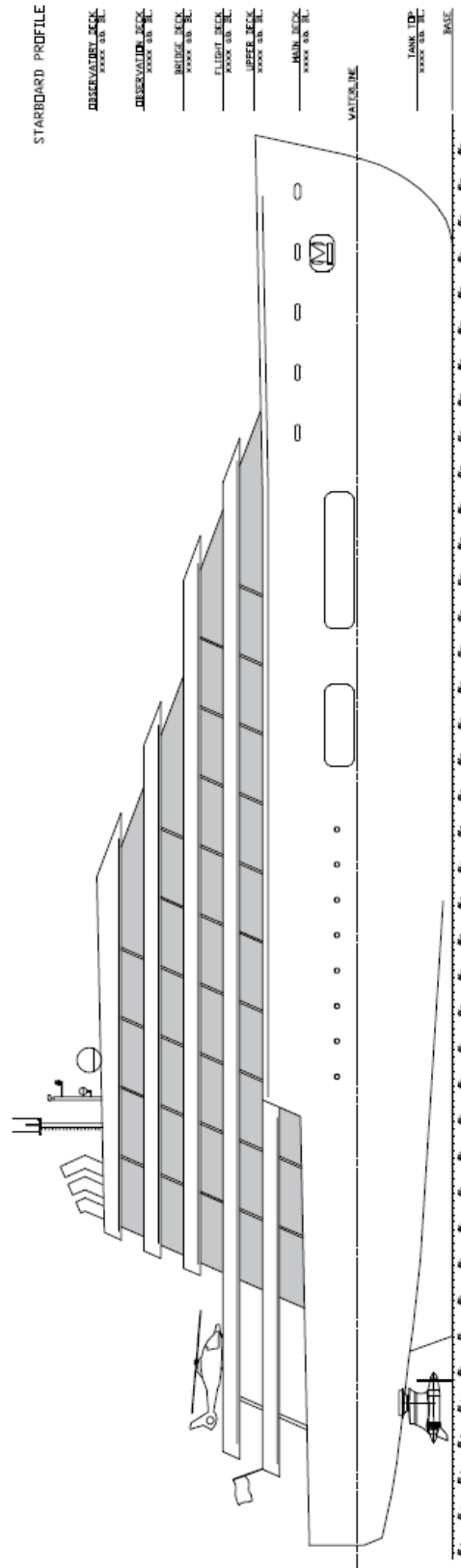
Figure 7 *Vessel general arrangement*
Slika 7 *Opći plan broda*

11. Design Ice Loads

For ships of all Polar Classes, a glancing impact on the bow is the design scenario for determining the scantlings required to resist ice loads. The design ice load is characterized by an average pressure, uniformly distributed over a rectangular load patch.

The parameters defining the glancing impact load characteristic are reflected in the class factors listed in Table 6 [Ref. 1].

Table 6 *Class factors for icebreaking bow forms*
Tablica 5 *Propisani faktori za pramce ledolomaca*

Polar Class	Crushing failure class factor	Flexural failure class factor	Load patch dimensions class factor	Displacement class factor	Longitudinal strength class factor
	C_C	C_F	C_D	C_{DI}	C_L
PC1	17,69	68,60	2,01	250	7,46
PC2	9,89	46,80	1,75	210	5,46
PC3	6,06	21,17	1,53	180	4,17
PC4	4,50	13,48	1,42	130	3,15
PC5	3,10	9,00	1,31	70	2,50
PC6	2,40	5,49	1,17	40	2,37
PC7	1,80	4,06	1,11	22	1,81

The loads in the bow area are functions of the hull angles measured at the upper ice waterline. The influence of the hull angles is captured through calculation of a bow shape coefficient, fa. The hull angles are defined in Figure 8 [Ref. 1].
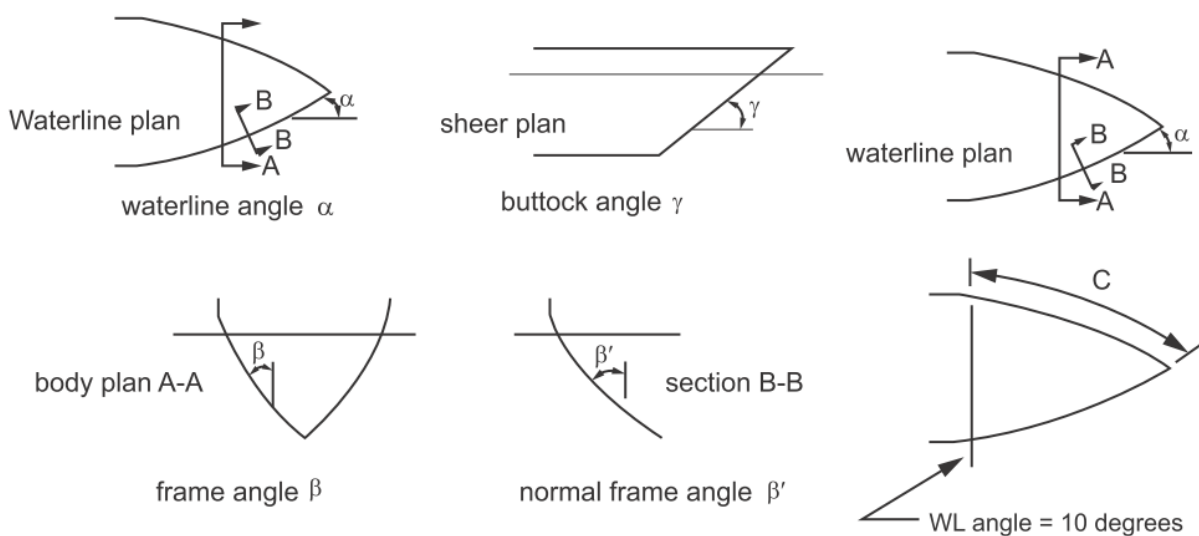
Figure 8 *Definition of hull angles*
Slika 8 *Definicija kuta trupa*

When the shape coefficient and other main particulars are defined, force, load patch aspect ratio, line load and pressure in different sub-regions can be calculated according to the rules [Ref. 1]. Sub-regions are equal divisions of the waterline length of the bow region. All before mentioned, forces, pressures etc. are calculated with respect to the mid-length position of each sub-region. Rules are also prescribed for hull areas other than the bow.

In the bow area, and the bow intermediate Ice-belt area, for ships with class notation PC6, corresponding design load patch (width and height) and pressure within the design load patch are calculated. Design load patch width is determined as the ratio of the maximum force and the maximum line load for each sub-region considered in bow area and bow intermediate area. Design load patch height is determined as the ratio of the maximum line load and the maximum pressure for each sub-region considered in bow area and bow intermediate area.

Regions other than the bow and bow intermediate are not divided into sub-regions. Therefore, the design load path width is calculated as ratio of force and line load, and the design load height is calculated as ratio of width and value of 3.6.

Associated with each hull area is an area factor that reflects the relative magnitude of the load expected in that area, see Table 7.

Table 7 *Hull area factors (AF)*
Tablica 6 *Faktori područja trupa (AF)*

Hull area		Area	Polar Class						
			PC1	PC2	PC3	PC4	PC5	PC6	PC7
Bow (B)	All	B	1,00	1,00	1,00	1,00	1,00	1,00	1,00
	Icebelt	BI i	0,90	0,85	0,85	0,80	0,80	1,00*	1,00*
Bow intermediate (BI)	Lower	BI l	0,70	0,65	0,65	0,60	0,55	0,55	0,50
	Bottom	BI b	0,55	0,50	0,45	0,40	0,35	0,30	0,25
Midbody (M)	Icebelt	M i	0,70	0,65	0,55	0,55	0,50	0,45	0,45
	Lower	M l	0,50	0,45	0,40	0,35	0,30	0,25	0,25
	Bottom	M b	0,30	0,30	0,25	**	**	**	**
Stern (S)	Icebelt	S i	0,75	0,70	0,65	0,60	0,50	0,40	0,35
	Lower	S l	0,45	0,40	0,35	0,30	0,25	0,25	0,25
	Bottom	S b	0,35	0,30	0,30	0,25	0,15	**	**

* See Pt 8, Ch 2, 10.2 Design ice load – General 10.2.3.

** Indicates that strengthening for ice loads is not necessary.

For this expedition yacht, in Provisional Rules for the Classification of Stern First Ice Class Ships [Ref. 2], the area factors for stern are shown for the bow and bow intermediate region, see Table 8.

Table 8 *PC Rule Area Factors for bow and bow intermediate regions applied to the stern of SFIC ships*
Tablica 7 *Faktori površine polarne klase za pramac i srednje pramčano područje za brodove sa klasifikacijom SFIC*

Ice Class assigned	Bow	Bow Intermediate Ice Belt	Bow Intermediate lower	Bow Intermediate bottom
PC1	0,85	0,85	0,65	0,50
PC2	0,85	0,85	0,65	0,45
PC3	0,85	0,80	0,60	0,40
PC4	0,85	0,80	0,55	0,35
PC5	0,85	0,80	0,55	0,30
PC6	0,85	1,00	0,50	0,25
PC7	0,85	1,00	0,50	0,25

A corrosion and abrasion allowance for polar classes is presented in Table 9.

Table 9 *Corrosion and abrasion allowance, t_s, for polar classes*
Tablica 8 *Dodatak za koroziju i abraziju, t_s, za polarne klase*

Hull area	t_s, in mm					
	With effective protection			Without effective protection		
	PC1 to **PC3**	**PC4** and **PC5**	**PC6** and **PC7**	**PC1** to **PC3**	**PC4** and **PC5**	**PC6** and **PC7**
Bow; Bow Intermediate Ice belt	3,5	2,5	2,0	7,0	5,0	4,0
Bow Intermediate Lower; Mid-body & Stern Ice belt	2,5	2,0	2,0	5,0	4,0	3,0
Mid-body and Stern Lower; Bottom	2,0	2,0	2,0	4,0	3,0	2,5

The process of calculation design ice loadings is schematically explained in Figure 9.

| | Glancing impact on the bow - class factors - PC6 (Pt 8, Ch 2, 10.3 of Ref. 1) | |

↓

| | Design ice load – pressure (Pa) over a rectangular patch (b x w) (Pt 8, Ch 2, 10.2 of Ref. 1) | |

↑

Areas		Shape
Bow area (B)		Buttock angle (γ) < 80° & normal frame angle (β') > 10 ° (Pt 8, Ch 2, 10.4.3 of Ref. 1)
Bow intermediate icebelt area (BIi)	Function of bow shape – shape coefficient (fai), total glancing impact force (Fi), line load (Qi), pressure (Pi) (Pt 8, Ch 2, 10.2.3 of Ref. 1)	Bow vertical sides & normal frame angle (β') = 0° - 10 ° (Pt 8, Ch 2, 10.4.4 of Ref. 1) · Bulbous bow (Pt 8, Ch 2, 10.2-8 of Ref. 1)
		Other bow forms – specially considered
Other areas	Independently of the hull shape, based on a fixed load patch aspect ratio, AR = 3.6 (Pt 8, Ch 2, 10.2.5 of Ref. 1)	

Figure 9 *Design ice load calculation flow chart*
Slika 9 *Tijek izračuna dizajn opterećenja ledom*

The ice exposed hull shape of the vessel and its associated ice zones are presented in Figure 10.

Figure 10 *Ice load zones*
Slika 10 *Zone opterećenja leda*

12. Local Scantlings Calculation

Scantlings for plating and secondary stiffening (ice framing) for the ice induced loading is to be calculated according rule formulae given in Pt 8, Ch 2, Sec 10 of [Ref. 1]. As specified in the rules, at this

moment no direct calculation can be used to substitute the values obtained according to mentioned rule formulae for these elements.

For each respective zone, and applied pressure and patch size (as described in Ch. 11) the scantlings are obtained as plate thicknesses and section moduli of plasticity for secondary stiffeners with its attached plating.

12.1. *Shell plate requirements*

The required minimum shell plate thickness depends on the orientation of framing and according to Pt 8, Ch2, 10.9.2 [Ref. 1] is calculated as:

$$t = t_{net} + t_s \text{ [mm]} \tag{1}$$

Where:

t_{net} – plate thickness [mm] required to resist ice loads = $f(s, b \text{ or } l, AF, K_p, P_a, \sigma_y)$

t_s – corrosion and abrasion allowance [mm] – Pt 8, Ch 2, 10.16,

s - transverse frame spacing [m] in transversely-framed ships or longitudinal frame spacing in longitudinally-framed ships, measured along the girth,

AF – hull area factor

K_p – peak pressure factor (plating),

P_a – average patch pressure [MPa]

σ_y – minimum upper yield stress of the material [N/mm²]

b – height of design load patch [m]

l - distance between frame supports [m]

12.2. *Framing scantlings requirements*

Regarding the plate stiffening, the rules prescribe the minimum for net effective shear area and net effective plastic section modulus of the stiffener, with its attached plating included.

The net effective shear area, depending on whether it is s a local frame in bottom structure and transverse local frame in side structure or a longitudinal local frame in side structure, is calculated in accordance with Pt 8, Ch 2, 10.10 to 10.12 [Ref. 1]. The net effective shear area is a function of $l_L \text{ or } b_1, s \text{ or } a, AF, K_t \text{ or } K_s, P_a, \sigma_y;$

Where:

l_L – length of loaded portion of span [m]

$b_1 = 1 - \frac{0.3 \cdot s}{b}$ [m], where b – height of design ice load patch

s – spacing of local frame [m]

a – effective span of longitudinal frame [m]

K_t – peak pressure factor (transverse framing)

K_s – peak pressure factor (bottom structures, side longitudinal, web frames and load carrying stringers)

The moduli of plasticity depend on whether the cross sectional area of the attached plating exceeds or not the cross sectional area of the local frame, and are calculated according to formulae given in Pt 8, Ch 2, 10.10 to 10.12 [Ref. 1]. The moduli of plasticity are a function of l_L, Y, s, AF, K_t or K_s, P_a, a, A_1 or A_4, σ_y;

Where:

$$Y = 1 - \frac{l_L}{a}$$

A_1 – greater of A_{1A} or A_{1B}

$$A_4 = \frac{1}{2 + k_w \left(\sqrt{1 - a_4^2} - 1 \right)}$$

12.3. *Framing structural stability*

Besides the net effective shear area and modulus of plasticity, structural stability of the plate stiffening also has to be ensured. To prevent local buckling of the web, the web height to net web thickness ratio of any stiffening member is to be the following:

- For flat bar sections:

$$\frac{h_w}{t_{wn}} \leq \frac{282}{\sqrt{\sigma_y}} \tag{2}$$

- For bulb, tee and angle sections:

$$\frac{h_w}{t_{wn}} \leq \frac{805}{\sqrt{\sigma_y}} \tag{3}$$

Where:

h_w – web height

t_{wn} – net web thickness

In addition, the following statement has to be satisfied:

$$t_{wn} \geq 0.35 t_{pn} \sqrt{\frac{\sigma_y}{235}} \tag{4}$$

Where:

t_{pn} – net thickness of the shell plate in way of framing member [mm].

Moreover, to prevent local flange buckling of welded profiles, the following criteria are to be satisfied. The flange width, b_f, is not to be less than five times the net thickness of the web, t_{wn}; and the flange outstand, b_o, is to meet the following:

$$\frac{b_o}{t_{fn}} \leq \frac{155}{\sqrt{\sigma_y}}$$
(5)

Where:

t_{fn} – net thickness of the flange [mm].

12.4. Rule software

Rule based formulae software "Rules Calc" can be used as a relatively automated tool for determination of local scantlings of plating and stiffening. An issue that was raised during this project was a discrepancy while calculating the modulus of plasticity for "built" profile sections. This has been mentioned more in detail in Ch. 14 of this article.

13. Direct Analysis of Primary Ship Structure

As stated in the rules (Pt 8, Ch 2, 10.13 of [Ref. 1]), when the primary structure is forming a grillage it is to be directly analyzed via linear or nonlinear static calculation.

The structure has been analyzed in order to check the maximum structural capacity of the primary members under the combined effects of bending and shear.

According to Pt 8, Ch2, 10.26 of [Ref. 1] the following criteria have to be fulfilled:

a) Web plates and flange elements in compression and shear to fulfil relevant buckling criteria in accordance with the applicable Ship-Right SDA procedures (Pt 3, Ch 16, 3 of [Ref. 1]),
b) Nominal shear stresses in member web plates to be less than $S_y/\sqrt{3}$,
c) Nominal von Mises stresses in member flanges to be less than $1.15 \cdot S_y$.

Where S_y is Yield Strength of the material.

13.1. Finite Element Assessment of Primary Structure

For checking the strength of the primary structure under ice induced loads, a linear finite element analysis has been conducted using Siemens Femap with NX Nastran solver.

Although only primary structural elements are to be analyzed through this FE model, shell plating and stiffeners have been modelled in order to represent adequate stiffness and transfer of loading from the secondary structure to the primary one.

While determining the model extent, it is important to have a good, rough feel of the grillage that the primary structure is forming along the shell ice boundary. This FE model, or a series of models, represent a larger portion of the shell structure subjected to various combinations of local, ice induced loadings. Also, as defined in Ch. 11, various parts of shell are loaded differently and with a different ice load patch size depending on their respective ice zone. From this point two alternatives are possible, modeling the complete ice affected shell of the vessel, actually to some extent more than half of the vessel using symmetrical boundary conditions and even more towards the ends of the vessel in order to minimize the effect of the boundary conditions. This solution would result in a large, rather complex model with several

thousand (or even more) loading conditions and therefore would result in bulky and difficult to manipulate FE models as well as increasing calculation and post processing time. The alternative is to determine areas of interest per ice zone and split up the FE models to several ones, typically covering each respective zone (or several if applicable). This way the loading combination number is decreased to a more reasonable level, the models are easier to handle and post process, the work can be split up more easily between different structural engineers or modelers. The smaller, isolated models also can accommodate smaller mesh size in order to represent certain structural details and minimize the approximation in appliance of ice pressure loading.

An overview drawing indicating model extents and typical ice patch dimensions and pressures is then drawn out for different zones (see Figure 11) in order to present the analysis more clearly and prove that all of the pressure combinations vs. the largest spans of primary member are analyzed.
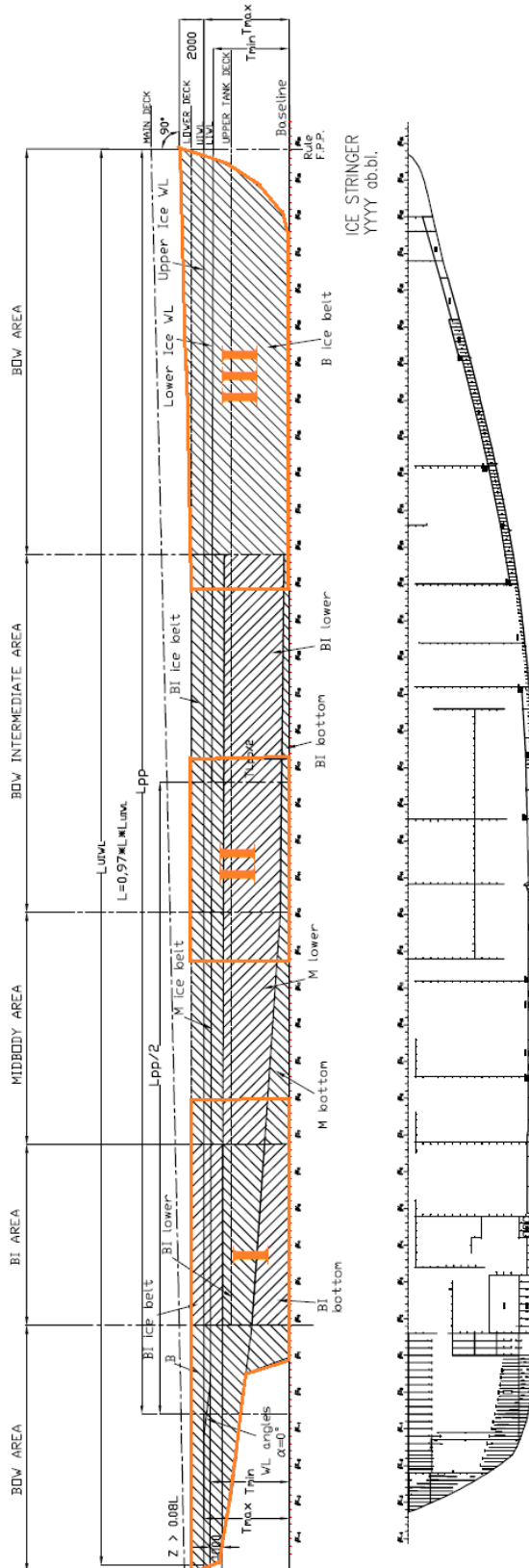
Figure 11 *FEA model extents*
Slika 11 *Opseg modela za analizu metodom konačnih elemenata*

The mesh size considered is also to be determined. The smaller the mesh size is, more correctly areas of adequate ice patch can be loaded to FE model applying pressure to the model. While there is no prescribed mesh size according to Rules, the chosen mesh size is 50x50 mm in order to adequately represent the response of the structure under ice induced loads.

The analysis has been done as a series of load cases where the corresponding ice patch (as described in Ch. 11) has been applied onto various locations of the shell plating in order to obtain worst case scenario stresses; i.e. locations where the capacity of these members under the combined effects of bending and shear is minimized (see Figure 12 to Figure 15).
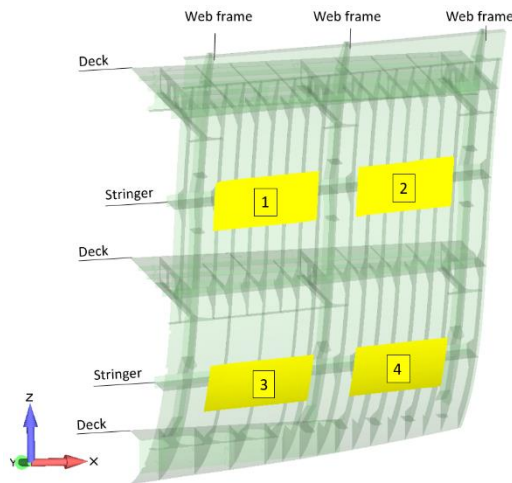
Figure 12 *Load patch position for checking maximum bending capacity of the stringer*
Slika 12 *Pozicije površina opterećnja za provjeru savojnog kapaciteta proveza*
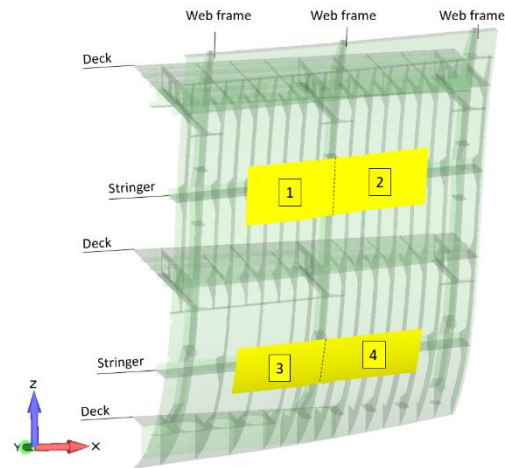
Figure 13 *Load patch position for checking the maximum shear capacity of the stringer*
Slika 13 *Pozicije površina opterećnja za provjeru smičnog kapaciteta proveza*
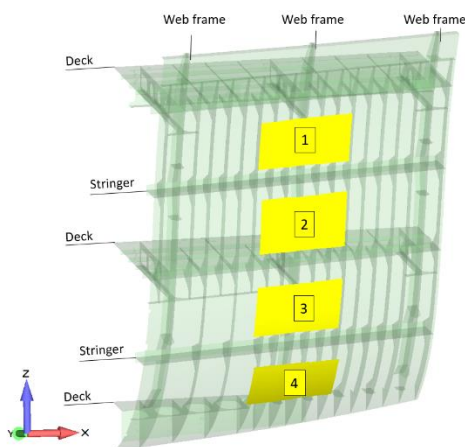
Figure 14 *Load patch position for checking maximum bending capacity of the web frame*
Slika 14 *Pozicije površina opterećnja za provjeru savojnog kapaciteta okvirnog rebra*
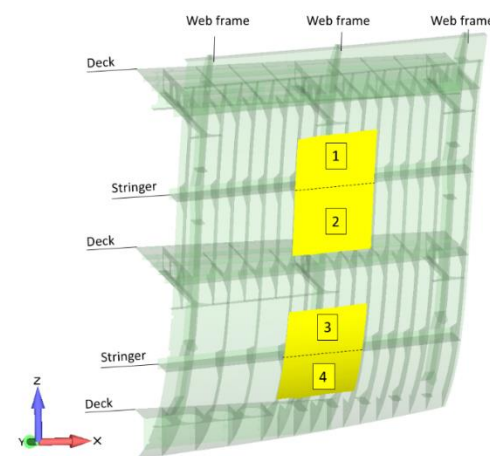
Figure 15 *Load patch position for checking maximum shear capacity of the web frame*
Slika 15 *Pozicije površina opterećnja za provjeru smičnog kapaciteta okvirnog rebra*

Only the primary members such as stringers, web frames, double bottom floors, bulkheads and longitudinal girders have been analysed, which were modelled using shell elements. The shell plating and secondary stiffening scantlings have been calculated according to Pt 8, Ch 2, 10.9 and 10.10 of [Ref. 1]. The analyses were conducted on partial ship models of sufficient extents in order to simulate the most accurate boundary conditions.

The plating and secondary stiffening is modeled in the FEA model only to provide more realistic deformation levels and load transfer.
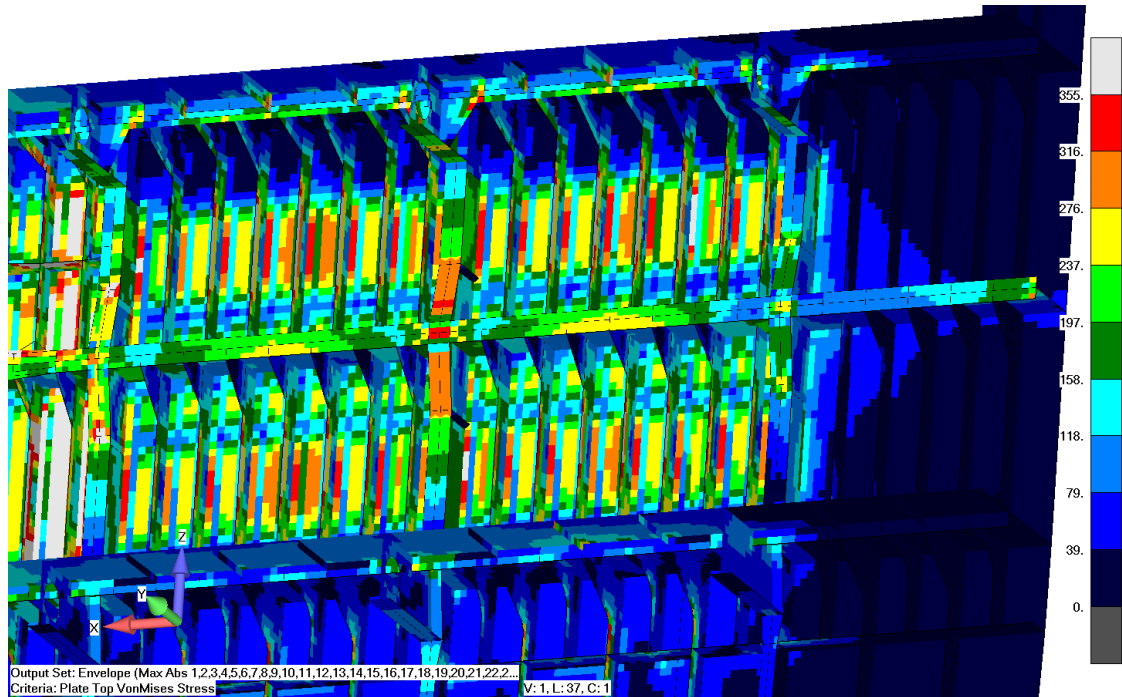
Figure 16 *FEA Von Mises stress levels for all shell ice fraing members [MPa]*
Slika 16 *Von Mises naprezanja za sve elemente pojačanja leda na oplati [MPa]*

The stress levels for these secondary members are not the object of this analysis and the output plots, according already stated acceptance criteria at the start of chapter 6, are adapted.
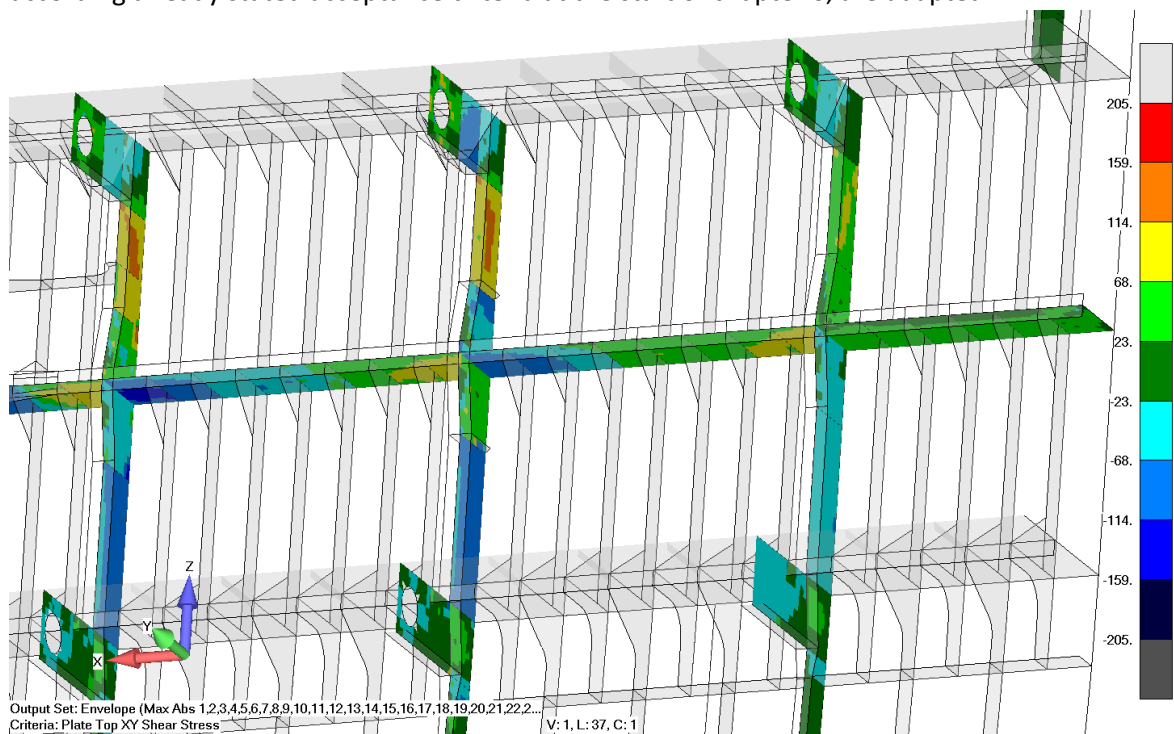
Figure 17 *FEA Shear stress levels for shell primary ice fraing members IWO ice loading [MPa]*

Figure 18 *FEA Von Mises stress levels for primary flange elements IWO ice loading [MPa]*
Slika 18 *Von Mises naprezanja za flanže primarnih elemenata oplate izložene opterećenjima leda [MPa]*

13.2. Buckling assessment

According to the Pt 8, Ch 2, 10.26.5(a) [Ref. 1] web plates and flange elements in compression and shear have to fulfil relevant buckling criteria in accordance with the applicable "Ship Right" SDA procedures.

The buckling stresses of plate panels are to be derived taking into account all relevant membrane axial and shear stress components. The ship structure consists of elementary plate panels, bounded at their edges by either a stiffening member (flat bar, HP, etc.) or a primary member. They can be categorized as unstiffened (UP) and stiffened (SP) panels. An unstiffened panel is normally defined as the plate bounded by stiffeners and primary supports, while a stiffened panel is normally defined as a component comprised of stiffeners with attached plating, see Figure 19.
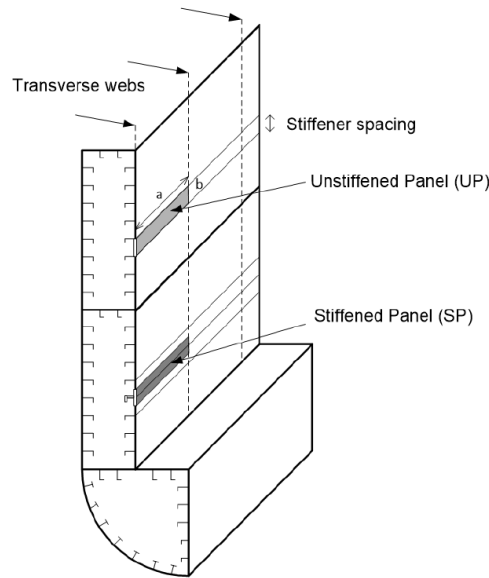
Figure 19 *Illustration of stiffened panel and unstiffened panel [Ref. 6]*
Slika 19 *Shematski prikaz ukrepljenog panela i neukrepljenog panela [Ref. 6]*

After obtaining results of a linear static analysis, for each elementary panel (consisting of multiple finite elements), an area-weighted average of stress is calculated to provide a longitudinal, transversal and in-plane shear stress as given in the guidance notes Ch 2, Sec 2 of [Ref. 6]. These stresses are then used in formulae to check if any buckling occurs in this structure, see Figure 20. For buckling assessment, compressive stress is assumed to be positive and tensile stress is assumed to be negative.
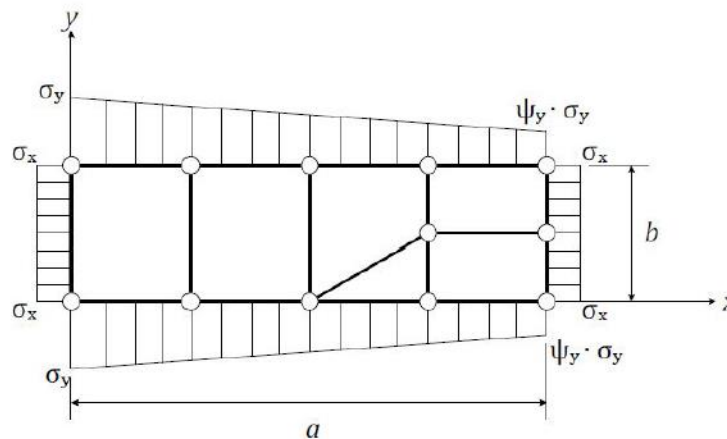
Figure 20 *Illustration of buckling working stresses [Ref. 6]*
Slika 20 *Shematski prikaz radnog naprezanja izvijanja [Ref. 6]*

For an unstiffened panel under combined in-plane buckling stresses (σ_x, σ_y, τ) the Factor of safety (Ω) for buckling assessment is to be determined from:

$$\Omega = \gamma_c \tag{6}$$

where

γ_c = the stress multiplier factor at failure calculated based on Ch 3, Sec 3, Buckling capacity of unstiffened panels [Ref. 6].

For a stiffened panel under combined in-plane buckling stresses (σ_x, σ_y, τ) and lateral pressure P, the Factor of safety (Ω) for buckling assessment is to be determined from:

$$\Omega = \min \left(\gamma_{ca}, \gamma_{cb}, \gamma_{cc}, \gamma_{cd} \right) \tag{7}$$

where

γ_{ca} = the stress multiplier factor at failure calculated based on Chapter 3, Section 2, Overall stiffened panel buckling capacity for overall stiffened panel capacity [Ref. 6].

γ_{cb} = the stress multiplier factor at failure calculated based on Chapter 3, Section 3, Buckling capacity of unstiffened panels for plate capacity [Ref. 6].

γ_{cc} = the stress multiplier factor at failure calculated based on Chapter 3, Section 4, Buckling capacity of stiffeners for stiffener induced (SI) failure capacity [Ref. 6].

γ_{cd} = the stress multiplier factor at failure calculated based on Chapter 3, Section 4, Buckling capacity of stiffeners for attached plate induced (PI) failure capacity [Ref. 6].

Spreadsheets are made to calculate the stress multiplier factors γ_c according to the interaction formulae given in the Buckling Assessment Guidance Notes [Ref. 6].

The required factors of safety for buckling strength assessments are according to the "Ship Right" SDA Procedure for Container Ships Table 1.6.1 Maximum permissible membrane stresses [Ref. 6] and is given as:

$$\Omega \geq 1,2 \tag{8}$$

Note that at the time of calculating these buckling factors "Ship Right" SDA Procedure for Passenger Ships did not exist. Nowadays the buckling factors would be different based on these new rules.

The results are obtained via spreadsheets and macros for all buckling, in plane stressed elements and the attained Ω obtained according to above described procedure. The results are then loaded to FEMAP via load vector and presented as attained Ω for all considered elements.

The plate limit state for the buckling capacity of unstiffened plate panels, is based on the following formulae:

$$\left(\frac{\gamma_{c1}\sigma_x S}{\sigma_{cx}} \right)^{e_0} - B \left(\frac{\gamma_{c1}\sigma_x S}{\sigma_{cx}} \right)^{\frac{e_0}{2}} \left(\frac{\gamma_{c1}\sigma_y S}{\sigma_{cy}} \right)^{\frac{e_0}{2}} + \left(\frac{\gamma_{c1}\sigma_y S}{\sigma_{cy}} \right)^{e_0} + \left(\frac{\gamma_{c1}|\tau|S}{\tau_c} \right)^{e_0} = 1 \tag{9}$$

$$\left(\frac{\gamma_{c2}\sigma_x S}{\sigma_{cx}} \right)^{2/\beta_p^{0.25}} + \left(\frac{\gamma_{c2}|\tau|S}{\tau_c} \right)^{2/\beta_p^{0.25}} = 1 \qquad \text{for } \sigma_x \geq 0 \text{ and } \sigma_y < 0 \tag{10}$$

$$\left(\frac{\gamma_{c2}\sigma_y S}{\sigma_{cy}} \right)^{2/\beta_p^{0.25}} + \left(\frac{\gamma_{c2}|\tau|S}{\tau_c} \right)^{2/\beta_p^{0.25}} = 1 \qquad \text{for } \sigma_y \geq 0 \text{ and } \sigma_x < 0 \tag{11}$$

$$\left(\frac{\gamma_{c2}|\tau|S}{\tau_c} \right) = 1 \qquad \text{for } \sigma_x < 0 \text{ and } \sigma_y < 0 \tag{12}$$

with

$$\gamma_c = \gamma_{c1} \qquad \text{for } \sigma_x \geq 0 \text{ and } \sigma_y \geq 0 \tag{13}$$

$$\gamma_c = \min \left(\gamma_{c1}, \gamma_{c2} \right) \qquad \text{for } \sigma_x < 0 \text{ and } \sigma_y < 0 \tag{14}$$

where

σ_x = applied normal stress to the plate panel, in N/mm^2

σ_y = applied normal stress to the plate panel, in N/mm²

τ = applied shear stress to the plate panel, in N/mm²

σ_{cx} = ultimate buckling stress, in N/mm², in direction parallel to the longer edge of the buckling panel as defined in Ch 3, Sec 3.1, Plate panel 3.1.3 [Ref. 6]

σ_{cy} = ultimate buckling stress, in N/mm², in direction parallel to the shorter edge of the buckling panel as defined in Ch 3, Sec 3.1, Plate panel 3.1.3 [Ref. 6]

τ_c = ultimate buckling shear stress, in N/mm², as defined in Ch 3, Sec 3.1, Plate panel 3.1.4 [Ref. 6]

γ_{c1}, γ_{c2} = stress multiplier factors at failure for each of the above different limit states

B = coefficient given in Table 3.3.1 Definition of coefficients B and e_0 [Ref. 6], **Table 10**

S = 1.0 for additional factor of safety

e_0 = coefficient given in Table 3.3.1 Definition of coefficients B and e_0 [Ref. 6], **Table 10**

β_p = plate slenderness parameter taken as $\beta_p = \dfrac{b}{t_p}\sqrt{\dfrac{\sigma_{0\_p}}{E}}$

Table 10 *Definition of coefficients B and e₀*
Tablica 9 *Definicija koeficijenata B i e₀*

Applied stress	B	e₀
for $\sigma_x \geq 0$ and $\sigma_y \geq 0$	$0.7-0.3\beta_p/\alpha^2$	$2/\beta p^{0.25}$
for $\sigma_x < 0$ and $\sigma_y < 0$	1.0	2.0

The reference degree of slenderness is to be taken as:

$$\lambda = \sqrt{\frac{\sigma_{0\_p}}{K\sigma_E}} \qquad (15)$$

where

K = buckling factor, as defined in Table 3.3.3 and Table 3.3.4 [Ref. 6].

The boundary conditions for plates are to be considered as simply supported, see Figure 21. If the boundary conditions differ significantly from simple supports, a more appropriate boundary condition may be applied according to the alternative cases given in the Table 3.3.3 [Ref. 6].
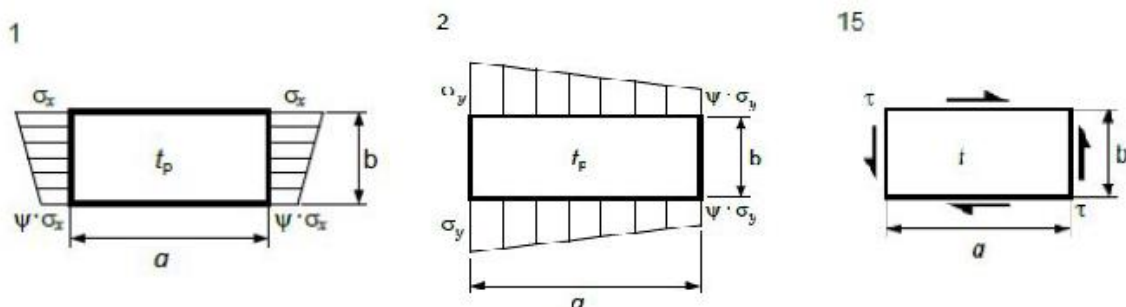
Figure 21 *Buckling cases for plane plate panels [Ref. 6]*

54

The buckling capacity of a longitudinal stiffener is to be checked for the following limit states:

- Stiffener induced failure (SI)

- Associated plate induced failure (PI)

The effective length of the stiffener, l_{eff}, in mm, is to be taken equal to:

$l_{eff} = \frac{1}{\sqrt{3}}$: stiffener fixed at both ends

$l_{eff} = 0.75l$: stiffener simply supported at one end and fixed at the other

$l_{eff} = l$: stiffener simply supported at both ends

The effective width of attached plating of stiffeners b_{eff}, in mm, is to be taken as:

$$b_{eff} = \min(C_x b, x_s s) \tag{16}$$

where

C_x = reduction factor defined in Table 3.3.3 [Ref. 6].

b = width of plate panel, in mm

s = stiffener spacing, in mm

$$x_s = min \left| \frac{1.12}{1+\frac{1.75}{\left(\frac{l_{eff}}{s}\right)^{1.6}}} ; 1 \right| \qquad \text{for } \frac{l_{eff}}{s} \geq 1 \tag{17}$$

$$x_s = 0.407 \left(\frac{l_{eff}}{s}\right) \qquad \text{for } \frac{l_{eff}}{s} < 1 \tag{18}$$

In order to account for the decrease in stiffness due to local lateral deformation, the effective web thickness of flat bar stiffener, in mm, is to be used for the calculation of the net sectional area, A_s, the net section modulus Z, and the moment of inertia I, of the stiffener and is taken as:

$$t_{w\_red} = t_w \left(1 - \left(\frac{2\pi^2}{3}\right)\left(\frac{h_w}{s}\right)^2 \left(1 - \frac{C_x b}{s}\right) \right) \tag{19}$$

The net section modulus Z of a stiffener, in cm³, including effective width of plating, b_{eff}, is to be taken equal to:

- The section modulus calculated at the top of the flange for stiffener induced failure (SI)
- The section modulus calculated at the attached plating for plate induced failure (PI)

The net moment of inertia, I in cm⁴, of a stiffener including effective width of attached plating b_{eff} is to comply with the following requirement:

$$I \geq \frac{s t_p^3}{12*10^4} \tag{20}$$

Bulb profiles may be considered as equivalent angle profiles, see Figure 22.
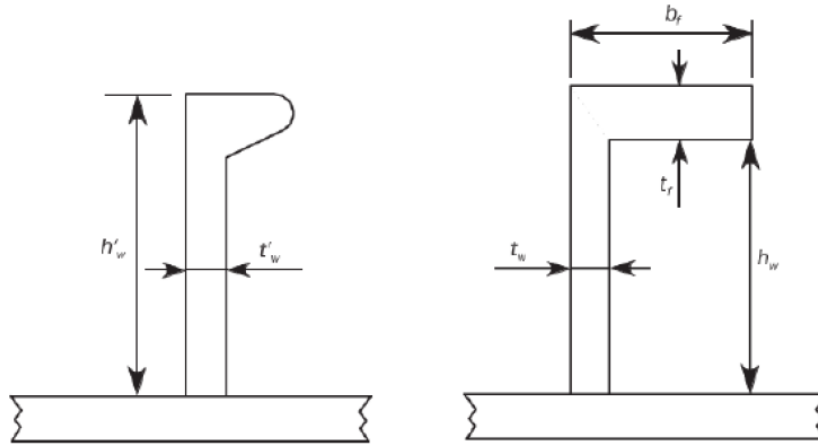
Figure 22 *Idealization of bulb stiffener [Ref. 6]*
Slika 22 *Idealizacija bulb profila [Ref. 6]*

When $\sigma_a + \sigma_b + \sigma_w > 0$, the ultimate buckling capacity for stiffeners is to be checked according to the following interaction formula:

$$\frac{\gamma_c \sigma_a + \sigma_b + \sigma_w}{\sigma_0} = 1 \qquad (21)$$

where

σ_a = effective axial stress, in N/mm², at mid-span of the stiffener, defined in Ch 3, Sec 4.3, Stiffener buckling capacity 4.3.2 [Ref. 6].

σ_b = bending stress in the stiffener, in N/mm², defined in Ch 3, Sec 4.3, Stiffener buckling capacity 4.3.3 [Ref. 6].

σ_w = stress due to torsional deformation, in N/mm², defined in Ch 3, Sec 4.3, Stiffener buckling capacity 4.3.4 [Ref. 6].

σ_o = specified minimum yield stress of the material, in N/mm²

$\quad\quad \sigma_{o\_s}$ = for stiffener induced failure (SI)

$\quad\quad \sigma_{o\_p}$ = for plate induced failure (PI)

Regarding the buckling capacity of primary supporting members, the web plate adjacent to the opening on both sides is to be considered as individual unstiffened panels as shown in Table 3.5.1 Reduction factors [Ref. 6].

The interaction formulae of Ch 3, Sec 3, Buckling capacity of unstiffened panels [Ref.6] are to be used with:

$$\sigma_x = \sigma_{av}$$
$$\sigma_y = 0$$
$$\tau_x = \tau_{av} \qquad (22)$$

where

σ_{av} = area-weighted average compressive stress, in N/mm², in the area of web plate being considered, i.e. P1, P2 or P3 as shown in Table 3.5.1 of [Ref. 6], see Figure 23.

For the application of the mentioned Table 3.5.1 of [Ref. 6], the area-weighted average shear stress is to be taken as:

- Opening modelled in primary supporting members:

  τ_{av} = area-weighted average shear stress, in N/mm^2, in the area of web plate being considered, i.e. P1, P2 or P3 as shown in Table 3.5.1 of [Ref. 6].

- Opening not modelled in primary supporting structure:

  τ_{av} = area-weighted average shear stress, in N/mm^2, given in Table 3.5.1 of [Ref. 6].

The equivalent plate panel of web plate or primary supporting members crossed by perpendicular stiffeners is to be idealized as shown in Figure 24. This is also applicable for other slot configurations provided that the web of collar plate is attached to at least one side of the passing stiffener.
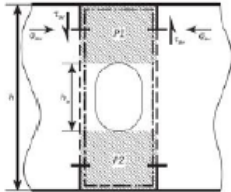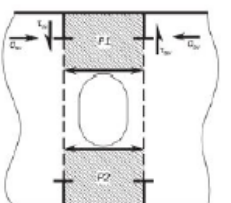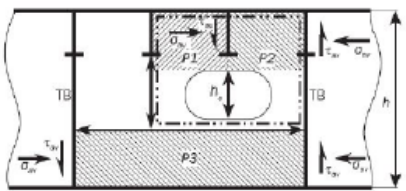
Configuration	C_x, C_y	C_τ	
		Opening modelled in PSM	**Opening not modelled in PSM**
(a) Without edge reinforcements: 	Separate reduction factors are to be applied to areas P1 and P2 using case 3 or case 6 in *Table 3.3.3 Buckling factor and reduction factor for plane plate panels*, with edge stress ratio: $\Psi = 1,0$	Separate reduction factors are to be applied to areas P1 and P2 using case 18 or case 19 in *Table 3.3.3 Buckling factor and reduction factor for plane plate panels*.	When case 17 of *Table 3.3.3 Buckling factor and reduction factor for plane plate panels* is applicable: A common reduction factor is to be applied to areas P1 and P2 using case 17 in *Table 3.3.3 Buckling factor and reduction factor for plane plate panels* with: $\tau_{av} = \tau_{av}(\text{web})$
			When case 17 of *Table 3.3.3 Buckling factor and reduction factor for plane plate panels* is not applicable: Separate reduction factors are to be applied to areas P1 and P2 using case 18 or case 19 in *Table 3.3.3 Buckling factor and reduction factor for plane plate panels* with: $\tau_{av} = \tau_{av}(\text{web})h/\left(h - h_0\right)$
(b) With edge reinforcements: 	Separate reduction factors are to be applied for areas P1 and P2 using C_x for case 1 or C_y for case 2 in *Table 3.3.3 Buckling factor and reduction factor for plane plate panels* with stress ratio: $\Psi = 1,0$	Separate reduction factors are to be applied for areas P1 and P2 using case 15 in *Table 3.3.3 Buckling factor and reduction factor for plane plate panels*.	Separate reduction factors are to be applied to areas P1 and P2 using case 15 in *Table 3.3.3 Buckling factor and reduction factor for plane plate panels* with: $\tau_{av} = \tau_{av}(\text{web})h/\left(h - h_0\right)$
(c) Example of hole in web: 	Panels P1 and P2 are to be evaluated in accordance with (a). Panel P3 is to be evaluated in accordance with (b).		

where

h = height, in m, of the web of the primary supporting member in way of the opening

h_0 = height, in m, of the opening measured in the depth of the web

$\tau_{av}(\text{web})$ = weighted average shear stress, in N/mm^2 over the web height h of the primary supporting member

Note 1: Web panels to be considered for buckling in way of openings are shown shaded and numbered P1, P2, etc.

Figure 23 *Reduction factors [Ref. 6]*
Slika 23 *Redukcijski faktori [Ref. 6]*
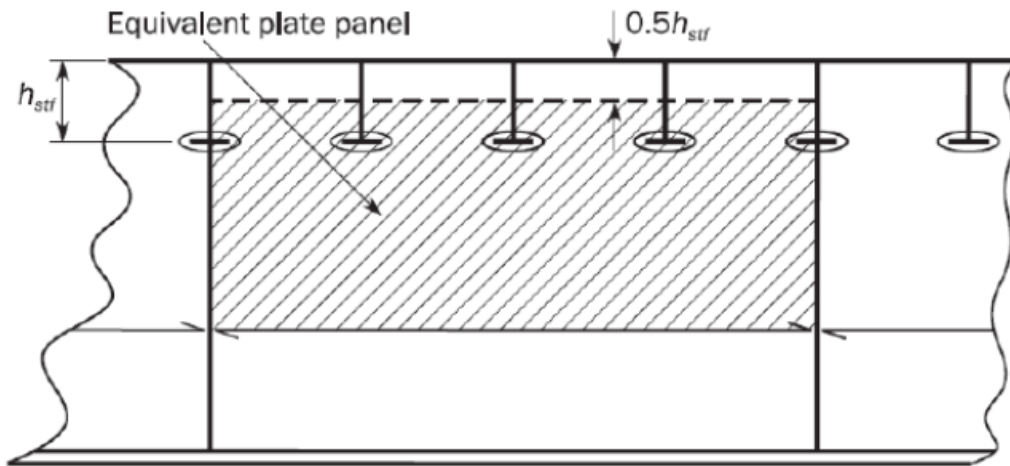
Figure 24 *Web plate idealization [Ref. 6]*
Slika 24 *Idealizacija okvira [Ref. 6]*

For the passenger ships there is an extra guidance in Ch 6, Sec 2 Buckling panel modelling [Ref. 6] that indicates the use of Tables 6.2.1, 6.2.2 and 6.2.3 for the buckling panels of the longitudinal and transverse structural members. In Figure 25, Figure **26** and Figure **27** it can be seen which assessment method is to be used for which plate panels.

Structural member	Assessment method	Normal panel definition
Outer shell envelope, including outer bottom, bilge and side shell Other longitudinal members, including inner bottom, decks and longitudinal effective structures	SP-A (see Ch 3, 3.1 Plate panel 3.1.4) (Note: For transversally stiffened bilges, the method in Ch 3, 3.2 Curved plate panel can be used)	Length: between web frames Width: between primary supporting members
Double bottom girders	SP-B (see Ch 3, 3.1 Plate panel 3.1.4)	Length: between web frames Width: web depth
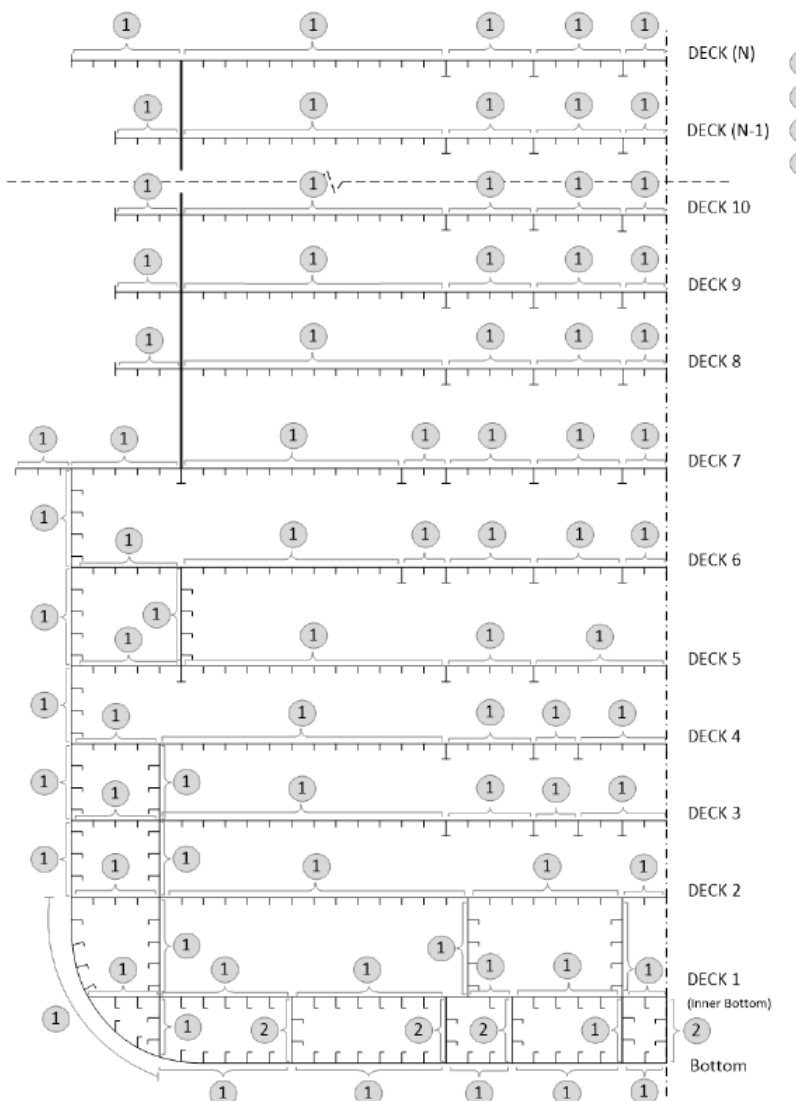
Figure 25 *Longitudinal structural members [Ref. 6]*
Slika 25 *Uzdužni strukturalni elementi [Ref. 6]*

Structural member	Assessment method	Normal panel definition
Double bottom floors, Side transverse, Side shell in way of openings Transverse webs with web stiffeners	SP-B (see Ch 3, 3.1 Plate panel 3.1.4)	Between local supporting members
Irregularly stiffened panels (e.g. web panels in way of bilge) Transverse webs without web stiffeners	UP-B (see Ch 3, 3.1 Plate panel 3.1.4) (special case I: see Ch 3, 3.1 Plate panel 3.1.7, Case 20) (special case II: see Ch 3, 5 Buckling capacity of primary supporting members)	Between local supporting members
Pillars	Column Buckling (see Ch 3, 6.1 Struts, pillars and cross ties)	Between local supporting members
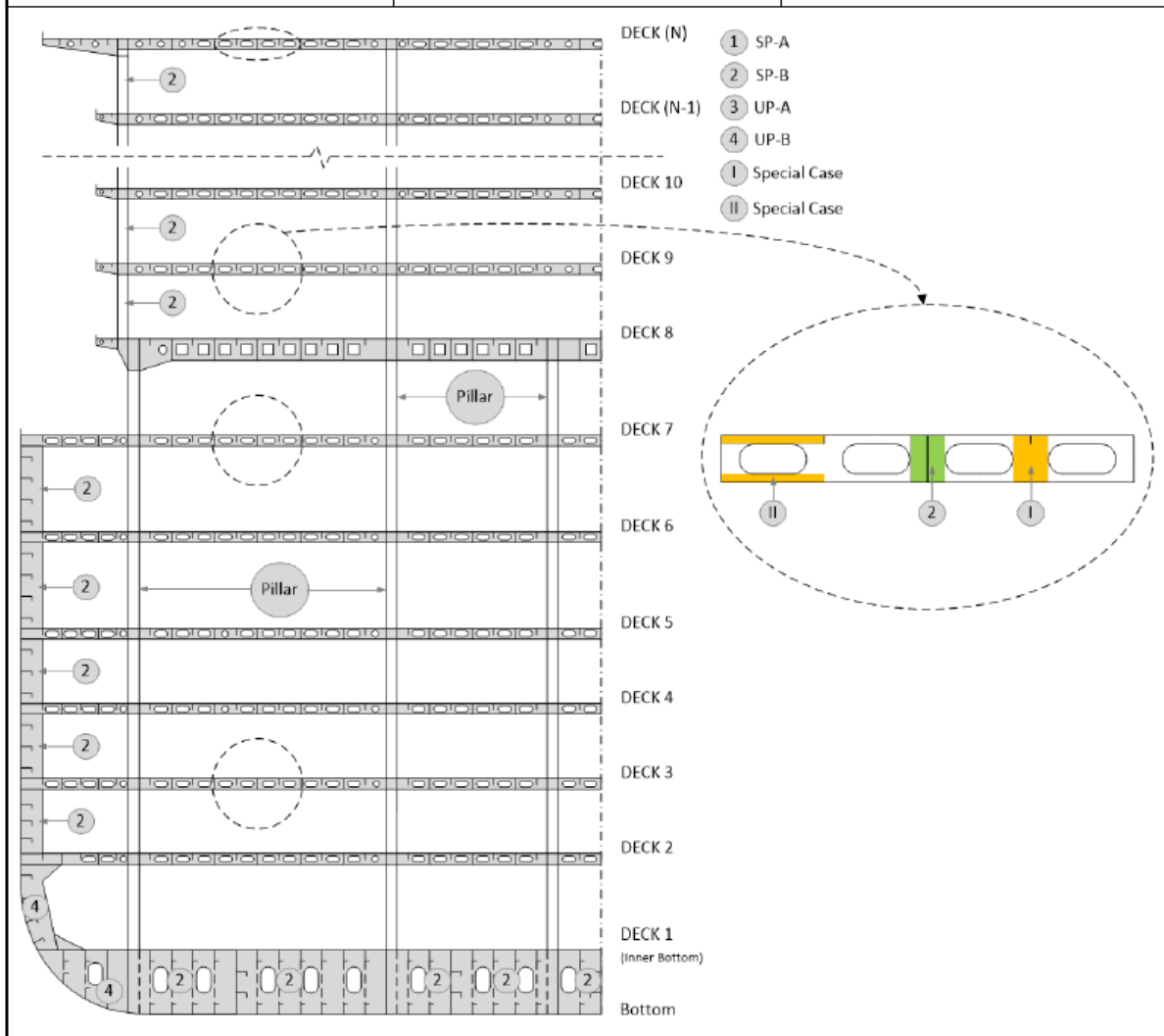
Figure 26 *Transverse webs [Ref. 6]*
Slika 26 *Poprečni okviri [Ref. 6]*

Structural member	Assessment method	Normal panel definition
Regularly stiffened panels	SP-A (see Ch 3, 3.1 Plate panel 3.1.4)	Between local supporting members
Irregularly stiffened panels, e.g. web panels in way of bilge	UP-A (see Ch 3, 3.1 Plate panel 3.1.4)	Between local supporting members
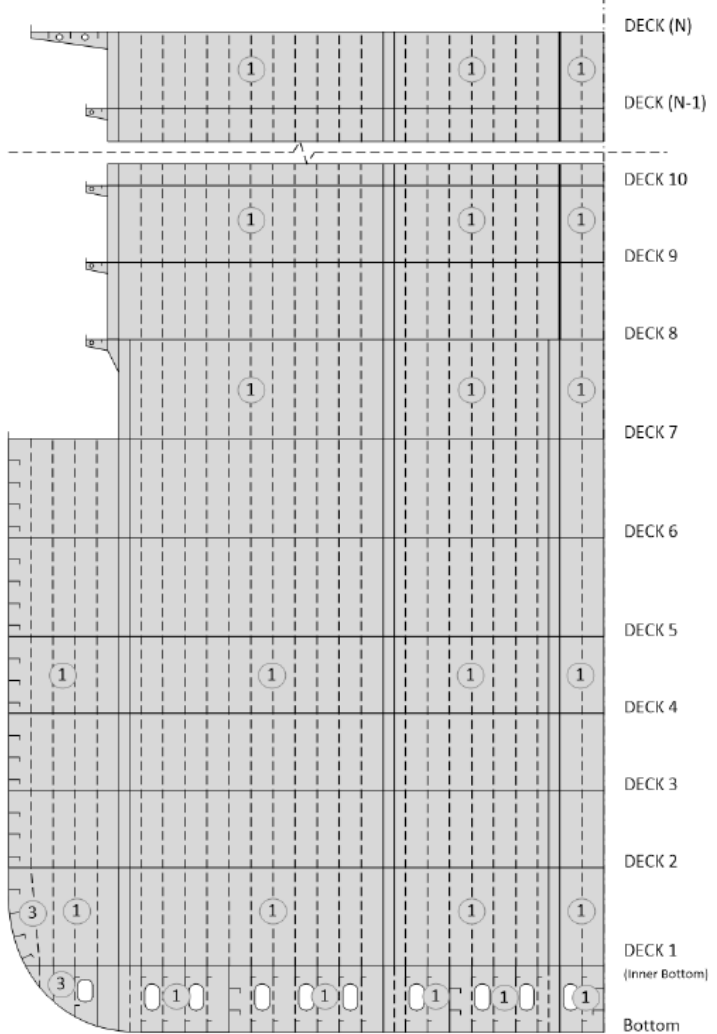
Figure 27 *Transverse bulkheads [Ref. 6]*
Slika 27 *Poprečne pregrade [Ref. 6]*

In general there are certain simplifications used for large openings. Based on Ch 6, Sec 2 Buckling panel modelling [Ref. 6], the assessment method of the plate panels around large openings takes the calculation to Ch 3, Sec 3.1 or Ch 3, Sec 5 [Ref. 6] (both mentioned in a previous chapter) which ultimately leads again back to Ch 3, Sec 3.1.

Buckling procedure for one portion of a frame, see Figure 28, will be explained in further text.
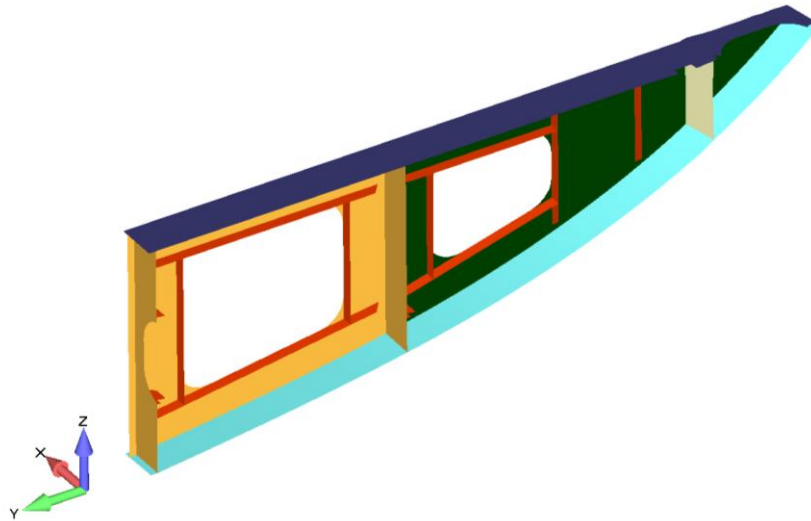
Figure 28 *Example portion of a ship frame*
Slika 28 *Primjer dijela rebra broda*

In Figure 29 it can be seen how this example portion of a frame is divided into elementary plate panels. Each elementary plate panel consists out of multiple finite elements whose orientation can be seen in 29. Element orientation is always in such way so that the X direction is in the direction of a longer side of the panel.
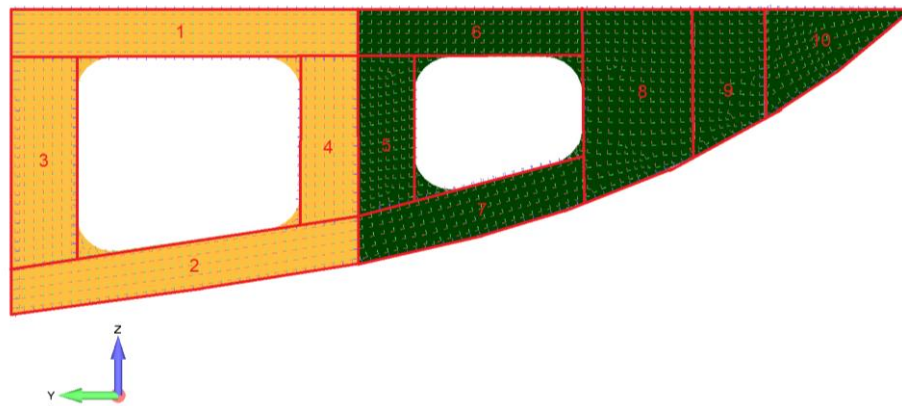
Figure 29 *Example portion of a ship frame divided into elementary plate panels*
Slika 29 *Primjer dijela rebra broda podijeljen na elementarne pločaste panele*
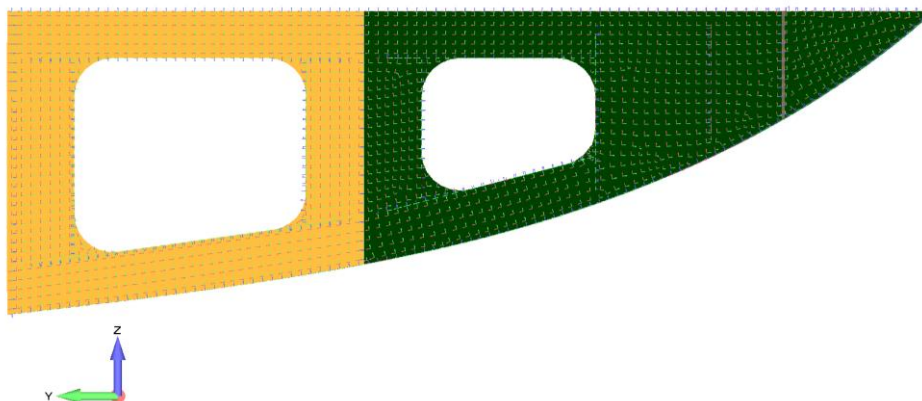
Figure 30 *Example portion of a ship frame with finite element orientation*

Stress distribution for X, Y normal stress and shear XY stress, from FEMAP, can be seen in Figure 31, Figure 32 and Figure 33. Since every finite element has its own stress value, stress averaging across each panel is done.
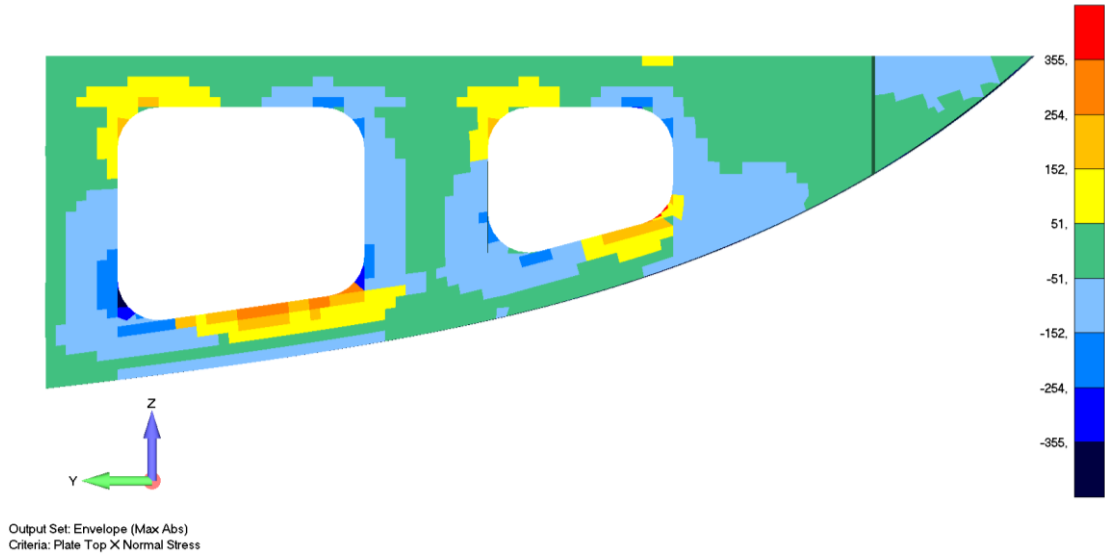
Figure 31 *X normal stress [N/mm^2] on a portion of a ship frame*
Slika 31 *Normalno naprezanje [N/mm^2] u X smjeru dijela rebra broda*
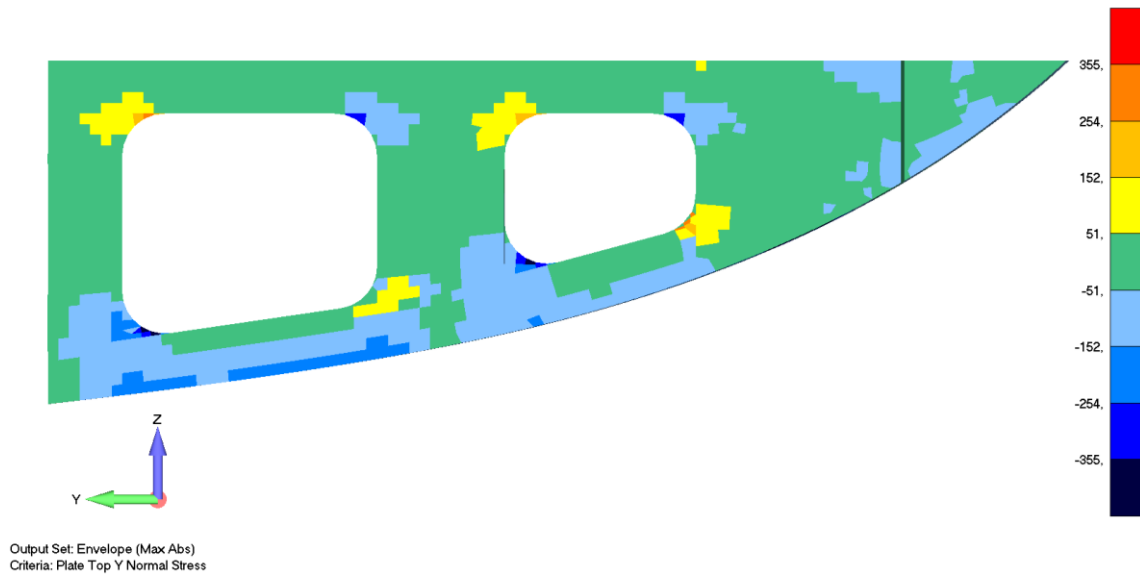
Figure 32 *Y normal stress [N/mm^2] on a portion of a ship frame*
Slika 32 *Normalno naprezanje [N/mm^2] u Y smjeru dijela rebra broda*

Output Set: Envelope (Max Abs)
Criteria: Plate Top XY Shear Stress
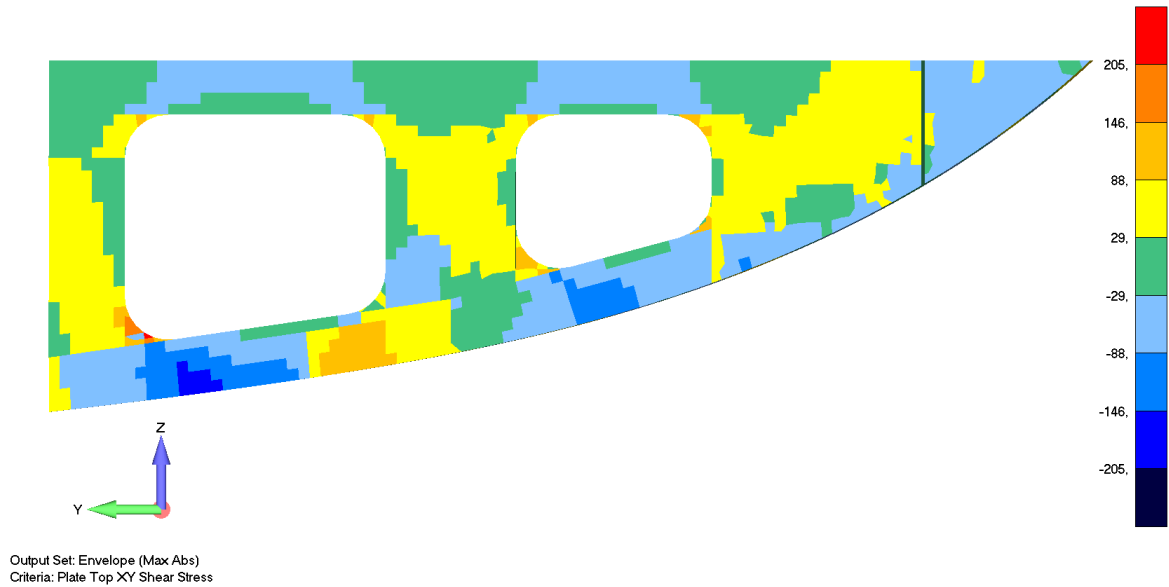
Figure 33 *XY shear stress [N/mm^2] on a portion of a ship frame*
Slika 33 *Smično naprezanje [N/mm^2] u XY ravnini dijela rebra broda*

From Figure 26 it can be seen that for this portion of a frame the special case II is to be used. This case is referencing Ch 3, Sec 5 [Ref. 6] and the Figure 23. From here it can be seen that panels 1 – 2 and 6 – 7 are to calculated while panels 3 – 4 and 5 – 8 will take their buckling factors. Calculation goes back to Table 3.3.3 [Ref. 6] from which corresponding buckling cases are used and buckling factors obtained. In Figure 34 buckling factors for portion of a frame are shown.

Output Set: Buckling stresses
Criteria: Buckling safety factor
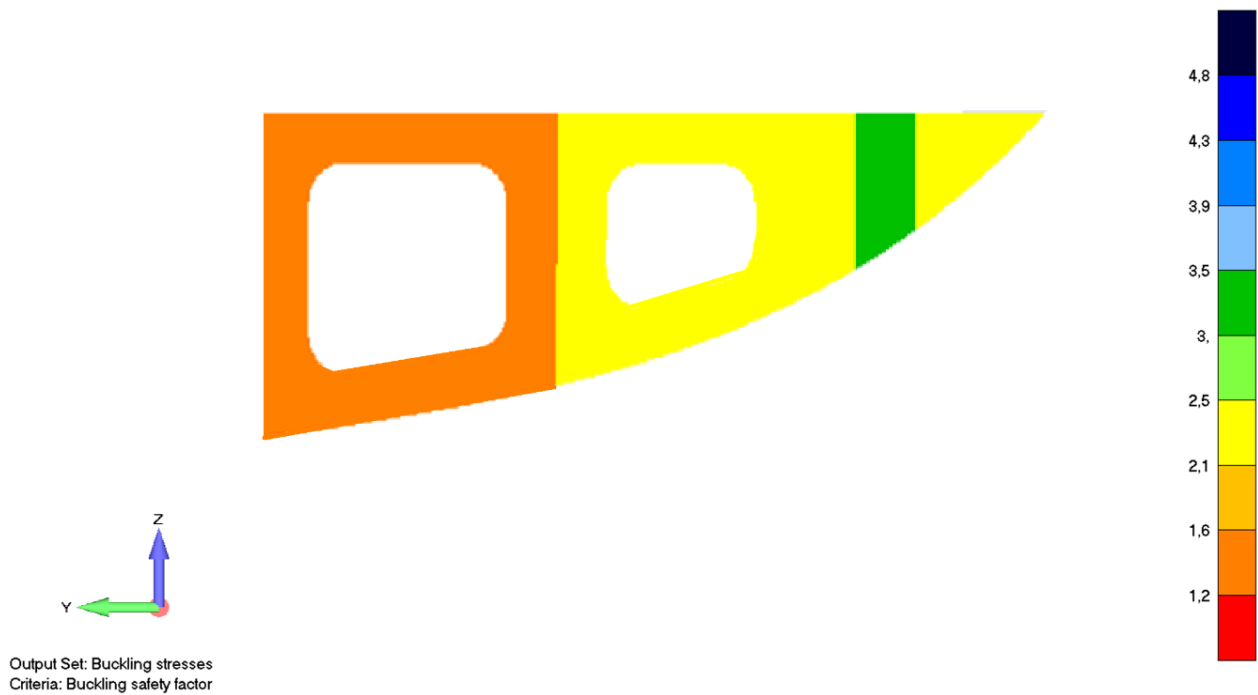
Figure 34 *Calculated buckling factors on a portion of a ship frame*
Slika 34 *Izračunati faktori izvijanja dijela rebra broda*

14. Points of Attention

14.1. Plated Structure in way of ice loads

According to Pt 8, Ch 2, 10.15 of [Ref. 1], plated structures are stiffened plate elements in contact with the hull and subject to ice loads for which the following criteria has to be met:

- Thickness of the plating and the scantlings of attached stiffeners to ensure the end fixity for the shell framing

- The stability of plated structure to withstand the ice loads defined in Pt 8, Ch2, 10.7 of [Ref. 1] (pressure within a design load patch)

These above mentined criteria are applicable to an inboard extent which is lesser of:

- Web height of adjacent parallel web frame or stringer, or

- 2.5 times the depth of framing that intersects the plated structure

An example of a shell adjacent deck plating with a seam can be seen in **Figure 35**, depicting the reinforced area near the shell.

Figure 35 *Shell adjacent deck plating*
Slika 35 *Paluba do oplate*

The question is whether the deck and web plating should or shouldn't be checked for buckling.

The following figures present an example of high Y normal stresses (see **Figure 36** and Figure **37**) and accompanying buckling factors in a deck (see Figure 38).

Output Set: Internalize Set 50 - NX NASTRAN Case 50
Criteria: Plate Top Y Normal Stress

Figure 36 *Y normal stress [N/mm^2] in deck for one load case*
Slika 36 *Normalno naprezanje u Y smjeru [N/mm^2] u palubi za jedan slučaj opterećenja*

Figure 37 *Y normal stress [N/mm²] in deck*
Slika 37 *Normalno naprezanje u Y smjeru [N/mm²] u palubi*
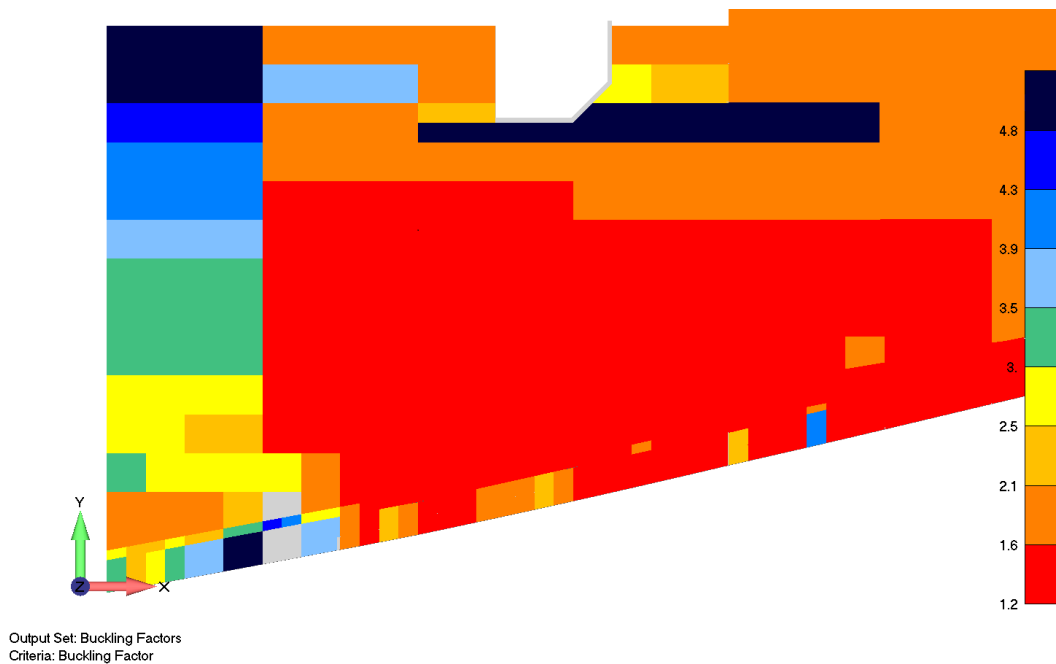
Figure 38 *Deck buckling factors*
Slika 38 *Faktori izvijanja palube*

14.2. *Y normal stress*

In Ch. 0, in Figure 32 it can be seen that Y normal stresses are high due to the direction of the ice load, which results in severe buckling factors due to the geometry of the unstiffened panel. According to Ch 3, 5.1.3 of [Ref. 6], Y normal stress is to be taken as zero, while the Table 3.5.1 of [Ref. 6] implies otherwise. That is another point that should be addressed in the rules in a more precise way. In this case study, Y normal stresses have been taken into account for calculating the buckling factors for panels of these cases.

14.3. The shell-adjacent longitudinal profile under ice loads

The deck structure is subjected to a rule deck load and minor global loading, but the shell adjacent longitudinal deck profile (marked red in Figure 40, an isometric view of the structure in question (shown in Figure 39) is connected to the shell via plating through ice framing and brackets, therefore it will also experience severe transverse loading due to the ice load or the connection reinforced accordingly with the introduction of transverse stiffening. Consequently the before-mentioned longitudinal profile has to be replaced by a larger profile. Question here is which criteria is used to dimension the deck longitudinal profiles? Yield limit, or a rule-based direct approach similar to secondary ice stiffening?

Consequently, by taking the yield stress limit criteria into account, the before-mentioned longitudinal profile has to be replaced by a larger profile, while also introducing transverse HP's for the given highly stressed region. Comparison of the von Mises stress criteria before and after the profile was enlarged and transverse stiffening added can be seen in Figure 41 and Figure 42 respectively.
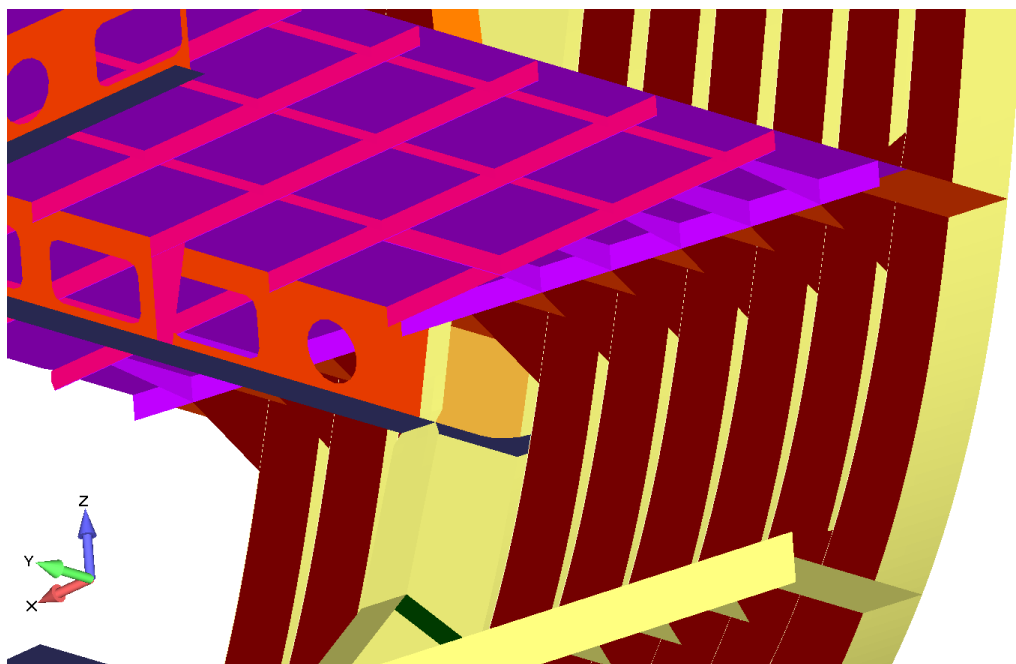
Figure 39 *Part of a FEA model structure*
Slika 39 *Dio strukture u modelu za analizu metodom konačnih elemenata*
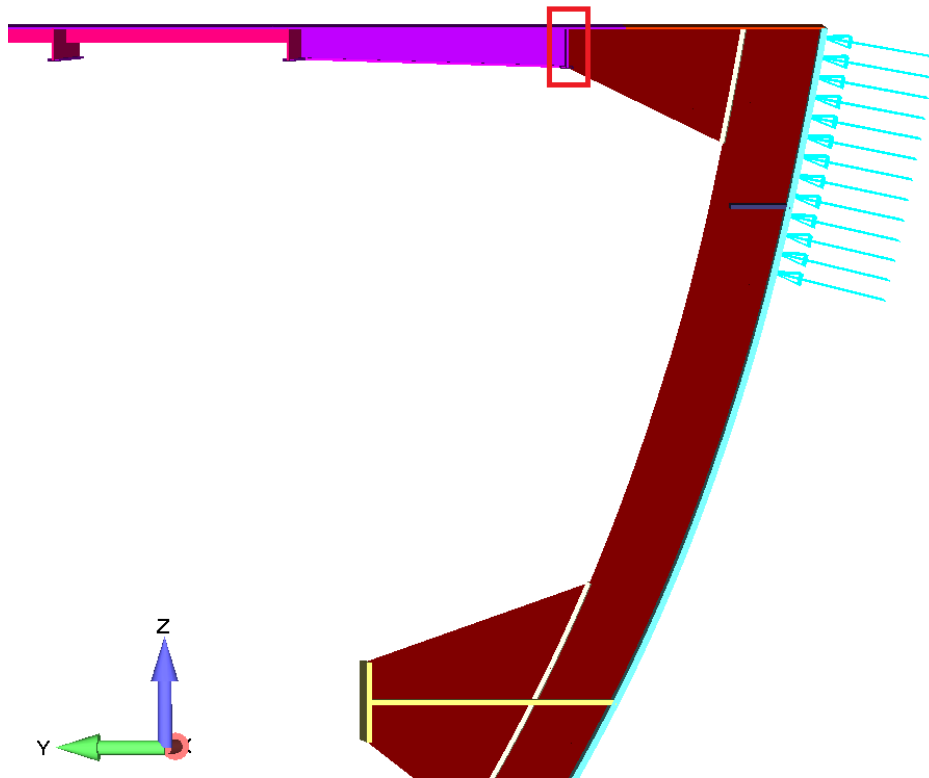
Figure 40 *Longitudinal profile severely loaded due to ice load*
Slika 40 *Uzdužni profil jako opterećen uslijed površine opterećenja leda*
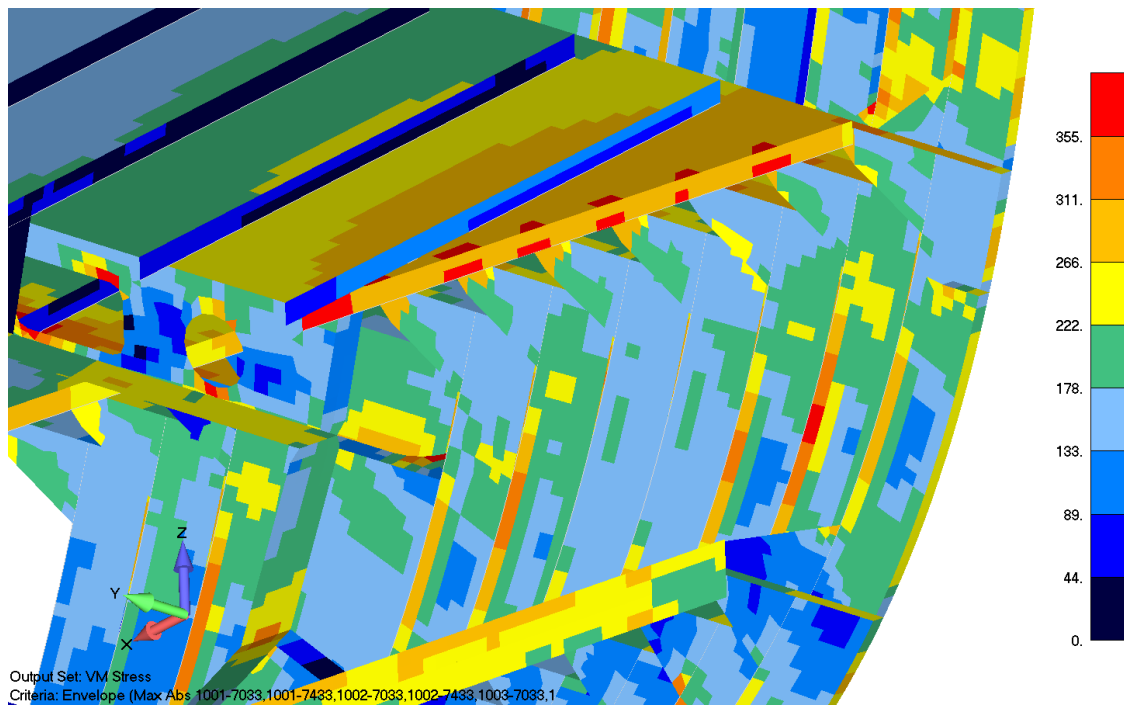
Figure 41 *von Mises stress before enlarged profile and anti-buckling strips*
Slika 41 *von Mises naprezanje prije pojačavanja profila i dodavanja traka protiv izvijanja*
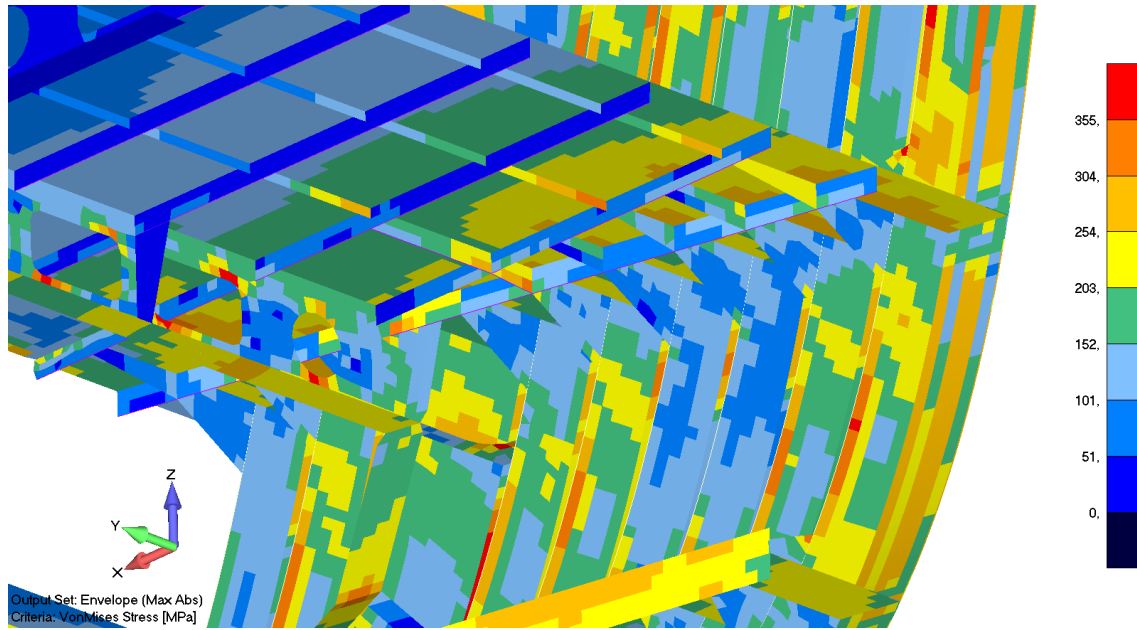
Figure 42 *von Mises stress after enlarged profile and anti-buckling strips*
Slika 42 *von Mises naprezanje nakon pojačavanja profila i dodavanja traka protiv izvijanja*

14.4. Plastic section modulus calculation in "Rules Calc"

It must be noted that the calculation for the actual net effective plastic section modulus (Z_p) of a "built" transverse or longitudinal frame, see Figure 43 (for cases when the cross-sectional area of the attached plate flange exceeds the cross-sectional area of the local frame, as described in Pt 8, Ch2, 10.10.9 of [Ref. 1]) in "Rules Calc" (v. 2018.0.0.6) gives incorrect values, larger than in reality, for profiles with height of local web frame (h_w) larger than 300 mm. Therefore, the calculation for larger profiles has been done manually.
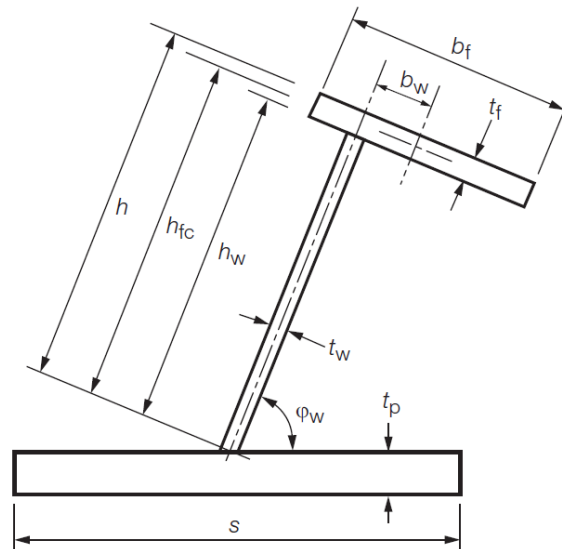
Figure 43 *Stiffener geometry [Ref.1]*
Slika 43 *Geometrija profila [Ref.1]*

Additionally, an example of replacement of bent profiles with built profiles is given in Figure 44.
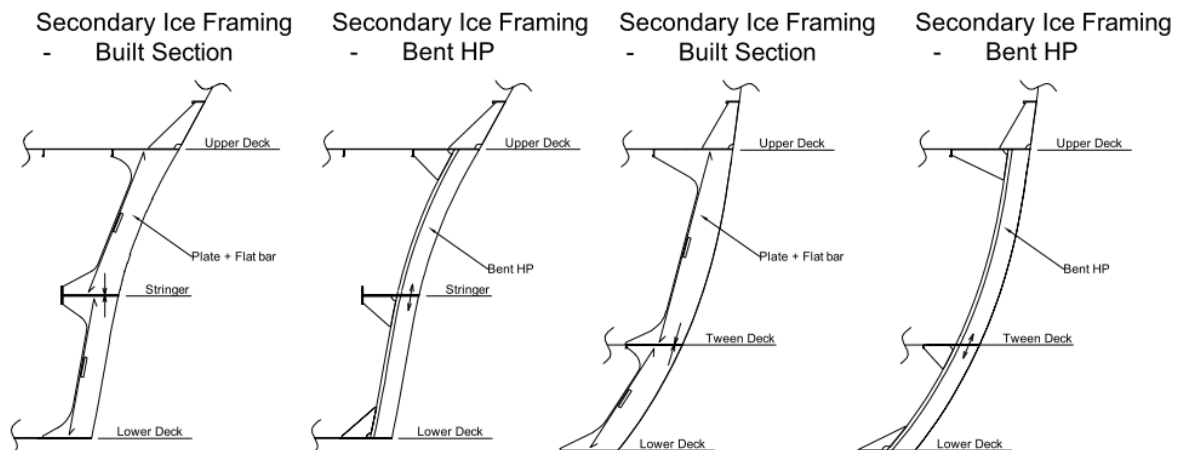
Figure 44 *Example of application of built instead of bent profiles*
Slika 44 *Primjer korištenja sastavljenih umjesto savijenih profila*

15. Conclusion

The methodology of Polar class PC6, SFIC hull structure scantling calculation is presented in this document. Given that the scantling calculation for secondary ice framing is rule based, and as already indicated, cannot be substituted by direct calculation more detailed examples were given for the primary structural members in way of ice loading strength assessment. A linear static analysis was conducted for the polar yacht case study and acceptance criteria presented as well as a prescribed buckling methodology according LR-SDA procedure.

In chapter 7 of the article several items are addressed that required additional consideration according provided rules from the classification society regarding primary structure strength assessment. Mainly this refers to the extent of buckling assessment of "plated structures" as referred to in the rules, the prescribed normal stresses used for buckling assessment of web plating with large and the acceptance criteria of the end connections of secondary stiffening ice framing.

These items were addressed directly towards the class society during the design stage of the polar expedition yacht case study and certain yielding or buckling limits were set as stated in chapters 6 and 7 respectively.

The IACS polar class rules are relatively new and the number of these vessels has increased in recent years. It is expected that in the coming years feedback from the polar vessels currently in operation will provide additional information regarding hull structure behavior under ice induced loading. This could possibly lead to further refinement of the existing classification rules.

REFERENCES

[1]   Lloyd's Register – Rules and Regulations for the Classification of Ships, July 2019
[2]   Lloyd's Register – Rules and Regulations for the Classification of Stern First Ice Class Ships, July 2019
[3]   Daley, Claude (April 2014) – Ice Class Rules: Description and Comparison
[4]   Finish Maritime Administration - ICE CLASS REGULATIONS 2008 (FINNISH-SWEDISH ICE CLASS RULES
[5]   TRAFI/708629 - GUIDELINES FOR THE APPLICATION OF THE 2017 FINNISH-SWEDISH ICE CLASS RULES – Helsinki, 8 January 2019
[6]   ShipRight Design and Construction - Guidance Notes for ShipRight SDA Buckling Assessment, June 2019

IHC BEAVER - Custom built Cutter Suction Dredger

Maja Radolović [a], Robert Grubiša 2[b]*

a IHC Engineering Croatia, Nikole Tesle 9, Pula
b IHC Engineering Croatia, Milutina Barača 7, Rijeka
* Corresponding Author, r.grubisa@royalihc.com

Abstract

IHC Beaver® is trademark representing series of small cutter suction dredgers (CSD) designed to answer demand for small sturdy dredgers of standard type which can be quickly supplied ready for service. Some custom built dredgers are designed and delivered as tailor made vessels along with wide range of Standard IHC Beavers®. The design of the IHC Beavers® is continuously improved using the latest technological developments and feedback from customers.

Custom designed and built CSD for maximum dredging depth of 15 m and power of submerged dredge pump of 400 kW is presented in the paper. IHC in-house basic and detail engineering using resources in the Netherlands and Croatia have been done with special attention paid to a simple and quick transportation, assembly and dismantling systems. Some important stability cases are presented as well.

Key words: Dredging; Engineering; Stability

Sažetak

IHC Beaver® (IHC Dabar) je zaštićeno ime serije malih usisnih jaružala projektiranih kao odgovor na zahtjeve tržišta za malim robusnim jaružalima standardnog tipa spremnih za isporuku i eksploataciju u kratkom roku nakon narudžbe. Uz standardne izvedbe usisnih jaružala, određeni broj takvih malih plovnih naprava posebno se prilagođavaju zahtjevima pojedinih naručitelja. Projekt i izvedba IHC Beavera® se stalno unapređuje korištenjem najnovijih tehnoloških dostignuća i povratnih informacija od strane korisnika.

Usisno jaružalo projektirano i izgrađeno prema posebnom zahtjevu za najveću dubinu kopanja od 15m uz snagu uronjene usisne pumpe od 400 kW predstavljeno je u ovom radu. Osnovni i detaljni projekt napravili su IHC-ovi stručnjaci u Nizozemskoj i Hrvatskoj. Posebno se pazilo na mogućnost jednostavnog i brzog transporta, te sastavljanja i rastavljanja jaružala. Zahtjevi za stabilitet ovakvih plovnih naprava su posebno prikazani.

Ključne riječi: Jaružanje; Projektiranje; Stabilitet

1. Introduction

Dredging activity has always been a special scope and has great importance in the maritime industry, and in 19th century started revolutionary development and evolution of cutter suction dredgers and suction hopper dredgers. Growth of dredging market in last decades has a strong connection with the mayor global trends:

- o Growing world population

- o Expansion of global trade

- o Rising sea level

- o Higher energy demand

- o Growing tourism and leisure

All of these trends means that there will be greater demand for safe, economic and sustainable logistic. Capital dredging like reclamation projects (from extension of ports to creation of offshore islands) and maintenance dredging became growing activity. Maintenance dredging is a broader term which includes clearing of deposits and cleaning, widening or deepening of a waterways or channels, and it is one of the oldest dredging activities. Regular maintenance dredging is of huge importance in coastal regions which have large tidal activity and also in water bodies which are susceptible to become silted with sediments, sand and mud. As sufficient port capacity is vital for economic growth, the maintenance of ports and their approaches must provide a constant navigable water depth. The maintenance of the water depth also helps to protect river valleys from flooding.

Therefore, designing maintenance dredging vessels are one of the great important activities for Royal IHC.

2. IHC Beaver® Cutter Suction Dredgers (CSDs)

2.1. Standard IHC Beaver®

IHC designs and builds a variety of standardized and custom-built CSDs called IHC Beaver®. These are capable of dredging compacted soil types and materials, such as clay and rock. High accuracy and a continuous rate of production ensure that IHC Beavers® dredgers are ideal for many dredging jobs, such as port and waterway maintenance, land reclamation, lakes dredging, port construction. IHC also designs, engineers and manufactures all of major equipment for CSDs. This is hugely beneficial to customer, who receives a unique package of integrated dredging solutions.

IHC Beaver® dredgers are the latest generation of small preconfigured cutter suction dredgers (CSDs), well known for its robust construction and excellent performance. Some of main IHC Beaver® features are:

- o Reliability and fuel efficiency
- o High productivity
- o Easy transportable
- o Short delivery time – deliverable from the stock
- o Cost effectivity
- o Live –cycle support
- o High levels of productivity and discharge over long distances

IHC offers wide range of demountable cutter section dredgers consist of basic models, with dredging depth from 6 to 18 m, suction pipe diameter from 260 to 650 mm and with available pump power from 250 to 1700 kW.

They are equipped with state-of-art technology and offer some of the following features:

- o Dismountable and transportable over land
- o Suitable for single-handed operations
- o Easily customized with a wide range of additional equipment
- o Low emission and environmentally friendly operation

With different characteristics and different cutter heads IHC Beaver® can be used for various types of soil: hard soil, cohesive soil, non cohesive soil. The desired production rate of IHC Beaver® will

determine design, size and type of soil the vessel can dredge. Beavers has a high accuracy and continuous rate of production, either they are been used for dredging rocks or sand or gravel, or for construction and reclamation works. The production capacity design is directly related to the hardness of the material that the Beaver is going to dredge.

But sometimes a standard vessel does not meet all customer's requirements or wants to be adjusted to special scope of work. Considering specific requirements, standard products can be customized for many different applications and feature a wide range of optional extras like increasing dredging depths, adding anchor booms, spud carriage installation, swivel bends and automation.

3. Custom Beaver project no. 15052

3.1.   General description and project requirements

Custom built IHC Beaver® dredger Project no. 15052 is an electric dismountable wheel suction dredger type IHC Beaver® 600 ordered by the client from Colombia. It is intended to work on ponds and other smaller restricted internal waters. The dredger is designed to remove overburden by dredging to expose gold bearing sediments. With a total power of 800kVA the dredger is capable to operate to a dredging depth of 15 meters and is fitted with a dredging wheel to handle the sticky clay of the overburden.

It consist of three pontoons hull, one main pontoon housing machinery room, and two side pontoons. All parts are dimensioned to allow that vessel can be transported by road, rail or sea. If pontoons are transported to working location disconnected, pontoons are always completely assembled and fully tested afloat before delivery, and ready for operation when arrived on site. The IHC Beaver® is equipped with a connection-disconnection system for pontoons, achieved using bolts at deck level, and hooks at the bottom and can be simple and quick assembled.

There is no permanent crew. Cabin for one operator is provided on top of the deck house.

Main particulars of the vessel is given in the table below.

Table 11 Project No.15052 – Main particulars

Length overall, ladder up	34,30 m
Length over pontoons	26,00 m
Breadth over pontoons	6,97 m
Depth at side	1,50 m
Average draught, approx.	1,10 m
Max. dredging depth	15,0 m
Inside dia. of suction and discharge pipes	450 mm
Power of submerged dredge pump shaft	400 kW

General arrangement of the dredger is given on following figures.
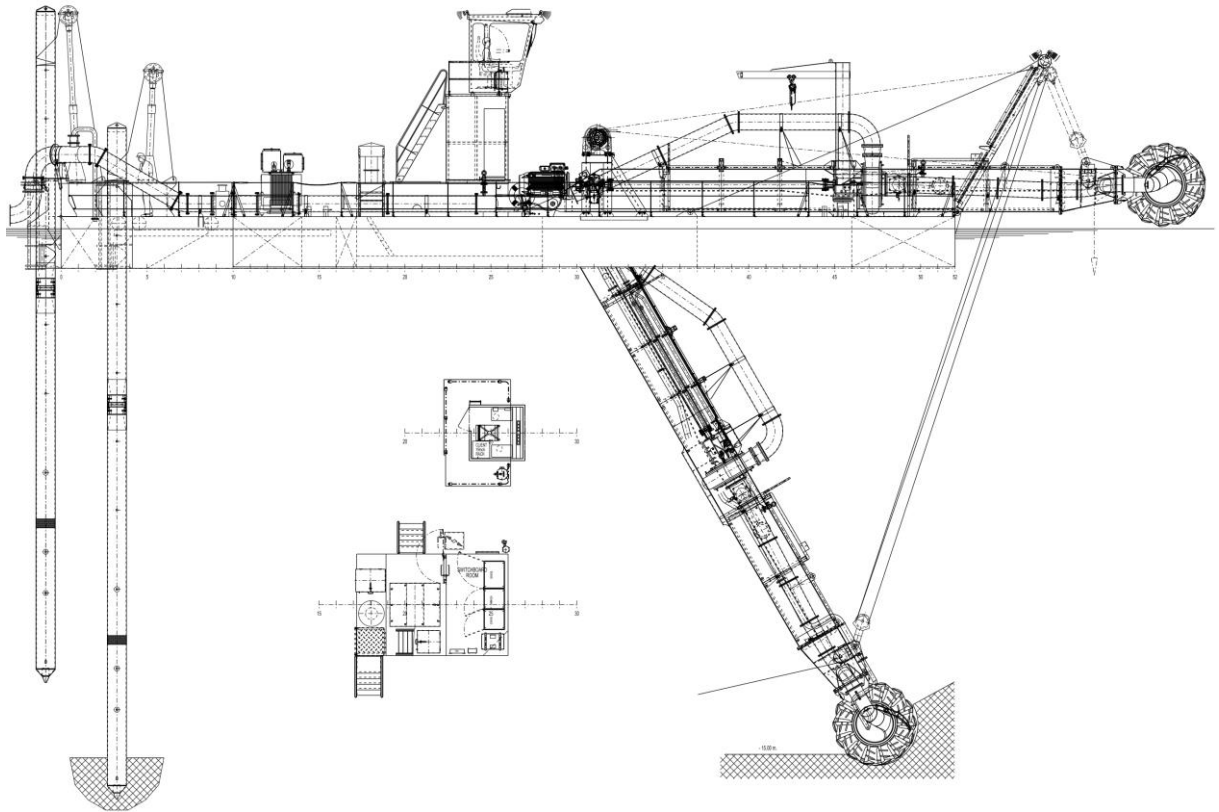
Figure 1 *Longitudinal view of Pr. No.15052*

SIDE PONTOONS DIMENSIONS
21.00 x 1.97 x 1.46 m

MAIN PONTOON DIMENSIONS
14.00 x 2.95 x 2.46 m
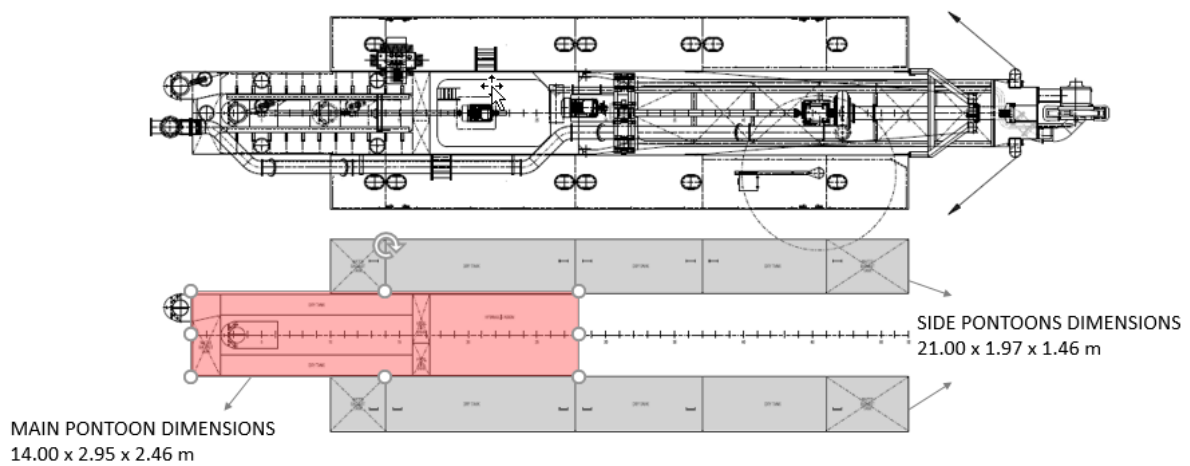
Figure 2 *Top view of Pr. No.15052*

Due to the specific work of gold mining, there were some specific project requirements according to the existing standard IHC Beaver® :

- o Increased dredging depth to 15m
- o Larger transformer, with design capacity of 80% of anticipated load
- o Submerged dredge pump, electrically driven
- o Production measuring device
- o Spud divide
- o Increased dredging pipe diameter and swivel bend
- o Steel frame at rear of dredger to enable push transport

3.2. Design challenges

Beside above mentioned technical requirements, specific design requirements for the Project No. 15052 was also:

- o Length of the side pontoons just enough to provide necessary buoyancy and low freeboard sufficient for safe operation of the dredger.
- o Transportation of the assembled vessel to Colombia as deck cargo by ship.

3.3. Lightship calculation

Detailed lightship distribution, including centers of gravities, is very important due to the small size of the floating object. Although Project No. 15052 is intended to operate on ponds and restricted internal waters, the freeboard has to be reasonably enough for the purpose taking into account various operational scenarios. At least 3-5% of margin to the calculated/estimated lightship to be taken into account.

3.4. Stability rules and regulations

IHC Beaver® dredger under Project No. 15052 for Colombian company is not required to be built under classification societies rules and regulations. Also, there is no national or international stability rules and regulations for such type of small dredgers operating on the internal waterways, small lakes, ponds etc. Although IHC Beaver® dredgers (including custom built Pr.No.15052), as well as other similar small floating working objects, are not so complex as sea-going vessels, stability must not be underestimate in order to obtain technical sound final product.

Therefore, set of custom stability criteria made up of existing ones has been internally agreed in IHC for particular IHC Beaver® dredger taking into account size and operational environment.

Bureau Veritas inland navigation stability rules are often used as they are written originally or they are modified to suite the specific custom IHC Beaver® .

Stability criteria for Project No.15052 has been set as follows:

Table 12 Stability criteria applied for Project no. 15052

Value	BV Inland navigation Rules	Added criteria for Pr.No.15052
GZ curve area	0.024 m*rad up to the angle of heel of 27 deg. (or immersion of the first unprotected opening)	
Minimum righting lever (GZ)	0.10 m in the positive area of righting lever curve	
Initial metacentric height (GM$_0$)	0.10 m	
Wind speed used for calculation of wind heeling moment		27.8 knots
Angle of heel due to the wind heeling moment		< 10 deg.
Freeboard midship (including heel due to the wind)		>= 0.300 m
Freeboard on aft and fore ends (including heel due to the wind)		>=0.100 m

Added criteria are dealing with the freeboard of the vessel at the equilibrium stage with and without the effect of the wind heeling moment. 100mm of freeboard on the fore and aft end of the vessel has been established as absolute minimum value. The original selected length of the side pontoons has been increased to satisfy the freeboard requirement as stated above.

The wind speed used for the calculation of the wind heeling moment is 27.8 knots which is upper limit of the Beaufort 6 range. It is not expected that the small IHC Beaver® dredger will perform any operational activities in such weather condition.

3.5.   *Hoisting and transportation of the dredger*

Decision to deliver and transport the dredger "in one piece" has been made later during the design process so evaluation of various scenarios of hoisting the vessel has been done. Finite element (FE) model in FEMAP has been made in order to evaluate stress and deformation levels as well as necessary scantlings of couplings between the pontoons, cutter ladder and gantry. Several scenarios of hoisting have been evaluated. FEM model of the dredger with spuds on deck and removed control cabin is showing on following photos. Results of this analysis have been used for proper dimensioning of hull structure and connecting elements between parts of the dredger. Hoisting scenario with lifting wires attached to the one hook has been tested as a proof that it could be used later during the site to site transportation, if needed.
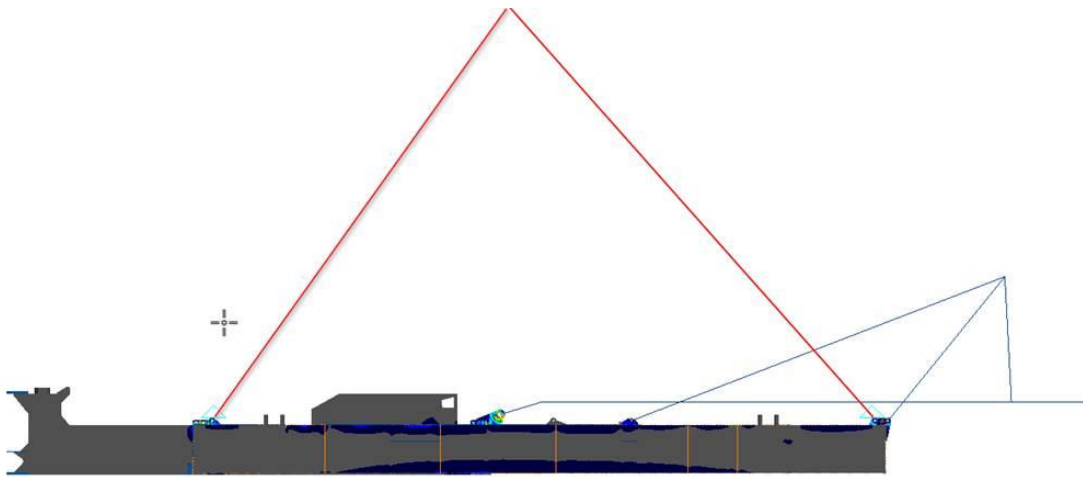
Figure 3 *Hoisting eyes positions*
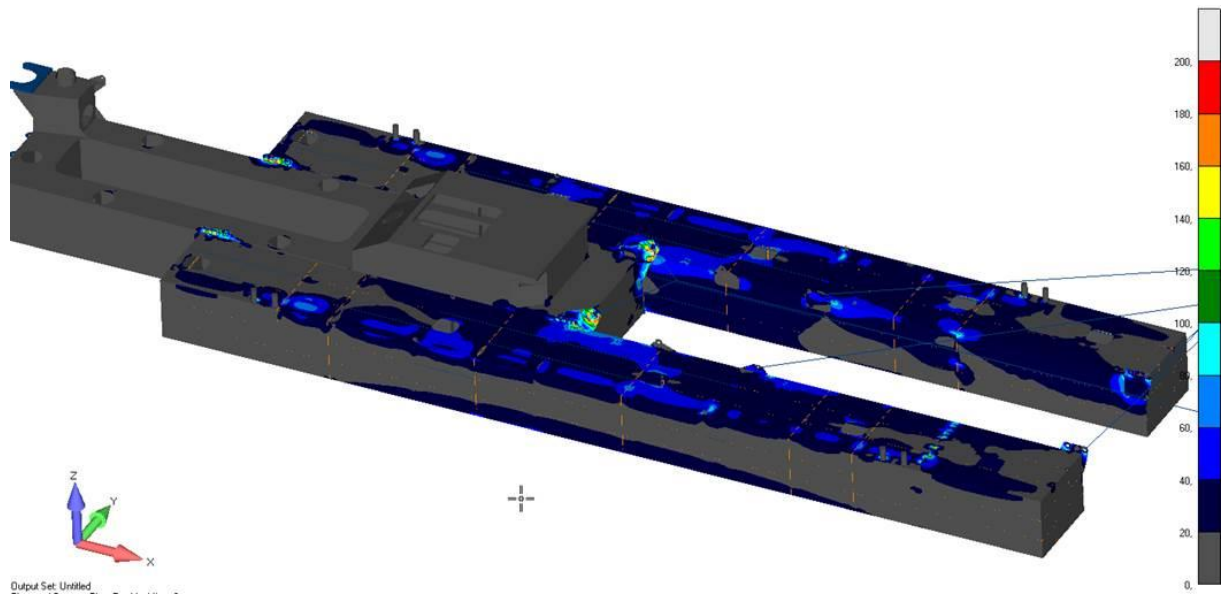
Figure 4 *Stress levels (MPa)*
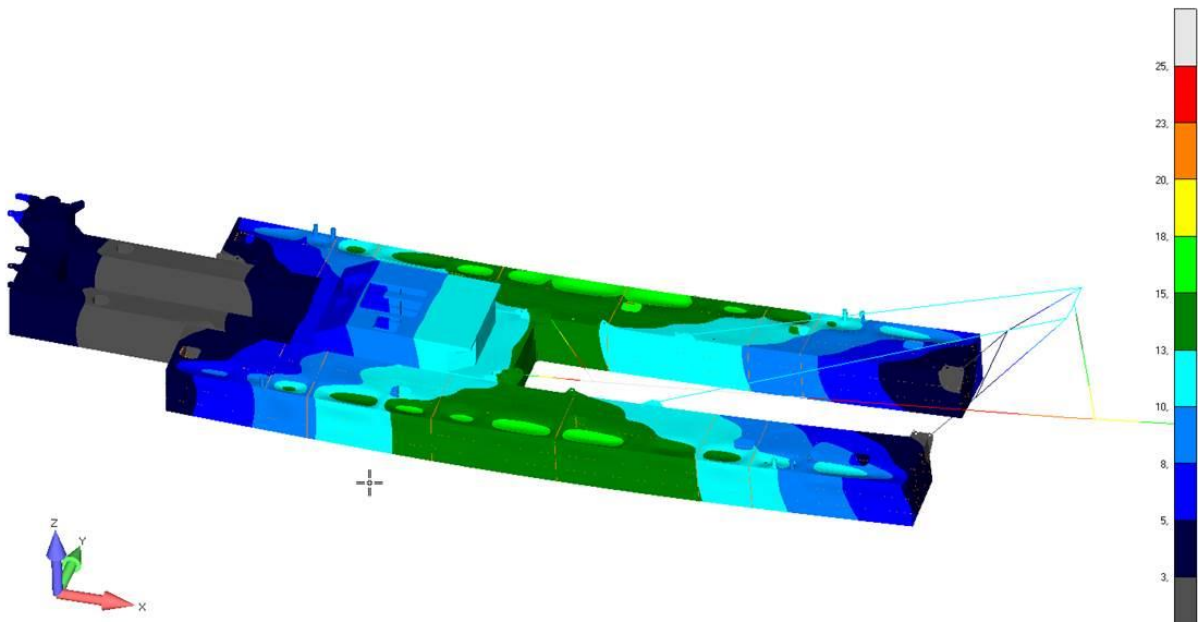
Figure 5 *Deformation levels (mm)*

Lowering of the dredger into the water for the very first time in the Shipyard has been done using shipyard crane with two hooks as visible on the following figure. Cutter ladder and spuds have been installed after the launching.

Figure 6 *Lowering the dredger for the first time into water in the Shipyard*

3.6.   Launching

Project No. 15052, as well as other standard IHC Beaver® dredgers, is relative small floating object with the primary function of dredging on the specific site in relative calm water and weather conditions. It has not their own propulsion. It is transported from one working site to the another by towing/pushing or it has to be disassembled and transport by road.

Launching of such crafts on different sites is done using various techniques. If the adequate crane is not available than pushing it into the water by means of truck, tractor or other suitable vehicle is common practice. Temporarily "slipway" with rolling devices are often used.

Launching of another standard IHC Beaver® 40 dredger (slightly smaller than Project No.15052) is shown on following figures.

Figure 7 *Preparing the "slipway"*

Figure 8 *Crawler heavy vehicle used for pushing the IHC Beaver® dredger into the water*

Figure 9 *IHC Beaver® on-site launching*

3.7. *Equipment technical particulars*

Main components of IHC Beaver® project No. 15052 are: cutter ladder, one ladder gantry, control cabin, dredge pump, diesel engines and auxiliary power units, discharge line and the spuds. The dredging wheel is driven by a radial piston hydraulic motor.

The dredger is moved forward by means of a spud carriage installation.

Two spuds are operated by means of a hydraulic ram.

Two separate swing winches and the ladder hoisting winch are each driven by hydraulic motor.

The submerged pump is electrically driven.

Oil for the hydraulic system is supplied by hydraulic pumps.

Mentioned machinery is mounted in and on main pontoon, so in that way the minimum number of parts has to be dismantled when dredger is transported. On deck a transformer is placed to which the shore supply cable should be connected. Electromotor an the hydraulic installation are remote controlled from the dredge master deck, so that all dredging controls can be operated by one man.
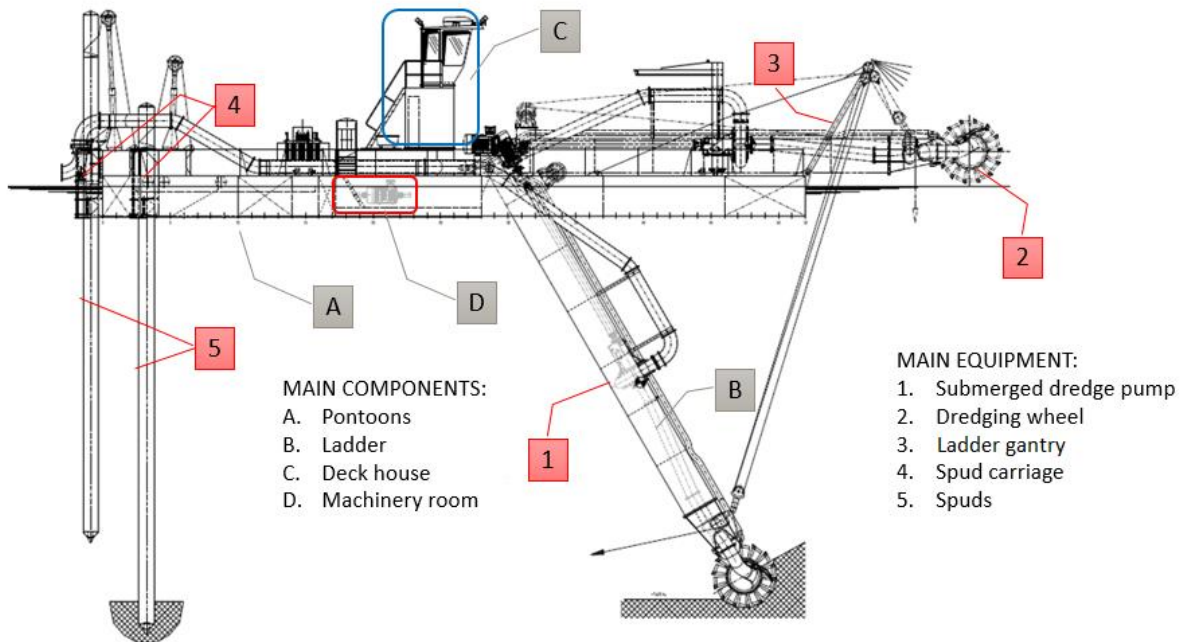
Figure 10 *Project No.15052 main components*

3.8. *Submerged dredge pump*

The effectiveness (cost) of dredging today depends greatly on the performance of the pumps. IHC has a wide range of different dredge pumps, all developed, designed and produced at IHC. All pumps are designed to reduce of wear and increase the ease of maintenance.

At project No.15052, submerged dredge pump is installed, and the main characteristic is underwater placement for increased production and bigger dredging depth. This is single walled conventional pump, electrically driven, complete with support and control systems.

Table 13 Installed dredge pump characteristics

Type	Single walled, 3 bladed
Speed (nominal)	418 rpm

Speed(maximum)	459 rpm
Power	550HP (400kW)
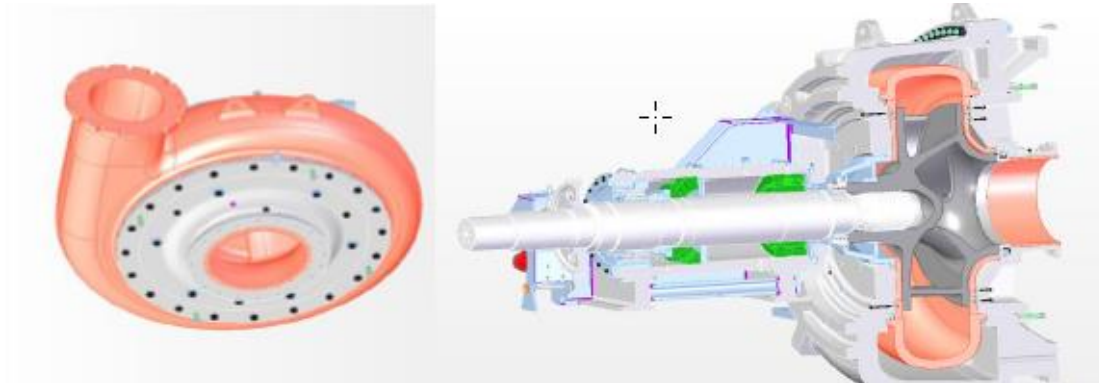
Figure 11 *Submerged dredge pump*

Figure 12 *Pump testing*

3.9. *Dredging wheel*

Dredging wheel can be used for different soil types, primary sand and clay and have constant feed rate ideal for mining operation. They have high slurry density (70%). Wheels are also part of standard IHC Beaver® components and can be executed in version with upward and downward cutting model, and the bucket can be fitted either with smooth cutting edges or replaceable teeth. The dredging wheel consist of

a hub and a ring connected by bottomless bucket which excavate the soil. Standard dredging wheels are available in a power range from 20 to 1000kW and outputs up to 10000 t/h.

Advantages of this kind of unit are:

- o High production and low spillage
- o Low sensitivity to debris such as rocks and tree stumps
- o Constant and equal production in both directions of swing
- o Reduced risk of large clay ball formation
- o High mixture density
- o Low operating costs

On project No.15052 standard dredging wheel with power of 100kW, and is driven by radial piston hydraulic motor.

Table 14 Installed dredging wheel characteristics

Type	Under cutting, smooth edges
Diameter	2400 mm
Speed	7.5 - 15 - 18.6 rpm
Power at shaft	100kw
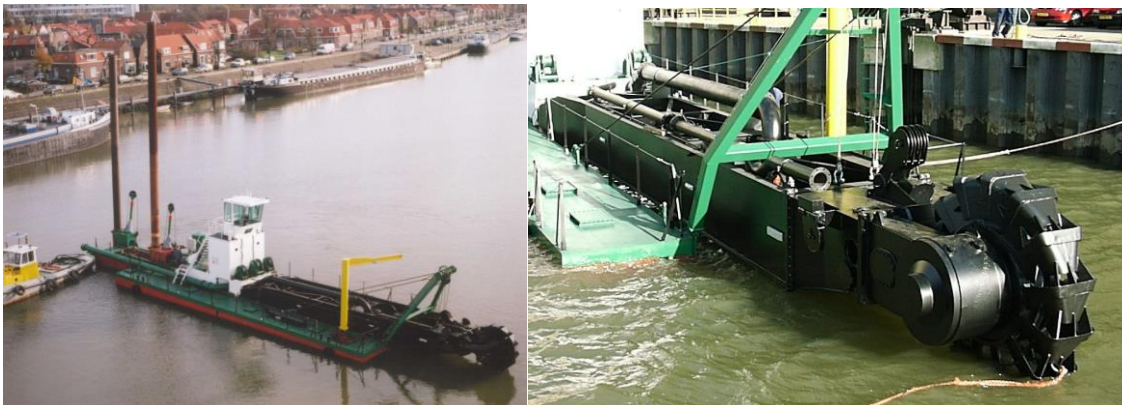
Figure 13 *Dredging wheel (photos taken from sister dredger already in exploitation)*

3.10. *Dividable spuds*

The requirement of increasing dredging depth from 15 to 19.5 led to a modified design of spuds from two dividable parts, with bolt connection. Lower part is made of 2 welded segments and upper part is made of 3 welded segments, with dredging depth of 15m and diameter of 559 mm.
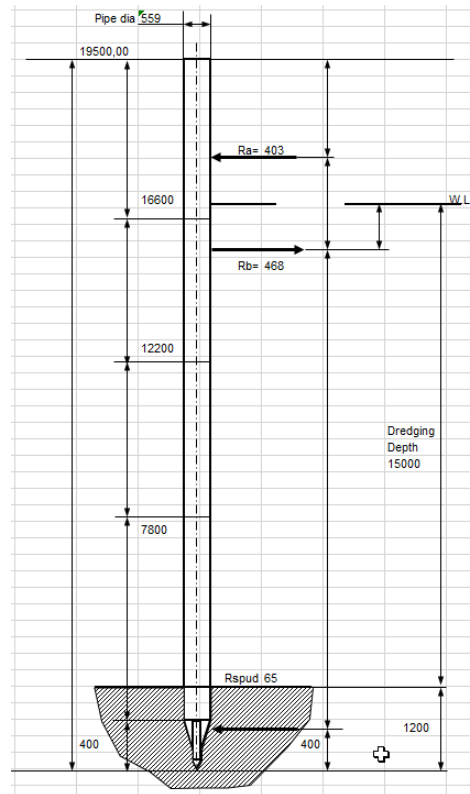
Figure 14 *Spud dimensions*

4. Conclusion

Because of expansion and everyday growth of capital and maintenance dredging work it is necessary to maximize uptime and performance and to minimize operational expenses. In order to have a competitive product on the market, standardized vessels that can be delivered quickly with low cost and a wide range of options are designed and offered. New features can be incorporated in the standard design and then engineered and produced in the short time if there is a need to meet some specific individual customer requirements. Vessel can be transported worldwide by road or rail, or completely assembled like project No.15052. Operation then can be started quickly, due to integrated equipment in main pontoon and vessel overall dimensions.

REFERENCES

[1]   Information taken from relevant documentation for IHC Pr.No.15052.

[2]   IHC Beavers® presentation papers and IHC website: https://www.royalihc.com/en/products/dredging/cutter-dredging/ihc-beaver-cutter-suction-dredger

MODULAR DECK SYSTEM FOR RORO VESSELS – RAMSSES H2020 R&D PROJECT

Vito Radolović[a], Josip Andrišić[a]*

a Flow Ship Design d.o.o., Anticova 9, Pula
* Corisponding Author, josip.andrisic@flowship.eu

Abstract

This paper will give an overview of the demonstration case Modular Deck System for RoRo Vessels developed within RAMSSES (Realisation and Demonstration of Advanced Material Solutions for Sustainable and Efficient Ships) EU funded project under HORIZON 2020. The research and development is addressed to the construction of internal strength decks on RoRo vessels introducing FRP (Fibre reinforced plastic) pultruded profiles and FRP sandwich technology. Reducing the weight of decks results in many benefits regarding general ship design due to large number of decks. Improved flexibility in the ship design, where weight could be traded for ship size, scantlings, cargo capacity, speed, installed power and weight, integration of structures and outfitting. Optimising the deck structure design using innovative materials and geometry results in more efficient production as well. With respect to ship operational aspects such as Fuel oil consumption and CO_2 emission reduction due to ship lightweight reduction leads to increased propulsion efficiency. The overall objective at RAMSSES is to develop optimised structure of RO-RO/Car-carrier using RAMSSES defined deck modules with respect to production optimisation as main objective followed by weight reduction, joint development, Fuel oil consumption and CO_2 emission reduction.

Key words: *RAMSSES; RoRo vessel; pultruded profiles; lightweight; production optimisation*

Sažetak

Članak daje pregled demonstracijskog slučaja modularnog sustava paluba RoRo brodova koji se razvija u sklopu projekta RAMSSES (Realisation and Demonstration of Advanced Material Solutions for Sustainable and Efficient Ships) koji je financiran sredstvima EU unutar HORIZON 2020. Istraživanje i razvoj unutar ove radne cjeline odnose se na konstrukciju unutarnjih paluba RoRo brodova. Smanjenje težina paluba stvara mnoge prednosti na opće karakteristike broda s obzirom da ti tipovi brodova imaju značajan broj paluba. Neke od prednosti su fleksibilnost prilikom osnivanja broda gdje se smanjenjem težine mogu povećati same dimenzije, korisna nosivost, brzina, ili smanjiti potrebna porivna snaga te bolja integracija strukture i opreme. Optimiziranjem strukture palube primjenom inovativnih materijala i geometrije rezultira i efikasnijom proizvodnjom. Ako se promatra brod u službi, smanjenje potrošnje goriva i smanjenje CO_2 zbog smanjene težine broda, dovodi do povećanja propulzijske efikasnosti. Sveobuhvatni cilj unutar RAMSSES-a je razviti optimiziranu strukturu RO-RO broda odnosno broda za prijevoz automobila primjenom RAMSSES palubnih modula kroz optimizaciju proizvodnje kao primarni cilj, uz dodatne ciljeve smanjenja težina, zajedničkog razvoja te smanjenja potrošnje goriva i ispuštanja CO_2.

Ključne riječi: *RAMSSES; RoRo brod; pultrudirani profili; smanjenje težine; proizvodnje optimizacija*

1   Introduction

Imperative on efficient transportation drives the development of new ligthweight structural solutions with the goal of energy consumption and greenhouse gasses emissions reduction. This paper will give an overview of the Work package 14's Modular Deck System for RoRo Vessels, which is one of thirteen demonstration cases developed within the R&D project RAMSSES (Realisation and Demonstration of Advanced Material Solutions for Sustainable and Efficient Ships), funded by the European Union's HORIZON 2020 framework programme under grant agreement No 723246.

The research and development presented is addressed to the construction of internal strength decks on RoRo vessels introducing FRP (Fiber reinforced plastic) pultruded profiles and FRP sandwich technology. The development started back in the 2006. during the R&D project Delight Transport, funded by the European Union's FP6 framework programme, where a design of a composite car deck has been developed,

using sandwich technology. Five years after the project end, the benefits of the solution have been recognized by a shipowner, which results with a successful implementation on the Car carrier m/v SIEM CICERO for the construction of three fixed car decks, built and delivered at Uljanik Shipyard in the 2017. The inovative design from CICERO has been used as a starting point for the further development in RAMSSES project,. The project started in 2017. and will be finished in 2021.

1.1   Problem definition

RoRo vessels have numerous internal strength decks. Clearances between decks are fixed and defined by cargo requirements (height of cars, trucks). Reducing the weight of decks results in many benefits regarding general ship design due to large number of decks (lower ship height, lower vertical centre of gravity (VCG), lower equipment number etc.). Improved flexibility in the ship design, where weight could be traded for ship size, scantlings, cargo capacity, speed, installed power and weight, integration of structures and outfitting. Optimising the deck structure design using innovative materials and geometry results in more efficient production as well (shorter lead times, improved reliability, and quality)

1.2   Technical approach

With respect to ship operational aspects such as fuel oil consumption and CO_2 emission reduction ship lightweight reduction leads to increased propulsion efficiency. In addition, depending on the design requirements, main engine installed power can be reduced for the same cargo intake or cargo intake can be increased. Reduced ship weight in the ship upper zone leads to better stability performance and less ballast required to fulfil stability requirements, where the total cargo in take can be additionally increased.

The first step to the full application of RAMSSES modules was to implement the hybrid transport structure approach with steel and GRP profiles application in the design and production of deck structures. The overall objective was to develop optimised structure of a Vehicle carrier using RAMSSES defined deck modules with respect to production optimisation as main objective followed by weight reduction, joint development, fuel oil consumption and CO_2 emission reduction.

The innovative design was evaluated with respect to the conventional steel design as well as to the alternative design using GRP sandwich panels already implemented at Uljanik newbuilding No 513 (m/v SIEM CICERO, delivered June 2017), Figure 1., which was used as base design for the developments at RAMSSES.

Figure 15 *Uljanik newbuilding No 513 (m/v SIEM CICERO, delivered June 2017).*

1.3 Results and achievements

In the novel RAMSSES design fixed car decks on a Car Carrier were designed by implementing composite modules using FRP pultruded profiles technology. Uljanik newbuilding No 513 (Car Carrier m/v SIEM Cicero) was chosen as base design, where innovative deck structure design, including composite sandwich panels is implemented at Decks 10, 11 and 12.

Full application of RAMSSES modules started with the implementation of the new developed module using pultruded profile technology by replacing the composite sandwich panel on a base design. In addition, alternative deck structure designs were recognised for further development at RAMSSES.

The first step was to define the data needed for the design such as deck structure arrangement, boundary condition, loading and design criteria.

Followed by the design alternatives assessment in the detail design stage, RAMSSES deck was further developed.

With respect to the production and assembly process, assessment on the integration of the RAMSSES design alternative into shipyard process was performed considering several scenarios. Further adjustments will be done according to the data collected from the full scale demonstrator production process.

New developed designs were evaluated with respect to the conventional steel design as well as to the composite design implemented on Uljanik newbuilding No 513 (base design).

Finally, the novel structural design will be further evaluated through laboratory tests (mechanical tests, full-scale and small-scale fire tests) as well as tests on the full-scale demonstrator.

At this stage of the project the production of the small scale and full-scale specimens is ongoing. Preparations for the full-scale demonstrator were performed and the production started.

2 Requirements and case definition

2.1 Case definition

The purpose of this application case is to reduce the production cost and lead time as well as to decrease the weight of the three upper decks (decks 10, 11 and 12) in a Car carrier; see Figure 2. This way both the structural weight of the ship and the vertical centre of gravity will be also lowered. Clearances between decks are fixed and defined by cargo requirements (height of cars, trucks). Reducing height and weight of deck structures is a very demanding task but it can result in many benefits regarding general ship design due to large number of decks (lower ship height, lower VCG, lower equipment number etc.).
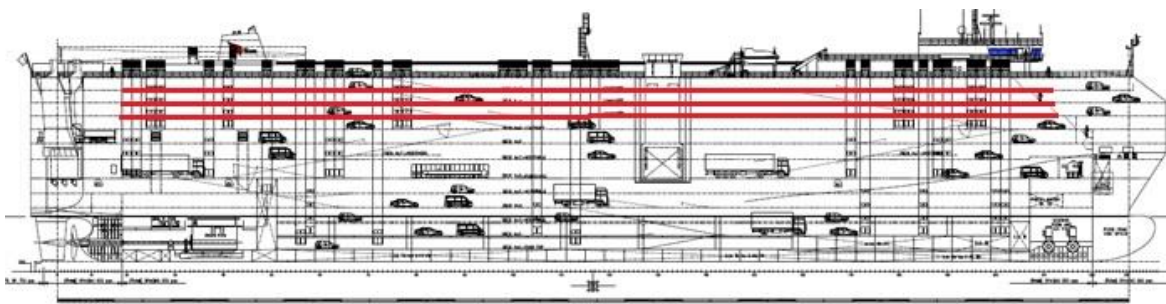
Figure 16 *Uljanik newbulding No 513 – composite decks 10,11 and 12*

In a conventional steel design a cargo deck is designed with steel deck plating stiffened by transversal web frames and longitudinal stiffeners. In the Innovative deck structure design at Uljanik newbuilding No 513 (base design), composite structure is implemented at Decks 10, 11 and 12. The structure arrangement consists of steel supporting grillage and composite sandwich panels (GRP, with PVC core, vacuum infused), Figure 3, Figure 4. Composite panel connection to supporting structure is designed as flexible with bolts. Same deck design will be base design for further development at RAMSSES.

Figure 17 *Composite sandwich panel*

Figure 18 *Uljanik newbuilding No 513 – decks 10,11 and 12 view*

2.1.1 Technical approach

The way to the full application of RAMSSES modules was to implement the new developed module using pultruded profile technology analysing different design alternatives, which can be defined as follows:

1. Composite module designed to replace the composite sandwich panel according the base design (small composite module)
2. Composite module designed to replace the composite sandwich panel and part of steel supporting structure according to the base design (large composite module)

The first step was to develop a composite module using pultruded profile technology by replacing the composite panel in the base design (Design alternative 1). In parallel to the First design alternative possibilities for further design development was investigated. Such as possibility to use FRP pultruded profiles for part of supporting structure, made of steel on base design, combination of different designs such as steel, composite sandwich panels and extruded profiles as well (Design alternative 2). Hypothetic design solutions investigated are illustrated on Figure 5 to Figure 8.
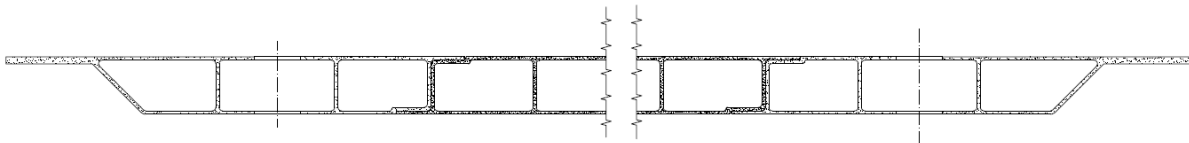
Figure 19 *Design alternative 1 – composite module hypothetic design solution –cross section)*
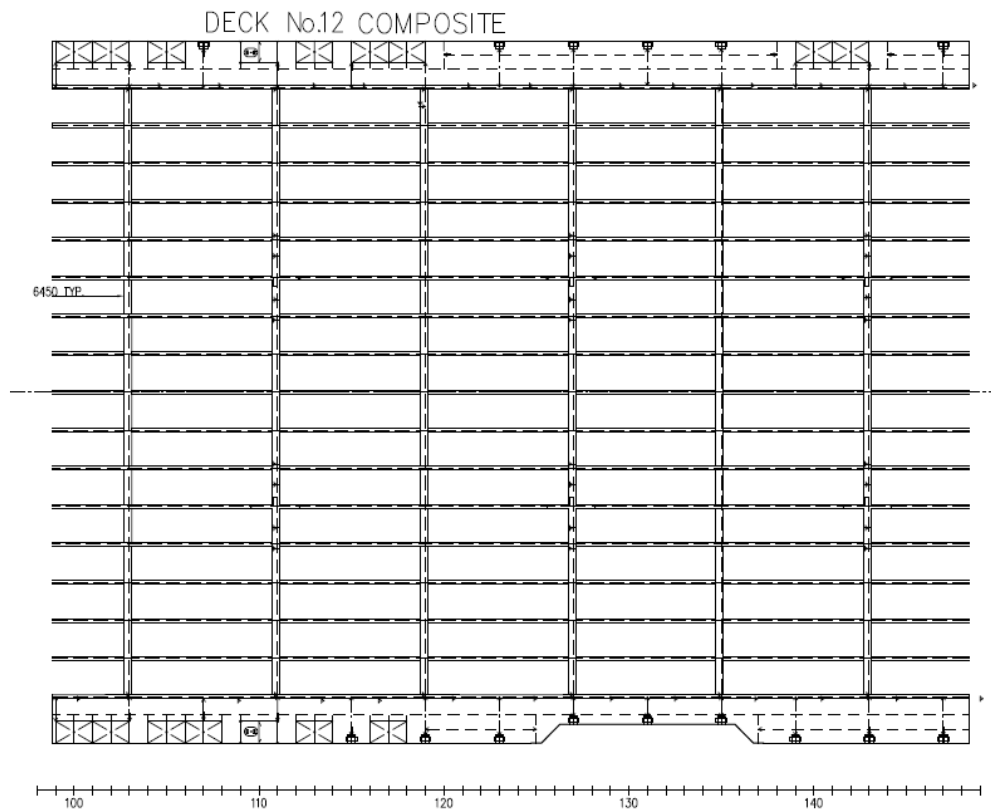
Figure 20 *Design alternative 1 – steel structure arrangement – Deck top view*
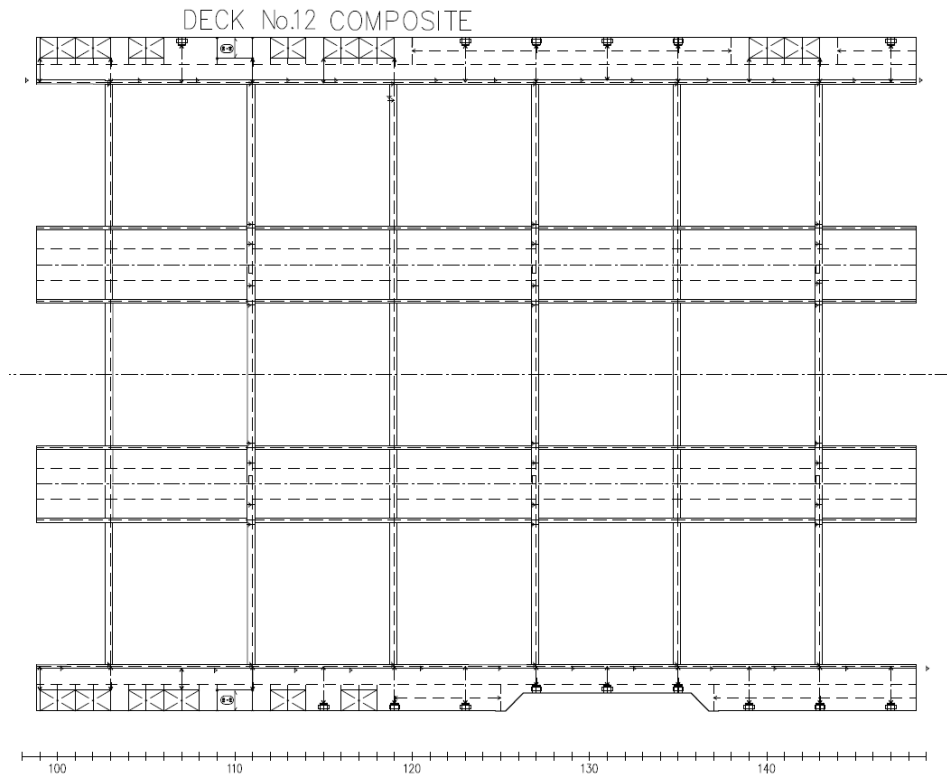
Figure 21 *Design alternative 2 – steel structure arrangement– Deck top view*
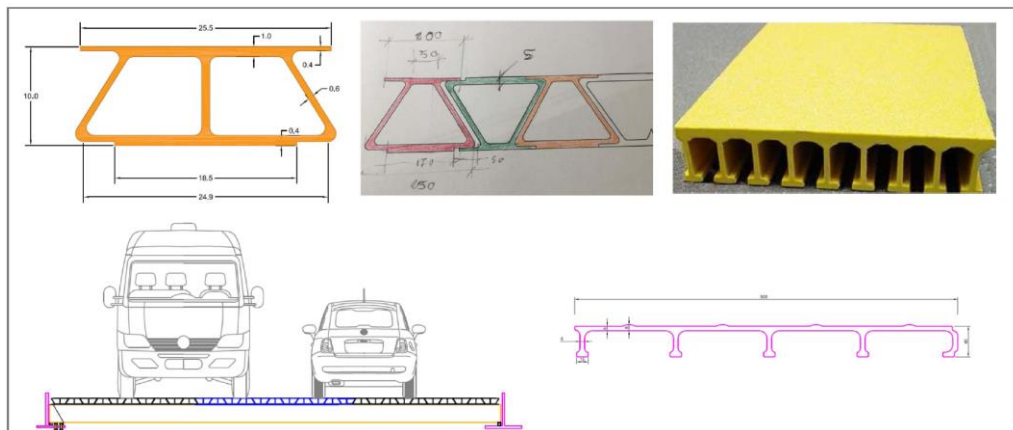
Figure 22 *FRP pultruded profiles geometry and arrangement – hypothetic solutions*

2.1.2 **Pultrusion** process

Pultrusion is a continuous process for manufacturing composite materials with constant cross-section. The term is a compound word, combining "pull" and "extrusion". As opposed to extrusion, which pushes the material, pultrusion works by pulling the material.

The pultrusion process is based on the balance between the pulling speed of the puller devices and the resin polymerization times: if the catalysis occurs too quickly, the material becomes hard within the heated mould (die), blocking the traction process.

On the contrary if the catalysis is too slow, the material will be released from the die yet gelled and the tensile force to which it will be subjected will cause the deformation of the profile.

The mechanical properties of the profiles depend on the quantity and type of raw materials (resins and fibers) that are used.

Many resin types may be used in pultrusion: both thermosetting (polyester, epoxy, acrylic, vinylester, etc.), thermoplastic (PVC, polyurethane, polyethylene, etc.) and various type of reinforced fibers.

FRP profiles made with the pultrusion process have excellent mechanical properties (such as tensile strength) in the direction of the fibers, unlike the mechanical properties in the transverse direction that are low. To increase the mechanical properties in the transverse direction is possible to add reinforcing mats (with fibers arranged in two or more preferential directions) in the composite mixture.

Extruded profiles and production facilities are illustrated on Figure 9 and Figure 10.

Figure 23 *Extruded profiles production facilities*
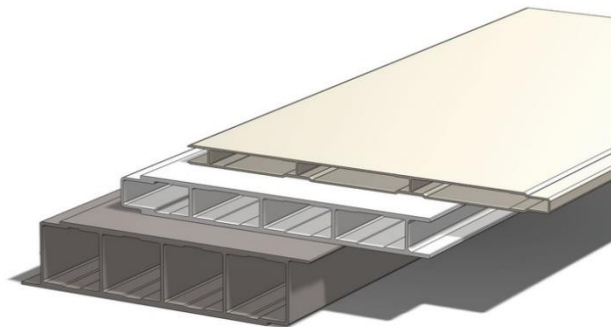
Figure 24 *Extruded profiles - examples*

2.1.3 FRP Profiles Properties

Profiles can be realized in various sections, shapes and colors, with constant cross-section along the length.

Use of FRP pultruded profiles can bring the following benefits: reduced weight, low assembly and transportation costs, reduced maintenance cost as maintenance is not required, significant corrosion and chemical resistance, electric and thermal insulation, insonorization, operational range (temperatures from -40° C to +120° C) , high mechanical resistance, acoustic insulation, electromagnetic transparency, durability.

Raw materials used in pultrusion process can be categorized as follows:

1.   Thermosetting Resins: Polyester, Vinylester, Epoxy. Acrylic
2.   Reinforcements
    a. Layout: Rovings, Mats, Reinforcing Mats, Wovens
    b. Type: Glass, Carbon, Aramidic, Polyester, Natural

3.   Fillers: Calcium carbonate, Quartz, Kaolin
4.   Catalysts and additive

2.2   Requirements

2.2.1 Geometry requirements

The composite module is to be designed to cover the opening formed by a load carrying steel grillage structure to form a deck surface. Composite modules are to be the same for all considered decks.

Geometry of the steel supporting structure will be defined according to the design alternative.

Supporting structure constraints are:

o   Length between deck transverses, LT= 13600 mm,
o   Breadth between deck longitudinal girders is not a constraint, at base design BL = 1750 mm,
o   Height, including structure height, building tolerance and static deflection (cargo load only, without own weight and without dynamic acceleration), H=330 mm
o   Transverse girder flange breadth BFT, is not a constraint, at base design BFT= 350 mm
o   Longitudinal girder flange breadth BFT, is not a constraint, at base design BFL= 180 mm

Opening in steel grillage dimensions to be covered with composite module:

o   Length between deck transverses flange, LC= LT- BFT
o   Breadth between deck longitudinal girder flange, BC= BL- BFL
o   Radius at opening corners, to be defined

Composite module constraints between girders are:

o   Height above deck plating line to be max. 5 mm

FRP profiles geometry constraints with respect to production:

o   Height > 0.5 m
o   Breadth > 1.2 m

Cargo lashing opening arrangement:

o   transversal distance between openings: 600 - 900 mm
o   longitudinal distance between openings: 600 -700 mm

2.2.2 **Boundary** Conditions

Boundary condition are to be investigated as have influence on the connection detail design with respect to FRP structure arrangement.

Boundary is considered as simply supported on the base design, due to the realistic nature of the interaction between sandwich panel and supporting grillage.

2.2.3 Loading

The cargo loading is defined and shown on Figure 11.
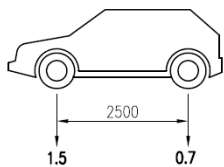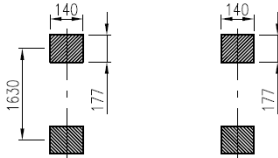
NAME	LOAD AT	AXLE LOAD (t)	TYRE PRINT (mm)	HOMMOGENOUS LOADING (t/m2)	DECK NO
PRIVATE CAR	SEA	L=4.8 m B=1.9 m 2500 1.5 0.7	140 1630 177 140 177	0.20	1 3 5 10 11 12 13

Figure 25 *Load cases – vehicle parking position*

With respect to the connection of the composite module to supporting structure, load case found to be critical is when four lashing forces acting on composite module not loaded with cargo in ship transverse direction.

2.3 Technical challenges

Main technical challenge foreseen is a design of a robust composite module that will allow standard shipbuilding tolerances at the steel part of the structure combined with an improved composite/steel arrangement, compared to the base design) with respect to:

- o production (less complex steel structure arrangement, building blocks, etc)
- o assembly (transport, joints)
- o cargo operation (flush deck, lashing)
- o cost (decreased production cost)

3 Product design

3.1 Concept design

Concept design is defined as the phase in structural design when geometry and topology are open to modification and structural variants are analyzed in accordance with the needs of the head designer. Benefits of optimization procedure in this phase are the biggest. For the concept designs, steel and composite part have been optimized with respect to weight, arrangement, connection and fire safety.

The first step was to develop the deck profile using pultruded profile technology, which is similar for all design alternatives considered at RAMSSES. In parallel to deck profile, possibilities for further design development have been investigated, such as possibility to use FRP pultruded profiles for part of supporting structure, made of steel on base design.

Starting from the two design alternatives, five concept designs were developed and analyzed:

- o 2 FRP profile types, FRP deck profile and FRP boundary, small composite module
- o 1A 1 FRP profile type, small composite module
- o 3 FRP profile types, FRP deck and FRP supporting profile, medium composite module
- o 2A 3 FRP profile types, FRP deck and FRP supporting profile, large composite module
- o 1 FRP profile type, FRP deck profile, large composite module (combination of 1 and 2)

For each design concept both steel and composite structure arrangement were defined where deck arrangement consists of the composite module supported by the steel grillage. Steel grillage is supported by two rows of pillars. Steel grillage and composite module arrangement have been variated resulting in five concept designs, illustrated on Figure 12.

1,1A (smal module) 2 (medium module) 2A (large module) 3 (large module)
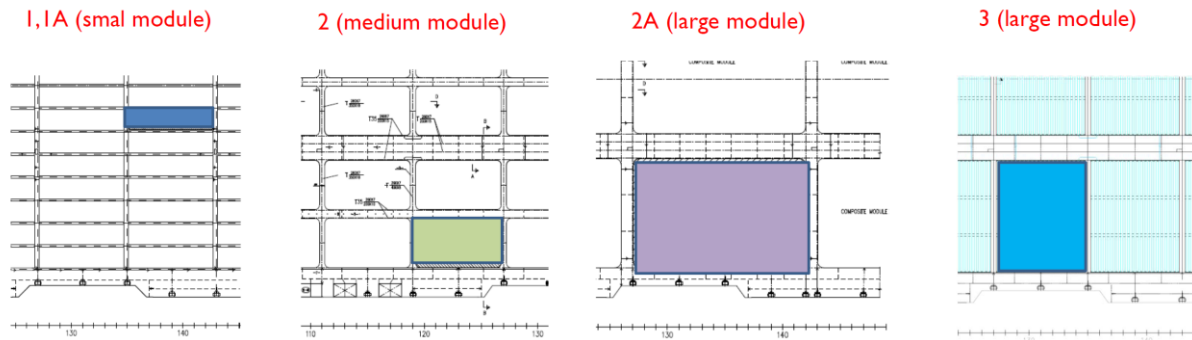
Figure 26 *Concept designs developed at RAMSSES*

3.1.1 Steel structure

For the design concepts, deck structure arrangement optimization has been performed with respect to weight, outfitting, production technology and cost.

Structure scantlings have been checked according to BV Rules and Regulations.

Arrangement of the steel beams has been variated in order to evaluate different sizes of the composite module. Main constraints were the pillar arrangement, ship side structure, outfitting (arrangement of the CO2 fire distinguishing system, two lines in longitudinal direction) and maximum allowable deflection of the structure.

3D beam structural analysis has been performed for the steel structure scantlings determination, for concept designs with medium and large module (2, 2A, 3), using DNV software NAUTICUS 3D Beam. For the concept designs with small module, structure scantlings from base design have been considered.

3.1.2 Composite structure

Depending on the design concept, different profile types and geometry for each type were considered. Composite profile types can be divided as follows:

Deck profile – forming composite module surface

Supporting profile – used as support of the deck profile and for connection to the steel structure

3.1.3 Design concept assessment

Selection of most promising concept designs for further development have been performed according to preliminary weight estimation, preliminary production cost analysis and production process criteria.

Summary of the assessment can be found below:

- 1
  - weight reduction of 8 % compared to the conventional steel deck
  - Increased weight for 17 % compared to the base design
  - Reduced deck production cost for 15 %
  - Simple transport and assembly of composite module on board
- 1A
  - No weight reduction compared to the conventional steel deck

96

- o Increased weight for 25 % compared to the base design

- o No production cost savings compared to the base design

- o Simple transport and assembly of composite module on board

- o 2

  - o weight reduction of 10 % compared to the conventional steel deck

  - o increased weight for 15 % compared to base design

  - o Reduced deck production cost for 18 % compared to the base design

  - o Flexibility in the lashing holes arrangement

  - o Special attention to be paid on the transport and assembly of composite module on board

- o 2A

  o Too big deflections od FRP supporting girders i.e. design of FRP supporting girders is not applicable

- o 3

  o weight reduction of 10 % compared to the conventional steel deck

  o increased weight for 15 % compared to base design with GRP sandwich modules

  o Reduced deck production cost for 20 % compared to the base design

  o Flexibility in the lashing holes arrangement

  o Special attention to be paid on the transport and assembly of composite module on board

  o Special attention to be paid on the interaction of the FRP module and steel supporting structure

Concept design 3 has been chosen for the detail design stage and further development. Main arguments that outweighed to concept design 3 are:

- size of the composite module – large composite module, bigger challenge at RAMSSES
- promising weight and production cost assessment results,
- number of different pultruded profiles used

Starting from the two design alternatives defined in the early project stage, five concept designs have been developed and analyzed where one has been selected for further development in the detail design stage: Concept design 3.

3.2   Detail design

Following concept design assessment results in the detail design stage RAMSSES deck has been further developed. Starting from the Concept design 3 deck arrangement (geometry and topology) the optimisation has been concentrated on refined structure scantlings optimisation for both steel and

composite module, definition of specific details with respect to outfitting (connection details, lashing) and fire safety, following the RAMSSES objectives.

Deck arrangement consists of the composite module supported by the steel grillage system and fixed part of steel arranged on the side shell and in the central part of the deck in way of the pillars (executed as a large box girder)). Composite module supporting steel grillage system consists of longitudinal girders (composite module supports) supported by transverse girders. Transverse girders are supported by the fixed part of the deck on the side and box girder in way of the pillars. In order to obtain a flat deck i.e. composite module and steel plating upper surfaces on the same level, the steel grillage supporting system is arranged in two heights. As composite module supports, longitudinal steel girders are lower in height where bottom edge is in line with the transverse steel girders and central box girders. At the central box girders and fixed deck at side shell, a flat bar is arranged to support the composite module. Bolt or riveted connection system of the Composite module to longitudinal supports is foreseen. Deck arrangement is illustrated on Figure 13 and Figure 14.
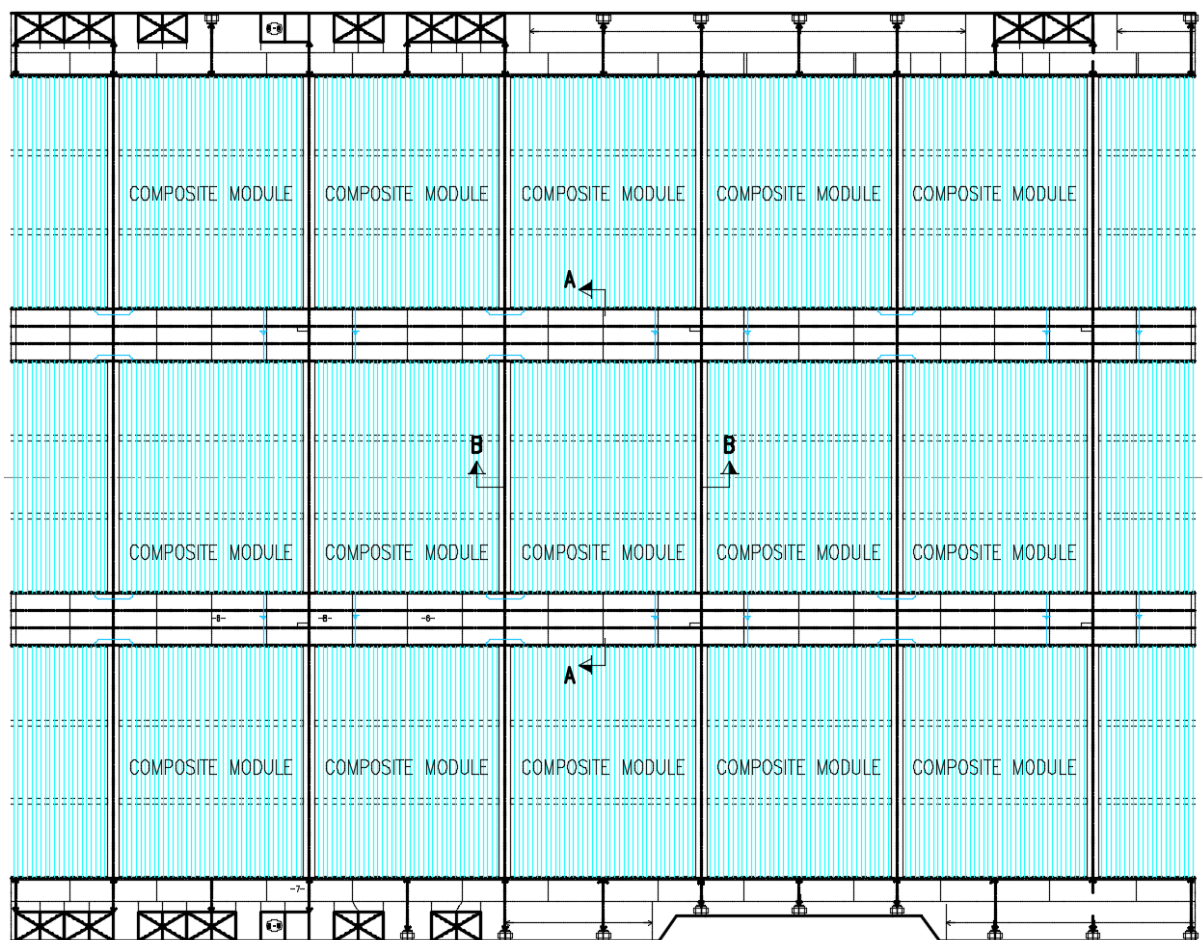
Figure 27 *RAMSSES deck arrangement*
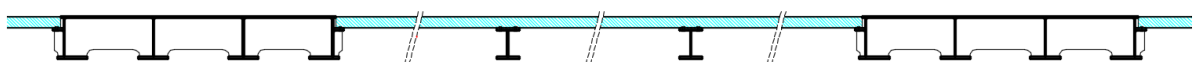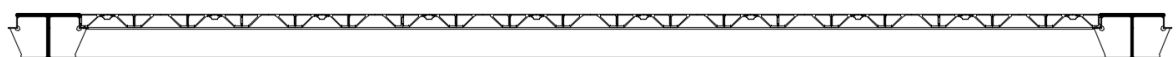
Figure 28 *RAMSSES deck arrangement – cross sections*

The first step was to finalise the composite deck profile design. Further, possible design improvements on the steel grillage supporting system have been investigated. Starting from the deck arrangement described above a second design alternative has been developed and analysed, where the main objective was to improve the design in way of production and connection between steel and composite module. Hence, steel grillage system where the height of the transverse girder reduced to be aligned with the longitudinal girders is developed. For both grillage arrangements, composite module and connection system is the same.

3.2.1   Steel structure arrangement and calculation

Deck structure arrangement optimization has been performed with respect to weight, outfitting, production technology and cost. Structure scantlings have been checked according to BV Rules and Regulations.

Arrangement of the steel beams from the concept design 3 has been further optimized, variating girder geometry (width, thickness, height, profile type: box, T). From the optimization results, two arrangements are selected for further assessment and final selection which can be presented as follows:

1. Grillage system in two levels, Figure 14

2. Grillage system in one level, Figure 15
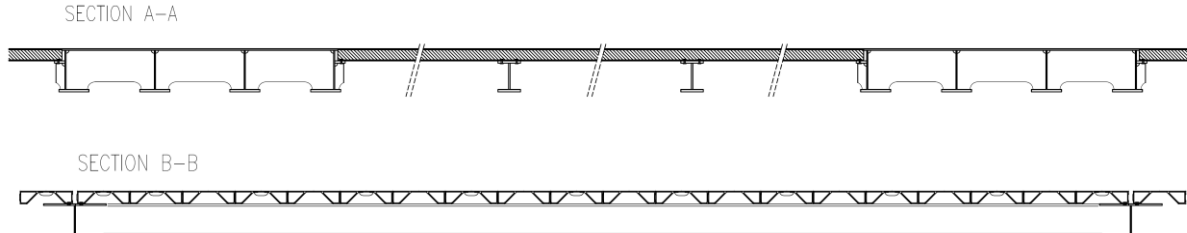
Figure 29 *RAMSSES deck arrangement – grillage system alternative 2 - cross sections*

3D beam structural analysis has been performed for the steel structure scantlings determination, using DNV software NAUTICUS 3D Beam. Grillage model is illustrated on Figure 16. Finally, Grillage system in two levels was selected for further developments. FEA will be performed to further optimize the structure.
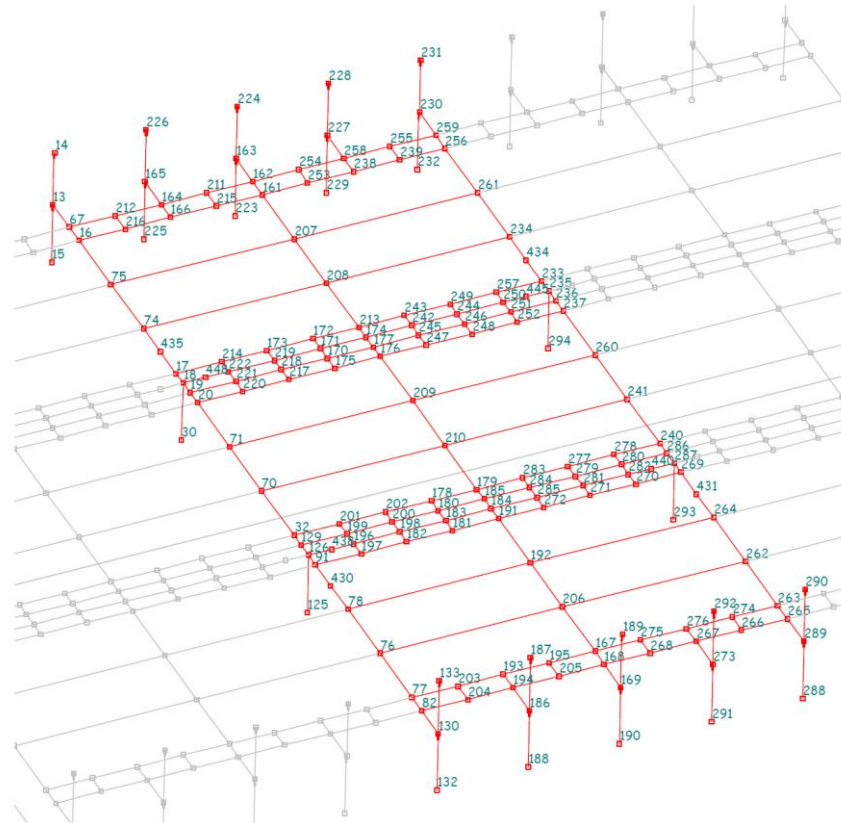
Figure 30 *3D beam – deck steel grillage model*

3.2.2 Composite module optimisation

The driver of the optimisation was based on the requirements to reduce the deformability of the FRP structure from one side and to extend the use of FRP as much as possible in order to reduce the overall weight. For solving this issue, it was decided to adopt a hybrid structure deck with steel beams supporting higher continuous FRP profiles (Concept design 3).

Deck profile geometry definition is led by production process technology restrictions and lashing opening arrangement requirements. The profile section is arranged in order to assure both the torsional stiffness of the deck and lashing opening outfitting, where the geometry had to be arranged for the lashing hole outfitting (steel protection) and cargo lashing equipment (hook) that require a thin surface. The contact area to be glued is articulated with a shear key shape in order to increase the connection between the profiles. Deck profile and Composite module geometry and arrangement are illustrated on and Figure **17** and Figure **32** *Composite module arrangement*

Calculation input data have been considered. Finite element analysis has been performed. The tool used to evaluate the FRP deck panel was SAP2000. Structure is discretized with combination of solid (frame) and shell elements. Deck profile is modelled with shell elements and deck profile supporting structure is modelled with solid (frame) elements. Calculation model is shown on Figure 19, where yellow represents the deck profile and blue represents the steel girders, deck module supporting structure. Typical load schemes are shown on Figure 20.

Figure 31 *Pultruded profile geometry*
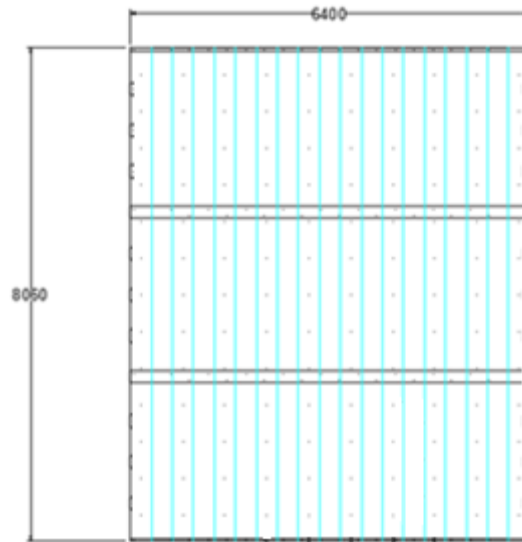
Figure 32 *Composite module arrangement*
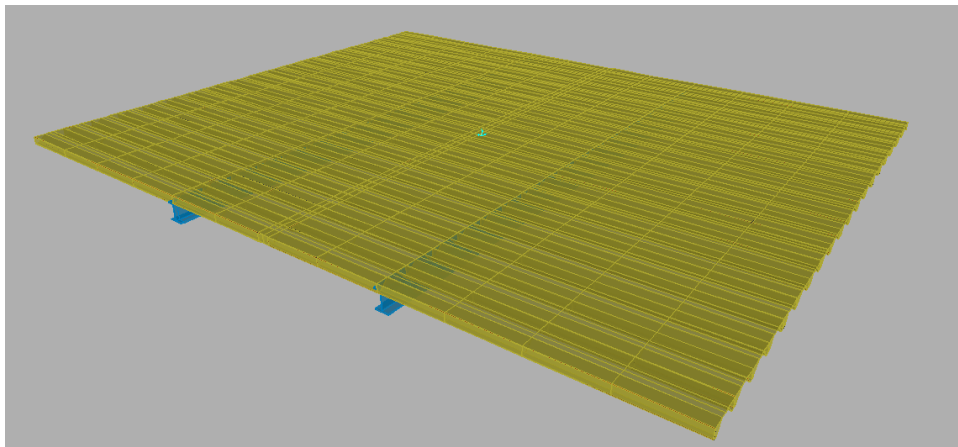
Figure 33 *FEA - Deck profile calculation model*
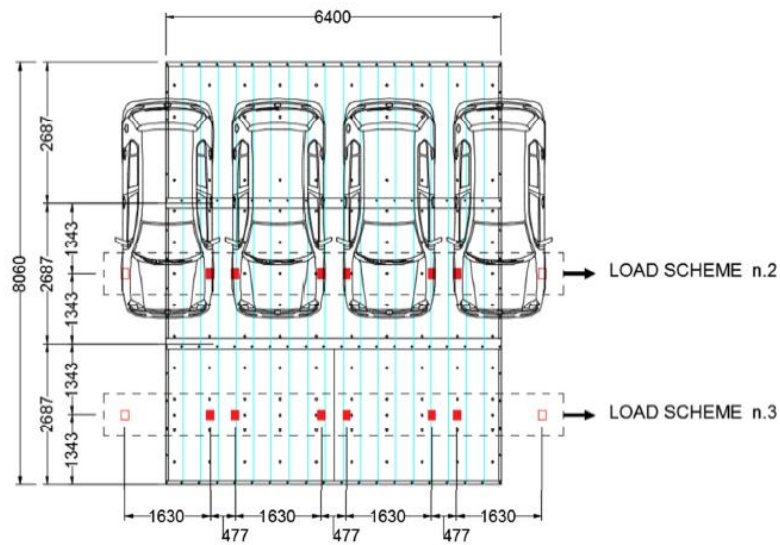
Figure 34 *FEA - Load Scheme*

Calculation results showed that the stress and deflection values are within the required limits. Calculation results are illustrated on Figure 21 and Figure 22.
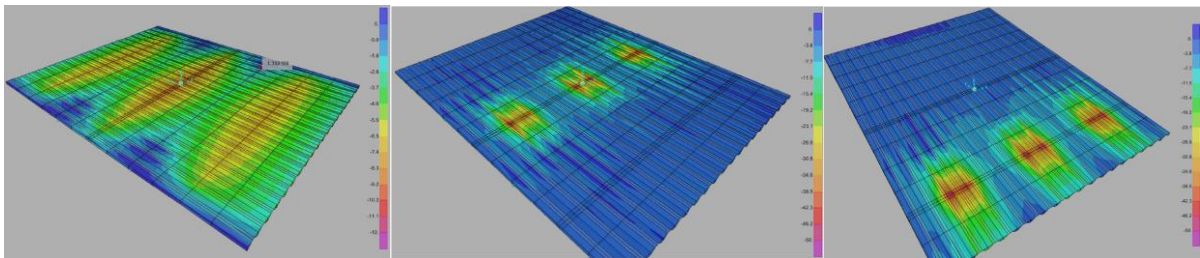
Figure 35 *FEA –stresses result overview: Load case1 (left), Load case 2 (Centre), Load case3 (Right)*
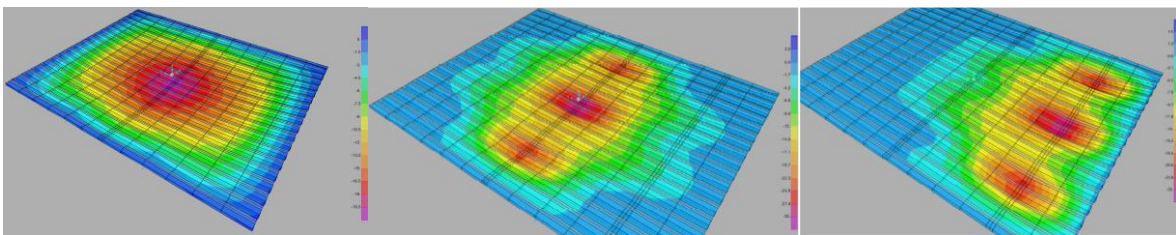
Figure 36 *FEA –deflection result overview: Load case1 (left), Load case 2 (Centre), Load case3 (Right)*

3.2.3 Connections

In the detail design stage connections were developed and optimized. Final connection solution between structural members was selected, which can be divided as follows:

Steel to steel

Standard shipbuilding welded connection.

Composite to composite

FRP pultruded profiles are bonded to each other in order to form a composite module to be assembled on the steel supporting structure. The connection area geometry of the profiles is additionally designed to improve the connection.

Composite to steel

Composite module riveted connection has been selected for further development. The connections are designed to withstand the design forces; deck load, local cargo lashing and global forces (deflections).

With respect to the connection of the composite module to supporting structure, load case found to be critical is when four lashing forces acting on composite module not loaded with cargo in ship transverse direction.

For the connection equipment, the expansion bolt (HOLLO BOLT) has been selected as final solution.
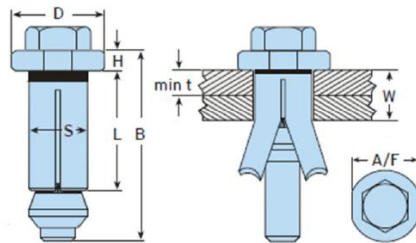
a) Hexagonal				Sleeve		Collar					Safe Working Loads (5:1 Factor of Safety)	
Product Code	Bolt Length	Clamping Thickness	Outer Ply	Length	Outer Ø	Height	Ø		Tightening Torque		Tensile	Single Shear
	B mm	W mm	min t mm	L mm	S mm	H mm	D mm	A/F mm	Nm		kN	kN
HB08-1	M8 x 50	3 - 22	-	30	13.75	5	22	19	23		4.0	5.0
HB08-2	M8 x 70	22 - 41	-	49	13.75	5	22	19	23		4.0	5.0

Figure 37 *Selected HOLLO BOLT*

3.2.4 Fire safety assessment

According to the requirements and experience from fire safety assessment conducted at the base design, RAMSSES deck arrangement has been preliminary evaluated. Main objective in order to improve fire safety properties is to execute the deck as much as possible gas tight. Critical points are openings in deck at cargo lashing equipment and at composite module boundaries.

To reduce the openings, different solutions are available either structural or outfitting. Final decision will be taken according to the fire tests results, where two different full scale specimens will be tested.

3.2.5 Weight calculation

After the structural calculation and optimization were performed, the weight calculation was done where the RAMSSES design was compared versus the conventional steel design and base design. Deck area considered in the calculation represents the part of the novel deck design including the composite modules and steel supporting structure i.e. modified structure arrangement compared to the conventional design. Selected deck areas are illustrated on 24, 25 and 26. Total deck weight summary is shown in Table 1.
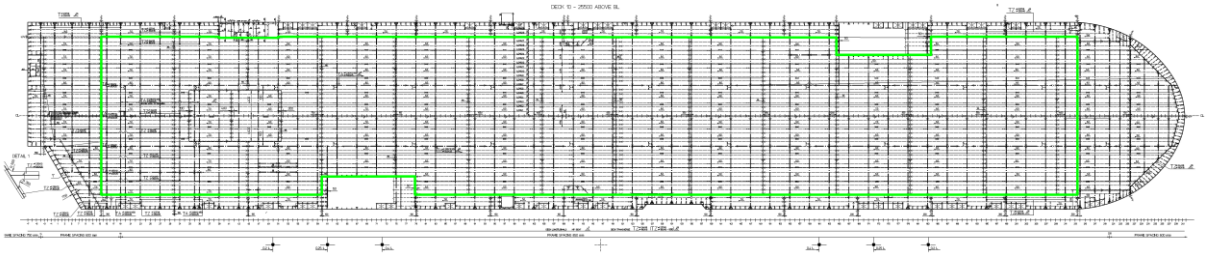
Figure 38 *Conventional steel deck*
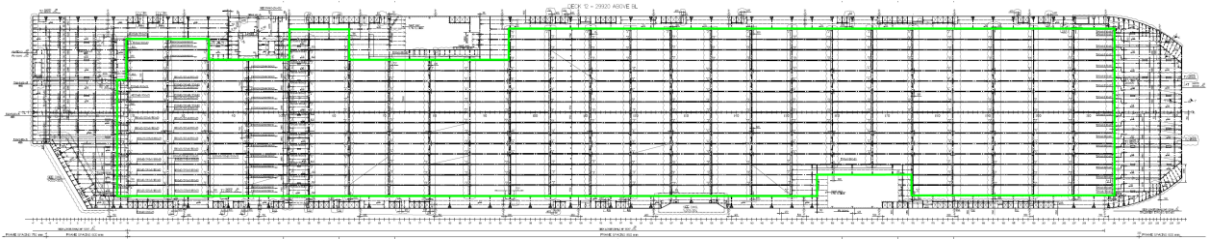
Figure 39 *Base design-composite GRP sandwich panels and steel*
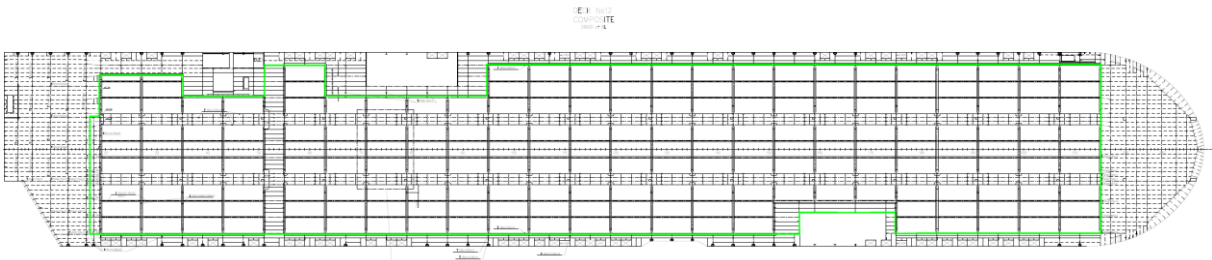
Figure 40 *Ramsses design - composite FRP pultruded profiles and steel*

Table 15 Weight calculation summary

	Conventional design - steel	Base design - Sandwich panels	RAMSSES design - pultruded FRP profiles
SPECIFIC WEIGHT			
Steel weight, kg/m2	80.3	48.01	50.43
Composite weight, kg/m2	0	13.07	18.59
Total weight, kg/m2	80.3	61.08	69.02
Total area (3 decks)	13290	13290	13290
TOTAL WEIGHT			
composite weight	0	174	247
steel weight, tonnes	1067	638	670
weight, tones	1067	812	917
RELATIVE DIFFERENCE			
composite weight	/	0%	42%
steel weight	67%	0%	5%
total weight	31%	0%	13%
RELATIVE DIFFERENCE			
composite weight/total	0%	16%	23%
steel weight	0%	-40%	-37%
total weight	0%	-24%	-14%

4 Process engineering

This chapter will summarize the possible production and assembly process for the design alternative of GFRP composite panels which study is ongoing at the time of writing this article.

For the production process of pultrusion profile, two busines models are analyzed where there are possibilities to produce the pultrusion panel in the shipyard or in a specialized factory out of the shipyard. According to the business models it has been determined what is the best approach to produce the pultrusion profile in term of time and cost from production and transportation point of view.

For the assembly process in the shipyard, the analysis on the lead time, resources, and the constraints in shipyards to enable the integration of design alternative panels into current assembly process has been performed, by using the Simulation Toolkit Shipbuilding (STS) of the Siemens simulation software Plant Simulation.

The hole process is applied on the different areas of the shipyard. In the STS the transportation by crane, forklift and carrier is also included in the simulation, so the time and therefore the lead costs of the drivers have been included in the resources of all personal statistics. As there are already methods for joining blocks or sections it is very suitable using this tool for the installation of the panels to the blocks as well as for the bonding process.

During the preparation of the simulation, total five scenarios were considered with respect to the composite module preassembly and assembly location. The scenarios have been reduced to two, as the installation after ship launching is restricted to the panel size. The first scenario is considering joining of all panels in the workshop and install them all in the slipway. The second scenario is analyzing the process to install the panels in the pre-block assembly. As there are restrictions of the hot work, this is not applicable for all the panels to some needs also be installed afterwards. It is examined that the second scenario will take more time but also avoiding the bottleneck in the slipway.

The complete process of assembly scenario 1 and 2 can be seen in Figure 41 *Pultrusion panel assembly process for scenario 1, and 2*

Process 1 (Assembly scenario 1,2)

Unloading the pallet from Truck into storage area

Parking area to storage area 77

Process 2 (Assembly scenario 1,2)

Pallet dismantling and transfer to bonding workshop

Storage area 77 to workshop OJ16

Process 3 (Assembly scenario 1,2)

Gluing process of subpanels (Surface preparation, adhesive application, sub panels join, and curing process)

Workshop OJ16

Process 4 (Assembly scenario 1)

Panel installation in slipway

Process 4 (Assembly scenario 2)

subpanel installation in Block Preassembly

P4

Process 5 (Assembly scenario 1)

Panel coating

Outfitting quay or P3

Process 5 (Assembly scenario 2)

±50% Panel installation in slipway

P3

Process 6 (Assembly scenario 2)

Panel coating

Outfitting quay or P3

Figure 41 *Pultrusion panel assembly process for scenario 1, and 2*

5   Demonstrator and Testing

The demonstrator was designed to represent the typical RAMSSES deck structure in full scale, as marked with red square on Figure 28.

Building and assembly process for the demonstrator will be equal to the process to be used in the shipyard, where feedback will be given to the production process assessment.
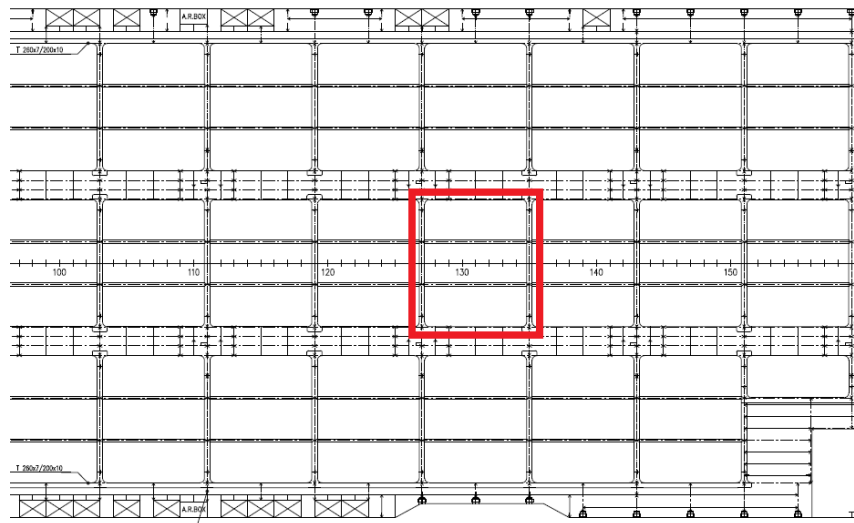
Figure 42 *Typical deck layout*

At the time of writing this article, the demonstrator production was ongoing. Steel component under construction is illustrated on Figure 29. Pultrusion facilities including the RAMSSES component forming dye and profile specimen are illustrated on Figure 30 and Figure 31.

Figure 43 *Demonstrator – steel structure under construction*

Figure 44 *Pultrusion process – RAMSSES forming dye*

Figure 45 *RAMSSES FRP profile*

Several test arrangements are planned and specified as follows:

- Bonding test
- Small scale fire tests
- Full scale fire tests
- Mechanical tests
- Tests on the demonstrator

Figure 46 *Test specimens*

6   Conclusion

In the novel RAMSSES design fixed car decks 10 to 12 on a Car Carrier were designed implementing composite modules using FRP pultruded profiles technology. Uljanik newbuilding No 513 (m/v SIEM Cicero) was used as base design. At the base design, innovative deck structure design, including composite sandwich panels has been implemented at Decks 10, 11 and 12.

The first step was to create the data needed to design the composite modules at decks 10-12. In addition, Deck structure arrangement, boundary condition, loading and design criteria were defined.

Full application of RAMSSES modules started with the implementation of the new developed module using pultruded profile technology where different design alternatives were investigated. Following the design alternatives assessment results in the detail design stage RAMSSES deck was further developed. Deck optimisation was concentrated on the composite module optimisation with respect to weight, outfitting (connection details, lashing) and fire safety, following the RAMSSES objectives. Steel structure was optimised with respect to the production process (arrangement) as main objective, resulting in two different designs. Further, with respect to fire safety, improvements on both steel and composite module were considered. Finally, the solutions were evaluated and final design selected where specific composite module details with respect to fire safety will be finally selected after the fire tests results. Weight calculation was performed, where the results are in line with the expected. In addition, Demonstrator was designed to represent the final RAMSSES deck design in full scale.

With respect to the production and assembly process, assessment on the integration of the RAMSSES design alternative into shipyard process was performed considering several scenarios.

New developed design was evaluated with respect to the conventional steel design as well as to the composite design implemented on Uljanik newbuilding No 513.

Finally, the novel structural design will be further evaluated through laboratory tests results (mechanical tests, fire tests), full scale tests on the demonstrator and lessons learned with respect to the full-scale demonstrator production process.

REFERENCES

[1]   Radolovic, V., Rahm, M., 2017, : Design of car decks with composite panels introduced on a 7000 cars car carrier, ELASS conference, Pula, Croatia. Available at: https://e-lass.eu/media/2017/10/E-LASS-Pula-carcarrier_v2_final_1.pdf

[2]   Radolovic, V., 2020, ; Deliverable 14.2 WP14 Results at MS6, RAMSSES Project

[3]   Bureau Veritas (Marine & Offshore Division). 2012. Rule Note NR 546 DT R00 E: Hull in Composite Materials and Ply-wood, Material Approval, Design Principles, Construction and Survey.

[4]   Bureau Veritas (Marine & Offshore Division). 2014. Rule Note NR 600 DT R00 E: Hull structure and arrangement for the classification of cargo ships less than 65 m and non-cargo ships less than 90 m.

[5]   Bureau Veritas (Marine & Offshore Division). 2014. Rule Note NR 467 DT R07 E: Rules for the classification of steel ships

"SKLAD" TRIMARAN CONCEPT FOR PROTECTION OF ADRIATIC SEA

Dario, Ban*[a], Marko, Liović [a]

a FESB-University of Split;
* Corisponding Author, darioban@fesb.hr

Abstract

Missile, countersubmarine patrol ship with displacement over 1000 tonnes is designed for Adriatic sea protection in 21st century, according to the LCS-2 trimaran concept (Littoral Combat Class), with wide helicopter deck. The central hull is based on semi-displacement hull series "Sklad" developed in "Brodarski Institut" in Zagreb, with stabilizing hulls ensuring survival of 3 neighboring compartments damage and superior seakeeping performances. The ship can achieve maximal speed of 50 knots using CODAG propulsion (2 Diesel + 1 Gas turbine) with 3 waterjet propulsors. The autonomy of the ship for cruising speed of 20 knots is 1000nm.

Key words: "Sklad" systematic series; trimaran; survival of 3 damaged compartments; helicopter deck; maximal speed 50 knots

Sažetak (Abstract in Croatian only for Croatian speaking authors)

Za potrebe nadzora Jadranskog mora u 21. stoljeću osnovan je raketni, protupodmornički patrolni brod istisnine preko 1000t, prema konceptu LCS-2 (Littoral Combat Class) trimarana, sa širokom helikopterskom palubom. Za formu centralnog trupa je odabrana sustavna serija poluistisninskih formi "Sklad" razvijana u "Brodarskom institutu" u Zagrebu, a brod je stabiliziran pomoćnim trupovima, čime brod može preživjeti naplavu 3 susjedna prostora te ima superiorna pomorstvena svojstva. Brod postiže maksimalnu brzinu od 50 čv CODAG pogonskim postrojenjem (2 Diesel motora + 1 Plinska turbina) s 3 vodomlazna propulzora. Za brzinu krstarenja broda od 20 čv, autonomija broda je 1000 nm.

Ključne riječi: sustavna serija "Sklad" ; trimaran ; preživljavanje naplave 3 prostora ; helikopterska paluba ; maksimalna brzina 50 čvorova

1. Uvod

Uvjeti nadzora mora u 21. stoljeću se mijenjaju prema višeslojnom sustavu podržanom komunikacijsko-informacijskom tehnologijom, koji će omogućiti nadzor zraka, mora i podmorja, cijele godine, u svim vremenskim uvjetima, slika 1. Klasičan, dosadašnji način nadzora prisustvom velikih pomorskih objekata će biti zamijenjen autonomnim rojevima zračnih, podvodnih i pomorskih dronova čije će se upravljanje i komunikacija obavljati s kopna i na glavnim brodovima (mother ships) manjih i većih dimenzija kao što je to opisano na interenet stranicama hrvatskog Klastera konkurentnosti obrambene industrije, [1], čiji je FESB član.

Glavni brod tog sustava bi bio višenamjenski ratni brod, kao platforma za prihvat dronova svih vrsta, te su zbog toga glavni projektni zahtjevi za taj brod široka radna paluba koja omogućuje prihvat AUV i ROV podvodnih objekata (eng. AUV – Autonomou Underwater Vehicle, ROV – Remote Operating Vehicle) i ASS plovila (eng. Autonomous Surface Ship), te slijetanja AAV i RPAS (eng. Autonomous Airborne Vehicles, Remotely Piloted Aircraft Systems), tj. dronova i helikoptera. Osim toga, brod mora biti operativan u Jadranskom moru na stanjima mora 6 i više, te imati doplov više od 1000 (nm). Kao ratni brod, on mora imati povećanu robusnost i preživljavanje i kod naplave od 3 susjedna prostora.
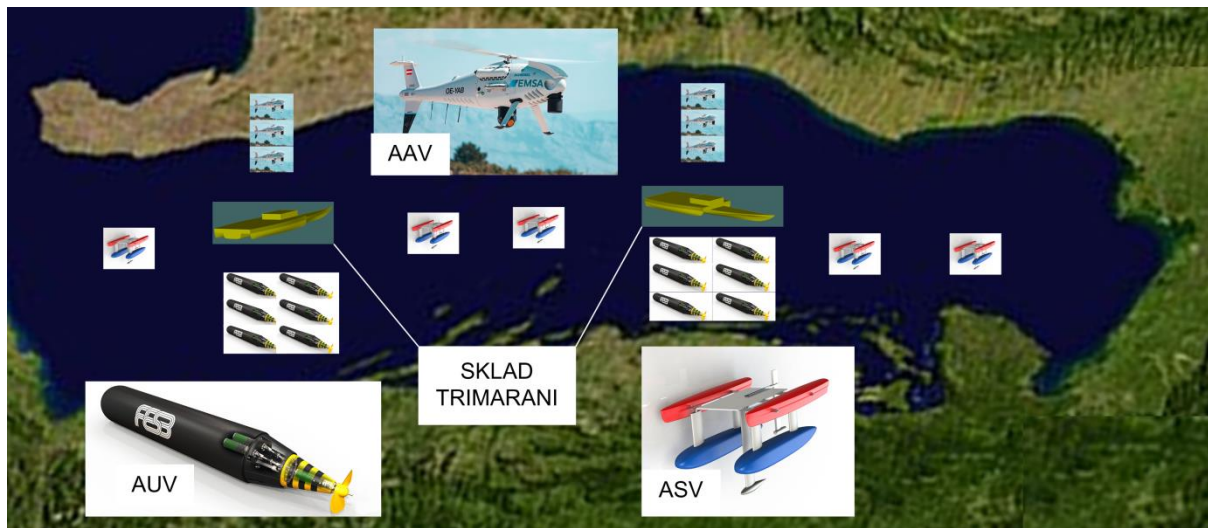
Figure 47 *Situation plan for Adriatic sea surveillance in 21st century*
Slika 48 *Raspored patrolnog sustava za nadzor Jadranskog mora u 21. stoljeću*

S obzirom na navedene projektne zahtjeve, kao mogući koncept koji ispunjava gornje zahtjeve, odabran je LCS-2 (Littoral Combat Class), [2], slika 2, koncept trimarana mornarice SAD, s glavnim, centralnim trupom oblika prema sustavnoj seriji polu-istisninskih formi „Sklad" razvijenoj u "Brodarskom institutu" u Zagrebu, [3]. Osiguranje poboljšanog stabiliteta te superiornih pomorstvenih svojstava ostvareno je ugradnjom pomoćnih trupova, čiji je optimalni oblik i veličinu tek potrebno odrediti. U ovom radu je pretpostavljen oblik pomoćnih trupova prema Wigleyevoj formi.

Figure 2 *US Navy LCS2*
Slika 2 *LCS mornarice SAD*

2. Forma "Sklad" trimarana

Brodarski institut u Hrvatskoj je razvio vrlo uspješnu sustavnu seriju polu-istisninskih brodskih formi „Sklad", [3], koja je razvijana i korištena kod projektiranja patrolnih, raketnih topovnjača HRM, te ostalih patrolnih i ratnih brodova Republike Hrvatske. Razvojem brodogradnje se u ovo vrijeme javlja potreba za nastavkom rada na seriji „Sklad" njenom primjenom kod višetrupaca, što bi omogućilo ponovnu izgradnju znastvene-istraživačke infrastrukture hrvatske civilne i vojne brodogradnje. S obzirom na koncept trimarana LCS-2 mornarice SAD uočena je mogućnost primjene serije „Sklad" u razvoju ophodnog/patrolnog broda trimarana za nadzor Jadranskog mora povećanog doplova.

Za koncept „Sklad" trimarana odabrana je puna istisnina od 1000 tona, maksimalne brzine od 50 čvorova, te autonomijom od 1000 nautičkih milja kod brzine krstarenja od 20 čvorova, čiji je opći plan prikazan na slici 3, a trodimenzionalni prikaz na slici 5.
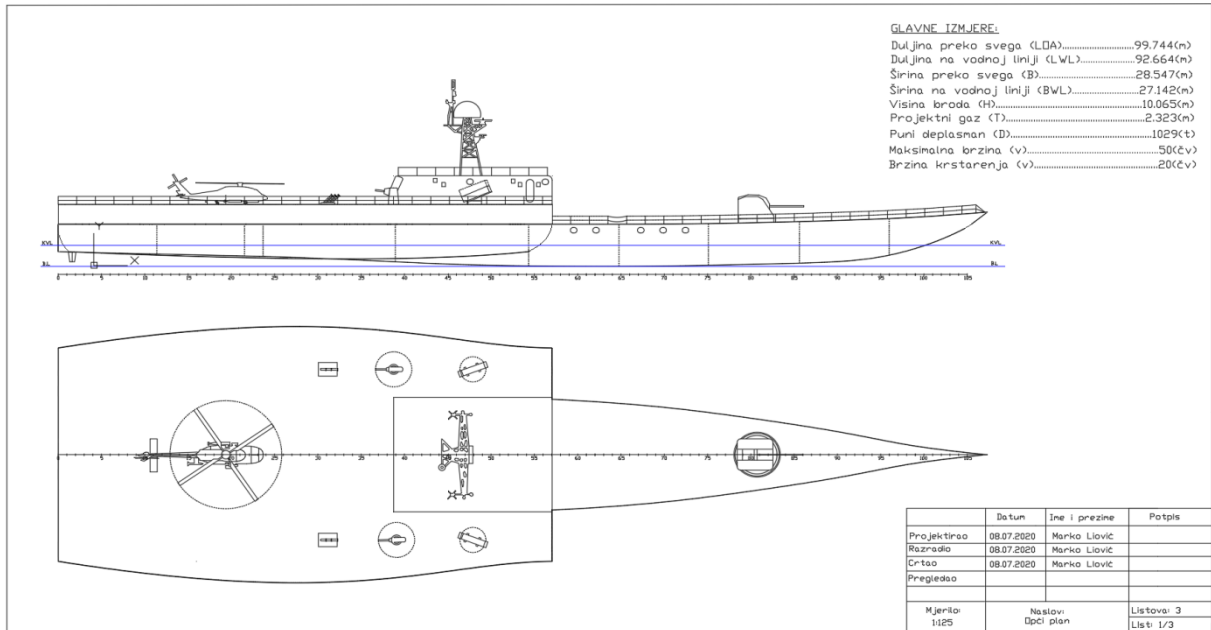
Figure 3 *Opći plan "Sklad" trimarana za nadzor Jadranskog mora*
Slika 3 *General arrangement of "Sklad" trimaran for Adriatic sea protection*

Središnji trup broda je odabran prema rasponu izmjera sustavne serije poluistisninskih brodova „Sklad" s L/B = 8, B/T = 3, te C_B = 0,35, čije su izmjere: L_{WL} = 92,94 (m), B_{WL} = 11,62 (m), T = 2,323 (m), s masenom istisninom od Δ = 900 (t), slika 4.
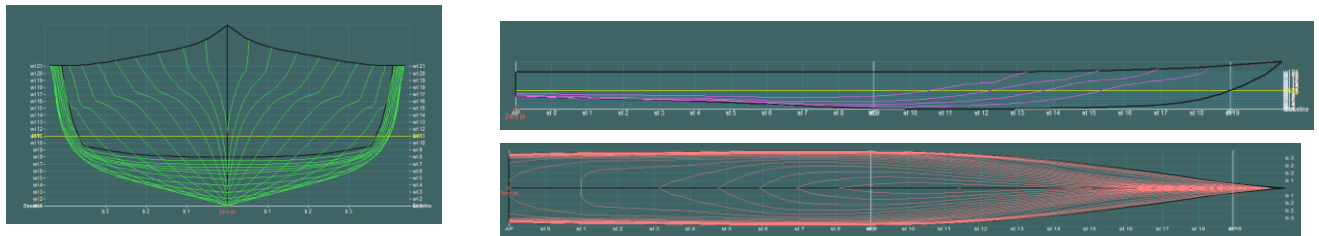
Figure 4 *Main Hull Lines Plan*
Slika 4 *Nacrt linija glavnog trupa broda*

Pomoćni trupovi su odabrani proizvoljno u svrhu provjere koncepta, u obliku Wigleyeve forme, s dimenzijama: L_{WL} = 51 (m), B_{WL} = 3,5 (m), te T = 1,5 (m), s masenom istisninom od Δ = 85,75 (t), te koeficijentom punoće C_B = 0,313.

Figure 5 *Ship drawing in perspective*
Slika 5 *Prikaz broda u perspektivi*

Razmak trupova je određen optimiranjem otpora broda pri brzini od 50 čvorova korištenjem računalne dinamike fluida u računalnom programu "Numeca", [4], slika 6, te je kao najpovoljniji određen razmak 14,815 (m), prema rezultatima u tablici 1.
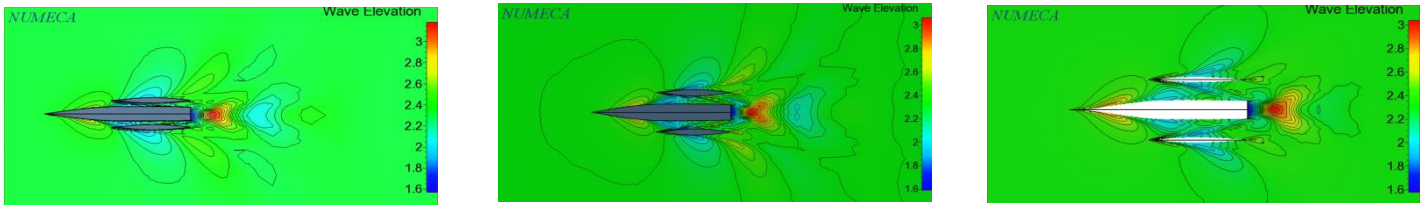
Figure 6 *CFD determination of side hulls distance from centre hull*
Slika 6 *Određivanje položaja pomoćnih trupova pomoću programa za proračun dinamike fluida*

Table 1 *The results of CFD calculation of ship resistance for different hull distances*
Tablica 1 *Rezultati proračuna otpora broda računalnom dinamikom fluida, za različite razmake trupova*

Razmak S (m)	Sila otpora, proračun (N)	Sila otpora, CFD (N)
S_1 = 11,852	183047,451	155015
S_2 = 14,815	183047,451	154893
S_3 = 17,778	183047,451	164079

Nakon definiranja svih prostora broda kao korisna površina palube dobijena je površina od oko 1000 (m²), što je superiorna vrijednost u odnosu na jednotrupac. Također, povećanim razmakom pomoćnih i glavnih trupova, omogućen je prihvat podvodnih i površinskih objekata, čime je ispunjen projektni zahtjev i jedna od osnovnih funkcija broda.

3. Ostala svojstva "Sklad" trimarana

Izborom forme glavnih i pomoćnih trupova omogućen je izbor pogonskog postrojenja te propulzora broda, kao i pripadno konstruktivno rješenje. Za materijal izrade trupa broda odabran je čelik, dok je nadgrađe od aluminija. U cilju ostvarenja zadane maksimalne brzine od 50 čvorova odabrana je CODAG pogonsko postrojenje s 2 MTU 20V 8000 M71L diesel motora s P_b = 9100 (kW), te 1 plinskom turbinom Rolls Royce MT30, ukupne kočene snage od 54560 (kW), te 4 pomoćna motora MTU 8V396 TE94. Pri brzini broda od 20 čvorova, autonomija broda je 1000 (nm).

Za propulzore su odabrani vodomlazni propulzori Wartsila 1500 za diesel motore, te Wartsila 2300 za plinsku turbinu sa ukupnim smještajem na slici 7.
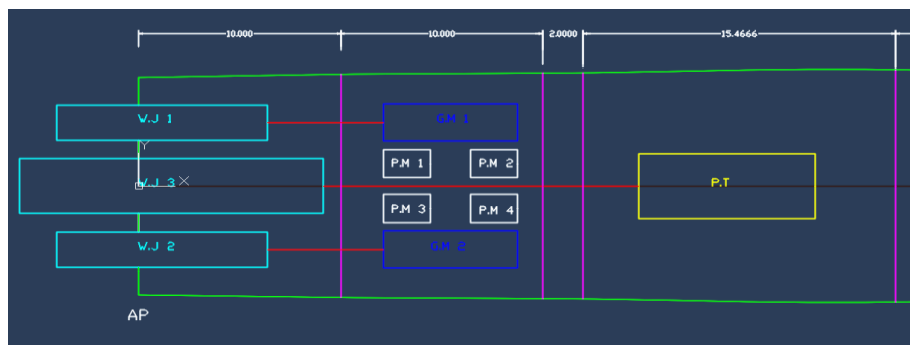
Figure 7 *CODAG propulsion system with waterjets*
Slika 7 CODAG pogonski sustav s vodomlaznim propulzorima

Provjerom nepotonivosti određeno je da brod preživljava naplavu 3 susjedna prostora, slika 8, što je provjereno asimetričnom naplavom broda, tj. oštećenjem jednog od pomoćnih trupova.
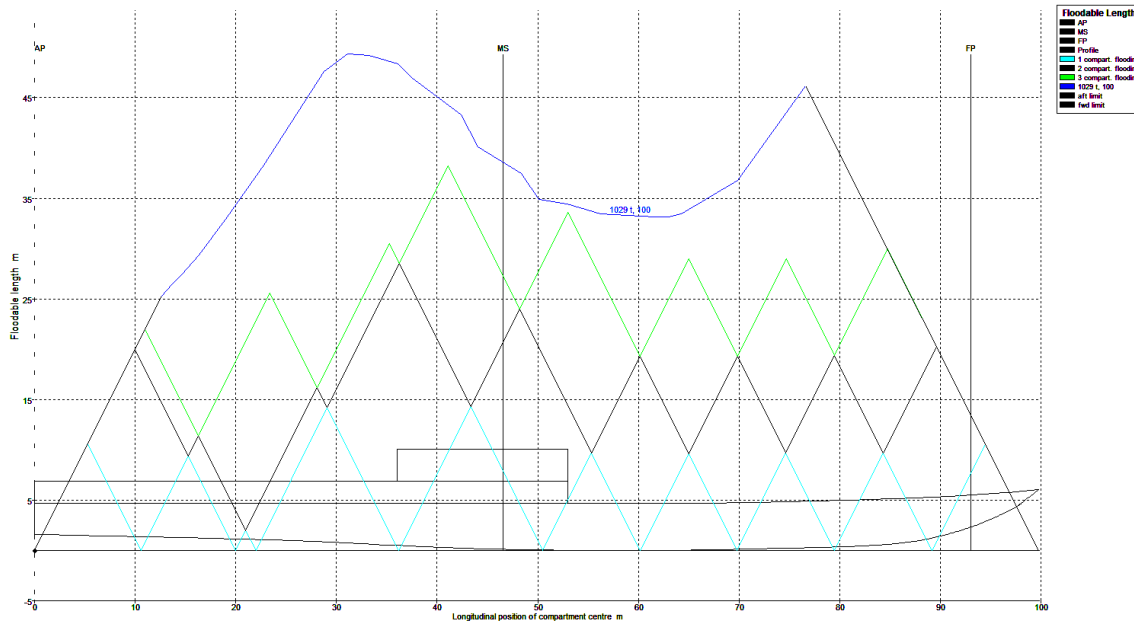
Figure 8 *Ship Survivability of 3 damaged compartments*
Slika 8 *Provjera preživljavanja naplave 3 susjedna prostora*

Na kraju su izračunata pomorstvena svojstva "Sklad" trimarana, [5], i uspoređena sa pomorstvenim svojstvima patrolnog broda jednotrupca, s formom trupa tipa "Sklad", [6], kako je to pokazano u tablici 2.

Table 2 *Comparisson of seakeeping results of trimaran and single hull "Sklad" ships*
Tablica 2 *Usporedba rezultata proračuna pomorstvenih svojstava "Sklad" trimarana i jednotrupca*

Stanje mora 6	Trimaran 20 (čv)	Jednotrupac 25 (čv)
Maksimalno vertikalno ubrzanje (m/s²)	1,375	10,781

4. Zaključak

Koncept "Sklad" trimarana kao patrolnog broda za nadzor Jadranskog mora u potpunosti zadovoljava zahtjeve nadzora mora u 21. stoljeću u uvjetima povećanog prometa svih oblika kretanja zrakom, na površini i pod morem. Velika površina helikopterske palube te široki razmak trupova omogućuju prihvat kako zračnih, tako i morskih i podmorskih autonomnih objekata u svrhu njihovog održavanja i punjenja energijom potrebnom za njihovo kretanje. Ovakav koncept konačno omogućuje obavljanje zadaća nadzora cijele godine uz superiorna pomorstvena svojstva te autonomiju potrebnu za nadzor cijelog Jadranskog mora.

LITERATURA

[1]   Internet stranice hrvatskog Klastera konkurentnosti obrambene industrije https://hkkoi.hr/index.php/fesb/

[2]   "USS Independence", (LCS-2), Wikipedia, Internet enciklopedia,

[3]   A. Gamulin, "Hidrodinamika i osnivanje oblika poludeplasmanskog broda (čamca)", doktorska disertacija, 1990.

[4]   Computational Fluid Dynamics software "Numeca",

[5]   M. Liović, "Osnivanje patrolnog broda za nadzor Jadrana tipa"Sklad" trimaran, istisnine 1000t, maksimalne brzine 50čv", Diplomski rad, FESB – Sveučilište u Splitu, 2020.

[6]   M. Liović, "Osnivanje raketne korvete za zaštitu Jadrana istisnine 500t, maksimalne brzine 50 čv", Završni rad, FESB – Sveučilište u Splitu, 2017.

AN OVERVIEW OF MEASURES FOR IMPROVING THE ENERGY PERFORMANCE OF SHIPS

Darin Majnarić[a], Lino Josip Novak[a], Roko Dejhalla[a]*

a Faculty of Engineering – University of Rijeka, Vukovarska 58, 51000 Rijeka, Croatia

* Corresponding Author, roko.dejhalla@riteh.hr

Abstract

A "green ship" is a term given to ships that contribute to the improvement of the present environmental situation. Maritime industry is one of the greatest contributors of the greenhouse effect and in order to reduce carbon emissions coming from it many actions were taken worldwide. The efforts taken by the International Maritime Organization (IMO) can be particularly pointed out, but there is number of other opportunities that can be applied to improve the energy efficiency of ships. Ship designers and shipbuilders have at their disposal a number of measures that could be used to increase the energy performance of ships. This paper focuses on some of these opportunities, some of which are regulated by mandatory regulations and rules while other are applied on a voluntary basis.

Keywords: ship; energy performance; improvement measures; overview;

Sažetak

"Zeleni brod" je pojam koji se dodijeljuje brodovima koji doprinose poboljšanju sadašnjie situacije u okolišu. Pomorska industrija jedan je od najvećih doprinositelja učinku staklenika. Kako bi se smanjile emisije ugljika koje proizlaze iz te industrije, poduzete su mnoge akcije širom svijeta. Posebno se mogu istaknuti napori Međunarodne pomorske organizacije (IMO), ali postoji niz drugih mogućnosti koje se mogu primijeniti za poboljšanje energetske učinkovitosti brodova. Projektantima i brodograditeljima na raspolaganju stoji niz mjera kojima bi se mogla povećati energetske značajke brodova. Ovaj se rad usredotočuje na neke od njih, od kojih su neke regulirane obveznim propisima i pravilima, dok se druge primjenjuju na dobrovoljnoj osnovi.

Ključne riječi: brod; energetske značajke; pregled mjera za poboljšanje;

1. Introduction

A comprehensive concept of a "green ship" implies a ship that will not harm the natural environment and that will meet the right criteria from the very beginning to the end, i.e. not only during the ship's service life but also during the building as well as going to the ship-breaking yard. The ships, by their function, spend most of their time sailing the seas so this concept mostly refers to a ship in service. Therefore, to make a ship "greener", one of the most important matters to do is to reduce greenhouse gas emissions (GHG).

The key findings from the Third IMO GHG Study 2014 pointed out that international shipping emitted 796 million tons of CO_2 in 2012, accounting for about 2.2% of the total global anthropogenic CO_2 emissions for that year, [1]. If the world maritime trade continues this trend of growth, those emissions have the potential to grow between 50% and 250% by 2050. Because of that, IMO is increasing its engagement in a global approach of enhancing the ship's energy efficiency and developing measures to reduce GHG emissions from ships.

Initial IMO Strategy on reduction of GHG emissions from ships reviews a reduction in total GHG emissions from international maritime shipping and identifies the following crucial steps [2]:

1) Implementation of further phases of the EEDI (Energy Efficiency Design Index) for new ships that should result in decreasing of the ship's carbon intensity;

2) Reduction of international shipping carbon intensity by at least 40% by 2030, with the target of 70% by 2050, compared to 2008;

3) To peak GHG emissions from international maritime shipping as soon as possible with the target to reduce the total annual GHG emissions by at least 50% by 2050 compared to 2008;

IMO regulations will evolve through the years and the newbuildings will have to comply with even more strict constraints. In addition to the environmental impact caused by a ship in regular service, the problems of the deliberate release of oil into the sea and accidents at sea that result with oil leakages are also being taken more seriously.

One of the prerequisites for "greener" ships would also be the modernization and equipping of coastal infrastructure. Ports and terminals should be equipped with modern transshipment and cargo handling facilities that would enable the fast and efficient loading and unloading of cargo on and off the ship so that ships could only be designed to carry out their basic task, to sail and to carry cargo by sea as efficient as possible.

This paper focuses on measures that could contribute to reducing the carbon footprint of merchant ships. The main aim is to maximize the energy efficiency of the ships in service, i.e. to reduce the GHG emissions to a minimum. To achieve that, it is important to define the main requirements, restrictions and regulations at the initial stage of ship design according to which the ship will be designed and built.

2. Measures for improvements

There are numerous measures that can be implemented to improve the energy performance of ships and Table 1. provides an overview of some of them. Some measures are discussed in more detail hereafter.

Table 1. Measures that could be used to increase the energy performance of ships

Ship design	Propulsion & Machinery	Operation & Maintenance
- Optimization of main dimensions and hull form	- Type of fuel	- Hull coating system and cleaning
- Optimization of hull appendages and openings	- Sulfur-cleaning scrubbers	- Energy saving lighting
- Air lubrication	- Waste heat recovery system	- Voyage performance management
- Optimization of ship structure	- Electric propulsion systems	- Ship speed reduction
- Reduction of main deck equipment	- Renewable energy propulsion: wind power, solar power	- Turnaround time in port

2.1. Ship design

Hull and appendages

In the context of ship design, the most fundamental and everlasting problem is the design of low resistance ship satisfying given requirements of deadweight and speed. All of the essential features of a ship, such as hydrostatics, stability, hydrodynamic characteristics, strength, and seakeeping mostly derive from the underwater ship hull form.

Ship owner's requirements often require a certain ship's deadweight at a given draught, resulting in excessive length, breadth and block coefficient. This results in a higher amount of construction material, higher main engine power, and thus higher fuel consumption, with a lower deadweight coefficient. For the given limited draught, due to the limited depth of ports or sea passages, reasonable main dimensions and optimal main dimension ratios and form coefficients should be chosen. The values of the main dimension ratios and block coefficient recommended in [3] are:

$5 < L/B < 8$, in accordance with value of Froude number defined as $Fr = V/(g \cdot L)^{1/2}$,

$8 < L/D < 10$, depending on the size of the ship,

$1,8 < B/T < 2,5$,

$0,6 < C_B < 0,8$, depending on the value of Fr and the size of the ship,

where L, B, D, T and C_B are ship's length, breadth, depth, draught and block coefficient, respectively.

Ship's length can be described as a function of displacement and speed, [4], and it is known as the most expensive dimension because it significantly influences the steel, accommodation, and outfitting mass. The steel mass increases, [3]:
- with the length on exponent $a \approx 2$,
- with the breadth on exponent $b \approx 2/3$,
- with the depth on exponent $c \approx 1/3$,

so the formula for calculating the mass of steel can be written as:

$$W_S = k \cdot L^a \cdot B^b \cdot D^c, \tag{1}$$

where k is the coefficient that depends on the type of ship. One of the accepted ways to reduce the ship's total resistance and thus fuel consumption is to increase L or to reduce B in order to obtain a satisfactory L/B ratio. To achieve good hydrodynamic characteristics, it is recommended not to have the value of L/B below 6.5. While the increase of the L/B ratio has a beneficial effect on reducing the total resistance, it negatively affects the ship's stability. The increase of L at the expense of other characteristics of the ship usually results with higher construction cost, so this suggests keeping L as short as possible, [4]. On the other hand, some research shows that a lengthening of a ship for 10 to 15% could result in the reduction of power demand by 10%, [5]. Both approaches have their advantages and disadvantages, but it is very likely that in practice the length of the ship will be determined from requirements which are not of a hydrodynamic nature.

A ship with a large draught can be fitted with a larger and higher efficient propeller rotating at the lower number of revolutions. Also, the larger draught allows the fitting of a larger rudder for improved steering and maneuverability. When designing new ship, the limiting of the draught should be avoided as much as possible, especially in cases where the space lost by reducing draught is compensated by an increase in the main dimensions and coefficients. This results in unreasonable ratios between main dimensions, such as $L/B > 8$ or $L/B < 5$, $L/D > 14$, $B/T > 2.5$, or even $B/T > 3$. Some experiments have confirmed that a ratio $B/T \approx 2.5$ is the best from both frictional and wave resistance point of view, [4].

The formulas for determining the block coefficient are usually based on the ship's relative speed, i.e. the Froude number Fr, which means that the higher the Fr the lower the C_B. However, C_B is a function of several factors and not only Fr. Ship's size and type determine the selection of C_B, in a way that larger ships usually require higher C_B. Also, a higher L/B ratio, for the same ship size and Fr tolerates slightly higher C_B due to the relatively smaller curvatures and less pronounced shoulders. The economics of shipbuilding generally follows the direction of higher C_B, and there are several reasons for that. Higher C_B makes it possible to get the same deadweight and cargo space with a smaller ship and consequently smaller mass of the lightship.

As for the hull appendages, only bilge keels will be briefly discussed here although there is a whole range of appendages on ships. The normally derived increase in resistance from 1 to 3% at the expense of the bilge keels can be accepted as a minimum that matches a special case when the bilge keels are placed in the water flow direction. Otherwise, in real service conditions, their resistance is even higher. However, there is still no device for reduction of rolling motions that could be an alternative for bilge keels, given their cost of installation, maintenance, and reliability of operation. On some ships, it is possible to reduce the length of the bilge keels, or even to completely leave them out. This could enable savings in both power and fuel consumption.

As for the hull openings, by installing a transverse pipe to place the bow thruster, the ship loses some of the displacement while the integrity of the hull is disrupted and the total mass is increased. The water flow disturbance from openings of the bow thruster tunnels and sea chests can be high, and this certainly increases the resistance. Therefore, it is beneficial to install scallops behind openings. Good design of all openings combined with proper location can give up to 5% lower power demand than one with poor design. For containership, corresponding improvement in total energy consumption could reach almost 5%, [5]. In some cases, the option of a merchant ship without the lateral thrust, which relies on the assistance of a local tugboat, could prove to be an optimal design.

Air lubrication

EEDI as an integral part of energy efficient ship concept has classified air lubrication as "Innovative Energy Efficiency Technologies" that can reduce ship resistance, [6]. Although technology is still between development and testing phase, confident data are available. A total of 18 full scale performance tests between 2002 and 2015 were identified. The net energy savings reported range approximately between 4% to 10%, [6]. These sea trials were not monitored and analyzed as required for EEDI trials so air lubrication system still needs official confirmation of effectiveness.

Reduction of equipment on main deck

Port infrastructure with modern transshipment and cargo handling facilities could enable to free the ships from deck cranes and transshipment facilities that have a permanent impact on the entire ship design. Cranes that are mounted on the ship's main deck take up a lot of space, increase its mass, and have a negative impact on a ship's stability. Besides that, it is necessary to reinforce the ship's structure under the cranes and this also unnecessarily adds mass. The operation of the ship's cranes increases the energy consumption of the whole system, and it is known that the energy produced on board is more expensive than that of the shore. Lastly, there are also maintenance costs that could expel some of the more important costs.

Structure

Optimization of structure requires a significant amount of additional working hours and usage of more expensive materials, but a reduction can have a large effect on fuel consumption i.e. savings. Furthermore, a decrease in structural mass means that there is an increase in available deadweight with which transport efficiency can be improved. Initial ship construction design

price will be higher but return on investment (ROI) will follow with the more profitable ship in operation.

There are two main ways of optimizing ship structure. Firstly, it can be implemented in the basic design of a ship. During the design of ship structure, rules and regulations of classification societies must be respected and followed. In the process of meeting rules and regulations there are a lot of doubtful places for which in common practice a designer will always take greater scantlings of structure elements and with that make the structure heavier.

That additional mass can be avoided with usage of finite element method with which doubtful element scantlings can be checked and most effective dimensions of structure element can be chosen. Described procedure can produce lighter ship structure but would require additional working hours and therefore result with more expensive ship at the beginning.

Another option is to use lighter materials with which considerable saving can be achieved. Materials that can be used to create light mass ships are high tensile steel (HTS), aluminum and composites. It was shown that usage of 10% more of HTS can reduce mass by 1.5% to 2%. With the mentioned reduction ships like tankers and bulk carriers can have an increase in deadweight and cargo payload of 0.2 to 0.3%, or fuel consumption per ton of cargo transported can be reduced 0.2% to 0.5%, [7]. While HTS is for now the best option for large cargo ships, aluminum and composite materials can be applied for the structure of ferries and Ro-Ro/Ro-Pax ships. Fiber reinforced plastic (FRP) can be applied to the structure and superstructure of high-speed crafts and can produce 30% to 70% mass savings which would then reflect on the fuel savings, [7]. An example of FRP implementation can be found on the car carrier that had top three of the 13 vehicle decks built from PVC foam-cored glass/polyester sandwich panels, [8]. In this case, these composite decks were 25% lighter than steel decks, which saved 230 tons overall. The lower vertical center of gravity reduced ballast requirement by 575 tons and total mass savings enabled 805 ton increase in payload which resulted with 4.5% reduction in fuel consumption.

2.2. Propulsion & Machinery

Heavy Fuel Oil

The powerful ship main engines burn huge amounts of heavy fuel every day to give thrust to heavily loaded ships. Fuel costs represent as much as 30 to 50% of the ship's total operating cost so these engines usually use low-grade heavy fuel oil to lower these costs.

The propulsion of marine diesel engines with heavy fuel has numerous negative effects on the ship, which are less frequently mentioned. Heavy fuel is stored in large tanks that require additional space on board, thus reducing usable space or increasing ship dimensions. This results in an increase in displacement and thus resistance and fuel consumption, as well as maintenance costs. It may be suggested to phase out the use of heavy fuel on ships and marine objects, by switching to just one type of fuel both for main engine and auxiliary machinery, i.e. marine diesel oil.

This would allow the reduction of the lightship's mass saving the space in the engine room. Heavy fuel supply systems are complicated and require a lot of auxiliary equipment such as additional tanks, pipelines, transfer pumps, heaters, purifiers, and measuring instruments. These systems also require crew members, that takes care of these equipments, which otherwise would not be necessary. All ship systems require permanent maintenance, which is especially important for ship propulsion and power supply systems. A lot of energy is wasted for the transport, heating and preparation of the heavy fuel, and also to power all the associated systems.

It is important to mention that the use of the heavy fuel for ship propulsion significantly shortens the engine life and its lower heating value, high amount of small particles and sulphur content increase the green house gas emissions. Most of the ships still use heavy fuel, which is also of lower quality compared to marine diesel oil and this results in much higher green house gas emissions. Switching to alternative fuels is happening slowly and gradually and such big changes require a lot of time.

Sulfur-cleaning scrubbers

As from January 1, 2020, the limit for sulphur in fuel oil used on ships operating outside designated emission control areas is reduced to 0.5% m/m (mass by mass), [9]. For ships that are in operation and have propulsion system based on oil fuel, sulfur cleaning scrubber is temporary solution between oil fuels and more eco-friendly fuels. Exact benefits of scrubbers are reduction of the SO_X emissions by at least 95% and particulate matter by at least 60%. Scrubbers can also reduce the NO_X emissions, but it is still unknown by how much, [10].

LNG fuel

In desire to gradually reduce usage of oil-based fuels on ships, maritime industry has found potential in liquefied natural gas (LNG) fuel. That is because even though renewable energy (solar, wind) may have some potential to reduce carbon emissions, they cannot meet the needs of commercial maritime shipping on their own. Currently, there are over 175 ships using LNG fuel in operation, [11], and this has shown environmental benefits like elimination of SO_X emissions, significant reduction of NO_X and particulate matter (PM) as well as a small reduction in GHG emissions, [12]. DNV GL forecast is that by the 2050 47% of energy for shipping will come from oil-based fuels, 32% from gas fuels and rest will be provided from biofuels and electricity, [13]. While technology of electric propulsion that run on batteries is in development, LNG has proven itself as good replacement and is certainly contributing to the "green ship" idea.

Waste heat recovery system

The usage of wasted heat can be directed in reduction of need of more energy that is coming from fuels. Appropriate waste heat recovery system should be selected for each ship separately based on engine type, engine power, demand for electricity etc. One of the possible methods to reduce the fuel consumption is to use steam generated in waste heat recovery boilers to meet the demand for heating and to feed turbochargers, [14]. Exhaust reduction can be 36.28% for NO_X and 16.88% for CO_2 while maintain a 5%-10% reduction in EEDI at 400,000 tons of deadweight. Furthermore, a saving of 16.1% was achieved by installing waste heat recovery system, [15].

Electric propulsion systems

Electric propulsion system is offering best alternative to conventional propulsion systems in today's time. Electric propulsion can be based on two different main propulsion systems; diesel driven or turbine (steam) driven propulsion. Main advantage of the electrical propulsion system is its environmental benefits from lower fuel consumption and emissions and the fact that it requires much less space for installation, [16].

It is worth mentioning electric ships powered by lithium-ion batteries which could present a major change in reduction in CO_2 emissions. There are currently several important electric ship projects which test this alternative to traditional fuels for maritime shipping. Implementation of this technology on ships is still in early phase but with the development of technology it can be expected more and more electric ships powered on batteries, [17].

Renewable energy propulsion – wind power

Mechanically propelled ships have pushed out sail ships from commercial maritime shipping, but as the industry is turning to green and renewable energy, former sail technology will probably be more and more present.

Technology of towing kites which are used like sails have already been implemented on commercial ships, Figure 1, even though technology is still in verification and optimization phase, [18, 19]. In the current state of development, large fuel saving are possible on slow-speed

ships like tankers and bulk carriers and savings in fuel consumption can be up to 30%. Issues that should be further addressed are safety and complexity of operation, [18].

Figure 1. Towing kite system, [20]

Besides towing kites, Flettner rotor places itself as potentially efficient wind propulsion technology. Flettner rotor is vertical cylindrical sail that works on principle of Magnus effect. This device is named after German aviation engineer and inventor Anton Flettner who studied in 1920s the effectiveness of spinning cylinders as a ship's propulsion system. Technology is still in testing phase and its actual impact on performance of commercial ships is still ongoing. There were few cases of open sea trials that were carried on by the companies Norsepower and Maersk on a product tanker "Maersk Pelican", [21], Figure 2. The Flettner rotors were implemented on bulk carrier "Afros", [22]. The reduction potential on fuel consumption of the main engine was estimated to be around 3% to 15%, [23].

Figure 2. Flattner rotors on board Maersk Pelican, [21]

Renewable energy propulsion – solar power

Over the last years solar panels which convert sunlight into electricity have been recognized as potential additional source of auxiliary power. The cost of implementing solar power units on ships on which usually there are no free flat areas is another negative aspect and it is not surprising that there has been no wider application in the maritime shipping industry. As an example of implementation of solar power units on commercial ship, NYK car carrier "Auriga

Leader" can be given, [24]. This ship has 328 solar panels on its top deck that provide 40 kilowatts of power, Figure 3. Today solar panels can be used only as additional power source.

Figure 3. NYK car carrier "Auriga Leader" (left), solar panels on the top deck (right), [24]

2.3. Operation & Maintenance

Hull coating system and cleaning

Harsh conditions in which ships operate cause corrosion and abrasion, especially of underwater parts of the hull which result in increased resistance and fuel consumption. Marine coating systems are used to protect materials from corrosion and abrasion. Additional segment of marine coating system other than protective one is to improve the flow of water over the hull in order to reduce resistance. To improve overall performance of the ship, high- performance coating system should be used and some producers claim that up to 10% improvement in speed can be achieved and up to 13% improvement in fuel economy as well, [25]. While the accuracy of information given by coating producers should be taken with caution, it is certain that coating systems have positive impact on overall ship performance.

Reduction in power consumption – lighting

Rapid increase of energy efficient lighting equipment was recorded in almost all industries and marine industry is no exception. It is important to take into consideration energy consumed by lighting because it is estimated that on usual merchant ship 5% of total consumed electrical power goes on lighting while on passenger ships it can be higher than 10%. The emission reduction potential on usual merchant ships is estimated to 3% of the total auxiliary engine consumption, [26].

The low energy halogen lamps, fluorescent tubes and LED (Light Emitting Diode) fall into the energy efficient lighting equipment that can be used on ships. In addition to the use of this type of lighting, it is also necessary to install controlled systems for dimming, automatic shut off, etc.

Some experiments done at bulk carrier proved "that the energy-efficient light sources provide remarkable advantages in comparison with the traditional light sources of ships." It was also stated that lighting system power capacity can be reduced by 65%, marine fuel consumption by 59.4% and lighting cost by 53% The CO_2, NO_X, SO_2, and PM emissions can also be decreased by 53% by more efficient lighting, [26]. All of the above is in line with the claims of companies manufacturing lighting equipment that the total energy for lighting on board ships can be reduced by 50%, [27, 28].

Voyage performance management

Energy saving operational decisions can be managed by crew or vessel management systems. Some of operational factors that have effect on overall energy consumption are "just in time speed", reduction of added resistance (wind, waves and current), weather routing, minimizing rudder movements and optimizing ballast carried and trim for lowest hull resistance.

Voyage speed optimization proves to be effective tool in energy saving management. The largest opportunities for reducing fuel consumption are present on fast ships while on other types of ships this depends on their speeds. According to some rough estimates, it turns out that 10% reduction in speed can result in 20% reduction in propulsion fuel consumption, [7].

Weather routing is another tool in energy saving management which can have significant impact on fuel consumption, but savings of route planning significantly depend on weather and voyage length. Percentage of fuel consumption varies significantly from case to case but saving can go up to around 30% and more, [29].

3. Conclusion

Ship designers and shipbuilders have at their disposal a number of measures that could be used to increase the energy performance of ships. Some of these measures are regulated by mandatory regulations and rules while other measures are applied on a voluntary basis. However, designers and shipyards are only one side in the whole process of ship design and construction, while the other side, most often crucial, is the investor, i.e. the ship owner who is usually not too inclined to some innovative solutions that have not yet been proven in the marine environment. There have been cases in the past where untested technologies, which at one point seemed to be very good solutions that could contribute to the fuel consumption reduction, in practice very quickly proved to be completely unsuitable for the marine environment.

When it is discussed about a "green ship", it is usually meant a ship that has the lowest carbon footprint. In that sense, a ship which is fuel efficient can be considered as a "green ship". From this viewpoint, the ship's engine room is the largest contributor to environmental impact. However, a "green ship" needs to be viewed much more broadly, not only as the ship's hull form with its appendages and an efficient propulsion system with low fuel consumption. As an example, an eco-friendly ship built with recycled materials that uses renewable energy can be mentioned. The above can be further broaden by many other entries, like zero discharge of gray or black water, etc., including the ports that should also become much more environmentally friendly.

Shipbuilding and the maritime industry are facing great challenges today, and these challenges will certainly intensify in the near future. This leads to a large number of questions that the industry will need to adequately answer.

5. ACKNOWLEDGMENTS

6. REFERENCES

[1]   Third IMO GHG Study 2014 – Executive summary and final report, www.imo.org, International Maritime Organization, 2015

[2]   Initial IMO Strategy on Reduction of GHG Emissions from Ships, Annex 11, Resolution MEPS.304(72), adopted on 13 April 2018

[3]   Belamarić, I., Brod i entropija, Književni krug, Split, 1998.

[4]   Papanikolau, A., Ship Design – Methodologies of Preliminary Design, Springer Dodrecht, Heidelberg, 2014.

[5]   "Boosting Energy Efficiency", Wärtsilä, Energy Efficiency Catalogue / Ship Power R&D, September 2008

[6]   "Air Lubrication Technology" (2019) https://ww2.eagle.org/content/dam/eagle/advisories-and-debriefs/Air%20Lubrication%20Technology.pdf (access on: May 2020.)

[7]   "Ship Energy Efficiency Measures Advisory" https://ww2.eagle.org/content/dam/eagle/advisories-and-debriefs/ABS_Energy_Efficiency_Advisory.pdf (access on: 23th of September 2020.)

[8]   Mason, K., Low weight on the high seas (2018) https://www.compositesworld.com/articles/low-weight-on-the-high-seas (access on: May 2020.)

[9]   "UNIFIED INTERPRETATIONS TO MARPOL ANNEX VI" (2019) http://www.imo.org/en/OurWork/Environment/PollutionPrevention/Documents/MEPC.1-Circ.795-Rev.4.pdf (access on: May 2020.)

[10]   Tran, T.A. (2017) Research of the Scrubber Systems to Clean Marine Diesel Engine Exhaust Gases on Ships, Tran, J Marine Sci Res Dev 2017, 7:6, DOI: 10.4172/2155-9910.1000243

[11]   "SEALNG: 175 LNG-Fueled Ships in Operation, 203 on Order" (2020), World Maritime News, https://www.offshore-energy.biz/sealng-175-LNG-fueled-ships-in-operation-203-on-order/ (access on: May 2020.)

[12]   "In Focus - LNG as ship fuel" (2015) https://www.dnvgl.com/publications/in-focus-lng-as-ship-fuel- 24731 (access on: May 2020.)

[13]   "Oil And Gas Forecast To 2050" (2017) https://eto.dnvgl.com/2017/oilgas (access on: May 2020.)

[14]   Behrendt, C., (2019) Conditions of Waste Heat Recovery in Marine Waste Heat Recovery Systems, Journal of Machine Construction and Maintenance, 4/2017 p. 141-147

[15]   Senary, K. et al. (2016) Development of a waste heat recovery system onboard LNG carrier to meet IMO regulations. Alexandria Engineering Journal Alexandria Engineering Journal, Volume 55, Issue 3, September 2016, Pages 1951-1960

[16]   McGeorge, H.D. (2014) "Marine Electrical Equipment and Practice". 2nd Edition, Butterworth-Heinemann, ISBN: 9780750616478

[17]   Grasso Macola, I. (2020) Electric Ships: the World's Top Five Projects by Battery Capacity, https://www.ship-technology.com/features/electric-ships-the-world-top-five-projects-by-battery-capacity/ (access on: May 2020.)

[18]   Houska, B., Diehl, M. (2007) Optimal Control of Towing Kites. Conference: Decision and Control, 2693 - 2697.

[19]   Duport, C., Deberque, M., Leroux, J., Roncin, K. (2017) Local Results Verification of a 3D Non-Linear Lifting Line Method for Fluid-Structure Interactions Simulation on a Towing Kite for Vessels, 11th Symposium on High-Performance Marine Vehicles HIPER'17, Zevenwacht, 11-13 September 2017

[20]   https://skysails-group.com/marine-division-media-lounge.html#&gid=1&pid=2, (access on: May 2020.)

[21]   "Rotor Sails Fitted on board Maersk's Tanker in a World's 1st"(2018) https://www.offshore-energy.biz/rotor-sails-fitted-on-board-maersks-tanker-in-a-worlds-1st/ (access on: May 2020.)

[22]   https://safety4sea.com/blue-planet-shipping-receives-green4sea-dry-bulk-operator-award/ (access on: May 2020.)

[23]   "Flettner Rotors - Applicability in the Maritime industry" (2018) https://www.maritimecyprus.com/2018/11/15/flettner-rotors-applicability-in-the-maritime-industry/ (access on: May 2020.)

[24]   Psaraftis, H. (2019) Sustainable Shipping a Cross-Disciplinary View: A Cross-Disciplinary View, DOI: 10.1007/978-3-030-04330-8, ISBN: 978-3-030-04329-2

[25]   https://www.hullspeed.us/ (access on: May 2020.)

[26]   Yiğit, K., Kökkülünk, G., Savaş, Ö. (2018) Comparative Analysis of Ship Lighting Systems in Terms of Economic, Environmental and Material Performance, Acta Physica Polonica A 134(1):189-191, DOI: 10.12693/APhysPolA.134.189

[27] "Full steam ahead for OSRAM" (2009) https://www.osram-group.com/media/press-releases/pr-2009/09- 03-2009, (access on: May 2020.)

[28] Norwegian NOx fond, (2015) www.nho.no/siteassets/nhos-filer-og-bilder/filer-ogdokumenter/nox-fondet/dette-er-nox-fondet/innvilget-stotte/webliste-til-fondet -- 050515-alleinnvilgede-soknader.pdf
(access on: March 2020)

[29] Cui, T., Turan, O., Boulougouris, E., (2016) Development of a ship weather routing system for energy efficient shipping, IAME 2016 Conference, Hamburg, Paper ID 115

CENTRE OF GRAVITY ENVELOPE EFECT ON INTACT AND DAMAGE STABILITY FOR HIGH SPEED CRAFTS

Marin, Smilović; Anton, Turk; Teuta, Duletić; Aleksandar, Vuković

MS Tech d.o.o Tometići 1/D, 51215 Kastav

msmilovic2107@gmail.com; aturk@riteh.hr; tduletic@metalsharkboats.com; avukovic@metalsharkboats.com;

Abstract

High speed crafts are designed and built for situations which require prompt reaction in order to save human life and/or property. Thus, wide range of severe operational conditions (i.e. fire, heavy seas, etc.) which can occur throughout craft's exploitation life shall be considered during initial design process. Determination of specific center of gravity position throughout initial design phase of high-speed craft, represents sophisticated task which significantly influences overall performance of the craft (speed, stability, seaworthiness, maneuverability, etc.). This article provides a brief overview of interdependence between craft's positive stability and its position of center of gravity. For purpose of presenting subject thesis in this paper, a referent designed and built working craft has been used. Centre of gravity envelope will be performed for subject working craft to show correlation of craft's damaged and intact stability in respect of position of CoG. Centre of gravity envelope will show acceptable area of CoG which allows positive stability necessary to meet International code of safety requirements for High-speed crafts by considering longitudinal, transversal and vertical axis. This article will provide comparison of positive stability areas with reference to CoG position for both, intact and damage stability.

Key words: Stability; Damage Stability; Intact Stability; Positive stability CG Envelope

Sažetak

Brze radne brodice se projektiraju i grade s ciljem zadovoljenja najrazličitijih stanja operacije koja traže promptnost reakcije ne bi li kvalitetno odradile zadaću spašavanja ljudskog života i/ili imovine. S tim u skladu velik raspon izazovnih stanja operacije brodice (kao što su gašenje požara, spašavanja prilikom teških stanja mora i sl.) koja se mogu pojaviti za vrijeme njezinog životnog vijeka, mora biti uzet u obzir prilikom procesa osnivanja brodice. Utvrđivanje točnog položaja težišta tijekom procesa osnivanja brze brodice predstavlja kompleksan zadatak koji ima značajan utjecaj na ključne performanse brodice kao što su brzina, stabilitet, pomorstvenost, upravljivost i sl. Predmetni članak daje sažet prikaz utjecaja pozicije težišta brze brodice na pozitivan stabilitet. Iznošenje predmetne teze kroz ovaj je rad dano korištenjem referentne radne brodice koja je projektirana i izgrađena upravo za takav tip operacije. Područje prihvatljivog položaja težišta tzv. težišna envelopa biti će određena za referentnu brodicu kako bi se dokazala korelacija stabiliteta brodice u oštećenom i neoštećenom stanju te položaja težišta. Težišna envelopa daje pregled prihvatljivog raspona položaja težišta koji rezultira sa pozitivnim stabilitetom potrebnim za zadovoljenje međunarodnih pravila za sigurnost brzih plovila po uzdužnoj, poprečnoj i vertikalnoj osi. Predmetni članak daje prikaz veze pozitivnog stabiliteta u ovisnosti od pozicije težišta za stabilitet u oštećenom i neoštećenom stanju.

Ključne riječi: Težišna envelopa, Stabilitet; Oštećeno stanje; Neoštećeno stanje; Brze brodice; Stabilitet plovila u ovisnosti o CG

1.   UVOD

Područje prihvatljivog položaja težišta tzv. težišna envelopa se koristi u projektiranju brzih radnih brodica kako bi se pokazala korelacija stabiliteta brodice u oštećenom i neoštećenom stanju te položaja težišta.

Područje položaja težišta brodice daje prihvatljiv raspon položaja težišta koji rezultira sa pozitivnim stabilitetom potrebnim za zadovoljenje Međunarodnih pravila za sigurnost brzih plovila po uzdužnoj, poprečnoj i vertikalnoj osi *„HSC 2000 Rules" (2)*.

U cilju izrade potrebnih proračuna, brodica je podijeljena na pet (5) prostora. Strojarnica brodice podijeljena je na dva (2) dijela. Kako radna brodica ima vodomlaznu propulziju koja je spojena sa glavnim motorom pomoću osovine, vodonepropusna pregrada nalazi se između motora i vodomlaznog propulzora. U odjeljku nakon strojarnice smješten je strukturni tank goriva. Potpalublje je odvojeno vodonepropusnom pregradom od prostora u kojem se nalazi strukturni tank i prostor koji služi kao spremište za sidro.

Pramčana sudarna pregrada pozicionirana je tako da se maksimalno iskoristi prostor u potpalublju te da se pritom zadovolje pravila klasifikacijskog društva DNV-GL (1).

2. NAMJENA I GLAVNE IZMJERE REFERENTNE BRODICE

Namjena referentne brodice korištene u predmetnom radu jest gašenje požara te sposobnost obavljanja funkcije traganja i spašavanja. Ista je lako upravljiva sa 3 člana posade i sposobna prevoziti do 6 vatrogasaca sa punom opremom. Brodica je ograničena maksimalnim gazom od 0,95 metara. Brodica ima vodomlaznu propulziju koju pokreću dva (2) motora na dizelski pogon.

Kormilarnica je zamišljena kao radno mjesto za kapetana koji upravlja brodom i časnika koji daljinskim putem kontrolira monitore za gašenje požara u čemu mu pomaže i glavni strojar. Iz kormilarnice se silazi u prostor gdje se nalaze sanitarije, kuhinja i mjesto za prijevoz vatrogasaca na intervenciju. Otvor na palubi dovoljan je za ulaz u potpalublje za vatrogasca sa punom opremom kao i za nosila sa unesrećenom osobom. Ispod kormilarnice nalazi se strukturni tank goriva kojem se može pristupiti iz kormilarnice.

3. SAŽETAK PROCESA OSNIVANJA BRODICE

Forma brodice je modelirana u programu Rhinoceros-Orca3D kako bi bila kompatibilna / iskoristiva prilikom unosa u program Maxsurf koji je korišten za daljnje detaljne proračune stabiliteta. Dimenzije su odabrane kao optimalne za vatrogasno plovilo kako bi se mogla smjestiti sva oprema potrebna za optimalno funkcioniranje i izvršavanje svrhe plovila. Odabrana dužina plovila je 15,35 metara, a širina iznosi 4,88 metara.
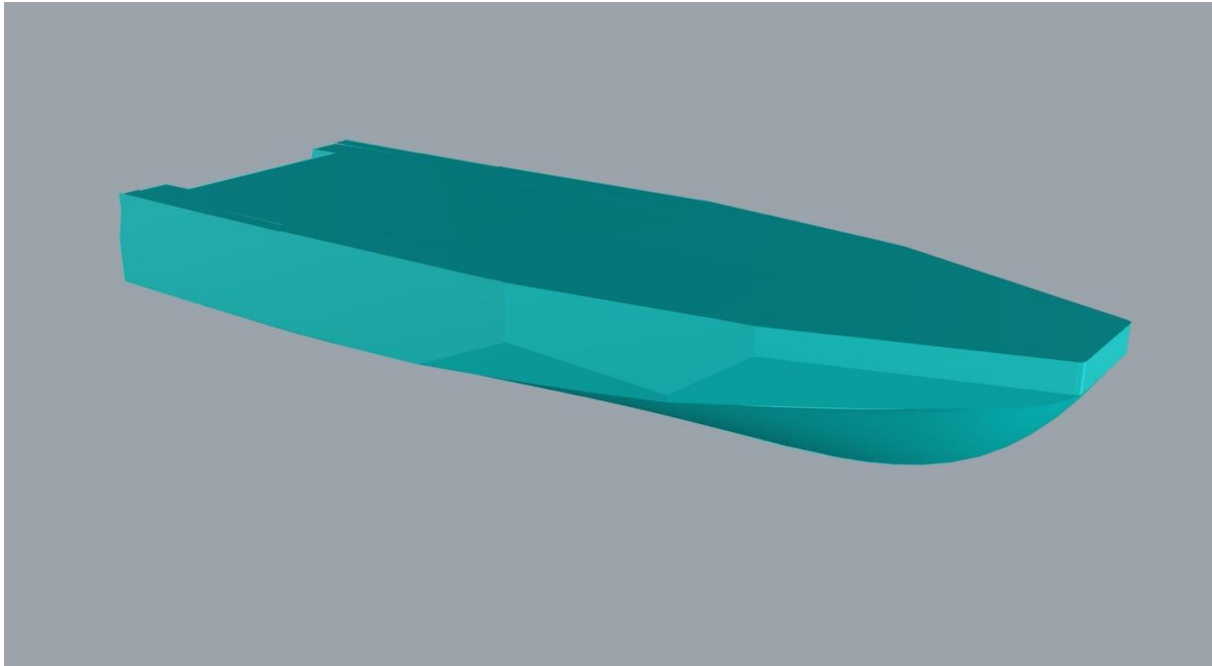
Slika 1. Prikaz form brodice

3.1.   HIDROSTATIKA

Hidrostatički proračun baziran je na gore modeliranoj formi. Masa brodice u punom opterećenom stanju iznosi 30,19 t. Rezultati hidrostatičkog izračuna za predmetnu masu brodice prikazani su u Tablici 1.

Draft Amidships, m	0,938
Displacement t	30,19
Volume (displaced) m^3	29,453
Heel deg	0,0
Draft at FP m	0,938
Draft at AP m	0,938
Draft at LCF m	0,938
Trim (+ve by stern) m	0,000
WL Length m	14,278
Beam max extents on WL m	4,882
Wetted Area m^2	66,629
Waterpl. Area m^2	54,766
Prismatic coeff. (Cp)	0,693

Draft Amidships, m	0,938
Block coeff. (Cb)	0,450
Max Sect. area coeff. (Cm)	0,650
Waterpl. area coeff. (Cwp)	0,786
LCB from zero pt. (+ve fwd) m	5,347
LCF from zero pt. (+ve fwd) m	5,819
KB m	0,615
KG m	1,800
BMt m	3,066
BML m	23,408
GMt m	1,881
GML m	22,223
KMt m	3,681
KML m	24,023
Immersion (TPc) tonne/cm	0,561
MTc tonne.m	0,471
RM at 1deg = GMt.Disp.sin(1) tonne.m	0,991
Max deck inclination deg	0,0000
Trim angle (+ve by stern) deg	0,0000
Density of Seawater tonne/m^3	1,025

Tablica 1. Hidrostatički podaci za istisninu 30,19t

Pravila klasifikacijskog društva koje definiraju pramčanu sudarnu pregradu definiraju razmak od pramčanog perpendikulara kako slijedi:

$$x_C \ (minimum) \quad = \quad 0.05 \ L \ (m)$$
$$x_C \ (maximum) \quad = \quad 3.0 + 0.05 \ L \ (m)$$

X_c (minimum) = 0,05 * 15,35 (m)

X_c=0,767m

X_c (maksimum) = 3 + 0,05 * 15,35 (m)

X_c (minimum) = 3,767m

Položaj pregrada definiran je u Tablici 2. kako slijedi:

	Aft (m)	Fore (m)
Jet Room	0	2
Engine Room	2	6,8
Tank Space	6,8	9,15
Galley	9,15	13,55
Anchor Locker	13,55	15,24

Tablica 2. Položaj pregrada

3.2. STABILITET BRODICE U NEOŠTEĆENOM STANJU

U preliminarnoj fazi osnivanja broda još se uvijek ne može dovoljno detaljno odrediti masa praznog plovila već se koristi detaljna baza podataka sličnih izgrađenih brodova i pokušava što kvalitetnije procijeniti masa u predmetnoj fazi. Definiran je preliminarni položaj uzdužnog težišta broda koji iznosi LCG = 5,5m. Prilikom prolaska prvog kruga projektne spirale predmetni podaci služe kao orijentacija u cilju odrađivanja centracije masa sa svim definiranim komponentama.

Brodica je projektirana po klasifikacijskom društvu DNV-GL koji se klasnom notacijom definira kao *"High Speed Light Craft"*. Klasifikacijsko društvo DNV-GL se u dokumentu *„Part 5 Ship types Chapter 6 Small service"* poziva na dokument koji treba slijediti prilikom proračuna stabiliteta *"2000 HSC CODE (International Code of Safey for High-Speed Craft 2000)"* uz dodatke za oštećeno stanje definirano u DNV-GL.

Zahtjevi vezani uz stabilitet nalaze se u Annexu 8, a izračunat je početni stabilitet, poluga stabiliteta, trim i dinamički stabilitet.

Kriteriji koje plovilo u neoštećenom stanju mora zadovoljiti su sljedeći:

- Ukoliko se maksimalna vrijednost poluge stabiliteta nalazi oko 15° - površina ispod poluge stabiliteta između 0° i 15° mora iznositi minimalno 0.07 mrad;
- Ukoliko se maksimalna vrijednost poluge stabiliteta nalazi preko 30° - površina ispod poluge stabiliteta između 0° i 30° mora iznositi minimalno 0.055 mrad;
- Ukoliko se maksimalna vrijednost poluge stabiliteta nalazi između 15° i 30° - površina ispod poluge stabiliteta računa se kao A= 0.055 + 0.001 (30° - Q_{max}) mrad, gdje je Q_{max} kut izražen u stupnjevima pri kojem poluga stabiliteta doseže svoj maksimum;
- Površina ispod krivulje poluge stabiliteta između 30° - 40° ili između 30° i kuta naplavljivanja, ovisno o tome koji nastupa prije mora biti minimalno 0.03 mrad;
- Iznos poluge stabiliteta mora biti minimalno 0.2 m pri kutu nagiba jednakom ili većem od 30°;
- Maksimalni iznos poluge stabiliteta mora biti na ne manje od 15°;
- Početna metacentarska visina ne smije biti manja od 0.15 m;

- Prilikom računanja dinamičkog stabiliteta pritisak P (N/m^2) uzrokovan vjetrom određuje se formulom 500 (V$_w$ / 26)^2 gdje je član V$_w$ definiran kao brzina vjetra (m/s) koja odgovara najgorem uvjetu u kojem se plovilo može naći. Kut nagiba zbog naleta vjetra ne smije biti veći od 16° ili 80% vrijednosti kuta pri kojem uranja paluba ovisno koja vrijednost nastupa prije.

Podaci o stanju krcanja brodice dani su u Tablici 3.

Item Name	Quantity	Unit Mass tonne	Total Mass tonne	Unit Volume m^3	Total Volume m^3	Long. Arm m	Trans. Arm m	Vert. Arm m
Full Load	1	30,200	30,200			5,500	0,000	2,100
Total Loadcase			30,200	0,000	0,000	5,500	0,000	2,100

Tablica 3. Stanja krcanja brodice

Izračunati trim za navedeno stanje krcanja prikazan je u Tablici 4.

Draft Amidships m	0,947
Displacement t	30,20
Heel deg	0,0
Draft at FP m	0,996
Draft at AP m	0,898
Draft at LCF m	0,938
Trim (+ve by stern) m	-0,098
WL Length m	14,358
Beam max extents on WL m	4,882
Wetted Area m^2	67,245
Waterpl. Area m^2	55,335
Prismatic coeff. (Cp)	0,724
Block coeff. (Cb)	0,441
Max Sect. area coeff. (Cm)	0,632
Waterpl. area coeff. (Cwp)	0,789
LCB from zero pt. (+ve fwd) m	5,510
LCF from zero pt. (+ve fwd) m	5,879
KB m	0,616
KG solid m	2,100
BMt m	3,098
BML m	24,082

GMt corrected m	1,614
GML m	22,598
KMt m	3,714
KML m	24,698
Immersion (TPc) tonne/cm	0,567
MTc tonne.m	0,479
RM at 1deg = GMt.Disp.sin(1) tonne.m	0,850
Max deck inclination deg	0,3951
Trim angle (+ve by stern) deg	-0,3951

Tablica 4. Proračun gaza i trima

Nadvođe broda za navedeno stanje krcanja prikazano je u Tablici 5.

Key point	Type	Freeboard m
Margin Line (freeboard pos = 0 m)		1,361
Deck Edge (freeboard pos = 0 m)		1,437

Tablica 5. Nadvođe broda

Točke naplavljivanja definirane su po HSC 2000 koji navodi kako svaki otvor koji ne može biti trajno vodonepropusno zatvoren mora biti uzet u obzir prilikom računanja stabiliteta. Također definirano je da se moraju uzeti u obzir i klizni prozori. Kao točke naplavljivanja uzete su točka ventilacije strojarnice i klizni prozor na kormilarnici. Točka ulaza u kormilarnicu nije uzeta u obzir iz razloga jer je na istoj visini kao i točka ventilacije strojarnice, a jedno se nalazi i više prema sredini broda pa naplavljivanje nastupa najprije na ventilaciju.

Točke naplavljivanja prikazane su na slici 2.
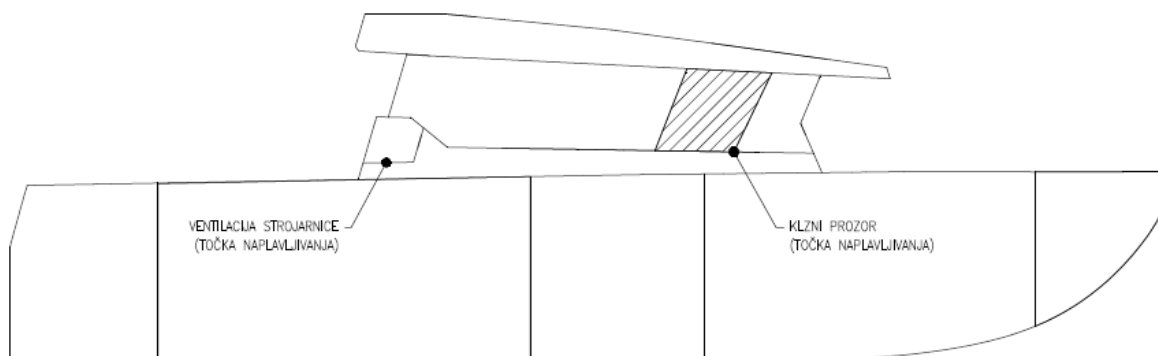
Slika 2. Točke naplavljivanja

Poluga stabiliteta prikazana je na Slici 3.
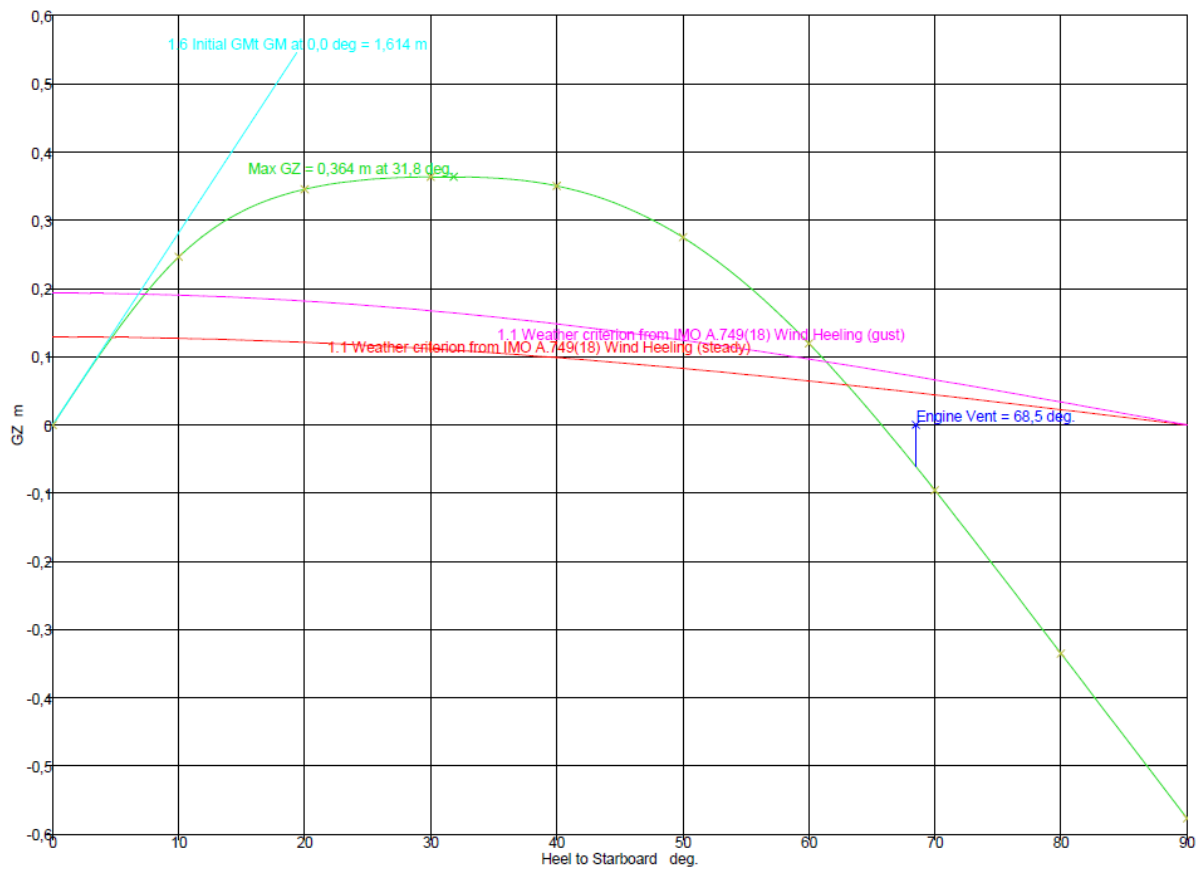
Slika 3. Poluga stabiliteta u neoštećenom stanju

Dinamički stabilitet broda definiran je u HSC 2000 Annexom 8. Kriterij prema kojem je odrađen proračun podrazumijeva vjetar od 26 čvorova. Kriteriji za neoštećeno stanje broda prikazani su u Tablici 6.

max GZ	31,8 deg.		
Kriterij stabiliteta u neoštećenom stanju	zahtijevana vrijednost	dobivena vrijednost	
površina ispod krivulje između 0° i 30° ako je maksimalni GZ oko 15°	/	/	
površina ispod krivulje između 0° i 30° ako je maksimalni GZ veći od 30°	0,055 m rad	0,139 m rad	zadovoljeno
površina ispod krivulje između 30° i 40°	0,03 m rad	0,0691 m rad	zadovoljeno

minimalni GZ na 30° ili više	0,2 m	0,364 m	zadovoljeno
maksimalni GZ	>15°	31,8°	zadovoljeno
početna metacentarska visina	>0,15 m	1,614 m	zadovoljeno
Dinamički stabilitet			
kut nagiba uslijed naleta vjetra	<16° ili <80% kuta urona palube	4,7° i 13,21%	zadovoljeno

Tablica 6. Kriteriji stabiliteta u neoštećenom stanju

3.3. STABILITET BRODICE U OŠTEĆENOM STANJU

Za proračun stabiliteta u oštećenom stanju potrebno je bilo koristiti model sa definiranim prostorima kako bi se mogao odrediti stabilitet broda. Stabilitet u oštećenom stanju računat je u programu Maxsurf koji funkcionira na principu metode izgubljene istisnine. Raspored prostora prikazan je na Slici 4. Raspored pregrada uzet je po dužini broda sa koordinatnim sustavom postavljenim na sjecištu osnovice i krmenog zrcala.
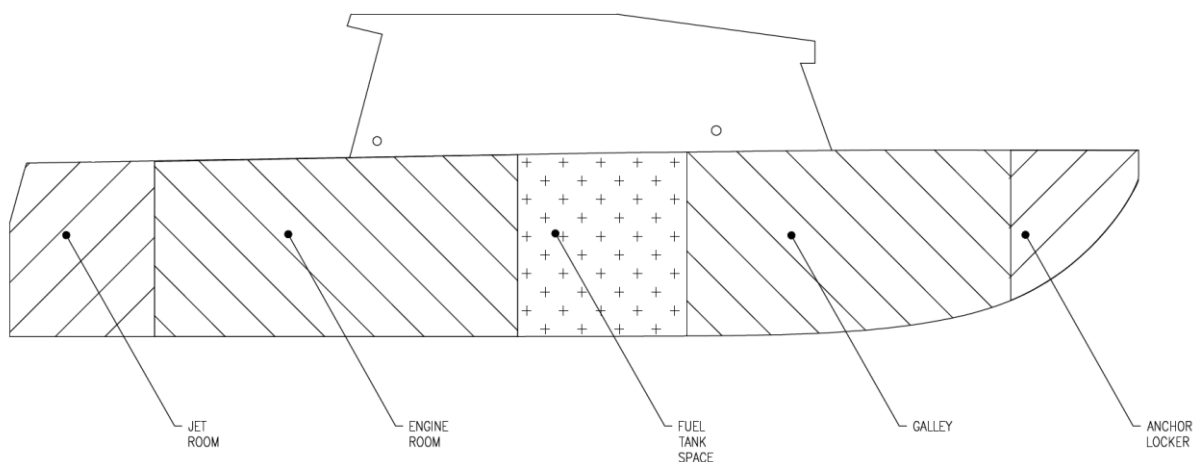
Slika 4. Kompartmenizacija brodice

Kriteriji koje plovilo u oštećenom stanju mora zadovoljiti su sljedeći:

- Opseg pozitivnog dijela poluge stabiliteta mora iznositi minimum 15° iznad kuta ravnoteže;
- Površina ispod krivulje poluge stabiliteta mora iznositi minimalno 0.015 mrad, mjereno od kuta ravnoteže do manje vrijednosti između kuta naplavljivanja i 27°;
- Preostala poluga stabiliteta biti će određena u pozitivnom opsegu stabiliteta s time da se u obzir uzme najveći prekretni moment između gomilanja putnika na jednu stranu, porinuća potpuno opremljene brodice za spašavanje na jednu

stranu i pritiska uzrokovanog vjetrom. Preostala poluga stabiliteta izračunava se preko formule

$GZ = \frac{prekretni\ moment}{istisnina} + 0.04\ (m)$ te ni u kojem slučaju ne smije biti manja od 0.1 m;

- U fazama naplavljivanja maksimalni iznos poluge stabiliteta mora iznositi minimalno 0.05 m, a opseg pozitivnih poluga stabiliteta mora iznositi minimalno 7°. U svim slučajevima samo jedan prodor vode i samo jedan utjecaj slobodnih površina je potrebno razmatrati.

Za proračun stabiliteta u oštećenom stanju napravljeno je 6 različitih stanja naplavljivanja odjeljaka.

Stanja naplavljivanja su raspoređena na sljedeći način:

1. Naplavljivanje prostora vodomlaznog propulzora
2. Naplavljivanje prostora strojarnice
3. Naplavljivanje prostora za tank goriva
4. Naplavljivanje prostora podpalublja
5. Naplavljivanje prostora za sidro
6. Kombinacija naplavljivanja prostora za tank i podpalublja

3.3.1. Naplavljivanje prostora vodomlaznog propulzora

Svi prostori su naplavljivani na način da su se ispunili morskom vodom definirane gustoće, prilikom toga nije korištena veličina oštećenja na trupu iz razloga jer je naplavljeno više slučajeva naplavljivanja. HSC 2000 definira permeabilnost za brodske prostore koji su prikazani u Tablici 7.

Spaces	Permeability
Appropriated to cargo or stores	60
Occupied by accommodation	95
Occupied by machinery	85
Intended for liquids	0 or 95*
Appropriated for cargo vehicles	90
Void spaces	95

* whichever results in the more severe requirements

Tablica 7. Permeabilnost prostora

Prostor vodomlaznog propulzora spada u permeabilnost od 85%.

Kriteriji koje mora ispuniti brodica za svaki potopljeni odjeljak i kombinaciju odjeljaka prikazan je u Tablici 8.:

Kriterij stabiliteta u oštećenom stanju			
DNV-GL	zahtijevana vrijednost	dobivena vrijednost	

Minimalno nadvođe do prve točke naplavljivanja	>0,3m	1,492	zadovoljeno
kut nagiba	<15°	0	zadovoljeno
HSC 2000			
između ravnoteže i točke gdje gubi stabilitet GZ mora imati opseg	>15°	53,7	zadovoljeno
Površina ispod krivulje između stanja ravnoteže i prvog kuta naplavljivanja (ili 27°,što je manje)	>=0,015mrad	0,096	zadovoljeno
GZ	>0,2m	0,332	zadovoljeno
tokom naplavljivanja Gzmax	>=0,05	0,332	zadovoljeno
tokom naplavljivanja opseg GZ	>=7°	53,7	zadovoljeno

Tablica 8. Naplavljivanje prostora vodomlaznog propulzora
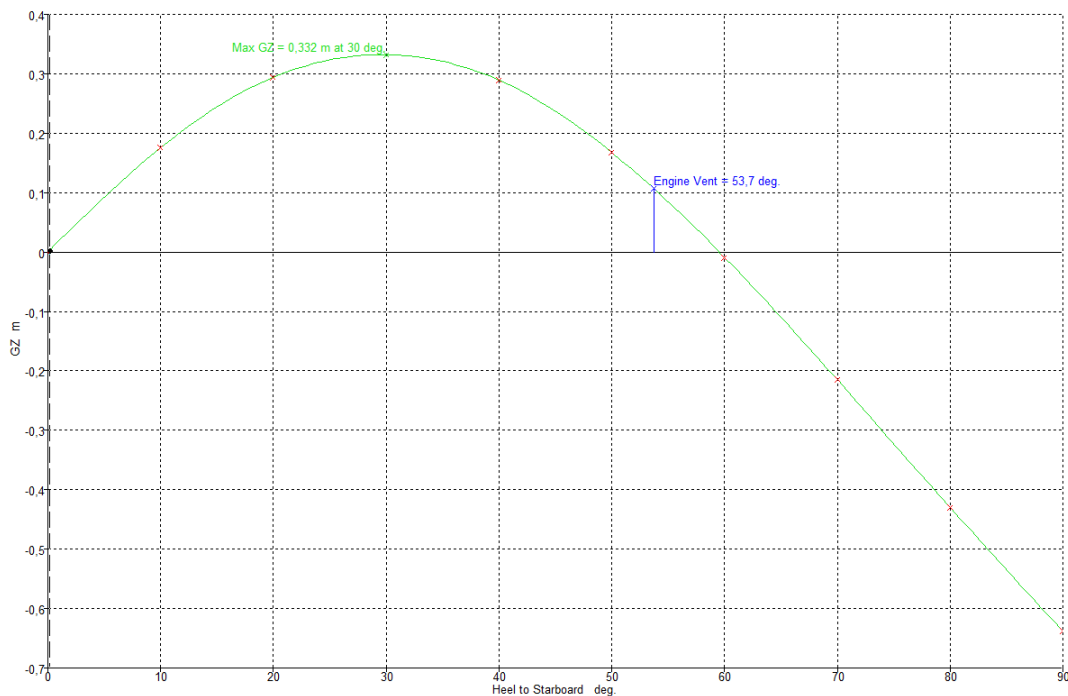
Slika 5. GZ krivulja naplavljivanja 1 odjeljka

137

3.3.2. Naplavljivanje prostora strojarnice

Kriterij stabiliteta u oštećenom stanju			
DNV-GL	zahtijevana vrijednost	dobivena vrijednost	
Minimalno nadvođe do prve točke naplavljivanja	>0,3m	1,638	zadovoljeno
kut nagiba	<15°	0	zadovoljeno
HSC 2000			
između ravnoteže i točke gdje gubi stabilitet GZ mora imati opseg	>15°	53,7	zadovoljeno
Površina ispod krivulje između stanja ravnoteže i prvog kuta naplavljivanja (ili 27°,što je manje)	>=0,015mrad	0,07	zadovoljeno
GZ	>0,2m	0,245	zadovoljeno
tokom naplavljivanja Gzmax	>=0,05	0,245	zadovoljeno
tokom naplavljivanja opseg GZ	>=7°	53,7	zadovoljeno

Tablica 9. Naplavljivanje prostora strojarnice
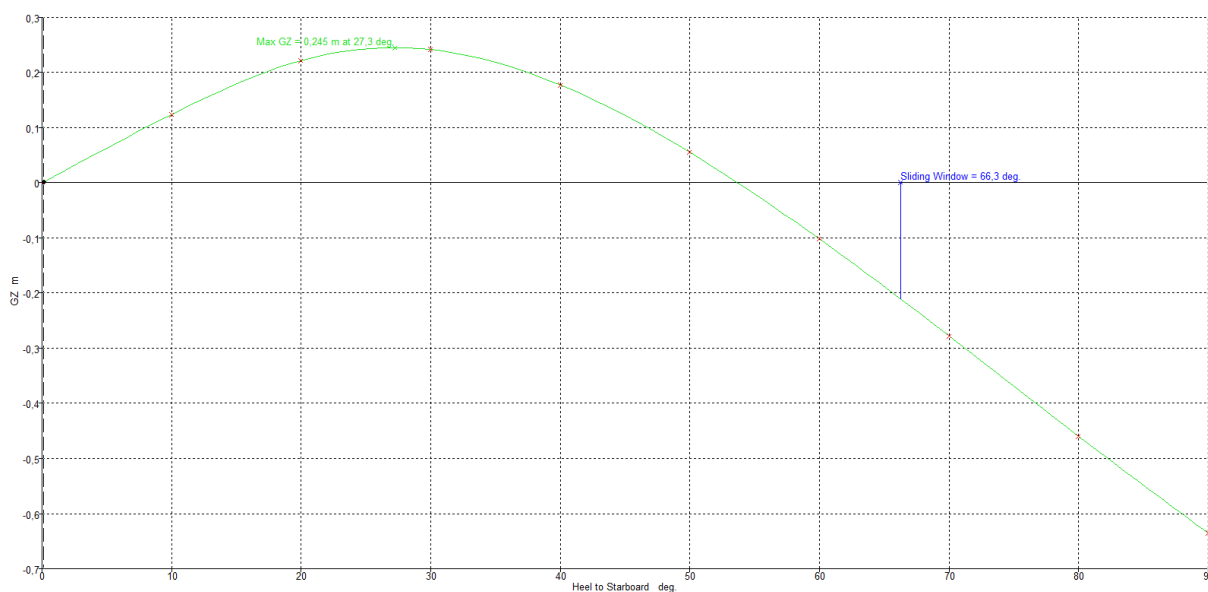
Slika 6. GZ krivulja naplavljivanja 2 odjeljka

3.3.3. Naplavljivanje prostora tanka

Kriterij stabiliteta u oštećenom stanju			
DNV-GL	zahtijevana vrijednost	dobivena vrijednost	
Minimalno nadvođe do prve točke naplavljivanja	>0,3m	1,651	zadovoljeno
kut nagiba	<15°	0	zadovoljeno
HSC 2000			
između ravnoteže i točke gdje gubi stabilitet GZ mora imati opseg	>15°	64	zadovoljeno
Površina ispod krivulje između stanja ravnoteže i prvog kuta naplavljivanja (ili 27°,što je manje)	>=0,015mrad	0,112	zadovoljeno
GZ	>0,2m	0,340	zadovoljeno
tokom naplavljivanja Gzmax	>=0,05	0,340	zadovoljeno
tokom naplavljivanja opseg GZ	>=7°	64	zadovoljeno

Tablica 10. Naplavljivanje prostora tanka
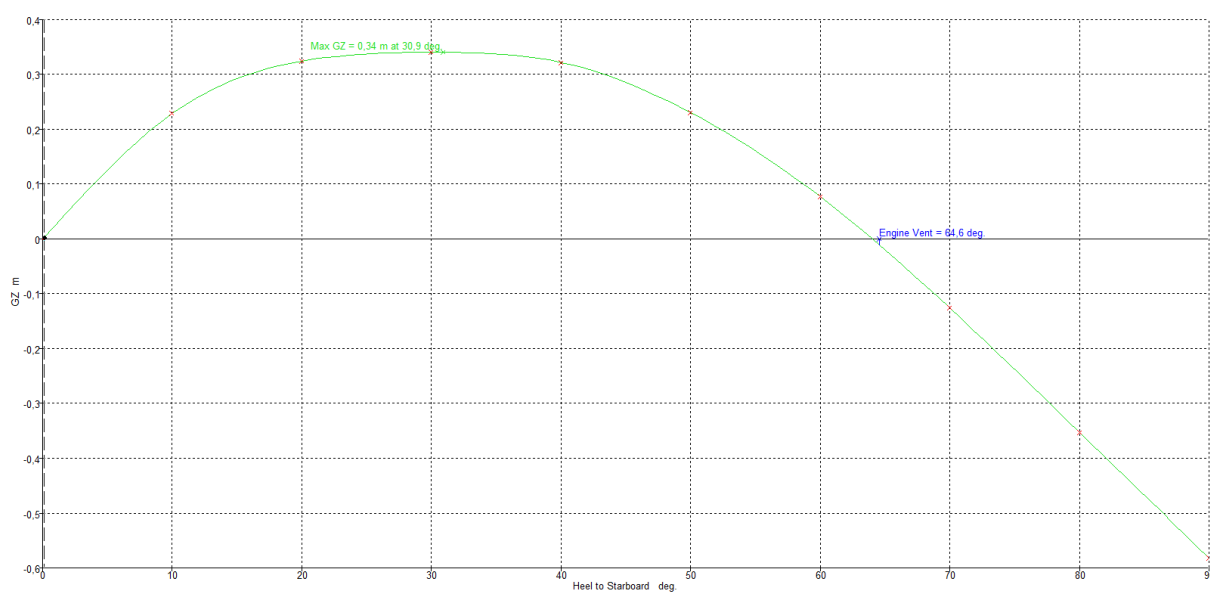
Slika 7. GZ krivulja naplavljivanja 3 odjeljka

3.3.4. Naplavljivanje prostora podpalublja

Kriterij stabiliteta u oštećenom stanju			
DNV-GL	zahtijevana vrijednost	dobivena vrijednost	
Minimalno nadvođe do prve točke naplavljivanja	>0,3m	1,651	zadovoljeno
kut nagiba	<15°	0	zadovoljeno
HSC 2000			
izmeđ ravnoteže i točke gdje gubi stabilitet GZ mora imati opseg	>15°	54,9	zadovoljeno
Površina ispod krivulje između stanja ravnoteže i prvog kuta naplavljivanja (ili 27°,što je manje)	>=0,015mrad	0,12	zadovoljeno
GZ	>0,2m	0,376	zadovoljeno
tokom naplavljivanja Gzmax	>=0,05	0,376	zadovoljeno
tokom naplavljivanja opseg GZ	>=7°	54,9	zadovoljeno

Tablica 11. Naplavljivanje prostora podpalublja
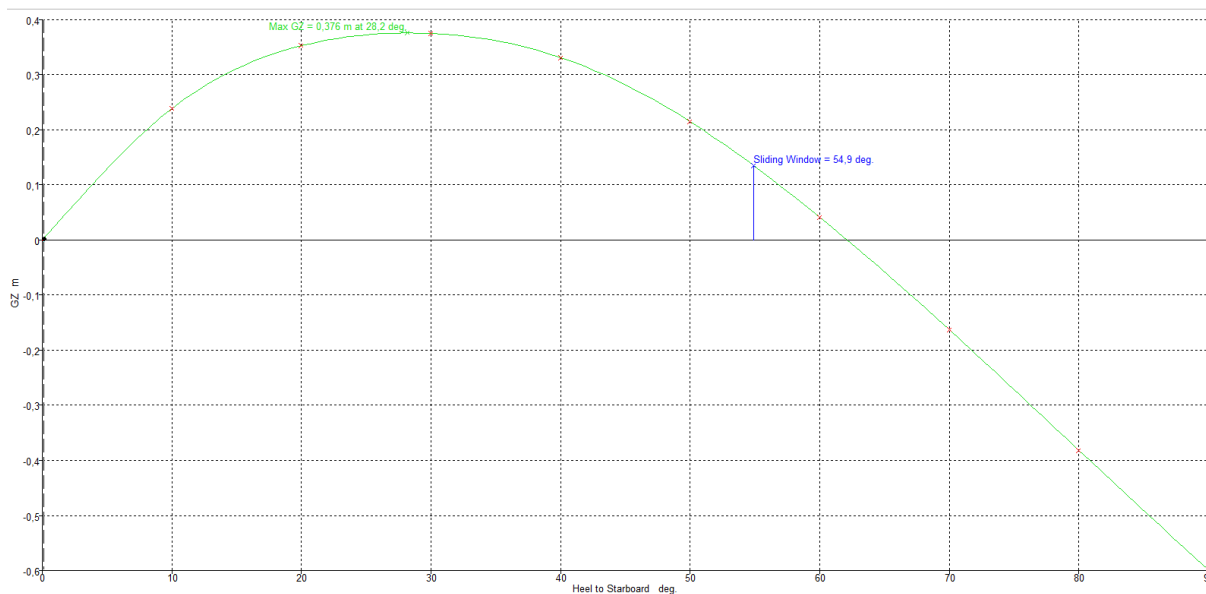
Slika 8. GZ krivulja naplavljivanja 4 odjeljka

3.3.5. Naplavljivanje prostora spreme za sidro

Kriterij stabiliteta u neoštećenom stanju			
DNV-GL	zahtjevana vrijednost	dobivena vrijednost	
Minimalno nadvođe do prve točke naplavljivanja	>0,3m	1,708	zadovoljeno
kut nagiba	<15°	0	zadovoljeno
HSC 2000			
izmeđ ravnoteže i točke gdje gubi stabilitet GZ mora imati opseg	>15°	65,8	zadovoljeno
Površina ispod krivulje između stanja ravnoteže i prvog kuta naplavljivanja (ili 27°,što je manje)	>=0,015mrad	0,119	zadovoljeno
GZ	>0,2m	0,364	zadovoljeno
tokom naplavljivanja Gzmax	>=0,05	0,364	zadovoljeno
tokom naplavljivanja opseg GZ	>=7°	65,8	zadovoljeno

Tablica 12. Naplavljivanje prostora spreme za sidro
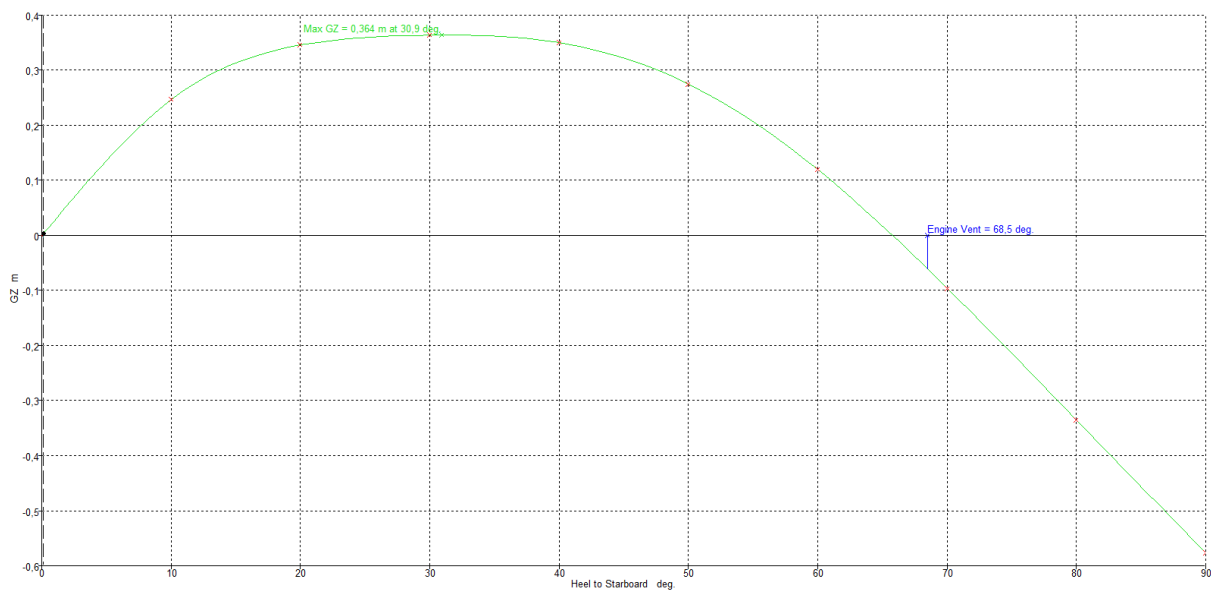
Slika 9. GZ krivulja naplavljivanja 5 odjeljka

3.3.6. Naplavljivanje prostora za tank i podpalublja

Kriterij stabiliteta u oštećenom stanju			
DNV-GL	zahtijevana vrijednost	dobivena vrijednost	
Minimalno nadvođe do prve točke naplavljivanja	>0,3m	1,708	zadovoljeno
kut nagiba	<15°	0	zadovoljeno
HSC 2000			
između ravnoteže i točke gdje gubi stabilitet GZ mora imati opseg	>15°	39,9	zadovoljeno
Površina ispod krivulje između stanja ravnoteže i prvog kuta naplavljivanja (ili 27°,što je manje)	>=0,015mrad	0,108	zadovoljeno
GZ	>0,2m	0,340	zadovoljeno
tokom naplavljivanja Gzmax	>=0,05	0,340	zadovoljeno
tokom naplavljivanja opseg GZ	>=7°	39,9	zadovoljeno

Tablica 13. Naplavljivanje prostora za tank i podpalublja
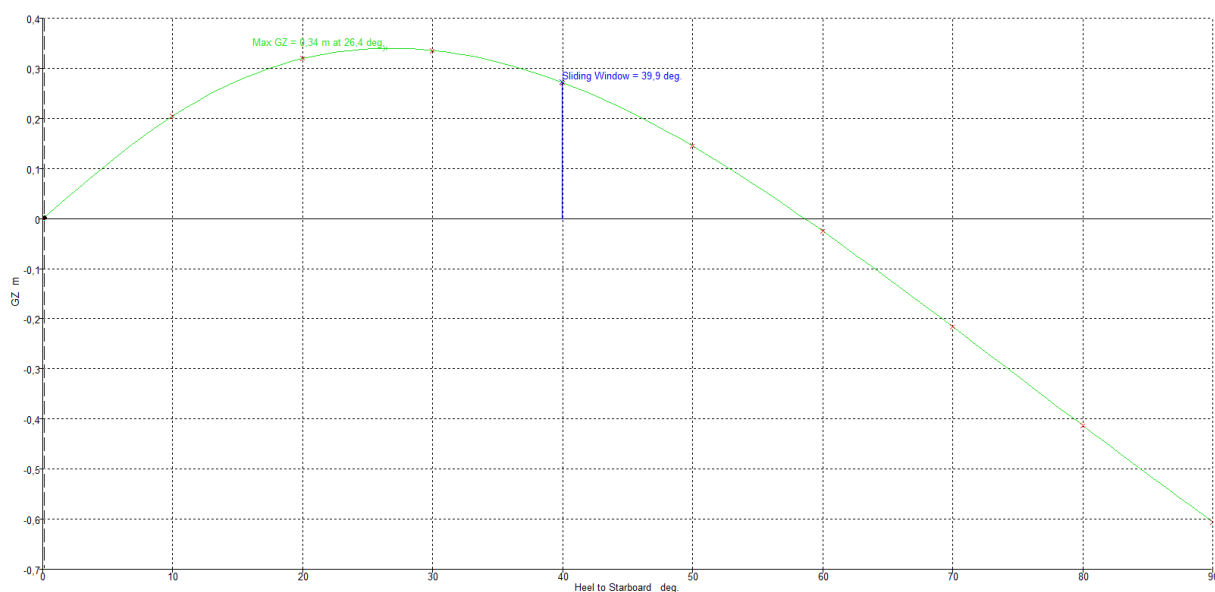
Slika 10. GZ krivulja naplavljivanja kombinacije 3 i 4 odjeljka

4.   PODRUČJE PRIHVATLJIVOG POLOŽAJA TEŽIŠTA (TEŽIŠNA ENVELOPA)

Prilikom sveobuhvatnog procesa osnivanja broda cilj je definirati područje prihvatljivog položaja težišta (težišnu envelopu) koja daje prikaz dopustivog raspona težina i položaja težišta unutar kojeg brod može sigurno operirati.

Ukoliko je kombinacija težine i težišta dopuštena samo unutar određenih ograničenja raspodjele poprečnih opterećenja koje bi se nenamjerno mogle premašiti, ta je opterećenja potrebno utvrditi za odgovarajuće kombinacije težina i težišta.

Područje položaja težišta brodice daje prihvatljiv raspon položaja težišta koji rezultira sa pozitivnim stabilitetom potrebnim za zadovoljenje Međunarodnih pravila za sigurnost brzih plovila po uzdužnoj, poprečnoj i vertikalnoj osi. Slika 11. daje prikaz područja prihvatljive pozicije težišta za stabilitet brodice u neoštećenom stanju.
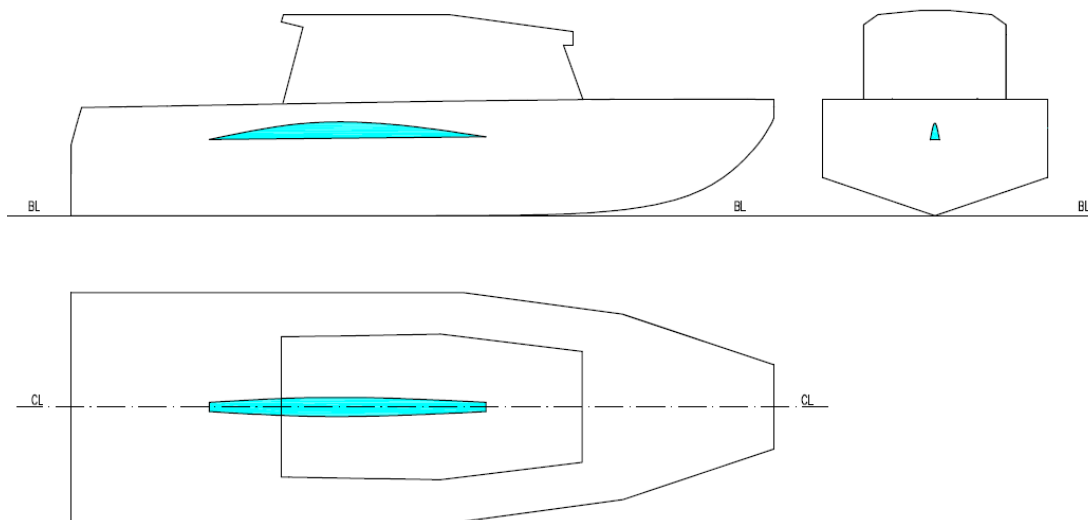
Slika 11. Područje prihvatljivog položaja težišta stabiliteta u neoštećenom stanju

Na slici 12. dat je raspon prihvatljivog područja položaja težišta brodice koji rezultira sa pozitivnim stabilitetom za sva stanja naplavljivanja u oštećenom i neoštećenom stanju.

Koncept težišne envelope je puno zastupljeniji u avio industriji odnosno projektiranju aviona. Težišna envelopa je klasificiran dokument koji se izrađuje u cilju sigurne operacije zrakoplova i sastavni je dio uputa za operiranje zrakoplovom. Do određene mjere ga se može promatrati i prilikom projektiranja brodova u cilju definiranja određenih operacijskih uvjeta i limita koje brod treba ispoštovati prilikom perioda eksploatacije.

Vertikalna pozicija težišta (VCG) ima utjecaj na oboje: uzdužni i poprečni stabilitet. Lateralni pomak pozicije težišta pogoršava stabilitet ljuljanja dok uzdužni pomak utječe na statički stabilitet.

Prilikom projektiranja prototipa rade se kontinuirane iteracije težišne envelope uslijed zaprimanja novih projektnih informacija i/ili promjena.
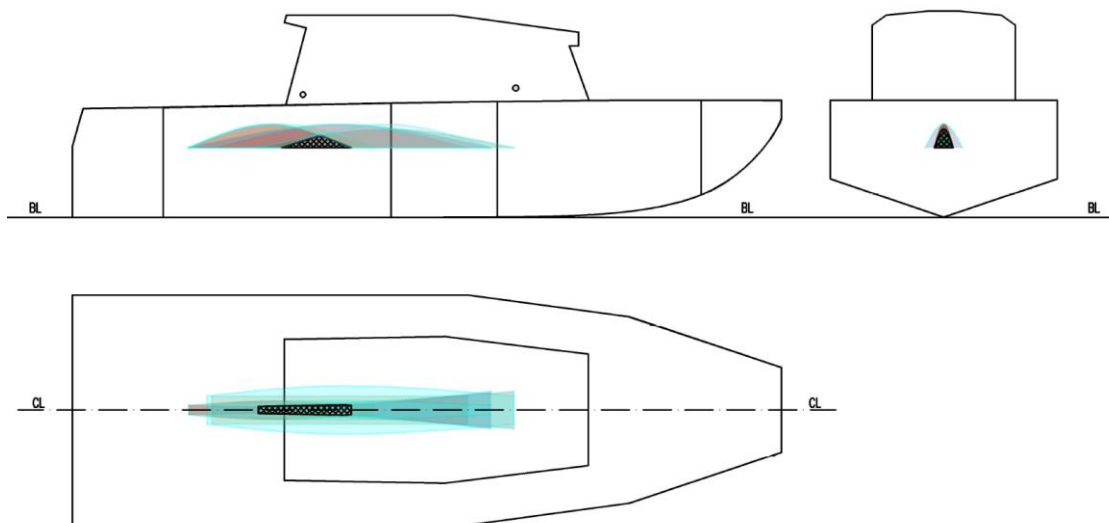
Slika 12. Područje prihvatljivog položaja težišta stabiliteta u oštećenom i neoštećenom stanju

5. ZAKLJUČAK

Cilj predmetnog članka bio je odrediti područje položaja prihvatljive pozicije težišta brodice koja rezultira pozitivnim stabilitetom. Područje prihvatljivog položaja težišta definirano je za referentnu brodicu kako bi se pokazala ovisnost stabiliteta brodice u oštećenom i neoštećenom stanju sa položajem težišta. Plovilo je zadovoljilo sve kriterije stabiliteta oštećenog i neoštećenog stanja kao i dinamički stabilitet. Pravila koja su definirala kriterije stabiliteta proizašla su iz klasifikacijskog društva DNV-GL koje daje smjernice na koja se pravila potrebno vezati kako bi brodica bila sigurna u plovidbi. Nakon podjele broda u prostore i definiranja točke naplavljivanja izrađen je proračun stabiliteta u oštećenom stanju za svaki odjeljak posebno i kombinaciju 2 odjeljka. Proračun je pokazao da prostor tanka i prostor podpalublja ne trebaju biti odvojeni vodonepropusnom pregradom što uvelike olakšava pristup tank goriva. Specifičan pristup tražio je prostor vodomlaznog propulzora gdje forma na krmi zatvara najveći volumen čime posljedično brod dobiva trim (stvara se moment zbog velike udaljenosti) i nije bilo moguće spojiti strojarnicu i navedeni prostor u jedan. Područje položaja težišta brodice dao je prihvatljiv raspon položaja težišta koji rezultira sa pozitivnim stabilitetom potrebnim za zadovoljenje međunarodnih pravila za sigurnost brzih plovila po uzdužnoj, poprečnoj i vertikalnoj osi.

6. LITERATURA

[1]   DNV-GL Rules for Classification- High Speed and light craft Part 5 Ship types Chapter 6 Small service craft

[2]   International Code of Safety for High-Speed Craft (2000) The Maritime and Coastguard Agency

STRUCTURAL ANALYSIS OF MASTS, BOWSPRIT AND STANDING RIGGING OF A THREE-MAST SCHOONER

Marin Palaversa*[a], Zdenko Šperanda[b]

a University of Zagreb, Faculty of Mechanical Engineering and Naval Architecture, Ivana Lucica 5, Zagreb, Croatia
b DIV Marine & Energy Solutions, Froudeova 5, Zagreb, Croatia
* Corresponding Author, marin.palaversa@fsb.hr

Abstract

This paper deals with structural analysis of masts, standing rigging and bowsprit of a three-mast passenger schooner. Loads that act on the structure as well as classification societies' acceptance criteria are described. Moreover, application of the loads on the finite element analysis model is demonstrated. At the end, finite element analysis of the structure is discussed: finite elements, boundary conditions, nonlinear and buckling analyses and the results.

Key words: structural design; finite element analysis; sail ship; masts; bowsprit; standing rigging

Sažetak

Ovaj članak se bavi analizom konstrukcije jarbola, opute i pramčanog kosnika trojarbolne putničke škune. Opisana su opterećenja koja djeluju na konstrukciju kao i kriteriji za evaluaciju propisani od strane klasifikacijskih društava. Pored toga, pokazana je i primjena opisanih opterećenja na model konačnih elemenata. Na kraju se prikazuje analiza konstrukcije metodom konačnih elemenata uz opis korištenih konačnih elemenata, rubnih uvjeta, nelinearne analize i analize izvijanja te rezultata.

Ključne riječi: projektiranje konstrukcije; metoda konačnih elemenata; jedrenjak; jarboli; pramčani kosnik; oputa

1. Introduction

Sailing ships dominated the world of shipping for centuries, from antiquity to the late 19th century. They were used for transporting people and goods, for exploring new lands and in wars. First sailing ships were square-rigged and were built by the Egyptians. Later, ships with fore-and-aft sails emerged. These employed the lateen sail that spread from the Eastern Mediterranean westwards. At the height of the age of sail, ships usually combined the square and the fore-and-aft sails as can be seen in Figure 1. The square sails were excellent for long ocean voyages where trade winds dominated. However, in coastal sailing with a variety of winds, their performance was rather poor. Thus, in coastal trading for-and-aft rigged ships were favoured.

Schooners are sailing ships with fore-and-aft sails, i.e. all sails are set aft of a mast or a stay, parallel to the ship's keel and can take the wind on either side [1]. The concept first emerged in the Netherlands, but their modern form was developed in the North America in the 17th century and soon became very popular. The largest schooner ever built had 7 masts, but they were usually two- or three-masted ships. However, with the advent of steam ships and later ships with internal combustion engines, sailing ships fell out of use so that classification societies even stopped the development of rules applicable to these ships in the first half of the 20th century (e.g. Lloyd's Register of Shipping issued its last rules for sailing ships in the mid 1920's [2]). In the 1980's a new wave of interest in sailing ships emerged primarily among those cruise shipping companies that

wanted to offer something authentic and new to its customers. This was followed by a number of orders of these ships in European shipyards [2]. They were aimed at Europeans with knowledge and interest in sailing and their intended service were one- or two-week cruises in the Caribbean [2]. The ship whose rig we shall deal with in this paper also belongs into this group. It is approximately 65 m long, 10 m wide and will carry 50 crew and passengers on board (Figure 2). Its rig consists of three masts, a bowsprit and a boom with corresponding standing and running rigging. Each mast has two spreaders and the bowsprit has a dolphin striker. Main and mizzen masts are designed with jumpers.

Figure 1 A barque with square sails on foremast and mainmast, the rest are fore-and-aft sails
Slika 1 Bark s križnim jedrima na pramčanom i prednjem jarbolu i letnim jedrima na ostalim jarbolima
(Source/Izvor: Anonymous - Vallejo Gallery, Public Domain,
https://commons.wikimedia.org/w/index.php?curid=79161068)

This paper deals with structural analysis of the masts, standing rigging and the bowsprit. Metal spars are usually manufactured from plane metal plates, rolled and tapered to obtain hollow, conical mast sections, with lengths typically between half a meter and a few meters. Mast sections are assembled into the whole mast. The length of the foremast on this ship is 34.23 m while the length of the mainmast and the mizzenmast is 32.06 m measured from the top of the mast foundation on deck. Outer diameters of the foremast sections range from 663 mm to 305 mm while their thickness is from 9 to 18 mm. This shows the slenderness of the mast structure.
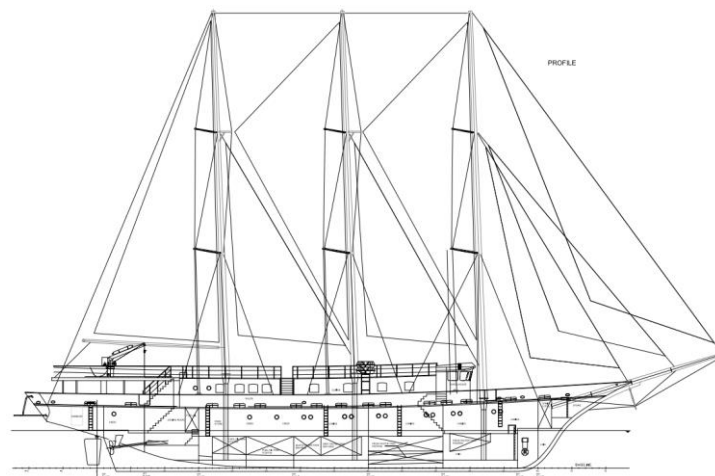
Figure 2 General arrangement plan
Slika 2 Opći plan

As this paper deals primarily with the masts, the bowsprit and the standing rigging will only be touched upon while other components of the rig will not be dealt with at all. The paper comprises a description of dominant loads on masts and standing rigging, their structural behaviour and classification society's acceptance criteria. It proceeds with the finite element analysis of the system (finite elements, boundary conditions, loads) and, at the end, the analysis' results are shown and briefly discussed.

2. Mast and standing rigging loads, structural behaviour and the classification society's acceptance criteria

Masts on a sailing ship represent, together with sails, the pillars of the ship's sailing system. Sails, used to move the sailing ship in a desired direction, are (at least partially) attached to the masts or to spars connected to the masts. This means that forces produced by the wind when it acts on the sails are transmitted to the masts via the attachment points. Wind forces together with inertial forces due to ship motions and gravity load act on the masts and all the other components attached or mounted on the masts. Masts, being very slender, are generally not capable to bear these loads within prescribed limits on their own and thus a system of wire ropes (called standing rigging) is used to limit their deformations. This means that we can identify the following loads acting on a sailing ship mast: wind forces from sails (point loads), wind loads on mast structure (distributed load), forces from standing rigging wire ropes, inertial forces (distributed body force) and gravity force (distributed body force).

Table 1 Sail forces
Tablica 1 Sile na jedra

Sail	Sail area (m²)	Total wind force (kN)	Tack force (kN)	Clew force (kN)	Head force (kN)
Flying jib	114	18.01	5.40	5.40	7.20
Outer jib	71	11.21	3.36	3.36	4.49
Inner jib	72	11.37	3.41	3.41	4.55
Main staysail	77	12.16	3.65	3.65	4.86
Fore fisherman	125	19.74	5.92	5.92	7.90
Mizzen staysail	78	12.32	3.70	3.70	4.93
Main fisherman	124	19.59	5.88	5.88	7.83
Spanker	155	24.48	7.34	7.34	9.79

Wind loads can be estimated by means of the following formula [2]:

$$F_S = \frac{1}{2} \cdot \rho \cdot A_S \cdot v_A^2 \cdot C \qquad (1)$$

where ρ is air density, A_S represents sail's area (see **Error! Reference source not found.**), v_A is apparent wind speed (represents a vectoral sum of true wind speed and ship speed), C is aerodynamic coefficient (lift for sails, drag for spars). The design apparent wind speed v_A can be obtained from Beaufort's scale and in this study it is 27 knots which correspond to the Beaufort wind force 6. The aerodynamic coefficient depends on the type of sail and can be found in [2]. Additionally, wind gust effects must be taken into account. They represent high but short (typically

10 s or so) variations in wind velocity and are usually accounted for by means of the gust coefficient that should be between 1.35 and 1.45 according to [3]. Once the force on sail is obtained, sail corner loads can be estimated. The following distribution of the sail forces is used: 30% of the total force is assigned to the tack, 30% to the clew and 40% to the head (Figure 3). For the purpose of the structural analysis, wind induced sail forces are assumed to act athwartship. Magnitude of sail forces is listed in Table 1.

Wind loads on spars are calculated by means of (1).

Inertial forces are calculated by means of standard procedures employed in classification societies' rules (e.g. see [2]).

Regarding standing rigging, it is important to bear in mind that standing rigging on this ship consists almost entirely of wire ropes. Wire ropes are not able to carry any load in compression. Moreover, they should never be allowed to reach a non-tension (slack) state as this can induce shock loads that result in wear and fatigue damage [2]. In order to achieve tension at all times, the standing rigging wire ropes are pretensioned using turnbuckles (see Figure 4) which in turn induces compression in spars even if no other loads are present. Value of wire rope pretension is usually between 5% and 20% of their break load.
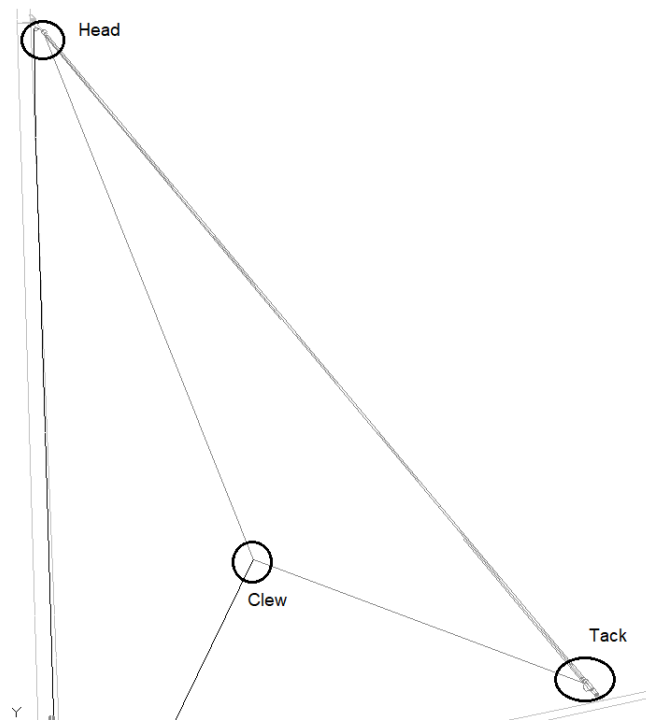
Figure 3 Sail's corners where reaction force is transmitted to other rig components
Slika 3 Kutovi jedara gdje se reakcijske sile prenose na druge dijelove snasti

When wire ropes represent sail stays (as in Figure 3), the sail acts on them producing a sag which in turn causes tension forces in the stay. The value of these forces depends on the sag of the stay. Over the years, appropriate value of the stay sag has been debated and it is now generally considered that for traditionally rigged vessels this value should be between 3% and 6% of the stay's length [2], in this study 4% of the stay's sag is used in the calculations. Once the sag value is assumed, the tension forces can be obtained by means of catenary response analysis. It is important to point out here that stays are attached to masts, bowsprit and ship structure (see Figure 4) and both the

pretension loads as well as the loads due to stay's sag are transmitted to these structures and should be taken into account when their structural response is analysed.
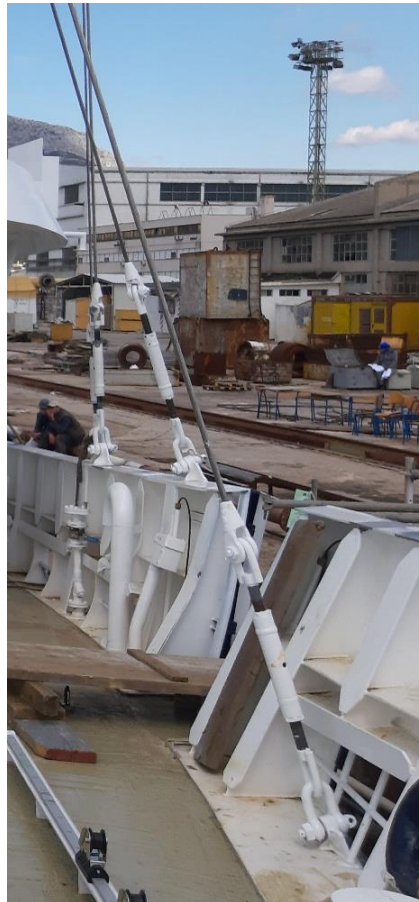
Figure 4 Standing rigging wire ropes attached to the ship structure (turnbuckles used for their pretension can be seen)

Slika 4 Čelična užad opute pričvršćena za konstrukciju broda (mogu se vidjeti zatezači koji se koriste za pritezanje)

Once the loads have been defined, one needs to determine load cases and establish structural evaluation or acceptance criteria before commencing any structural analysis. These are usually prescribed by the classification societies. In this study we use [3]. It defines two operating conditions: operational and survival. The most significant loads in operational load case (Figure 5) come from the wind loads on sails. In the analysis model, they are given as point loads on masts and bowsprit at sail lines' attachment points and as axial force in sail's stay due to the sag, in the analysis model these are assigned as temperature loads for jibs and staysails. Additionally, structure's weight is also taken into account and can be seen in Figure 5. Standing rigging ropes' pretension forces are usually modelled by defining prescribed displacements as can be seen in Figure 5 (only in wire ropes that stretch between two masts, they are modelled as temperature loads).

In survival condition the ship sails with stowed sails ("bare poles" condition) thus no wind force on sails is present. The loads present in this load case are inertial forces and wind loads on spars, spars' self-weight and standing rigging pretension forces. Regarding wind loads on spars, they are calculated by means of (1) with apparent wind speed of 63 m/s.
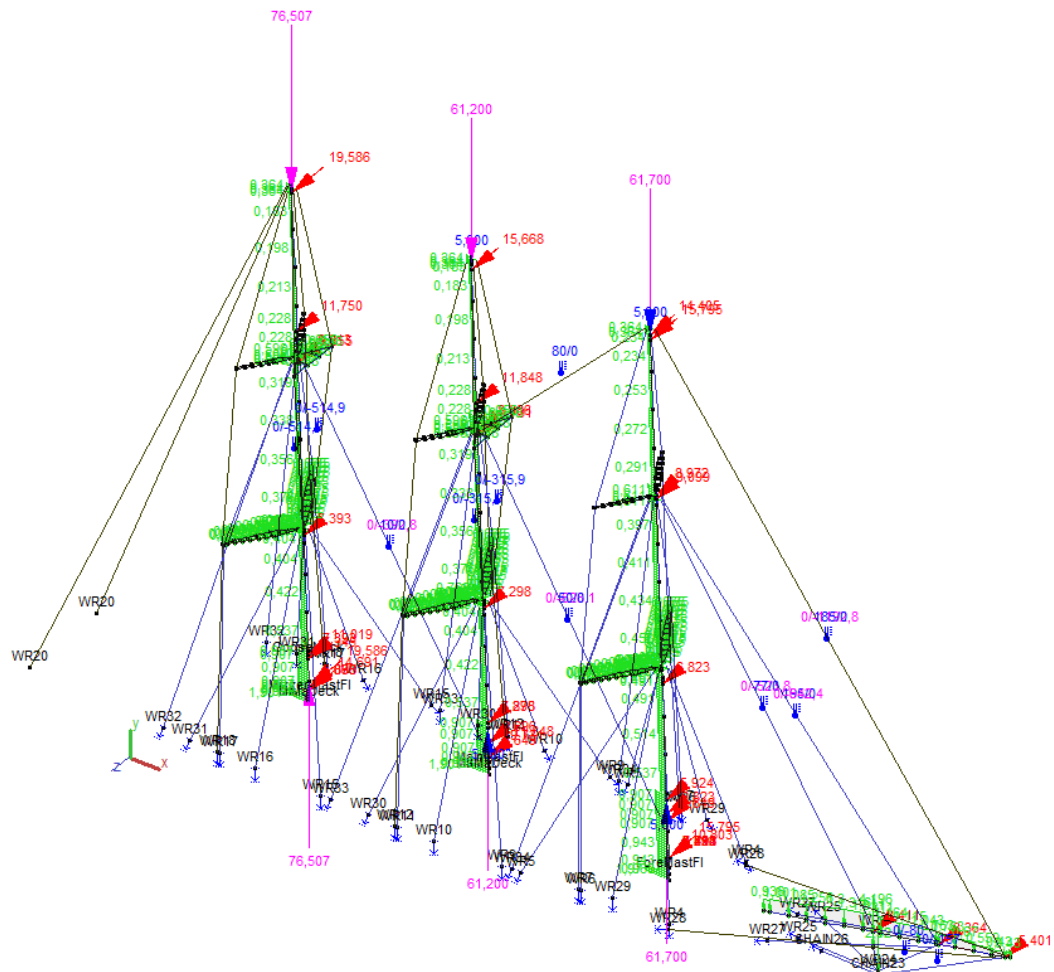
Figure 5 Operational load case loads
Slika 5 Opterećenja za operativni slučaj opterećenja

Classification society's acceptance criteria are given in form of limit direct and shear stresses for normal (σ_N, τ_N) and survival condition (σ_S, τ_S) [3]:

$$\sigma_N \leq \frac{175}{k} N/mm^2 \tag{2}$$

$$\sigma_S \leq \frac{215}{k} N/mm^2 \tag{3}$$

$$\tau_N \leq \frac{100}{k} N/mm^2 \tag{4}$$

$$\tau_S \leq \frac{115}{k} N/mm^2 \tag{5}$$

where *k* is the scantlings coefficient that is different than 1 if material other than mild steel is used. In this study, bowsprit is made of mild steel while masts are made of aluminium alloy 5083 (material properties can be found in Table 2). Thus, *k* = 1 for the bowsprit and for Al5083 can be calculated according to [3]:

$$k = \frac{235}{R_e} = 1.88 \tag{6}$$

Based on (6) and (2) to (5) the limit stresses for aluminium masts are:

$$\sigma_N \leq 87.77 \ N/mm^2 \tag{7}$$

$$\sigma_S \leq 114.36 \ N/mm^2 \tag{8}$$

$$\tau_N \leq 53.19 \ N/mm^2 \tag{9}$$

$$\tau_S \leq 61.17 \ N/mm^2 \tag{10}$$

Table 2 Properties of mild steel, aluminium alloy 5083 and wire rope material
Tablica 2 Svojstva običnog brodograđevnog čelika, aluminijske legure 5083 i materijala čelične užadi

Property	Mild steel	Al 5083	Wire rope
Modulus of elasticity (E), N/mm^2	206 000	68 000	128 000
Poisson's factor (ν)	0.30	0.33	
Yield strength (R$_e$/R$_{p0.2}$), N/mm^2	235	125	N/A
Tensile strength (R$_m$), N/mm^2	400	275	
Density (ρ), kg/m^3	7 850	2 700	7 920

Standing rigging wire ropes are characterised by their tension breaking force. The criterion used for the evaluation of wire rope's adequacy is called the material safety factor (*MSF*):

$$MSF = \frac{BRL}{T_{max}} \tag{11}$$

Equation (11) expresses ratio between the capacity of the wire rope, BRL, and maximum calculated tension force in the wire rope T_{max}. The required minimum value of *MSF* can be debated. We opted here for the following values: *MSF* should be greater than 2 for for-and-aft rigging and greater than 2.5 for transverse rigging as given in [4].

3. Finite element analysis of masts, standing rigging and bowsprit

Structural analysis of masts, standing rigging and bowsprit is carried out by means of the finite element method in software called Multiframe. In this chapter the finite element model is described as well as the types of the analyses and the results.

Rig consists of three masts: foremast, mainmast and mizzenmast (Figure 2) tilted aft by 2° (see Figure 8). Mast sections are of circular shape and are tapered along the height of the masts. Spars are modelled with beam finite elements (see Figure 6). As mast sections are tapered, the beam properties of FEs are averaged along its length as Multiframe does not support formulation of tapered beam elements. The bowsprit is modelled in the similar manner and tilted upwards by 12° (see Figure 8). Spreaders and jumpers are modelled with beam elements and as spreaders are hinged, appropriate releases are introduced in the model to the spreader elements. Properties of materials associated with bowsprit and masts FEs can be found in Table 2.

Standing rigging ropes are modelled as tension-only rod elements. Wire ropes are made of galvanised or stainless steel but the material and geometric properties of standing rigging ropes are not given in this paper for the sake of brevity as there are 38 ropes and, in order to be modelled correctly, beside the aforementioned properties, one must have their exact locations and points of attachment what would require full reproduction of the standing rigging plan (a part of it can be seen in Figure 8). However, for an interested reader, these are available on request.
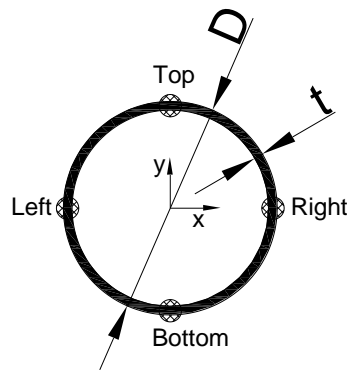
Figure 6 Beam FE cross-section
Slika 6 Poprečni presjek grednog konačnog elementa
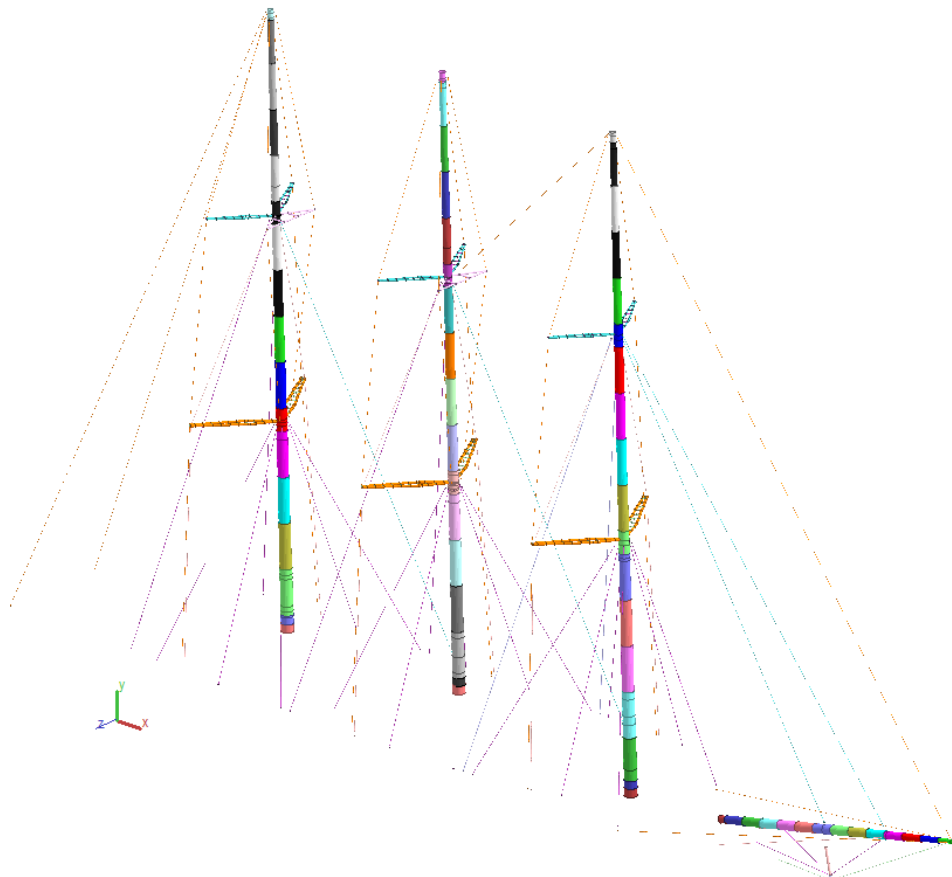
Figure 7 Finite elements' mesh
Slika 7 Mreža konačnih elemenata

152

Boundary conditions for masts are prescribed as fixed at their connection to deck. Bowsprit is pinned at its connections to deck and stem. Additionally, at its deck connection at frame 67 rotation about its longitudinal axis is constrained. Standing rigging is fixed to the deck structure. Dolphin striker is pinned at its connection to the stem.

Model loads and load cases are described in chapter 2.
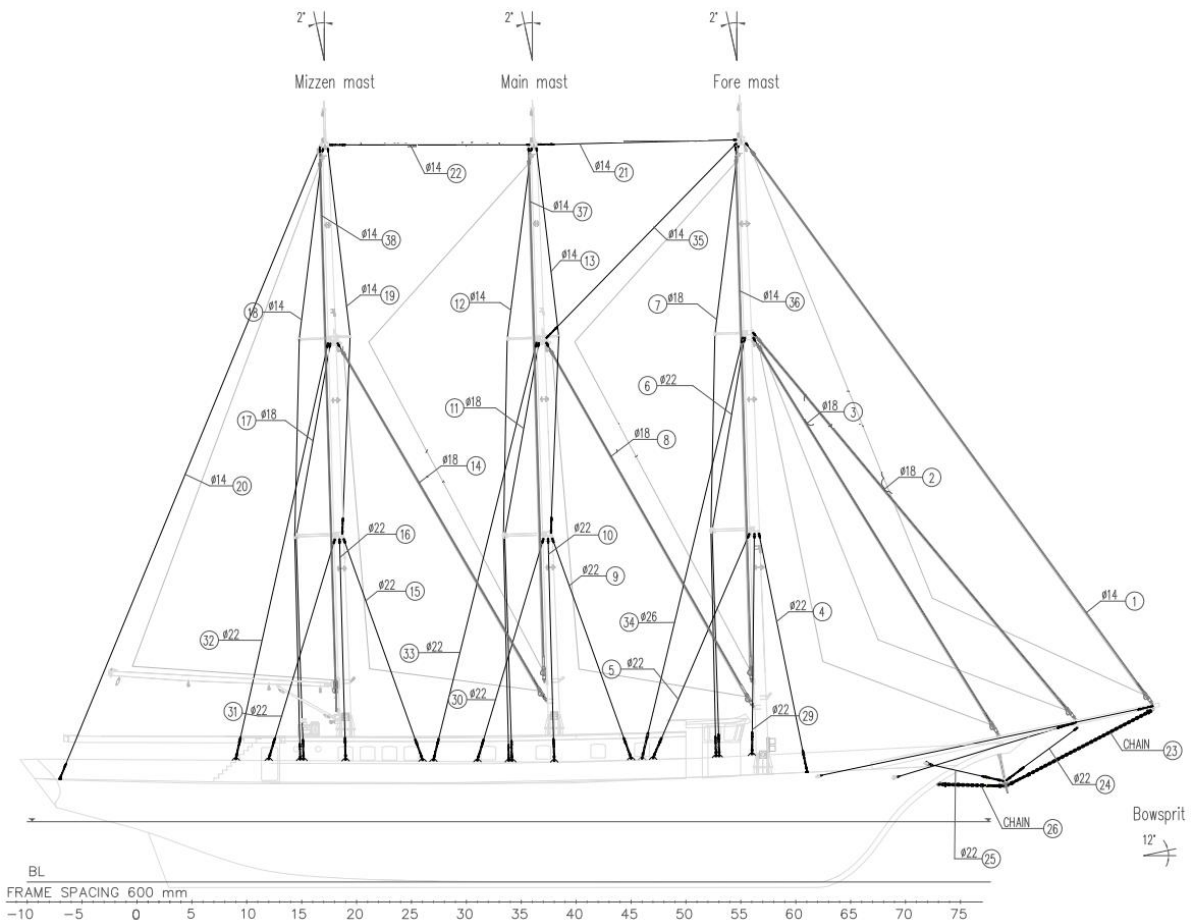
Figure 8 Standing rigging plan - side view of the ship
Slika 8 Plan opute – bočni pogled na brod

Two analyses are carried out in this study: geometrically nonlinear FE analysis to obtain displacements and stresses and the eigenvalue buckling analysis to asses system stability. The nonlinear analysis is required by the slender nature of the rigging system and nonlinear behaviour of the wire ropes.

4. Finite element analyses' results

Table 3 and Table 4 show the maximum stresses and deflections in both the masts and the bowsprit while Figure 10 to Figure 14 show their distribution. Additionally, the criteria given in equations (2) to (5) and (7) to (10) are presented for comparison. It is obvious that all the criteria are fulfilled. In the sequel we give the explanation for stresses in the tables:

- o σ_a – axial stress on a cross-section in mast/bowsprit caused by load components that act in mast/bowsprit longitudinal direction.

- $\sigma_{b,L}$ or $\sigma_{b,T}$ – bending stress on a cross-section in ship's longitudinal or transverse plane. For each FE it is given in points top/bottom and left/right (see Figure 6).
- $\sigma_{comb,L}$ or $\sigma_{comb,T}$ – total stresses ($\sigma_a + \sigma_{b,L}$ or $\sigma_a + \sigma_{b,T}$) on a cross section
- τ – shear stresses on a cross-section
- d – max deflection along mast/bowsprit

Figure 9 Bowsprit connection to deck and stem
Slika 9 Spoj pramčanog kosnika na palubu i statvu

Table 3 Structural response characteristics for masts
Tablica 3 Karakteristike odziva konstrukcije jarbola

Load case	Characteristic	Value	Location	Criterium (N/mm²)
Operational	σ_a	41 N/mm²	Foremast	N/A
	$\sigma_{b,L}$	55 N/mm²	Foremast	
	$\sigma_{b,T}$	47 N/mm²	Foremast	
	$\sigma_{comb,L}$	76 N/mm²	Foremast	≤ 88
	$\sigma_{comb,T}$	79 N/mm²	Mainmast	
	d	616 mm	Mizzenmast	N/A
Survival	σ_a	26 N/mm²	Mainmast	N/A
	$\sigma_{b,L}$	33 N/mm²	Foremast	
	$\sigma_{b,T}$	60 N/mm²	Foremast	
	$\sigma_{comb,L}$	47 N/mm²	Foremast	≤ 114
	$\sigma_{comb,T}$	74 N/mm²	Foremast	
	d	487 mm	Mainmast	N/A

Table 4 Structural response characteristics for bowsprit
Tablica 4 Karakteristike odziva konstrukcije pramčanog kosnika

Load case	Characteristic	Value	Criterium
Operational	σ_a	42 N/mm²	N/A
	$\sigma_{b,L}$	25 N/mm²	
	$\sigma_{b,T}$	88 N/mm²	
	τ	41 N/mm²	
	$\sigma_{comb,L}$	93 N/mm²	≤ 175
	$\sigma_{comb,T}$	116 N/mm²	
	d	60 mm	N/A
Survival	σ_a	21 N/mm²	N/A
	$\sigma_{b,T}$	17 N/mm²	
	$\sigma_{comb,L}$	20 N/mm²	≤ 215
	$\sigma_{comb,T}$	38 N/mm²	
	d	9 mm	N/A
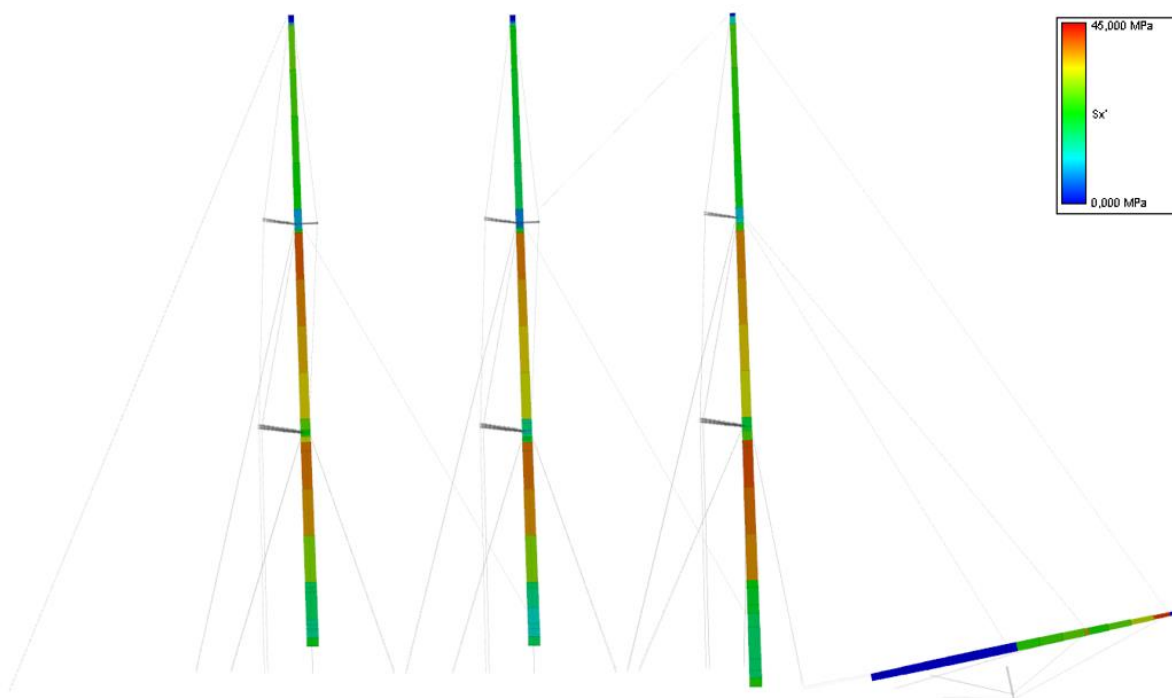
Figure 10 Axial stresses distribution for operational load case
Slika 10 Distribucija aksijalnih naprezanja za operacijski slučaj opterećenja

155
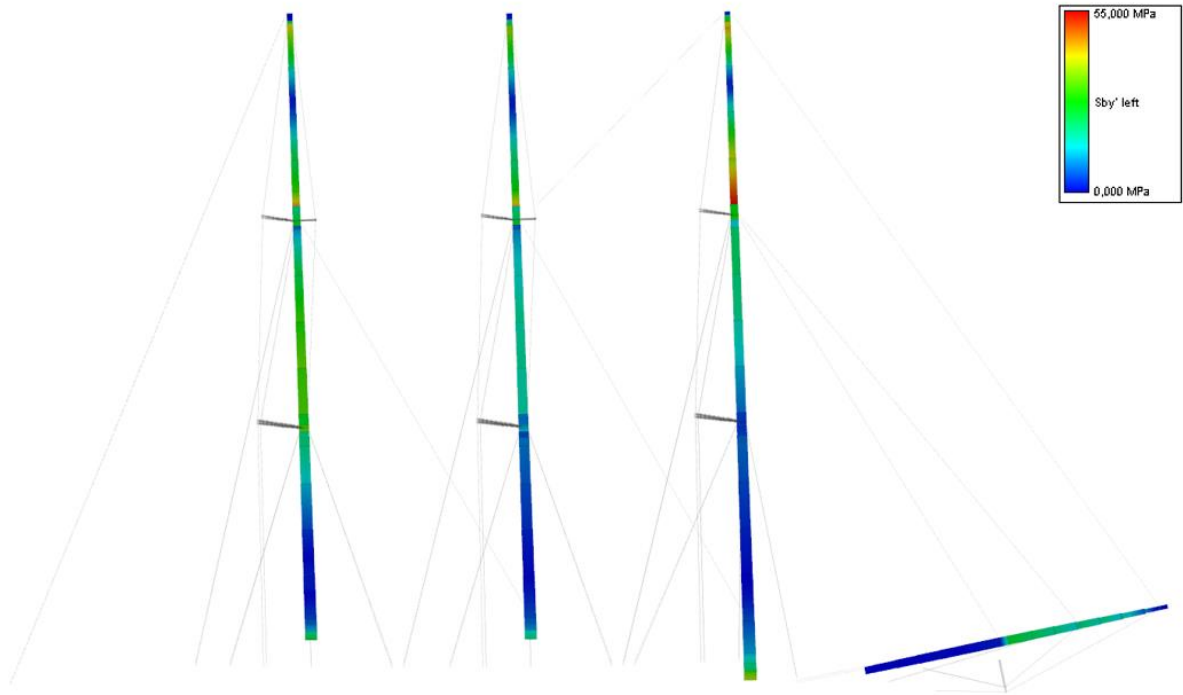
Figure 11 Bending stresses in ship's longitudinal plane for operational load case
Slika 11 Savojna naprezanja u uzdužnoj ravnini broad za operacijski slučaj opterećenja
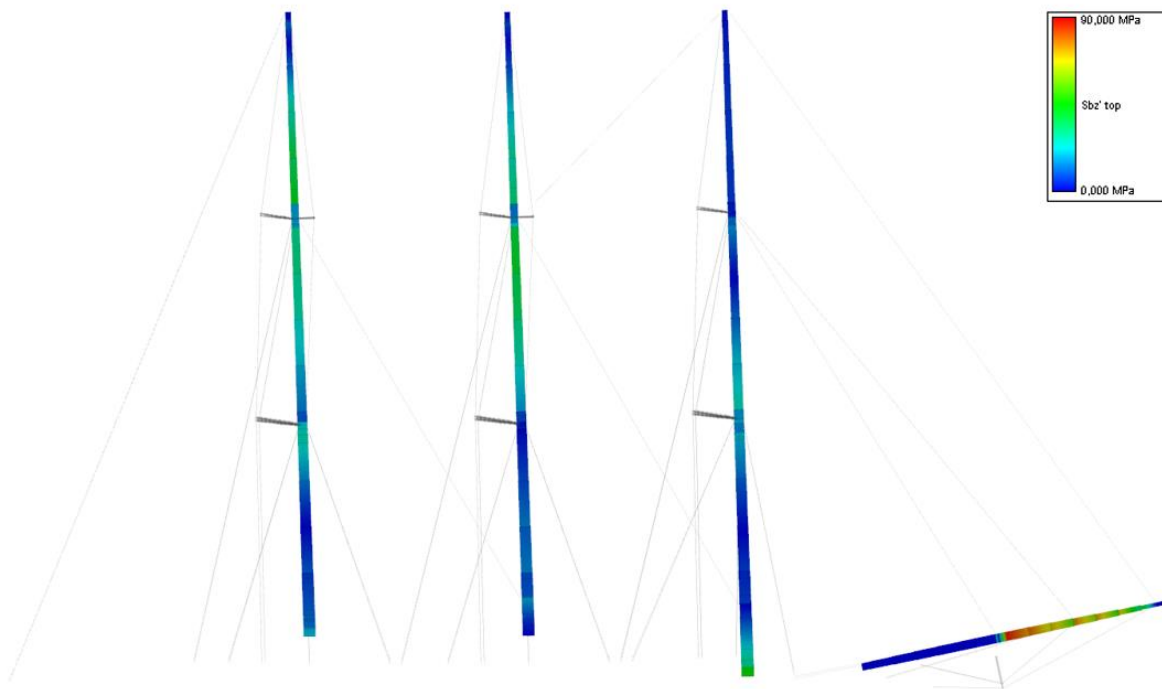
Figure 12 Bending stresses in ship's transverse plane for operational load case
Slika 12 Savojna naprezanja u poprečnoj ravnini broad za operacijski slučaj opterećenja
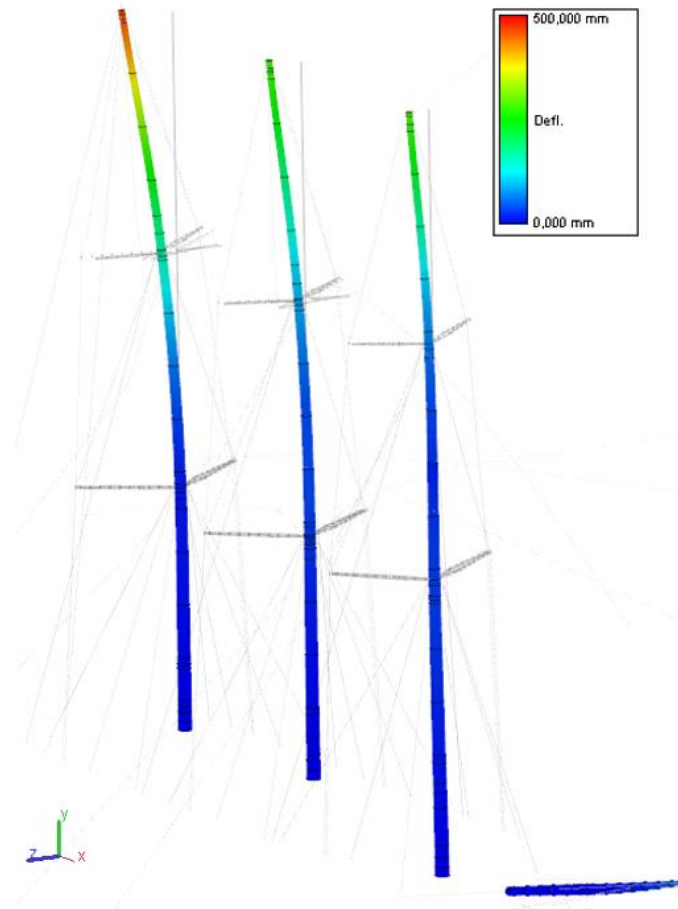
Figure 13 Deflections in operational load case
Slika 13 Pomaci u operacijskom slučaju opterećenja
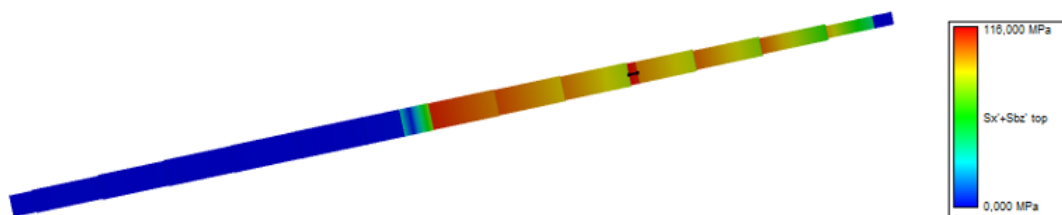
Figure 14 Maximum stresses in bowsprit
Slika 14 Najveća opterećenja u pramčanom kosniku

Regarding eigenvalue buckling analysis, the lowest eigenvalues are 7.4 in operational load case and 17 in survival load case. In both load cases the first buckling mode occurs in mizzenmast (Figure 15). In this study we have opted for [4] in determination of minimum allowable buckling eigenvalue. It is stated that for global stability analysis the lowest eigenvalue should be at least 3.1 which the proposed structure satisfies.

5. Conclusion

This paper has dealt with structural analysis of schooner's masts, bowsprit and standing rigging. It has been demonstrated that the proposed structure fulfils all the classification society's criteria and thus can be of use to designers in dealing with similar projects in the future. However, further

investigations are needed to explain its structural response in detail. Clearly, structural optimisation could be employed to reduce structural mass and enhance ship's stability and propulsion characteristics especially due to the nonlinearity of the problem.
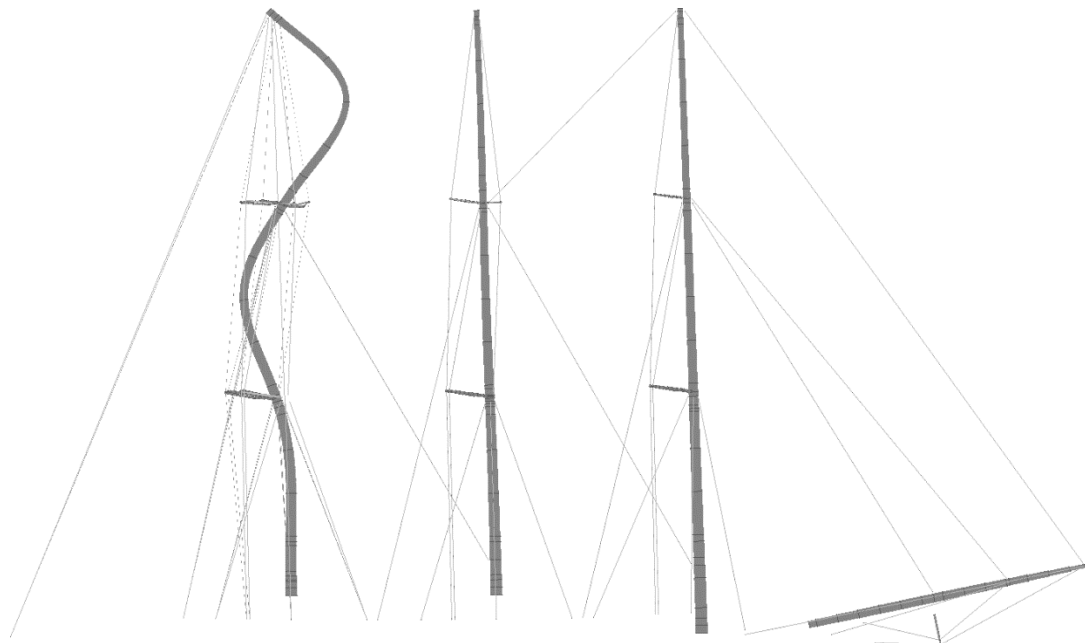
Figure 15 First buckling mode in operational load case
Slika 15 Prvi slučaj izvijanja kod operacijskog slučaja opterećenja

Acknowledgments

REFERENCES

[1]   The Editors of E. Britannica, "Encyclopædia Britannica," Encyclopædia Britannica, inc., 21 January 2011. [Online]. Available: https://www.britannica.com/technology/schooner. [Accessed 01 May 2020].

[2]   M. J. Gudmunsen, "The Verification of Masts and Rigging of Large Sailing Vessels," in *Proceedings of the 16th International Symposium on Yacht Design and Yacht Construction*, 2000.

[3]   NR 206 DNC R00 E: Classification of wind propulsion plants on board ships, Paris, France: Bureau Veritas, 1987.

[4]   DNVGL-ST-0412 Design and construction of large modern yacht rigs, Hovik, Norway: DNV-GL, 2016.

AN ARTIFICIAL NEURAL NETWORK APPROACH TO WIND LOADS ESTIMATION

*Marko Valčić [a], Jasna Prpić-Oršić *[a], Zoran Čarija [a]*

[a] Faculty of Engineering, University of Rijeka, Vukovarska 58, 51000 Rijeka, Croatia
* Corresponding Author, jasnapo@riteh.hr

Abstract

Various aspects of exposed ship structure have major impact on the accuracy of wind load estimation methods. Although several appropriate approaches for dealing with these issues have been proposed so far, there is still room for improvement. In that context, this paper presents an extension of previously proposed approach, which was based on Elliptic Fourier Descriptors (EFD) that are used for ship frontal and lateral closed contour representation. In previous research, the Generalized Regression Neural Network (GRNN) was trained with elliptic Fourier descriptors of a set of closed contours and non-dimensional wind load coefficients obtained from experimental wind tunnel tests. In this paper, training and testing sample is expanded with wind load coefficients derived from 3D steady RANS Computational Fluid Dynamic (CFD) analysis. In this way, the cheaper and faster calculation can bridge the gap between ship shapes for which calculations or experiments have already been made. The obtained neural network (NN) responses are well aligned with results of available experiments and obtained CFD results. Simulations used for this purpose were based on the analysis of the relationship of various container configurations on the deck of a 9000+ TEU container ship and associated wind forces and moments.

Key words: Computational Fluid Dynamics (CFD); Neural networks; Wind loads on ships

Sažetak

Različiti aspekti izloženog dijela konstrukcije broda imaju značajan utjecaj na točnost metoda procjene vjetrovnog opterećenja. Iako je do sada predloženo nekoliko prikladnih pristupa za rješavanje ovih problema, još uvijek ima prostora za poboljšanje. U tom kontekstu, ovaj rad predstavlja proširenje prethodno predloženog pristupa koji se temelji na eliptičnim Fourierovim deskriptorima (EFD), a koji se koriste za modeliranje vanjske zatvorene konture frontalnih i lateralnih projiciranih površina. U prethodnim istraživanjima, generalizirana regresijska neuronska mreža (GRNN) je bila trenirana s eliptičnim Fourierovim deskriptorima skupa zatvorenih kontura te s bez-dimenzijskim koeficijentima opterećenja vjetra dobivenih eksperimentalnim ispitivanjima u vjetrovnim tunelima. U ovom radu uzorak za treniranje i testiranje je proširen koeficijentima opterećenja vjetra dobivenima koristeći metode računalne dinamike fluida (CFD). Na taj način, jeftiniji i brži izračuni mogu premostiti jaz između različitih geometrijskih karakteristika brodskih formi za koje su proračuni ili eksperimenti već napravljeni u odnosu na one za koje nisu. Dobiveni odzivi neuronske mreže dobro su usklađeni s rezultatima dostupnih eksperimentalnih vrijednosti, kao i s rezultatima dobivenima pomoću računalne dinamike fluida. Simulacije korištene u tu svrhu temeljile su se na analizi odnosa različitih konfiguracija kontejnera na palubi kontejnerskog broda od 9000+ TEU s obzirom na odgovarajuće sile i momente uslijed djelovanja vjetra.

Ključne riječi: računalna dinamika fluida; neuronske mreže; vjetrovno opterećenje na brodove

1. Introduction

Although the load on ships and marine structures due to wind does not represent the most important part of environmental loads, it still plays an important role in many aspects of exposed marine structure exploitation. Accurate estimation of forces and moments caused by wind represents a challenge because of its implications for various analysis related to ship stability, ship speed estimation, maneuvering, station-keeping and berthing. Experimental research is still the best and most reliable approach. However, experiments are very demanding and expensive. It is

necessary to have a wind tunnel at disposal and build a ship model, which is lifelike as much as possible. Even then, the obtained results can be used only for that specific ship. Researchers realized quite early that it is necessary to systematically perform a series of experiments and then overcome the gap between them by some interpolation method.

Andersen [1] carried out an investigation of the influence of container configuration on the deck of a 9000+ TEU container ship on wind forces through a series of wind tunnel tests. She showed the influence of container configuration on longitudinal force.

Recently, computational fluid dynamics (CFD) is increasingly used in the assessment of the impact of wind on marine structures. Compared with wind tunnel testing, CFD has many advantages, of which the most obvious is lower cost and faster performance. Obviously, this doesn't mean that such tests can replace measurements in laboratory conditions, but they are very suitable for visualization of results and for preparatory calculations. However, the results can often be deceiving because they are affected by the mesh and input data selection as well as by the choice of the CFD method. Brizzolara and Rizzuto [2] used CFD methods to investigate the wind pressure field on superstructures of large commercial ships, in particular the suction area on the main deck caused by the presence of a negative pressure field.

Wnek and Guedes Soares [3] used a CFD code to analyse wind forces on a floating LNG platform and an LNG carrier. They compared obtained results with experimental ones and achieved a reasonable agreement. There are several other authors who have dealt with this kind of problem and a short overview can be found in Wnek and Guedes Soares [3]. Janssen et al. [4] presented 3D steady RANS CFD simulations of wind loads on a container ship, validation with wind-tunnel measurements [1], and an analysis of the impact of geometrical simplifications. For the validation, CFD simulations are performed in a narrow computational domain resembling the cross-section of the wind tunnel. Blockage effects caused by the domain boundaries are studied by comparing CFD results in the wind tunnel domain and a larger domain. Their study shows the importance of validating CFD simulations with measurements.

The approach to wind load estimation presented in this paper is based on elliptic Fourier features of a closed contour that can be used for describing ship frontal and lateral closed contours. The obtained set of data combined with the wind load coefficients data are used to train the approximating radial basis neural network. The methodology is simple to use and can capture variability of transverse and longitudinal ship contour. This approach of wind load estimation method, where Generalized Regression Neural Network (GRNN) is trained by elliptic Fourier descriptors of set of closed contours and wind coefficients, is proposed by Valčić and Prpić-Oršić [5]. In addition to that, the approach is now extended with the 3D steady RANS Computational Fluid Dynamic (CFD) analysis for the estimation of wind load coefficients during neural network deployment phase.

2. Hybrid methodology for wind loads estimation

2.1. Theoretical background

The wind load estimation method used in this paper consists of four basic parts. Hence, phases of image editing, pre-processing and data preparation for training, validation and testing of neural network should include the following steps [5]:

(*i*) Acquisition and pre-processing of vessel images

At first, the capturing of real images, i.e. bow and side vessel views with their transformations into a digital representation are required. This can be done by digital cameras, but other acquisition techniques can also be used as well, e.g. scanning or editing of existing photos and project/technical documentation, editing of 2D or 3D CAD models, etc. Pre-processing phase is based on further digital editing of photos/figures which can include: discarding of unimportant image parts, overall image enhancement, grey scale conversion, object segmentation, etc. It is convenient to emphasize that the most important part of pre-processing phase is image binarization, i.e. converting background colour to white and vessel colour to black or vice versa.

(*ii*) Feature extraction of frontal and lateral projections

This phase covers the procedure of obtaining the information about vessel outer contour from the vessel binarized image. For this purpose, Freeman chain encoding method was used [6].

(*iii*) Input and target data preparation for neural network training

Input data for the training of the GRNN [7], i.e. mathematical description of frontal and lateral ship projections, are prepared using Freeman chain encoding coupled with elliptic Fourier analysis. In terms of different number of harmonics used in this elliptic analysis, better approximation of analyzed closed contour can be obtained, but some caution is required in order to avoid undesirable overfitting. On the other hand, target data, i.e. appropriate wind load coefficients are prepared using both experimental data from wind tunnel tests [1] and CFD calculations [8].

(*iv*) Validating, testing and retraining of deployed neural network

In order to determine the mapping of elliptic Fourier descriptors to wind load coefficients, generalized regression neural network [7] has been used in this paper. Training and testing were conducted for the same container ship, but with different container configurations.

2.2. *Reference frames and notation of characteristic quantities*

Geographic reference frames are illustrated in Figure 1, where x_n and y_n denote North and East axis of North-East-Down (NED) reference frame {n}, while x_b and y_b denote surge and sway axis of body-reference frame {b}, respectively [9].
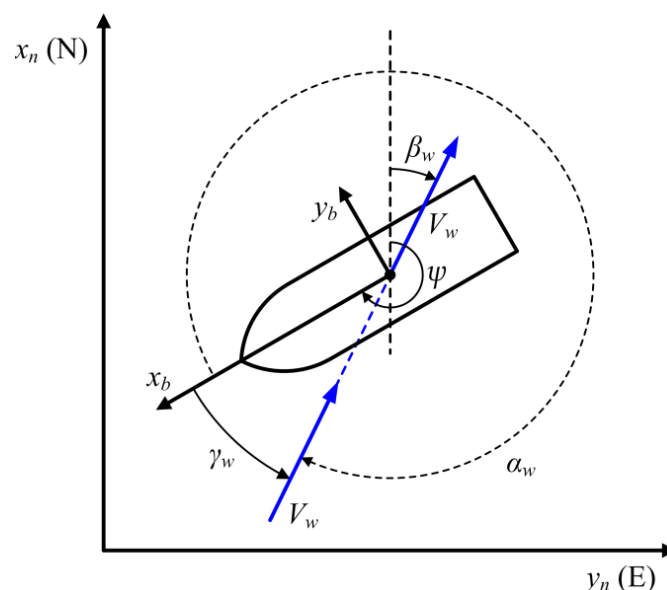
Figure 49 *Reference frames and notation*
Slika 1 Referentni koordinatni sustavi i notacija

The wind speed V_w and wind direction β_w are usually measured by the anemometers with respect to {n}, while the wind angle γ_w is defined in {b} with respect to x_b axis in a counter-clockwise direction.

2.3. Wind loads on marine vessel at rest

For a marine vessel at rest, i.e. with zero forward speed, the wind loads in surge, sway and yaw axis can be expressed in terms of the non-dimensional wind load coefficients $C_X(\gamma_w)$, $C_Y(\gamma_w)$ and $C_N(\gamma_w)$ according to

$$\begin{bmatrix} X_{wind} \\ Y_{wind} \\ M_{wind} \end{bmatrix} = \frac{1}{2}\rho_a V_w^2 \begin{bmatrix} C_X(\gamma_w)A_F \\ C_Y(\gamma_w)A_L \\ C_N(\gamma_w)A_L L_{oa} \end{bmatrix}, \tag{1}$$

where X_{wind}, Y_{wind} and M_{wind} are wind forces and moment in surge, sway and yaw, respectively, ρ_a is the air density, A_L and A_F are the vessel's frontal and lateral projected areas above the water line, respectively, and L_{oa} is vessel's length over all.

It is important to emphasize that if the vessel is moving at a forward speed U then (1) should be redefined in terms of relative wind speed and relative angle. In this paper, only the results from the model tests and CFD analyses have been used so the relativity of wind speed and angle can be neglected. It is presumed that the ship forward speed is equal to zero.

As mentioned previously, non-dimensional wind load coefficients are usually computed numerically or can be determined experimentally in wind tunnels using appropriate scaled vessel models and other necessary equipment. Based on (1), they can be expressed relative to the bow as

$$\begin{bmatrix} C_X(\gamma_w) \\ C_Y(\gamma_w) \\ C_N(\gamma_w) \end{bmatrix} = \frac{2}{\rho_a V_w^2} \begin{bmatrix} X_{wind}/A_F \\ Y_{wind}/A_L \\ M_{wind}/(A_L L_{oa}) \end{bmatrix}. \tag{2}$$

2.4. A method for wind load estimation based on EFDs and GRNN

Valčić and Prpić-Oršić [5] proposed a novel methodology for the estimation of the wind loads on ships based on EFDs and GRNN techniques. In comparison with the originally proposed methodology [5], this one, also shown in Figure 2, can be subdivided into three characteristic parts [8]:

(*i*) CFD analysis and numerical calculation of wind load coefficients

(*ii*) Model deployment based on CFD results, EFDs and GRNN

(*iii*) Additional independent testing and forthcoming application of deployed NN model.

Therefore, in the first part of this enhanced methodology, CFD analysis is used in order to calculate wind load coefficients for various container configurations on deck. Available experimental results are used for calibrating CFD model and for additional verification.

Afterwards, in the second part, it is necessary to build appropriate knowledge database for NN training, validation and testing. For this purpose, all available vessel images should be collected and edited in accordance to the criteria defined in sub-chapter 2.1. It is important to emphasize that vessel's length over all (L_{oa}), if necessary, can be used for image scaling, while frontal and lateral projected areas (A_F, A_L) can be used as control variables. Resulting binarized images of frontal and lateral projected areas should be prepared so the Freeman chain encoding can be performed in the simplest way possible.

Graphical representation of Freeman chain encoding is shown in Figure 3 (right up). Therefore, after the vessel image has been edited and binarized, the chain encoding can be performed from an arbitrary starting point.

Figure 2 *Model deployment and application phase*
Slika 2 Faza razvoja i faza primjene modela

163

Figure 3 *Vector representation of chain encoding and contour extraction based on Freeman chain encoding*
Slika 3 Vektorski prikaz kodiranja lanca i ekstrakcije konture temeljen na Freemanovom kodiranju lanca

An example of chain encoding procedure is presented in Figure 3, where yellow square indicates the starting point and each grey square presents one image pixel. Encoding can be performed both in clockwise or counter-clockwise direction, but for the purpose of this paper encoding is done in counter-clockwise direction. Thus, the chain code is of the form V= 6700000000000000000000000000000000000000000000021114444444532224466653222446666532224 46666532224466665322224466665322224466665322224466665322222244366666665322224466665322224466665. Afterwards, obtained chain-codes are used to calculate EFDs of frontal and lateral projected areas, as described in more detail in [5]. Hence, we need to distinguish two ordered quadruples of EFDs, i.e. an ordered quadruple (a_n, b_n, c_n, d_n) of EFDs for describing frontal projected area and an ordered quadruple (e_n, f_n, g_n, h_n) of EFDs for describing lateral projected area, where n = 1,2,…, N and N is the number of harmonics in Fourier expansion. Both of these quadruples are calculated using Freeman chain encoding and elliptic Fourier descriptors for images of frontal and lateral vessel profiles.

Description of the contour can be achieved by taking into consideration that the image plane defines the complex plane, i.e. each image pixel is represented by a complex number [10]. In order to determine the elliptic Fourier descriptors (EFDs) of a contour, it is necessary to obtain the Fourier expansion of the contour. The Fourier expansion can be performed by using the complex form proposed by Granlund [11] or trigonometric representation of Kuhl and Giardina [10]. The latter approach based on results of Kuhl and Giardina is used in this paper.

Calculated EFDs are foundation of knowledge database since they represent input parameters which contain all the required information about frontal and lateral vessel profile. Once the training, validation and testing of the GRNN is completed in a manner conventional in machine learning, the deployed GRNN model can be used in the forthcoming applications, i.e. in the case when the estimation of non-dimensional wind load coefficients for some new vessel or vessel's configuration is required. Considering very limited number of analyzed container configurations, leave-one-out cross-validation approach was used for this purpose. Thus, deployed GRNN model presents a multivariable non-linear mapping

$$[\text{EFDs}] \xrightarrow{\text{GRNN}} [C_X, C_Y, C_N] \tag{3}$$

i.e. the mapping of frontal and lateral contours described by EFDs to wind load coefficients.

With the appropriate number of harmonics N, close contour can be described very accurately. Figure 4 shows the ship contour (blue line) vs. contour based on different number (N = 10, 100) of

harmonics (red line). It is obvious that chosen contours can be very well captured with only 100 harmonics.

Figure 4 *Contour capturing with different number of harmonics N*
Slika 4 Rekonstrukcija konture s različitim brojem harmonika *N*

Finally, according to (3), the estimation of wind forces and moment can be easily performed by using previously deployed models, frontal and lateral projected areas (A_F, A_L) and filtered anemometer data (V_w, γ_w). It is also important to highlight the capability of this approach according to which it is possible to easily calculate the frontal and lateral projected areas if they are not known in advance. This calculation can be performed during the determination of EFDs.

If the wind load coefficients C_X, C_Y and C_N are already known for some arbitrary new vessel, they can be used either for additional independent testing in application phase or for retraining of deployed NN model in deployment phase in order to increase reliability, accuracy and overall performance.

3. Wind loads estimation with CFD

The ship geometry and the experimental conditions for the CFD simulations are set up according to Andersen set up for wind-tunnel measurements [1][5][8]. The target wind velocity profile, which is a power law with z_{ref} = 0.0222 m (equal to 10 m height in full scale), U_{ref} = 45 m/s, and α = 0.11 is estimated according the formula

$$U(z) = U_{ref} \left(\frac{z}{z_{ref}} \right)^{\alpha} . \tag{4}$$

For velocity profiles over the ocean, α is usually between 0.11 and 0.14, which is the target value for wind tunnel tests of ocean structures [8][12]. The wind load coefficients and corresponding forces and moments are obtained for the wind speed angle in range from 0° to 180°. Figure 5 shows graphic representation of velocity streamlines passing over bays.
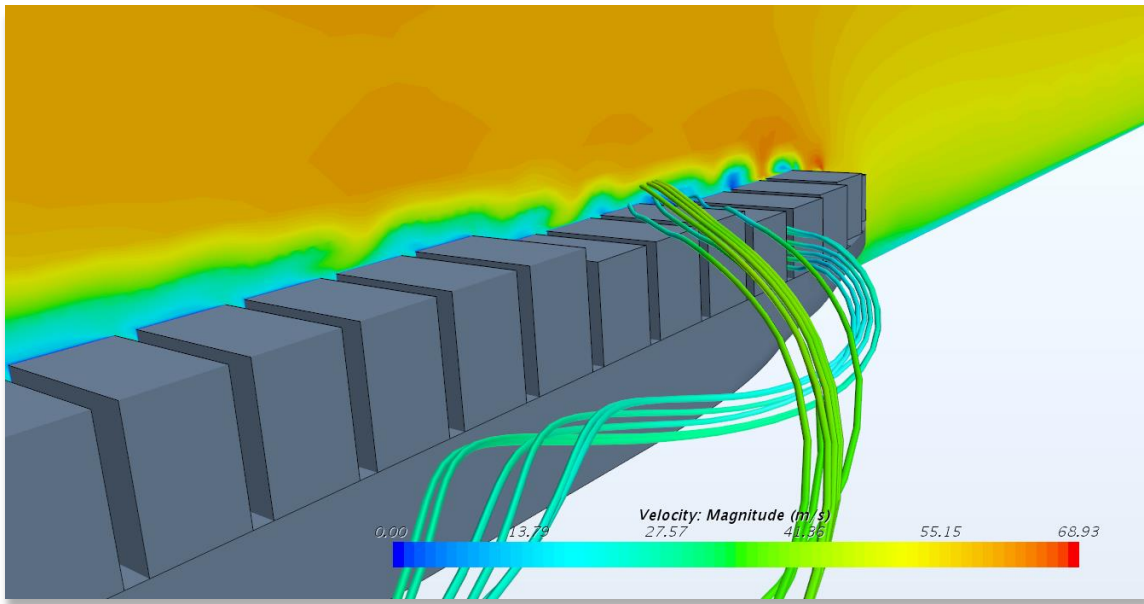
Figure 5 *CFD representation of velocity streamlines*
Slika 5 Prikaz strujnica brzina pomoću računalne dinamike fluida

4. Numerical results

The CFD calculation has been run for the 9000+ container ship, shown in Figure 6 [1], with the main characteristics: L_{oa} = 340 m, L_{pp} = 320 m, B = 45 m. The 17 different container configurations on the deck are shown in Table 1, where the first 13 configurations were analyzed in this paper.
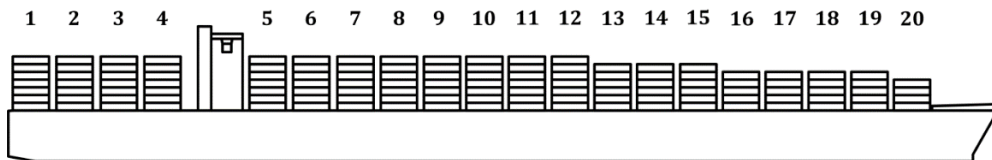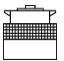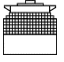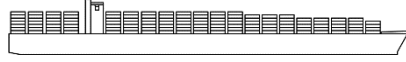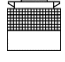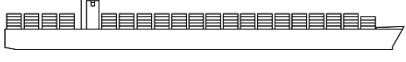
Figure 6 *Analysed container ship*
Slika 6 Analizirani brod za prijevoz kontejnera

Table 1 Container configurations
Table 1 Konfiguracije kontejnera

#	Frontal	Lateral	#	Frontal	Lateral
1			10		
2			11		
3			12		
4			13		

5			14		
6			15		
7			16		
8			17		
9					

In order to ensure the conditions of CFD numerical analysis as much similar as the conditions of the experiment, it was necessary to add a tunnel wall to the boundary conditions. Obtained results, as it can be seen in the following figures, are based on the calculation that has been performed for the two cases, i.e. in case with no influence of wind tunnel walls (uncorrected, blue line) and in case with the influence of wind tunnel walls (corrected, red line).

The findings indicate that uncorrected CFD results deviate somewhat from the experimental ones, especially in the transverse direction. However, the corrected values for the case with wind tunnel walls accounted are in line with those obtained experimentally. Those results are practically equable for the variability of ship lateral profile caused by different container configurations and indicate very good agreement.

It is important to emphasize that the GRNN was trained with 12 arbitrary configurations at a time and the responses are compared with respect to remaining 13-th vessel, as it is usual in leave-one-out cross-validation approach. In other words, the wind load coefficients of 13 analysed container configurations obtained as GRNN responses are compared with corresponding wind load coefficients obtained in experiment [1]. For instance, in Figures 7 and 8, for configurations #4 and #10, respectively, one can see visual comparison of wind load coefficients obtained by GRNN (green line) trained with corrected CFD values (red line), uncorrected CFD results (blue line) and Andersen experimental data (black line). The results clearly indicate that GRNN responses are in very good agreement with wind-tunnel measurements, as well as with corrected CFD results.
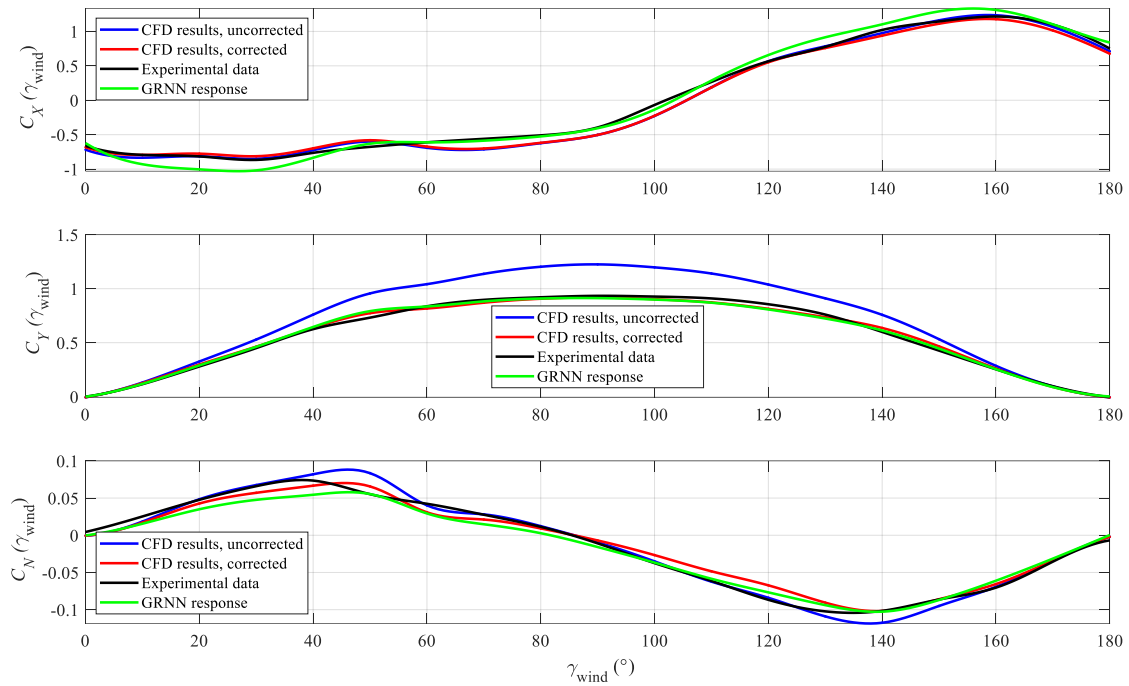
Figure 7 *Wind loads coefficients for configuration #4*
Slika 7 Koeficijenti vjetrovnog opterećenja za konfiguraciju #4
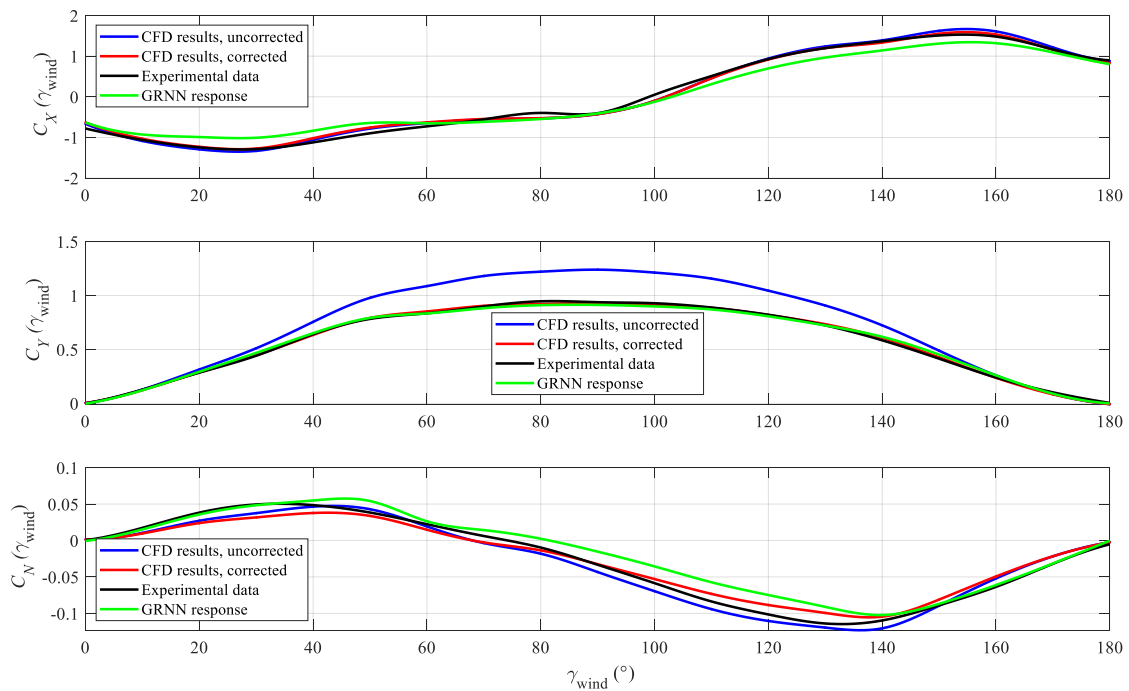
Figure 8 *Wind loads coefficients for configuration #10*
Slika 8 Koeficijenti vjetrovnog opterećenja za konfiguraciju #10

5. Conclusions

An enchanced method for estimating the wind loads on ships is presented in this paper. The method is based on Elliptic Fourier Descriptors (EFD), which are used for ship frontal and lateral closed contour representation. The Generalized Regression Neural Network (GRNN) is trained by elliptic Fourier descriptors of closed contours and wind load data derived from CFD analysis. The validation of CFD model is based on 13 different container configurations of 9000+ container ship for which the experimental results are known. The neural network is created with 13 container configurations so that the network is trained with 12 configurations, and the 13th one is used for testing. Thus, 13 trained networks were examined. The results show good agreement.

This approach takes into account all aspects of the variability of the above water frontal and lateral ship profile. It is very suitable for the assessment of wind loads on ships wherever one has a wind load database for a container ship with various container configurations. In this way, the cheaper and faster calculation can fill the gap between ship shapes above the water line for which calculations or experiments are performed. It is reasonable to believe that the network trained with larger database will provide more accurate results. Moreover, for the estimation of real forces acting on container ship the network should be trained with uncorrected values of wind loads coefficients.

Further research will be aimed toward the uncertainties and reliability analysis, as well to increasing the number of container configurations by means of verified CFD analysis in order to enlarge the available database for neural network training.

Acknowledgment

REFERENCES

[1]   Andersen, I.M.V. Wind loads on post-panamax containership. Ocean Eng. 2013, Vol. 58, 115-134.

[2]   Brizzolara, S., Rizzuto, E., Wind heeling moments on very large ships. Some insights through CFD results. In: Proceedings of the 9th International Conference on Stability of Ships and OceanVehicles, 2006, Rio de Janeiro, Brasil, pp. 781-793.

[3]   Wnek, A.D., Guedes Soares, C., CFD assessment of the wind loads on an LNG carrier and floating platform models. Ocean Eng. 2015, Vol. 97, 30-36.

[4]   Janssen, W.D., Blocken, B., van Wijhe, H.J., Journal of Wind Engineering and Industrial Aerodynamics 2017, Vol. 166, 106-116.

[5]   Valčić, M., Prpić-Oršić, J., Hybrid method for estimating wind loads on ships based on elliptic Fourier analysis and radial basis neural networks. Ocean Eng. 2016, Vol 122, 227-240.

[6]   Freeman, H., Computer Processing of Line-Drawing Images. Comput. Surv. 1974, Vol. 6 (1), 57-97.

[7]   Specht, D.F., A General Regression Neural Network. IEEE T. Neural Networ. 1991, Vol. 2 (6), 568-576.

[8]   Prpić-Oršić, J., Valčić, M., Čarija, Z., Hybrid wind load estimation method for container ship based on computational fluid dynamics and neural networks. J. Mar. Sci. Eng. 2020, Vol. 8 (7), 539.

[9]   Fossen, T.I., Handbook of Marine Craft Hydrodynamics and Motion Control. John Wiley & Sons Ltd, Chichester, UK. 2011.

[10]   Kuhl, F.P., Giardina, C.R., Elliptic Fourier Features of a Closed Contour. Comput. Vision. Graph. 1982, Vol. 18, 236-258.

[11]   Granlund, G.H., Fourier Preprocessing for Hand Print Character Recognition. IEEE T. Comput. 1972, Vol. 21, 195-201.

[12]   Norwegian Maritime Directory, 1997, Regulations for Mobile Offshore Units.

TOURIST CATAMARAN STRUCTURAL ANALYSIS

Parunov Ratko[*a], Parunov Joško[b]*

a Centre for Technology Transfer ltd., Ivana Lučića 5, 10000 Zagreb
b University of Zagreb, Faculty of Mechanical Engineering and Naval Architecture, I. Lučića 5, 10000, Zagreb
* Corresponding Author, ratko.parunov@gmail.com

_____

Abstract

Structural strength analysis of 30 m tourist catamaran is performed according to the Classification Society's Rules. The analysis consists in four parts, i.e. longitudinal, local, torsional and transverse strength calculations. MARS software is used for the longitudinal and local strength, while the finite element method is employed for the torsional and transverse strength calculation. Model loading and boundary conditions are taken in accordance to the Rules of Ship Classification Society. The results of the analysis show that all structural elements satisfy Rule strength requirements.

Key words: tourist catamaran, structural analysis, finite element method

Sažetak

Analiza čvrstoće konstrukcije turističkog katamarana duljine 30 m je provedena u skladu s pravilima klasifikacijskog društva. Analiza se sastoji od četiri vrste proračun, tj. proračuni uzdužne, lokalne, torzijske i poprečne čvrstoće. MARS program je upotrjebljen za proračun uzdužne i lokalne čvrstoće, dok je metoda konačnih elemenata korištena za proračun torzijske i poprečne čvrstoće. Opterećenja i rubni uvjeti za proračun definirani su pravilima klasifikacijskog društva. Rezultati analize pokazuju da svi konstrukcijski elementi zadovoljavaju kriterije čvrstoće klasifikacijskog društva.

Ključne riječi: turistički katamaran, strukturna analiza, metoda konačnih elemenata

_____

1. Introduction

The safety of passengers and crew members has always been a priority for the designers, engineers, classification societies and shipowners. The construction of each ship must be resistant to the maximum load in the area of navigation for which it is designed. To obtain validation that the scantlings and construction solutions are adequate for maximal loads in navigation, structural strength calculation should be performed. Strength analysis of ship structure in general consists of the verification of the global longitudinal strength, primary supporting members and local strength of plates and longitudinals and it is performed in accordance to the Rules of Classification Societies [1]. Different failure criteria are checked in the strength analysis, as the yielding, buckling and fatigue strength.

MARS software is often used for the longitudinal and local strength calculation [2]. Longitudinal strength calculation aims in checking the sectional modulus of transverse sections along the ship, considering structural elements contributing to the longitudinal strength. Local strength calculation consists in checking bending and buckling of longitudinals between web frames (with the effect of the global hull bending included) and local bending and buckling of

the plating between longitudinals and web frames (also including the effect of the global hull bending). In MARS software, all checking criteria necessary for these tasks are inherently implemented. MARS is therefore used for quick verification and dimensioning of structural elements and it very popular tool among ship designers.

Primary longitudinal and transverse supporting members often represent complex grillages and it is not possible to consider these structural elements individually, since their interaction is important. Using the finite element (FE) model it's possible to consider such interaction and to determine the stresses in these members.

In the present study, practical and efficient procedure for the structural strength analysis of the tourist catamaran with length between perpendiculars of about 30 m, breadth abt. 9.5 m, depth abt. 3.3 m and max. speed of 13 knots is described. Longitudinal and local strength analysis is performed using MARS. FE analysis of the torsional strength of the main deck platform between two hulls is carried out using FE software package FEMAP with NX Nastran V11.0. An additional FE check of the main deck structure loaded with a uniform pressure is also presented.

2. Calculation of the longitudinal and local strength

For the purpose of verification of the longitudinal and local strength, 2D model of the catamaran main frame is created in the program MARS. A model consisting of hull and deck elements, which contribute to the longitudinal strength, is shown in Figure 1. Ship is entirely built in higher strength steel AH32 with minimum guaranteed yield stress of 315MPa. Permissible normal stress for strength analysis under global loads reads 180 MPa, determined according to the applicable Rules [3].

The still water bending moment for catamaran in hogging reads 600 kNm. Vertical wave bending moment is 830 kNm. Both bending moments are determined using formulas from the Rules [3]. Therefore, total bending moment amounts 1430 kNm. Section modulus of the ship at bottom is calculated to be $0.065m^3$. Therefore, longitudinal stress caused by the global vertical bending reads 22 MPa, which is much lower than the permissible value.
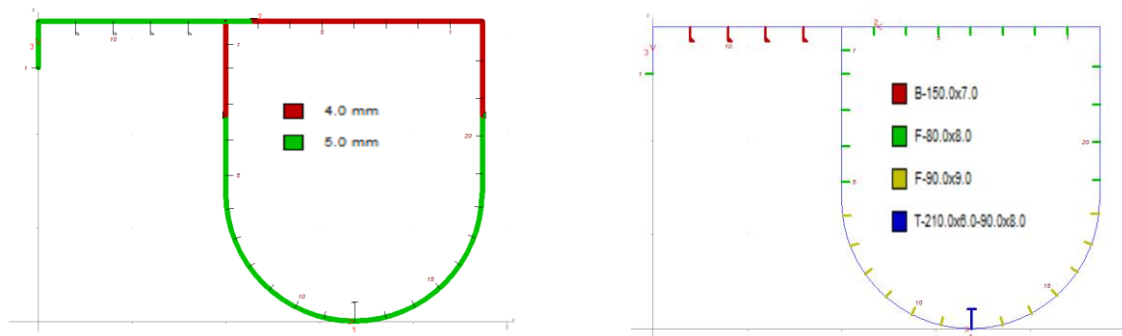
Figure 1 *MARS model of catamaran midship section (half of the complete section) left – plate thickness, right – stiffener scantlings*
Slika 1 MARS model glavnog rebra katamarana (polovica poprečnog presjeka) lijevo – debljine oploćenja, desno- dimenzije uzdužnjaka

As expected, longitudinal strength for such small ship is not an issue. The reason is that maximum vertical wave bending moment is achieved for the case when the wave length is approximately equal to the ship length. As the ship is only 30 m in length, waves equal to the ship length have small wave heights and therefore cannot produce large vertical wave bending moment.

The local strength of the plates and longitudinals was checked by the MARS program using Rules [4]. The results are shown in Figure 2. Although the plating and longitudinals fully satisfy Rule requirements, it can be noticed that the results for the local strength are closer to the allowable limit than stresses resulting from the vertical bending moments.
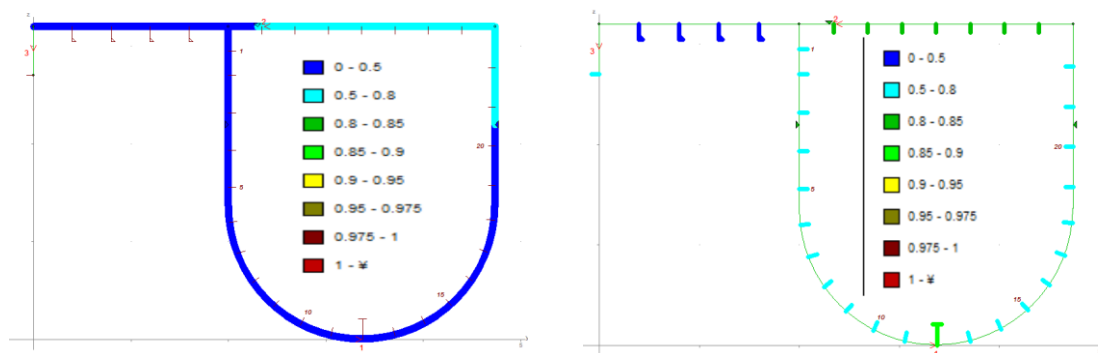
Figure 2 *Results of calculation in MARS (left plating, right longitudinals)*
Slika 2 Resultati MARS proračuna (lijevo opločenje, desno uzdužnjaci)

3. FE torsional and transverse strength calculation

3D FE model of the catamaran, used for torsional and transverse strength calculation is shown in Figure 3. The model is made in software FEMAP based on the relevant structural drawings. All plating, girders, and web frames are modelled by shell finite elements while the stiffeners and ordinary frames are modelled by bar finite elements. Mesh size is such to have one element between longitudinals. The model consists of 1440 nodes, 6220 plate elements and 5200 bar elements.
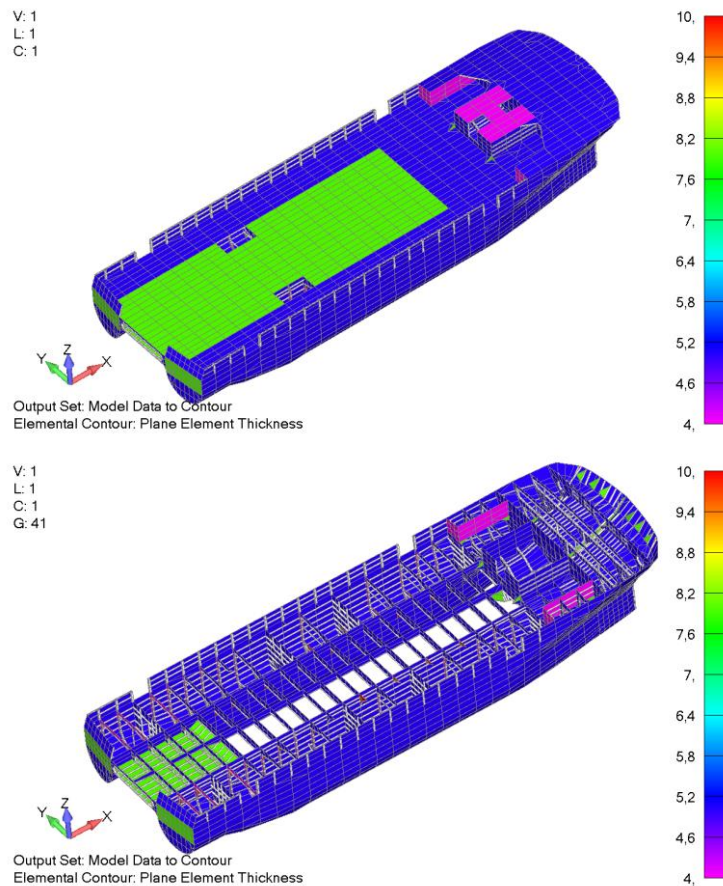
Figure 3 *3D FEM model of catamaran (up - full model, down – main deck omitted)*
Slika 3 3D MKE model katamarana (gore – cijeli model, dolje – ispuštena glavna paluba)

Loads and boundary conditions for the main deck torsional strength calculation are determined according to the BV Rule Note NR 600 [3]. It is assumed that in the quartering seas condition, catamaran encounters sinusoidal wave equal to the diagonal length of the ship [3]. Such oblique wave loading may be approximated by set of the opposite vertical forces acting on the perpendiculars of each of two hulls. Classification Society recommends simplified beam calculation model for this type of the analysis, which is shown in Figure 4. The magnitude of each vertical force is determined according to [3]. Boundary conditions are such that the main deck is clamped at the junction with one of the hulls.

In the present study, 3D FE model is used instead of the beam model in order to obtain more realistic stress distribution. Loading and boundary conditions on the 3D FE model, corresponding to the Rule recommended calculation model from Figure 4 is shown in Figure 5. One may observe opposite vertical loads at perpendiculars of one of two hulls and clamped boundary conditions at the connection of the main deck and the other one of two hulls.
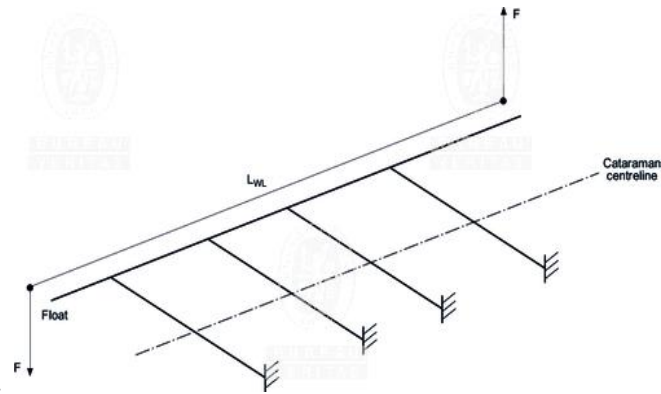
Figure 4 *Recommended calculation model for the torsional analysis* [3]
Slika 4 Preporučeni proračunski model za analizu torzije [3]
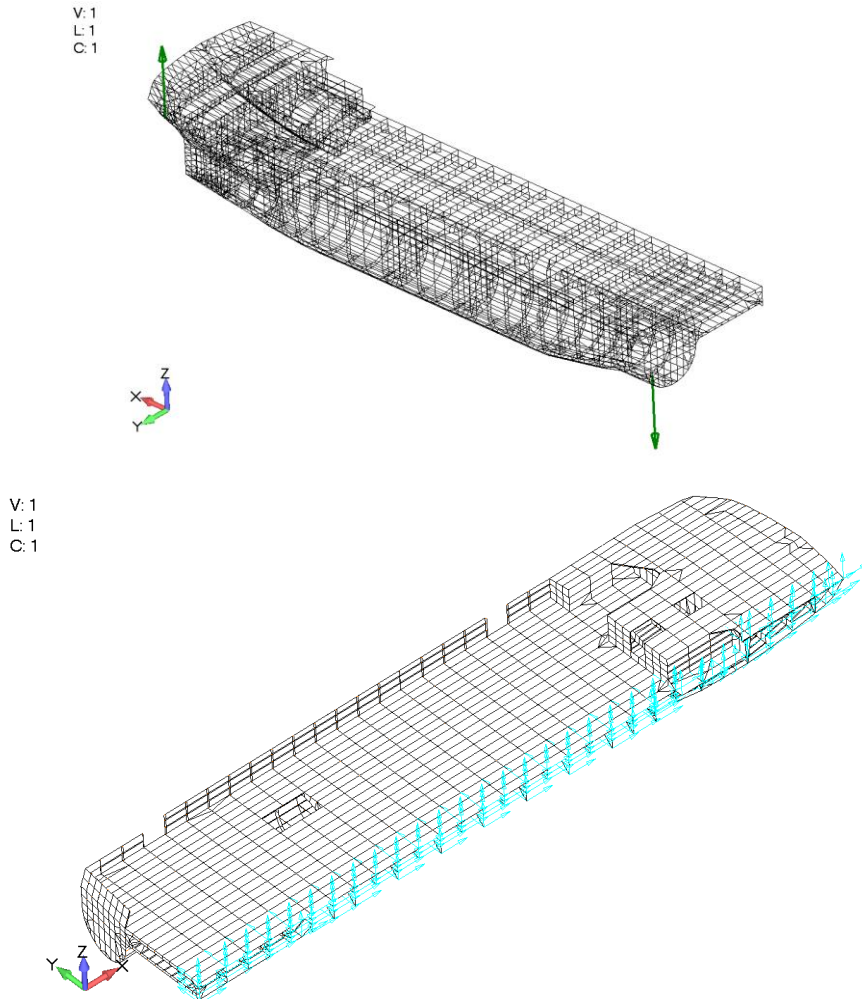
Figure 5 *Loading and boundary condition of 3D FEM model for torsional strength analysis (upper – loading with two opposite vertical forces, visible in green; lower – boundary conditions –prevented all deformations at the connection of the platform and one hull)*

It should be clarified that the presented analysis is practical approach enabling relatively fast analysis procedure. More sophisticated approach could be employed where catamaran may be loaded by hydrostatic and wave pressure. However, such approach, although presumably more accurate is time consuming and therefore outside of the scope of the present study.

Digging is type of the wave-induced loading that can be relevant for the catamaran hull, corresponding to the situation where the catamaran sails in quartering sea condition and has the fore end of the floats burying into the encountered waves [3]. This loading condition may be omitted if the main deck platform between hulls is extending close to the fore end. This is the case for the present ship (Figure 3) and digging is therefore not considered.

For the purpose of verification of the transverse strength of the main deck, the FE model is loaded with a surface distributed load of $16\,\mathrm{kN/m^2}$. The boundary conditions are set to prevent hull deformation at an appropriate distance from the main deck, so there is no effect on the results of the calculation. The model with the main deck pressure load is shown in Figure 6.
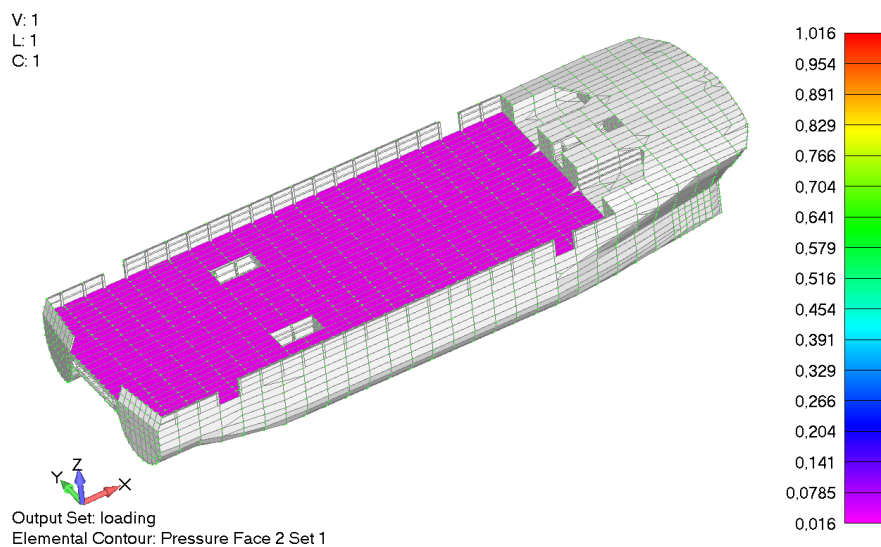
Figure 6 *The model with the main deck pressure load*
Slika 6 Model s opterećenjem glavne palube vanjskim tlakom

Figure 7 shows the results of FEM torsional analysis, i.e. von Misses stresses in the main deck structures (plate of the main deck and girders of the main deck). These stresses are low, with maximum value of 35 MPa, which is well below the permissible stresses of 180MPa.
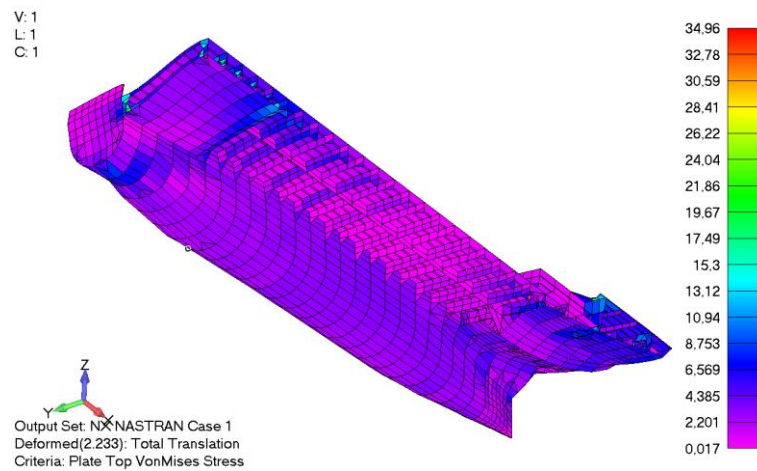
Figure 7 *Von Mises stresses in plating and girders for torsional loading*
Figure 7 Von Mises naprezanja u oploćenju i nosačima za torzijsko opterećenje

Figure 8 shows the axial stresses in flanges of main deck girders for torsional loading. These stresses are also low, with maximum value of 22 MPa.
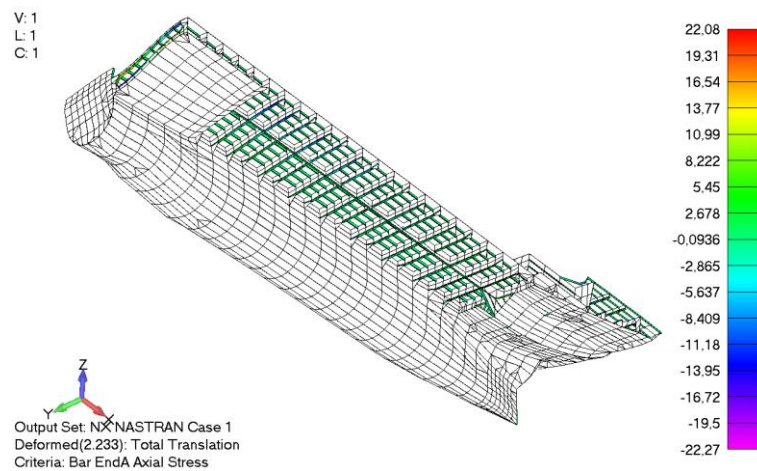
Figure 8 *Stresses in flanges of main deck girders for torsional loading*
Slika 8 Naprezanja u pojasnim trakama nosača glavne palube za torzijsko opterećenje

Results of the transverse strength analysis are shown in Figure 9. Von Mises stresses are at the level of 40 MPa, which is well under allowable stress of 180 MPa.
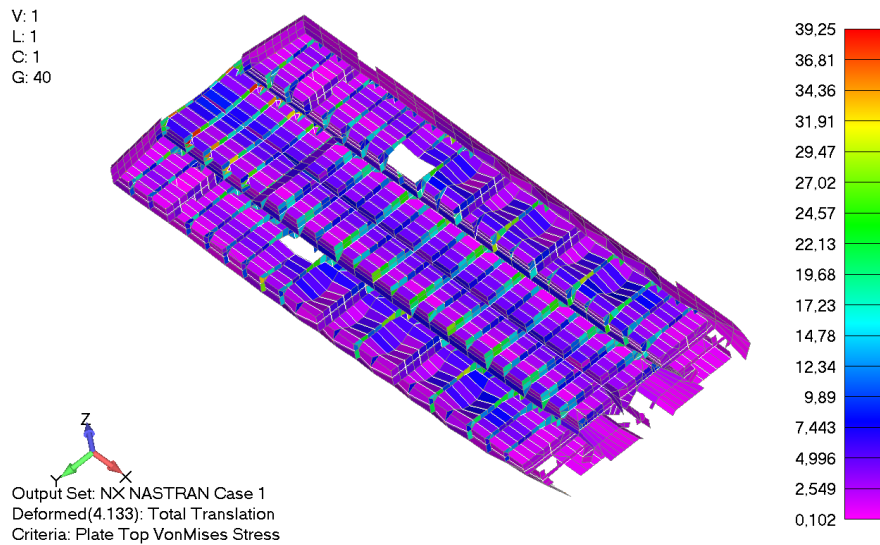
Figure 9 *Von Mises stresses in plating for deck pressure loading*
Slika 9 Von Misesova naprezanja u oploćenju za slučaj opterećenja palube vanjskim tlakom

Figure 10 shows the axial stresses in flanges of main deck girders. These stresses are also low, with maximum value of about 41 MPa.

Figure 10 *Stresses in flanges of main deck girders for deck pressure loading*
Slika 10 Naprezanja u pojasnim trakama nosača palube za slučaj opterećenja palube vanjskim tlakom

4. Conclusion

The practical procedure of the structural strength analysis of the tourist catamaran with length of about 30 m was presented. The whole procedure was done according to the Rules of

Classification Society. Longitudinal and local strength analysis was performed using MARS software. Torsional and transverse strength calculations of the main deck platform were carried out using FEM. Results of the longitudinal and local strength calculations showed that construction fully met the requirements of Ship Classification Rules. Results of FEM analysis of transverse and torsional strength showed that stresses in the main deck structure are acceptable.

Acknowledgments

REFERENCES

[1]   Hughes, O.F, Paik J.K., Ship Structural Analysis and Design, SNAME, 2010.
[2]   Bureau Veritas, MARS 2000, Version 2.9m Feb 11, 2018, Modeler User's Guide.
[3]   Bureau Veritas, "NR 600 Hull structure and arrangement for the classification of cargo ships less than 65 m and non-cargo ships less than 90 m", 2018.
[4]   Bureau Veritas, "NR 467 Rules for the classification of steel ships", 2018.

STRUCTURAL ASPECTS DURING CONVERSION FROM GENERAL CARGO SHIPS TO CEMENT CARRIERS

Paul Jurišić [a], Joško Parunov [b]

[a]   Croatian Register of Shipping (CRS); Marasovićeva 67, 21000 Split

[b]   Faculty of Mechanical Engineering and Naval Architecture; I. Lučića 5; 10000 Zagreb

* Coresponding author: Paul Jurisic, paul.jurisic@crs.hr

Abstract

During the major conversion from one to another ship type, a level of technical assurance is required through the design approval by national and international classification and statutory authorities, in order to keep adequate safety level and cost efficiency of converted ships further in their service. In this study is described general approach to convert general cargo or small-size container ships to cement carriers. The approaches taken by classification society CRS to carry out a comprehensive re-appraisal of conditions of ship, considering its history and present condition of the structure, is provided. Two case studies are presented where the strength assessment has been performed using 3D Finite Element model generated according to available hull drawings and thickness measurement reports. Results of the study are interpreted with respect to the structural modifications carried out during conversion process and some general conclusions are drawn.

Key words: *Ship structures; general cargo ships; cement carriers; major conversion; finite element method*

Sažetak

Tijekom velikih konverzija iz jednog tipa broda u drugi potrebno je u projektu definirati odgovarajući nivo tehničkog osiguranja uz odobrenje nacionalnih i međunarodnih klasifikacijskih i statutarnih tijela kako bi se održala razina sigurnosti i isplativosti obnovljenih brodova u njihovoj daljnjoj službi. U ovoj je studiji opisan opći pristup pri konverziji brodova za opći teret ili brodova za kontejnere malih dimenzija u brodove za prijevoz cementa. Predložen je pristup klasifikacijskog društva HRB u nastojanju da izvrši sveobuhvatnu procjenu stanja broda, uzimajući u obzir njegova akumulirana oštećenja u prošlosti i trenutno stanje konstrukcije. Predstavljena su dva primjera broda gdje su procjene čvrstoće provedene pomoću 3D modela konačnih elemenata generiranog prema dostupnim nacrtima konstrukcije trupa i izvješćima o mjerenju debljine. Rezultati studije objašnjeni su s obzirom na izvršenu strukturnu analizu provedenu tijekom postupka konverzije i izneseni su neki opći zaključci.

Ključne riječi: *Brodska konstrukcija, brod za opći teret, brod za prijevoz cementa, velika preinaka, metoda konačnih elemenata*

1. Introduction

The current trends in the global marine marketplace is that new building orders for bulk and cement carriers, oil tankers and container ships have significantly reduced, which resulted the need for life extension of these ships more important [1]. Before planning the conversion of existing ships, it would be necessary to perform condition assessment of a vessel, which requires structural analysis and determination of corrosion diminution based on the hull thickness measurement [2]. Classification societies have been developing software packages for ships in service that have integrated module for a corroded structure with using finite element method (FEM model) and taking into account the survey report from hull inspections.

The conversion occupies a special place among different variants of essential modernizations. It means dimensional modernization of the vessel with survey of all her parts as new ones, i.e. on compliance to requirements of the International Conventions and the Rules of Classification Society. Conversion allows remediating problems of essential life prolongation and maintaining the safety at a reasonable level and with smaller expense than it is necessary for new construction.

However, conversion requires the accounting of the some defects which were accumulated during operation of the vessel pre-conversion e.g. corrosion and mechanical wear of hull constructions and welded joints, especially local thinning which are badly documented and not considered at the traditional strength calculations, deformations of the inner bottom and inner side as a result of contact with cargo and cargo handling gauges in ports, deformation of the outer shell as a result of contact with ground at shallow water. Also, the accumulated fatigue damages at the zone of stress concentration, especially micro-crack and violations of crystal structure of material that cannot be found at surveys, as well as possible alternation of the mechanical properties of material of the hull (ageing) is to be consider.

In this study the conversion from general cargo ships to cement carriers is based on the principles of the scientifically based approach of definition of border between installation of new elements and usage of the old ones. In order to fully meet the set of the international and national requirements for building date of the vessel under conversion, the application of modern calculation methods and technologies have been performed. Two case studies are presented in this paper where the strength assessment has been performed using 3D Finite Element model generated according to available hull drawings and thickness measurement reports.

2. Cargo system of cement carriers

The cargo system of the subjected cement carriers for loading and discharge is supplied by the company Cargo Flex® and accompanying equipment is installed on board the ships during these conversions. The main office of Cargo Flex® is based in the Netherlands near Rotterdam which is the biggest industrial port of Europe. The dry bulk transfer system is designed for installation on-board of a self-discharging pneumatic dry bulk carrier. The system as offered is suitable for loading and transferring dry products, loading can be done by gravity, pneumatically and mechanically, while discharging can be done pneumatically directly into a silo or shed, or mechanically directly into the trucks. Cargo Flex® loading and discharging equipment are generally located in four, 40 feet containers, secured to the existing hatch covers with the existing container twist locks and supporting structure. The Flex dry bulk transfer system is a fully automated system which can be controlled via the local control panels.

Loading of the dry bulk into the atmospheric cargo holds will take place from shore, the dry bulk will be loaded into the atmospheric cargo holds via the delivered air slides (by gravity) or optional by means of pneumatic transportation. The air slides has been fed mechanically or by gravity with a maximum feeding rate or alternatively the cargo holds can be loaded pneumatically by using the quick connection couplings for example 8 (eight) on ship PS, 8 (eight) on ship SB and 4 (four) on the general loading line leading to the air slides.

The new installed batch tank room comprises steel plates and stiffeners have been fitted into ship holds no. 1 and 2. The batch tank room bulkheads penetrate the hatch covers and are sealed using collar plates. Two batch tanks, which function during the unloading process, are fitted inside tank rooms. The cargo loading and discharge system is supplied by the company Cargo Flex® and an accompanying Cargo Flex® equipment is installed on board the ship during this conversion. Cargo Flex® loading and discharging equipment is generally located in four, 40 feet containers, secured to the existing hatch covers with the existing container twist locks and supporting structure. Two new vent houses have been added to the permanently welded hatch covers to accommodate the cargo hold vents and filter units and two new deck's cranes are also fitted on the top existing hatch coamings in order to improve the cargo handling, during the cargo loading/unloading sequences.

3. Cargo ships chosen for conversion

The observed two ships are originally built as general cargo ships in which the inner bottom is continues from aft bulkhead in engine room to forward bulkhead in fore peak. Inner bottom and hull are strengthening for carrying heavy cargo. Double bottom and double side area may be used as ballast tanks. The both ships have the holds designed for carrying containers and heavy cargo, while first ship has only one rectangular hold and second has three holds.

The first one originally had only one hold of 52,6 m in length and 10,2 m in breadth. In that large amount hold a new corrugated bulkhead is fitted. Consequently, the ship now has two separate holds for the cement cargo load. General arrangement after major conversion of the first one converted ship with originally built three container holds is shown on the Figure 1.
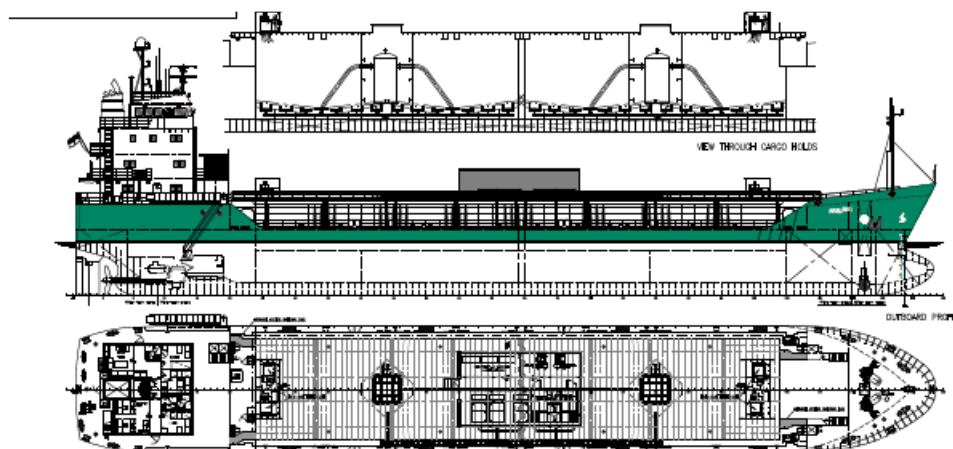
Figure 1 General arrangement of the ship no.1 after major conversion

Slika 50 Opći plan broda br.1 poslije velike konverzije

Each of the holds are fitted with a raised steel hold bottom, supported by transverse and longitudinal structure, which will form the base for the fluidizing beds, respectably new inner bottom and located above the existing tank top. The new raised hold bottom is outfitted with a fabric covering, fitted to the hold bottom plate with a series of studs, flat bars and rubber protection strips. This arrangement forms a fluidizing bed for the aeration of the cement cargo. This conversion has not included any changed of the existing water ballast system. Consequently, the water ballast tanks have not been changed, also. Local structure (stiffeners and frames) of some ballast tanks has been reinforced in way to accommodate new fluidizing bed but without change in the tank's capacity.

The original vessel's single skin hatch covers have their wheels, seals and hydraulic cylinders. Those elements have been removed and sides of hatch covers has been reinforced with thicker insert plates and welded to the existing hatch coamings using an arrangement of flat bars and half tube connections. The cargo hatch covers (eight pcs.) are permanently connected to each other and reinforced with longitudinal stiffeners, thus creating a new continuous trunk deck.

Table 16 Main characteristic of two observed general cargo ships
Tablica 1. Glavne karakteristike dva analizirana broda za opći teret

		Ship no. 1	Ship no.2
Length	Loa	85.4 m	121.9 m
Breadth	B	12.8 m	19.2 m
Depth	D	6.5 m	9.1 m
Draught	Tsc	5.6 m	7.52 m
Deadweight	DWT	3000 tons	7650 tons

General arrangement before and after major conversion of the second one converted ship with originally built three containers holds is shown on the Figure 1.
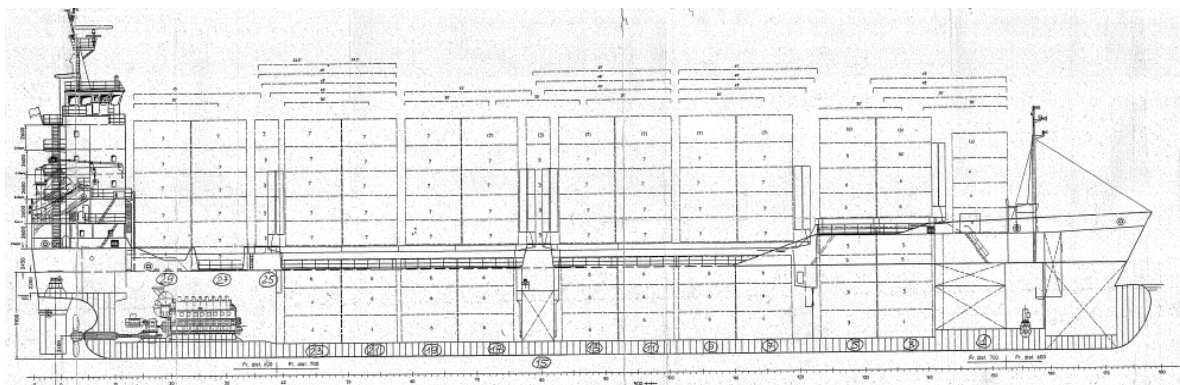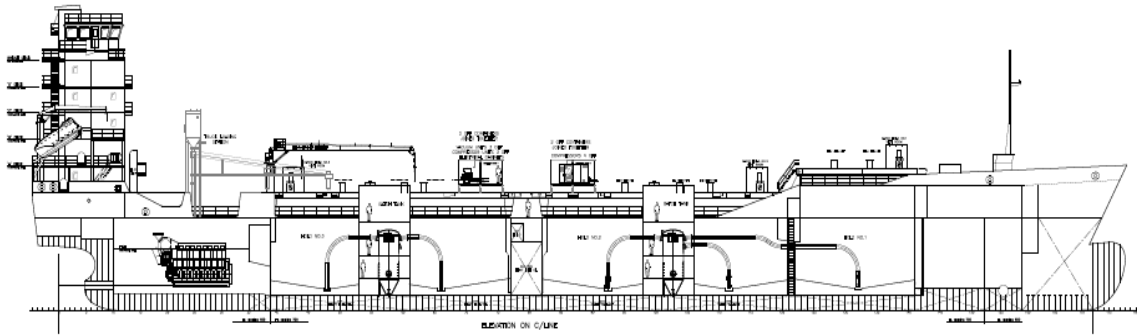
Figure 2 General arrangement of the ship no.2 before (up) and after(down) major conversion

Slika 2 Opći plan broda br.2 prije (gore) i poslije (dolje) velike konverzije

4. Structural analysis of conversion from general cargo ships to cement carriers

The strength analyses of the ships structure are performed by the finite element method employing the programming system Femap/NX Nastran. The model, calculations and post-treatments are carried out using VeriSTAR Hull Version 5.14 r1 [7]. Since the structure is very complex the coarse mesh model is created in order to analyse behaviours of the primary structure. Fine finite element mesh is required which is adapted to the structure topology as much as possible. The structure is modelled by the quadrilateral orthotropic shell element with four nodes each with six degrees of freedom including secondary stiffeners, and the beam elements in accordance with structure drawings. Each beam element consists of 2 nodes with 6 degrees of freedom. The FE analysis has been carried out based on the project documents and models, shown in Figure 3 and 4.
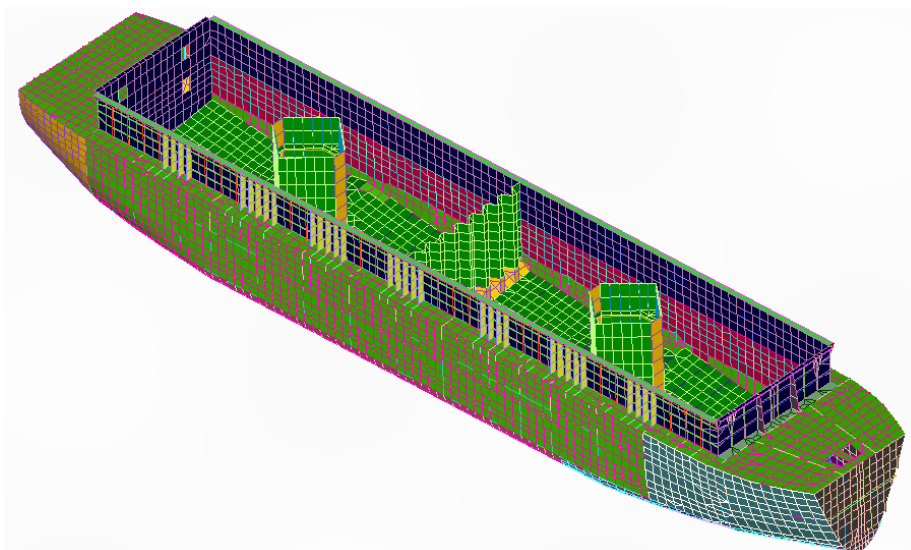
Figure 3 3D FE model of the ship no.1 after major conversion

Slika 3 3D FE model broda br.1 poslije velike konverzije
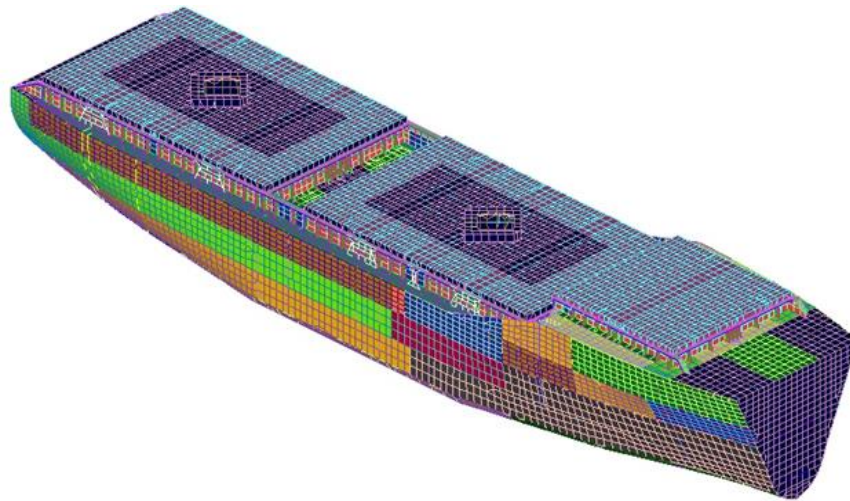
Figure 4 3D FE model of the ship no.2 after major conversion

Slika 4 3D FE model broda br.2 poslije velike konverzije

Three types of the shipbuilding steel are used for FEM model purpose of ship no. 2 , with the following properties:

Grade A (mild steel) in hull general

Young's modules $\qquad$ E = 206 000 MPa

Poisson's ratio $\qquad$ ν = 0.3

Yield stress $\qquad$ σ_Y = 235 MPa

Density of steel ρ = 7,85E-009 t/mm³

Grade D32 (high tensile steel) in sheer strake and main deck plates and lower part of hatch coamings.

Yield stress $\qquad$ σ_Y = 315 MPa

Grade E36 (high tensile steel) in upper part of hatch coamings (60 mm thick plates).

Yield stress $\qquad$ σ_Y = 355 MPa

5. Calculation Data and Assumptions

All calculations are performed with the following assumptions:

- Static analysis,

- Small displacements,

- Linear behaviour of material.

The stress levels are analysed according to the Von Mises stress criterion. Whilst the buckling level is analysed for the following cases:

- Uni-axial compression,

-      Shear,

-      Flexural, compression & shear,

-      Bi-axial compression.

5.1. Loading conditions, cargo and equipment loads

On the FE model, first step was to define mesh size and to idealize the structural members of the ships, and then the loads have been applied to FE model based on the Rule requirements. Also, the loads as grouped solid masses and concentrated vertical forces have been applied on the installed equipment such as the batch tanks in the cargo holds region. After that the model was balanced in a way that the hydrostatic equilibrium was reached, and finally the model was controlled to achieve the bending moments (SWBM) and the shear forces (SWSF) in the still water following the diagrams obtained from submitted Stability Report of the designer (OSD IMT designed office company).

The reduced (net) thickness of all structural members has been used in relation to as-built thicknesses shown on the submitted hull drawings, see Figure 5.
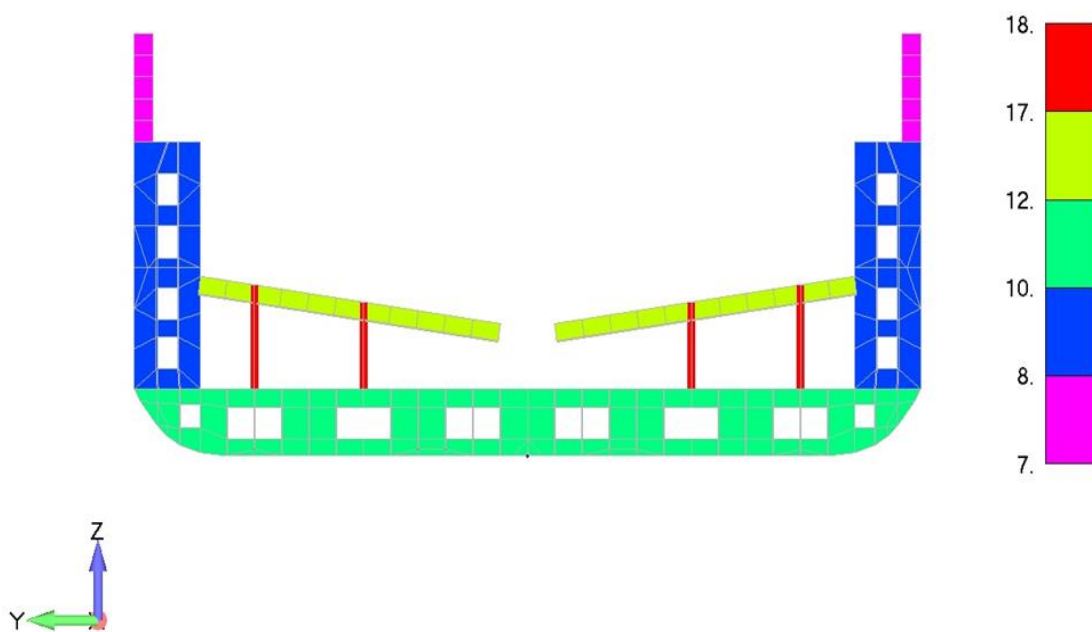
Figure 5 Transversal section model gross thickness in cargo hold of the ship no.2

Slika 5 Poprečni presjek na modelu broda br.2 u skladištu tereta

The longitudinal, transversal and local strengths have been analysed for three loading conditions, respectively ship no.2:

1) LC1   Ballast case or the light ballast of the ship, in the hogging conditions.

2) LC2 Full load for Sea going with deadweight of 7650 tons in the sagging   conditions.

3) LC3 Partially load for Sea going with deadweight of 900 tons in the sagging   conditions.
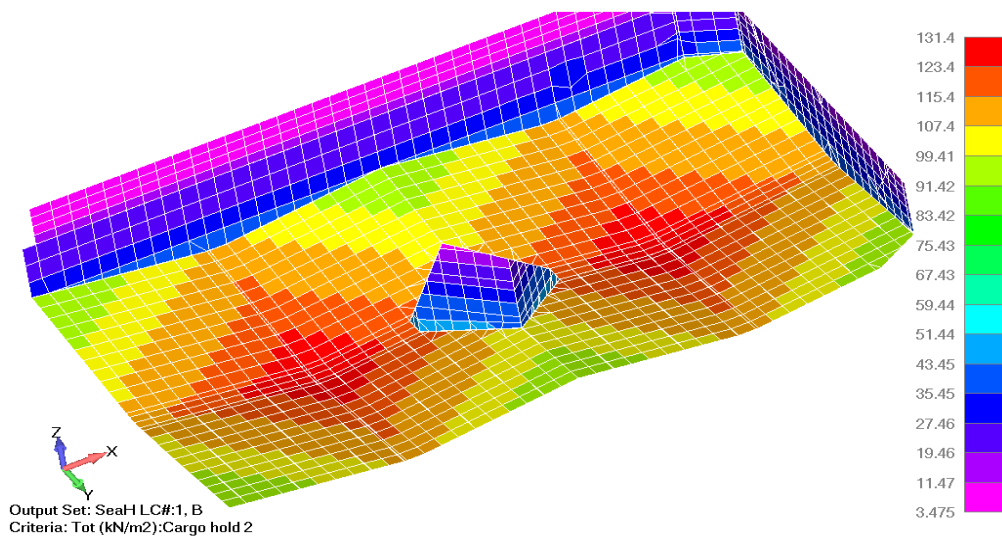
Figure 6 Static + dynamic cargo loads on the hold no.2 (fluidizing bed) of the ship no.2

Slika 6 Statičko+dinamičko opterećenje teretomu skladištu br.2 za brod br.2

5.2. Structural response of FEM model

The structural response in the form of hull displacements, stresses and adequacy parameters are verified in accordance with the requirements of the Croatian Register of Shipping Rules (CRS), Part 2-Hull.

This analysis focuses on the new and existing tank top and the existing hatch covers and coamings regions. The three-hold length FEM model reduces the adverse effects of the boundary conditions to a minimum in the assessed middle hold. The results directly output from the software are interpreted regarding the model characteristics and the criteria have been checked. The following chapters describe the heavy loaded areas.

The existing hatch covers becomes the structural part of the main deck by welding with their coamings. Based on that in sagging conditions (full load sea going), the hatch covers start showing high values of buckling ratios above permissible levels given by Rules requirement. The problem is solved by adding longitudinal stiffeners. Separate analysis was performed for hatch covers exposed to green water loads, showing acceptable stress levels. The analysis model and results are shown in Figure 7.
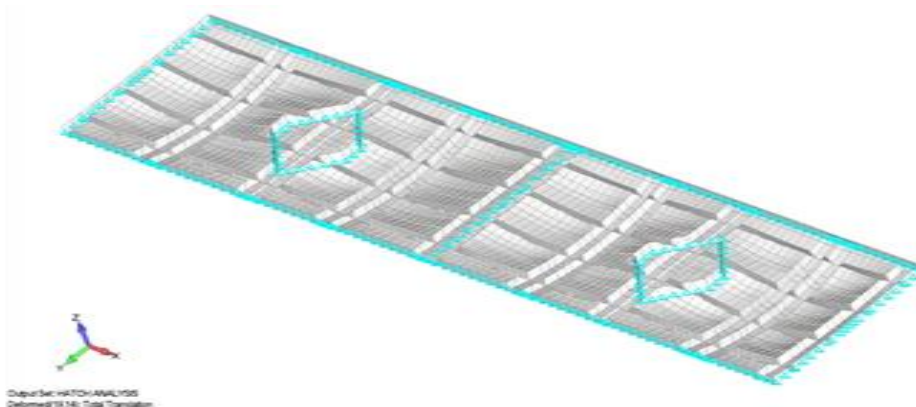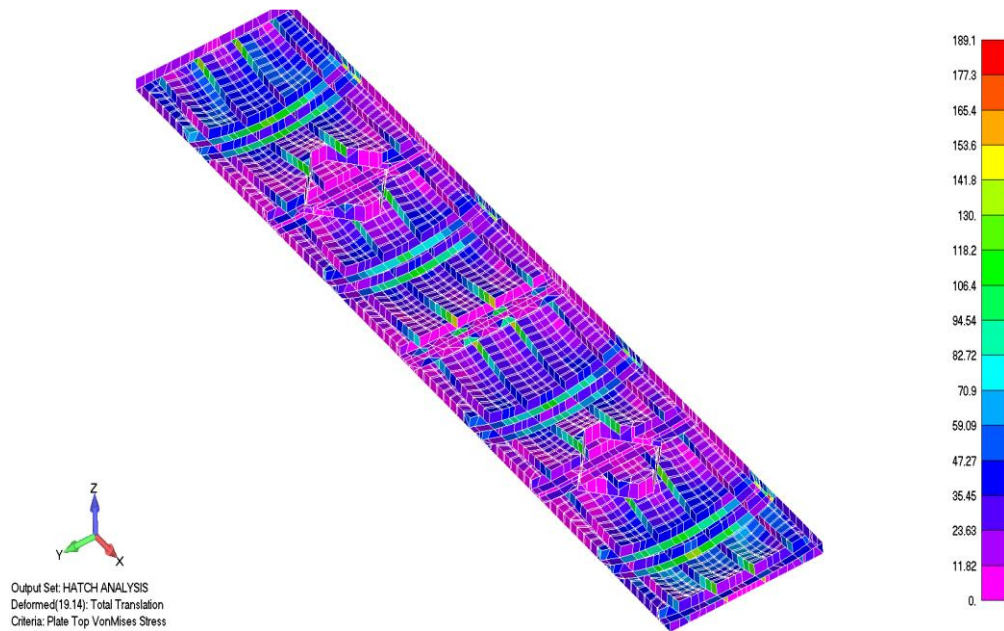
Figure 7 Hatch covers due to green water loads, boundary conditions (up) and VM stress (down)

Slika 7 Konstrukcija poklopaca teretnog grotla analizirana na valno opterećenje i VM naprezanja za brod br.1

In the case of observed loading conditions, maximum stress levels are regularly obtained in new tank top area (fluidising bed) and the transverse floors, as well as in the vertical ordinary frames in the side ballast tanks of the existing hull structure. However, all stresses are below permissible values, see Figure 8, and yielding ratio which is to be below 1 in Figure 9.
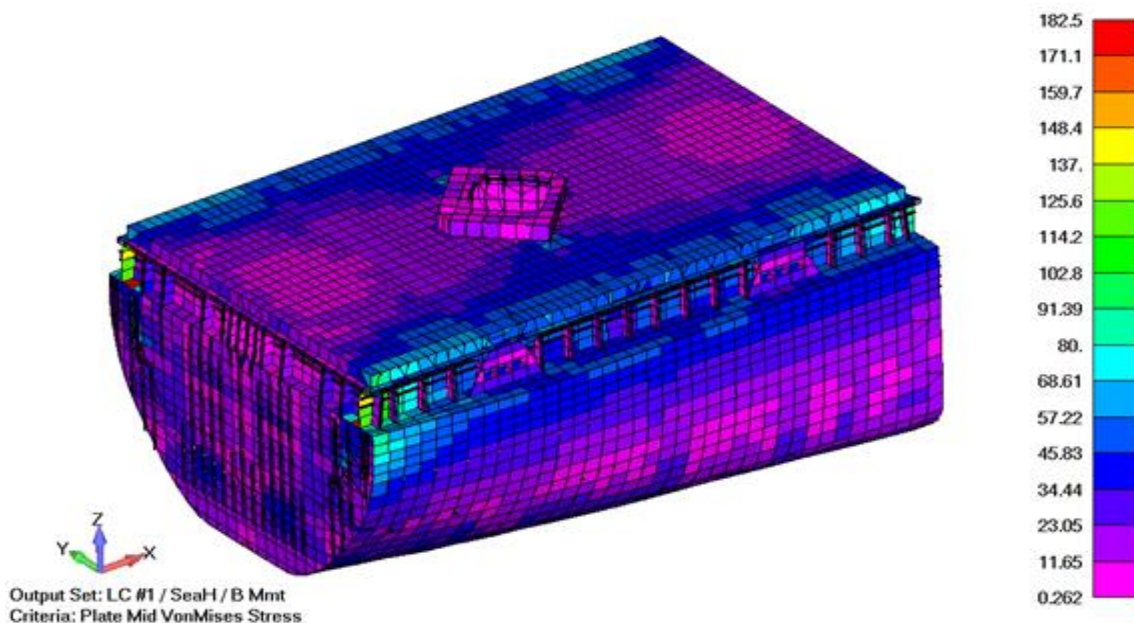
Figure 8 Von Mises stress in plate elements for Hold 3, LC2 (sagging case) ship no.2

Slika 8 Von Mises naprezanja u plošnim elementima skladišta tereta 3 za brod br.2
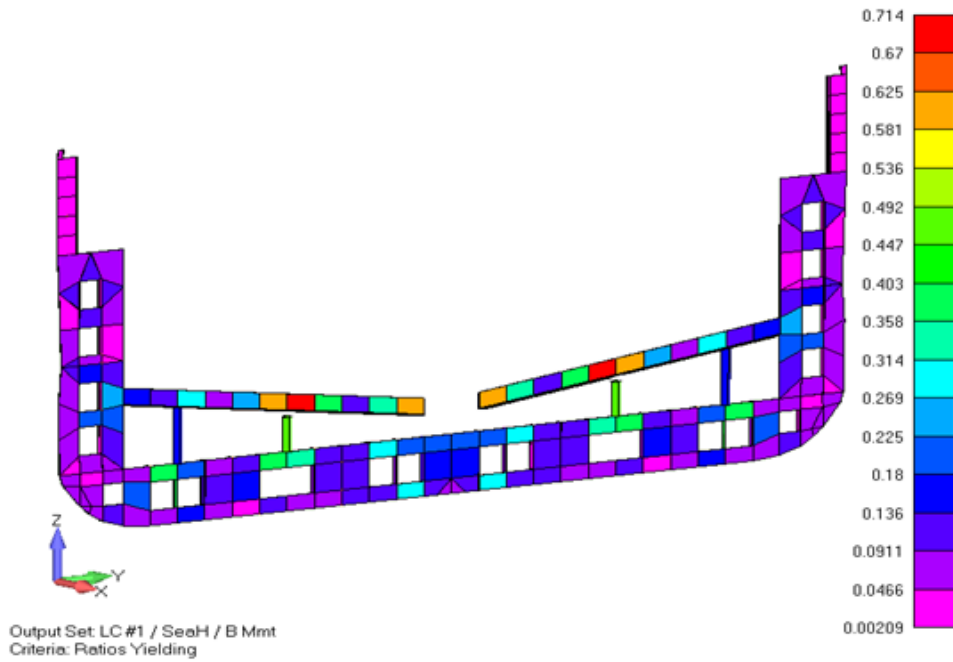
Figure 9 Yielding ratios in web frame of Hold 3/ Fr.55, LC2 (sagging case) ship no.2

Slika Omjer naprezanja tečenja u okvirnim rebrima skladišta tereta 3 /R.55 za brod br.2

The girder system of the double bottom and ship's sides shall have been checked based on the increased design sea pressure and increased cargo weight in the holds and find that are not exceeding allowable stresses with reference to the Rules, see Figure 10.
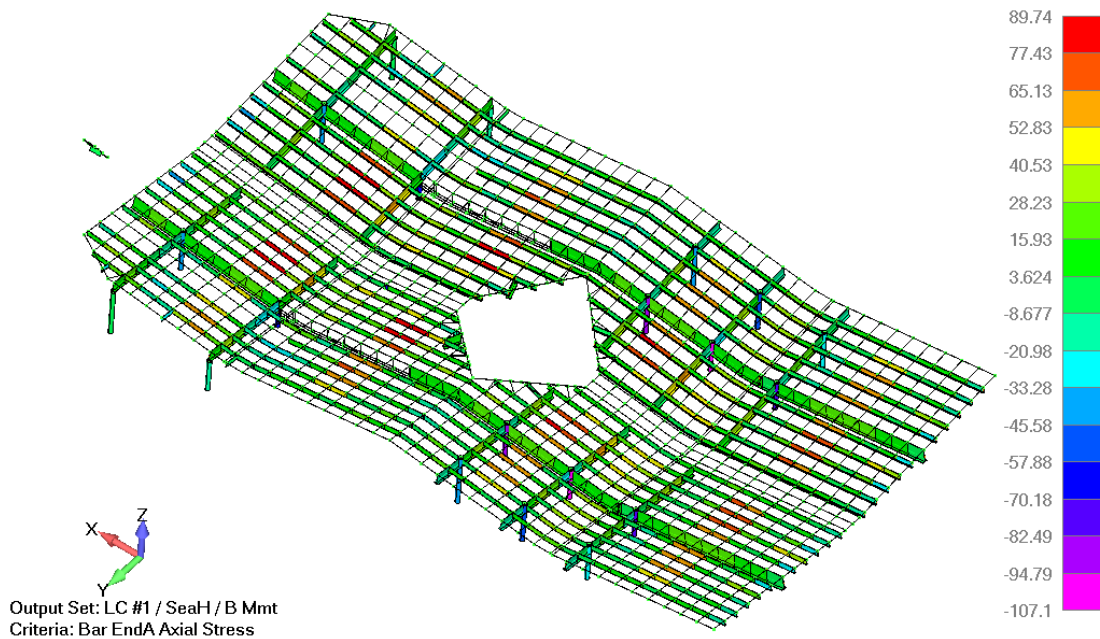
Figure 10 Axial stress in bar elements of new tank top (fluidizing bed) for Hold 2, LC2, ship no.2

Slika 10 Aksijalna naprezanja tečenja u grednim elementima novog pokrova dvodna skladišta tereta 2 za brod 2

Also, the corrosion margin is not included for the hatch covers plates due to high level of buckling ratio. Therefore, no thickness reduction is allowed during the hull elements measuring on the vessel periodical surveys for above-mentioned elements. We note that existing hatch covers will become the structural part of the main deck by welding with their coamings, see Figure 11.
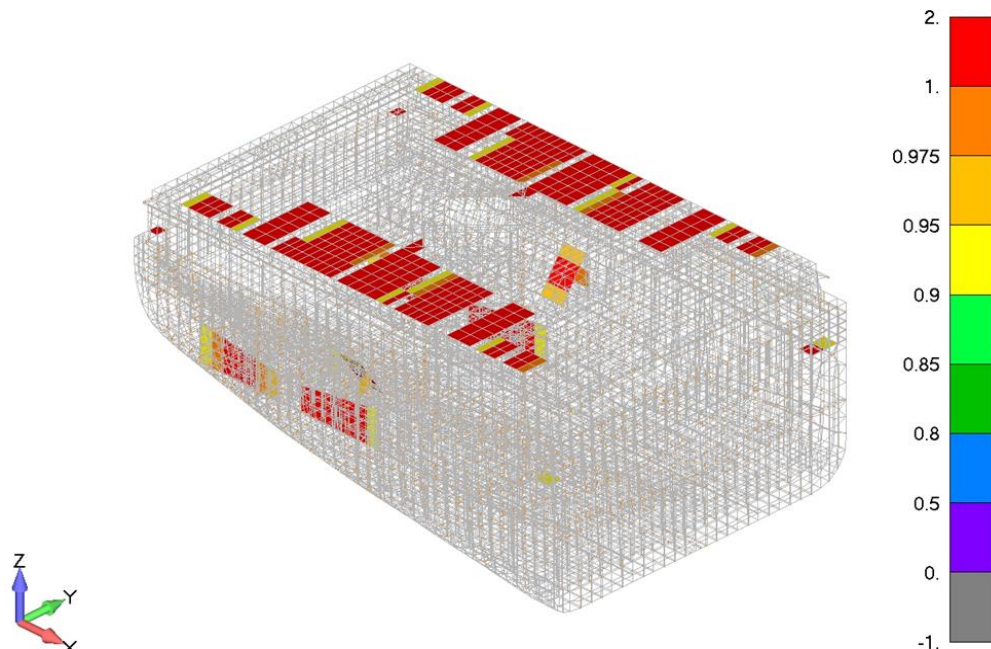
Figure 11 - Buckling ratios of the assessment area > 0.9, for Hold 3, all load cases, ship no.2

Slika 11 Provjera omjera izvijanja s vrijednostima iznad 0.9 u području skladišta tereta 3 za sve slučajeve opterećenja za brod br.2

6. Conclusion

The strength assessment of two general cargo ships, under the major conversion to cement carriers, has been performed with 3D Finite Element method (FE). The 3D FE model of the cargo region of the ship is generated according to available hull drawings and thickness measurement reports provided by the owner. Wave bending moment and shear forces are calculated in according to the Rules requirement and generated using Veristar Hull software automatic functions.

The behaviour of the ship's structure in terms of stress level and other safety criteria has been found satisfactory in all considered load cases. Distributions of stresses obtained for selected load cases in all cases have satisfied CRS requirements. Maximum von Mises equivalent stress on FE element was obtained through automatic checking of all critical locations. Under observed loading conditions, the combined stresses in the ship's structure elements are not exceeding allowable stress of 175 N/mm2 as per CRS Rules [4].

Finally, the maximum stress ratios through all loading cases are within the limits of the permissible values indicating an appropriate and redundant structural design of the ship structure. The obtained results show that the ships can be exploited with the intended design loading condition, homogeneous cargo cement loading condition. However, due to the safety reasons and bearing in mind ship age, it is recommended to avoid alternative cargo loading, respectively successive completely empty one hold and completely full another holds during the cement loading/unloading.

REFERENCES

[1]   PARUNOV J., URODA T., SENJANOVIĆ I., "Structural Analysis of a General Cargo Ship", Brodogradnja 61; 2010.

[2]   Hess, P., Aksu, S., Blake, J., Boote, D., Caridis, P., Egorov, A., Jurisic, P., Murayama, H., Rye Anderson, M., Tammer, M. Committee V.7 Structural Longevity. In: 20th International Ship and Offshore Structures Congress (ISSC 2018), Mirek Kaminski and Philippe Rigo (Eds.), Delft, Belgium and Netherlands, Taylor & Francis Group, London (UK), 2018

[3]   HUGHES, O. S., PAIK, J.K., "Ship structural analyses and design", Trans. SNAME, New Jersey 2010.

[4]   CROATIAN REGISTER OF SHIPPING, Rules for the direct calculations, Rules for the classification of ships, Part 2 – HULL, Annex D,

[5]   BUREAU VERITAS, - Rules for the Classification of Steel Ships PART B, January 2019.

[6]   DET NORSKE VERITAS, DNVGL-CG-0156, Class Guideline for conversion of ship, Edition February 2016.

[7]   FEMAP/NX NASTRAN ver.11.3.2, Structural Dynamics Research Corporation, Exton (USA) 2015.

COMPARATIVE EVALUATION OF REVERSE CHARACTERISTICS OF A SHIP EQUIPPED WITH PROPELLER OF VARIABLE PITCH

Vishnevskii Leonid *, Togunjac Anatolii **

*Krylov State Research Centre, St. Petersburg, Russia
**Morskay Technika, St. Petersburg, Russia
* Vishli@yandex.ru,**Togunjac-branko@yandex.ru

Abstract

The report examined the process of reverse of a ship equipped with a variable pitch propeller (VPP) according to the following scenario: the initial stage, which includes stopping freely rotating propellers and an active stage with a propulsion device, which provides braking force when propellers is working at reverse mode. The method allows obtaining of comparative data related to emergency braking of a ship equipped with a fixed-pitch propeller (FPP) and VPP. Systematic calculations have been performed that show the effectiveness of the use of VPP from the point of view of improving the reverse characteristics of the ship compared to the same ship, but equipped with a VPP.

Key words: emergency ship stop; pitch variable propeller; run out distance

_____

1.   Introduction

Recently, considerable attention has been paid to variable pitch propellers (VPP). A distinctive feature of such movers is the mobility of the blades on the hub, for example, in the plane of the mover's disk. Extensive research has been carried out on VPP and it has been shown that they have several advantages over traditional fixed pitch propellers (FPP) [8]. Moreover, prototypes of such propellers were created, confirming their positive qualities, see Fig. 1.

A   **B**   **C**
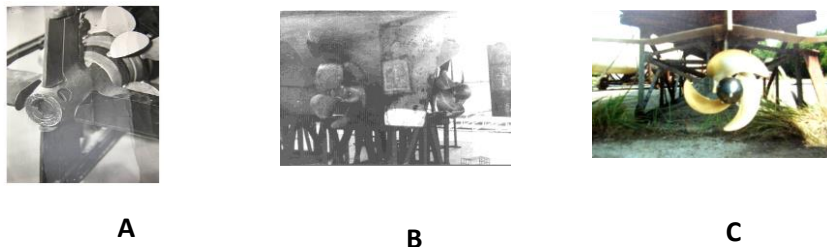
Figure 1 *Marine objects equipped with VPP: A - autonomous uninhabited underwater vehicle (AUUV), B - minesweeper and C - hydrofoil boat*
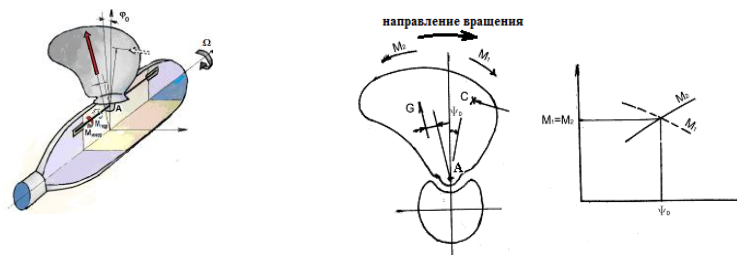
Figure 2 *Scheme explaining the work of VPP*

Fig. 2 is a diagram explaining the principle of operation of VPP. More detailed information on them is contained in [8]. This paper presents the results of a study of the reversible characteristics of a vessel equipped with the indicated propellers.

As you know, the reverse characteristics of the vessel are one of the main characteristics, on which the safety of its navigation largely depends. Therefore, as a rule, they are included in the program of acceptance tests of the ship upon transfer to the ship owner. Evaluation of these characteristics is important at the design stage of the ship, it also affects the choice of type of propeller, which it will be equipped with she [3,4,5].

Of the variety of maneuvers the most important is the emergency stop of the ship. Therefore, in this work, we consider comparative data in the indicated mode (Crush stop) when maneuvering ship equipped with alternately propellers: fixed pitch (FPP), variable pitch (VPP). Design features of the latter are given in [2]. Upon further evaluation, it is assumed that the time required for issuing commands and their execution for emergency braking are the same for an engine with a VFF and an engine with a VPP. Also, the interaction of propellers with the hull is not taken into account.

... ..To achieve this aim, the process of emergency stop of the ship, we consider the following scenario, without taking into account the interaction of propeller with the hull [7]. We divide this scenario into two periods and introduce certain assumptions.

The first period (initial period) will include the time period from the moment the main engine is turned off until the propellers stop rotating and they set in the reverse speed, which ensures the processing of braking power;

To the second period we assign the time period for which the forward speed of the ship to go to zero.

As the studies showed, the duration of the first period is not more than 0.4 seconds for a wide class of ships. Based on this, the ship run-off assessment can be started from second period.

2.   Asstssment of duration of the 2-nd period

For the estimated assessment of the 2nd period, we accept the following conditions: the speed of the propellers must correspond to the frequency at which the power consumed for the emergency stop of the ship is processed [1,2]. It should be emphasized that in the selected scenario, the

rotational speed of the propeller is set based on the reversed power value, and is not determined by solving the equation for the speed of the propulsion device.

The equation of moving of the ship is written as:

$$m\frac{dv}{dt} = -P - cv^2,\qquad(1)$$

where m is the mass and the added mass of the water of the ship;

v - ship speed during the second period;

P - braking force of the propellers on the reverse mode;

c - coefficient of proportionality of the quadratic resistance of the ship vs speed.

This paper does not introduce the assumption that the force P is constant during braking, as it is the case in [1]. Therefore, we find P as a function of the speed of the ship v. To do this, having set the value of v and the expected value of the advanced ratio J corresponding to the mode of movement of the ship on the reverse, we will determine from the corresponding diagrams of the action curves of the mover K_Q. Further, according to given power spent on the reversing Ne and the diameter of the propeller D, the rotation frequency n is determined, which allows one to determine the advanced ratio J of the next approximation. Repeating the indicated procedure, K_Q, n, and J are found in succession. As the calculations showed, the process converges quickly, usually 2-3 approximations are enough. Based on the value of J found in this way, K_t and K_Q are found for the selected value of velocity v. Then the braking force P at a given power Ne and a selected speed v is determined from the expression

$$P = K_T \rho n^2 D^4 = \frac{K_T}{K_Q^{2/3}} \rho^{1/3} (Ne/2\pi)^{2/3} D^{2/3},\qquad(2)$$

where ρ is the density of water;

Ne - consumed power during the reverse of the shipl;

D is the diameter of the propeller,

K_T, K_Q are the thrust and moment coefficients of the propeller.

After performing such calculations for each given speed, and then, constructing an approximation dependence of the velocity, we obtain the analytical dependence of P on the velocity v. It can be

seen from (2) that the braking force depends on the ratio $\dfrac{K_T}{K_Q^{2/3}}$ and the diameter of the propeller D

to the degree of 2/3 for the considered reverse power Ne. Fig 3 shows the dependences $\dfrac{K_T}{K_Q^{2/3}}$ for

Ne = 50, 100, and 200 kW. The corresponding analytical dependencies are also presented there. To build them, we used the experimental data of the propellers related to their operation at reverse mode with A_E / A_0 and Z = 3 and given in [1] and see fig. 9 as well.

It should also be noted that if you write down the ratio of the braking force created by the VPP to the same force, but created by the FPP, it will depend only on the ratio of the diameters to the power of 2/3. Indeed, as analysis has shown (see fig. 3), the ratio $\left(\dfrac{K_T}{K_Q^{2/3}} \right)_{ВИШ} \Big/ \left(\dfrac{K_T}{K_Q^{2/3}} \right)_{ВФШ}$ is close to 1, built for propellers that process various power in the entire range of reversal modes.
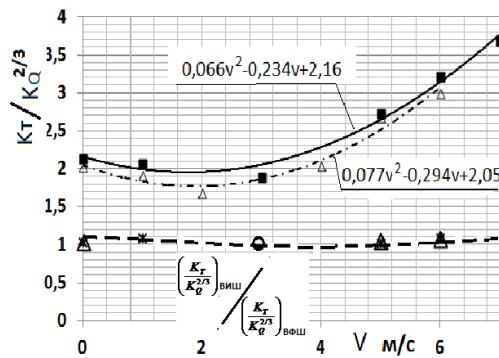
Figure 3 *Approximate dependences of $K_T / K_Q^{2/3}$ on speed V.*

Designations relate to: ■ *- propeller H / D = 1,0;*

Δ - to the propeller H / D = 1.4;

Δ O ✳ *- to propellers processing power of 200, 100, 50 kW*
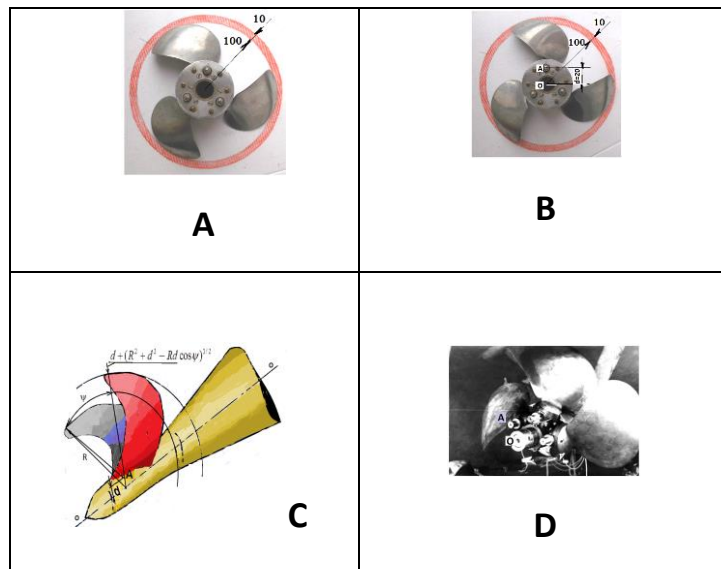
Figure 4 A.- *Model of the right 3-bladed VPP with blades displaced relative to the hub in the plane of the mover's disk to the extreme left position; **B** - the same model with blades in the extreme right position. **C**.- sketch of VPP with blades installed in working position 1 and with blades mounted on the hub in position during reverse. **D** - 5-bladed VPP of the minesweeper, passed the full scale test.*

Thus

$$\frac{P_{ВИШ}}{P_{ВФШ}} = \left(\frac{D_{ВИШ}}{D_{ВФШ}}\right)^{2/3} . \qquad (3)$$

This ratio shows that due to the design features of the VPP in the reversal mode $D_{VPP} > D_{FPP}$ (see Fig. 4), the braking force of the V_{PP} will be greater in comparison with the same force created by the VPP under the condition of the same processing power by the propellers. The constructed analytical dependences make it possible to relatively easily integrate equation (1) in order to obtain comparative data related to its reversible characteristics of the VPP.

3. Integration of equation (1)

Based on the foregoing, we represent the braking force P in the form of a quadratic dependence

$$P = \alpha v^2 + \beta v + \gamma . \qquad (4)$$

Then (1) it may be rewritten as

$$\frac{dv}{-(\alpha + c)v^2 - \beta v - \gamma} = \frac{dt}{m}$$

or

$$\frac{dt}{m.}\Big|_{T_1}^{T_2} = -\frac{2.}{\sqrt{4(\alpha+c)\gamma-\beta^2}}\,arctg\,\frac{2(\alpha+c)v+\beta}{\sqrt{4(\alpha+c)\gamma-\beta^2}}\Big|_{v_1}^{v_2}.$$

Taking $T_1 \sim 0$ due to the short duration of the first period, as well as $v_2 = 0$ (ship stop), we obtain solution (1) in the form to determine the duration of the second period T_2

$$T_2 = \frac{2m}{\sqrt{4(\propto+c)\gamma-\beta^2}}\,arctg\left\{\frac{V_1\sqrt{4(\propto+c)\gamma-\beta^2}}{2\gamma+\beta V_1}\right\} \quad (5)$$

to determine the current value of the speed V_2 in the second period

$$V_2 = \frac{V_1\sqrt{4(\propto+c)\gamma-\beta^2}-(2\gamma+\beta V_1)tg\left\{\frac{\sqrt{4(\propto+c)\gamma-\beta^2}}{2m}t\right\}}{\sqrt{4(\propto+c)\gamma-\beta^2}+[2(\alpha+c)V_1+\beta]tg\left\{\frac{\sqrt{4(\propto+c)\gamma-\beta^2}}{2m}t\right\}}. \quad (6)$$

In the case $\alpha = \beta = 0$, expressions (5) and (6) can be simplified and written accordingly in the form.

$$T_2 = \frac{m}{\sqrt{c\gamma}}\,arctg\left\{V_1\sqrt{\frac{c}{\gamma}}\right\}, \quad (7)$$

$$V_2 = \frac{V_1\sqrt{c\gamma}-\gamma tg\left\{\frac{\sqrt{c\gamma}}{m}t\right\}}{\sqrt{c\gamma}+cV_1 tg\left\{\frac{\sqrt{c\gamma}}{m}t\right\}}. \quad (8).$$

An analysis of expressions (5, 6) and (7, 8) showed that the main contribution to T_2 and V_2 is made by the coefficient γ. In other words, the main contribution to these quantities is made by the coefficient γ in the expression for P (see formula (4)), i.e. the amount of braking force is determined mainly by the mooring mode, i.e. for v = 0 (see formula (4)). To confirm what was said in fig 5 it is shown the calculated dependences of the velocity V_2 on time t. It can be seen that the exact values (formula (6)) and approximate values (formula (8)) coincide quite well. In fig. 5, these values are indicated by "1" and "2", respectively. This served as the basis for systematic calculations based on the data below and to use the formula (10). At the same time, the comparative data presented in Fig. 5 also confirm that the assumption expressed in [1] that it is possible to take the braking force constant, equal to the mooring mode, when solving equation (1), is fair. Moreover, the data presented in this figure illustrate the small influence of the H / D pitch ratio under the condition that they constantly process the braking power. Compare the designations "1" and "3" related to the pitch ratio H / D = 1.0 and 1.4, respectively, and presented in fig. 5. This gives reason to use the reverse diagrams obtained for the FPP and contained in [1].
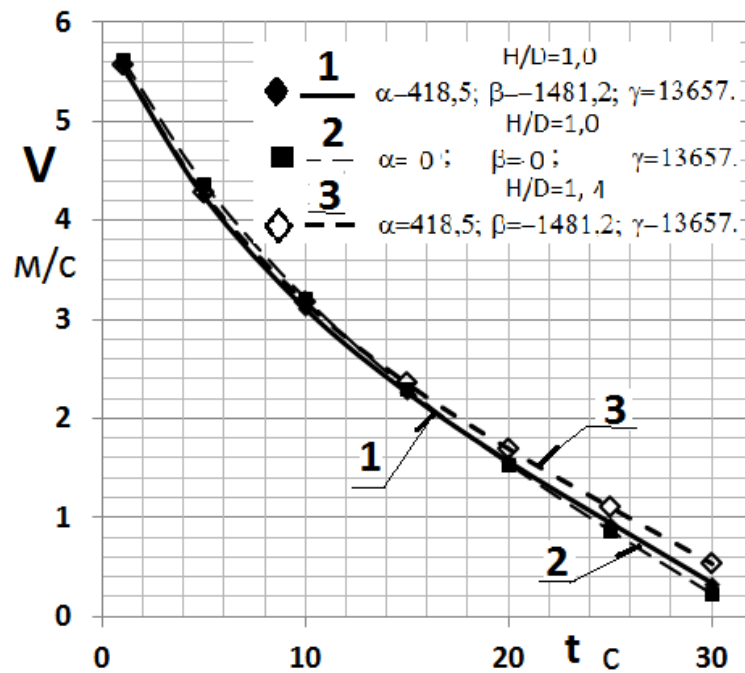
Figure 5 *V₂ velocity change with time t*

To obtain comparative data related to the VPP compared to the FPP regarding the braking force, braking time and run out of the ship, we use the initial data and formulas (7) and (8) below.

Determine the braking distance of stopping ship equipped with a propeller in the second period

$$S = \int_{T_1}^{T_2} V_2 dt = V_1 \int_{T_1}^{T_2} \frac{dt}{1 + V_1\sqrt{\frac{c}{\gamma}}\,tg\left[\frac{\sqrt{c\gamma}}{m}t\right]} - \sqrt{\frac{\gamma}{c}} \int_{T_1}^{T_2} \frac{tg\left[\frac{\sqrt{c\gamma}}{m}t\right]}{1 + V_1\sqrt{\frac{c}{\gamma}}\,tg\left[\frac{\sqrt{c\gamma}}{m}t\right]}$$

Assuming $tg\left[\frac{\sqrt{c\gamma}}{m}t\right] \approx \frac{\sqrt{c\gamma}}{m}t$ it's easy to find the desired expression for the path traveled

$$S \approx V_1 \int_{T_1}^{T_2} \frac{dt}{1 + \frac{V_1 c}{m}t} - \frac{\gamma}{m} \int_{T_1}^{T_2} \frac{tdt}{1 + \frac{V_1 c}{m}t} = \frac{m}{c}\left[1 + \frac{\gamma}{V_{\cdot 1}^2 c}\right]\ln\left(1 + \frac{V_1 c}{m}t\right) - \frac{\gamma}{V_1 c}t\Big|_{T_1}^{T_2}. \quad (9)$$

Let us draw up a relation for the braking paths of ship equipped alternately with VPP and FPP. Omitting the intermediate obvious calculations, we find

$$\frac{S_{ВИШ}}{S_{ВФШ}} = \frac{\frac{m}{c}\left[1 + \frac{\gamma_{ВИШ}}{V_{.1}^2 c}\right]\ln\left(1 + \frac{V_1 c}{m}t\right) - \frac{\gamma_{ВИШ}}{V_1 c}t}{\frac{m}{c}\left[1 + \frac{\gamma_{ВФШ}}{V_1^2 c}\right]\ln\left(1 + \frac{V_1 c}{m}\right) - .\frac{\gamma_{ВФШ}}{V_1 c}t} = \frac{\gamma_{ВФШ}}{\gamma_{ВИШ}}$$

Taking into account the previously obtained ratios

$$\gamma_{ВИШ} = \gamma_{ВФШ}\left(\frac{D_{ВИШ}}{D_{ВФШ}}\right)^{\frac{2}{3}},$$

$$D_{ВИШ} = D_{ВФШ}\left\{\frac{d}{R} + \sqrt[2]{1 + \left(\frac{d}{R}\right)^2 - 2\left(\frac{d}{R}\right)\cos\Psi}\right\} \quad (9a)$$

we can write

$$\frac{S_{ВИШ}}{S_{ВФШ}} = \left\{\frac{d}{R} + \left[1 + \left(\frac{d}{R}\right)^2 - 2\left(\frac{d}{R}\right)\cos\psi\right]^{\frac{1}{2}}\right\}^{\frac{2}{3}}. \quad (10)$$

From (10) it can be seen that the stopping distance of aship equipped with a VPP is shorter than the same path, but the ship equipped with a FPP. This reduction is determined by the relative distance of the axis of rotation of the blade on the hub d / R (point A in fig. 4 -B) from the axis of rotation of the propeller (point O in the same figure). In fig. 6 it shows the percentage reduction in run-out during reversal of a ship with a VPP compared with the case of equipping its FPP depending on the parameters ψ and d / R. It can be seen that it can be very significant if, when designing VPP for a given project of ship, it is necessary to include the maximum possible parameters ψ and d / R.
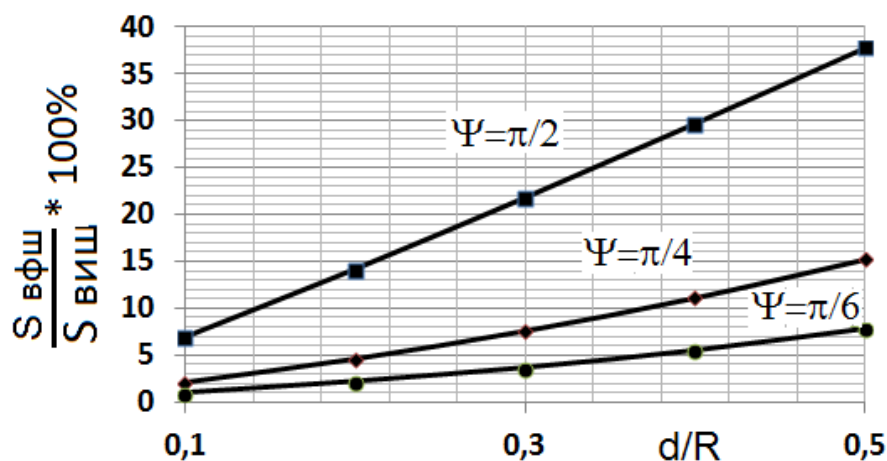
Figure 6 *Percentage reduction in run-out during reversal of a ship with a VPP compared with the case of equipping its FPP depending on the parameters ψ and d / R*

Omitting the intermediate calculations according to the initial data given below, systematic calculations of the comparative characteristics of the reversal of a marine vessel equipped with alternating VSS and VFSh were carried out, see Fig. 7 and 8.
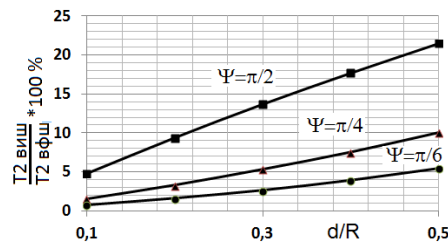
Figure 7 *Percentage reduction in the time of reversal of ship with a VPP compared with the case of a FPP depending on the parameters ψ and d / R*
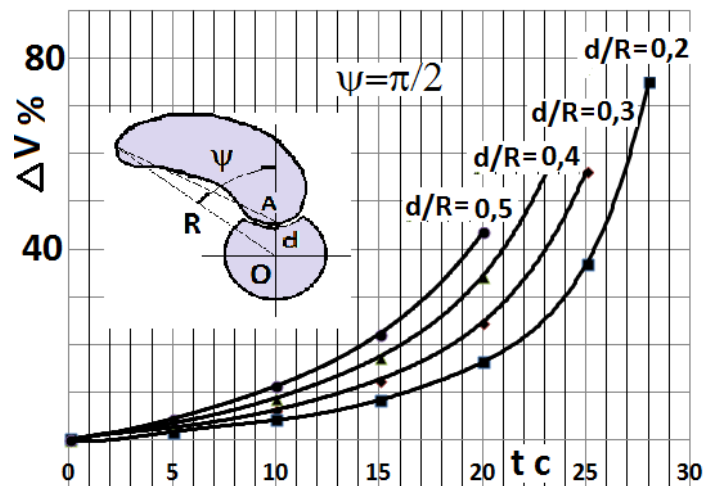
Figure 8 *Loss of interest with VPP the ship speed emergency braking it in relation to the same loss, but in the case of the same ship with FPP*

From the presented calculated data it is seen that due to the design features of the VPP due to the increasing diameter compared with the diameter of the FPP, its braking force of the propulsion device during reversal increases. This is due to such parameters of the VPP blades as their skew characterized by the angle ψ, and the relative distance d / R from the axis of the moving. An increase in these parameters leads to a decrease distance of run out and braking time of the ship.

4. Used data in evaluating comparative characteristics of ship

The following characteristics were used as initial data when performing design estimates for the reverse of the ship given in this paper:

The mass of the ship together with the added mass of water: M = 100000 kg;

Power of the main engines: 2 * Ne = 221kW;

Power during braking: 2 * Netor = 100 kW

Full forward speed: V_1 = 6 m / s;

Diameter of propeller: 1 m;

Resistance at full speed: R = 30000 N;

The rotational speed of the propeller when the ship is in full ahead speed: 10 s^{-1};

It should be especially noted that VPP when working in reverse provide a fixed installation of the blades on the stops due to its design features, and it works as a FPP in these modes.

To estimate the time of the first period, the well-known approximate formula was used:

$$J_1 = 28*10^5*\gamma*D^5*k_v*\frac{A_E}{A_0}(\frac{A_E}{A_0}+3)$$ to calculate the moment of inertia of the propeller;

where γ is the specific gravity of the propeller material;

D is the diameter of the propeller;

A_E / A_0 - disk ratio propeller;

k_v - coefficient taking into account the mass of the propeller due to the added mass.

During the calculations, along with the above values of the characteristics of the calculated small-tonnage vessel, the following data were adopted: J = 39 kgm^2;

$n_0 = 10$ s^{-1} $\rho = 1000$; kg / m3; D = 1.1 m; V_0 = 6 m / s; K_Q = 0.04; λ = 0.7. The hydrodynamic characteristics in reverse operating modes were borrowed from [1] and are shown in fig. 9.
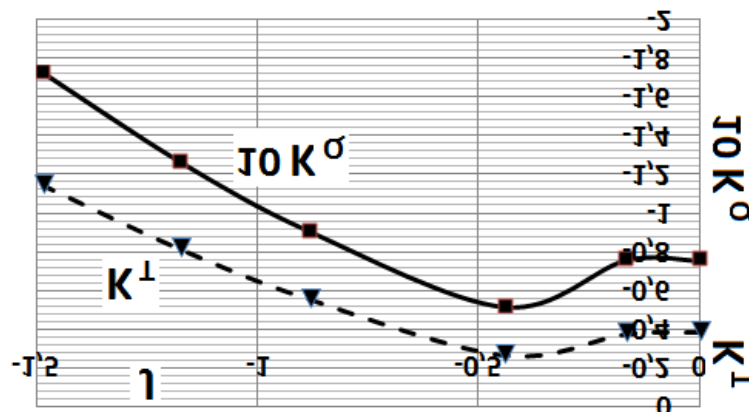
Figure 9 *Curves of the propeller, borrowed from [1].*

H / D = 1.0; A_E / A_0 = 0.8; Z = 3

From the presented results it is seen that the most effective braking of the ship is carried out by the VPP. Due to the shifting of the blades during reversal, they move to an increased diameter, causing greater braking force. In this mode, they operate as an FPP with a larger diameter compared to an FPP designed at the same full speed.

5. Conclusion

Estimating the reverse characteristics of ship equipped with the propulsion system considered above, it can be argued that equipping its VPP is preferable for emergency braking of the ship in comparison with the same shipl, but equipped with a FPP. Since, as you know, VPP along with its adaptability to various conditions of the vessel's navigation, as a result of which more efficient

processing of power is ensured, it will ensure more safe operation of the ship. This state of affairs is due to the design feature of the VPP, in which the blades are mounted fix in position on the hub, providing the propeller with a bigger diameter than the FPP in the process of reverse. Obtaining the maximum possible reduction in the running out of a ship with VPP during reverse depends on the design parameters of the propulsion device, in particular, on the distance of the axes of rotation of the blades relative to the hub from the axis of rotation of the propeller. To the aforesaid, it should be added that a smaller distance of running out of minesweeper with a VPP was visually observed during comparative full scale test, which took place at the end of the last century. During these tests, FPP was used as VPP with blades fixed on the hub in a constructive position. A photograph of a full-scale VPP, which has passed full scale test, is presented in Fig. 4-D.

6. References

[1] Басин А.М., Миниович И.Я. Теория и расчет гребных винтов. Ленинград, Судпромгиз 1963.

[2] Вишневский Л.И., Тогуняц А.Р. Корабельные лопастные движители, новые технические решения, результаты исследования. Судостроение, Санкт-Петербург, 2012.

[3] Бискуп Б.А., Бушковский В.А. Оценка прочности гребных винтов с откидкой контура лопасти на режимах реверса // Труды ЦНИИ им. акад. А.Н. Крылова, вып. 8(292), СПб, 1998, с. 60 – 67.
[4] Яковлев А.Ю., Васильев Ю.М. Метод расчета экстренного торможения судна с помощью нескольких движителей различных типов // Труды Крыловского государственного научного центра, вып. 90 (374), 2015, с. 27 – 38.
[5] Яковлев А.Ю. Численное моделирование и проектирование новых типов движителей. Труды Крыловского ГНЦ, 387, 2019, с. 32-50

[6] Бронштейн Н.Н., Семендяев К.А. Справочник по математике. Издательство Наука, М. 1964.

[7] Котлович В.М., К вопросу о квазиреверсивных испытаниях судовых движителей в опытовом бассейне. Труды Крыловского государственного научного центра, вып. 389, 2019, с. 37 – 48.
[8] Вишневский Л.И., Тогуняц А.Р. Гидродинамика корабельных лопастных движителей, инновационные решения, Санкт-Петербург, 2020.

TOWARD OPERABILITY ANALYSIS OF A PASSENGER SHIP IN THE ADRIATIC SEA BASED ON THE JONSWAP-ADRIATIC WAVE SPECTRUM

Marko Katalinić*[a], Joško Parunov[b], Antonio Mikulić[b]

a University of Split - Faculty of Maritime Studies, Ruđera Boškovića 37, 21000 Split, Croatia
b Faculty of Mechanical Engineering and Naval Architecture, Ivana Lučića 5, 10000 Zagreb, Croatia
* Corresponding Author, marko.katalinic@pfst.hr

Abstract

The paper demonstrates an operability analysis based on a slamming criterion of a passenger ship intended for sailing in the Adriatic Sea. The seakeeping calculations are performed by a boundary-element-method, potential flow solver, to obtain the vessel's motion at sea. A full range of ship-to-wave headings are considered for a ship at its design speed and at rest. The applied Adriatic wave climate is the newly developed JONSWAP-Adriatic wave spectrum, while a sea state table is based on a database which contains satellite measurements and numerical simulation results for the entire Adriatic over 24 years. The proposed wave spectrum presents an optimization of JONSWAP spectrum parameters and Tabain's modal frequency expression, for offshore Adriatic conditions. The results are interpreted to find out those sea states where the selected bow slamming criteria are not satisfied. By knowing the frequency of occurrence of such sea states it is possible to determine the yearly time fraction when the ship will not be able to operate at its full operational profile due to weather conditions. This methodology is intended to serve to ship owners and operators, as well as designers, for evaluating if a certain ship is appropriate for operating in a region of interest.

Key words: Slamming, Operability analysis; Adriatic Sea; JONSWAP-Adriatic wave spectrum

Sažetak

U radu je prikazana analiza operabilnosti putničkog broda, na temelju kriterija udaranja pramca, namijenjenog plovidbi Jadranskim morem. Proračuni pomorstvenosti su provedeni potencijalnom teorijom, 3D panel metodom, kako bi se dobile prijenosne funkcije odziva broda na valovima. Razmatran je puni raspon relativnih kurseva broda na valove pri putnoj brzini i u mirovanju. Primijenjena je klima valova Jadranskog mora predložena JONSWAP-Adriatic spektrom i tablicom stanja mora prema bazi podataka koja obuhvaća satelitska mjerenja i numeričke simulacije za cijeli Jadran kroz 24 godine. Predloženi valni spektar predstavlja optimizaciju JONSWAP spektra i Tabainovog izraza za modalnu frekvenciju, za uvijete Jadrana. Rezultati su interpretirani tako da pokažu na kojim stanjima mora brod ne udovoljava razmatranom kriteriju udaranja pramca. Poznavanjem učestalosti pojavljivanja takvih stanja mora ,moguće je odrediti udio vremena prikladan za plovidbu akvatorijem za koji je namijenjen.

Ključne riječi: Udaranje pramca; Operabilnost; Jadransko more; JONSWAP-Adriatic spektar valova

1. Introduction

Frequency of exceedance of the bow slamming limit criteria, as one of the common seakeeping operability criteria, is assessed and presented for a liner ship (such a ferry, ro-pax or cruise ships) intended for operation in the Adriatic Sea. The underlying information about the sea environment is information about the frequency of occurrence of different sea states in the Adriatic taken from a wave database. The given example vessel, used for the analysis (as presented in Figure 45 and Figure 46) has the main characteristics similar to the vessels considered for procurement or construction within the "larger ferry category", typically used for passenger transport on the east coast of the Adriatic. The same methodology can be applied retroactively to existing or new ships

sailing on established liner or circular routes in order to estimate the number of days per year during which the ship may not sail and achieve its purpose, i.e. to justify the investment.

Main particulars of the analysed vessel:

L_{OA} = 114   m   length over all

B = 18.7 m   width

T = 5.0   m   draft

Δ = 6565t   displacement

v_{max} = 17   kn   max. speed
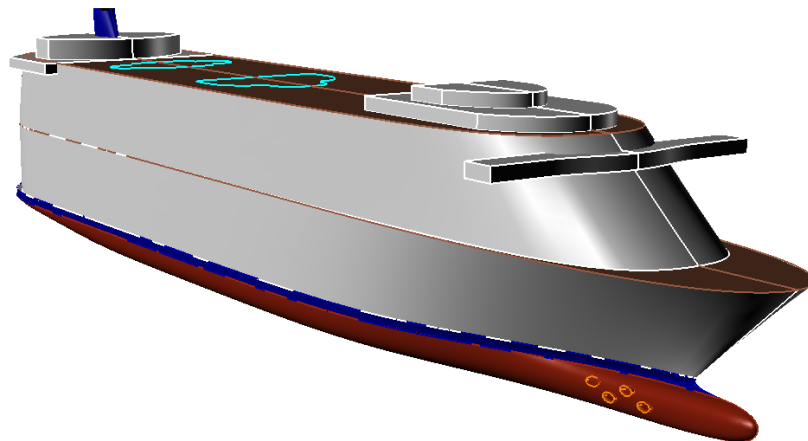
Figure 45 *Geometric model of the case study vessel*
Slika 1 Geometrijski model analiziranog broda
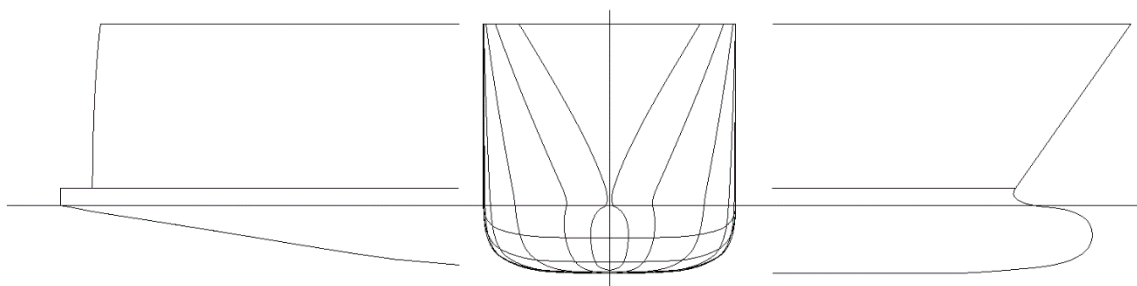
Figure 46 *Ship lines for seaworthiness analysis (not in scale)*
Slika 2 Linije broda za analizu pomorstvenosti (nije u mjerilu)

Ship operability studies are usually focused on the most frequent operating conditions and less often on extremes. Accordingly, it is assumed that the ship response in a seaway may be determined by reasonable accuracy with the linear seakeeping theory. Therefore, seaworthiness is analysed in

the frequency domain (strip theory or 3D panel methods) [1]. Ship responses are initially calculated on individual harmonic waves, while the response in realistic sea waves is then obtained by spectral analysis. In this way, a database of transfer functions is created, which represents the response of the ship to harmonic waves of unit amplitude. Multiplying the encountered wave spectrum by the square of the transfer function the response spectrum is obtained. Spectral moments are then determined by integrating the response spectrum, and then significant values of ship motions, velocities and accelerations are determined by well-known standard expressions [2].

The seakeeping calculation was performed with the Ansys AQWA software package based on the 3D panel method, employing potential theory (inviscid, irrotational and incompressible fluid is assumed). The influence of hull appendages such as rudders, skegs or bilge keels is neglected and viscous damping is not implemented in the calculation model.

The inertial characteristics of the ship were estimated with respect to the total mass, assuming that the mass is homogeneously distributed across the volume.

Ixx = 154 269 $\quad$ tm^2

Iyy = 3 927 039 tm^2

Izz = 4 057 781 tm^2

Metacentric height: GM =1.94 m

The calculation model mesh is defined as structured mesh with a basic element size of 1.0 meter (Figure 47), in order to capture geometry transitions across the hull. Likewise, the elements size is related to the frequency range considered within the calculation (a finer resolution mesh is required for considering higher frequencies, i.e. shorter waves).
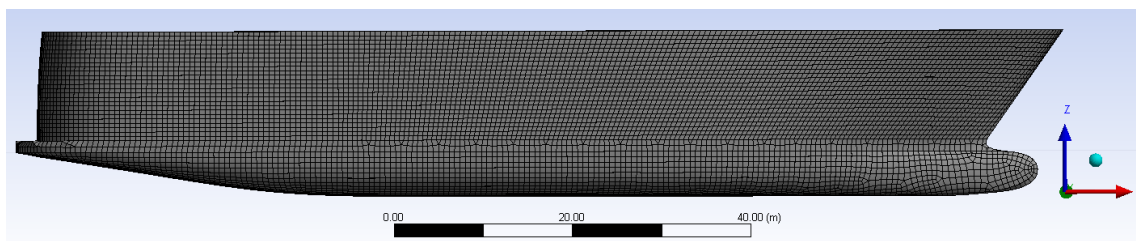
Figure 47 *Geometry model mesh*
Slika 3 Mrežni model broda

2. Hydrodynamic analysis

The calculation of the hydrodynamic coefficients (additional mass and damping) and the hydrodynamic excitation (Froud-Krylov and diffraction component) was performed for individual incident wave directions separately at the assumed cruising speed (v = 17 kn) and a ship at rest (v = 0 kn).

The calculation of the hydrodynamic coefficients, excitation forces and moments is preceded by the calculation of basic hydrostatic characteristics, which serve also as a verification of the hydrodynamic model. The results confirmed the given displacement with an acceptably small deviation resulting from the discretization of the geometry and, among other, provide insight into the position of the centre of buoyancy, waterline surface characteristics and the hydrostatic stiffness matrix for 6 degrees of freedom.

The calculation results provide insight into the transfer functions, hydrodynamic (Froude-Krylov and diffraction) forces and motions and pressures. Pressure distribution along the free surface and the hull wetted surface is shown in Figure 48.
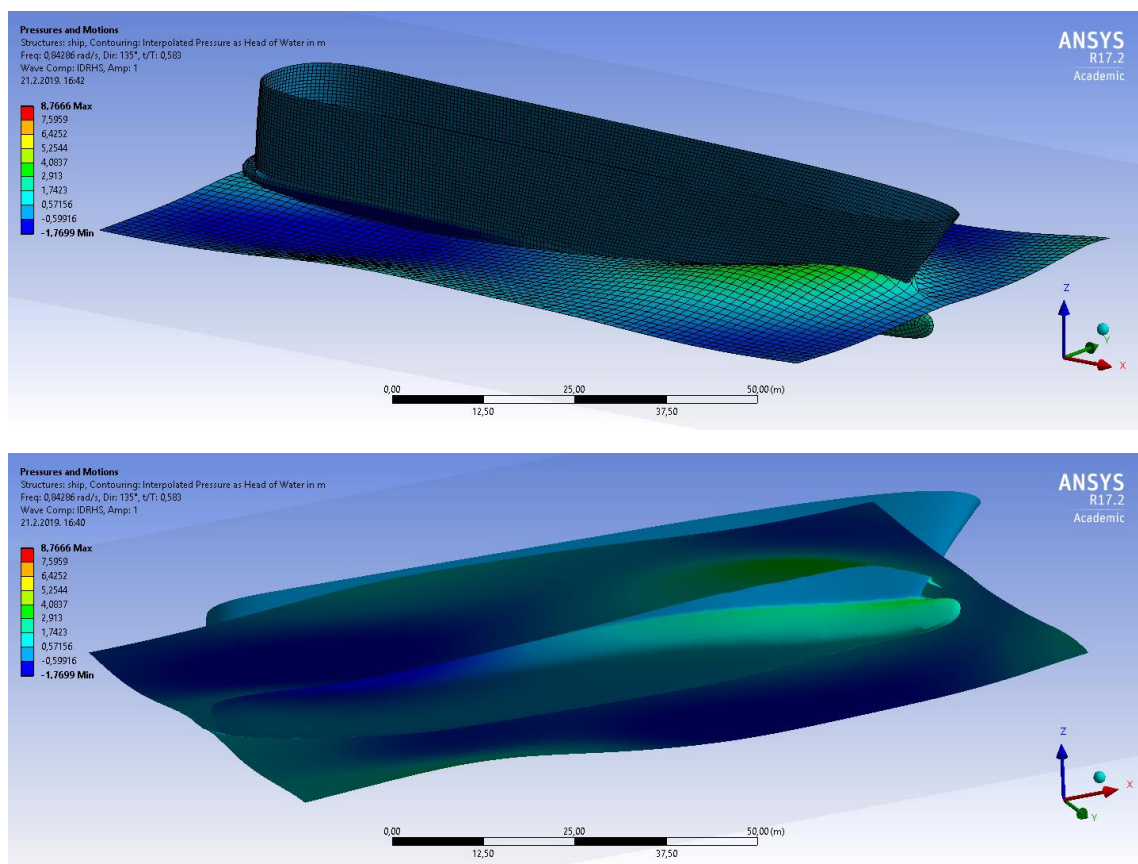
Figure 48 *Pressures across the ship wetted surface and motion response to a harmonic wave. Example: Hs = 2m / ω = 0.843 rad / s; at an angle of 45 deg to the bow at a speed of 17 kn*
Slika 4 Tlakovi na oplakanoj površini broda i odziv na harmonijskom valu. Primjer: Hs = 2m / ω = 0,843 rad/s; pod kutem od 45 deg u pramac pri brzini od 17 kn

Transfer functions of heave motion for zero speed case are presented in Figure 5, while transfer functions of relative vertical bow motion are shown in Figure 6.
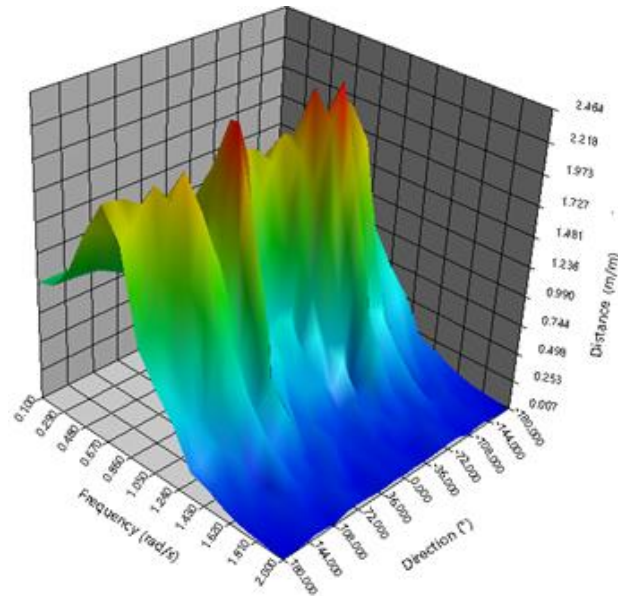
Figure 49 *Heave transfer function for the ship at rest (v = 0)*
Slika 5 Prijenosna funkcija poniranja za brod u mirovanju (v = 0 kn)
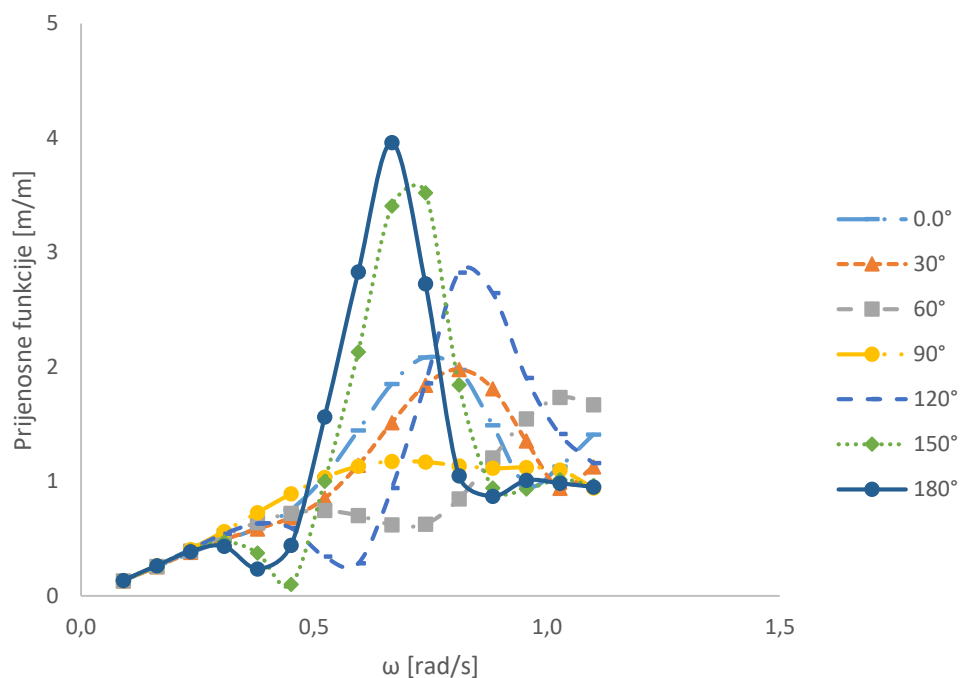
Figure 50 *Transfer functions of relative vertical bow motion for different incoming wave directions (180° represent incoming bow waves) at cruising speed v = 17 kn*
Slika 6 Prijenosne funkcije relativnog vertikalnog pomaka u točki na pramcu za razne nailazne kuteve (180° predstavlja valove u pramac) pri putnoj brzini v= 17 kn

Transfer functions are determined depending on ship speed and the heading relative to the dominant wave propagation direction. The results for relative wave elevation at the bow are derived from coupled heaving and pitching motion, with the aim of determining the limiting conditions at sea with respect to the bow slamming seakeeping criteria. The slamming criterion is defined according to [2]

$$p = exp\left[-\left(\frac{d_p^2}{2m_{0\_r}} + \frac{v_{kr}^2}{2m_{0\_v}}\right)\right] < 0,03 \qquad (1)$$

where

d_p = 5.0   m   draft at bow

v_{kr} = 3.11   m/s   critical vert. bow motion speed, as per $v_{kr} = 0,093\sqrt{gL}$

m_{0_r} zeroth-moment response spectrum of relative vertical motion

$m_{0\_v} = m_{2\_r}$ zeroth-moment response spectrum relative vertical velocity

The slamming criterion represents joint probability of keel emergence and exceedance of the critical relative vertical velocity at bow. It is mainly used for ships with higher block coefficient that are prone to bottom slamming, while for slender hulls it is recommended to consider the bow flare slamming.

3. Adriatic wave spectrum and sea state table

Basic seakeeping theory implies that both a mathematical description of a waves and a physical model of the ship response are necessary to evaluate ship behaviour in a seaway. As for the wave description, the newly proposed JONSWAP-Adriatic wave spectrum [3] is adopted as well as the sea state table which states frequency of occurrence of different sea states in the Adriatic Sea. The underlying wave database which served to derive the previously mentioned combined 24 years of satellite altimetry measurements and numerical hindcast of surface waves across 39 uniformly distributed locations across the entire basin [4] as shown in **Figure 51**.

Figure 51 *Locations in the Adriatic Sea available in the WW (OCEANOR-Fugro) database*
Slika 7 Lokacije na Jadranskom moru dostupne u WW (OCEANOR- Fugro) bazi podataka

The sea state table valid for the Adriatic as a whole, i.e. data merged and sorted for all 39 locations together is shown in Table 1.

Table 17 Sea state table for the entire Adriatic Sea

Table 51 Tablica stanja mora - Cijeli Jadran

Tp / Hs	0.0 - 0.5	0.5 - 1.0	1.0 - 1.5	1.5 - 2.0	2.0 - 2.5	2.5 - 3.0	3.0 - 3.5	3.5 - 4.0	4.0 - 4.5	4.5 - 5.0	5.0 - 5.5	5.5 - 6.0	6.0 - 6.5	Sum
0 - 1	0	0	0	0	0	0	0	0	0	0	0	0	0	0
1 - 2	0	0	0	0	0	0	0	0	0	0	0	0	0	0
2 - 3	221186	65034	754	7	0	0	0	0	0	0	0	0	0	286981
3 - 4	149331	225790	32459	1233	39	1	1	0	0	0	0	0	0	408854
4 - 5	36859	130876	80830	19669	1732	109	7	1	0	0	0	0	0	270083
5 - 6	17747	52597	54473	38089	15605	3194	469	54	3	0	0	0	0	182231
6 - 7	10379	24193	20917	17297	14389	8836	3255	731	183	32	5	2	1	100220
7 - 8	3704	8591	8993	6373	4838	3810	3141	1879	701	215	54	18	10	42327
8 - 9	1863	3459	3515	2727	1930	1361	956	677	470	197	78	13	8	17254
9 - 10	1174	1055	1115	819	654	495	336	231	156	92	48	26	3	6204
10 - 11	376	434	420	294	217	120	98	64	40	22	6	2	1	2094
11 - 12	363	105	107	81	91	31	26	16	10	9	5	2	1	847
12 - 13	434	39	23	10	8	10	7	7	2	2	1	1	0	544
13 - 14	0	0	0	0	0	0	0	0	0	0	0	0	0	0
Sum	443416	512173	203606	86599	39503	17967	8296	3660	1565	569	197	64	24	1317639

The applied JONSWAP-Adriatic spectrum is wave spectrum formulation proposed based on the 24-year database. It is obtained by optimizing the original JONSWAP spectrum expression coefficients to best describe Adriatic Sea conditions and simplifying it to a one-parameter equation using Tabain's modal frequency formulation, also with optimized coefficients, in respect to the 24-year database [3]. JONSWAP-Adriatic spectrum follows as:

$$S(\omega) = 0{,}8626 \frac{5}{16} \frac{H_s^2 \omega_m^4}{\omega^5} exp\left[-\frac{5}{4} \left(\frac{\omega_m}{\omega} \right)^4 \right] 1{,}78^{\,exp\left[-\frac{1}{2} \left(\frac{\omega - \omega_m}{\sigma\, \omega_m} \right)^2 \right]} \tag{2}$$

Where

$$\omega_m = 0{,}52 + \frac{1{,}4}{H_s + 0{,}7}$$ modal (peak) frequency

$$\sigma \begin{cases} \sigma_a = 0,06 \; za \; \omega \leq \omega_m \\ \sigma_b = 0,08 \; za \; \omega > \omega_m \end{cases} \quad \text{spectral width coefficient}$$

Comparison of the proposed JONSWAP-Adriatic wave spectrum (J-A) and Tabain's wave spectrum most often used within the shipbuilding community for the Adriatic Sea is shown in Figure 52. It may be seen that spectral peak of J-A spectrum is shifted toward higher frequency, while in the same time J-A spectrum is distributed over larger frequency band compared to the Tabain's spectrum.
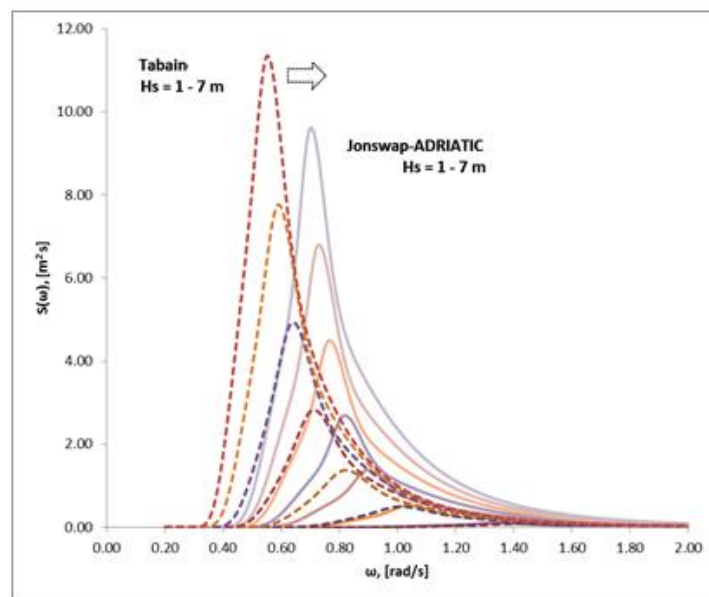
Figure 52 *Comparison of Tabain's wave spectrum and the JONSWAP-Adriatic spectrum for an improved description of the waves of the Adriatic Sea based on data from numerical re-analysis and satellite altimetry measurements [3]*
Slika 8 Usporedba Tabainovog spektra valova i JONSWAP-Adriatic spektar za unaprijeđeni opis valova Jadranskog mora na temelju podataka numeričkih re-analiza i mjerenja satelitskom altimetrijom [3]

4. Results

Multiplying the wave spectrum by the square of the transfer function the response spectrums are obtained and from them the spectral moments are calculated in order to determine the probability of bow slamming (Equation (1)). Since such a system is linear, the limit value of the criteria can be found by varying the significant wave height *Hs*, which defines the wave spectrum.

It is considered that after the probability of bow slamming exceeds the given threshold value, the ship's captain will reduce speed or change course. Slamming causes discomfort to crew and passengers and induces transient vibrations through the hull. These vibrations can significantly contribute to the global hull loads especially in slender ships and ships with an open cross-section. It should be clarified that the bow slamming criteria is just one of the applicable seakeeping criteria. When building or contracting a new ship, it is extremely important to determine all relevant criteria with regard to the ship's intended purpose. In general, from the point of view of seaworthiness, operability criteria can be classified into three categories: comfort, operability and survivability [2].

The criteria of maximum allowable probability of bow slamming belongs into the operability category and was chosen for this study to methodologically present how to estimate time fraction when ship is not fully operable (speed reduction, course alterations or staying in harbour). For a comprehensive assessment of a passenger ship, additional criteria, in particular comfort criteria, which are more strict than the operability criteria, should be included in the design and analysis at the time of ship acquisition, making the analysis more complex.

The limit values of the significant wave heights for bow slamming are shown by a polar plot in the Figure 53.
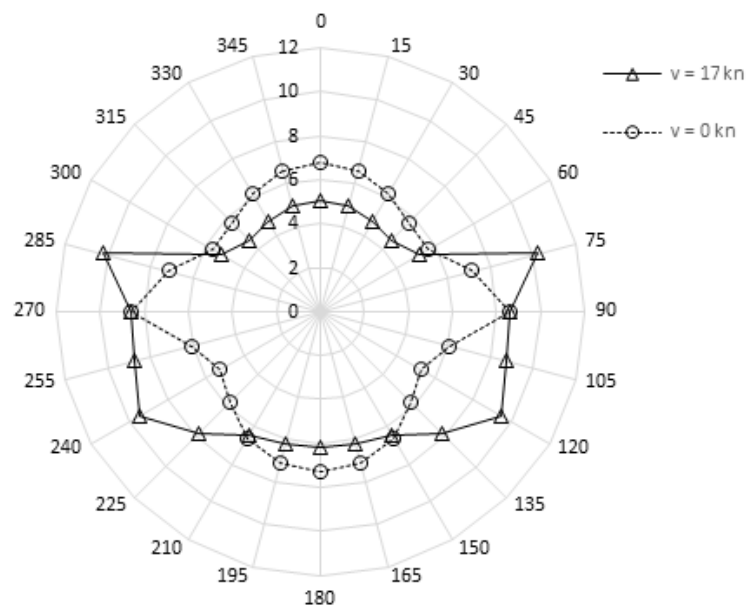
Figure 53 *Polar plot of limit significant wave height H_s[m] depending on relative ship-to-wave heading according to the bow slamming operability criteria*
Slika 9 Polarni dijagram granične značajne valne visine H_s [m]s obzirom na relativni kurs broda u odnosu na valove prema kriteriju udaranja pramca

The bow slamming limit condition for the considered vessel at cruising speed of 17 kn will first be exceeded at significant wave height H_s = 4.55 meters, with waves incoming at 45° to bow. A deviation from that relative ship-to-wave course (e.g. to 75°) causes significant difference in response. The most favourable course to recommend to the ship's master, according to the applied methodology and with regard to the selected criteria, without sped alteration, is what is colloquially known as "the stern quarter". Such suggestion corresponds well to known good maritime practice.

By comparing a certain limit value of H_s with the sea state table valid for the Adriatic basin as whole, it is easily possible to determine that H_s > 4.55 meters occurs 0.05% of the time, i.e. 0.183 days per year. In other words, such a ship, on an annual basis, at certain heading at cruising speed will not meet the selected criteria for an average of 2.2 hours, and will have to modify the operating profile.

The previous conclusion, however, needs to be considered strictly in the context of the one selected and applied criteria – bow bottom slamming. A wider analysis should also consider effects

such as propeller emergence, green water on deck, engine overheating due to additional resistance with incoming high waves or excessive roll in beam seas, limit accelerations, crew and passenger comfort criteria, etc. According to a question-and-answer survey among professional seafarers [5] 61% stated that the decisive seakeeping criteria to modify the ship operation profile (speed or course change) is excessive rolling followed with 33% for excessive bow slamming. The exact list of criteria should always be custom tailored to a specific ship [6,7,8] with regard to its characteristics, area of navigation and purpose.

5. Conclusion

A case study example for passenger ship operability, in terms of frequency of exceedance of the bow slamming limit criteria, in the Adriatic Sea is presented. The newly developed JONSWAP Adriatic wave spectrum is used for the description of the local sea conditions. Methodology of estimating the fraction of time a ship will not be able to operate in the intended region is described. Only the slamming seakeeping criterion is applied in the paper, but extension to other criteria is straightforward. The approach is useful for ship owners and operators in the decision-making process, when a new ship is acquired for known operational environment.

REFERENCES

[1]   Grin, R.Voyage simulation techniques as a design tool for cruise vessels, RINA 2011, London

[2]   Prpić-Oršić J, Čorić V. Pomorstvenost plovnih objekata. Zigo, Rijeka. 2006.

[3]   Katalinić M, Ćorak M, Parunov J. Optimized Wave Spectrum Definition for the Adriatic Sea. Naše more. 2020 Mar 11;67(1):19-23.

[4]   Katalinić M, Parunov J. Wave statistics in the Adriatic Sea based on 24 years of satellite measurements. Ocean engineering. 2018 Jun 15;158:378-88.

[5]   Mudronja L, Katalinić M, Vidan P, Parunov J. Route planning based on ship roll in numerically modelled heavy seas. In 22. simpozij Teorija i praksa brodogradnje, in memoriam prof. Leopold Sorta (Sorta 2016) 2016 Jan 1.

[6]   Tezdogan T, Incecik A, Turan O. Operability assessment of high speed passenger ships based on human comfort criteria. Ocean Engineering. 2014 Oct 1;89:32-52.

[7]   Sayli A, Alkan AD, Nabergoj R, Uysal AO. Seakeeping assessment of fishing vessels in conceptual design stage. Ocean Engineering. 2007 Apr 1;34(5-6):724-38.

[8]   Tello M, e Silva SR, Soares CG. Seakeeping performance of fishing vessels in irregular waves. Ocean Engineering. 2011 Apr 1;38(5-6):763-73.

COMPARISON OF WAVE DATA FROM DIFFERENT SOURCES IN THE NORTH ADRIATIC SEA

Maro, Ćorak*ᵃ, Marko, Katalinić ᵇ, Joško, Parunov ᶜ, Antonio, Mikulić ᶜ

a University of Dubrovnik, Maritime Department, Ćira Carića 4, 20000, Dubrovnik
b University of Split, Faculty of Maritime Studies, Ul. Ruđera Boškovića 37, 21000, Split
c University of Zagreb, Faculty of Mechanical Engineering and Naval Architecture, I. Lučića 5, 10000, Zagreb
* Corisponding Author, maro.corak@unidu.hr

Abstract

Wave data obtained from measurements by research tower ACQUA ALTA are compared with those obtained by numerical re-analysis and satellite measurements contained in Oceanor database, for almost the same location in the north part of the Adriatic Sea. Databases are briefly described in the first part of the paper and then comparative analysis of significant wave heights is performed. For each year (1979-2019) maximum significant wave height and time of occurrence are extracted from each of two databases. Significant wave height and peak wave periods are further presented in the form of wave scatter diagrams. Comparative analysis presents basis for the future analysis of uncertainties of long-term extreme wave conditions caused by wave data from different sources.

Key words: Adriatic Sea, Significan wave height, Peak frequency, Scatter diagram ;

Sažetak (Abstract in Croatian only for Croatian speaking authors)

Podaci o valovima dobiveni mjerenjima na tornju ACQUA ALTA uspoređeni su s numerički analiziranim satelitskim mjerenjima u OCEANOR bazi podataka, za skoro jednaku poziciju u sjevernom dijelu Jadranskog mora. Baze podataka su kratko opisane u prvom dijelu rada, a zatim je napravljena komparativna analiza značajnih valnih visina. Za svaku godinu (1979 – 2019) izvučena je maksimalna značajna valna visina skupa s vremenom javljanja. Značajna valna visina i vršni periodi su nadalje prikazani u obliku dijagrama stanja mora. Komparativna analiza predstavlja osnovu za buduću analizu nesigurnosti dugoročnih uvjeta uzrokovanih valnim podacima iz različitih izvora.

Ključne riječi: Jadransko more, Značajna valna visina, Vršna frekvencija, Dijagram stanja mora;

1. Introduction

Accurate knowledge of wave statistics is crucial for safety analysis of marine structures. Wave statistics is used for long-term analysis of marine structure's motions and loads in order to analyse their fatigue behaviour or extreme responses. Wave statistics is created based on wave data collected using different types of long-term wave measurements, observations or numerical predictions. Due to various method employed in their acquisition, wave data can differ even if they refer to the same geographical location. Uncertainty of wave data collected from different sources can have considerable impact on design and analysis of ships and marine structures [1], [2]. Therefore, such uncertainty became focus of the interests of scientific and engineering community in the recent years [3]. It was found that uncertainty in wave data may be divided into measurement, statistical (sampling variability) and modelling uncertainties, which are still not fully quantified today.

The present paper presents comparison of two validated and recognized databases containing wave data collected from different sources at almost the same location. First database analysed consists of 39 years of directional wave time series recorded since 1979 at the ACQUA ALTA oceanographic research tower, located in the Northern Adriatic Sea [4]. Second database is OCEANOR WorldWaves atlas, which is developed primarily based on satellite measurements,

validated by in-situ measurements by wave buoys and hindcasted by numerical wave modelling [5]. OCEANOR database is available for the period 1992-2019 for 39 locations in the Adriatic Sea. One of available locations is fairly close (about 38 km) to the ACQUA ALTA, without any natural obstacle between them as presented in Figure 1.
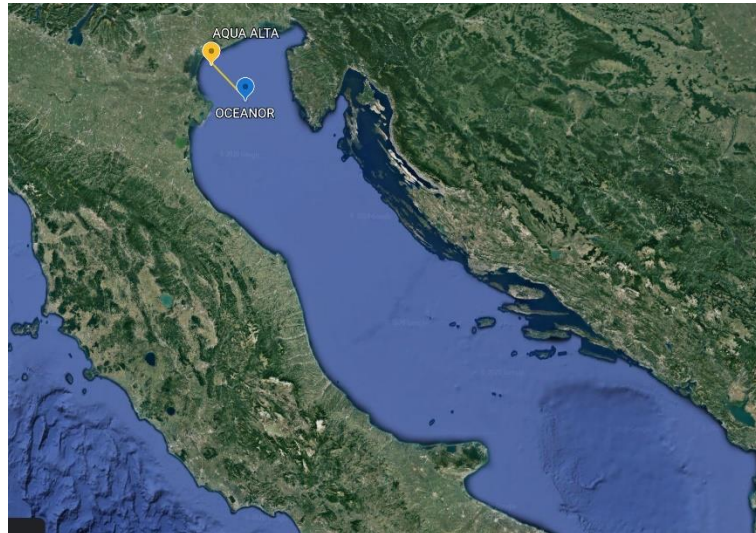
Figure 1 *The distance between ACQUA ALTA tower and OCEANOR location #3. Source Google: Earth Pro*
Slika 1 Udaljenost između ACQUA ALTA tornja i OCEANOR lokacije broj 3 Izvor Google: Earth Pro

The aim of the paper is to make comparative analysis of these two databases with respect to the most important wave parameters used in design of marine structures. Thus, maximum yearly significant wave heights from each of two databases are extracted and compared. Also, wave scatter diagrams, containing frequencies of occurrence of sea states defined by significant wave height and peak wave period are analysed. Results of the comparative analysis may provide valuable input for further analysis of long-term extreme values and associated uncertainties [3].

The paper is organized in the following way. After introduction, description of underlying databases is provided. After that, comparison of results is presented together with the discussion. Finally, appropriate conclusions are drawn.

2. ACQUA ALTA database

A database of the in-situ measurements is available from ACQUA ALTA, an oceanographic research tower located in the Northern Adriatic Sea as presented in Figure 2.
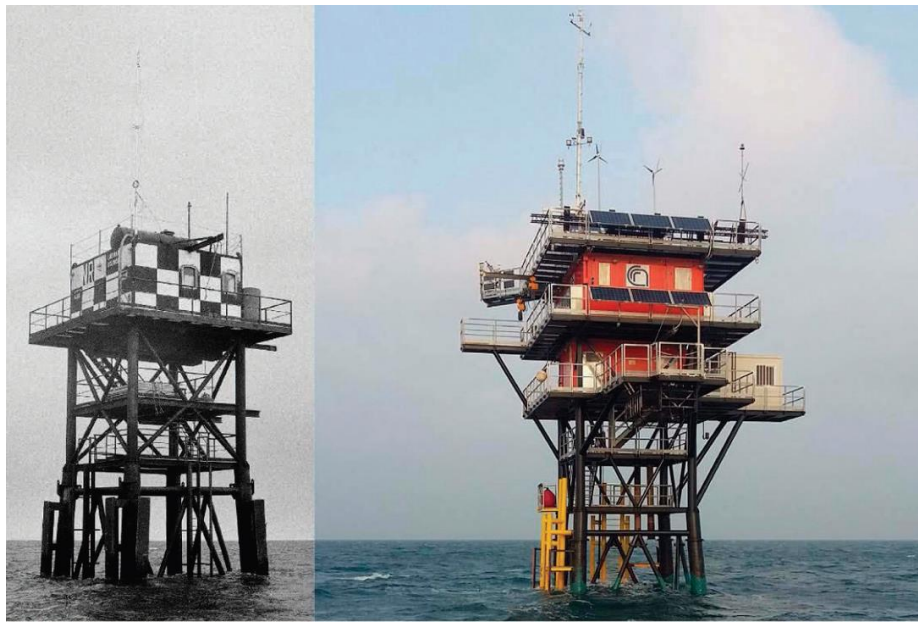
Figure 2 *The ACQUA ALTA oceanographic tower years 1970 and 2017). Source [4]*
Slika 2 ACQUA ALTA oceanografski toranj, Izvor [4]

The database is extensively used and reported in literature [4]. The complete set of basic wave parameters is available in open-source format. Measurements comprise data from 39 years (exactly 438 912 measurements), in three-hour intervals, starting from 1979 to 2017. The measuring tower is located 16 km of Venice (latitude/longitude: 45.3° / 12.5°) at a depth of 16 meters.

3. Fugro-Oceanor database

WorldWaves (WW) database is developed in Fugro-Oceanor, an industrial leader in the field of met-ocean analysis for the offshore industry. WW provides wind and wave data for the global domain from 1979 up to the present. The database is developed by combining numerical wave model hindcast results with the available satellite altimetry data. While satellite altimetry could be considered a more accurate data source (it is extensively verified by buoy in-situ measurements where possible) it is non-homogenous in space and time depending on satellite tracks and overflight time (Figure 3). The space and time homogeneity is thus acheived by underlying the numerical wave model results from the WAM model run at ECMWF (European Centre for Medium range Weather Forecast), i.e. calibrating the numerical model results with appropriate satellite altimetry data [5].
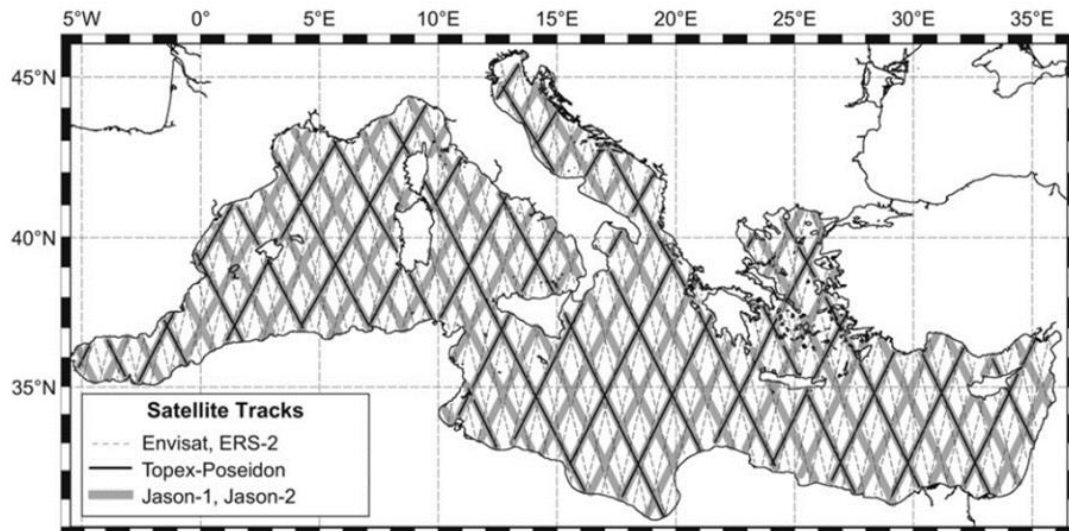
Figure 3 *Satellite tracks over ground. Wave measurement missions over the Mediterranean. Source: Liberti L, Carillo A, Sannino G. Wave energy resource assessment in the Mediterranean, the Italian perspective. Renewable Energy. 2013 Feb 1;50:938-49.*
Slika 3 Satelitska mjerenja iznad zemlje. Misija mjerenja valova iznad Mediterana. Izvor Liberti L, Carillo A, Sannino G. Wave energy resource assessment in the Mediterranean, the Italian perspective. Renewable Energy. 2013 Feb 1;50:938-49.

For the Adriatic Sea, 39 uniformly distributed location across the basin are available in 0.5° lat./long. resolution. At each location, 12 physical wave and wind parameters are available at 6-hour intervals (four per day). Each location contains a total of 38600 records, starting in September 1992 and ending in January 2019.

4. Results of the analysis

Comparative analysis of previously described wave databases is performed where the accent is given on few types of information used in design of marine structures. Firstly, maximum significant wave heights are extracted and compared for all available years from database sets. However, since available records from ACQUA ALTA tower exists until the end of 2017, while the OCEANOR data set starts from the beginning of 1992 the comparison could be performed only in these 26 years (1992-2017). Results are presented in Figure 4 from which it can be concluded that maximum wave height in specified time reads 5.6 m and it is recorded in OCEANOR database during 1993. In the same year, the maximum *Hs* measured at ACQUA ALTA reads 4.0 m. The agreement between recorded maximum *Hs* is much better in 1992 where wave heights of 4.69 m and 5.15 m are observed on the same day and hour (09.12.1992. 0.00 h) on ACQUA ALTA and OCEANOR, respectively. The maximum recorded *Hs* over all data in OCEANOR database is observed in 2018 and reads 5.76 m, while the maximum *Hs* at ACQUA ALTA tower was recorded in 1992 as previously discussed.
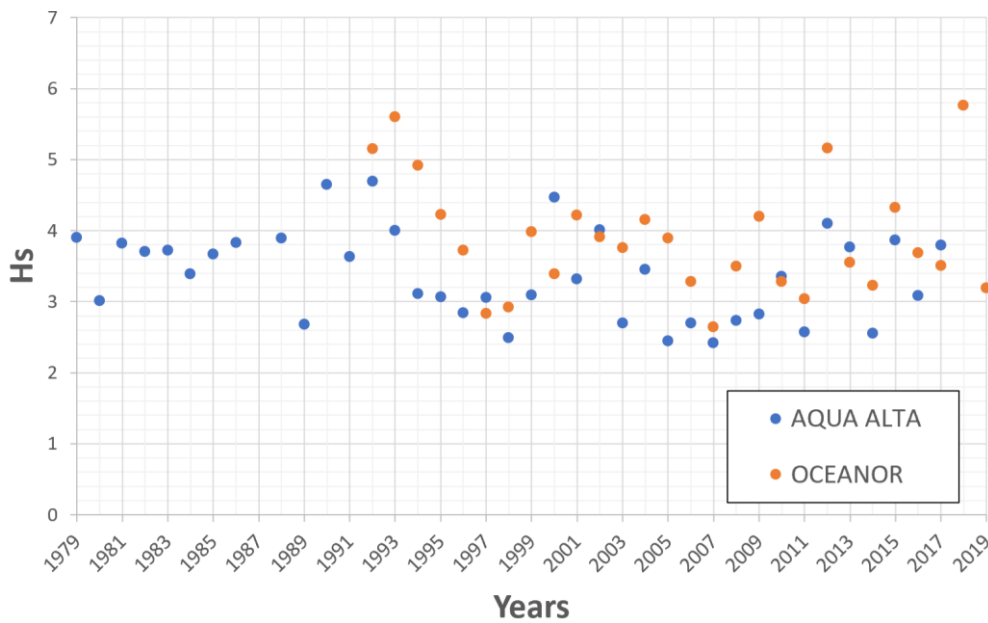
Figure 4 *Maximum significant wave heights for ACQUA ALTA and OCEANOR location*
Slika 4 Maksimalne značajne valne visine na ACQUA ALTA i OCEANOR lokaciji

Closer look to the processed records reviles that qualitative agreement between time series of *Hs* in two databases is much better compared to the single maximum *Hs* observed as point in time. Such comparison is shown in Figure 5 for December in 1992 and January in 1993. Although discrepancies were recorded in maximum *Hs*, both records clearly show that, based on diagram peaks three storms occurred during that period. Generally, OCEANOR database provides somewhat larger *Hs* through all analysed years. This may be explained by the fact that the exact location of the OCEANOR is little more exposed to open waters with larger water depth compared to the ACQUA ALTA tower.
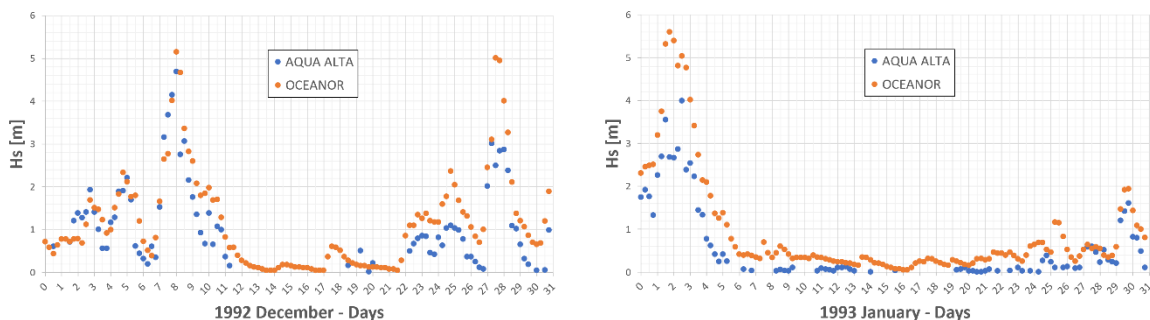
Figure 5 *Time series of Hs for December (1992) and January (1993) on considered locations*
Slika 5 Vremenska promjena *Hs* u prosincu 1992. i siječnju 1993. na promatranim lokacijama

Next, frequencies of occurrence of sea states defined by significant wave height and peak wave period are analysed and presented in the form of scatter diagrams. OCEANOR scatter diagram contains 38600 sea states, while ACQUA ALTA scatter diagram is constructed from 78800 data. Results are given in Figure 6. where we can notice that OCEANOR has a wider spread of significant wave heights and peak wave periods. Majority of sea states in ACQUA ALTA are accumulated

216

between *Hs* = 0 – 1.5 m and *Tp* = 1.5 – 5 s, while OCEANOR wave heights are located between 0 – 2.5 m for peak periods of 1 – 5.5 s.

a)

b)

Figure 6 *Scatter diagrams plot for (a) ACQUA ALTA and (b) OCEANOR*
Slika 6 Plot tablice stanja mora za (a) ACQUA ALTA i (b) OCEANOR

Finally, angular modal spectral frequency for seas states from two datasets is analysed to detect which location has the steeper waves. Analysis is based on Tabain`s modal frequency formulation which is optimized for two considered locations as described by Katalinić et al. [6].

Relationship between *Hs* and *Tp* is shown in Figure 7 for two databases. Since Figure 5 shows large scatter of angular frequencies for a given significant wave height the Tabain`s formulation is optimized in order to find best average fit of specified logs.
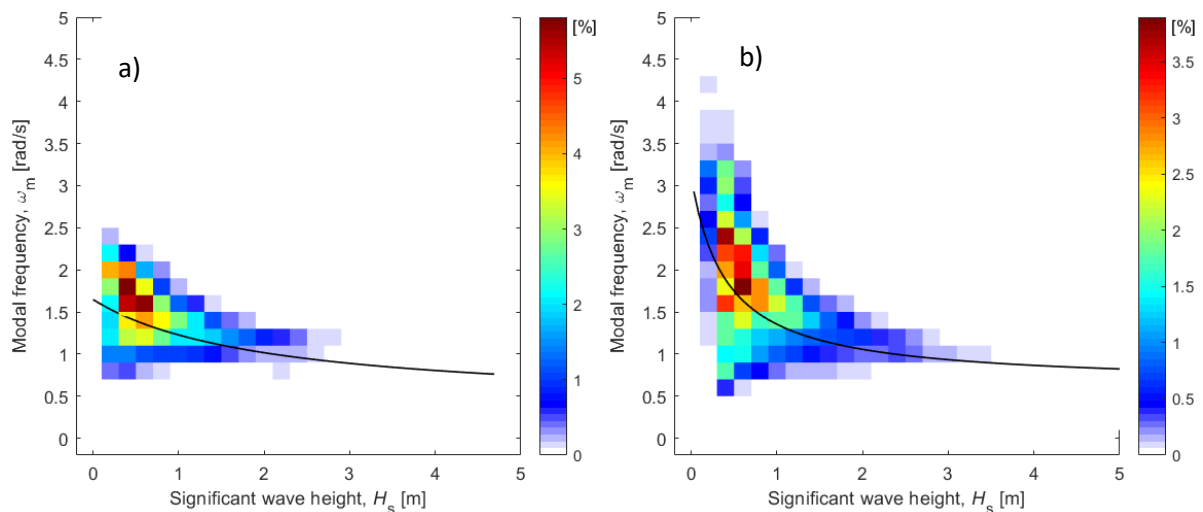
Figure 7 *Frequency of occurrence distribution of significant wave height and modal frequency for (a) ACQUA ALTA and (b) OCEANOR*
Slika 7 Učestalost pojavljivanja značajne valne visine u ovisnosti o modalnoj frekvenciji za (a) ACQUA ALTA i (b) OCEANOR

Original Tabain`s expression for modal frequency as a function of a significant wave height reads:

$$\omega_m = a + \frac{b}{H_S + c} \tag{1}$$

where coefficients a, b and c are given in Table 1. Such formulation is optimized by nonlinear least square method in order to find the best possible agreement with two considered database sets. After optimization, the coefficients of the best fit are found as given in Table 1.

Table 1 Coefficients for modal frequency formulation

Table 1 Koeficijenti za jednadžbu modalne frekvencije

	Tabain formulation	ACQUA ALTA	OCEANOR
a	0.32	0.38	0.64
b	1.8	2.54	1.01
c	0.6	2.01	0.41

The original and optimized results, together with Tabain`s original formulation are presented in Figure 8 from which it can be concluded that OCEANOR database provides a somewhat steeper waves compared to the ACQUA ALTA tower. Also, the agreement between two optimised curves is much better for larger wave heights while there are significant discrepancies between two databases for lower values of *Hs*. This could be explained by a wider spread of sea states across peak periods for OCEANOR database. However additional analysis to explain these differences are needed.
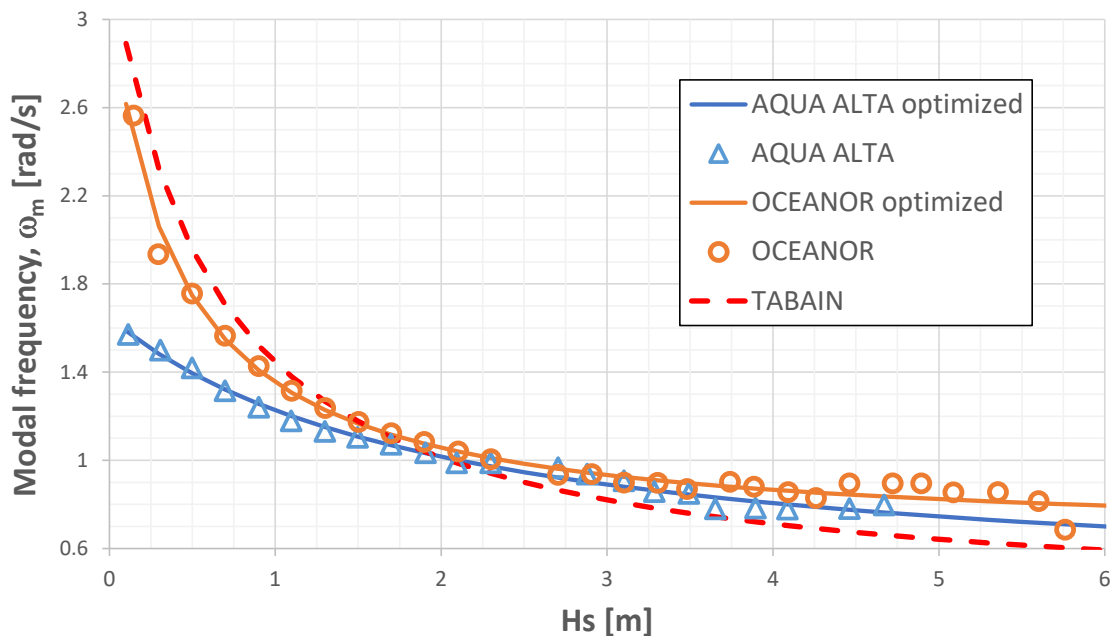
Figure 8 *Comparison of optimised and original Tabain`s spectral modal frequency formulations*
Slika 8 Usporedba optimiziranih i originalnih Tabain-ovih izraza za modalnu frekvenciju

5. Conclusions

The comparison of wave data collected by two different sources for the location in the Northern Adriatic Sea is presented. Analysed wave data sources are measurements from fixed wave tower station and satellite measurements complemented by numerical re-analysis.

Results of the study show that measured yearly extreme significant wave heights from satellite measurements and numerical re-analysis overestimate measurements from fixed wave tower in average by 17%. Differences in wave scatter diagrams created by two data sets are also important and can impact on design and analysis of marine structures. Modal frequency of wave spectra is higher in OCEANOR database, resulting in the steeper waves for the same significant wave height.

Although databases do not refer to the exacly the sam geographic location, the reasons for these differences are not completely clear and it should be studied in the future research.

Acknowlegments

REFERENCES

[1]   Vettor R.; Soares CG. 2016. Assessment of the Storm Avoidance Effect on the Wave Climate along the Main North Atlantic Routes. Journal of Navigation 69(1): 127–144.

[2]   Schirmann, ML.; Collette MD.; Gose JW. 2019. Impact of weather source selection on time-and-place specific vessel response predictions. Trends in the Analysis and Design of Marine Structures - Proceedings of the 7th International Conference on Marine Structures, MARSTRUCT 2019: 33– 41.

[3]   Bitner-Gregersen, EM; Dong, S; Fu T.; Ma N.; Maisondieu C.; Miyake R.; Rychlik I., 2016. Sea state conditions for marine structures' analysis and model tests. Ocean Engineering 119: 309–322.

[4]   Pomaro A. et al. 2018, 39 years of directional wave recorded data and relative problems, climatological implications and use. Sci. Data 5:180139 doi: 10.1038/sdata.2018.139.

[5]   Katalinić, M.; Parunov, J. 2018, Wave statistics in the Adriatic Sea based on 24 years of satellite measurements, Ocean engineering, 158, 378-388 doi:10.1016/j.oceaneng.2018.04.009.

[6]   Katalinić, M.; Ćorak, M.; Parunov, J. 2020, Optimized wave spectrum definition for the Adriatic Sea, Naše more 67(1), pp. 19-23.

THE IMPACT OF ANTIFOULING COATINGS ON SHIP PERFORMANCE

Andrea Farkas[a], Nastia Degiuli[a], Ivana Martić[a], Ivan Gospić[b]*

a University of Zagreb, Faculty of Mechanical Engineering and Naval Architecture, Ivana Lučića 5, Zagreb, Croatia
b University of Zadar, The Maritime Department, Ulica Mihovila Pavlinovića 1, Zadar, Croatia
* Corresponding Author, nastia.degiuli@fsb.hr

Abstract

Energy efficiency is one of the main goals that must be met within the preliminary design of the ship, as well as for existing ships. Recently, the International Maritime Organization (IMO) has introduced regulations such as the Energy Efficiency Design Index (EEDI), the Ship Energy Efficiency Management Plan (SEEMP), and the Energy Efficiency Operational Index (EEOI) to reduce emissions in shipping industry. There are various measures to increase the energy efficiency of a ship, and one of them is the application of coatings with low surface roughness. In this paper, the impact of the application of two types of antifouling coatings from the ship resistance and effective power point of view is analyzed. Grigson roughness function and Granville similarity law scaling method are applied to determine frictional resistance coefficient of an oil tanker and a container ship in full-scale. The obtained results point out the advantages of coatings with low surface roughness regarding the effective power and thus the energy efficiency of the ship.

Key words: antifouling coatings; ship resistance; Granville similarity law scaling method; oil tanker; container ship

Sažetak

Energetska učinkovitost predstavlja jedan od glavnih ciljeva koji se moraju ispuniti u okviru preliminarnog projekta broda, kao i za postojeće brodove. U posljednje vrijeme Međunarodna pomorska organizacija (IMO) je uvela propise kao što su Projektni indeks energetske učinkovitosti (EEDI), Plan upravljanja energetskom učinkovitošću broda (SEEMP), kao i Operativni indeks energetske učinkovitosti (EEOI) kako bi se smanjila emisija štetnih plinova u pomorskoj industriji. Postoje razne mjere za povećanje energetske učinkovitosti broda, a jedna od njih je primjena premaza s manjom hrapavošću. U ovom radu, analiziran je utjecaj primjene dvije vrste antivegetativnih premaza sa stajališta otpora broda i efektivne snage. Primjenjena je Grigsonova funkcija hrapavosti te Granvilleova metoda zakona sličnosti za određivanje koeficijenta otpora trenja tankera i kontejnerskog broda u naravi. Dobiveni rezultati ukazuju na prednosti primjene premaza s manjom hrapavošću sa stajališta efektivne snage, a tako i energetske učinkovitosti broda.

Ključne riječi: antivegetativni premazi; otpor broda; Granvilleova metoda zakona sličnosti; tanker; kontejnerski brod

1. Uvod

Svjetska pomorska trgovina u posljednjih nekoliko godina bilježi porast, čemu u prilog ide i poboljšanje svjetske ekonomije. U 2017. godini se pomorska trgovina povećala za 4%, što je bio najbrži rast u posljednjih 5 godina. Pored toga, u 2017. godini zabilježena je stopa rasta od 3,3% u globalnoj tonaži svjetske flote, nakon 5 godina stagnacije. Trenutno je svjetska flota uglavnom pogonjena gorivom na bazi ugljikovodika i stoga se ne može izbjeći emisija stakleničkih plinova. Međunarodna pomorska organizacija (eng. International Maritime Organisation, IMO) usvojila je strategiju u travnju 2018. godine prema kojoj bi smanjenje ukupne godišnje emisije stakleničkih plinova do 2050. godine bilo najmanje 50% u usporedbi s ukupnom godišnjom emisijom stakleničkih plinova u 2008. godini [1]. Stoga je energetska učinkovitost jedan od glavnih ciljeva koji se moraju

ispuniti u okviru preliminarnog projekta broda, kao i za postojeće brodove. U posljednje vrijeme IMO je uveo propise kao što su projektni indeks energetske učinkovitosti (eng. Energy Efficiency Design Indeks, EEDI), plan upravljanja energetskom učinkovitošću broda (eng. Ship Energy Efficiency Management Plan, SEEMP), kao i operativni indeks energetske učinkovitosti (eng. Energy Efficiency Operational Indeks, EEOI) kako bi se smanjila emisija štetnih plinova u pomorskoj industriji [2]. Stoga je smanjivanje potrošnje goriva presudan parametar za budućnost pomorske industrije, ne samo sa stajališta brodovlasnika, već i sa stajališta zaštite okoliša [3]. Za postojeće brodove, brodovlasnici mogu primijeniti operativne mjere energetske učinkovitosti kao što su smanjenje brzine; optimizacija rute plovidbe; optimizacija čišćenja trupa; primjena premaza s manjom hrapavošću; primjena alternativnih goriva, Fletnerrovih rotora, zmajeva, jedara, vjetro turbina, uređaja za uštedu energije itd. Međutim, sa ciljem primjene određene mjere uštede energije, brodari procjenjuju povrat ulaganja. Izračun povrata ulaganja vrlo je složen, pa je pomorska industrija u potrazi za općim metodama i modelima za procjenu potencijalnih ušteda energije [4]. Iako je dokazano da smanjenje brzine značajno poboljšava energetsku učinkovitost broda, troškovi uzrokovani plovidbom smanjenom brzinom doveli su do neisplativosti provedbe ove mjere na tržištu. Primjena raznih uređaja temeljenih na obnovljivim izvorima energije može biti vrlo efikasna metoda za smanjenje emisije štetnih plinova, ali zbog velikog broja nepoznanica vezanih uz tehnologiju, pouzdanost, sigurnost, kao i zbog nedostatka praktične primjene u stvarnosti, široka primjena ovih uređaja još uvijek nije ostvarena [5]. Optimizacija rute plovidbe je važna operativna mjera, jer može smanjiti emisije štetnih plinova, ali i povećati sigurnost putovanja. Međutim, vremenske uvjete nije moguće kontrolirati te ova metoda ovisi o vremenskoj prognozi. Također, izloženost lošim vremenskim uvjetima se može svesti na minimum samo ukoliko se trajanje putovanja poveća [6]. Iako postoje razne mjere za sprječavanje obraštaja na trupu broda, primjena antivegetativnih premaza je najčešće primjenjivana mjera [7]. Danas postoje dva glavna pristupa u prevenciji obraštaja s antivegetativnim premazima, tj. biocidni i nebiocidni premazi [8]. Biocidni premazi polako otpuštaju ugrađene biocide u more i tako sprječavaju prianjanje mikroorganizama na površinu [9]. Tradicionalno, većina antivegetativnih premaza sadrži tributilin (TBT) ili bakar. Osamdesetih godina se smatralo da je problem obraštaja riješen primjenom TBT-a. Međutim, zbog štetnog utjecaja TBT-a na okoliš, IMO je zabranio antivegetativne premaze na bazi

TBT-a od 2008 godine. Stoga se trenutno biocidi temelje na bakru, ali se smatra da će se korištenje i tih antivegetativnih premaza također zabraniti zbog njihovog utjecaja na okoliš [10]. Iz tog razloga se naglasak stavlja na razvoj nebiocidnih premaza [11]. Nebiocidni premazi se nazivaju još i neobraštajući premazi. Ovi premazi onemogućuju potpuno prianjanje obraštaja na trup broda te na taj način omogućuju otpuštanje obraštaja tijekom plovidbe ili uklanjanje primjenom jednostavnog mehaničkog čišćenja [12]. Osim sprječavanja pojave obraštaja na trupu broda, antivegetativni premazi utječu na otpor trenja broda, budući da svaki premaz ima određenu hrapavost, koja uzrokuje porast hrapavosti, a samim time i otpor trenja broda. Budući da otpor trenja predstavlja dominantnu komponentu ukupnog otpora broda, čak i relativno malo smanjenje otpora trenja može uzrokovati značajnu uštedu u potrošnji goriva, a time i smanjenje emisije stakleničkih plinova. Stoga je u posljednje vrijeme sve više istraživanja usmjereno na ispitivanje otpora trenja raznih antivegetativnih premaza [13-17]. Utjecaj hrapavosti antivegetativnog premaza na otpor trenja broda određuje se preko funkcije hrapavosti uz pretpostavku da je utjecaj hrapavosti ograničen na unutarnji dio turbulentnog graničnog sloja. Funkcija hrapavosti definirana je kao smanjenje srednjeg profila brzine u inercijalnom podsloju. Budući da ne postoji univerzalna funkcija hrapavosti, koja bi mogla opisati sve vrste hrapavosti, potrebno je provesti eksperimentalna ispitivanja pojedinih tipova hrapavosti. U radu [18], moguće je uočiti kako Grigsonova funkcija hrapavosti predstavlja najbolji model funkcije

221

hrapavosti za antivegetativne premaze, odnosno površinu trupa broda s antivegetativnim premazom. Kada se odredi model funkcije hrapavosti, tj. kada se funkcija hrapavosti prikaže u ovisnosti o Reynoldsovom broju na temelju hrapavosti, primjenom Granvilleovog zakona sličnosti moguće je odrediti porast otpora trenja za određenu hrapavu površinu definiranu tom funkcijom hrapavosti.

U ovom radu je na temelju eksperimentalnih ispitivanja ploča premazanih s dva tipa antivegetativnih premaza [17] te primjenom Grigsonove funkcije hrapavosti i Granvilleovog zakona sličnosti određen otpor trenja te ukupni otpor tankera i kontejnerskog broda. U istraživanju [17], autori su proveli mjerenja otpora trenja za tri stanja izvorne hrapavosti površine ploča: laboratorijsko stanje, niska razina hrapavosti i visoka razina hrapavosti. U ovom radu su stoga određeni prirasti otpora trenja za navedena tri stanja izvorne hrapavosti površine trupa broda. Pokazane su prednosti primjene antivegetativnog premaza s manjom hrapavošću sa stajališta efektivne snage.

2. Metoda

Utjecaj hrapavosti antivegetativnih premaza na efektivnu snagu broda istražen je na temelju određivanja porasta koeficijenta otpora trenja. Naime, hrapavost antivegetativnog premaza modelirana je pomoću Grigsonove funkcije hrapavosti definirane izrazom:

$$\Delta U^+ = \frac{1}{\kappa}\ln\left(1 + k^+\right) \tag{1}$$

gdje je κ von Karmanova konstanta, a k^+ Reynoldsov broj na temelju hrapavosti.

Reynoldsov broj na temelju hrapavosti računa se prema izrazu:

$$k^+ = \frac{k u_\tau}{\nu} \tag{2}$$

gdje je k skala hrapavosti, u_τ brzina trenja, a ν koeficijent kinematičke viskoznosti.

Veća hrapavost antivegetativnog premaza ogleda se kroz veću vrijednost skale hrapavosti. Izbor skale hrapavosti vrlo je važan za definiciju modela funkcije hrapavosti. Skala hrapavosti odabire se na način da vrijednosti funkcije hrapavosti odgovaraju unaprijed određenom modelu funkcije hrapavosti, pod uvjetom da su vrijednosti funkcije hrapavosti i model funkcije hrapavosti međusobno usklađeni [19]. Vrijednosti skale hrapavosti za dvije vrste antivegetativnih premaza za razna stanja površine podloge na koju su ti premazi aplicirani dane su u [16]. Yeginbayeva i Atlar [16] ispitivali su otpor trenja ploča premazanih s tri vrste premaza, sa ciljem određivanja skale hrapavosti odnosno modela funkcije hrapavosti za te premaze.

U ovom radu, ispitan je utjecaj dva premaza, Intersleek 1100 SR te Interspeed 6400, budući da su ova dva premaza trenutno aktualna na tržištu. Intersleek 1100 SR predstavlja napredni neobraštajući premaz (eng. Fouling Release, FR) od fluoropolimera, tj. ne biocidni premaz s patentiranom tehnologijom otpuštanja biofilma, koja omogućuje otpuštanje biofilma tijekom plovidbe. Interspeed 6400 predstavlja premaz s topljivom matricom (eng. Controlled Depletion Polymer, CDP) bez TBT-a, odnosno na bazi bakra te predstavlja tipični biocidni premaz. Danas je većina brodova svjetske flote premazana upravo biocidnim premazima. Mnogobrojni su procesi koji ili pojedinačno ili u kombinaciji uzrokuju hrapavost trupa. Ti procesi mogu se podijeliti u dvije faze: prva faza se događa tijekom isporuke, a druga se javlja kod brodova u službi, uključujući i rutinsko čišćenje trupa u suhom doku. Stoga, svježe aplicirani antivegetativni premazi imaju veću hrapavost

od one koju bi imali u idealnim, laboratorijskim uvjetima na pjeskarenoj ploči. Iz tog razloga su Yeginbayeva i Atlar [16] simulirali uvjete hrapavosti površine trupa broda postavljanjem umjetne hrapavosti u formi zrnaca pijeska na površinu ispitivanih ploča, koje su potom premazivali antivegetativnim premazima. Takvo modeliranje hrapavosti trupa temeljilo se na iskustvu International Paint Ltd i njihovoj analizi baze podataka od 845 pojedinačnih ispitivanja hrapavosti trupa broda provedenih između 2003. i 2014. godine. Stoga su Yeginbayeva i Atlar [16] ispitivali hidrodinamička svojstva antivegetativnih premaza za tri stanja površine podloge. Važno je napomenuti da su antivegetativni premazi aplicirani sprejanjem, nakon što su prethodno ploče premazane primerom i antikorozivnim premazom prema preporuci proizvođača premaza. Dobivene vrijednosti skale hrapavosti za navedena tri stanja površine ploče te za FR i CDP premaz dane su u Tablici 1.

Table 1 Roughness length scale of investigated antifouling coatings

Table 1 Skale hrapavosti ispitanih antivegetativnih premaza

Premaz	Stanje površine	Skala hrapavosti, μm
FR	laboratorijsko	1,20
CDP	laboratorijsko	4,80
FR	niska hrapavost	4,49
CDP	niska hrapavost	11,70
FR	visoka hrapavost	5,10
CDP	visoka hrapavost	14,98

Porast koeficijenta otpora trenja određen je primjenom Granvilleovog zakona sličnosti, koji predviđa povećanje koeficijenta otpora trenja ploče duljine jednake duljini broda primjenom određenog modela funkcije hrapavosti. Grafički prikaz procedure skaliranja koeficijenta otpora trenja za hrapavu ploču prikazan je na Slici 1.

Koeficijent otpora trenja glatke ravne ploče prema Schoenherrovoj liniji otpora trenja glasi:

$$\frac{0.242}{\sqrt{C_{F0}}} = \log(Re\,C_{F0}) \tag{3}$$

gdje je C_{F0} koeficijent otpora trenja glatke ravne ploče, a Re je Reynoldsov broj.

Linija otpora trenja za hrapavu ploču dobije se pomicanjem linije otpora trenja za glatku ploču za udaljenost $\Delta U^+ / \ln(10/\kappa)$. Potom se ucrtavaju dvije krivulje: krivulja konstantne vrijednosti $L^+_{\text{ploče}}$ te krivulja konstantne vrijednosti L^+_{broda}, koja je pomaknuta od krivulje $L^+_{\text{ploče}}$ za udaljenost $\log\left(L_{\text{broda}} / L_{\text{ploče}}\right)$. Linija konstantne krivulje $L^+_{\text{ploče}}$ određuje se prema:

$$L^+_{\text{ploče}} = \frac{L_{\text{ploče}}u_\tau}{\nu} \tag{4}$$

gdje je $L_{\text{ploče}}$ duljina ispitivane ploče koja iznosi 0,6 m.
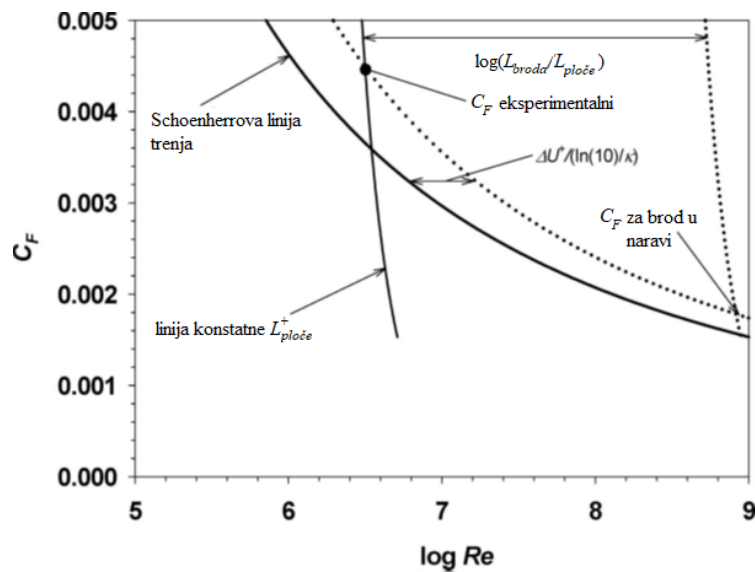
Figure 1 *Graphical representation of Granville's similarity scaling law*
Slika 1 Grafički prikaz Granvilleovog zakona sličnosti

Nakon što se odredi koeficijent otpora trenja hrapave ploče koja ima duljinu jednaku duljini broda $\left(C_{F0R} \right)$, moguće je odrediti porast koeficijenta otpora trenja kako slijedi:

$$\Delta C_F = C_{F0R} - C_{F0} \tag{5}$$

Koeficijent ukupnog otpora broda premazanog određenim antivegetativnim premazom određen je prema:

$$C_T = (1+k) C_{FR} + C_W \tag{6}$$

gdje je k faktor forme, C_{FR} koeficijent otpora trenja broda premazanog određenim antivegetativnim premazom, a C_W koeficijent otpora valova.

Koeficijent otpora trenja broda premazanog određenim antivegetativnim premazom računa se na sljedeći način:

$$C_{FR} = C_F + \Delta C_F \tag{6}$$

gdje je C_F koeficijent otpora trenja broda određen pomoću korelacijske linije model-brod ITTC 1957.

Efektivna snaga broda dobije se kao umnožak ukupnog otpora broda i brzine broda.

3. Ispitivani brodovi

U ovom radu je provedena analiza utjecaja antivegetativnih premaza na efektivnu snagu tankera i kontejnerskog broda. Kriso Very Large Crude Carrier 2 (KVLCC2) je veliki tanker za prijevoz nafte koji može prevesti 300000 tona sirove nafte. Predstavlja drugu varijantu Kriso tankera KVLCC s

modificiranim krmenim rebrima, koja su U-oblika. Kim i sur. [20] su proveli opsežna modelska ispitivanja sa ciljem određivanja otpora, značajki strujanja, značajki valova te propulzijskih značajki KVLCC2 broda. Duisburg Test Case (DTC) je post-panamax kontejnerski brod koji može prevesti 14000 TEU kontejnera. Moctar i sur. [21] proveli su opsežna ispitivanja sa ciljem određivanja otpora, propulzijskih značajki te mjerenja prigušivanja ljuljanja DTC broda. Nacrt rebara dva ispitana broda prikazan je na Slici 2. Glavne značajke ova dva broda dane su u Tablici 2.
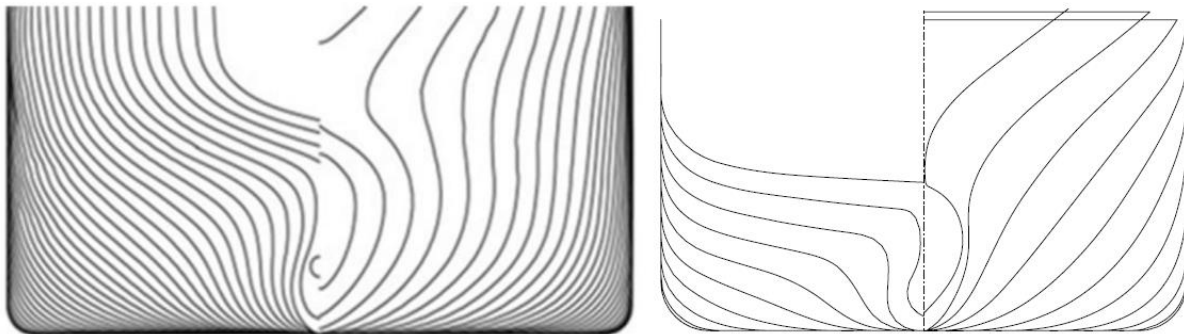
Figure 2 *Body plan of KVLCC2 (left) and DTC (right)*
Slika 2 Nacrt rebara KVLCC2 (lijevo) [22] i DTC (desno) [21]

Table 2 The main particulars of investigated ships

Table 2 Glavne značajke ispitivanih brodova

Značajka	KVLCC2	DTC
duljina između perpendikulara, m	320	355
duljina na vodnoj liniji, m	325,5	356,1
širina, m	58	51
gaz, m	20,8	14,5
istisnina, t	320750	177977
oplakana površina, m^2	27467	22032
blok koeficijent	0.8098	0.661
Froudeov broj	0,1423	0,2179
projektna brzina, čv	15,5	25

Kao što je moguće uočiti na Slici 2, oba ispitana broda imaju bulb te krmeno zrcalo. Ova dva broda predstavljaju tipične forme modernih trgovačkih brodova, pri čemu KVLCC2 predstavlja znatno puniju tankersku formu, dok DTC predstavlja finiju kontejnersku formu.

4. Rezultati i diskusija

Rezultati modelskih ispitivanja KVLCC2 [20] i DTC [21] prikazani su u Tablici 3. Treba napomenuti da je faktor forme za DTC određen primjenom računalne dinamike fluida za mjerilo modela. U Tablici 3 dane su vrijednosti za mjerilo modela. U ovom radu je pretpostavljeno da su faktor forme te koeficijent otpora valova jednaki za mjerilo modela te brod u naravi.

Table 3 Results of towing tank tests

Značajka	KVLCC2 [20]	DTC [21]
geometrijsko mjerilo	58	59,4
$10^3 C_T$	4,11	3,67
$10^3 C_F$	3,45	3,048
k	0,16	0,094
$10^3 C_W$	0,108	0,336

Vrijednosti koeficijenta otpora trenja za ravnu ploču duljine jednake duljini KVLCC2 i DTC broda određene su pomoću jednadžbe (3) te iznose 0,001393 za KVLCC2 i 0,001304 za DTC. Vrijednosti koeficijenta otpora trenja za KVLCC2 i DTC određene su prema korelacijskoj liniji model-brod te iznose 0,001392 za KVLCC2 i 0,001303 za DTC. Nakon što su određene vrijednosti koeficijenta otpora trenja, izračunati su porasti koeficijenta otpora trenja za određene antivegetativne premaze, a potom i koeficijenti ukupnog otpora. Dobiveni rezultati prikazani su u Tablicama 4 i 5. U Tablicama 4 i 5 dani su porasti koeficijenta otpora trenja, koeficijent otpora trenja i koeficijent ukupnog otpora za brod s određenim stanjem površine trupa broda, kao i dobiveni relativni porasti koeficijenata otpora trenja i koeficijenta ukupnog otpora u odnosu na brod s glatkom površinom trupa. Treba napomenuti da stanje površine trupa 1 predstavlja laboratorijsko stanje, stanje 2 predstavlja nisku hrapavost površine, a stanje 3 visoku hrapavost površine. Na Slici 3 prikazane su dobivene vrijednosti efektivne snage KVLCC2 i DTC brodova za razna stanja površine trupa. Kao što je moguće uočiti iz Tablica 4 i 5, kao i Slike 3, koeficijent ukupnog otpora kao i efektivna snaga značajno su manji za slučaj kada je površina trupa ispitanih brodova premazana FR premazom. Također se može uočiti da se povećavanjem hrapavosti površine trupa s laboratorijskog stanja na stanje visoke hrapavosti, razlike u efektivnoj snazi brodova koji su premazani FR i CDP premazom povećavaju. Tako dobivena efektivna snaga za laboratorijsko stanje površine trupa KVLCC2 premazane FR premazom iznosi 12408 kW, dok za CDP premaz iznosi 13001 kW, a za DTC premazan FR premazom iznosi 43369 kW, a CDP premazom iznosi 45760 kW. Ove razlike značajno su veće pri hrapavom stanju trupa, odnosno za stanje visoke hrapavosti efektivna snaga KVLCC2 premazanog FR premazom iznosi 13043 kW, dok za CDP premaz iznosi 14117 kW, a za DTC premazan FR premazom iznosi 45924 kW, a CDP premazom iznosi 49808 kW. Ovo se može pripisati dobrim svojstvima FR premaza Intersleek 1100 SR, koji iako apliciran preko početno hrapave površine, ne uzrokuje značajan porast hrapavosti, kao što i tvrdi proizvođač

premaza [23]. Ovo je vrlo važno svojstvo antivegetativnog premaza, s obzirom da hrapavost trupa broda znatno poraste tijekom službe. Stanje površine 2, odnosno niska hrapavost površine najviše odgovara početnom stupnju hrapavosti trupa broda prilikom apliciranja antivegetativnog premaza. Za ovaj slučaj efektivna snaga KVLCC2 premazanog FR premazom je za -6.35% manja u odnosu na efektivnu snagu KVLCC2 premazanog CDP premazom, dok je kod DTC ova razlika čak i veća te iznosi -6.53%.

Table 4 Results for different hull surface conditions for KVLCC2

Table 4 Rezultati za razna stanja površine trupa KVLCC2

Stanje površine trupa	$10^3 \Delta C_F$	$10^3 C_{FR}$	$10^3 C_{TR}$	ΔC_F, %	ΔC_T, %
FR 1	0,027	1,420	1,755	1,958	1,835
FR 2	0,094	1,487	1,833	6,773	6,348
FR 3	0,105	1,497	1,844	7,513	7,042
CDP 1	0,100	1,492	1,839	7,150	6,702
CDP 2	0,201	1,594	1,957	14,462	13,555
CDP 3	0,236	1,628	1,996	16,924	15,864

Table 5 Results for different hull surface conditions for DTC

Table 5 Rezultati za razna stanja površine trupa DTC

Stanje površine trupa	$10^3 \Delta C_F$	$10^3 C_{FR}$	$10^3 C_{TR}$	ΔC_F, %	ΔC_T, %
FR 1	0,039	1,342	1,804	2,973	2,406
FR 2	0,123	1,426	1,896	9,429	7,630
FR 3	0,136	1,439	1,910	10,427	8,438
CDP 1	0,130	1,433	1,904	9,949	8,051
CDP 2	0,244	1,547	2,029	18,724	15,153
CDP 3	0,284	1,587	2,072	21,762	17,612
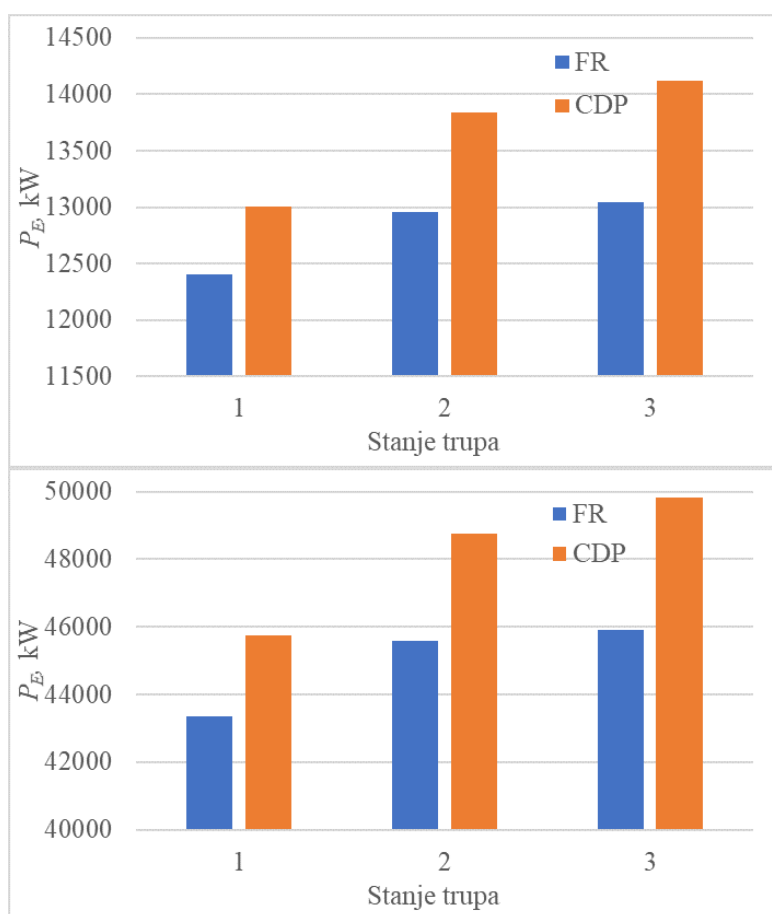
Figure 3 *Effective power for different surface conditions of KVLCC2 (upper) and DTC (lower)*
Slika 3 Efektivna snage za razna stanja površina broda KVLCC2 (gore) i DTC (dolje)

5. Zaključci

U ovom radu provedeno je istraživanje utjecaja antivegetativnog premaza na hidrodinamičke značajke dva trgovačka broda. Temeljem eksperimentalnih ispitivanja određene su skale hrapavosti dva antivegetativna premaza za tri različita stanja površine: laboratorijsko stanje, stanje niske hrapavosti i stanje visoke hrapavosti [16]. Primjenom navedenih skala hrapavosti i Grigsonovog modela funkcije hrapavosti te Gravilleove metode zakona sličnosti određeni su porasti koeficijenta otpora trenja za dva antivegetativna premaza i tri stanja površine trupa broda. Jedan premaz predstavlja neobraštajući premaz s manjom površinskom hrapavošću, dok drugi premaz predstavlja biocidni premaz na bazi bakra s topljivom matricom. Nakon što su određeni porasti koeficijenta otpora trenja, izračunati su koeficijenti ukupnog otpora kao i efektivne snage za navedena stanja površine trupa broda. Dobiveni rezultati ukazuju na prednosti primjene premaza s manjom hrapavošću sa stajališta efektivne snage, a tako i energetske učinkovitosti broda.

REFERENCES

[1]   United Nations Conference on Trade and Development. Review of maritime transport 2018 (Report, United Nations). New York: United Nations Conference on Trade and Development, 2018.

[2] Demirel, Y.K., Turan, O., Incecik, A., 2017. Predicting the effect of biofouling on ship resistance using CFD. Applied Ocean Research. 62, 100–118.

[3] Farkas, A., Degiuli, N., Martić, I., 2018. Assessment of hydrodynamic characteristics of a full-scale ship at different draughts. Ocean Engineering. 156, 135–152.

[4] Tillig F., Ringsberg J.W., Mao W., Ramne, B., 2017. A generic energy systems model for efficient ship design and operation. Proceedings of the Institution of Mechanical Engineers, Part M: J Engineering Maritime Environment. 231(2), 649–666.

[5] Rehmatulla, N., Parker, S., Smith, T., Stulgis, V., 2017. Wind technologies: Opportunities and barriers to a low carbon shipping industry. Marine policy. 75, 217-226.

[6] Adland, R., Cariou, P., Jia, H., Wolff, F. C. 2018. The energy efficiency effects of periodic ship hull cleaning. Journal of Cleaner Production. 178, 1-13.

[7] Stojanović, I., Farkas, A., Alar, V., Degiuli, N. 2019. Evaluation of the Corrosion Protection of Two Underwater Coating Systems in a Simulated Marine Environment. JOM. 71(12), 4330-4338.

[8] Ventura, C., Guerin, A.J., El-Zubir, O., Ruiz-Sanchez, A.J., Dixon, L.I., Reynolds, K.J., Dale, M.L., Ferguson, J., Houlton, A., Horrocks, B.R., Clare, A.S. 2017. Marine antifouling performance of polymer coatings incorporating zwitterions. Biofouling 33, 892-903.

[9] Mathiazhagan, A., Joseph, R., 2011. Nanotechnology-a New prospective in organic coating-review. International Journal of Chemical Engineering and Applications, 2(4), 225.

[10] Zhang, Z. P., Song, X. F., Cui, L. Y., Qi, Y. H., 2018. Synthesis of polydimethylsiloxane-modified polyurethane and the structure and properties of its antifouling coatings. Coatings, 8(5), 157.

[11] Ba, M., Zhang, Z., Qi, Y., 2018. Fouling release coatings based on polydimethylsiloxane with the incorporation of phenylmethylsilicone oil. Coatings, 8(5), 153.

[12] Chambers, L. D., Stokes, K. R., Walsh, F. C., Wood, R. J., 2006. Modern approaches to marine antifouling coatings. Surface and Coatings Technology, 201(6), 3642-3652.

[13] Schultz, M.P., 2004. Frictional resistance of antifouling coating systems, Journal of Fluids Engineering, 126(6), 1039-1047.

[14] Ünal, U.O., 2015. Correlation of frictional drag and roughness length scale for transitionally and fully rough turbulent boundary layers, Ocean Engineering, 107, 283–298.

[15] Niebles Atencio, B., Chernoray, V., 2019. A resolved RANS CFD approach for drag characterization of antifouling paints, Ocean Engineering, 171, 519–532.

[16] Yeginbayeva, I.A., Atlar, M. 2018. An experimental investigation into the surface and hydrodynamic characteristics of marine coatings with mimicked hull roughness ranges, Biofouling, 34(9), 1001–1019.

[17] Erbas, B. 2019. The turbulent boundary layer and frictional drag characteristics of new generation marine fouling control coatings, Brodogradnja, 70(4), 51-65.

[18] Andersson, J., Oliveira, D. R., Yeginbayeva, I., Leer-Andersen, M., Bensow, R. E., 2020. Review and comparison of methods to model ship hull roughness. Applied Ocean Research, 99, 102119.

[19] Demirel, Y. K., Khorasanchi, M., Turan, O., Incecik, A., Schultz, M. P., 2014. A CFD model for the frictional resistance prediction of antifouling coatings. Ocean Engineering, 89, 21-31.

[20] Kim, W. J., Van, S. H., Kim, D. H., 2001. Measurement of flows around modern commercial ship models. Experiments in fluids, 31(5), 567-578.

[21] Moctar, O. E., Shigunov, V., Zorn, T., 2012. Duisburg Test Case: Post-panamax container ship for benchmarking. Ship Technology Research, 59(3), 50-64.

[22] Farkas, A., Degiuli, N., Martić, I., 2020. An investigation into the effect of hard fouling on the ship resistance using CFD. Applied Ocean Research, 100, 102205.

[23] International Intersleek 1100 SR. https://www.international-marine.com/product/intersleek-1100sr, pristupljeno 11.9.2020. godine

MEANS OF PERFORMANCE IMPROVEMENTS OF TWO-STAGE BLADE PROPULSORS

Togunjac Anatolij-Branko R.*; JSC "Scientific and Production Enterprise "Marine Equipment"; Kanonersky Isl. 41,St.Petersburg,198184Russia;e-mail:togunjac.branko@yandex.ru

Anchikov Sergei L.; JSC "Scientific and Production Enterprise "Marine Equipment"; Kanonersky Island 41, St. Petersburg, 198184Russia; e-mail spb_ morteh@mail.ru

Vishnevsky Leonid I.; Krylov State Research Centre; Moskovskoye Shosse 44, St. Petersburg, 198158 Russia; e-mail vishli@yandex.ru

Abstract

The paper contains brief description of two-stage multifunctional propulsors (TSMP) and steering thruster with contra-rotating propellers (CRP) in the development of which authors directly participated and protected by patents. It is schematic shown how works TSMP on the different modes of operation. The data of model tests of the TSMPs in the Krylov State Research Center are presented, which confirmed the feasibility of the adopted design solutions that provide improved operational characteristics of a vessel. The layout of the TSMP for the conceptual design of a transport vessel is presented. The design features of the steering thrusters with CRPs, affecting their operational characteristics, are considered. Solutions for improving operational characteristics of steering thrusters with CRPs are substantiated, and the expected improvement in their hydrodynamic efficiency is estimated. The prospects for the use of steering thrusters with CRPs are assessed on the example of the Russian Civil Fleet.

Key words: contra-rotating propellers, two-stage multipurpose propulsor, hydrodynamic efficiency

1. Introduction

Among the large variety of two-stage blade propulsors we would like to concentrate on the designs of propulsors that are able to operate in reactive mode and change thrust direction in a wide angular range. Such propulsors are called multifunctional as they provide a ship with the following modes of operation: full speed, maneuverability at all speeds, slow speed with steerability. The ways of improving performance characteristics of two-stage blade propulsors are illustrated by the examples of patented construction designs that were developed with direct involvement of the authors of the present article. The performance characteristics of propulsors are understood, first of all, as hydrodynamic efficiency and built-in reliability of the construction. These properties of propulsors have been extremely vital during all the history of their development and are not of minor importance today as it is confirmed by the International Maritime Organization (IMO) requirements towards energy efficiency of ships[1] [1] and marine environment protection. The proposed two-stage multifunctional blade propulsors (TSMP) can be divided into two types: propulsors with rear stage in the form of a dual-mode contra propeller, and propulsive-and-steering units (PSU) with electrically driven coaxial contra-rotating propellers (CRP). Let us consider successively these types of propulsors, results of model tank tests and proposed means of improving their performance characteristics.

---

[1] Attained Energy Efficiency Design Index – EEDI is compared with the required EEDI [1]. In accordance with the IMO rules Attained EEDI ≤ Required EEDI.

2.Two-stage multifunctional blade propulsors with dual mode contra propeller

The first construction design of TSMP with dual mode contra propeller as well as the mode of movement and maneuvering of a ship equipped with such propulsor were patented in 1997 [2]. The novelty of this technical solution resided in the fact that the rear stage of the propulsor represented by a contra-rotating propeller could work both in reactive and active (without power transfer to the contra propeller) modes. Fig.1 illustrates the principal modes of operation of a TSMP with dual mode contra propeller. The ability of TSMP rear stage to function in two modes (reactive and active) saves energy at full speed (fig. 1a) and provides maneuvering at slow speed (fig. 1c, d) acting as a steering thruster. Besides, this solution made it possible to back up components of a propulsion unit which is crucial for the safety of navigation.
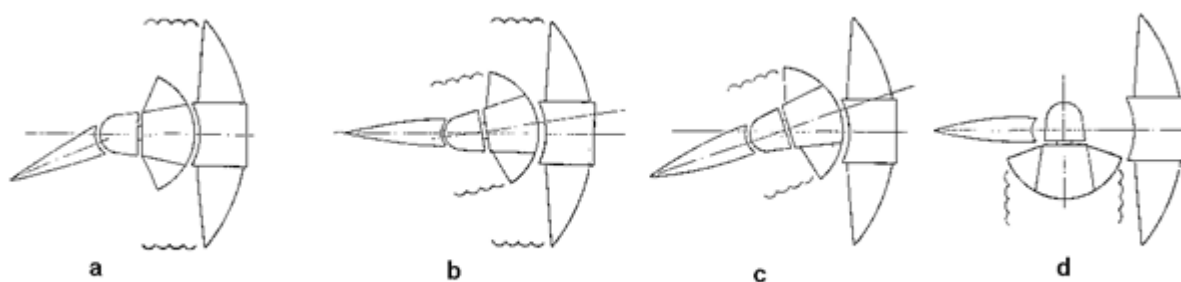
Figure 1 *The principal diagrams showing the multifunctional propulsor operation at different modes: a – full speed and maneuvering, fixed contra propeller; b- propulsor is operating in counter rotating propellers mode; c - low or emergency speed and maneuvering, contra propeller is working in reactive mode (puller propeller); d - maneuvering, contra propeller in reactive mode (pusher propeller); ∩∩∩∩ - reactive mode*

The implementation of the technical solution stated in the patent [2] implies solving of a number of engineering problems both in hydrodynamics (to develop a blade system for dual mode contra propeller) and in mechanics (to develop special mechanical appliances for steering thruster).

The hydrodynamics of a two-stage contra propeller which is operating periodically at two essentially different flow conditions (reactive and active) have not been investigated yet. Rational approach to the development of the two-stage contra propeller blades required to analyze the propeller's hydrodynamic in case of boundary variants of blades geometry i.e. blades designed for energy saving mode (fig. 1a) and for reactive mode (fig. 1c). Not of minor interest was to find an appropriate geometry (compromise geometry) of blades taking due consideration of the specific conditions of flow passing throw them in reactive and active modes.

The first estimation was made for a contra propeller designed to operate in energy-saving mode (fig. 1a). At the account of nonoptimal distribution of radial load in reactive mode efficiency losses equaled 8-12% [3],[4]. It resulted from the fact that blades were designed to operate in active mode. Experimental tests in the cavitation tunnel for special propulsors (KTSP) of the Krylov State Research Centre (KSRC) demonstrated (fig.2) that efficiency losses exceeded estimates and totaled 16-17% [5], [6].

Figure 2 *Model of TSMP with contra propeller in the working section of KTSP, energy-saving mode, see fig. 1a*

Testing of the TSMP with dual mode contra propeller was continued in the towing tank of the Krylov Shipbuilding Research Centre (KSRC) using a fishing vessel model [7], fig.3. The rudder installed behind the TSMP expectedly improved propulsive performance of the vessel in the reactive mode of contra propeller operation and hydrodynamic losses caused by nonoptimal geometry of the contra propeller designed for energy-saving mode reduced down to

a   b

Figure 3 *The TSMP model with contra propeller installed behind the hull of the tested model: a- energy-saving mode, full speed simulation, see fig.1a; b – slow speed simulation, see fig.1c*

3% [6],[7]. Comparing trials were performed on a small diameter controllable pitch propeller [8] geometry of which was found optimal for slow speed mode. Considerable improvement of the TSMP hydrodynamic efficiency in comparison with the test data obtained during trials in the uniform flow inside the KTSP can be explained by the fact that the rudder was installed behind the contra propeller (rudder eliminates negative effect of hub vortex, recovers energy of

contra propeller rotating slipstream and levels out deficiencies in the geometry of blades) and by positive effect of the radial distortion of the flow behind the tested model.

The main results of the TSMP model trials are as follows [4],[6],[9]:

– TSMP is able to provide energy saving by 6-7% in case the contra propeller is designed with consideration of the complete spin-up of the flow generated by screw propeller at full speed (i.e. active mode);

– attempts to find compromise solutions while choosing the contra propeller geometry of blades showed that the load-drop at the peripheral sections of the contra propeller blades results in a rather modest improvement of hydrodynamic efficiency in reactive mode (for $\approx$ 1%) and considerably eliminates energy-saving effect (more than twofold);

– efficient operation of the propulsor at slow or emergency speed (see fig.1) requires the following layout onboard: the rudder shall be located behind the contra propeller (after the rear stage of the TSMP);

– in case the rudder is placed behind the contra propeller designed for active mode of operation, this propeller will be efficient in reactive mode as well, but will underperform for $\approx$ 3% an optimal screw propeller of small diameter (i.e. equal to the contra propeller diameter) in terms of hydrodynamic efficiency.

The model trials of the TSMP hydrodynamics demonstrated that the design of the propulsor proposed in the patent № 2098316 [2] has certain drawbacks and can be improved. Let us concentrate on these drawbacks and discuss two improved TSMPs developed on the basis of a prototype design [2].

Testing of contra propeller hydrodynamics in reactive mode showed that its hydrodynamic efficiency considerably depends upon the presence of the rudder behind the contra propeller. When a pusher contra propeller creates transverse thrust T (see fig. 1d) during mooring operations for instance, the hydrodynamic efficiency of the TSMP according to the patent [2] decreases due to the flow spin-up losses because when the contra propeller turns for 90^0 there is no rudder behind it. According to the patent [2] the hydrodynamic efficiency of the puller contra propeller will decrease due to the fact that the components of rudder use to impede the contra propeller wake flow formation. The Fig.4 shows TSMP design which is free from these drawbacks due to a small rudder (see fig.4, position 4) and to a cut in the rudder. This propulsor is protected by the utility model certificate № 147957 [10].

a   b
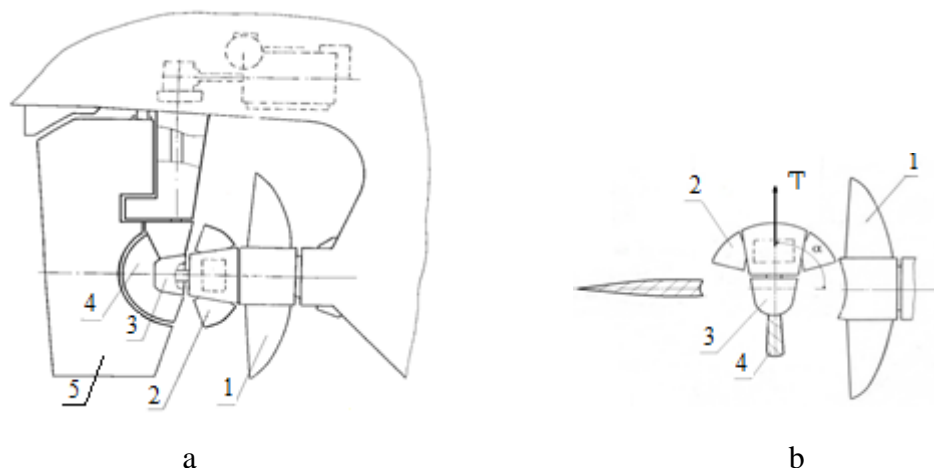
Figure 4 *Two-stage blade propulsive-and steering unit [10]:*

A – side view, full speed; b- conditional topside view, maneuvering and mooring;
1- Screw propeller; 2 – contra propeller; 3- hub fairing; 4- small rudder; 5 – rudder

Another drawback of the TSMP [2] is low hydrodynamic efficiency of contra propeller in backward running mode. Reverse thrust is achieved when contra propeller changes direction of its rotation i.e. similar to fixed pitch propeller principle of operation. As this takes place, conditions of contra propeller's blades flowing become extremely unfavorable for the achievement of maximal hydrodynamic efficiency: the leading edge of blade turns into trailing edge, and the suction surface of blade turns into pressure surface. To eliminate this problem in the TSMP construction as it is stated in the patent [11] the pitch-changing mechanism of the contra propeller has an optional capability to move blades through their feathered position and to set the pitch enabling the contra propeller to provide astern motion without changing the direction of its rotation, fig.5. In this case the suction surface of a blade is not changing its role which considerably improves the propulsion performance of contra propeller. For instance, the model trials of contra propellers   in mooring mode of operation demonstrated that the thrust increased for 50% [9], [12].

a   b
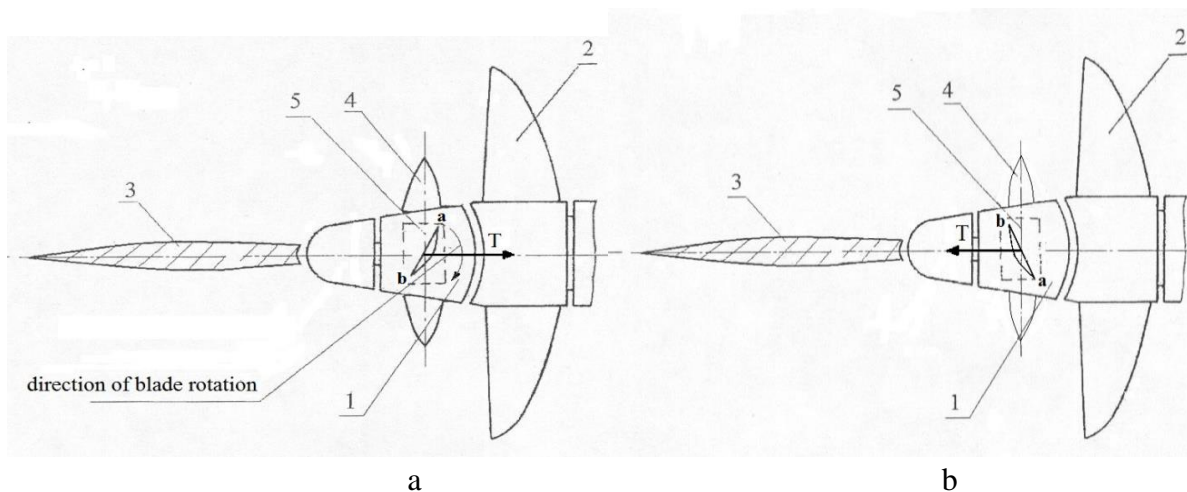
Figure 5 *TSMP with dual-mode contra propeller in three-set option [11]:*
a– forward movement; b- revers;
1- contra propeller; 2- screw propeller; 3 – rudder; 4 – contra propeller blade; 5- pitch-changing mechanism

Currently the implementation of the TSMP with dual-mode contra propeller is in its initial phase. The conceptual design of transport refrigerator (TR-1500) with TSMP dual-mode contra propeller developed by the Giprorybflot Institute was one of the first attempts to promote the implementation [13], [14]. For example, the following layout of the after end of transport vessel was proposed, fig.6.

234
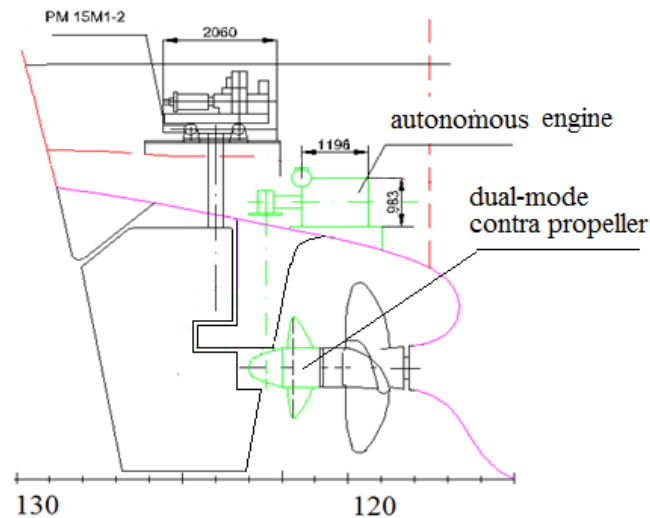
Figure 6 *After end of TP-1500 vessel with alternative propulsive unit equipped with dual-mode contra propeller as a propulsor*

This study proved that it is quite appropriate to arrange both propulsive unit and steering engine in one lay-out (see fig.6). It was proposed to use the Caterpillar C9 Acert 375 kW marine diesel engine in the alternative propulsive plant. The diesel engine arrangement is of no obstacle to the installation of Russian-manufactured RM 15 M1-2 steering engine. The autonomous diesel engine and steering engine must be located at different height levels but not be installed on the same deck. The advantages of equipping the TR15000 with the TSMP with dual-mode contra propeller are as follows:

– required power is reduced by $\approx$ 6% ($\approx$200 kW) at full speed equal to 14.5 knots;
– the alternative propulsive unit is able to provide emergency speed of not less than 7 knots (in case of the main propulsion unit failure), and, accordingly, the vessel will get an additional RP-1A symbol of the Russian Shipping Register indicating the due duplication of ship's propulsion system components;
– rear-stage of the TSMP functions as a steering thruster at slow speed and during mooring and, consequently, it is not necessary to install a stern tunnel thruster or azimuthing retractable thruster onboard the vessel .

Another step on the way to the implementation of the discussed propulsor is the detailed technical design of 500 kW propulsive-and-steering unit with dual mode contra propeller (PSU500) developed by the «VINT» Research, Development and Production Facility [9].

3. Propulsive-and- Steering Units with Electric Power Transmission to Coaxial Contra Rotating Screw Propellers (CRP)

The world shipbuilding industry of today is widely using propulsive-and- steering units (PSU) with coaxial contra-rotating propellers (CRP) [15]. The popularity of CRPs is explained by their high hydrodynamic efficiency: they exceed single screw propellers in terms of efficiency by 10-12 %. Among the most well-known PSUs of the type are British Rolls Royce Contaz thrusters (power range 1800– 5200 kW), Finnish Steerprop (800 –25000 kW) and

Swedish Volvo Penta (190–660 kW) thrusters. All the enlisted PSUs have mechanical power transmission to CRPs. Another step on the way of improving propulsors' performance is the development of a PSU with electrical power transmission to CRP. Electric power transmission will eliminate the drawbacks of mechanical transmission and will give the following positive results [6]:

– propulsor blade system will be able to sustain considerable torque overloads and remove restrictions for operation under ice conditions and this, in turn, will help to spread the use of CRPs onboard ice class ships;

– hydrodynamic efficiency of CRP will increase at the modes of operation that differ from the design mode and it especially important for PSUs operating in a wide range of different service conditions;

– PSUs with two electric motors will be provided with an option of additional duplication of propulsive plant components and, consequently, the safety of operation will improve.

Construction designs of PSUs with electrical transmission were proposed in Russia as early as in 1998[16], [17], and its first implementation took place in Japan in 2004 for «The Super Eco-Ship» innovative vessel [18]. However information about the results of the PSU operation onboard vessel is absent.

Modern trends in the field of electrical engineering make it possible to predict development in the nearest future of efficient and reliable electric motors for power transmission to CRP as part of PSU. At the same time, certain solutions in the field of hydrodynamics call for more detailed study aimed at the development of efficiently operating CRPs as a component of multifunctional propulsors. Such R&D studies shall foresee:

– defining of CRP hydrodynamic performance at large loads including mooring operations provided the screw propellers have uniform torque;

– study of CRP operation in reverse modes;

– study of CRP operation in a nozzle (ducted CRP).

The use of nozzles is an evident engineering solution to improve the hydrodynamic efficiency of CRP at large loads. The propulsors protected by the patents [16], [17], fig.7 foresee (as an option) installation of such nozzles.
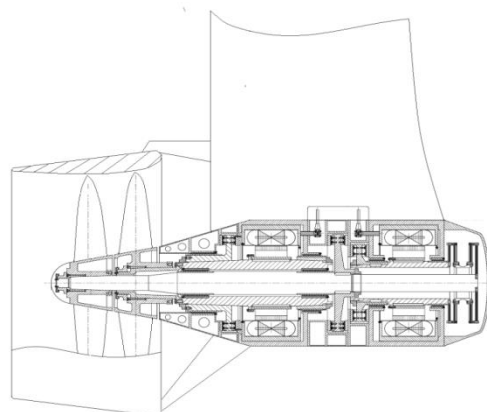
Figure 7 *PSU with electrical transmission to CRP in a nozzle according to the Russian Federation patent № 2 115 589, [16]*

The representative illustration of the nozzle positive effect on hydrodynamic efficiency is shown in fig.8 as the dependence of the efficiency factor (η_P) of various blade

propulsor designs on the load specified by thrust-load coefficient $C_T = 2T/\rho V_A^2 A_0$ (where T– screw propeller thrust, ρ – water density, V_A– speed of advance, A_0– propeller disc area) [19].
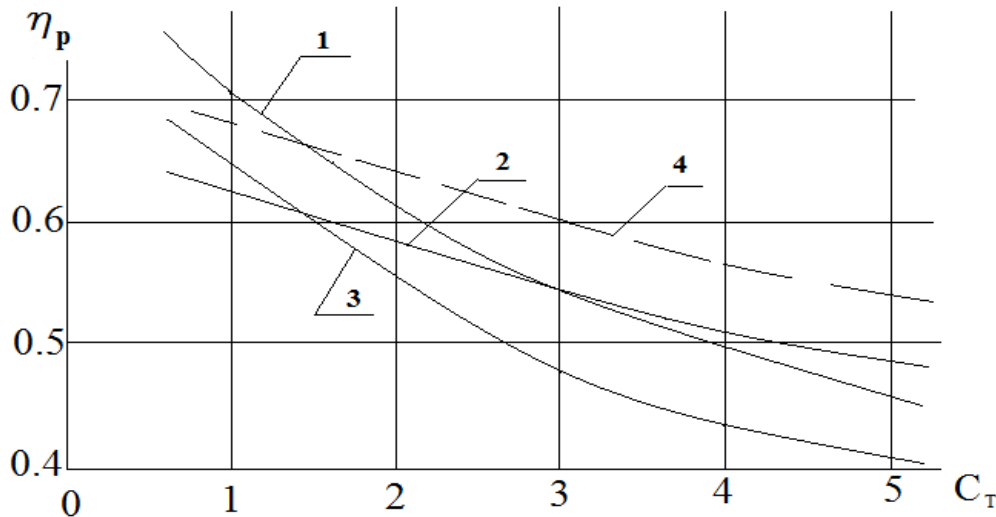
Figure 8 *Comparison of the efficiency factors (η_p) of various types of propulsors, disc ratio $A_E/A_0 \approx 1.0$: 1 – coaxial contra rotating screw propellers (CRP); 2 – propulsive unit consisting of a single screw propeller and nozzle; 3 – single screw propeller; 4 – propulsive unit consisting of contra rotating screw propellers (CRP) and nozzle (expected relationship).*

The expected relationship $\eta_p= f(C_T)$ for ducted CRPs (fig.8, position 4) was derived from the assessment that was performed as a part of hydrodynamic research and showed the advantage of open CRPs over single screw propellers both open or ducted. The research demonstrated that efficiency factor of CRPs within the load range $C_T = 0.6–5.0$ exceeds for 10– 12 % the efficiency factor of an open single screw propeller in case all the conditions for the equality of single screw propellers disc ratio and accumulative value for CRPs are provided [19]. It is supposed that similar advantage will be demonstrated by ducted CRP and ducted single screw propeller. According to the estimation, ducted CPRs will preserve advantage in case its load corresponds to $C_T > 1.5$. If load $C_T = 2.0$ than efficiency advantage will make appr. 5%, and if $C_T > 3.0$ it will exceed 10% (see fig.8). More precise efficiency factor ratio can be defined during comparative model tests complemented with the research aimed at finding the most optimal shape of nozzle and rational lay-out of CRPs inside it.

PSU with transmission of electrical power to CRPs represent new generation of propulsors and currently there are all the backgrounds for their development. Let us consider possible application of PSU with electrical power transmission to CRPs as an alternative option to existing azimuthing thrusters electrical power transmission on single screw propeller. Ships built at Russian shipyards and ships sailing under the Russian flag (predominantly these are supply vessels, tankers and ice-breakers) widely use Azipod type propulsive units of ABB company. Table.1,[20].

Table1 Use of PSUs with electrical power transmission to single screw propeller onboard Russian ice class ships

Type of ship, number of sister ships	Length L_{OA}, м	Ice class RMRS[2]	Propulsor, Power, kW	Speed, V_s, knots,
Norilsky Niekel, Containership	169	Arc 7	Azipod, 13 000	15.5
Vsilij Dinkov, Tanker 2	257	Arc 6	Azipod, 2x10 000	15.7
Mikhail Ulianov, Tanker, 1	257	Arc 6	Azipod, 2x8 500	16.0
Christophe de Margerie, Gas carrier	299	Arc 7	Azipod, 3x15 000	19.5
Shturman Albanov, Tanker, 6	245	Arc 7	Azipod, 2x11 000	14.0
Boris Sokolov, Tanker, 1	214	Arc 7	Azipod, 2x11 000	13.0
Aleksandr Sannikov, Ice-breaking Supply Vessel ,1	121	Icebreaker 8	Azipod, 2x7500 (stern) 1x 6500 (bow)	16.0
Ob' Harbour Ice-breaker	89.5	Icebreaker 7	Azipod, 2x3000(stern), 2x3000(bow)	15.0
Feodor Ushakov, Ice-breaking Supply Vessel, 3	99.9	Icebreaker 6	Azipod, 2x6500	16.0

Making choice in favor of PSU with power electrical power transmission to CRPs to be installed on similar ships shall be based upon comparative estimation of hydrodynamic efficiency of propulsors. It is possible to expect energy-saving up to 10–12% if the disc ratio of to-be-replaced single screw propeller A_E/A_0 not less than 0.8–1.0. These are the types of screw propellers that are usually used in line with Azipod type PSUs. Alongside with the types of ships that are highly recommended to be equipped with PSUs with electrical power transmission to CRP (enlisted in Table 1) it would be reasonable to add passenger vessels as well.

4. Conclusion

The two-stage multi-functional blade propulsors (TSMP with dual-mode contra propeller and PSU with electrical power transmission to CRPs) that were considered in this paper by the authors belong to one of the most technically challenging types of propulsors and are passing currently the very initial phase of their implementation. The driving force of research and design works is the hydrodynamic efficiency advantage of two-stage propulsors which is for 4-12 % better than that of traditional propulsors with one stage. The following conclusions result from research studies that were performed with the purpose to improve operational characteristics of TSMP:

---

[2] RMRS – Russian Maritime Register of Shipping

1. The design of TSMP with dual-mode contra propeller and small rudder according to the patent [10] demonstrates at slow speed and at mooring operations high hydrodynamic efficiency due to the elimination of the negative effect of hub vortex and spin-up of flow after the contra propeller.

2. The design of TSMP with dual-mode contra propeller with three pitch settings according to the patent [11] additionally provides the possibility for the vessel to move astern without changing the direction of contra propeller rotation while blade pitch is set by bringing blades through feathered position which is mostly favorable for minimizing hydrodynamic losses in this mode of operation.

3. The designs of PSU with electrical power transmission to ducted CRPs according to the patents [16], [17] require additional hydrodynamic research aimed at finding the most optimal shape of nozzle and rational lay-out of CRPs inside it.

The performed estimates show that when load corresponds $C_T > 3.0$, hydrodynamic efficiency advantage from using CPR in nozzle will exceed 10%.

With regard to the current interest of marine industry in energy saving and safety of navigation, and taking into consideration advances in electrical engineering it is possible to forecast further development of such propulsors by leading manufactures of marine engineering equipment in the nearest future.

REFERENCES

[1] IMO Train the Trainer (TTT) Course on Energy Efficient Ship Operation. Module 2–Ship Energy Efficiency Regulation and Related Guidelines. IMO, London, January 2016.

[2] *Тогуняц А.Р.* Способ движения и маневрирования судна. Патент № 2098316, Официальный бюллетень ВНИИПИ «Изобретения», №34, 1997.

[3] *Togunjac A.R., Kaprancev S.V.* Estimation of Hydrodynamic Efficiency of Fishing Vessel's Two-Stage Multipurpose Propulsor.Proceedings of 13th Interjnational Scientific and Professional Congress Theory and Practice of Shipbuilding, SORTA-1998, Zadar, 1998, p.181-190.

[4] *Вишневский Л.И., Тогуняц А.Р.* Корабельные лопастные движители: Новые технические решения, результаты исследований. СПб: Судостроение, 2011.

[5] *Togunjac A.R., Vishnevsky L.I., Morenshildt K.V.* Hydrodynamics Characteristics of the Dual-Mode Contra Propellers. Proceedings of the XXI Symposium on Theory and Practice of Shipbuilding in Memoriam prof. Leopold Sorta, Baška, October 2-4, 2014, p.291-300.

[6] *Вишневский Л.И., Тогуняц А.Р.* Гидродинамика корабельных лопастных движителей. Инновационные решения. СПб: «Реноме», 2020.

[7] *Togunjac A.R., Vishnevsky L.I., Kaprancev S.V.* Model Hydrodynamic Investigation of Two-Stage Multipurpose Propulsor Behind the Ship. Proceedings of the XXII Symposium on Theory and Practice of Shipbuilding in Memoriam prof. Leopold Sorta, Trogir-Seget Donji, Croatia, October 6-8, 2016, p.215-223.

[8] ОСТ 5.4129-75. Комплекс движительный гребной винт - направляющая насадка. Методика расчёта и правила проектирования.

[9] *Тогуняц А.Р. , Вишневский Л.И.* Двухступенчатый лопастной движитель с двухрежимным контрпропеллером и его конструктивные решения. Труды Крыловского государственного научного центра. Т.3,№ 389.2019. С.83-94.

[10] *Тогуняц А.Р., Вишневский Л.И.* Двухступенчатый лопастной движительно-рулевой комплекс. Патент на полезную модель № 147957. Официальный бюллетень «Изобретения. Полезные модели», № 32, 2014.

[11] *Тогуняц А.Р., Вишневский Л.И., Анчиков С.Л.* Способ проектирования двухрежимного контрпропеллера в трёх установочном варианте и двухрежимный контрпропеллер в трёхустановочном варианте. Патент на изобретение № 2569996. Официальный бюллетень «Изобретения. Полезные модели» № 34, 2015.

[12] *Тогуняц А.Р., Вишневский Л.И.* Модельные исследования гидродинамических характеристик двухрежимного контрпропеллера на швартовах как средства активного управления. Морской вестник.2017.№ 1(61). С.11-13.

[13] *Тогуняц А.Р., Вишневский Л.И., Седых Е.А.* Опыт концептуального проектирования морских судов с альтернативной пропульсивной установкой, оснащённой двухрежимным контрпропеллером. Научно-техн. сб. Российского морского регистра судоходства.2015. Вып.40/41.

[14] Togunjac A.–B., R., Vishnevsky L.I., Sedykh E.A. The conceptual design experience of seagoing ships with alternative propulsion system, equipped with dual-mode contra propeller. Journal of Shipping and Ocean Engineering. 2016, March-April. Vol.6, No.2.

[15] *Тогуняц А.Р., Анчиков С.Л., Вишневский Л.И.* Соосные гребные винты в зарубежном и отечественном судостроении. Морской вестник.2019.№ 4(72). С.44-49.

[16] *Бедекер В.Ф., Тогуняц А.Р.* Судовая движительно-двигательная установка типа "поворотная колонка". Патент № 2 115 589. Официальный бюллетень «Изобретения», № 20, 1998.

[17] *Бедекер В.Ф., Тогуняц А.Р.* Судовая движительно-двигательная установка типа "поворотная колонка". Патент № 2 119 875. Официальный бюллетень «Изобретения», № 28, 1998.

[18] The Super Eco-Ship. Class NK Magazine. 57th Edition 2005.

[19] *Турбал В.К.* Применение движителей новых типов на морских транспортных судах. Проблемы прикладной гидромеханики судна. Л.: Судостроение, 1975.

[20] *Штрек А.А.* Опыт компании Aker Arctic по созданию современных судов для Арктики. Тенденции развития арктического судостроения. Международный форум «Судостроение в Арктике». Архангельск, 14-15 июня 2018 г.

EXISTING 14000M^3 TRAILING SUCTION HOPPER DREDGER (TSHD) CONVERSION/45M LENGTHENING TO A 21000 M^3 TWIN HOPPER-TSHD

Marko, Pirija; Robert, Grubiša

IHC Engineering Croatia d.o.o., Milutina Baraća 7, 51000 Rijeka
m.pirija@royalihc.com ; r.grubisa@royalihc.com

Abstract

Trailing Suction Hopper Dredgers (TSHD) are one of the core products of IHC. They are used for dredging of soft soil as well as reclamation of material from the sea bed. Seldom ship-owners aim to increase hopper capacity for added capacity of dredge spoil to be transferred to a specific location thus increasing the payload.

This article covers a major conversion of an existing, IHC built TSHD, with an aim of increasing its hopper capacity from 14000m^3 to 21000m^3 by elongating the vessel with 45m, from the original 135,95m to 180,95m in length between perpendiculars. The new, elongated vessel, is designed with two hoppers divided approximately at the middle of the vessel. This article cover the design basis, feasibility study for different design and arrangement options, as well as basic engineering activities for the chosen conversion design option for this particular elongation. An overview is given of the basic engineering activities and deliverables for this major conversion, including statutory drawings, ship stability, longitudinal strength, FEM and buckling analysis.

Key words: Dredging; Twin Trailing Suction Hopper Dredger ;Feasibility; Engineering; Conversion; FEM

Sažetak

Usisna jaružala sa skladištem jedan su od osnovnih prozvoda tvrtke IHC. Namjena im je iskop nekoherentnog materijala sa morskog dna poput šljunka ili pijeska kao i ponovna ugradnja (iskrcaj) tog materijala. Često brodovlasnici žele povećati kapacitet skladišta postojećih usisnih jaružala zbog povećanja nosivosti/isplativosti spomenutih brodova.

Ovaj članak opisuje konverziju postojećeg usisnog jaružala sa skladištem, originalno izgrađenog u IHC-u, sa ciljem povećanja skladišnog kapaciteta iskopanog materijala sa 14000m^3 na 21000m^3 putem produljenja postojećeg broda za 45m, sa postojećih 135,95m na 180,95m duljine između okomica. Novi, produljeni brod, je projektiran sa dva skladišna prostora odijeljenima u sredini broda. Ovaj članak obuhvaća razradu idejnog projekta, studiju provedivosti za nekoliko projektnih opcija, kao i osnovne aktivnosti prilikom izrade klasifikacijske dokumentaciju u vidu dobivanja odobrenja od strane klasifikacijskog društva. Dan je i pregled osnovnih projektnih aktivnosti za ovu konverziju uključujući izradu osnovnih nacrta produljenja, proračuna stabiliteta i uzdužne čvrstoće, proračuna čvrstoće MKE metodom kao i proračun izvijanja brodske strukture.

Ključne riječi: Jaružalo ; Usisno jaružalo; Isplativost; Projektiranje; Konverzija; FEM

6. List of Abbreviations and Symbols

Abbreviation	Designation	Chapter
API	Application programming interface	6
BV	Bureau Veritas	4
COG	Center of gravity	6
D1	Design option 1	5
D2	Design option 2	5
FEA	Finite element analysis	6
FEM / MKE	Finite element method / Metoda konačnih elemenata	2
FO	Fuel oil	6
GA	General arrangement	3
IMO	International Maritime Organization	5
PS	Portside	3
SB	Starboard	3
SW	Still Water	5
SWBM	Still Water Bending Moment	4
SWSF	Still Water Shear Force	
TSHD	Trailing Suction Hopper Dredger	2
US	Ultrasound	6
WBM	Wave Bending Moment	
WSF	Wave Shear Force	

Symbol	Designation	Chapter
B	Moulded breadth, (m)	4
C	Wave parameter	4
C_B	Block coefficient	4
D	Total damage due to fatigue	6
D_{aBD} , D_{bBD} , D_{cBD}	Elementary damage ratios for load cases "a", "b" and "c" respectively, in "Ballast" dredging condition	6
D_{aBT} , D_{bBT} , D_{cBT}	Elementary damage ratios for load cases "a", "b" and "c" respectively, in "Ballast" navigation condition	6
D_{aF} , D_{bF} , D_{cF} , D_{dF}	Elementary damage ratios for load cases "a", "b", "c" and "d", respectively, in "Fully laden" dredging condition	6
D_{BD}	Cumulative damage ratio for ship in ballast condition while sailing in the operating area	6
D_{BT}	Cumulative damage ratio for ship in ballast condition while sailing in the navigation area	6
D_{DC}	Total damage due to dredging cycle	6
D_F	Cumulative damage ratio for ship in operating area at dredging draught	6
D_W	Damage due to waves	6
F_M	Distribution factor	4
F_Q	Distribution factor	4
H_S	Maximum significant wave height, (m)	3
k	Material factor	4
K_{cor}	Corrosion factor	6
L	Rule length, (m)	4
$M_{W,V,H,D}$	Wave bending moment, hogging conditions, (kNm)	4
$M_{W,V,S,D}$	Wave bending moments, sagging conditions, (kNm)	4
N_{fat}	Number of cycles leading to fatigue failure at the notch stress range	6
$Q_{W,V,H,D}$	Vertical wave shear force, (kN)	4

s	Length of the shorter side of the plate panel, (m)	4
T_{fl}	Design fatigue life, in years	6
α_D	Part of the ship's life in operating area	6
α_{FD}	Part of the ship's life in full load con. while in operating area	6
α_0	Sailing factor	6
α_1	Part of the ship's life in full load condition	6
α_2	Part of the ship's life in ballast condition and in operating area	6
$\Delta\sigma_{N,D}$	Notch stress range	6
n_C	Number of dredging cycles in the ship's life	6
n_{CD}	Number of dredging cycles per day	6
n_D	Navigation coefficient in dredging situation	4
$\sigma_{N,D,1}$	Notch stress in considered detail for fully laden condition in still water without accelerations	6
$\sigma_{N,D,2}$	Notch stress in considered detail for empty condition (hopper open to sea or discharged) in still water without accelerations	6

1. Introduction

Trailing Suction Hopper Dredgers are one of the core products of IHC. TSHD's are used for dredging of soft soil from the sea bed. The excavated material is gathered in an open structural tank formally known as a „hopper" tank. The material is then discharged from the hopper in several ways, via bottom doors in the bottom of the vessel, via bow coupling connection and a discharge pipeline or via bow coupling nozzle also known as „rainbowing". Sometimes the dredged material (mostly mud or sand) is to be reused on shore and TSHD's vessels are an efficient and preferred solution for these types of duties given their large storage capacity and quick discharge possibilities.

Figure 52 *Images of typical means of Hopper Discharging; From left to right – Bottom Doors; Rainbowing; Bow coupling connected to floating pipeline*
Slika 45 Prikaz tipičnih načina iskrcaja iskopanog materijala iz skladišta; Sa desnog na lijevo – Iskcaj kroz vrata u dnu broda; Iskrcaj preko pramčane sapnice; Iskrcaj preko pramčane konekcije za plutajući cjevovod

Given the demands of certain building sites where large capacities of sand are needed to be reused onshore, a need for increased hopper capacity takes ship-owners to reassess the exiting vessel capacity in order to increase the vessels profitability.

2. Original Vessel

Original vessel is a 14000 m³ TSHD with twin screws, driven by two 8700kW diesel engines, with a service speed of 15 knots. Profile view, Main Deck and double bottom from the original GA and main particulars are given below.
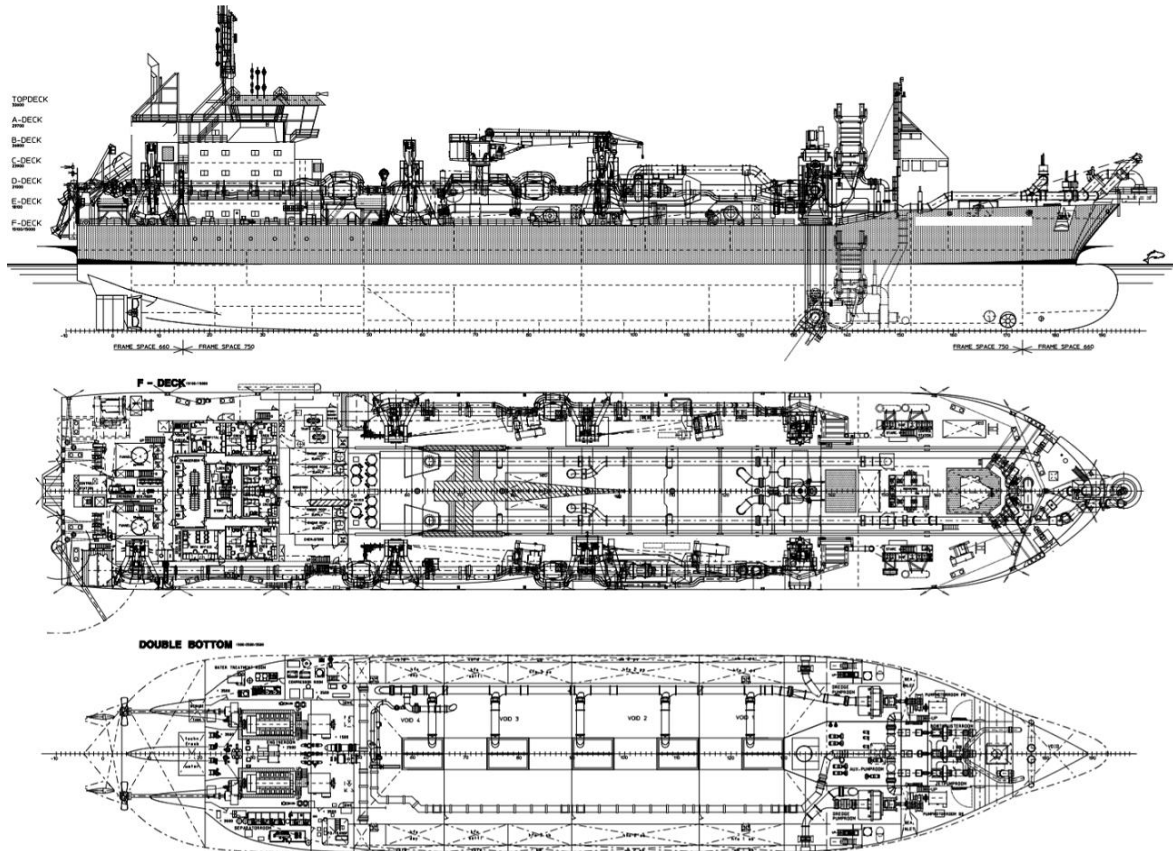
Figure 53 *Profile view, Main Deck and Tank top – original TSHD*
Slika 46 *Prikaz uzdužnog pogleda, glavne palube i pogleda na dvodno – originalno jaružalo*

Table 18 *Main Particulars – Original TSHD*

Length Overall Abt.	156.00 m
Length Between Perpendiculars	135.95 m
Breadth moulded	28.00 m
Depth moulded	15.00 m
Summer Draught moulded	9.24 m
Dredging Draught moulded – DRI (unrestricted dredging)	12.02 m
Dredging Draught moulded – DRII (Dredging within 15 miles from shore or 20 miles from port with Hs<3.5m)	12.84 m
Design Deadweight Abt.	19125 t
Dredging Deadweight Abt.	28395 t

Hopper volume to overflow	14000 m³
Hopper volume to coaming	15850 m³
Dredging depth PS/SB	55.8/83.7 m

3. Project constraints

3.1. Hopper capacity increase

The basic project objective was increasing hopper capacity to 21000 m3. The initial calculations had shown that in order to cope with the increase in total bending moments ship is to be consisted of two hoppers (twin hopper vessel) with a void space amidships to provide additional buoyancy to the vessel thus decreasing the sagging moment loading on the vessel. Preliminary capacity calculations resulted in an estimate of ship length increase of 45 m.

3.2. Rule Minimal Thickness Criteria

A really obvious project constraint regarding existing hull structure in the very beginning was to check for the non-compliant scantlings of the existing situation calculated with the targeted, new ship length. The rule formulae state the minimal thicknesses for primary structural elements as a function of ship length which leaves little room to accommodate for this when lengthening the vessel. An example is given on the following table as given in the rules [Ref.1 and 2]:

Table 19 Example of *Minimal Thickness Overview from the Rules and Regulations [Ref.2]*

Plating	Minimum net thickness, in mm
Keel	$5,1 + 0,040\ L\ k^{1/2} + 4,5\ s$
Bottom • transverse framing • longitudinal framing	$4,3 + 0,036\ L\ k^{1/2} + 4,5\ s$ $3,4 + 0,036\ L\ k^{1/2} + 4,5\ s$
Inner bottom outside hopper spaces	$2,0 + 0,025\ L\ k^{1/2} + 4,5\ s$
Side • below freeboard deck • between freeboard deck and strength deck	$2,5 + 0,031\ L\ k^{1/2} + 4,5\ s$ $2,5 + 0,013\ L\ k^{1/2} + 4,5\ s$
Strength deck within 0,4L amidships • transverse framing • longitudinal framing	 $2,5 + 0,040\ L\ k^{1/2} + 4,5\ s$ $2,5 + 0,032\ L\ k^{1/2} + 4,5\ s$
Hopper well • transverse and longitudinal bulkheads • cellular keel plating	$2,7 + 0,034\ L\ k^{1/2} + 4,5\ s$ $2,7 + 0,034\ L\ k^{1/2} + 4,5\ s$

A list of several non-conformities found was immediately prepared and discussed with the classification society in the start of the feasibility stage. The agreement with class authority upon their view on the findings was that the non-compliance with the minimal thicknesses can be waved for a lengthened vessel subject to:

- All relevant loading conditions are to be considered for both dredging draught and international draught
- Allowable hull girder normal stresses and buckling criteria to be complied with throughout the length of the vessel
- Minimum section modulus is to be complied with within 0.4 L amidships
- Midship section moment of inertia is to be complied with

3.3. Hull Girder Loads

One of the other basic constraints was naturally a big increase in the vertical wave bending moments for the vessel, given that the Rule given wave bending moment is a function of ship length squared as given in the rule formulae [Ref.2]. The following formulae are applied for the dredging situation still water bending moments.

$$M_{W,V,H,D} = 190 F_M n_D C L^2 B C_B 10^{-3} \text{ (kNm)} \tag{1}$$

$$M_{W,V,S,D} = -110 F_M n_D C L^2 B (C_B + 0,7) 10^{-3} \text{ (kNm)} \tag{2}$$

These are to be used for dredging conditions while the international draft (navigation) bending moments are slightly differently formulated. The increase of roughly 76% on the Vertical Wave bending moment resulted in introduction of wave limitation in order to cope with the increase on the total bending moments. This difference can be partly reduced (roughly 25%) with introducing dredging operating limitations according rule values given in the following table:

Table 20 *Coefficient n_D in dredging situation*

Operating area	L ≤ 110 m	110 m < L ≤ 150 m	150 m < L ≤ 180 m	n_D
dredging within 8 miles from shore	N.A.			1/3
dredging over 8 miles from shore with ...	$H_S \leq 1,5$ m	$H_S \leq 2,0$ m	$H_S \leq 2,0$ m	1/3
dredging within 15 miles from shore or within 20 miles from port	N.A.			2/3
dredging over 15 miles from shore with ...	$H_S \leq 2,5$ m	$H_S \leq 3,0$ m	$H_S \leq 3,5$ m	2/3
dredging over 15 miles from shore	N.A.			1

Note 1:H_S : Maximum significant wave height, in m, for operating area in dredging situation, according to the operating area notation assigned to the ship (see Pt A, Ch 1, Sec 2, [4.6.3]).
Note 2: N.A. = Not Applicable

The value of still water bending moments was then to be checked via different loading scenarios (density of spoil and hopper filling) to determine adequate DR I dredging draft with a n_D limitation of 2/3, corresponding to dredging within 15 from shore and within 20 miles from port or dredging over 15 miles from port with a significant wave height less or equal to 3.5 m. The remainder of the difference in bending moments was to be dealt with by a draft/loading limitation of the dredging condition. After initial SWBM calculations, the draft for DRI was to be set at 12.1m in order for the still water bending moments values be under check for the existing hull structure capacity. The

connection areas of the new and existing sections would most likely need reinforcements according preliminary check of total bending moments.

The increase in horizontal wave bending moments was also noted and according preliminary calculations this increase can be accommodated.

The value of vertical wave shear forces according rule formulae [Ref.2] also lead to the increase in the global shear forces for approximately 32% .

$$Q_{W,V,H,D} = 30 F_Q n_D CLB(C_B + 0.7)10^{-2} \text{ (kN)} \tag{3}$$

The introduced dredging wave limitation also provided a decrease in the vertical wave shear force distribution although given the new design of a twin hopper vessel still water shear force peaks were expected.

3.4. Existing Hull Reinforcement method

Existing Hull reinforcement design philosophy was determined early on during client meetings. Naturally, the project price was one of the main drivers and variables in the feasibility study and the business case in general. Preference for hull reinforcement was to reinforce in the easily accessible areas to minimise manual work with a lot of loose items.

In order to check the most affordable reinforcement method an early check of critical sections was carried out in Mars 2000, BV software. This was also carried out to check for possible bottlenecks stress-wise in the existing construction that would be potential "show-stoppers" for this elongation.

The material used was to be kept the same as on the original vessel. The bulk of the hull construction is Grade A steel, whereas the coaming is executed with Grade AH36 steel.
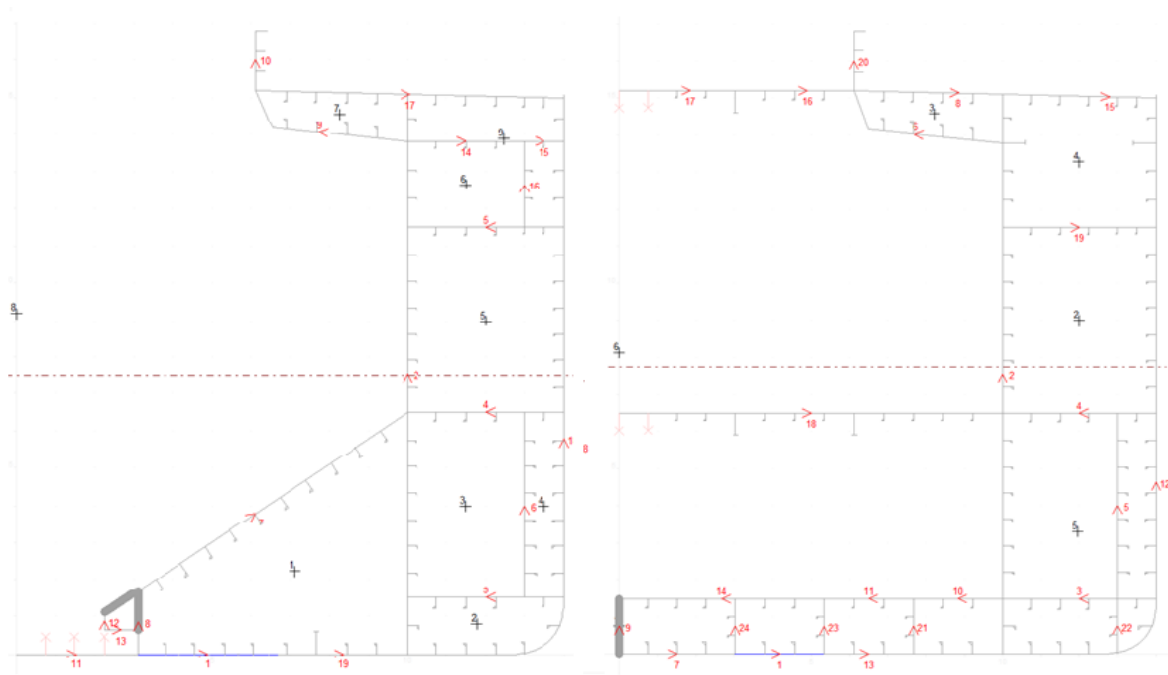
Figure 54 *Typical hopper and store space cross sections represented in Mars 2000 Software*
Slika 47 *Prikaz tipičnih poprečnih presjeka kroz prostor skladišta iskopanog materijala i centralnog (suhog) skladišta prikazanih u Mars 2000 računalnom programu*

According preliminary global strength calculations major reinforcements were to be provided for the bottom and main deck areas of the existing hull section. The means increasing the section modulus at the top was generally the coaming girder reinforcement given its effectiveness and ease of access. In the bottom the means of reinforcement was to be carried out by addition of bottom doubler strips on the outside bottom shell. This method was used for one of the fleets vessel elongation previously and proved to be an effective and cost worthy solution.

Another point of attention were the connection points of the hoppers to the store space in the middle. Given that large hopper sloped bulkheads were to stop at this buoyancy section, now to be used as a store space, the effectiveness of these large longitudinal elements were not sustained. A tank top was to be fitted in a large part of the new section thus overlapping in a certain limited length with the termination of the sloped hopper bulkheads. Special consideration was to be paid to these areas.

Shear loading was to be checked in a number of load cases to check against existing vessel capacity for the major vertical shear force carrying members, mainly longitudinal hopper bulkhead and side shell.

3.5. Statutory requirements and key arrangements

In the very start certain statutory drawings and requirements needed to be checked as well in order to determine possible bottle necks or show stoppers.

A variety of preliminary arrangement drawings and calculations were made and key items checked including:

o   Trim & Stability calculation

o   Freeboard calculation

- o Equipment number calculation
- o Field of Visibility
- o Mooring and Anchoring Arrangement
- o Ship lengths and draughts
- o Watertight subdivision
- o Dredge equipment arrangement
- o Balance of power and systems check
- o Escape route plan
- o Arrangement of lifesaving appliances
- o Navigational lights and signals

An identified minor obstruction around the bow coupling area was communicated to the Class and Flag authorities and a solution agreed in installing a cctv camera on the fore part of the vessel to enhance visibility forward.

Mooring and anchoring equipment was checked and the anchor chain diameter needed a slight increase as well as some mooring fittings needed to be added amidships.

Watertight boundaries were checked and preliminary damage stability calculation was done. The major watertight boundaries were found compliant to the rules and regulations.

A preliminary layout was done for the reinstallation of the dredge equipment and a feasibility check of the system was started in order to determine possible bottle necks in the mission equipment. No major obstacles were found. This led to the definition of the optimal cutting line. This was determined to be at approximately 0.36 L in order to keep existing pump gantry interface intact and minimize the suction tube system refit. An additional overflow for the extra hopper in the aft was to be accommodated using similar diameter as for the existing one, but was to be designed as a more recent, simpler arrangement, standard IHC overflow design. The existing loading and unloading pipelines were to be extended and the check of the system shown no obstacles were to be found there as well. This was also determined for the jet water system.

The installed power on board as well as needed capacity for heating was checked and found sufficient to accommodate this elongation.

No major obstacles were found in means of escape and arrangement of lifesaving appliances. Some improvements regarding the position of accommodation and pilot ladders have been done later during the project on the lengthened vessel.

The navigational lights and signals according COLREG regulations required no modifications.

3.6. Ship Mission Additional Preferences

Additional constraint was the ship mission in discharging dredged material to an on shore site via Bow coupling connection. It was reported from the fleet captains and it seemed operationally logical

to aim for trim to the aft in order for the vessel to reach the shore discharge site bow first and connect to the floating pipeline or use the rainbowing discharge nozzle.. This unloading is known in dredge master colloquialisms as "beaching the vessel". A preference in discharging the twin hoppers was also emptying of the forward hopper prior to the aft one. This results in asymmetric loading conditions but these cases realistically can happen only within 8 miles from shore so these asymmetric still water loading conditions were to be superimposed with vertical wave bending moments using a coastal area coefficient n_b limitation of 1/3, corresponding to dredging within 8 miles from shore or dredging over 8 miles from shore with a significant wave height less or equal to 2 m.

Figure 55 *"Beaching" of a TSHD*
Slika 48 *Prikaz iskrcaja materijala na obalu*

Multiple spoil densities were to be loaded to the stability models in order to determine the filling levels for the different density mixtures. While loading the hoppers the mixture (sand and water) density is maintained and monitored and the adjustable overflow levels in the hoppers ensure to make it possible to obtain higher mixture densities.

The ship-owner decided that in between the aft and forward hoppers, roughly set as a dry void space, a store are shall be designed to be used for spare parts of the dredging system, dredge pipelines etc.

This demarked the start of the feasibility phase where multiple design options were put to test and two design options were analysed more in detail in order to choose a preferred one.

4. Feasibility Study

Two designed options were roughly designed in order to asses these designs in the feasibility study stage. The first one called D1, envisioned a slightly larger forward hopper resulting in fairly symmetrical loading across the vessel. A second design option envisioned a larger hopper to the aft and a smaller hopper forward.

A rough representation of the mentioned design options is given in the following subchapters.

4.1. Design Option 1

As already mentioned, the design option 1 envisioned a larger forward hopper.
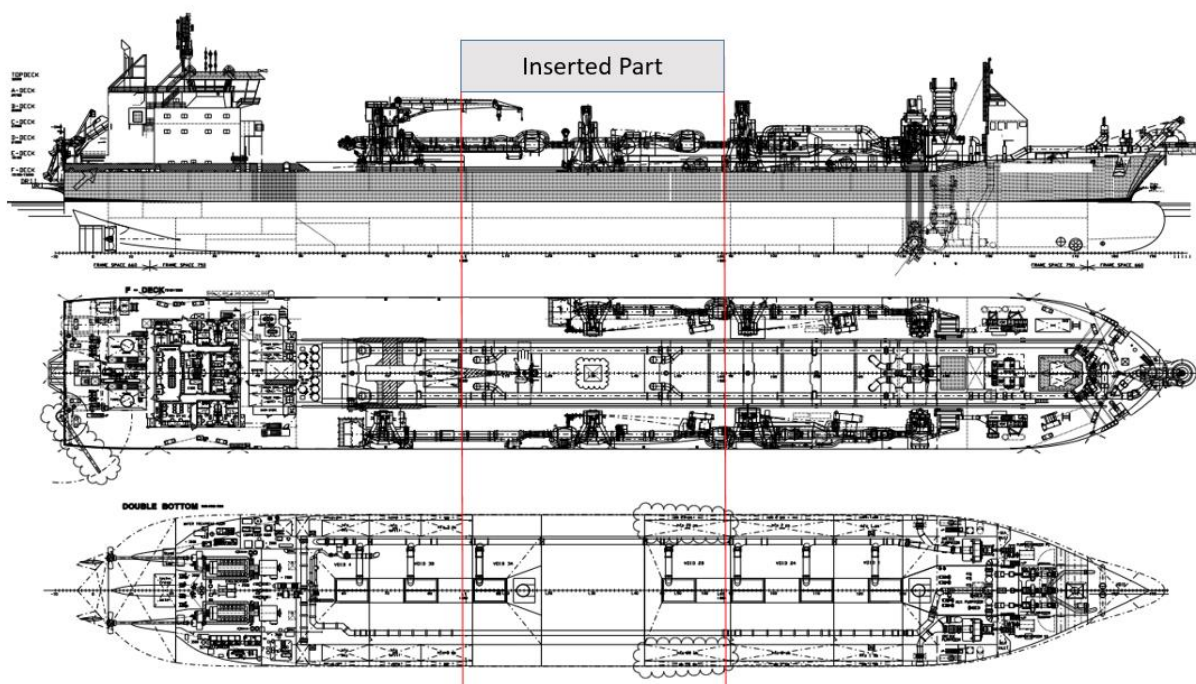
Figure 56 *Profile view, Main Deck and Tank top – Twin TSHD - Design 1*
Slika 49 *Prikaz uzdužnog pogleda, glavne palube i pogleda na dvodno – jaružalo sa dva skladišta – Projektna opcija 1*

A stability model was made using Delftship software in order to check the requirements for IMO code on intact stability for international draft, as well as stability criteria for dredging draft according to DR68 [Ref .3]. These criteria were met. Preliminary checks for damage stability were also conducted and the watertight subdivision was found adequate.

From the made stability model global bending moments and shear forces were obtained in order to check the existing hull structure and determine scantlings for the added part of the hull.

This configuration of the hoppers resulted in a fairly evenly loaded vessel with an expected slightly higher sagging bending moment in the larger forward hopper. The envelope curves were introduced to encompass a large number of loading conditions analysed in the stability model.

The loading conditions are presented for the dredging loading conditions only, given that the both design options are found of insignificant differences for loading conditions on international draft.

Figure 57 *Still Water Bending Moments - Symmetrical loading - Design 1*

Slika 50 *Prikaz momenata savijanja na mirnom moru – Simetrično krcanje skladišta – Projektna opcija 1*

Figure 58 *Still Water Bending Moments - Symmetrical loading - overloaded - Design 1*

Slika 51 *Prikaz momenata savijanja na mirnom moru – Simetrično krcanje skladišta – prekrcan – Projektna opcija 1*

Figure 59 *Still Water Bending Moments - Asymmetrical loading in the aft hopper included - Design 1*

Slika 52 *Prikaz momenata savijanja na mirnom moru – Asimetrično krcanje skladišta – Projektna opcija 1*

Figure 60 *Still Water Bending Moments - Asymmetrical loading in the aft hopper included - overloaded – Design 1*

Slika 53 *Prikaz momenata savijanja na mirnom moru – Asimetrično krcanje skladišta – prkrcan – Projektna opcija 1*

This design however resulted in a fore trim of the vessel when the hoppers were evenly loaded. This is beneficial only for the water flowing towards the overflows while loading the hoppers. It was found non-beneficial for discharging while "beaching" the vessel . The usage of ballast in the aft was not preferred according feedback from the fleet managers. The vessel was to be loaded in such a way in order to achieve even keel or slight trim to the aft, and asymmetrically unloaded – fore prior to aft hopper. This led to investigation of more loading in the aft hopper and even overloading conditions to check the sensitivity of the design. The increase of the bending moments in the aft resulted in an increase of the sagging envelope curve for roughly 8%).

The total bending moments maximum values were governed by the Symmetrical loading on even keel superimposed to the n_D limitation of 2/3, as given in Table 3. An overview of governing bending moments is shown on the following graph.

Figure 61 *Overview of governing bending moments - Design 1*

Slika 54 *Prikaz glavnih momenata savijanja – Projektna opcija 1*

The total bending moments were then cross-checked for needed reinforcement along the ships length as a function of the total bending moment. Given that sagging loading is identified as most severe for this vessel sagging moment was plotted against theoretical bending moment capacity for each section regarding it's obtained section modulus. The red dots indicated the current section modulus for a section in the existing hull part and the green arrows indicated the needed reinforcement for the given section. The black vertical continuous lines indicate the new hull section, whereas the dotted black vertical lines indicate the boundaries of the aft hopper and the forward hopper respectively.

Bending Moments

Figure 62 *Validation of section moduli plotted as permissible bending moment - Design 1*

Slika 55 *Validacija momenta otpora prema dozvoljenom momentu savijanja – Projektna opcija 1*

The shear forces increase was noticed in the added store area and a variety of load cases were made (combinations of hopper loading and unloading) to check the longitudinal extent of the shear force increase amidships. For the asymmetrical loading a separate set of loading conditions were introduced and the increase in shear, rather expectedly rose even higher.

Still Water Shear Forces
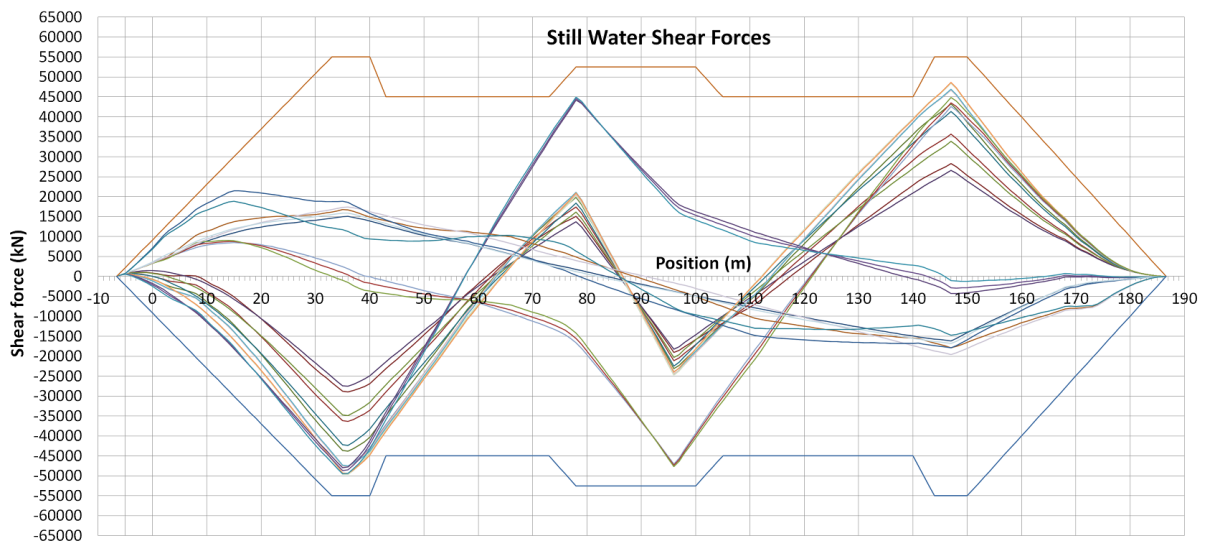
—LC1 Lightship
—LC7L Tdrd s.g. 1.2 t/m3 100% C.
—LC7L Tint s.g. 1.2 t/m3 10% C.
—LC8S Tdrd s.g. 1.4 t/m3 100% C.
—LC8S Tdrd s.g. 1.4 t/m3 10% C.
—LC9S Tdrd s.g. 1.6 t/m3 100% C.
—LC9S Tdrd s.g. 1.6 t/m3 10% C.
—LC10S Tdrd s.g. 1.8 t/m3 100% C.
—LC10S Tdrd s.g. 1.8 t/m3 10% C.
—LC11S Tdrd s.g. 2.0 t/m3 100% C.
—LC11S Tdrd s.g. 2.0 t/m3 10% C.
—LC12S Tdrd s.g. 2.2 t/m3 100% C.
—LC12S Tdrd s.g. 2.2 t/m3 10% C.
—LC13L Tdrd s.g. 1.674 t/m3 100%

—LC13L Tdrd s.g. 1.773 t/m3 10%
—LC13L Tdrd s.g. 1.773 tm/3 10% C; hopper aft HOTS
—LC13L Tdrd s.g. 1.773 t/m3 50% C; hopper aft HOTS
—LC13L Tdrd s.g. 1.773 t/m3 100% C; hopper aft HOTS
—LC13L Tdrd s.g. 1.773 t/m3 10% C; hopper fwd HOTS
—LC13L Tdrd s.g. 1.773 t/m3 50% C; hopper fwd HOTS
—LC13L Tdrd s.g. 1.773 t/m3 100% C; hopper fwd HOTS
—LC3 Hopper Empty 100% Consumables; FP full
LC3 Hopper Empty 10% Consumables; FP full
—LC3 Hopper Empty 100% Consumables; wb aft full
LC3 Hopper Empty 10% Consumables; wb aft full
—LC3 HOTS 100% Consumables; FP+wb aft full
—Envelope hog
—Envelope sag

Figure 63 *Still Water Shear Forces - Symmetrical loading - Design 1*

Slika 56 *Prikaz smičnih sila na mirnom moru – Simetrično krcanje skladišta – Projektna opcija 1*
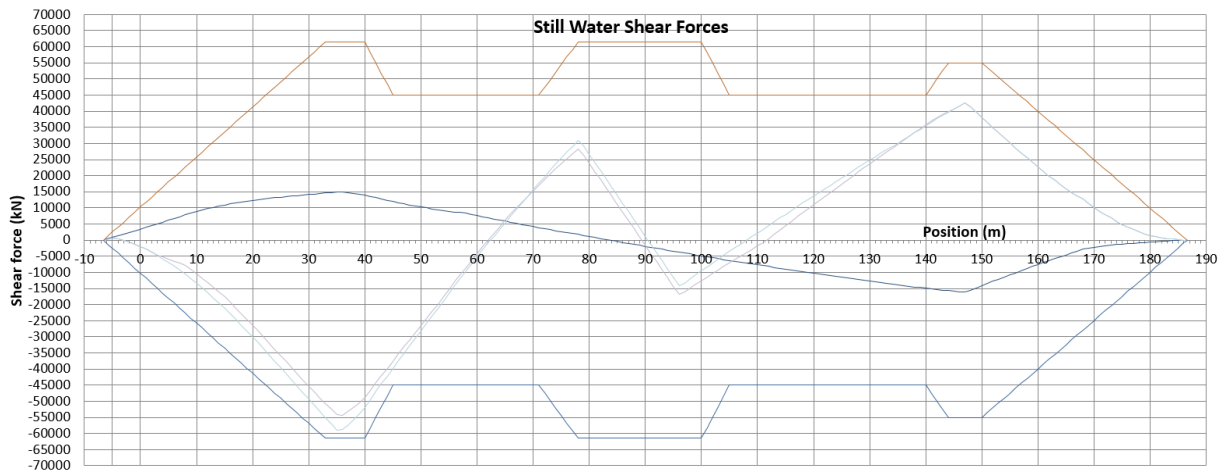
—LC1 Lightship
—LC12S Tdrd; s.g. 2.2 t/m3; 100% consumables hopper aft full; trim -0.5m
—LC12S Tdrd; s.g. 2.2 t/m3; 10% consumables hopper aft full; trim -0.5m
—Envelope hog
—Envelope sag

Figure 64 *Still Water Shear Forces - Symmetrical loading – overloaded - Design 1*

Slika 57 *Prikaz smičnih sila na mirnom moru – Simetrično krcanje skladišta – prkrcan – Projektna opcija 1*

Figure 65 *Still Water Shear Forces - Asymmetrical loading - Design 1*

Slika 58 *Prikaz smičnih sila na mirnom moru – Asimetrično krcanje skladišta – Projektna opcija 1*

Figure 66 *Still Water Shear Forces - Asymmetrical loading - overloaded - Design 1*

Slika 59 *Prikaz smičnih sila na mirnom moru – Asimetrično krcanje skladišta – prkrcan – Projektna opcija 1*

The governing loading conditions amidships regarding total shear force were found to be the asymmetric loading conditions, whereas in the aft and forward hopper bulkhead areas the governing loading conditions were symmetrical loading. The existing vessel hull girder shear

Capacity was fairly utilised but preliminary assessed with minor reinforcements-if any.

4.2. Design Option 2

As already mentioned, the design option 2 envisioned a larger aft hopper.
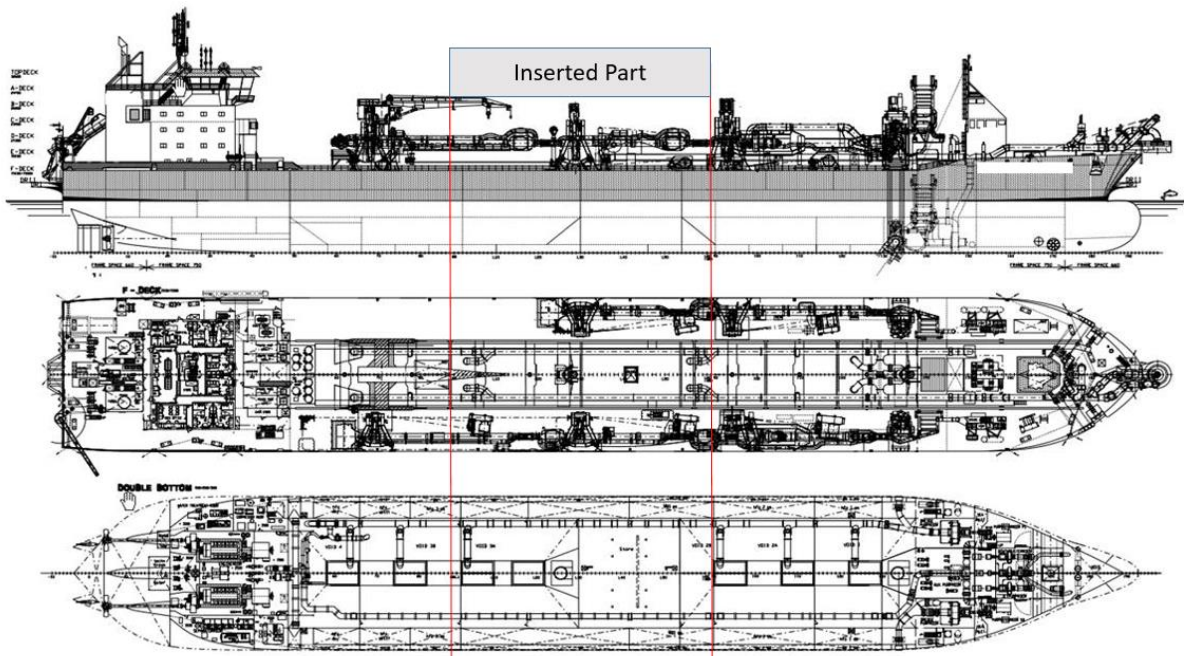
Figure 67 *Profile view, Main Deck and Tank top – Twin TSHD - Design 2*

Slika 60 *Bočni pogled, pogled na glavnu palubu i pokrov dvodna - Jaružalo – Projektna opcija 2*

A stability model was made in order to check for the requirements for IMO code on intact stability for international draft, as well as stability criteria for dredging draft according to DR68 [Ref .3]. These criteria were met. Preliminary checks for damage stability were also conducted and the watertight subdivision was found adequate.

From the made stability model global bending moments and shear forces were obtained in order to check the existing hull structure and determine scantlings for the added part of the hull.

This configuration of the hoppers resulted in a fairly unevenly loaded vessel regarding global bending moments with a larger bending moment increase in the aft hopper. On the first look it seemed rather as an unconventional design especially regarding bending moments. This design however, offered the possibility to "trim" the envelope sagging SW moment curve given that the tests for sensitivity of the design shown this configuration offers a lot of safety when overloading the vessel both aft and fore.
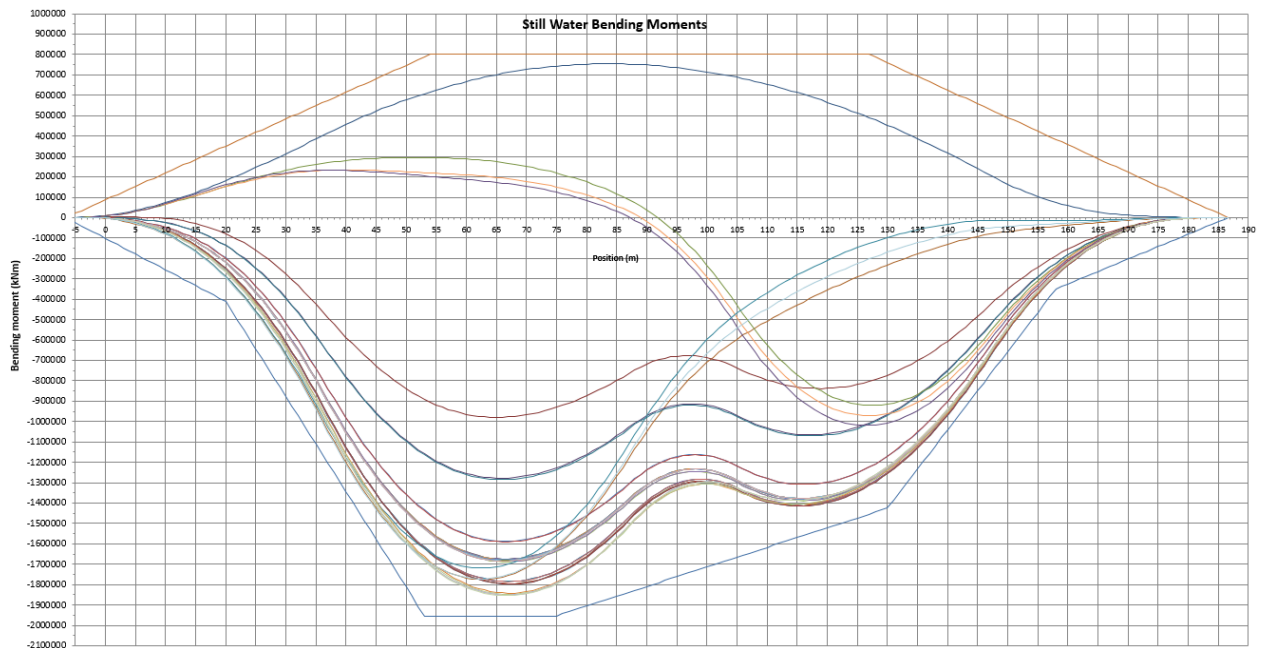
Still Water Bending Moments

—LC10S Tdrd; s.g. 1.8 t/m3; 100% consumables hopper aft full
—LC13L Tdrd; s.g. 1.75 t/m3;100% consumables hopper fwd
—LC1 Lightship
—LC7L Tdrd s.g. 1.2 tm3 100% C.
—LC8L Tdrd s.g. 1.4 tm3 100% C.
—LC8S Tdrd s.g. 1.4 tm3 100% C.
—LC9L Tdrd s.g. 1.6 tm3 100% C.
—LC9S Tdrd s.g. 1.6 tm3 100% C.
—LC10L Tdrd; s.g. 1.8 t/m3; 100% consumables
—LC10S Tdrd; s.g. 1.8 t/m3; 100% consumables
—LC10L Tdrd; s.g. 1.8 t/m3; 10% consumables
—LC10S Tdrd; s.g. 1.8 t/m3; 10% consumables
—LC11L Tdrd; s.g. 2.0 t/m3; 100% consumables
—LC11S Tdrd; s.g. 2.0 t/m3; 100% consumables
—LC11L Tdrd; s.g. 2.0 t/m3; 10% consumables
—LC11S Tdrd; s.g. 2.0 t/m3; 10% consumables
—LC12S Tdrd; s.g. 2.2 t/m3; 100% consumables
—LC12S Tdrd; s.g. 2.2 t/m3; 10% consumables

—LC13L Tdrd; s.g. 1.665 t/m3; 100% consumables
—LC13S Tdrd; s.g. 1.662 t/m3; 100% consumables
—LC13L Tdrd; s.g. 1.776 t/m3; 10% consumables
—LC13S Tdrd; s.g. 1.769 t/m3; 10% consumables
—LC13L Tdrd; s.g. 1.75 t/m3; 10% consumables hopper aft HOTS
—LC13L Tdrd; s.g. 1.75 t/m3; 50% consumables hopper aft HOTS
—LC13L Tdrd; s.g. 1.75 t/m3;100% consumables hopper aft HOTS
—LC13L Tdrd; s.g. 1.75 t/m3; 10% consumables hopper fwd HOTS
—LC10L Tdrd; s.g. 1.8 t/m3; 10% consumables hopper aft full
—LC10S Tdrd; s.g. 1.8 t/m3; 10% consumables hopper aft full
—LC11L Tdrd; s.g. 2.0 t/m3; 100% consumables hopper aft full
—LC11S Tdrd; s.g. 2.0 t/m3; 100% consumables hopper aft full
—Envelope sag
—Envelope hog
—LC11L Tdrd; s.g. 2.0 t/m3; 10% consumables hopper aft full
—LC11S Tdrd; s.g. 2.0 t/m3; 10% consumables hopper aft full
—LC12S Tdrd; s.g. 2.2 t/m3; 100% consumables hopper aft full
—LC12S Tdrd; s.g. 2.2 t/m3; 10% consumables hopper aft full
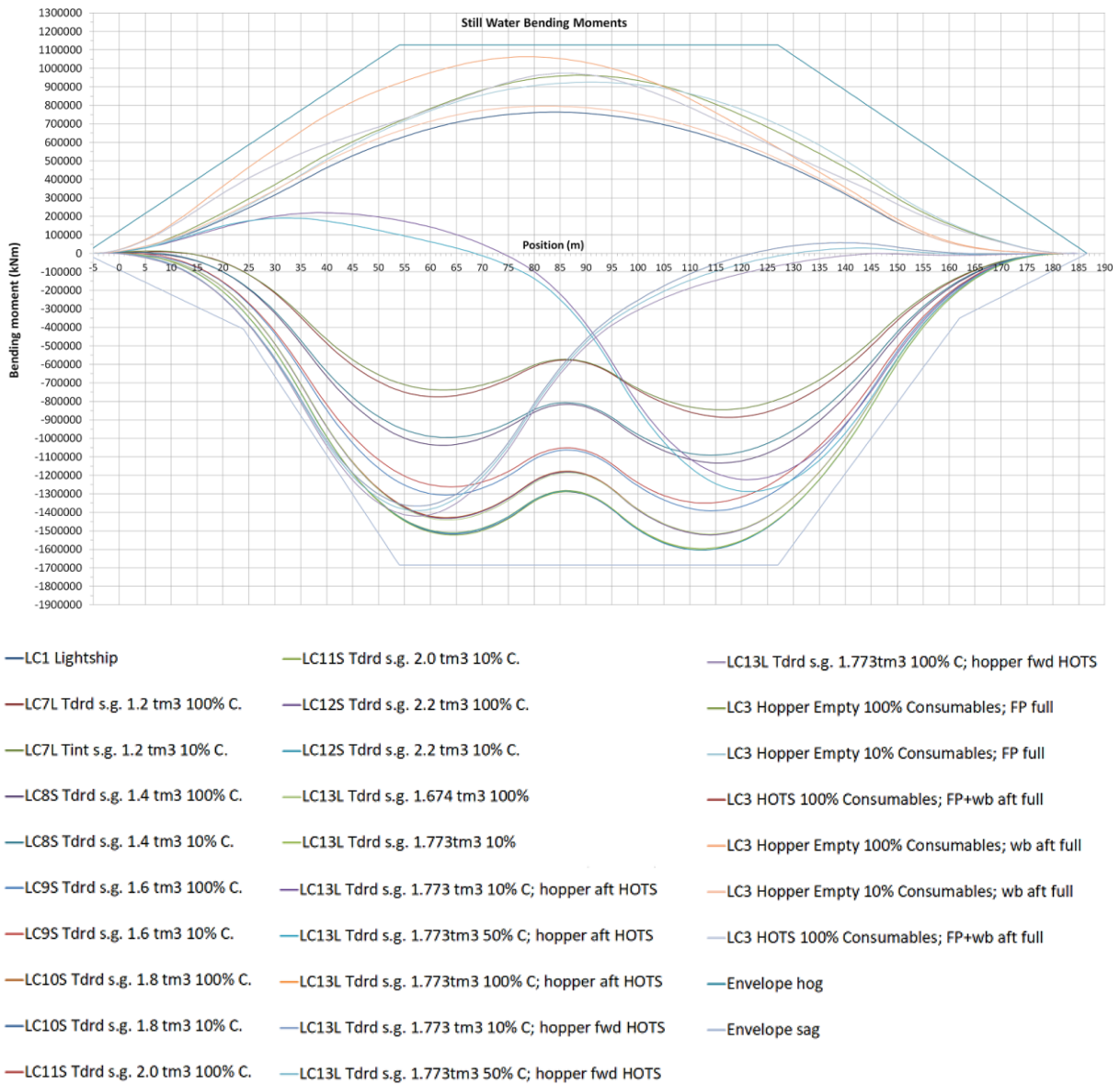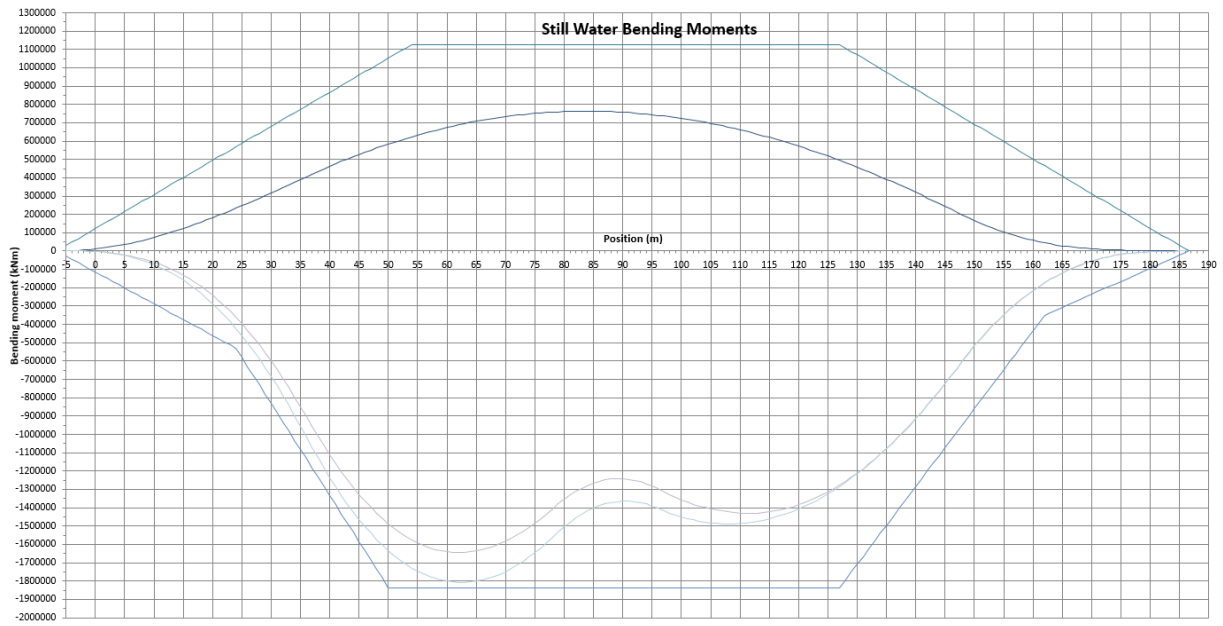—LC13L Tdrd; s.g. 1.75 t/m3; 50% consumables hopper fwd HOTS

Figure 68 *Still Water Bending Moments - Symmetrical loading - Design 2*

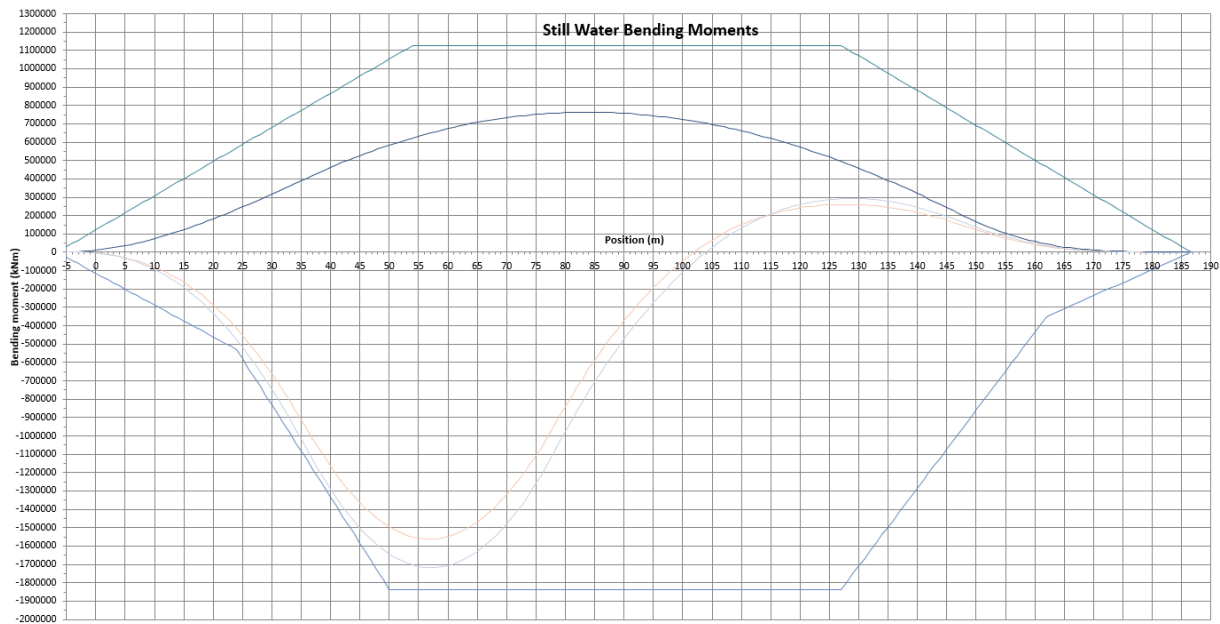**Slika 61** *Prikaz momenata savijanja na mirnom moru – Simetrično krcanje skladišta – Projektna opcija 2*

Figure 69 *Still Water Bending Moments - Asymmetrical loading - Design 2*

Slika 62 *Prikaz momenata savijanja na mirnom moru – Asimetrično krcanje skladišta – Projektna opcija 2*

The loading of the forward hopper was far lesser than in Design option 1 that and the aft trim and even keel and the preferred aft trim is more easily obtained. The design was also tested for overloading for both Symmetric and Asymmetric conditions and these were plotted against the envelope curves of the sagging still water bending moments.
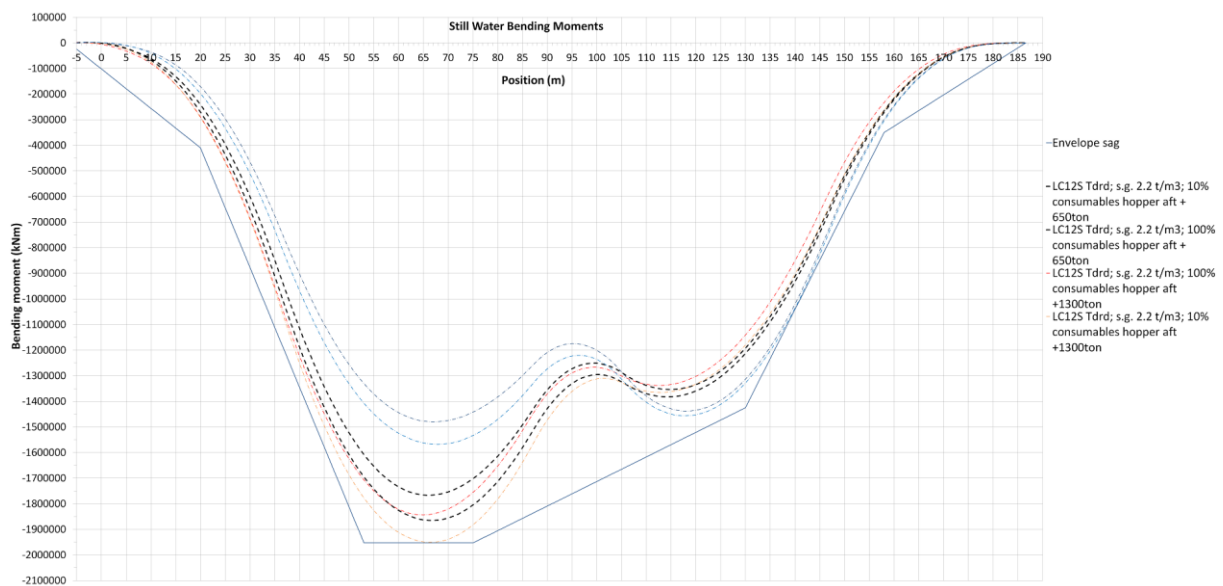
Figure 70 *Still Water Bending Moments - Symmetrical loading overload cases - Design 2*

Slika 63 *Prikaz momenata savijanja na mirnom moru – Simetrično krcanje skladišta - prekrcan – Projektna opcija 2*
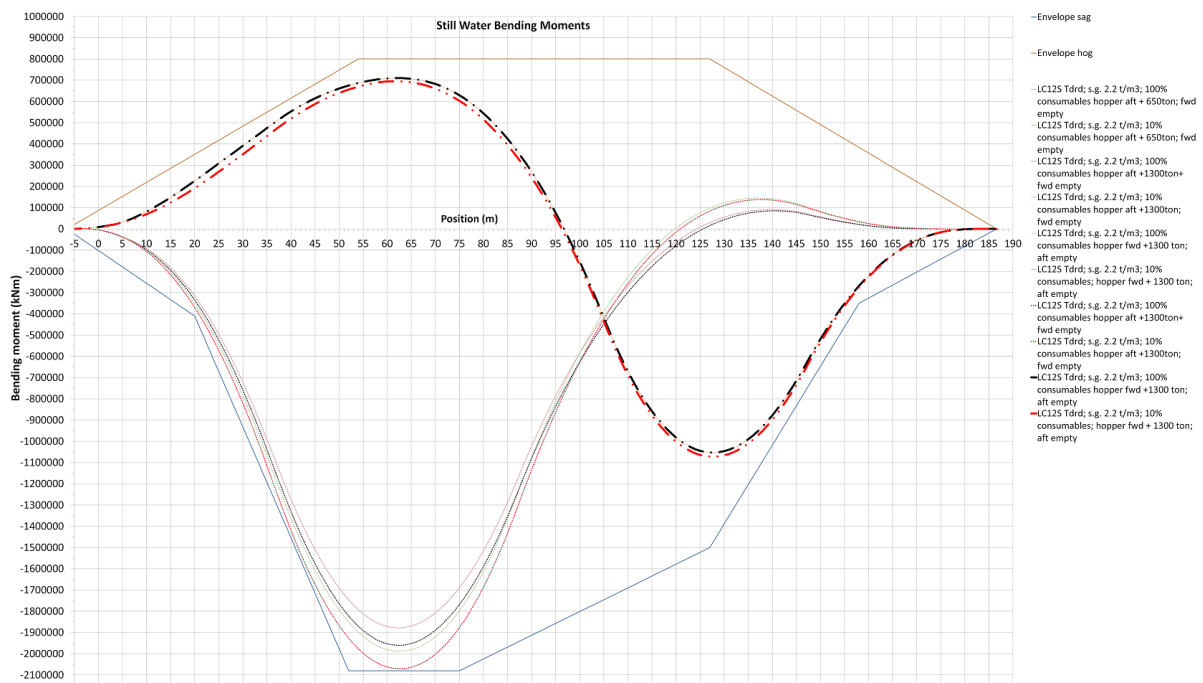
Figure 71 *Still Water Bending Moments - Asymmetrical loading overload cases - Design 2*

Slika 64 *Prikaz momenata savijanja na mirnom moru – Asimetrično krcanje skladišta – prekrcan - Projektna opcija 2*

The overload cases tested the envelopes to check the reserve and the sensitivity of the design. The increase in reserve was not needed given that the overloading of 1300t (around 11%) was still inside the envelope design curves. This was calibrated and cross checked further during the project to check the reserve and the loading manual limitations for uneven filling of the hoppers.

The total bending moments maximum values were governed by the Symmetrical loading on even keel superimposed to the n_D limitation of 2/3, as given in Table 3. An overview of governing bending moments is shown on the following graph.
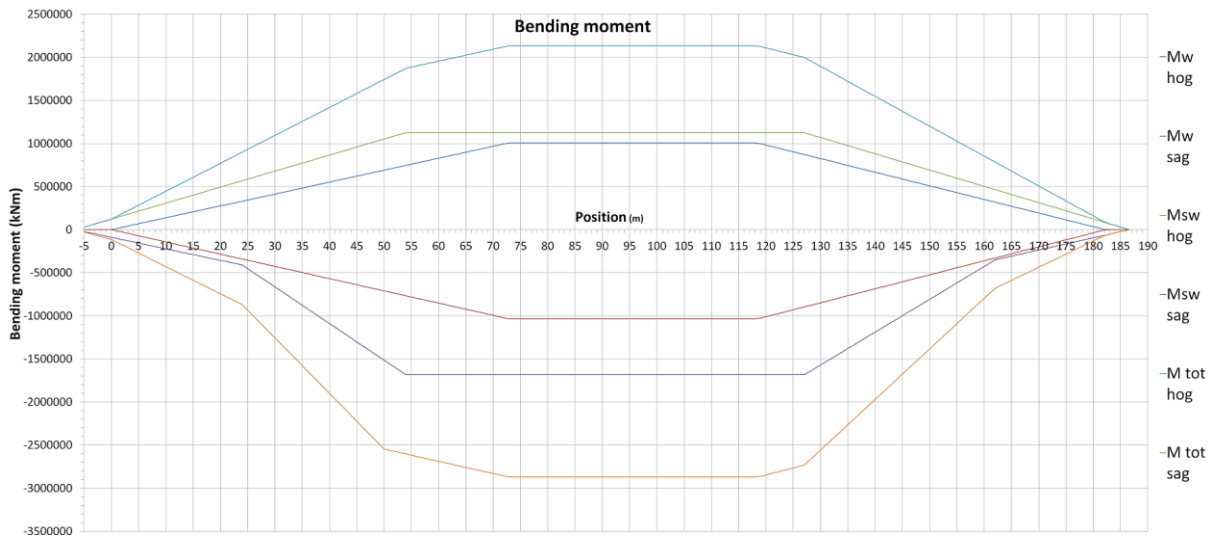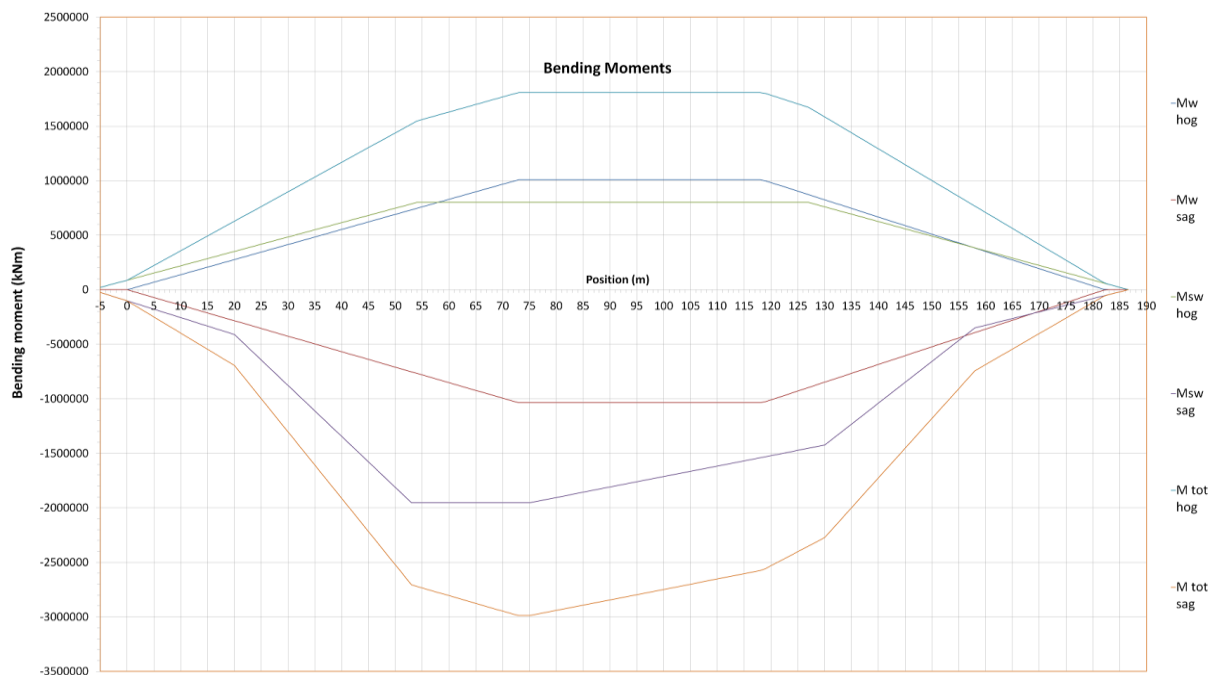

Figure 72 *Overview of governing bending moments - Design 2*

Slika 65 *Prikaz glavnih momenata savijanja – Projektna opcija 2*

The total bending moments were then cross-checked for needed reinforcement along the ships length as a function of the total bending moment. Given that sagging loading is identified as most severe for this vessel sagging moment was plotted against theoretical bending moment capacity for each section regarding it's obtained section modulus. The red dots indicated the current section modulus for a section in the existing hull part and the green arrows indicated the needed reinforcement for the given section. The black vertical continuous lines indicate the new hull section, whereas the dotted black vertical lines indicate the boundaries of the aft hopper and the forward hopper respectively.
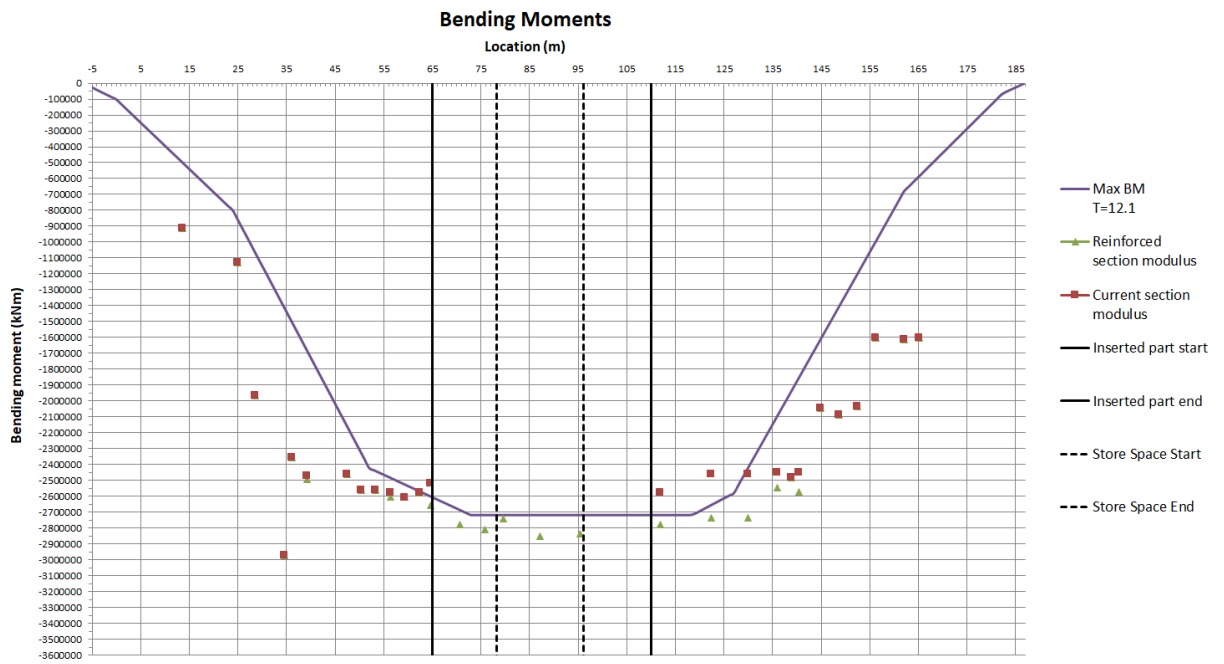
267

Figure 73 *Validation of section moduli plotted as permissible bending moment - Design 2*

Slika 66 *Validacija momenta otpora prema dozvoljenom momentu savijanja – Projektna opcija 2*

Similar to design option 1, the shear forces increase was noticed in the added store area and a variety of load cases were made (combinations of hopper loading and unloading) to check the longitudinal extent of the shear force increase amidships. For the asymmetrical loading a separate set of loading conditions were introduced and the increase in shear, rather expectedly rose even higher. The increase of shear force near the aft hopper bulkhead rose higher than on design 1 option.

Still Water Shear Forces

Legend:
- LC1 Lightship
- LC7L Tdrd s.g. 1.2 tm3 100% C.
- LC8L Tdrd s.g. 1.4 tm3 100% C.
- LC8S Tdrd s.g. 1.4 tm3 100% C.
- LC9L Tdrd s.g. 1.6 tm3 100% C.
- LC9S Tdrd s.g. 1.6 tm3 100% C.
- LC10L Tdrd; s.g. 1.8 t/m3; 100% consumables
- LC10S Tdrd; s.g. 1.8 t/m3; 100% consumables
- LC10L Tdrd; s.g. 1.8 t/m3; 10% consumables
- LC10S Tdrd; s.g. 1.8 t/m3; 10% consumables
- LC11L Tdrd; s.g. 2.0 t/m3; 100% consumables
- LC11S Tdrd; s.g. 2.0 t/m3; 100% consumables
- LC11L Tdrd; s.g. 2.0 t/m3; 10% consumables
- LC11S Tdrd; s.g. 2.0 t/m3; 10% consumables
- LC12S Tdrd; s.g. 2.2 t/m3; 100% consumables
- LC12S Tdrd; s.g. 2.2 t/m3; 10% consumables
- LC13L Tdrd; s.g. 1.665 t/m3; 100% consumables
- LC13S Tdrd; s.g. 1.662 t/m3; 100% consumables
- LC13L Tdrd; s.g. 1.776 t/m3; 10% consumables
- LC13S Tdrd; s.g. 1.769 t/m3; 10% consumables

Figure 74 *Still Water Shear Forces - Symmetrical loading - Design 2*

Slika 67 *Prikaz smičnih sila na mirnom moru – Simetrično krcanje skladišta – Projektna opcija 2*

Still Water Shear Forces

Figure 75 *Still Water Shear Forces - Asymmetrical loading - Design 2*

Slika 68 *Prikaz smičnih sila na mirnom moru – Asimetrično krcanje skladišta – Projektna opcija 2*
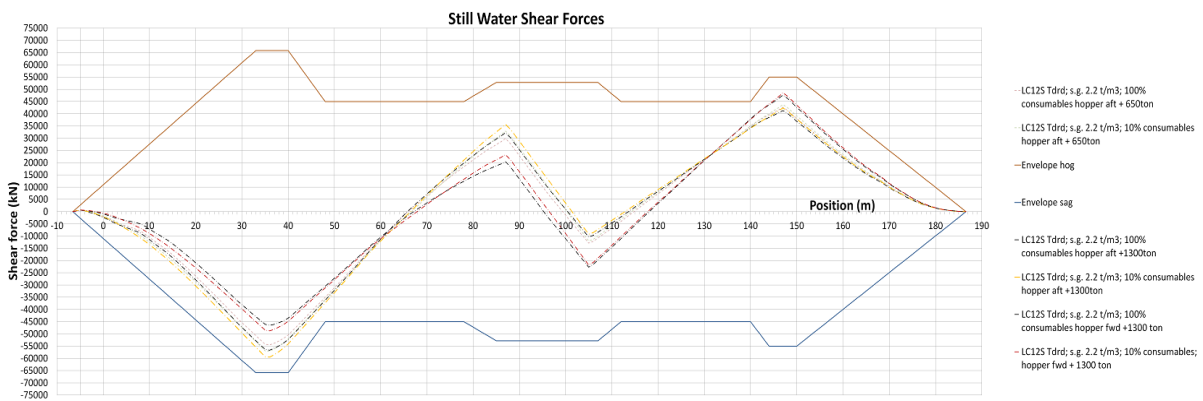
Figure 76 *Still Water Shear Forces with overload - Symmetrical loading - Design 2*

Slika 69 *Prikaz smičnih sila – Simetrično krcanje skladišta – prekrcan – Projektna opcija 2*
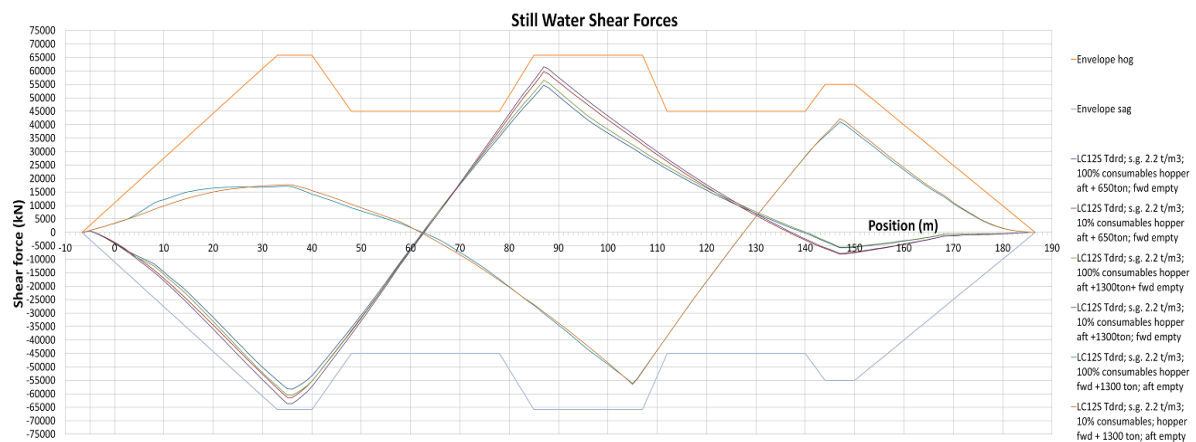
Figure 77 *Still Water Shear Forces with overload - Asymmetrical loading - Design 2*

Slika 70 *Prikaz smičnih sila – Asimetrično krcanje skladišta – prekrcan – Projektna opcija 2*

270

The governing loading conditions amidships regarding total shear force were found to be the asymmetric loading conditions, whereas in the aft and forward hopper bulkhead areas the governing loading conditions were symmetrical loading. The existing vessel hull girder shear capacity was found non-compliant in the aft hopper bulkhead connection area. Reinforcements to major global shear carrying members were to be investigated and carried out. The total shear force comparison (SWSF+WSF) for both designs is given in the following chapter.

4.3. Comparison of the design options

The two design options were analysed and preliminary reinforcement sketches and strength calculations were made. This was very important for estimation of the steel weight of the added part and reinforcements as well as the end price of the elongation.

The steel estimation for the added hull parts including reinforcements in the existing hull were estimated. These are presented in the following table.

Table 21 *Steel mass comparison - D1 – D2*

Design Option	Design 1	Design 2
Mass of new section [t]	2040	2102
Mass of needed reinforcements [t]	35	38
Total Added Mass [t]	2075	2140

It is visible that the weight of reinforcements is rather similar but the new section weight increase will be larger for the D2 option. The amount of reinforcement was drawn in a preliminary sketch and compared especially in way of reinforcement extent.
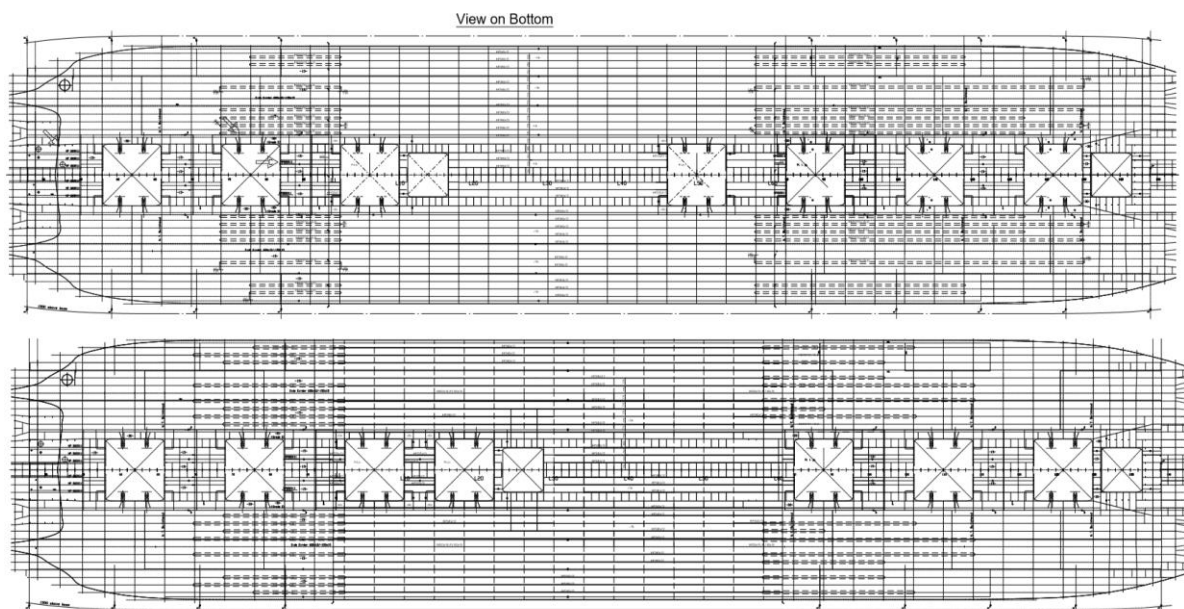
Figure 78 *Comparison of bottom reinforcement Design 1 and 2*

Slika 71 *Usporedba ojačanja dna – Projektna opcija 1 i 2*
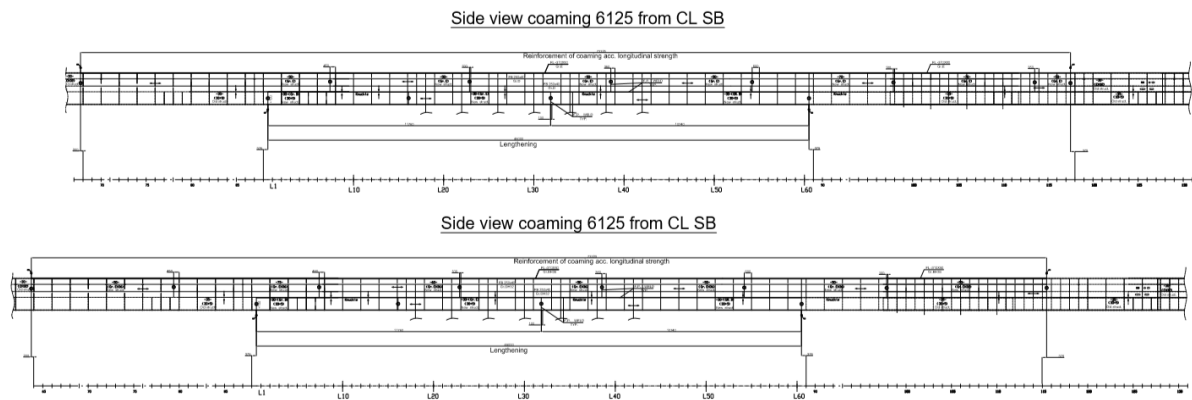
Figure 79 *Comparison of coaming reinforcement Design 1 and 2*

Slika 72 *Usporedba ojačanja pražnice – Projektna opcija 1 i 2*

The overview and comparison of bending moments and shear forces is also given to add to the insight of the needed reinforcements.
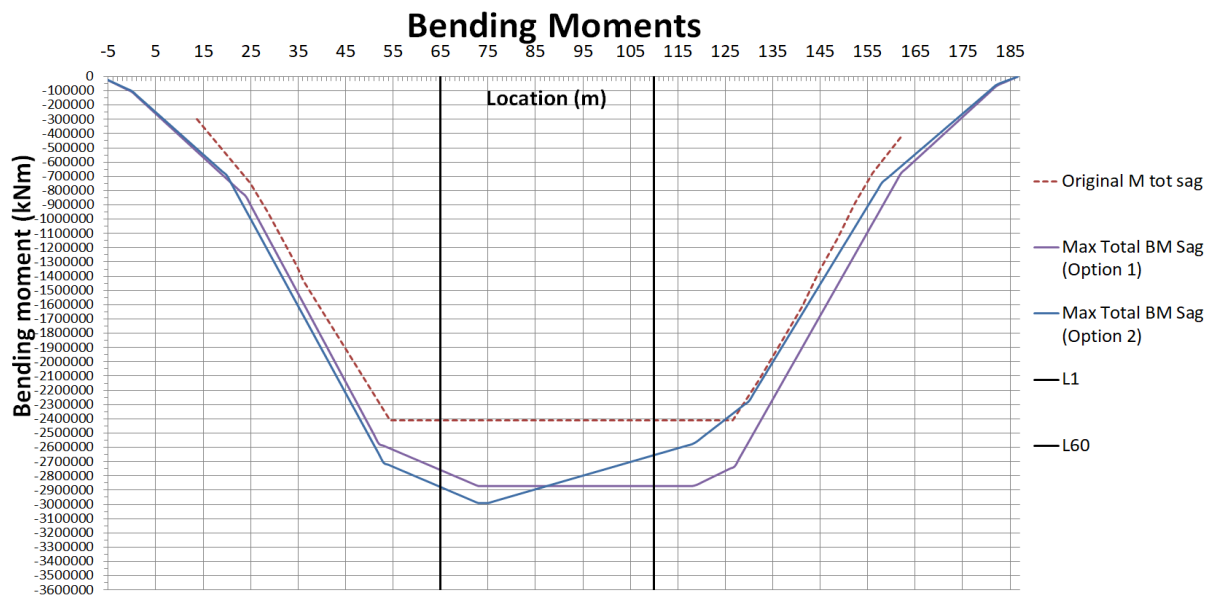
Figure 80 *Comparison of sagging bending moments Design 1,2 + Original Vessel*

Slika 73 *Usporedba momenata svijanja – Projektna opcija 1, 2 i originalni brod prije produženja*

273

Figure 81 *Comparison of shear forces Design 1,2 + Original Vessel*

Slika 74 *Usporedba smičnih sila – Projektna opcija 1, 2 i originalni brod prije produženja*

The increase in bending moments in the aft part for Design 2 is the most severe load increase for this conversion at all. The reinforcement requirements both for coaming structure and bottom reinforcement are substantial. According preliminary strength calculations, Design 2 option would require reinforcement for global shear in way of reinforcing the several existing longitudinal hopper bulkhead plate strakes in the vicinity of the aft hopper bulkhead. On top of all of this Design 2 is a heavier option (65t or approx. 3%).

The advantage of design 2 is less sensitivity for overloading of the aft hopper and amount of reinforcement of the forward hopper, given that the forward hopper is substantially less loaded. The fact that the added, new part of the hull is added more to the aft (elaborated under chapter 3) was also an added benefit to this design option and a disadvantage for the Design option 1.

An important aspect the ship-owner wanted checked was the trim of the vessel for different loading scenarios of arrival to shore discharge, so with full hoppers.
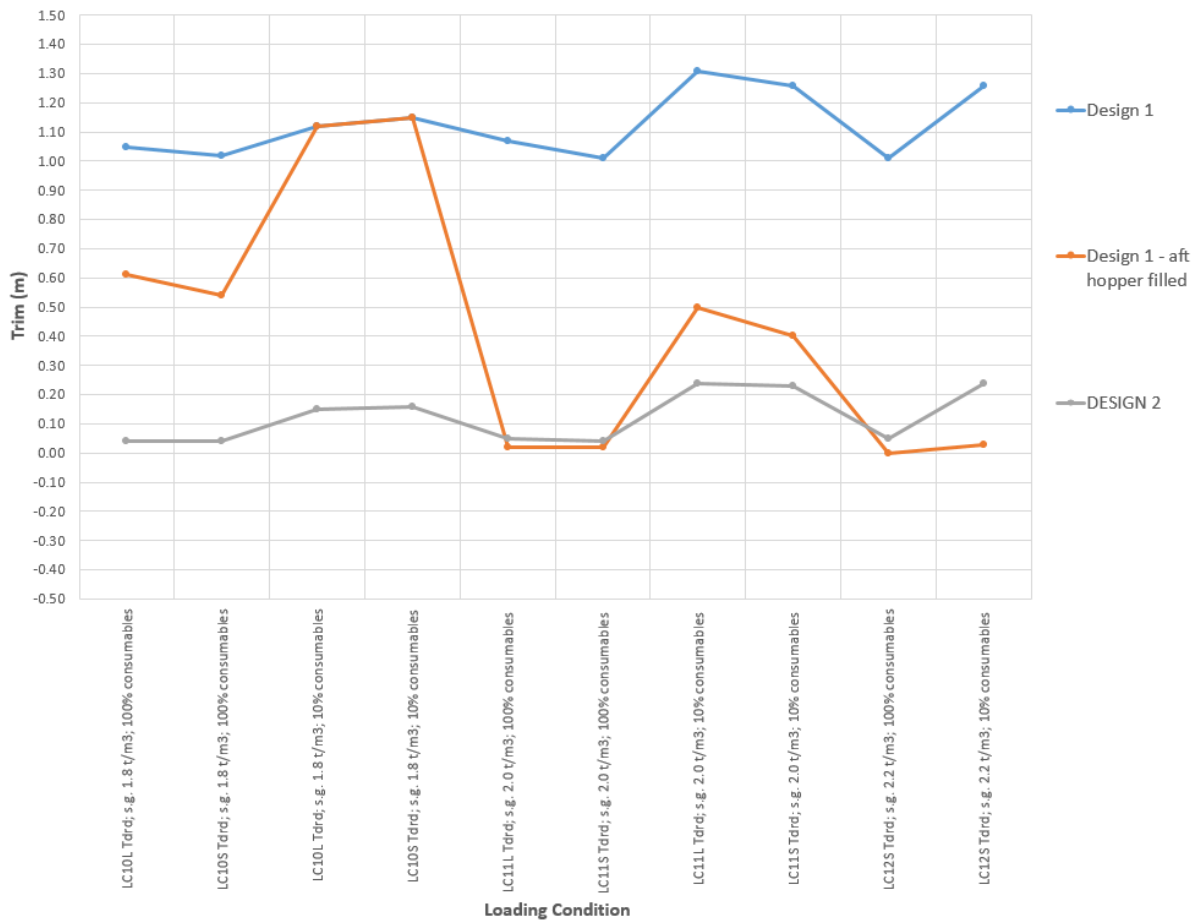
Figure 82 *Comparison of trim Design 1,2*

Slika 75 *Usporedba trimova – Projektna opcija 1 i 2*

The chart above shows different trims for various hopper fillings densities. As it indicates, even keel was easily obtained for Design 2. Design 1 aft hopper needed to be loaded more in order to obtain an even keel.

With all of the mentioned parameters reviewed the owner decided to execute the conversion according design option 2.

5. Basic Design

The end of feasibility stage demarked the start of basic design. A lot of activities were continued with certain activities started. Given that the repair shipyard was not known at that stage, as usual for these, conversion projects, project standards were set combining old, as built standards, new best practices as well as keeping in mind ease of procurement and fabrication for the projected location of the conversion yard.

Certain key activities and their respective milestones are touched briefly in the following chapter in order to give a representation of the general scope of the engineering package required for this particular conversion.

5.1. Ship Stability

6.1.1 Intact Stability

A stability model was made in the feasibility phase. This model was slightly refined and detailed in order to check for the requirements for IMO code on intact stability for international draft, as well as stability criteria for dredging draft according to "GUIDELINES FOR THE ASSIGNMENT OF REDUCED FREEBOARDS FOR DREDGERS DR-68 rev.1" [Ref.3] [Ref .3]. These criteria were met.
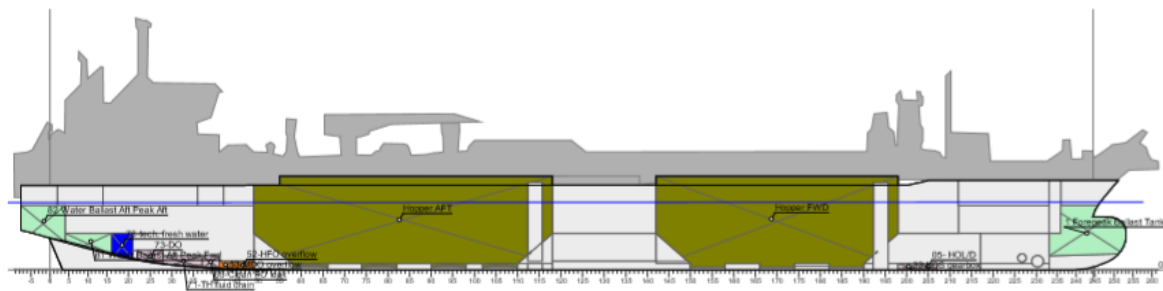
Figure 83 *Symmetrically loaded hoppers - stability model representation*

Slika 76 *Simetrično krcanje skladišta – prikaz modela za stabilitet broda*
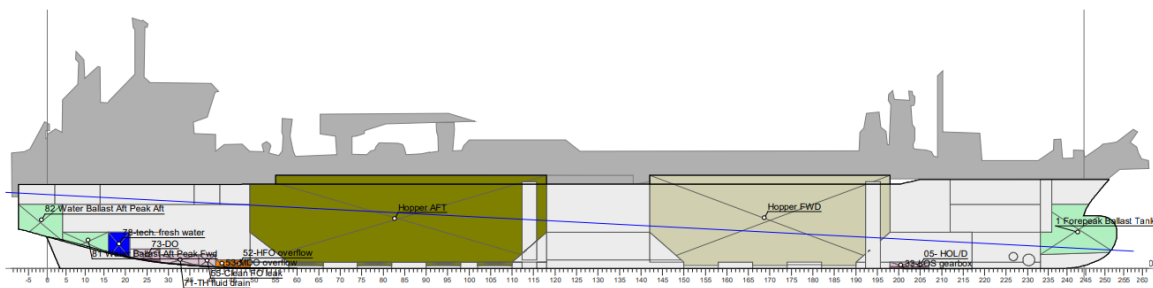
Figure 84 Asymmetrically loaded hoppers - stability model representation

Slika 77 *Asimetrično krcanje skladišta – prikaz modela za stabilitet broda*

From the stability model still water bending moments and still water shear forces were also calculated for a variety of loading conditions as already mentioned in Chapter 4. A large number of

hopper loading and unloading scenarios was loaded to the model to recheck the sensitivity of the structural design.

6.1.2 Damage Stability

Probabilistic damage calculations were also done to calculate the attained subdivision index and cross check it to the required subdivision index. A plan of watertight compartments was drafted out and the subdivision was set in the stability model as well as down-flooding and connection points.
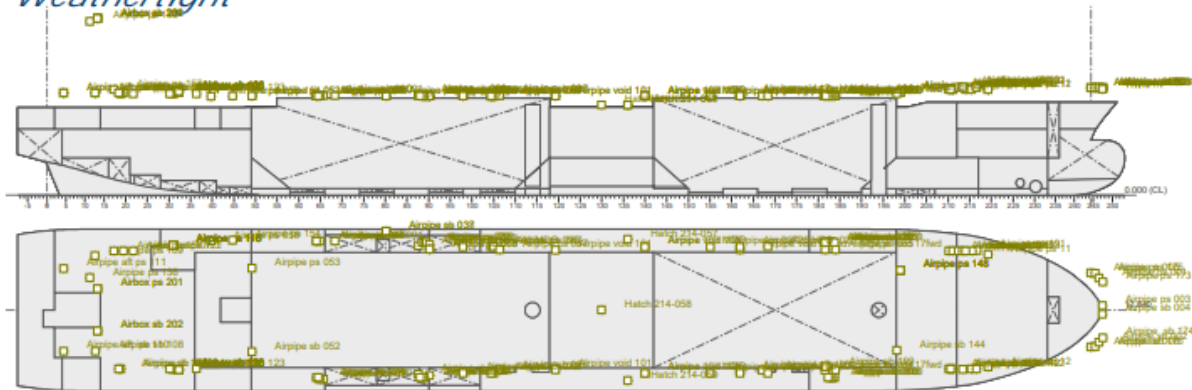
Figure 85 Weathertight and downflooding openings representation – Stability model

Slika 78 *Vodonepropusni otvori i točke progresivnog naplavljivanja – prikaz modela za stabilitet broda*

The probabilistic stability calculation was carried out according to Solas 2020 MSC.421(98) and found compliant.
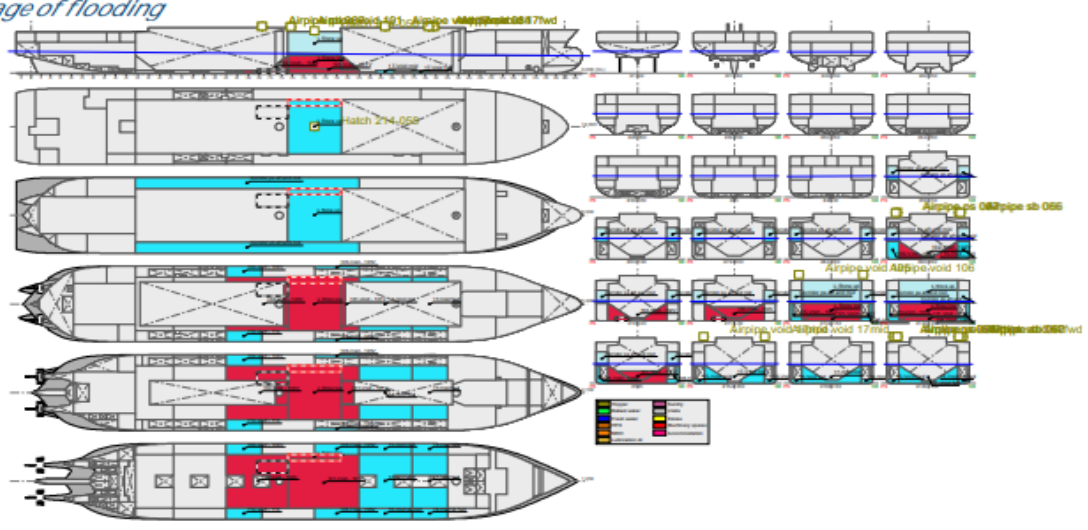
Figure 86 Flooding condition representation – Stability model

Slika 79 *Stanje naplave broda – prikaz modela za stabilitet broda*

Special attention was taken for the mid part of the vessel (the added store space) where a watertight tank top was introduced. The hopper unloading pipeline needed to be accommodated through this store space without bends so a recess in the tank top needed to be accommodated.

5.2. Hull Structure

6.2.1 Construction plans

With reference to the old/existing part of vessel as already approved structure, new main frame needed to be drafted out with regard to the increased hull girder loading and modified geometry amidships.

Alongside this, a lengthened vessel construction plan was to be drafted out with particular level of detail for the new, added section as well as the reinforced areas of the existing vessel.

Structural calculations for this conversion were already done in Mars 2000, BV Software, as well as rough beam grillage calculations for primary structure in way of added section amidships.
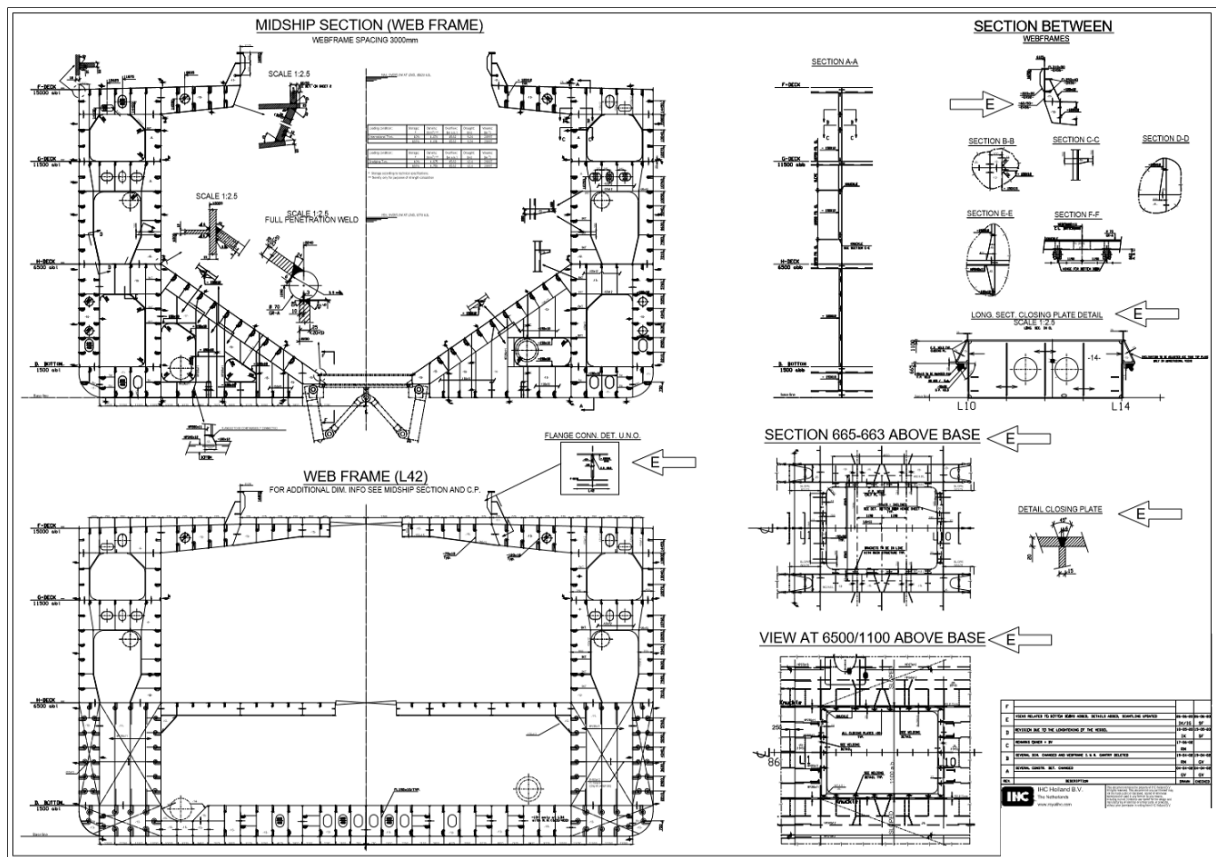
Figure 87 Main Frame Drawing Sheet Example

Slika 80 *Primjer nacrta glavnog rebra*

The list of submitted structural plans for Class appraisal of this conversion was to include:

o   Main Frame Drawing

o   Construction plan Midship

o   Shell Expansion

o   Welding List

o   Interface Drawing – Foundations in way of Gantries and winches

An interesting aspect reanalysed in this conversion project was the usage of owner wear allowances. Quite frequently owner wear allowances are used in the hopper area, on top of rule minimum required gross thicknesses, thus increasing steel weight significantly.

Regarding this topic, the owner monitored the wear on all of the ship's plating and documented periodically each thickness measurement conducted on the vessel. The worst wear reported was in the longitudinal hopper side bulkhead plate strakes, slightly higher from the mid-height of the hopper. This corresponds with the adjustable overflow lowest position when the sea water is flowing out in order to increase the spoil mixture density. The top streaks of the hopper area shown little or no wear what so ever. The bottom hopper plating wear was also far milder than expected in the design stage of the original vessel.

This led to a decrease in the owner allowance in the hopper area. In the existing vessel this went in favour of the gross scantling of the existing hopper areas.

6.2.2 Finite element analysis

During preliminary calculations and construction sketches in the feasibility stage, a meeting was set up with the classification society in order to determine required extent of finite element method (FEM) and fatigue calculations. Alongside the main frame preliminary drawing, a preliminary construction plan layout was submitted for information indicating the means of executing the hull construction of this conversion. Alongside the construction plans, a preliminary longitudinal strength assessment was submitted also for information, indicating the hull girder loading.

During these meetings the transition of the hoppers towards the store space area, and the loss of longitudinally effective members was identified of particular interest to be checked through a 3D Finite Element Calculation model. Also the aft hopper, given its higher loading in comparison to the forward one, was to be represented in larger extent in the FEA model.

Areas of the transition from single bottom structure to double bottom structure were also found interesting to analyse in this model, especially in way of the recess needed to accommodate straight hopper unloading pipeline route.

Also, as identified in preliminary beam calculations, the double bottom deformation levels of the store area tank top under maximum sea pressures was to be looked at in the global model.

Based on global FEA model stress plots and response of certain structural details, areas of particular interest for fatigue life expectancy assessment were to be highlighted.
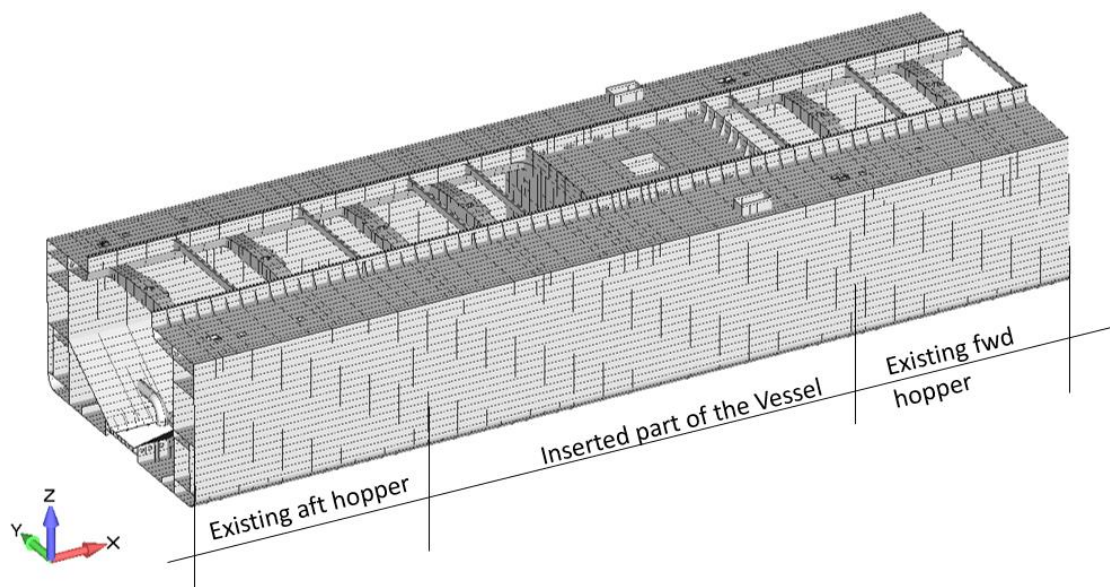
Figure 88 FEA Model Extent

Slika 81 *FEA model koji se promatrao*

The FEA model was made in Siemens Femap software. Model mesh consisted of shell elements representing primary members and plating and beam elements representing secondary stiffeners. Performed analysis was linear static with NX Nastran solver.
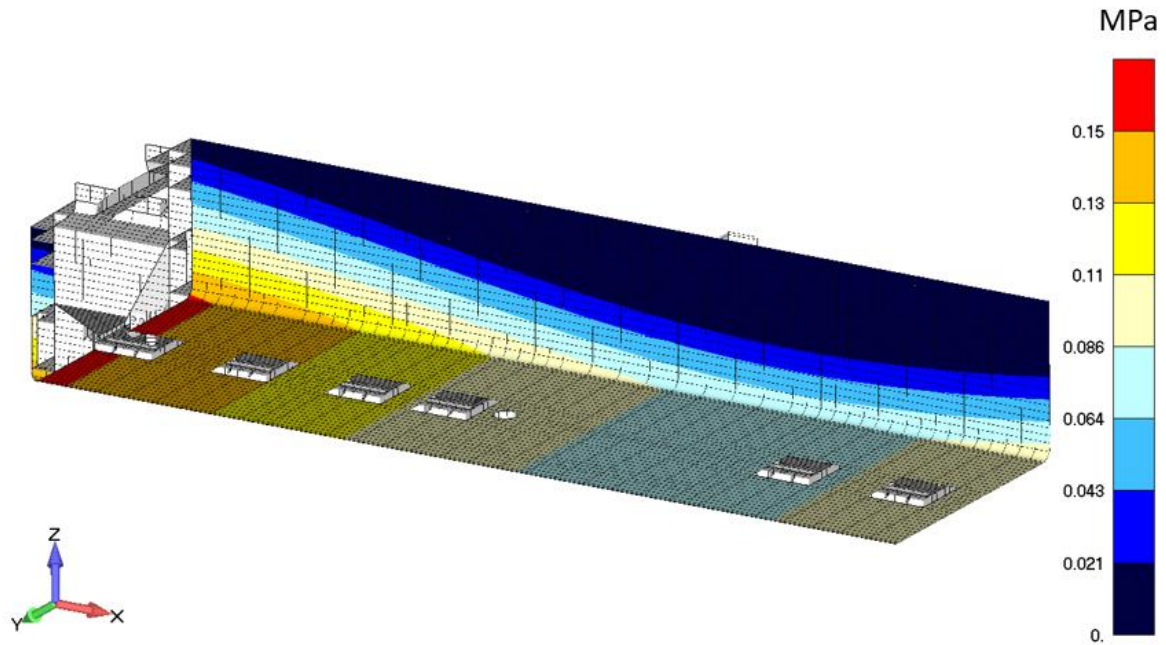
Output Set: END NODES - X3
Elemental Contour: Pressure Face 2 Set 301

Figure 89 FEA Model Sea pressure example on wetted surfaces

Slika 82 *FEA model – primjer prikaza tlaka mora na oplakanu površinu*

Given the foretold interest in details of the connection parts to the new store space the mesh size in these connection parts was generally set at 150x150mm in order to more accurately represent primary element transitions and connections.
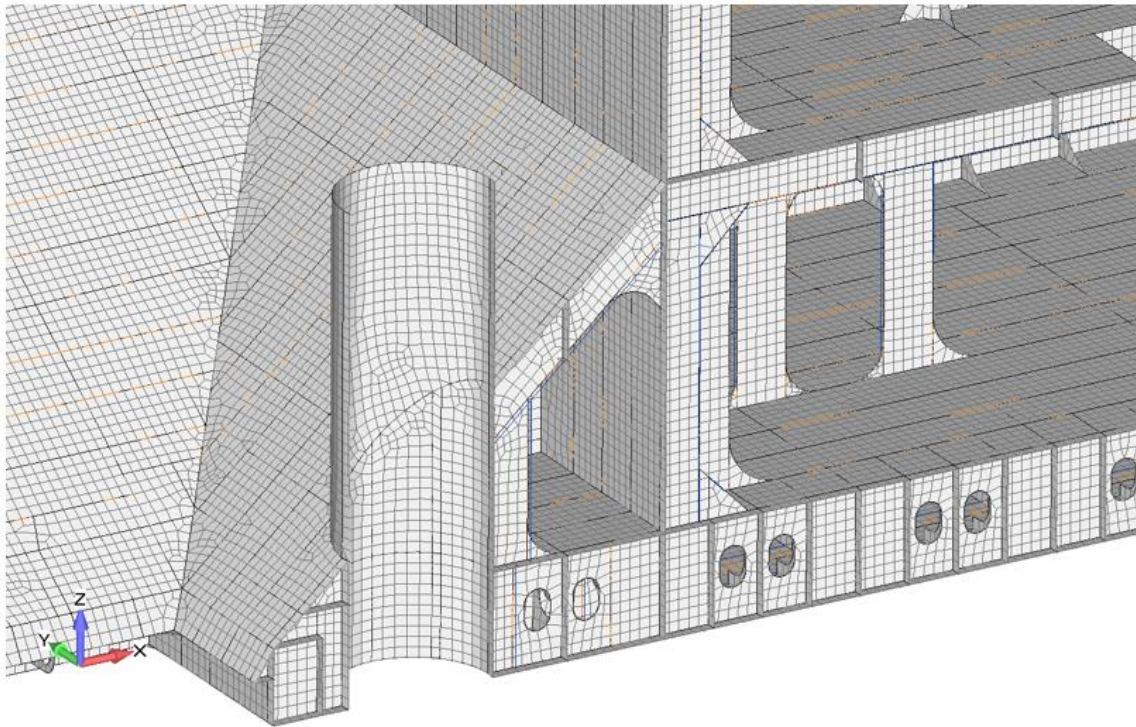
Figure 90 FEA Model mesh size in the hopper connection area around the overflow

Slika 83 *FEA model – veličina mreže (elemanta) na području ukrcajnog skladišta oko cijevi preljeva*

Boundary and loading conditions were set according rule requirements and validated against stability loading conditions superimposed with wave induced loadings.
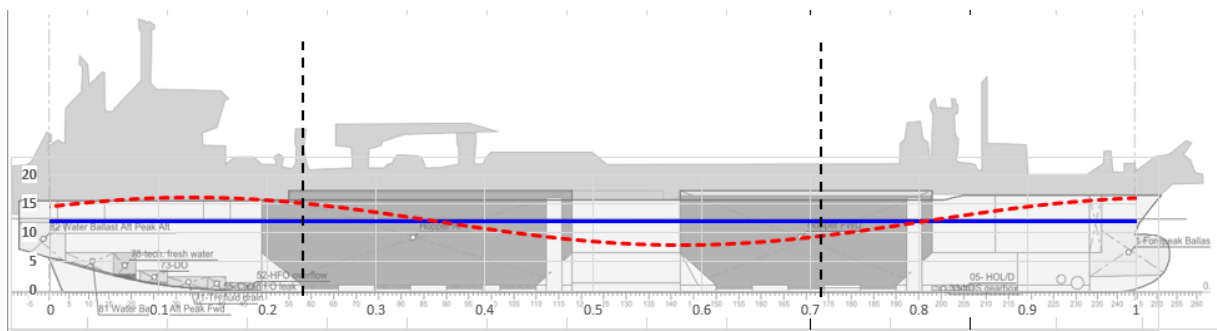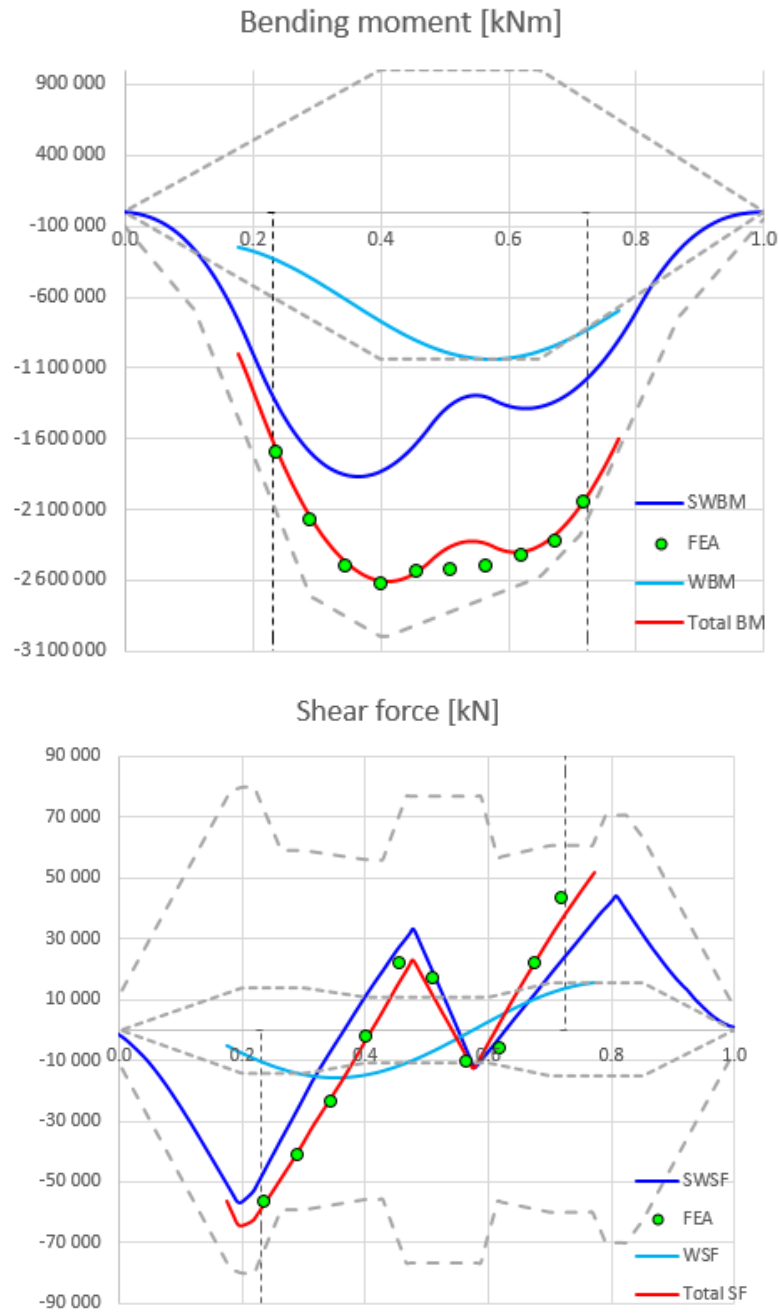
Figure 91 FEA Model loading condition validation – example symmetrical sagging loading

Slika 84 *FEA model – validacija stanja krcanja – primjer simetričnog progibnog opterećanja*

Output Set: NX NASTRAN Case 3
Elemental Contour: Plate Top VonMises Stress
Second Contour: Plate Bot VonMises Stress
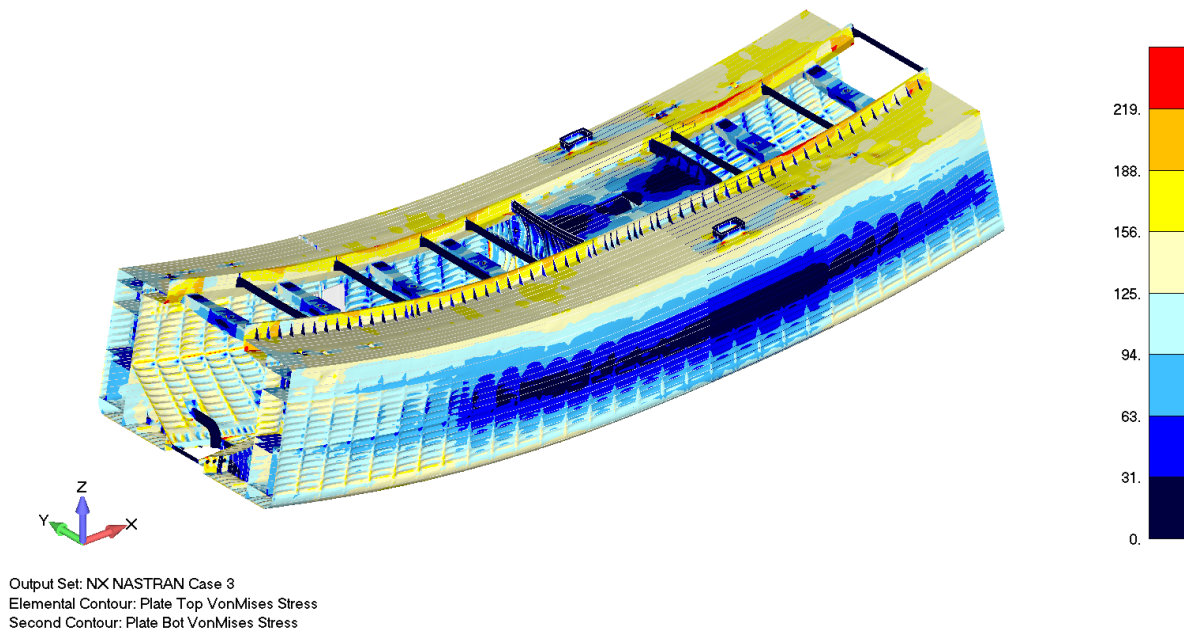
Figure 92 FEA Model stress level plot example for a symmetrical sagging load case

Slika 85 *FEA model – primjer prikaza vrijednosti opterećenja za simetrično progibno opterećenje*

After a conducted finite element analysis the global behaviour of the elongated vessel was found compliant to withstand the hull girder loadings. Several areas were highlighted in order to check in way of fine mesh for structural details and several were to be analysed for fatigue life assessment.

Buckling assessment was also conducted for most critical areas in way of compressive and shear stresses.

6.2.3   Buckling Assessment

Buckling assessment of the elongated vessel was performed using the FEA model stress levels according rule formulation as given in Rules and Regulations Pt B, Ch7.Sec 1, Pt 5 [Ref 1].

Based on the finite element results for the midship model, for each plate panel that meets certain geometrical criteria a buckling calculation has been performed. In this chapter the used methodology is explained.

The worst compressive and shear stresses identified in the global FEA model were found for amidst the aft hopper and the store part amidships respectively so buckling unity checks were conducted for that area.

The midship of the hopper dredger consists of a large number of elementary plate panels, bounded at their edges by either a stiffening member (flat bar, bulb profile, etc.) or a primary member. For each of these panels a critical buckling stress can be determined, which depends on the geometry of the panel, the mechanical properties of the material, and the way of constraining the edges. Because of the large number of panels present in the midship model, a software tool has been developed to aid in the hand calculation of buckling stresses and limits for these panels.

284

Basically it is an automated tool developed on basis of previously used API scripts to obtain normal and shear stress average levels from Femap. These were then loaded into rule based developed spreadsheets in order to check for the buckling unity factor of the panel considered. The results were then loaded back to Femap for presentation purposes. In latest years, an upgraded version of this tool has been developed automatically doing the unity checks and creating output plots.

In short, this tool applies the following steps:

i.   For each surface (considering it a panel) in the midship model the geometry is determined, as well as the edge constraints along each edge curve, while indicating whether it is a secondary or primary member attached to the edge.

ii. Then for each plate element on the surface the finite element stresses are expressed in the coordinate system of the panel, and an area-weighted average of these stresses are calculated to yield a longitudinal stress, a lateral stress and a shear stress average. When an element is loaded in tensile, the element stress component is taken equal to zero.

iii. With opposing edges equally constrained and always one set of edges considered primary and one set secondary, a total of six different buckling scenarios are subsequently tested. These are:
   o Buckling due to normal stress on primary edges only
   o Normal stress on secondary edges only
   o Shear stress only
   o Primary edge normal stress plus shear stress
   o Secondary edge normal stress plus shear stress
   o Biaxial stress plus shear stress

iv. For each of the six buckling scenarios the critical buckling stress of the panel is calculated, and a buckling unity check is found by dividing the appropriate panel stress component (from the FE result data) by this critical buckling stress. When the resulting factor is below 1 the panel will not buckle.

v.   The maximum value of the six buckling unity checks is loaded back to the FE model into a result set, to enable visualisation of the buckling unity checks for the midship model.

vi. This process is repeated for each load case in the model, and subsequently plots are shown to visualize the buckling unity checks for the vessel.

Examples of output plots of buckling factors obtained for elementary plate panels is given on the following figures.
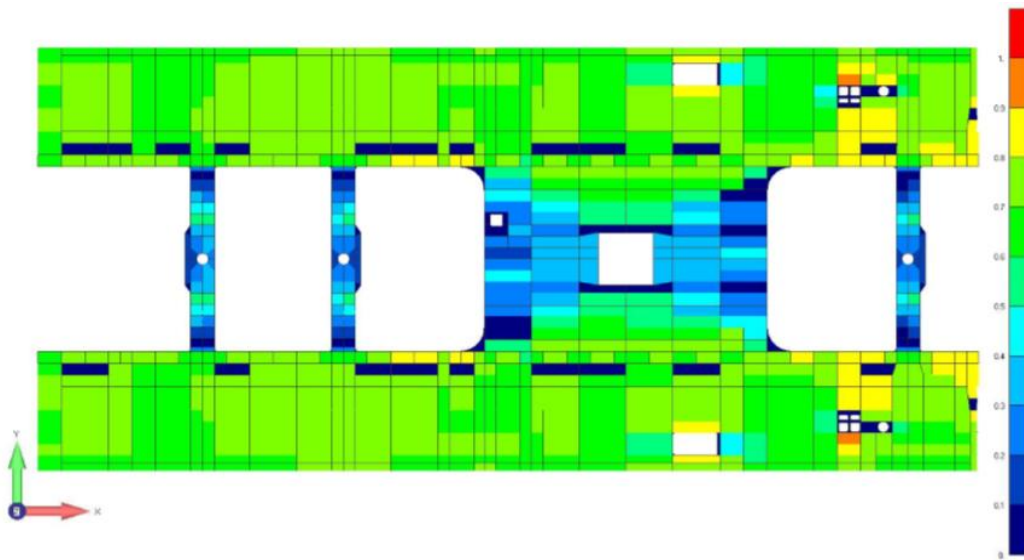
Figure 93 Main Deck Panel Buckling Factor - Automated tool plot example for a sagging loading condition

Slika 86 Faktor izvijanja limova na glavnoj palubi – primjer prikaza za progibno opterećenje
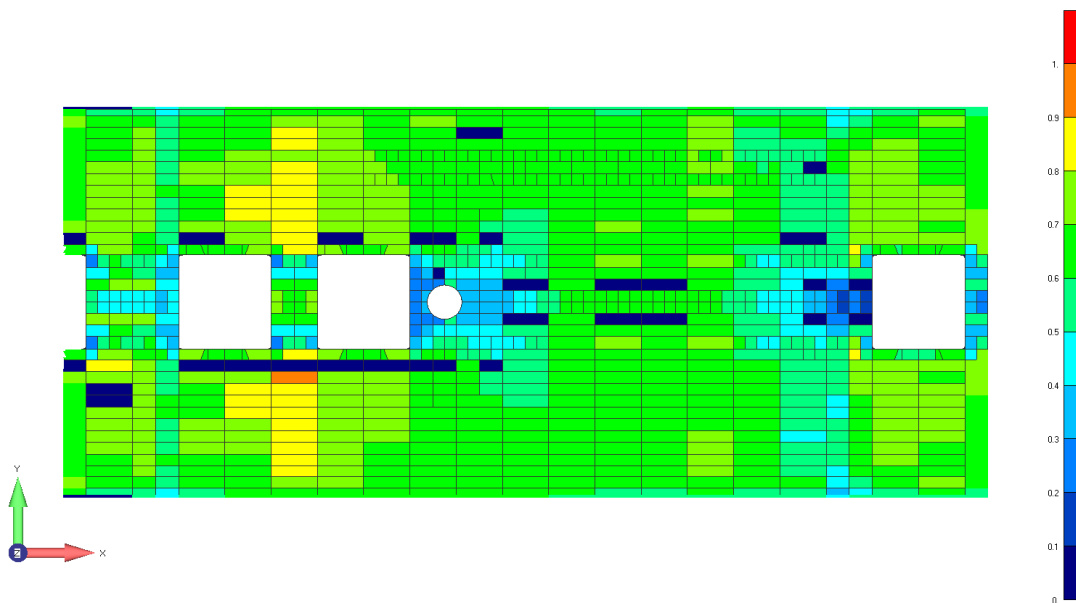
Figure 94 Bottom Panel Buckling Factor - Automated tool plot example for a hogging loading condition

Slika 87 Faktor izvijanja limova na oplati dna – primjer prikaza za pregibno opterećenje

6.2.4   Fatigue Life Assessment

Fatigue assessment was conducted for several details identified by the global model stress level plots. These were the:

- o Detail 1 - Connection radii of the main deck to the store space
- o Detail 2 - Web Frame connections to tween deck
- o Detail 3 - Connection of longitudinal and transverse hopper bulkheads
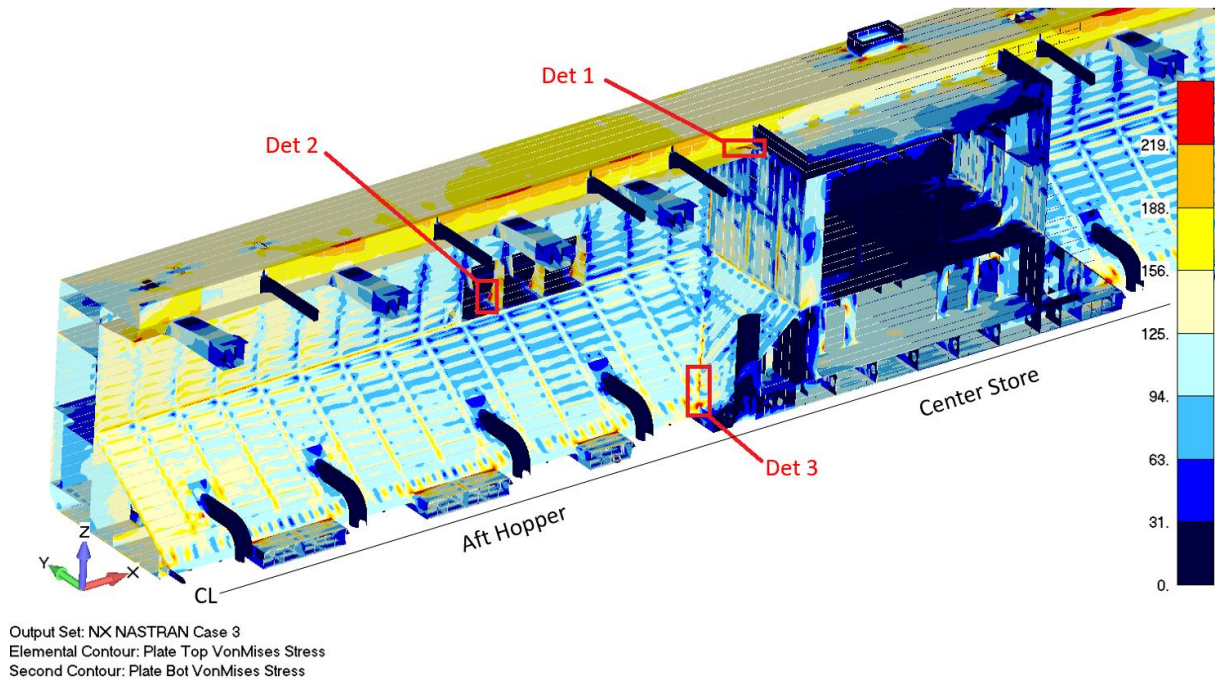
Figure 95 Representation of FEA model details to be assessed for fatigue

Slika 88 *Pozicije detalja u FEA modelu koji se trebaju razmatriti na zamor materijala*

The fatigue assessment has been done in accordance with Pt B, Ch 7, Sec 4 of the steel ship rules of Bureau Veritas [Ref. 1] and according the additional information note: 'Fatigue strength of welded ship structures'[Ref. 4]. In the mentioned rules a number of assumptions are made for the fatigue calculation of general cargo vessels, container vessels and bulk carriers. However, some of the assumptions made for the mentioned vessels are not valid in the case of a dredger given that still water stresses are not varying slowly during each voyage as assumed for general cargo vessels, container vessels and bulk carriers. Also dredgers have different types of loading conditions compared to other ship types.

Given the mentioned above and based on previous hopper dredger fatigue assessments, an information note – Guidance on fatigue check for dredgers is referenced [Ref. 5].

It is elaborated in the guidance note that the damage contribution of dredger loading-unloading sequence can occur multiple times a day and the changes in the still water bending moments, especially while unloading, occur very rapidly. In addition, during these dredging cycles the still water

bending moment changes from the maximum sagging to the maximum hogging moment. Therefore the still water stress cycle cannot be considered static, or very low frequency or of negligible magnitude (as given in [Ref. 4]) and is to be included in the fatigue assessment. Based on the cumulative damage principle of Miner the damage due to loading/unloading cycles can be considered separately from the standard (Wave induced) damage calculation and added to this.

Here it is important to define the operational profile of the vessel in means of operational percentage in transit (navigation conditions on international draft) and operational percentage in dredging situations. These are suggested to be:

- o   Part of sailing time in transit (20%)
- o   Part of sailing time dredging (80%)
  - -   While dredging fully laden (50%)
  - -   While dredging in ballast (50%)

The total damage due to fatigue is calculated as a sum of damage due to waves and damage due to dredging cycle is given in equation 4.

$$D = D_W + D_{DC} \tag{4}$$

Where:

D_W: Damage due to waves

D_{DC}: Damage due to dredging cycle

a.   Total damage due to waves

$$D_W = K_{cor}[\alpha_1 D_F + \alpha_2 D_{BD} + (1 - \alpha_1 - \alpha_2)D_{BT}] \tag{5}$$

Where:

$\alpha_1 = \alpha_D \alpha_{FD}$:   Part of the ship's life in full load condition

$\alpha_2 = \alpha_D(1 - \alpha_{FD})$: Part of the ship's life in ballast condition and in operating area

α_D: Part of the ship's life in operating area, generally to be taken equal to   0.80

α_{FD}: Part of the ship's life in full load condition while in operating area, generally to be taken equal to 0.5

D_F: Cumulative damage ratio for ship in operating area at dredging draught (full load), taken equal to:

$$D_F = \frac{1}{6}D_{aF} + \frac{1}{6}D_{bF} + \frac{1}{3}D_{cF} + \frac{1}{3}D_{dF} \qquad (6)$$

D_{BD}: Cumulative damage ratio for ship in ballast condition while sailing in the operating area, taken equal to:

$$D_{BD} = \frac{1}{3}D_{aBD} + \frac{1}{3}D_{bBD} + \frac{1}{3}D_{cBD} \qquad (7)$$

D_{BT}: Cumulative damage ratio for ship in ballast condition while sailing in the navigation area(transit), taken equal to:

$$D_{BT} = \frac{1}{3}D_{aBT} + \frac{1}{3}D_{bBT} + \frac{1}{3}D_{cBT} \qquad (8)$$

D_{aF}, D_{bF}, D_{cF}, D_{dF} : Elementary damage ratios for load cases "a", "b", "c" and "d", respectively, in "Fully laden" dredging condition, defined in Ch 7, Sec 4, Pt 3.1.1. [Rev 1] and considering the dredging draught T_D and the navigation coefficient n_D

D_{aBD}, D_{bBD}, D_{cBD} : Elementary damage ratios for load cases "a", "b" and "c" respectively, in "Ballast" dredging condition, defined in Ch 7, Sec 4, Pt 3.1.1. [Rev 1] and considering navigation coefficient n_D

D_{aBT}, D_{bBT}, D_{cBT} : Elementary damage ratios for load cases "a", "b" and "c" respectively, in "Ballast" navigation condition, defined in Ch 7, Sec 4, Pt 3.1.1. [Rev 1] and considering the navigation coefficient n

K_{cor} : Corrosion factor, taken equal to:

- o $K_{cor} = 1.5$ for cargo oil tanks
- o $K_{cor} = 1.1$ for ballast tanks having an effective coating protection
- o $K_{cor} = 1.0$ otherwise

b. Total damage due to dredging cycle

$$D_{DC} = K_{cor} \frac{n_C}{N_{fat}}$$
(9)

Where:

n_C: number of dredging cycles in the ship's life, taken equal to:

$$n_C = 365 T_{fl} \alpha_0 \, \alpha_D n_{CD}$$
(10)

Where:

α_0: sailing factor, taken equal to 0.85

T_{fl}: Design fatigue life, in years, taken equal to 20

n_{CD}: number of dredging cycles per day. In general can be taken equal to 6

N_{fat}: number of cycles leading to fatigue failure at the notch stress range. Taken as:

$$N_{fat} = \frac{K}{\Delta\sigma_{N,D}{}^3}$$
(11)

$$K = K_p \qquad\qquad \text{for } \Delta\sigma_{N,D} > S_Q$$
(12)

$$K = K_p^{5/3} \cdot 10^{-14/3} \qquad \text{for } \Delta\sigma_{N,D} < S_Q$$
(13)

Where:

$$K_p = 5.802 (\tfrac{22}{t})^{0.9} 10^{12}$$
(14)

$$S_q = (K_p 10^{-7})^{1/3}$$
(15)

$\Delta\sigma_{N,D}$: notch stress range, taken equal to:

$$\Delta\sigma_{N,D} = |\sigma_{N,D,1} - \sigma_{N,D,2}|$$
(16)

$\sigma_{N,D,1}$: Notch stress in considered detail for fully laden condition in still water without accelerations, increased with the average notch stress amplitude induced by wave action (sagging) during the transit period.

$\sigma_{N,D,2}$: Notch stress in considered detail for empty condition (hopper open to sea or discharged) in still water without accelerations, increased with the average notch stress amplitude induced by wave action (hogging) during the transit period.

Notch stress range is calculated according the procedure given in Ch7,Sec4, Pt 4.3.1 [Ref1]

Based on the above described fatigue assessment method fatigue assessment the mentioned details were found compliant.

5.3. Basic diagrams, statutory and arrangement drawings

After the initial check of lengthening impact for statutory drawings, a number of arrangement drawings were made either for approval or for owner and detail engineering reference. These include:

- o   Intact stability calculation
- o   Damage stability calculation
- o   Freeboard calculation
- o   Equipment number calculation
- o   Plan of watertight compartments
- o   Plan of tanks, manholes and ladders
- o   Compartment numbers, doors and hatches
- o   Plan of marks and dock plugs
- o   Overview sounding tubes
- o   Mooring and Anchoring arrangement
- o   Overview deck crane
- o   Structural fire protection
- o   Lifesaving appliances and escape route plan
- o   Navigation bridge visibility plan
- o   Overview of stairs
- o   Arrangement of hoisting beams
- o   Plan of hull sections
- o   Docking plan

Number of diagrams for this conversion was done including:

- o Diagram FO filling/transfer/overflow

- o Air/Sounding diagram

- o Diagram bilge/ballast

- o Diagram scupper and drain

- o Diagram air lines

- o Diagram Fuel oil consumers

- o Diagram Instrument air

- o Diagram Sludge/dirty and leak oil

- o Diagram US sounding

- o Diagram Thermal oil

- o Diagram sea cooling water

- o Diagram grease system

- o Diagram Jet water

- o Diagram firefighting/deck washing

- o Diagram gland/flushing

- o Diagram hydraulic watertight doors

- o Diagram gas/oxygen

- o Diagram tracing

- o Diagram Hydraulic systems

- o Ventilation plan

The major effect on the systems was in terms of jet-water and bilge lines as well as elongation of the dredge lines which led to modification of the gland and flushing system. New added store spaces needed to be vented and heated so the capacity calculations and arrangements were made without significant changes to the existing power capacity on board.

The electrical system also needed a slight modification where the new midsection was to be fitted with an electric cabinet. The mid part winches and the traveling deck crane cable drum were to be modified due to the extension and certain deck penetrations were to be repositioned. The electrical scope was drafted and an external vendor was to carry out the works.

5.4. Interfaces of mission equipment

The new section was a target for placing as much mission equipment as possible there given that large foundations would be executed integrated in the newly built section. In the feasibility stage it was already determined to move the cutting line more aft in order to keep the existing pump gantry and it's foundation intact. That was one of the first constraints.

During basic engineering a feasible suggestion regarding the SB drag-head gantry (longer suction tube option) was to elongate the suction tube in order to fit the drag-head gantry to the existing vessel intermediate gantry foundation. This way a lot of difficult labour on the existing vessel could be avoided. This is presented on the following figure where the suction tubes and the gantries are plotted in cyan while the new position of the SB drag-head gantry is indicated in red.
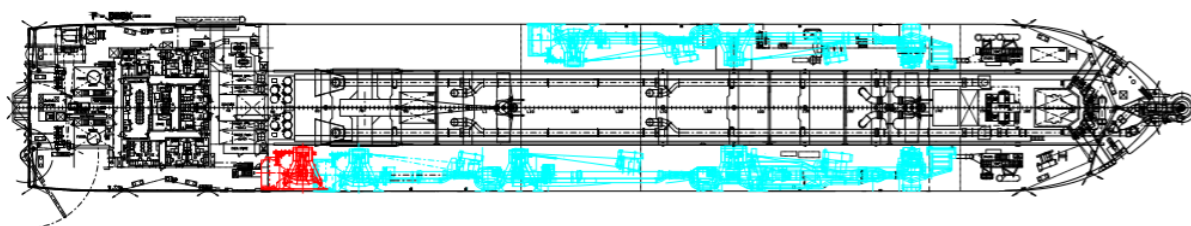
Figure 96 Representation of SB suction tube extension

Slika 89 *Prikaz produženja usisne cijevi na SB strani broda*

The original gantry system is executed as a "free fall" system guided to the outboard position by the self-weight of the suction tube so it was of major importance to check the COG's of the new arrangement and the geometrical compliance of the new arrangement.
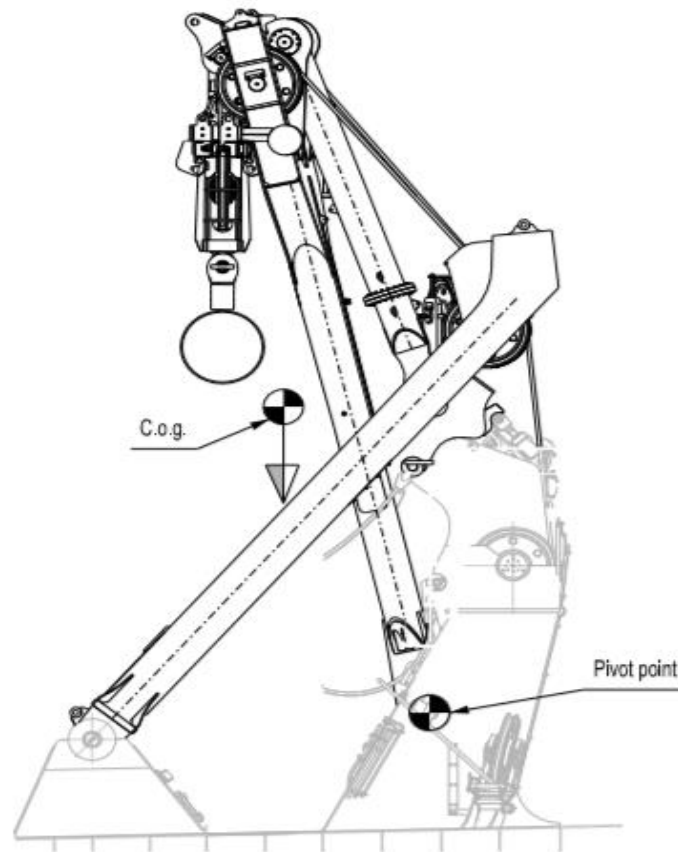
Figure 97 Representation of System COG and pivot point of a gravity gantry

Slika 90 *Prikaz težišta sustava i prekretne točke dizalice*

The investigation found that the suction tube and gantry system can be modified in order to execute the new drag-head gantry in the indicated position as shown on Figure 46. This required a slight elongation of the lower part of the SB suction tube. The A frames and the movable parts of the gantry were to be reused from the existing gantry. Due to minor geometrical misalignments the fixed part of the gantries and the pivot points on main deck were to be produced anew.

Apart for the already mentioned SB drag-head gantry all of the other suction tube system equipment requires modification solely in the new, added ship section. On the following figure a rough representation is given of the gantries and winches on main deck where the red, vertical lines represent part of added section of the hull.
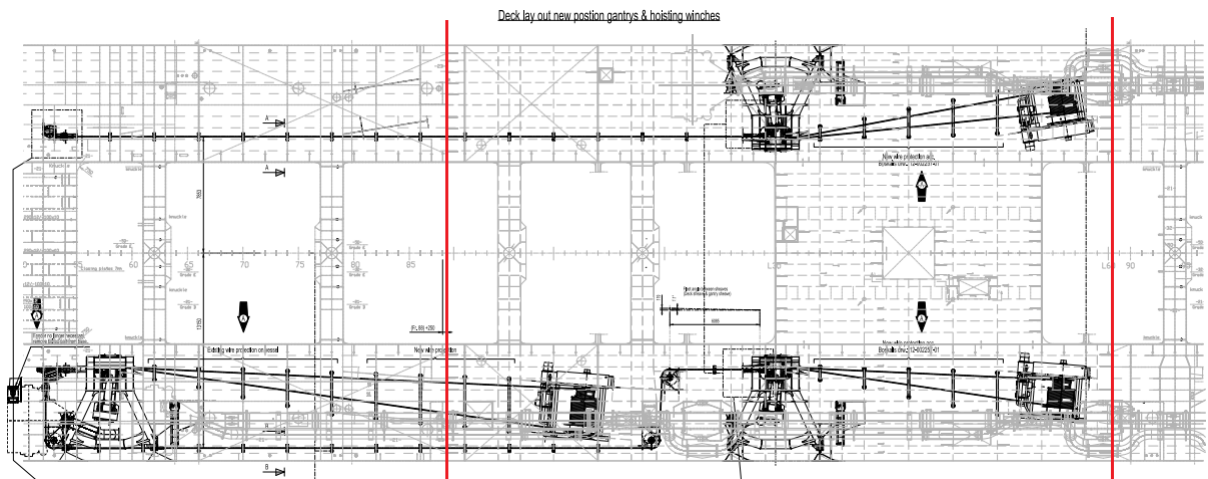
Figure 98 Deck layout of gantries and hoisting winches

Slika 91 *Prikaz pozicije dizalica i vitala na palubi*

These foundations were checked on a FEA sub-model derived from the global one.

The additional major engineering change with regards to mission equipment design was the new aft hopper adjustable overflow design. The existing overflow, now located in the forward hopper is a relatively bulky, complex overflow design outfitted with two small bottom doors that provided overloading in the hopper and opening the doors when the sand has sunk with water remaining on top levels. Then the bottom doors are opened to drop the excess of water and thus increasing spoil density.
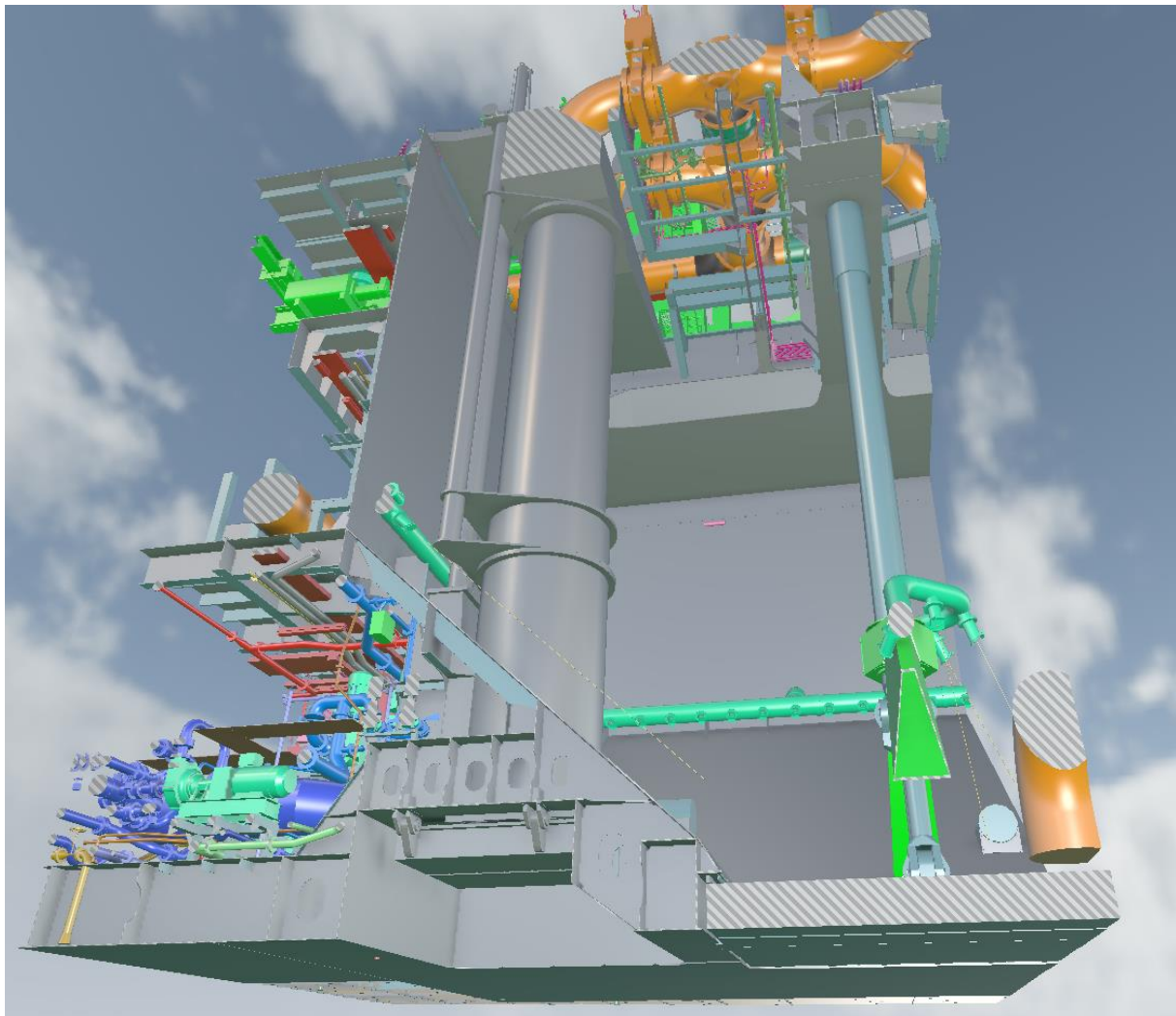
Figure 99 3D model view on the existing overflow design and integration in the fore hopper

Slika 92 *Prikaz 3D modela integracije postojeće cijevi preljeva s pramčanim ukrcajnim skladištem*

The aft overflow is to be executed with a more modern, less robust version of an IHC overflow. It is to be provided with a so called "green" valve in order to limit the intake of air in the overflow with adjusting the water levels and executed without the bottom doors.
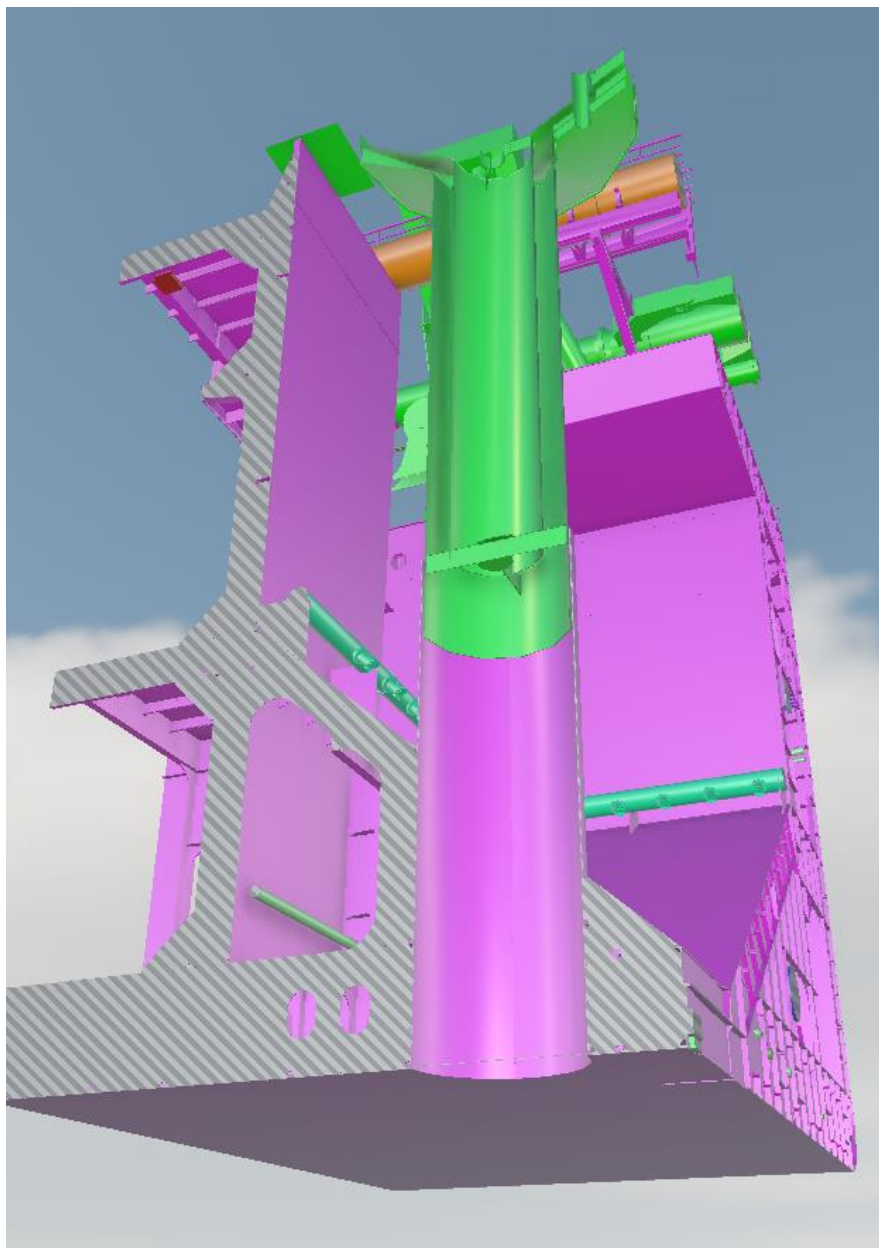
Figure 100 3D model view on the new overflow design and integration in the aft hopper

Slika 93 *Prikaz 3D modela dizajna nove cijevi preljeva i njene integracije u krmeno ukrcajno skladište*

The mission equipment activities also included repositioning and engineering of the horizontal sheaves for guidance of the wire towards the drag-head gantry swell compensator, check and repositioning of the hopper unloading pipes as well as introducing additional T-pieces, integration of two additional bottom doors and more minor activities. The two major integration activities were presented in this chapter.

5.5. Approval and Detail engineering

After the send outs of major basic engineering deliverables towards class and owner detail engineering was to be done in IHC delivering a complete engineering package.

IHC delivered Hull Section drawings with production information: plate parts and list of profiles including bending templates etc., pipe spools and outfitting drawings for the complete conversion.

The lead time in total from the start of the feasibility stage to the detail design delivery was roughly 4,5 months. Class approval of major plans was received roughly 3,5 months after the start of the feasibility stage.

6. Conclusion

The TSHD elongation described in this article is an example of a dynamic conversion project executed within a couple of months from feasibility stage to plan approval from the classification society. This article covered the basic engineering activities to efficiently assess and execute this project. In house developed engineering tools and integrated mission equipment design, and also shipbuilding "know-how" make the process smoother in offering a complete engineering package. The client identified the benefits of executing the complete engineering package in IHC. Given that the complete engineering was done in house the tight lead time for this conversion was met. With this the owner received a complete engineering package for tendering of the conversion process to a yard location of his choosing.

REFERENCES

[1]   Bureau Veritas, Rules For the Classification of Steel Ships, Part B – Hull and Stability, NR 467.B1 DT R12E, January 2020.

[2]   Bureau Veritas, Rules For the Classification of Steel Ships, Part D – Service Notations, NR 467.D1 DT R12E, January 2020.

[3]   Guidelines for the Assignment of Reduced Freeboard for Dredgers DR-68, rev. 1, IMO, 8th of March 2016.

[4]   Bureau Veritas, Guidelines for the Fatigue Assessment of Steel Ships and Offshore Units, NI 611 DT R00 E, September 2016.

[5]   Bureau Veritas, Guidance on Fatigue Check for Dredgers, September 2015.

OOFEM – Application of Open-Source Software in Ship Structural Analysis

Marin Palaversa*[a], Pero Prebeg[a], Jerolim Andric[a]

a University of Zagreb, Faculty of Mechanical Engineering and Naval Architecture, Ivana Lucica 5, Zagreb, Croatia
* Corresponding Author, marin.palaversa@fsb.hr

Abstract

This paper deals with use of open-source software in ship structural analysis. Some advantages and disadvantages of open-source software over standard commercial software are discussed. Object-oriented programming is briefly explained and its importance and benefits in software development are demonstrated on examples from OOFEM. After that, major characteristics and code architecture of OOFEM are described. Role of structural analysis in ship structural design is touched on. Classification societies' requirements on finite element analysis of ship structures are identified and OOFEM is assessed w.r.t them. An upgrade to OOFEM's library of finite elements is proposed based on the foregoing discussion.

Key words: ship structural design; ship structural analysis; finite element analysis; open-source software; FEM software

Sažetak

Ovaj se članak bavi upotrebom softvera otvorenog kôda u analizi brodskih konstrukcija. Raspravlja se o nekim prednostima i nedostacima softvera otvorenog kôda nasuprot standardnim komercijalnim softverima. Ukratko je objašnjeno objektno-orijentirano programiranje te su njegova važnost i benefiti kod razvoja softvera prikazani na primjerima iz OOOFEM-a. Nakon toga su opisane glavne karakteristike i arhitektura kôda OOFEM-a. Ukratko je opisana uloga analize konstrukcije u projektiranju brodskih konstrukcija, prepoznati su zahtjevi klasifikacijskih društava prema analizi metodom konačnih elemenata te je izvršena procjena OOFEM-a prema ovim zahtjevima. Predložena je nadogradnja biblioteke konačnih elemenata OOFEM-a na temelju prethodne rasprave.

Ključne riječi: projektiranje brodske konstrukcije; analiza brodske konstrukcije; analiza metodom konačnih elemenata; softver otvorenog kôda; MKE softver

List of abbreviations

CS – classification society

FE – finite element

FEA – finite element analysis

FEM – finite element method

OO – object-oriented

OSS – open-source software

1. Introduction

Structural analysis is part of ship structural design process [1]. Its primary aim is to determine response of ship's structure to loads imposed on it [1]. Since the second half of the 20th century, a

great development has occurred in field of the rational ship structural analysis (i.e. structural analysis based on first-principles methods such as the finite element method) [1].

There is a lot of good commercial software available on the market that is routinely applied to ship structural problems every day. A survey [2] conducted among structural designers that work in the field of offshore structures revealed that the most widely used software for structural analysis based on the finite element method (FEM) are ANSYS, Nastran (MSC's and Siemens's) and Abaqus respectively. No open-source software (OSS) was reported by any company that took part in the survey. On the other hand, 25% of all users that employ computational fluid dynamics' analyses in their work reported that they use OpenFOAM, OSS based on the finite volume method.

In this paper we present some advantages and disadvantages of using OSS in ship structural analysis. Importance of object-oriented (OO) design of its code architecture is discussed and benefits it brings are demonstrated on finite element analysis (FEA) software called OOFEM. At the end, we touch on a role of ship structural analysis within overall ship structural design process and the most important requirements that classification societies (CSs) impose on FEA software.

2. Open-source and object-oriented FEA software – benefits and challenges

When we talk about OSS, there are two associations that immediately cross our minds, namely that such software is free (no license fees) and that a user has access to its code. The former adds to cutting down the costs while the latter gives us opportunity to extend it (e.g. add new finite elements). However, these are not all of the opportunities offered by OSS, which is also rarely, as we shall see, totally free. A detailed discussion on open-source and object-oriented software in ship structural design is given in [3]. Here, we shall go only through some basic aspects of the subject.

When one plans to work with new software, it is important to determine total cost of ownership (TCO) of the software. License fees are an element of the TCO and are usually non-existent for OSS, but additional costs such as training, support and development costs must be taken into account. Training courses or similar introductory workshops can vary in price significantly: e.g. the price of OOFEM training course is 800 € per person[3] while that of OpenFOAM is 1200 € per person[4]. Development costs are related primarily to the amount of work that must be done in order to arrive from an initial state of software code to the desired one. E.g. when we started to work with OOFEM, it did not have any 2D finite element (FE) suitable for analysis of thin-walled structures so we had to identify the suitable FE, design a software implementation based on its theory given in scientific papers and books and implement it in OOFEM following OOFEM's guidelines and code structure which amounts to considerable work and time.

Development costs mentioned in the foregoing paragraph are directly related to activity (or inactivity) of users' community associated with the project. As a user works with the software, chances are that he will run into problems and usually the only support to rely on is the project's community. This is especially important in the beginning and is further augmented by the fact that OSS is notorious for lack of high-quality documentation. Most of OSS projects have online communities in form of Internet forums, user-groups, mailing lists, etc. These are generally regarded as benefits of using OSS because a user gets support totally free. On the other hand, no

---

[3] Source: http://www.oofem.org/en/courses
[4] Source: https://www.openfoam.com/training/schedule.php

one guarantees that there will be an active community in the first place. Thus, it is important to assess the activity of the community before opting for particular OSS. This is facilitated by the fact that most data that one needs for such assessment is publicly available. One of such assessment measures described in [3] is related to activity of project's Internet forum that can be measured by number of users registered during a time period, number of posts without an answer during a time period, etc. E.g. fraction of forum threads without an answer (in time period ranging from one week to one month before the date of data collection) on OOFEM's forum was 40% which is quite high if compared with that of 20% on OpenFOAM's forum [3], which definitely must be taken into account if this is the only support a user can rely on.

The next assessment measure for an open-source project is activity of its developers. It can be carried out very easily if the project is located on Github, Bitbucket or a similar service. Some of the measures are number of commits in a time period, number of active forks, etc. [3] E.g. the number of commits to OOFEM's repository on Github was 9 (in a 30-days period prior to the date of data collection) while that of another FEA software called FreeFEM was 92 (these and other data can be found in [3]). They show that FreeFEM's developers' community is more active or, at least, that it was more active in the surveyed period. Additionally, one should take care of these measures even in a longer time perspective because if a project dies out, no new code is developed. This is especially important if one just wants to use the software (and not to develop it) because, without an active developers' community, the software can become unusable due to bugs that are not fixed, lack of adaptability to new operating systems or their new features, etc.

The last set of assessment criteria is related to programming language(s) and design of code architecture. Most of open-source FEA software developed in last two or three decades has been written in C++ programming language. However, older software (e.g. Code Aster) could be written in Fortran. This is of less importance today as Fortran now enables object-oriented programming paradigm, but it may represent an obstacle if a user does not have time to spend on learning a new programming language.

```
for ( GaussPoint *gp : * iRule ) {
    this->computeBmatrixAt(gp, bi, iStartIndx, iEndIndx);
    this->computeConstitutiveMatrixAt(d, rMode, gp, tStep);
    dij.beSubMatrixOf(d, iStartIndx, iEndIndx, jStartIndx, jEndIndx);
    if ( i != j ) {
        this->computeBmatrixAt(gp, bj, jStartIndx, jEndIndx);
    } else {
        bj = bi;
    }

    dV  = this->computeVolumeAround(gp);
    dbj.beProductOf(dij, bj);
    if ( matStiffSymmFlag ) {
        answer.plusProductSymmUpper(bi, dbj, dV);
    } else {
        answer.plusProductUnsym(bi, dbj, dV);
    }
}
```

Figure 1 *Equation mimicking demonstrated on a code snippet from OOFEM*
Slika 1 Tehnika oponašanja jednadžbi prikazana na komadu kôda iz OOOFEM-a

Beside the programming language, design of software's code architecture is of paramount importance when choosing software that one plans to change or upgrade because it contributes to software's extensibility and maintainability as will be demonstrated. In our case, as already mentioned, it is necessary to add new FEs to OOFEM's existing library of FEs and it represents a prime example of software's extension. Once a new code is written, chances are that some

errors (bugs) will occur and they will have to be fixed. This is what is meant by maintainability. Both the enhanced maintainability and extensibility are supported by greater readability of OO code versus procedural code. For engineering software this is best demonstrated by the equation mimicking [4]. Figure 1 shows a code snippet from OOFEM that calculates stiffness matrix of a FE. It can be easily understood even by someone who cannot program because portions of code that execute a sequence of operations that together lead to a desired result are grouped within a method (e.g. instead of seeing a number of operations with hard-to-understand names, a method for computation of strain – displacement matrix **B**, named *computeBmatrixAt*, literally explains what is done and what result to expect). Furthermore, not only methods but also data that methods need in order to execute correctly are packed together in an object. This concept in OO programming is called encapsulation. It facilitates readability of code because it is close to way people see things and not computers or, as [5] states, "object-oriented thinking lends itself to an anthropomorphic view of objects".

Methods (operations) and attributes (data) of an object can be accessible either only from within the object or from other objects as well. Those who belong to the former make up object's implementation while the latter belong to object's interface. Concept of class's (or object's) interfaces is an important one because they represent a means of communication between objects. Because objects communicate only through their interfaces, deciding what goes to an interface and what stays in the implementation is very important. When something changes in object's interface, all other objects that use the changed method or attribute must adopt the same changes (e.g. if a list of parameters of a method changes, all methods of other objects that invoke the changed method will have to adapt). Thus, we try to keep interfaces to a minimum [6]. On the other hand, this enables us to change method's implementation and, if the interface remains the same, nothing needs to be changed in related objects. This greatly contributes to code's maintainability.

Another great benefit of OO programming is code reuse, which also enhances software extensibility. This is supported primarily through inheritance, polymorphism and composition, all being important OO concepts. Inheritance enables one object to inherit methods and attributes of another object which means that they do not have to be re-written when a new class is created. Inheritance is not limited to only one child class (or subclass), which can lead to creation of large class hierarchies typical for object-oriented code. Polymorphism is related to different implementations of a method inherited from a superclass (parent class) in subclasses (child classes). This is primarily used for defining common interfaces. More on all of these concepts can be found in [5] and [6]. Later, in Chapter 3, we shall demonstrate their use on examples from OOFEM.

3. Description of some OOFEM characteristics

OOFEM is OSS for calculations in structural mechanics, fluid dynamics and thermodynamics based on the finite element method (FEM). It is published under GNU Lesser General Public License. Its code architecture is OO and written in C++ programming language. It is developed to be easily extensible, modular (to support teamwork), maintainable, portable over available platforms (Linux and Windows) and its computational performance similar to programs written in C and Fortran [7]. It supports parallel execution and comprises interfaces between many mesh generators, FEM solvers, etc.

In this chapter, we shall describe fundamental classes of OOFEM and show how a new FE can be added to the existing OOFEM library of FEs. This will also demonstrate the way in which concepts of OO programming briefly explained in the foregoing chapter are realised in practice and benefits we can whence derive.

3.1. *Fundamental classes of OOFEM*

Fundamental classes of OOFEM are associated with basic building blocks of the FEM, formulation of the problem and its solution. There are 5 fundamental classes of OOFEM: *Domain*, *FEMComponent*, *EngngModel*, *NumericalMethod* and *SparseMtrx*.

FEMComponent class is a basic abstract class for all components that define physical problem solved by means of the FEM (frames 2 and 3 in Figure 2), which include: FEs (class *Element*) and their cross-sections (class *CrossSection*), boundaries associated with DOFs (class *DofManager*), boundary (class *GeneralBoundaryCondition*) and initial conditions (class *InitialCondition*) and materials (class *Material*).

Meaning of *DofManager* class might be confusing at first so we shall explain it. This class is a basic abstract class for element boundaries that have degrees-of-freedom (DOF) associated with them. For almost all FEs used in ship structural analysis these are simply nodes. However, some FEs can have DOFs associated with e.g. their sides and this is the reason why the basic class of an entity that "manages" DOFs associated with a FE is not a node. Hierarchy of classes related to *DofManager* class can be seen in Figure 3.

We shall now take a closer look at classes denoted by the grey colour in Figure 2. These classes provide a way to obtain solution to the problem formulated by classes in frames 2 and 3. *Domain* class contains information about all building blocks of the FEM: elements, cross-sections, DOFs, etc. If the program runs on multiple threads, it has multiple *Domain* objects. *EngngModel* class represents a finite element analysis (called engineering model). We might say that if *Domain* knows everything about the problem, *EngngModel* knows what to do with it. Figure 4 shows partial UML diagram of *EngngModel* class and its subclasses. The subclasses are related to particular problems and solutions, e.g. structural, fluid, linear, nonlinear, etc. *EngngModel* interacts, on one hand, with *Domain* object(s) that gives it access to problem's description and, on the other hand, with classes used for storing global stiffness matrix and solving the problem. This way, the analysis, the storage and the solution (solver) are made independent of each other as they indeed are. The analysis primarily takes care of physical meaning of the elements, DOFs, boundary conditions, etc. and it needs to formulate the problem based on data provided by the *Domain*. The solver depends only on mathematical characteristics of the system it needs to solve while the storage can be of any relevant matrix storage format bearing in mind only that certain combinations of matrix storage formats and solvers are more efficient than others [8]. Such code architecture adds on an easier implementation of new solvers or matrix storage formats without having to change anything in *EngngModel*. This is one of the powerful features of OO programming that will be more dealt with in the following subchapter.
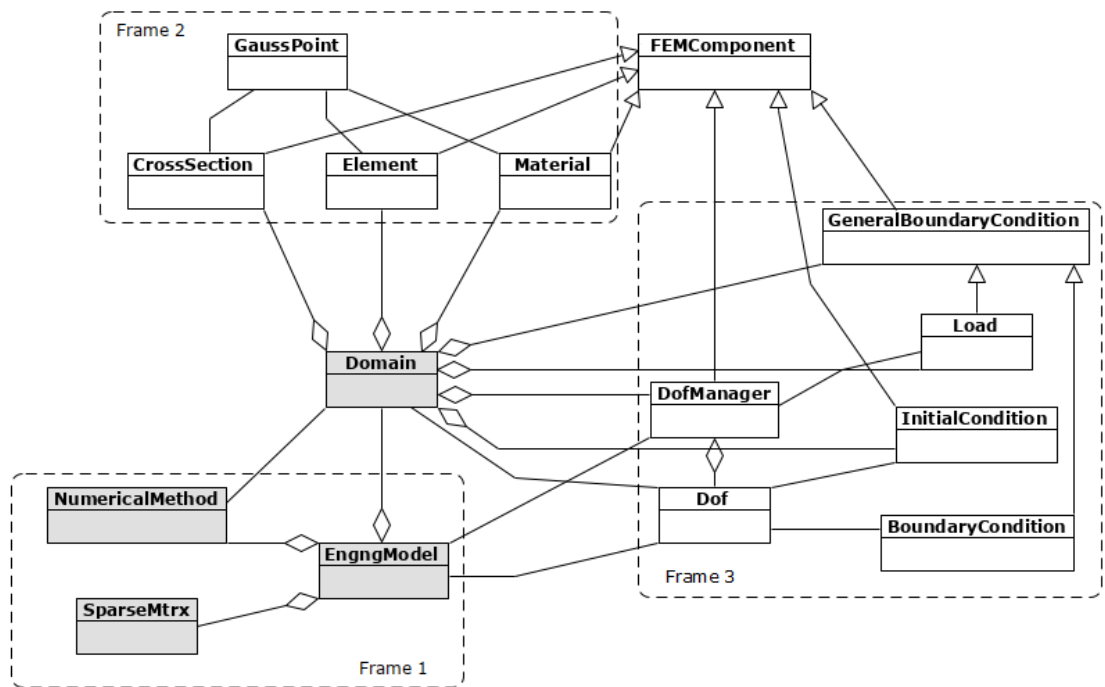
Figure 2 *UML diagram of fundamental classes of OOFEM*
Slika 2 UML dijagram temeljnih klasa OOFEM-a
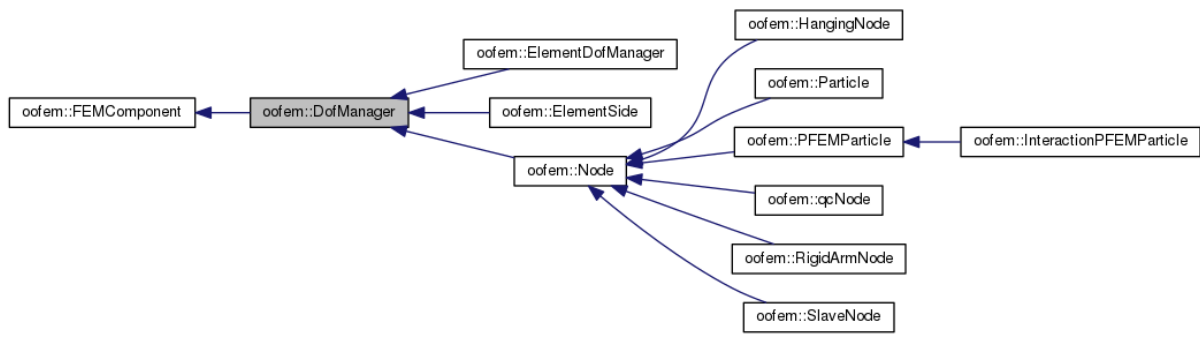
Figure 3 *Hierarchy of classes associated with* DOFManager *class*
Slika 3 Hijerarhija klasa povezana s klasom *DOFManager*

EngngModel

-ndomains : int
-numberOfSteps : int
-numberOfEquations : int
-renumberFlag : boolean

+EngngModel(i : int, _master : EngngModel* = NULL)
+~EngngModel()
+giveDomain(n : int) : Domain2*
+setDomain(i : int, ptr : Domain2*, iDeallocateOld : boolean = true) : void
+giveNumberOfDomains() : int
+setNumberOfEquations(id : int, neq : int) : void
+giveOutputStream() : FILE*
+terminateAnalysis() : void
+solveYourself() : void
+solveYourselfAt(tStep : TimeStep*)
+terminate(tStep : TimeStep*)
+initializeYourself(tStep : TimeStep*) : void
+giveNumberOfDomainEquations(di : int, num : UnknownNumberingScheme&) : int
+instanciateYourself(dr : DataReader&, ir : InputRecord&, outFileName : char*, desc : char*) : int
+saveContext(stream : DataStream&, mode : ContextMode) : void
+updateSolution(solutionVector : FloatArray&, tStep : TimeStep*, d : Domain2*) : void
+updateMatrix(mat : SparseMtrx&, tStep : TimeStep*, d : Domain2*) : void
+forceEquationNumbering() : int
+assemble(answer : SparseMtrx&, tStep : TimeStep*, ma : MatrixAssembler&, s : UnknownNumberingScheme&, domain : Domain2*) : void
+assembleVector(answer : FloatArray&, tStep : TimeStep*, va : VectorAssembler&, mode : ValueModeType, s : UnknownNumberingScheme&, domain : Domain2*, eNorms : FloatArray* = NULL) : v...
+outputNodes(file : FILE*, domain : Domain2&, tStep : TimeStep*, setNum : int) : void
+outputElements(file : FILE*, domain : Domain2&, tStep : TimeStep*, setNum : int) : void

StructuralEngngModel   StationaryTransportProblem   FluidModel   StaggeredProblem   TransientTransportProblem

NonLinearDynamic   StaticStructural   LinearStatic   LinearStability   CBS   StokesFlow   SUPG   FluidStructureProblem

Figure 4 *UML diagram of partial hierarchy of classes associated with* EngngModel *class*
Slika 4 UML dijagram djelomične hijerarhije klasa povezanih s klasom *EngngModel*

3.2. Extending OOFEM's library of FEs

Class hierarchy of FEs available in OOFEM begins with *FEMComponent* class mentioned in the foregoing subchapter. This class, common to FEs, materials, boundary and initial conditions, etc., declares methods and attributes common to all of them. Naturally, a set of those is rather small. If we take a look at UML diagram in Figure 5, we shall see that there are methods such as *initializeFrom* for entity's initialization based on input record data (input file), *checkConsistency* that checks some important properties of an entity before it is used by another object, methods for printing entity's data, etc. It can also be seen that most methods in this class are written in italics. Italic typeface denotes abstract (or virtual) classes according to the UML 2.0 standard. This means that no implementation is provided for these methods here; they are used only to define a common interface while their implementation is provided in child classes (subclasses) by making use of OO programming's concept of polymorphism.

FEMComponent

#number : int
#domain : Domain*

+FEMComponent(n : int, d : Domain*)
+~FEMComponent()
+giveNumber() : int
+setNumber(num : int) : void
+initializeFrom(ir : InputRecord&) : void
+giveInputRecord(input : DynamicInputRecord&) : void
+saveContext(stream : DataStream&, mode : ContextMode) : void
+restoreContext(stream : DataStream&, mode : ContextMode) : void
+printOutputAt(file : FILE*, tStep : TimeStep*) : void
+printYourself() : void
+checkConsistency() : int

Element

#numberOfDofMans : int
#dofManArray : IntArray
#material : int
#crossSection : int
#bodyLoadArray : IntArray
#boundaryLoadArray : IntArray
#globalNumber : int
#numberOfGaussPoints : int

+Element(n : int, aDomain : Domain*)
+~Element()
+giveLocationArray(locationArray : IntArray&, s : UnknownNumberingScheme&, dofIds : IntArray* = NULL) : void
+giveNumberOfNodes() : int
+giveCharacteristicMatrix(answer : FloatMatrix&, type : CharType, tStep : TimeStep*) : void
+giveCharacteristicVector(answer : FloatArray, type : CharType, mode : ValueModeType, tStep : TimeStep*) : void
+computeLoadVector(answer : FloatArray&, load : BodyLoad*, type : CharType, mode : ValueModeType, tStep : TimeStep*) : void
+computeOfPrimaryMasterDofs() : int
+giveRotationMatrix(answer : FloatMatrix&) : boolean
+computeVolumeAround(gp : GaussPoint*) : double
+computeVolume() : double
+computeArea() : double
+computeLength() : double
+giveDofManager(i : int) : DofManager*
+giveMaterialMode() : MaterialMode
+checkConsistency() : int
+giveIntegrationRule(i : int) : IntegrationRule*
+computeNumberOfDofs() : int
#computeGaussPoints() : void

StructuralElement

+StructuralElement(n : int, d : Domain*)
+~StructuralElement()
+giveCharacteristicMatrix(answer : FloatMatrix&, type : CharType, tStep : TimeStep*) : void
+giveCharacteristicVector(answer : FloatArray&, type : CharType, mode : ValueModeType, tStep : TimeStep*) : void
+computeMassMatrix(answer : FloatMatrix&, tStep : TimeStep*) : void
+computeStiffnessMatrix(answer : FloatMatrix&, rMode : MatResponseMode, tStep : TimeStep*) : void
+giveInternalForcesVector(answer : FloatArray&, tStep : TimeStep*, useUpdatedGpRecord : int = 0) : void
+computeStrainVector(answer : FloatArray&, gp : GaussPoint*, tStep : TimeStep*) : void
+checkConsistency() : int
+computeLoadVector(answer : FloatArray&, load : BodyLoad*, type : CharType, mode : ValueModeType, tStep : TimeStep*) : void
+computeConstitutiveMatrxAt(answer : FloatMatrix&, rMode : MatResponseMode, gp : GaussPoint*, tStep : TimeStep*) : void
+giveStructuralCrossSection() : StructuralCrossSection*
+computeStressVector(answer : FloatArray&, strain : FloatArray&, gp : GaussPoint*, tStep : TimeStep*) : void
+computeBmatrixAt(gp : GaussPoint*, answer : FloatMatrix&, lowerIndx : int = 1, upperIndx : int = ALL_STRAINS) : void
+computeNmatrixAt(iLocCoord : FloatArray*, answer : FloatMatrix&) : void

NLStructuralElement

#nlGeometry : int

+NLStructuralElement(n : int, d : Domain*)
+~NLStructuralElement()
+giveGeometryMode() : int
+computeFirstPKStressVector(answer : FloatArray&, gp : GaussPoint*, tStep : TimeStep*) : void
+computeCauchyStressVector(answer : FloatArray&, gp : GaussPoint*, tStep : TimeStep*) : void
+computeStiffnessMatrix(answer : FloatMatrix&, rMode : MatResponseMode, tStep : TimeStep*) : void
+giveInternalForcesVector(answer : FloatArray&, tStep : TimeStep*, useUpdatedGpRecord : int = 0) : void
+computeDeformationGradientVector(answer : FloatArray&, gp : GaussPoint*, tStep : TimeStep*) : void
#checkConsistency() : int

FMElement

TransportElement

Truss1d

SpringElement

BeamBaseElement

Structural3DElement

Quad1Mindlin

Structural2DElement

AxisymElement

PlaneStrainElement

MITC4Shell

#interp_lin : FEI2dQuadLin
#GtoLRotationMatrix : FloatMatrix<3, 3>
#drillCoeff : double = 0.

+MITC4Shell(n : int, d : Domain*)
#computeGaussPoint() : void
#computeStiffnessMatrix(answer : FloatMatrix&, rMode : MatResponseMode, tStep : TimeStep*) : void
#computeBmatrixAt(gp : GaussPoint*, answer : FloatMatrix&) : void
#computeNmatrixAt(iLocCoord : FloatArray&, answer : FloatMatrix&) : void
#computeConstitutiveMatrixAt(answer : FloatMatrix&, rMode : MatResponseMode, gp : GaussPoint*, tStep : Ti...
#computeStressVector(answer : FloatArray&, strain : FloatArray&, gp : GaussPoint*, tStep : TimeStep*) : void
-giveDirectorVectors() : array<FloatArrayF<3>, 4>
-giveThickness() : array<double, 4>
-giveMidplaneIPValue(gpXY : int, type : InternalStateType, tStep : TimeStep*) : FloatArray

PlaneStressElement

+PlaneStressElement(n : int, d : Doma...
+~PlaneStressElement()
+giveMaterialMode() : MaterialMode
+computeStressVector(answer : Float...
+computeConstitutiveMatrixAt(answer...
#computeBmatrixAt(gp : GaussPoint*,...

Figure 5 *UML diagram of partial hierarchy of classes associated with* FEMComponent *class*
    Slika 5 UML dijagram djelomične hijerarhije klasa povezanih s klasom *FEMComponent*

Going down the class hierarchy of Figure 5 we come to *Element* class. This class represents a FE no matter if it is employed in structural analysis, fluid mechanics (*FMElement*), thermodynamics (*TransportElement*) or any other field where the FEM is used to solve governing equations. Thus, the *Element* class declares only those attributes and methods that are common to all the FEs: *giveNumberOfNodes*, *computeVolume*, *computeArea*, *computeNumberOfDofs*, etc. For example, calculation of element's stiffness matrix is declared only in one of *Element*'s child classes, namely *StructuralElement* class. What would happen if, e.g., *computeStiffnessMatrix* were declared at *Element* class's level or *computeVolume* at *StructuralElement*'s level? The former would mean that all child classes of *Element* class inherit it. So, a *FMElement* would have a *computeStiffnessMatrix* method that it, obviously, does not need and it would only be a burden on computer's memory and would hinder code's readability and thus maintainability. If the latter were true, then *computeVolume* would have to be rewritten in all classes at the same hierarchical level, i.e. *FMElement*, *TransportElement*, etc. This would hinder code reuse, a benefit of OO programming that we have discussed. Thus, we can argue that one of the most delicate decisions when designing software's code architecture by applying OO paradigm is to find a right place in class hierarchy for each attribute and method because the opposite cancels out benefits of OO programming.

Going further down the hierarchy tree, we come to *StructuralElement* class which represents a base class for all FEs used in structural analysis (linear, non-linear, static, dynamic…). It declares methods for typical operations encountered in solid mechanics when the FEM is used: *computeMassMatrix*, *computeStiffnessMatrix*, *computeLoadVector*, *computeConstitutiveMatrixAt*, etc. It can be seen that the aforementioned method *computeStiffnessMatrix* is declared as abstract at this level and is implemented in subsequent classes (e.g. *NLStructuralElement*). The reason why it is declared at this level lies in fact that all FEs used in structural mechanics have a stiffness matrix. Thus, it is sensible to provide a common interface here. However, because the stiffness matrix is not calculated in the same manner for all structural FEs, the implementation of the method is left for lower classes, e.g. we can see that the implementation is provided within *NLStructuralElement* class.

NLStructuralElement class is a parent class for all 2D and 3D elements (e.g. plate and shell elements) whose stiffness matrices are calculated as $\int_{V^e} \boldsymbol{B}^T \boldsymbol{D} \boldsymbol{B}\, \mathrm{d}V$ (where $\boldsymbol{B}$ is the strain-displacement matrix, $\boldsymbol{D}$ is the constitutive matrix and V^e is FE's volume). In case of some minor departures from this procedure, the method can be overridden in *NLStructuralElement*'s child classes as it is the case with MITC4 FE.

Classes at the lowest level in the hierarchy of *NLStructuralElement* are related to concrete membrane (e.g. *PlaneStressElement*, *PlaneStrainElement*…), shell and plate (e.g. *MITC4Shell*, *Quad1Mindlin*…) and 3D (*Structural3DElement*) elements. Some methods appear for the first time only at this level, e.g. *computeBmatrixAt*. Again, in order to understand why this level is a right level for the foregoing method, we need to think about which elements calculate the strain-displacement matrix $\boldsymbol{B}$ in the same way (e.g. calculation of $\boldsymbol{B}$ matrix for a plate element differs from that of a plane stress element because it depends on assumptions given by the chosen plate theory). All of these examples demonstrate benefits of using OO programming concepts of inheritance and polymorphism. An underlying concept of encapsulation enables creation of all

307

these classes in the first place. A bit less obvious is use of composition which we shall not go into here (see more in [5] and [6]).

We have mentioned that two objects communicate with each other over their interfaces. We have also said that all attributes and methods declared as public of an object make up object's interface. There are a few benefits of such an approach. One of the main benefits is that when something changes within one object, it can still be accessed by other object(s) if its interface remains the same. This greatly contributes to the maintainability of the code because a developer changes only what is relevant not having to go through large portions of code to check whether something else must be changed too.

Let's consider the following example. There are two methods, one within an *EngngModel* object that solves the governing equations (e.g. *solveYourself* in Figure 4) and the other one that computes and returns FE's stresses (*computeStressVector*). During solution of the problem, the *EngngModel* method invokes *computeStressVector* of a FE used in the analysis. As we can see in Figure 5 *computeStressVector* is declared as public (little plus sign next to it) in *StructuralElement* class, which means that it belongs to *StructuralElement*'s interface, and therefore it can be seen and accessed from a method that belongs to another object. It can also be seen that it is declared as abstract (italic typeface) and that it is inherited by *StructuralElement*'s subclasses where it retains the same name, return type and a list of parameters, which means that the interface remains the same for all "structural FEs" (child classes of *StructuralElement*). Thus, when the *EngngModel*'s method wants to know stresses of any *StructuralElement*, it literally uses the same call (the same code). If we had different formats of *computeStressVector* for each element, different call code would be needed in the *EngngModel*'s method. Also, when we change way of stresses' calculation for an existing FE or when we add a new FE, nothing needs to be changed in the calling method (that of *EngngModel* in this example) as long as it inherits the *StructuralElement*'s method *computeStressVector*. This adds to code maintainability tremendously because the programmer does not have to make changes in all other calling methods too. The whole process is facilitated by declaring general interfaces by means of abstract methods whose implementation is provided in subclasses, which represents a prime example of using inheritance and polymorphism in practice.

4. FEA software in ship structural design

FEA software is of vital importance in direct ship structural analysis based on the FEM. Furthermore, the ship structural analysis is a part of ship structural design process. In this process, the structural analysis' software interacts with other software such as software for structural evaluation, definition of structural loads, structural optimisation, etc. The structural evaluation software incorporates CSs rules and is used for determination of structural adequacy. Examples of structural evaluation software can be found in [9], where Lloyd's Register's rules pertinent to structural design of RoRo ships are implemented in software employed in structural design and analysis of a livestock carrier, and [10], where Common Structural Rules (CSR) of International Association of Classification Societies (IACS) and Bureau Veritas's rules are implemented in software used in the rational structural design of a bulk carrier (see Figure 6 and Figure 7). The latter also implements an optimisation algorithm that seeks to determine an optimum structure based on sequential linear programming method. In the foregoing studies, FEA software called MAESTRO (more on MAESTRO can be found in [1]) was used. Since the researchers did not have access to its source-code, they were limited in selection of sensitivity

analysis methods used for structural optimisation [10]. If they had had access to the source-code of the FEA software, they would have been able to implement a, possibly, more efficient method as explained in [3]. Thus, we can argue that use of open-source FEA software within the rational ship structural design brings additional benefits, beside those present when only structural analysis is considered. This subject is dealt with in more details in [3].

While FEAs of ship structures were carried out only occasionally in the past, they have been made mandatory for many ship types since the advent of CSR by the IACS which, e.g., require direct strength analysis of ship's structure by means of the FEM for all bulk carriers and tankers whose length is 150 m or more [11]. Furthermore, DNVGL [12] requires FEA for container vessels, ro-ro and car carriers, large cruise vessels (L > 150 m), etc. Additionally, FEA is required in case of novel designs of ship structures or structural elements, for fatigue and buckling assessment, etc. For these reasons, CSs have come up with a set of criteria for FEAs of ship structures that we touch on in the sequel, following their description as given in [12].
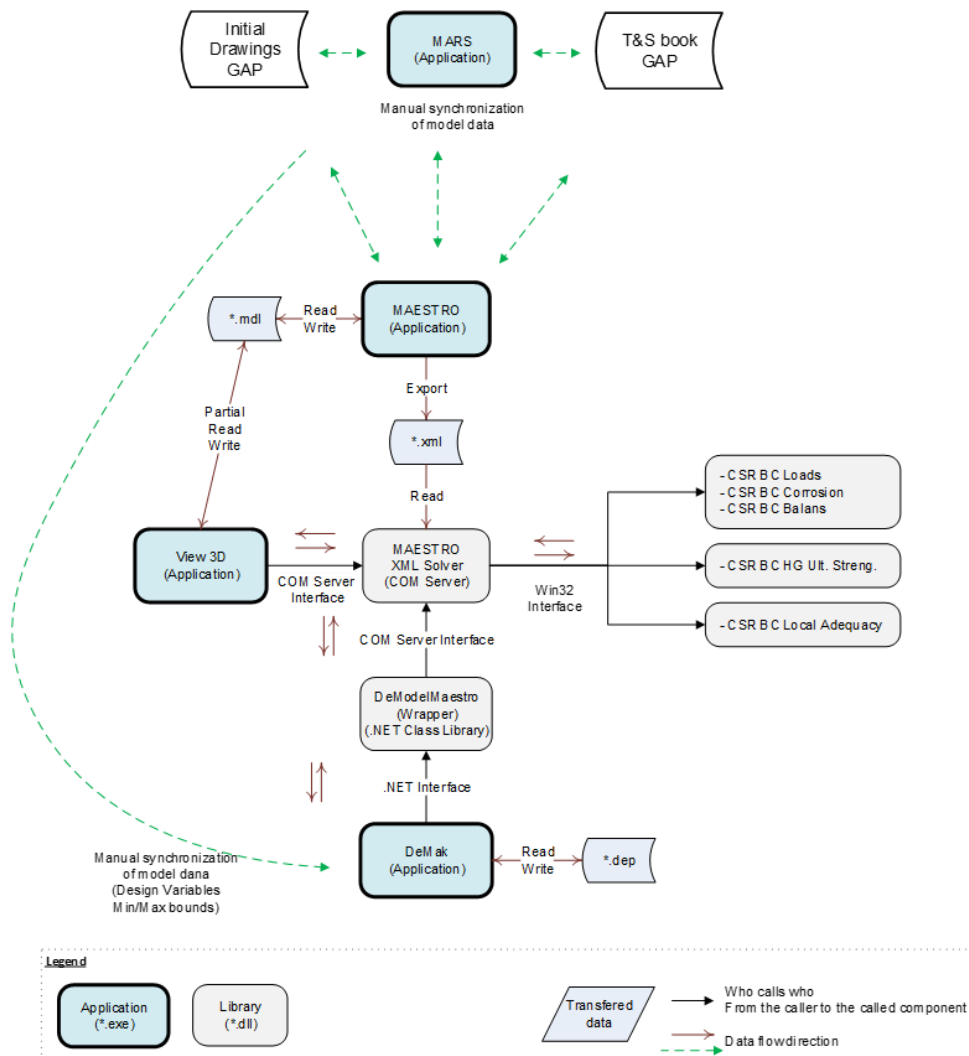
Figure 6 *Structural analysis' software (MAESTRO in the example from [10]) within the rational ship structural design*
Slika 6 Softver za analizu konstrukcije (MAESTRO u primjeru iz [10]) unutar racionalnog projektiranja brodske konstrukcije

From CS's point of view "any recognised software can be used provided that all specifications on mesh size, element type, boundary conditions, etc. can be achieved with this computer program" [12]. A FEA software must comprise following FEs: rod (truss) elements, beam elements, membrane elements and shell elements [12]. CSs requirements on these FEs can be found in Table 1.

Beside FEs, there are requirements on loads and boundary conditions as well. FEA software must support following load types: point (concentrated), pressure (distributed) and body (e.g. gravitational and inertial forces) loads. A user must be able to specify three forces (one force in direction of each axis) and three moments (one moment about each axis) in every grid point [12]. Furthermore, he must be able to define different load combinations that act simultaneously on ship's structure called load cases.

The supported boundary conditions must include fixed (clamped) and pinned ends as well as combinations of constrained translations and rotations. Special boundary conditions including rigid links and end-beams should also be available [12].

All element types, reactions in boundary conditions, shear, in-plane, axial and von Mises stress should be available for analysis' report [12]. Moreover, a user should have a possibility to see compliance of analysis' results with design criteria including plate and stiffened panel buckling analysis [12].

Based on the foregoing CSs requirements, it is possible to assess OOFEM's capabilities at time before any upgrades to its code are made. This is very important, as demonstrated in Chapter 2, because it determines an amount of work that needs to be invested before software is ready for use in ship structural analysis. Additional requirements may come from one's research interests where FEA software may be only a part of a broader set of tools as described in [3]. However, we shall make a brief assessment only w.r.t CSs requirements mentioned above.
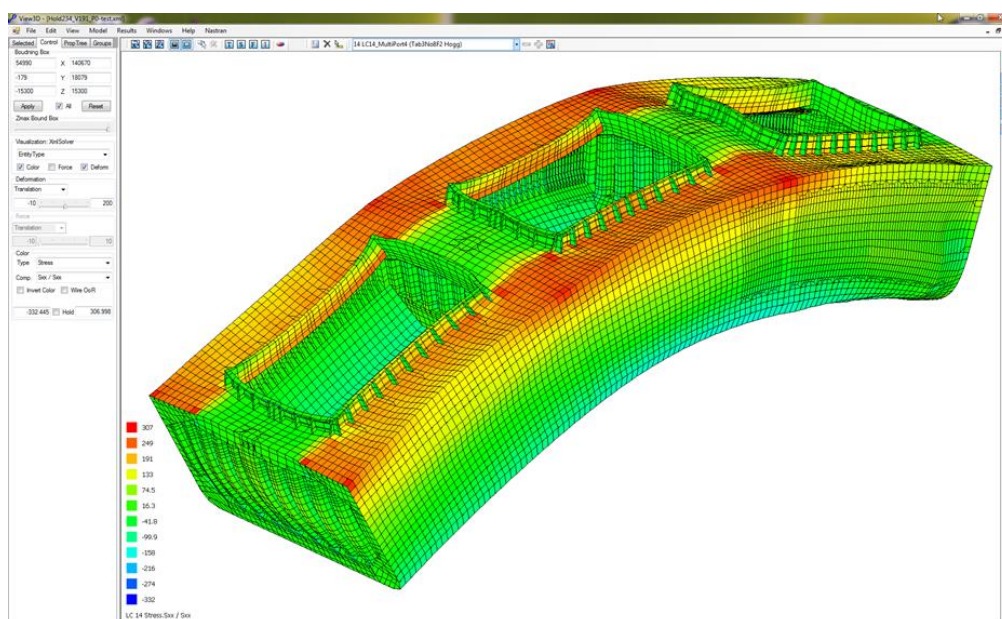
Figure 7 *Structural response of a three-cargo hold FE model of bulk carrier described in [10] from visualisation software View3D based on analysis' results imported from FEA software*
Slika 7 Odziv konstrukcije MKE modela tri skladišta broda za prijevoz rasutog tereta opisanog u [10] iz softvera za vizualizaciju View3D prema rezultatima analize uvezenima iz MKE softvera

As explained in [13], regarding boundary conditions and load cases, we have not found any deficiencies w.r.t CSs requirements. When it comes to loads, OOFEM can model both concentrated and distributed loads. However, distributed loads are evaluated by means of numerical integration of the load vector (see more in [14]). In many engineering applications, distributed loads are modelled by equal distribution to all nodes ("intuitively" as termed in [14]). In our examples, this is probably not a major difference because CSs usually regard distributed loads as equally distributed, but it might be different from something that a user has got used on. So, we plan to implement such a definition of distributed loads.

Most of the additional work will probably go into extension of OOFEM's library of FEs because no satisfactory membrane and plate/shell FE was found in OOFEM. When we started to use OOFEM, it comprised, as explained in [3], the following 4-node quadrilateral membrane, plate and shell elements (terminology according to [15]) of interest in the analysis of thin-walled structures: PlaneStress2d, QdktPlate and MITC4Shell. We conducted a series of simple tests with these FEs and their properties were found to be unsatisfactory [13]. Thus, our plan is to implement membrane and plate/shell FEs whose properties are close to properties of similar FEs in commercial software widely used in ship structural analysis (e.g. Nastran and Ansys). Furthermore, it is necessary to implement a beam FE based on Euler-Bernoulli beam theory and to change the way beam FEs are described in OOFEM, namely instead of asking a user to provide beam's cross-sectional properties directly (area, moments of inertia, etc.), he will specify characteristic dimensions of beam's cross-section while the properties will be calculated by a software procedure.

Table 1 CSs requirements on FEs used in ship structural analysis (according to [12])

Tablica 1 Zahtjevi klasifikacijskih društava prema konačnim elementima koji se upotrebljavaju u analizi brodskih konstrukcija (prema [12])

Finite element	Characteristics	Remarks
Rod (truss)	1D; axial stiffness; constant cross-section along length	N/A
Beam	1D; axial, torsional and bi-directional shear and bending stiffness; constant cross-sectional properties along length	
Membrane	2D; bi-axial and in-plane stiffness; constant thickness	Inner angles between 45° and 135°; aspect ratio close to 1 (never to exceed 3 for 4-node and 5 for 8-node FEs); shape functions should include "incompatible modes"; use of triangular elements should be avoided; assessment based on membrane (in-plane) stresses
Shell	2D; in-plane (membrane) and out-of-plane (bending) stiffness; constant thickness	

5. Conclusion

In this paper we deal with benefits and challenges of open-source software (OSS) from point of view of ship structural analysis. It is emphasized that OSS is rarely totally free. Activity of users' community and software developers associated with an OSS project is of paramount importance

for future work on the software. Some measures that can help in assessing these are proposed. Moreover, code architecture of prospective OSS is important. In this regard, we take a closer look on object-oriented (OO) programming paradigm. It is shown that it contributes greatly to readability and reusability of the code, which enhances software's extensibility and maintainability. This is all demonstrated on examples from OOFEM.

OOFEM, OSS for FEA, is described, its fundamental classes and their interactions as well as its code structure related to classes that describe FEs. At the end, we touch on role and position of structural analysis within ship structural design process and go through the most important requirements of CSs on FEAs and then use them to assess capabilities of OOFEM at its initial state, i.e. before any changes are made to the code from our side.

REFERENCES

[1]   Hughes OF, Paik JK. Ship Structural Analysis and Design. New Jersey: SNAME; 2010.

[2]   Committee IV.2 Design methods. In: Kaminski, ML, Rigo, P, editors. Proceedings of the 20th International Ship and Offshore Structures Congress (ISSC 2018), Amsterdam: IOS Press, 2018.

[3]   Palaversa, M, Prebeg, P, Andric, J. Opportunities of Using Open-Source FEA Software in Ship Structural Design. In: Bertram, V, editor. 19th Conference on Computer Applications and Information Technology in the Maritime Industries – COMPIT '20; Pontignano, Italy, 17.8.-19.8.2020. Hamburg: TUHH; 2020 [in print]

[4]   Chen, G, Xiong, Q, Morris, PJ, Paterson, EG, Sergeev, A, Wang, Y-C. OpenFOAM for Computational Fluid Dynamics. Notices of the AMS, 2014 Apr; 61(4): 354-63.

[5]   Rouson, D, Xia, J, Xu, X. Scientific Software Design: The Object-Oriented Way. New York: Cambridge University Press; 2011.

[6]   Weisfeld, M. The Object-Oriented Thought Process. 4th ed. Boston: Addison-Wesley; 2013.

[7]   Patzak, B, Bittnar, Z. Design of object-oriented finite element code. Advances in Engineering Software. 2001; 32: 759-67.

[8]   Nguyen, DT. Parallel-Vector Equation Solvers for Finite Element Engineering Applications. New York: Springer SBM; 2002.

[9]   Andric, J, Piric, K, Prebeg, P, Andrisic, J, Dmitrasinovic, A. Structural design and analysis of a large 'open type' livestock carrier. Ships and Offshore Structures, 2018; 13 (S1): 167-81.

[10]   Andric, J, Prebeg, P, Andrisic, J, Zanic, V. Structural optimisation of a bulk carrier according to IACS CSR-BC. Ships and Offshore Structures. 2018; 15(2): 123 – 37.

[11]   Common Structural Rules for Bulk Carriers and Oil Tankers. London: IACS; 2018.

[12]   DNVGL-CG-0127 Finite element analysis. Hovik: DNVGL; 2015.

[13]   Palaversa, M, Prebeg, P, Andrić, J. REMAKE Project Deliverable 2.1 - Definition of Requirements for OOFEM Upgrade, Zagreb: University of Zagreb, Faculty of Mechanical Engineering and Naval Architecture; 2019.

[14]   MacNeal, RH. Finite Elements: Their Design and Performance. New York: Marcel Dekker; 1994.

[15]   Patzak, B. OOFEM Element Library Manual [Internet]. Prague: CTU; 2018 [cited 2019 March]. 62 p. Available from: http://www.oofem.org/resources/doc/elementlibmanual/elementlibmanual.pdf

How the *Digital Revolution* could affect the shipbuilding world

Pérez Fernández, Rodrigo; *SENER; rodrigo.perez@sener.es*

Toman, Mirko; *SENER; mirko.toman@sener.es*

ABSTRACT

The marine structures are developed with *Computer Aided Design* (CAD) tools, but every day we are looking for integrated development of the product involving all its Life Cycle.

If all the equipment items and other components of the vessel are designed considering the *Internet of Things* (*IoT*), the shipbuilding Industry will have technology that allows to share their situation, diagnosis, functionality…The *CAD* system could use this information for knowing whether they are working properly or if its performance could be improved. It is also possible to identify whether it is necessary to make maintenance of the object, or if it is necessary to replace it because its life ends, or because it´s working wrongly. It will also be possible to know how their performance affects the functioning of the whole product, the ship or boat.

The growth of the *IoT* is linked to the increase of information and the management of *Big Data*, with the property that somehow *IoT* identifies information to a specific purpose, while the concept of *Big Data* is more generic. The possibilities are countless, but the beginning must be in the initial design. It is necessary to consider what is needed to correctly fulfil the mission of each of the elements. These requirements must be configurable in the initial design from where it will be extended to relations between each of them with other entities. *CAD* is one of the first steps, because it is where begins to collect systematically the concept of each component.

Key words: *Digital Transformation; IoT; shipbuilding CAD; Big Data; Industry 4.0. Open Source.*

1. STATE OF THE ART

Today the *Digital Revolution*[5] in shipbuilding, like in any other industry, is mostly apply to improve five main areas: performance, flexibility, productivity, supply chain and customization.

---

[5] *The Digital Revolution is the shift from mechanical and analogue electronic technology to digital electronics which began anywhere from the late 1950s to the late 1970s with the adoption and proliferation of digital computers and digital record keeping that continues to the present day. Implicitly, the term also refers to the sweeping changes brought about by digital computing and communication technology during (and after) the latter half of the 20th century. Analogous to the Agricultural Revolution and Industrial Revolution, the Digital Revolution marked the beginning of the Information Age.* [33]

The process is not *new* nevertheless what is new is the huge momentum that the industry is taking thanks to the fast evolution of internet, the *IoT*[6] and the *Digital Transformation*[7] that push the traditional scope of the Shipbuilding beyond its traditional limits and bringing new business opportunities with new processes, services and products based on these technological enhancements.

We may say that the *Shipbuilding Digital Revolution* started more than *50* years ago with the *Enterprise Resources Planning* (ERP) when its main task was to calculate the salaries of the several thousands of workers (earliest 1960s). It was soon followed by the *Computer Aided Design* (CAD) and *Manufacture* (CAM) together with the *Product Data Management* (PDM) (mid 1960s), lately evolved at what is known as *Product Life Cycle* (*PLM*).

More recently, the *PLM* introduced the concept of *Digital Twin*, initially just for products (*Product Digital Twin*) and then extended and include production facilities, processes and the whole Shipyard (*Digital Twin Production*).

Those *Digital Twins* may also include what we may call *Digital Twin Performance* online connected (or not) with their *Digital Twins* and capable to simulate, train or show operational processes and physics. In some cases, the *Digital Twin Performance* may run under simplified version of its real counterparts, like diagrams and dashboard that keep tracking of real equipment, systems and services or immersed in a very sophisticated emulation of the *3D world* by means of *Virtual Reality* and *Augmented Reality*.

In all these different solutions, the introduction of *IoT* brings a new dimension of possibilities thanks to the great amount of accurate online data. This great amount of data requires a deep analysis and optimization processes assisted by the *Big Data*[8]. In addition, this *Big Data* empower the *Artificial Intelligence*[9] (AI) because it requires a great amount of information (data) in order to calibrate its algorithms and create great results in so many fields and applications.

It is very interesting to study how all this technologies are interconnected, particularly in this paper will review what could be the role of the *CAD/CAM* in relation with the other technologies and how is expected to evolve in this splendid *Ecosystem* of new applications and new technologies.

---

[6] *The Internet of Things (IoT) is a system of interrelated computing devices, mechanical and digital machines, objects, animals or people that are provided with unique identifiers (UIDs) and the ability to transfer data over a network without requiring human-to-human or human-to-computer interaction. [15]*

[7] *Digital Transformation is the deliberate and ongoing digital evolution of a company, business model, idea, process, or methodology, both strategically and tactically. [24]*

[8] *Big Data is a field that treats ways to analyze, systematically extract information from, or otherwise deal with data sets that are too large or complex to be dealt with by traditional data-processing application software. Data with many cases (rows) offer greater statistical power, while data with higher complexity (more attributes or columns) may lead to a higher false discovery rate. Big Data challenges include capturing data, data storage, data analysis, search, sharing, transfer, visualization, querying, updating, information privacy and data source. Big Data was originally associated with three key concepts: volume, variety, and velocity. When we handle Big Data, we may not sample but simply observe and track what happens. Therefore, Big Data often includes data with sizes that exceed the capacity of traditional software to process within an acceptable time and value. [17]*

[9] *AI. Colloquially, the term artificial intelligence is often used to describe machines (or computers) that mimic cognitive functions that humans associate with the human mind, such as learning and problem solving.*
In the twenty-first century, AI techniques have experienced a resurgence following concurrent advances in computer power, large amounts of data, and theoretical understanding; and AI techniques have become an essential part of the technology industry, helping to solve many challenging problems in computer science, software engineering and operations research. [18].

Traditionally the role of the *CAD/CAM* tools are the early definition of the product, its validation and the generation of information for production, accurate and automatically.

With the arrival of the *Industry 4.0*, see figure 1, the *CAD/CAM* evolve and generate the *Digital Product Twin*. This *Digital Product Twin* has to be validate against its *Digital Product Performance*. This new business process model will provide a most accurate estimation of the cost and planning. It is also possible to consider the operative of the ships and maintenance, and in the future it may be reasonable that the Shipbuilding offer the *Ship as a Service*, in fact many ship-owners have their shipyards or are very related with some and the new *Digital Revolution* would empowering them.

Fig.1 - Related Industry 4.0 Technologies in a Shipbuilding CAD environment. [1]

All this processes are demanding a high level of integration, traditionally the Industry had initiatives that create standards with the objective to allow this interexchange of information between different solutions, it is partially possible but difficult if we may considered the logic that supports the different *CAD/CAM* applications (*CAD data Exchange*[10]).

In the case of the Shipbuilding there are many sources (*CAD, ERP, PLM, Digital Twin, IoT,..*) in different format: files, transactional database and not transactional databases, etc. and this information must be cleaned and integrated in some sort of pool of data, most probably generated by means of *Big Data*.

---

[10] *CAD data exchange is a modality of data exchange used to translate data between different Computer-aided design (CAD) authoring systems or between CAD and other downstream CAx systems.*

Many companies use different CAD systems internally and exchange CAD data with suppliers, customers and subcontractors. Transfer of data is necessary so that, for example, one organization can be developing a CAD model, while another performs analysis work on the same model; at the same time a third organization is responsible for manufacturing the product. The CAD systems currently available in the market differ not only in their application aims, user interfaces and performance levels, but also in data structures and data formats therefore accuracy in the data exchange process is of paramount importance and robust exchange mechanisms are needed.

The exchange process targets primarily the geometric information of the CAD data but it can also target other aspects such as metadata, knowledge, manufacturing information, tolerances and assembly structure. [19].

This pool of data shall feed the different *AI* algorithms and some automatic actions would be done, as well as some valuable processed information shall be transferred to adequate business areas and decision makers.

Ideally, these processes must be inside a framework that accomplished high *Cybersecurity Standards*[11] (for obvious reasons); include *Blockchain*[12] to certify transactions and approvals, and many applications and data available at the *Cloud Computing*[13] in order to facilitate its implementation, maintenance and distribution worldwide.

Covering so many technological areas is difficult for a single company even for a big corporation; up to some year ago, the corporations developed the whole scope of products and services but due the acceleration of the market the big corporations started to acquire new technologies and products that commonly nourished in small and agile companies, by purchasing them.

This strategy has its drawbacks, since it is difficult to integrate the new products, typically developed under different platforms and by highly dynamic employees within the rigid Corporation structures and methods. Meanwhile the *Digital Revolution* seems to be in favour of those companies that interchange information with others within some sort of *Digital Ecosystem*[14] that encourage the

---

[11] *Cybersecurity refers to three things: measures to protect information technology; the information it contains, processes, and transmits, and associated physical and virtual elements (which together comprise cyberspace); the degree of protection resulting from application of those measures; and the associated field of professional endeavour. Virtually any element of cyberspace can be at risk, and the degree of interconnection of those elements can make it difficult to determine the extent of the cybersecurity framework that is needed. Identifying the major weaknesses in U.S. cybersecurity is an area of some controversy. However, some components appear to be sources of potentially significant risk because either major vulnerabilities have been identified or substantial impacts could result from a successful attack - in particular, components that play critical roles in elements of critical infrastructure, widely used commercial software, organisational governance, and the level of public knowledge and perception about cybersecurity. There are several options for broadly addressing weaknesses in cybersecurity. They include adopting standards and certification, promulgating best practices and guidelines, using benchmarks and checklists, use of auditing, improving training and education, building security into enterprise architecture, using risk management, and using metrics. These different approaches all have different strengths and weaknesses with respect to how they might contribute to the development of a national framework for cybersecurity. None of them are likely to be widely adopted in the absence of sufficient economic incentives for cybersecurity [20].*

[12] *Blockchain Technology, structure was first described in the Bitcoin white paper as a peer-to-peer distributed time-stamp server. The author, Satoshi Nakamoto (possible a fictitius name), wanted to create a peer-to-peer electronic cash system that did not need a nerwork of banks to operate. Satoshi descibed "blocks" and "chains" as a way to organmizing and securing records, such that once entries had been made into a shared database, they could be proved mathematically correct and to have mainned unchanged. [21].*

[13] *Coud Computing refers to the hardware, systems software, and applications delivered as services over Internet. When a cloud is made available in a pay-as-you-go manner to the general public, we call it a Public Cloud. The term Private Cloud is used when the cloud infraestructure is operated solely for a business or an organization. A compisition of the two types (private and public) is called Hybrid Cloud. [22].*

[14] *We view Digital Ecosystems to be the digital counterparts of biological ecosystems, exploiting the self-organising properties of biological ecosystems, which are considered to be robust, self-organising and scalable architectures that can automatically solve complex, dynamic problems. Digital Ecosystems are a novel optimisation technique where the optimisation works at two levels: a first optimisation, migration of agents (representing services) which are distributed in a decentralised peer-topeer network, operating continuously in time; this process feeds a second optimisation based on evolutionary computing that operates locally on single peers and is aimed at finding solutions to satisfy locally relevant constraints. We created an EcosystemOriented Architecture (EOA) of Digital Ecosystems by extending Service-Oriented Architectures (SOAs) with distributed evolutionary computing (DEC), allowing services to recombine and evolve over time, constantly seeking to*

development of new applications in less time and reaching millions of users. Such kind of *Ecosystems* are been nourished under the *Open Source Development Model*[15].

There are lots of reasons why people choose open source over proprietary software, but the most common ones are [2]:

- *Peer review*: Because the source code is freely accessible and the open source community is very active, open source code is actively checked and improved upon by peer programmers. Think of it as living code, rather than code that is closed and becomes stagnant.

- *Transparency*: Need to know exactly what kinds of data are moving where, or what kinds of changes have happened in the code? Open source allows you to check and track that for yourself, without having to rely on vendor promises.

- *Reliability*: Proprietary code relies on the single author or company controlling that code to keep it updated, patched, and working. Open source code outlives its original authors because it is constantly updated through active open source communities. Open standards and peer review ensure that open source code is tested appropriately and often.

- *Flexibility*: Because of its emphasis on modification, you can use open source code to address problems that are unique to your business or community. You aren't locked in to using the code in any one specific way, and you can rely on community help and peer review when you implement new solutions.

- *Lower cost*: With open source the code itself is free—what you pay for when you use a company like Red Hat is support, security hardening, and help managing interoperability.

- *No vendor lock-in*: Freedom for the user means that you can take your open source code anywhere, and use it for anything, at any time.

- *Open collaboration*: The existence of active open source communities means that you can find help, resources, and perspectives that reach beyond one interest group or one company.

This *Ecosystems* share ideas, documentation, code, tools between developers and offer a potential pool of millions of users, and interestingly, successful *Ecosystems* retro-feed themselves by creating new and more enhanced solutions that increase the demand by attracting more users, creating a symbiosis that promoted the products at a huge speed.

The *Open Source* is a community distributed worldwide, Neither is new, *Linux*[16] was leading this concept for nearly *30* years; what is new is that the big companies such as *Google*, *Windows*, *IBM*, etc.

---

improve their effectiveness for the user base. Individuals within our Digital Ecosystem will be applications (groups of services), created in response to user requests by using evolutionary optimisation to aggregate the services. These individuals will migrate through the Digital Ecosystem and adapt to find niches where they are useful in fulfilling other user requests for applications. Simulation results imply that the Digital Ecosystem performs better at large scales than a comparable SOA, suggesting that incorporating ideas from theoretical ecology can contribute to useful self-organising properties in digital ecosystems. [32]

[15] An open source development model is the process used by an open source community project to develop open source software. The software is then released under an open source license, so anyone can view or modify the source code. [2]

[16] Linux is clone of the Unix OS, which has been popular in academic and business environments for years. Linux consists of a kernel, which is the core control software, and many libraries and utilities that rely on the kernel to provide features with users interact, The OS is available in many distributions, which are collections of a specific

are entering into these communities providing a great set of tools and code making a huge impulse to the *Open Source Community*.

In some cases, this apparently chaos, is reorganized thanks to some initiatives that offer Projects and create *Free Software Foundations* or open repositories like *Github*[17], *Eclipse*, *Apache*, *GNOME*, *KDE*, *GNU Project/Linux Foundation*, *Mozilla*, *Google Open Source*, *Microsoft Azzure*, *Lotus*, etc.

These *Foundations* facilitate the integration between different projects, version control, documentation, etc.

Like any other *Ecosystem*, some communities thrive bringing some projects to the top, and other perish, or more academically are abandoned. There are many reasons for leaving a *Digital Ecosystem*, big companies disclosure an already similar and better working code/product, key developers abandon the community in favour of other projects, etc. Therefore, the election of a good *Digital Ecosystem* will be a critical factor.

Some key factor for choosing a good *Digital Ecosystem* are: fair licensing, openness, wide and assorted number of projects, proper information distribution and truly open governance.

Business Model based on *Open Source* has mostly follow two main streams:

- *Services Model*[18]: implement, customize and maintain the *Open Source* applications
- *Licensing Model*: licensing partially or completely the software.

There are different ways of licensing software, shown in following *figure 2*, developed under the *Open Source Model* that may go from the *Public Domain*, *Non-protective Free* and *Open Source Software* (FOSS), *FOSS Protective license*, Proprietary and up to the *Trade Secret*.

---

kernel with specific support programs. Popular Linux distributions include Arch, CentOS, Debian, Fedora, Gentoo, Mandriva, Open SUSE, Red Hat, Slackware, SUSE Enterprise, and Ubuntu, but there are hundreds-if not thousands-of Linux distributions. [23]

[17] *GitHub is the leading code-hosting platform with literally millions of open cource projects having their code hosted on it. In conjunction with Git, it provides the means for a productive development workflow and is the preferred tool among developers. [31]*

[18] *Service Model: As the companies providing the services are guaranteed of regular (usually monthly) recurring revenue from subscriptions, they are able to finance ongoing development with reduced risk (historically most software companies derived the majority of their revenue from users upgrading, and had to invest upfront in developing sufficient new features and benefits to encourage users to upgrade), and delivering more frequent updates often using forms of agile software development internally.*
The change to the subscription model also reduces software piracy - which is a major benefit to the vendor. [16]
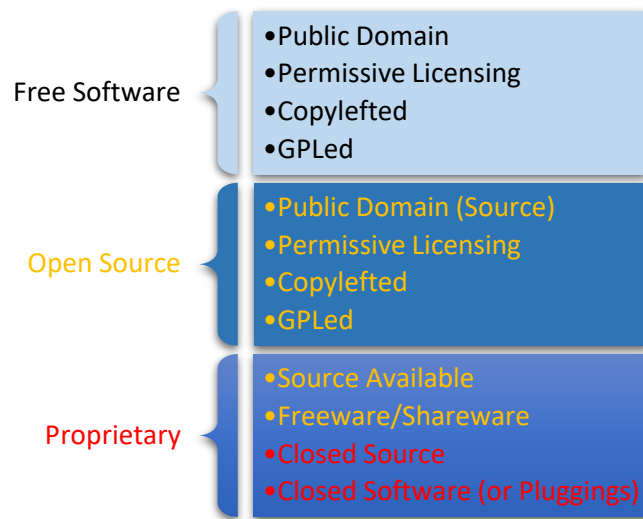
Fig.2 - Licensing software. Source: Freeware

2. DIGITAL TWIN

Digital Twin is a widespread concept that belongs to the *Industry 4.0 Ecosystem* but, what does it means and what is it for?nThis concept means the connection between the real asset and the design, the virtual world [3].

There are industries where this concept is widely applied, but shipbuilding industry is still starting with it. Aero-generators, energy platforms, airplane engines are nowadays the most common cases where we can find *Digital Twin* applied to, with two possible approaches: create a *Digital Twin* of the product and create a *Digital Twin* of a complete factory and control the facility through its *Digital Twin*. An example is *Azure Digital Twin* [4].

According to a *Gartner´s study* [5]*, Digital Twin* is used by the *24%* of the organizations with *IoT* technologies in production or with undergoing *IoT* projects and in the next three years, another *42%* is planning to implement it.

Many technologies, most of them described in this paper, are necessary to make possible a real effective *Digital Twin*, but *IoT* could be considered the most important, without forgetting the most basic and important technology necessary to make the *Industry 4.0* works, the communications infrastructure and, as always when we talk about data, security.

Digital Twin means a continuous and bidirectional exchange of Data between the real asset and the model, with the objective to have a real-time synchronization between those worlds.

Virtual to *Real Asset* data flow usually comes from a *Control Centre* that manages the data provided from the real world reflected into de virtual design. That *Control Centre* could interact with the real asset with a direct command executed through a console that will be converted in a digital signal that activates an actuator or by transmitting an order to a human operator.

Real Asset to *Virtual data flow* will be possible with a combination of sensors sending information through the communication infrastructure and human operators sending data by using Apps normally designed for devices that allow mobility and wireless connection.

Human or automatic processes (if the virtual asset includes *AI* or some automatic program that simply has an output depending on some input parameters) can manage both communication flows.

At the basis of the *Digital Twin*, the model is a must.

There are different ways to have it:

- *Spherical photographs*: it is a *360°* horizontal and *180°* vertical photograph that can be reproduced in an interactive way into a *3D* representation. This technology is the same used for *Street View* (*google*) available in *Google Maps*. There are special cameras that can take this kind of photographs, but it is also possible to generate a spherical photograph with standard cameras and specific software that can compose all those pictures taken from a fix position rotating the camera and taking all the necessary pictures to cover the complete surroundings.

  This is the most economical way to have a digital representation of the infrastructure. This solution is adopted when it is necessary to include the *Digital Twin* for *Industry 4.0* purposes and there is no *3D Model* of the facilities.
  This solution is also the fastest one, but the quality of the results and the possibilities are much more reduced than the other solutions.
  One of the most obvious disadvantages is that it is not valid for taking any kind of measurement. This technology only provides a conditioned visualization and navigation environment since the possibilities of movement are limited to the movement from one sphere to other following specific directions.
  Nonetheless, it could be enough for cases where it is only necessary a navigable virtual environment where it is possible to attach information provided by sensors, for example.

- *3D Scanning*: This method is widely explained in the paragraph that talks about *3D Printing*.

- *3D CAD* Model: This is the best option for a new infrastructure, or for a facility that already has the *3D Model* that can be easily updated to current situation and be used as *Digital Twin* without excessive effort.

The combination of *3D CAD* Model and *3D Scanning* is possibly the most interesting. With both technologies, it is possible to measure, and this is a very important advantage.
Shipyard is not a static scenario, that is why the best option is a *Digital Twin* based in *3D Model*s generated with a *CAD* system and when necessary with models generated by using *3D Scanning* technologies by transforming the clouds of points in volumes and surfaces.
This *Digital Twin* made of independent geometries, will be the best virtual environment to simulate and optimize processes, but also the best way to synchronize reality and the virtual world.
There are many applications for the *Digital Twin* and some of them are listed below:

- Remote monitoring and control of assets.

- Simulation of processes in a virtual environment.

- Training purposes.

- An updated *3D Model* of the facilities.

- Personnel, supply, assets real time control monitoring.

- Register of all the historical data and the possibility to analyse all that information in order to extract conclusions and decide actions to improve performance, for example.

- By combining historical data and algorithms, it will be possible to generate predictive models that can alert us about a dangerous or anomalous situation. The *Digital Twin* will provide the knowledge of all the dependencies between all the elements of the facility and the information about the monitored parameters. With that global information it will be possible not only the analyse situation of an asset but also predict the repercussions in the complete chain where that asset belongs to.

This concept can be implemented in an easiest way if all the stakeholders adopts *Digital Twin*; in fact, this is the real future of this concept, create a *Plug and Play Digital Twin Ecosystem*. It means that an asset will be ready to be implemented into a *Digital Twin* facility in a natural way, just install the physical asset into the facility, make the login of the new asset into the data system to acquire the information that comes from sensors and include the *3D Model* provided by the vendor into the virtual facility. The *3D Model* will include properties, parameters a direct link to the information provided by its sensors and will include operational information and predictive models that will be working during its operational life in order to be possible an early detection of problems.
The *Digital Twin* of the asset will also include:

- Digital manuals to be consulted by using *Augmented Reality*, infographic animations that provide step-by-step instructions for disassembly and inspection, etc.

- Programmed alerts for periodical inspections and maintenance operations.

- The possibility for manufacturers to link to the data of that asset, analyse its operating data to make real time recommendations and use that information to design new assets with improved characteristics.

An example of this *Plug and Play Ecosystem*: if a *Shipyard 4.0* needs storage racks, the provider of that asset will sold us a storage rack with its *Digital Twin*, which should include the *3D Model* to be directly implemented into the *Digital Twin* of the facility.
A fully equipped storage rack for *Industry 4.0* should include, for example, *RFID* antennas to detect the *RFID* tags attached to the components that will be stored and those antennas will send the information of the quantity of stored components to a logistics application that will manage instantly the situation and take decision autonomously buying new components if necessary.
To reach this *Digital Twin Ecosystem* the key factor is the definition of Standards, a common language to make possible an easy and fast integration of the real and virtual assets into a more complex *Digital Twin*. It is important to assume that a fully integrated *Digital Twin* is not always reachable and it will be frequent to find partial implementations that consists just in data acquisition from machines in order to analyse and use for different purposes, but once reached this first step, it will be easier to move in the *Digital Twin* direction.

3. BLOCKCHAIN

Cloud Computing requires transfer of sensitive data through an external network to our system, where it is processed and the response, which can include even more delicate data, used in the client system.

Some crypto processes are required to hide this data to curious, or even malicious, people. These processes require a secured channel, a double check to validate the information and some special operations all developed in the *Cybersecurity* paradigms.

Based on those paradigms, in 2009, the *Blockchain* methods, designed in 1991, are applied to cryptocurrency opening a new interchange trusted world, which ends with the bank intermediary requirement in monetary transactions. [6]

This *Cybersecurity* paradigm opens a new tool for distributed and shared work in all the industries, even more in shipbuilding, and its huge security requirements sibling, naval shipbuilding.

Blockchain technology offers a secure channel that requires an invitation, special program which knows all connection data, and where every operation performed is validated for all available connections and saved in a non-modifiable way, and where all the agents have a full copy of these operations, generating a trusted work methodology.

A *CAD* tool that includes the possibility of a *Blockchain* creation per each distributed work, and which locks items based on the assignation to a *Blockchain* operation can be included in the new era of *Industry 4.0*.

4. VIRTUAL REALITY AND AUGMENTED REALITY

Both *Augmented Reality* and *Virtual Reality* are technologies that cannot be considered as new, especially *Virtual Reality*, whose origins go back to the *Second World War*.

Until not long ago, the use of *Virtual Reality* in industrial area was something very rare, due to among other, to the high cost of this technology, but up to now and thanks to the recent progress in computer sciences, miniaturization, storage, graphic processing and the new high-resolution screens as well as technology is cheaper, *Virtual Reality* and *Augmented Reality* have revived.

Today, and thanks to the possibility of using smartphone for watching/interact in *Virtual Reality* environments or visualize *Augmented Reality* contents, these technologies are available to everyone [7] [8], without need of having a very powerful device. Another sector that drives these types of technologies are the video games world, creating increasingly real environments in which the users can feel really immersed thanks to *Virtual Reality* glasses and the tracking system allow a deeper immersion allowing to transfer the own individual movements (action in real environment linked to the action in real world). Technologies as the developed in the Leap Motion [9], in which on time scanning of the user's hands can be made, creating a duplicate in *Virtual Reality* copying fingers' movement, evolve at high speed to make the experience to be more immersive.

Besides *Virtual Reality* and *Augmented Reality*, also exist *Mixed Reality*, *Hybrid Reality* or *Merged Reality*. This concept is newer than the preceding's and which potential is out of question, consists in in the combination of the physical world and virtual world in a way that all of them coexist. This assumes that in these types of environments can happen a complete interaction between reality and virtual environment. Nevertheless, *Augmented Reality* is the technology that may seem to have more power in industrial sectors, proving in the cases it has been implemented that:

- Significant error reduction.

- Increase in productivity.

- Drop in employee injuries.

- Reduction of ergonomics issues.

- Favour collaborative environment.

- Improves efficiency.

- Etc.
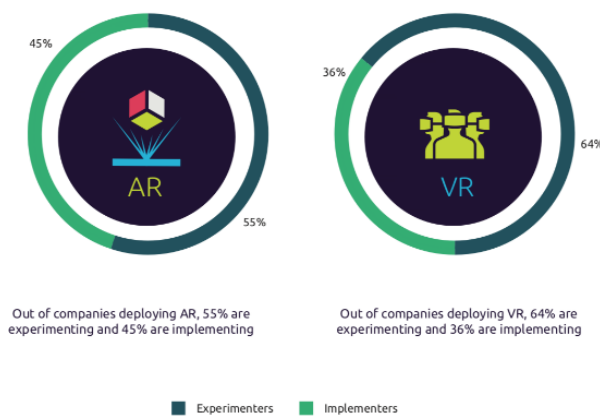
Fig.3 - Out of companies deploying AR/VR, implementation levels by organization category. [10]

The use of these technologies is more present and every day more important in automotive technology and aerospace industry. In other industries, the progress is slower, as for instance in the shipbuilding, but for *Digital Twin*, *Virtual Reality* and *Augmented Reality* comes along and *Digital Twin* is an unstoppable wave in *Industry 4.0* and *Shipyard 4.0*.

In *figure 3* we may appreciate as principal implementations of the companies are *Augmented Reality*, while at experimentation *Virtual Reality* overpasses *Augmented Reality* and in *figure 4*, below, it can be seen the implementation level of both technologies country by country.
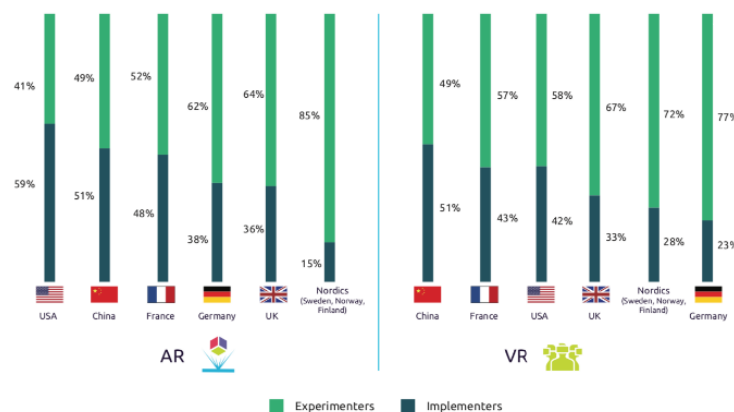
Fig.4 - Out of companies deploying AR/VR, implementation levels by country. [10]

A fundamental facet of both technologies and that conditions completely its use, is the device that will allow to access to *Augmented Reality* or *Virtual Reality*.

323

Augmented Reality consists in the superposition of digital elements over physical world; this way, digital elements add new details to real world thus creating an augmented experience of the reality. The devices with which this superposition can be reached can be divided into two groups depending on their limitations that their use means for the development of other activities simultaneously to visualization:

- Restrictive: Smartphones and Tablets.

- Not restrictive: Smart Glasses and other types of head-mounted devices.

The first ones are quite affordable devices, available to all types of users but they have the important disadvantage that the user who accesses the *Augmented Reality* with this type of device will not be able to execute tasks with their hands at the same time, as at least one of them must be used for holding the device.

These types of devices do not exploit the potential of *Augmented Reality* completely, although it is true that for those uses that require complex operations needing user interfaces that combine different operations in which *Augmented Reality* is only a small part of the features that provides, this type of device is the best option, especially Tablets. Smartphones have an excessively small screen, and, except for the portability, it does not provide a greater advantage compared to a Tablet.

The true potential of *Augmented Reality* can be obtained with *Smart Glasses* devices, that allow to combine *Augmented Reality* and true reality, without interaction with our hands, although that is not entirely true as these devices normally have touch pads and/or buttons to access to functionalities and interact with overlapping contents to reality.

The combination of this type of devices and the technologies of gestural recognition and natural language interpretation is what will allow exploiting the *Augmented Reality* in its maximum expression since in this way, the immersion is total and the interference of these devices in other types of actions that can be made by the operator is minimal or non-existent. The devices that are closest to this line are *Magic Leap* [11] for industrial use, *Hololens2* [12] and *Glass* [13].

Google Glass is, due to its dimensions and lightness, a device that is nearer the ideal while working on site. *Hololens & Magic Leap* that can also work with mixed reality, are heavier devices and less ergonomic when working with them, and also not suitable to work when ruggedized equipment is needed or there is a hazardous environment for sensible devices, as can be a shipyard.

Hololens and *Magic Leap* are more suitable for office environment or exceptional use during construction outside.

However, *Virtual Reality* creates its own pure digital surround in which the user is immersed, providing a sensorial experience that can be at several levels:

- Visual: Complete visualization and integration of the user within virtual environment, with visualization capacity in any direction.

  This integration can be in a:

  - Camera-way only, moving around virtual scenario, being the camera's movement the conductor, controlled or not by the own user.

  - Or through a digital avatar so the user can see through the avatar's eyes and it experiences the interactions of the avatar itself with the scenario, under the effect of the obstacles of the environment or the possibilities of interaction with virtual objects.

- Auditive: These virtual environments use the audio for augmenting the immersion experience, playing with sounds from the different elements existing in the virtual scenario with environments generally very well-achieved scenarios in which sounds are very reliable about position of them in the location.

- Tactile: There are many devices developed and that are being developed so the tactile experience is really immersive, and the user is able to perceive what he touches with his virtual hands or even with the rest of the body with integral suits. This way, user is physically conscient of the reality, something that only exists virtually, and can interact with the object in a completely natural way: perception of hardness, texture, etc.

- Olfactory: A field also under work.

Another important factor for *Virtual Reality* is how we interact with it. We already saw that tactile experience is a way to interact with these environments, but this interaction is also possible without so deep immersion level but offering easiness enough in handling for a person for doing it efficiently. The simplest way is by means of a typical cursors system to go forward and backwards, as well as by menus that can show up if we observe an object and can push a button or even if the system determines that the time that you observe an object is enough to display a menu linked to that object or information of it.

In a second level, we could place the devices that a user can hold with his hands, as controllers and see those devices in the virtual world so the interaction with the surround is through them. We can see this technology in famous *Oculus rift* and *HTC vive*, shown a picture of both in *figure 5*.
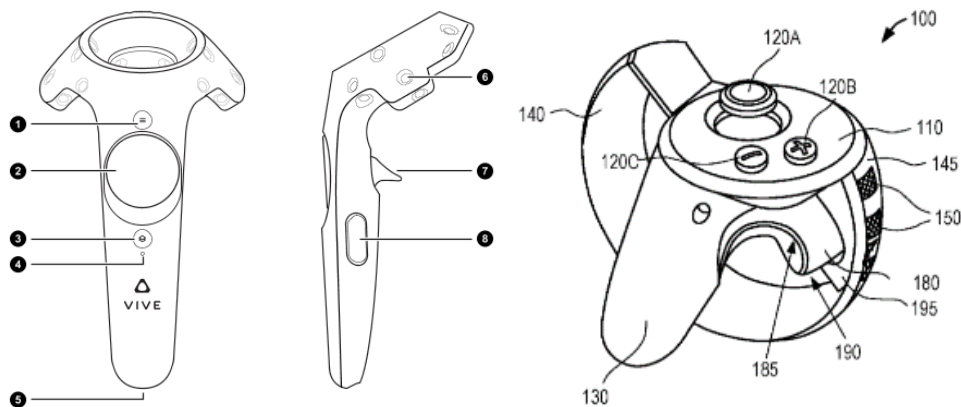
Fig.5 - HTC vive (left) [source: www.vive.com] and Oculus Rift (right). [14].

In a third level we could place *Leap Motion* [11], a device that scans user's hands and is capable of identify each finger in real time, making a *3D plot* of the hands in the virtual scenario and being this representation what interacts with the environment. Most advanced and immersive devices are gloves and even full suits.

Another essential interaction level is the own user's movement within scenario. Tracing systems are the most interesting as they allow to position in space, determine to what height you are (bended, standing still…), and to approach to virtual objects normally to see details.

Augmented Reality application in Industry could be wide, and in part also offers many of the possibilities that *Virtual Reality* proposes but it is necessary to distinguish in each case what is the best option.

It has been proved that *Augmented Reality* is really good at:

- Give instructions of a determined process to an operator while working with an equipment.

- Being able to preview a disassembly process step by step for a concrete equipment that is existent and that is the one the operator will work with, so he can execute each step with aid of *Augmented Reality* in that moment.

- Applications for remote assistance, to have available a system that allows to contact with an assistant in real time, with you being in front of the problem and that the camera of your *Augmented Reality* device shows the assistance the problem you are facing in real time so that the assistant can recommend you next steps.

Augmented Reality has a strong link with reality; this doesn't happen the same way with VR, but if this *Virtual Reality* is used over *Digital Twin*, the link is stronger.

This link with reality consists on the exploiting and visualization of the information generated by *IoT*. *Augmented Reality* allows as well to overlap the information generated by the *IoT* infrastructure directly, see history, trends, forecasts, warnings…. Never-ending possibilities that *Digital Twin*, through *Virtual Reality* could also offer remotely, being able in a future, who knows, to reach a completely remote management of a complex infrastructure interacting with *Digital Twin*.

Already said, repair and maintenance works along with design and assembly are the principal activities where these types of technologies can provide added value.

Concerning repair and maintenance works, main applications can be found in:

- Digital manuals visualization, videos etc. integrated into the virtual scenario in *Virtual Reality* or overlapped to reality in *Augmented Reality*.

- Remote assistance. Facing a problem that the user cannot solve, he can contact to an assistant that can see what he sees and recommend actions.

- Visualization of hidden elements by physical barriers overlapping *3D Model* of these hidden geometries versus reality where cannot be seen, and also interact with that virtual element to request information, move… thanks to *Augmented Reality*.

- Allow to reproduce assembly/disassembly tasks or other types of operations, visualize explicative infographics on a machine's functionality etc.

- In design and assembly, watch digitally stored information of the design.

- Simulate the behaviour of a determined asset in conditions generated by a virtual scenario.

- Visualization of the models in different conditions, surrounds, applying different materials, colours etc. To analyse the aspect it could have in real conditions and take decisions.

- Overlap *3D Model* on the real model.

- Multiuser collaborative environments to take decision around a design/prototype so costs for creating one or several real prototypes are reduced.

Although *Augmented Reality* requires of a more complex implementation within the productive protocols of a company, it has been proved that the results obtained are more profitable as the case is more complex.

Virtual Reality has been the most widely used and along longest time especially in training environments, design checks, commercial, etc. It continues to be string in these areas, but now more homogeneously, as this technology is more affordable than several years ago, and also, the evolution of the implied technologies has made the experience to be more immersive and powerful.

The area of training is the one that foresees more application in combination with Gamification concept as tool to speed up and strengthen workers training.

This idea has special interest when operating with complex infrastructures that require high quality training for both working skills as working in safe and security conditions; Scenarios could be created where users could prove their knowledge, detecting as well critical points, leading to a redesign if the analysis of the generated data within the virtual scenario shows any problem.

Another important use of *Virtual Reality* is the possibility of visualization of a prototype prior to manufacture.

This possibility also exists with *Augmented Reality*, but in this case it seems more interesting as we can position the prototype in different scenarios under different conditions or lightings, and if we add the chance of having a collaborative environment where several users can interact on the same prototype, not even being at the same place, the potential is enormous. This methodology has been proved greatly efficient where implemented, especially in automotive industry as it minimizes email exchange and meeting numbers to agree design features among all parties.

But being these technologies outstanding and with enormous potentials, it is decisive that it fits to a purpose in each case, as the implementation effort compensates and really add value.

In any case, it is not enough to will to implement these technologies, they must be supported on an infrastructure already technified in respect to equipment and also concerning people involved, as they have to be able to work and take the outmost of the advantages that these technologies represent.

When speaking of technological infrastructure necessary we mean:

- Availability of contents, being these contents: specifications, metrics, parameter values and sensor data, manuals, geometries, schemas, etc.

- Minimize risks of implementation supporting on expert companies on these types of technologies.

- Fully understand that in the cases where objective is to ubiquitous access to information and use these technologies exploiting their potential in collaborative working environments is basic, as well as with *IoT*, to have an infrastructure of communications being able to give an answer to the needs of this type of technologies.

- Last, to search integration with other systems that were being used in the company and that are part of the process as part of the productive process (*PLM*, *SAP*, *ERP*, etc.).

At the moment that we speak about the need of communication networks that allow access to data, we have to remind ourselves that it is a must that so named networks comply with all security standards that protects information.

CONCLUSIONS

The *Digital Revolution* presents major advantages for a Shipbuilding *CAD/CAM* mostly derived from the possibility to collaborate in many business areas with different *Open Source Projects* an integrate new technologies in a relative easy, cheap and specially fast way. Some of this business areas and technologies maybe:

- *AI: TensorFlow[19], H2O Sparkling Water[20], Acumos[21], AI Explainability 360[22], Caffe, NumPy, Keras, Weka, etc.*
- *Engineering simulation: OpenFOAM, OpenSIM, etc.*
- *IoT: Zetta, Arduino, Node-RED, Flutter, M2MLabs, ThingsBoard, Kinoma, Kaa IoT, etc.*
- *Simulation and Control of robots (cobots[23]): ROS[24].*
- *ERP: ADempiere, Apache OFBiz, WebERP.*
- *Virtual Reality: OpenSpace3D, Google's ARCore, Holokit, ApertusVR.*
- *Augmented Reality: Google's ARCore, AR.js, ARToolKit.*
- *Manufacturing and Risk Management: Odoo.*
- *Big Data: Hadoop, Apache Spark, Cassandra, RapidMiner, MongoDB, Apache SAMOA.*
- *Datamining: Orange, Rapid Miner, Weka, Knime, dataMelt, Apache Mahout.*
- *Collaborative Tools: Teamwork Projects, VisionProject, Workfront, Odoo, Qualio, Redmine.*
- *Supply Chain, Logistic and Traffic: Apache OFBiz, OpenBoxes, OpenLMIS, Odoo,*
- *Blockchain: Hyperledger, Ethereum, Corda, OpenChain.*
- *Cibersecurity; Apache, IBM Cloud Pak, OpenTitan, Vuls, ModSecurity.*
- *Cloud Computing: Apache Mesos, CloudStack, OpenStack, Eucalyptus, AppScale, Docker Hub, Kubernetes, Apache Kafka.*

---

[19] *TensorFlow is an end-to-end open source platform for machine learning. It has a comprehensive, flexible ecosystem of tools, libraries and community resources that lets researchers push the state-of-the-art in ML and developers easily build and deploy ML powered applications. [26]*

[20] *Sparkling Water allows users to combine the fast, scalable machine learning algorithms of H2O with the capabilities of Spark. Spark is an elegant and powerful general-purpose, open-source, in-memory platform with tremendous momentum. H2O is an in-memory platform for machine learning that is reshaping how people apply math and predictive analytics to their business problems. Integrating these two open-source environments provides a seamless experience for users who want to make a query using Spark SQL, feed the results into H2O to build a model and make predictions, and then use the results again in Spark. For any given problem, better interoperability between tools provides a better experience. [27].*

[21] *Acumos AI is a platform and Open Source framework that makes it easy to build, share, and deploy AI apps. Acumos standardizes the infrastructure stack and components required to run an out-of-the-box general AI environment. This frees data scientists and model trainers to focus on their core competencies and accelerates innovation. ([25]).*

[22] *AI Explainability 360 is a comprehensive toolkit that offers a unified API to bring together state-of-the-art algorithms that help people understand how machine learning makes predictions. [28].*

[23] *The industrial robots that might come to mind when you think of physical bots operating in 4-Ds type environments need separation from humans to operate safely. However "collaborative robots", known by the shorthand "cobots" are meant to operate in conjunction with, and in close proximity, to humans to perform their tasks. [30].*

[24] *The Robot Operating System (ROS) is a set of software libraries and tools that help you build robot applications. From drivers to state-of-the-art algorithms, and with powerful developer tools, ROS has what you need for your next robotics project. And it's all Open Source. [29].*

- *Databases: Apache Hive, ProgresSQL, MySQL, MariaDB, CockroachDB, Neo4j, RethinkDB, Redis, SQLite, Timescale, CouchDB.*
- *Digital Twins: Eclipse Ditto, CONTACT Elements for IoT,*
- *PLM: ARAS, OpenPLM, Odoo, Openbom.*
- *2D CAD: LibreCAD, SolveSpace, QCAD, NanoCad.*
- *3D CAD: FreeCAD, OpenSCAD, BRL-CAD, HeeksCAD, OnShape, Solcespace, Varkon, OpenCascade, JS Sketcher, OpenVSP, 3D Slash.*
- *Numerical Simulation: Salome, GNU Octave, FreeMat.*

After the review of all this technology, it is possible to have an idea of the magnitude and complexity of the changes that *Industry 4.0* is demanding.

In most cases, it is an unavoidable step that must be taken to remain competitive, but with the adoption of only a part of what is exposed; it could mean a too risky and complex step that should be studied carefully before taking any decision.

Some of these technologies are in early stages for industrial implementation but it is important to be aware and analyse what can offer and what can be useful for each case.

Most of the different technologies exposed in this paper are well known since long, but the true potential came a few years ago with the improvements in the communications infrastructures, that is why a concept like *Digital Twin* is something that seems reachable. Now with *5G*, it is expected that *IoT* will grow in an exponential way and its true potential will arise, which will also means the *Digital Twin* impulse.

In any case, although *5G* and *WiFi* promises to be the definitive revulsive for *IoT*, not all the cases could be solved with this technology, or at least, only with this, so it will be necessary to study carefully the conditions to decide the best communications infrastructure or even conclude that there is no feasible solution. Shipyards and ships are both cases where the conditions are not favourable for *IoT* deployment, particularly because of the important presence of metallic materials, one of the worst allies for WiFi communications. The highest the frequencies are, the worst *WiFi* behaviour will be in spaces surrounded by metallic materials, and this means that *5G* and *WiFi 6* should be studied carefully for these cases or similar ones.

Therefore, the first challenge for a correct implementation of *Industry 4.0* technologies is the network.

Platforms like *Raspberry PI*, *Arduino* and others, were key factors for the evolution of *IoT* technologies and its democratization thanks to an innovative *Ecosystem* where all kind of developers, Universities and Companies were able to contribute to the *IoT* evolution. This is maybe the second main factor for the *Industry 4.0*, the *IoT* technology is more accessible, both economically and technically for companies and persons, but *IoT* will reach its full potential when a true standard is stablished, a common language that makes easier for developers to create *IoT* devices, exchange information, and create infrastructures easily scalable and sustainable.

Other technologies like *Virtual Reality* have reappeared mainly thanks to the Game Development Industry and the lower cost of technology derived from the evolution of flat screens and miniaturization among other factors. *Virtual Reality* seems to have an important

future for training and simulation purposes, but its implementation in companies has a lower interest compared with *Augmented Reality*.

Ubiquitous access to information, immediacy, and remote operation of assets … nowadays these possibilities are in the hand of everyone, and this means a deep change in the Industrial world but also for the human being.

However, are our industries and infrastructures ready for this? Are we ready for this?

We are experiencing an incredibly rapid technological evolution that leads to an exponential growth of data acquisition that needs more and more storage space, and *IoT* will increment the data inputs that, with the new *5G*, it is expected to become even more.

According to a report by the *IDC* consultancy the data volume will reach *175 Zettabytes* in 2025 which means *175 times* the information generated in 2011 and the growth is exponential, as can be seen in the *figure 6*.
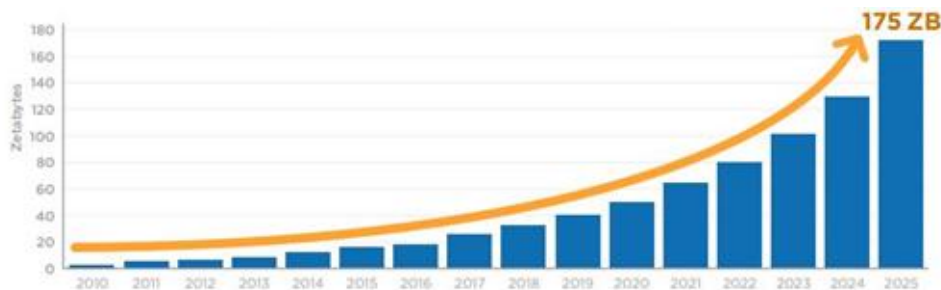
Fig.6 - Annual Size of the Global Datasphere.

Source: IDC report: The Digitization of the World from Edge to Core

The report ensures that the most of this information will be stored in the cloud and confirms that biggest contribution to this enormous increment of that will be a consequence of more than *150,000* million of devices connected to the network, in other words, *IoT*.

This perspective reinforces the ideas explained in this paper about the experience in the *e-Flow project* that describes the importance to filter the relevant information from the origin, by pre-processing the information in order to store only the useful information or simplify by using some kind of codification.

Another representative information provided by this report is about the intensity with which the people will interact with connected devices, *4,800 interactions/day* in 2025, which means practically a permanent connectivity through the network; a big jump from the *1,426 interactions/day* expected for 2020.

This entire connected world is a natural environment for the new and future generations and this means that the future workforce will be totally immersed in these technologies and they will be dependent on it.

In the not too distant future, it is possible that the concept of transhumanism becomes a reality, in a certain way we are already living the approach to that new reality because an enhanced human is what we are creating with this technological evolution. Devices like exoskeletons, google glass… are changing the human capabilities and here is another important actor of the entire *Industry 4.0 Ecosystem*, the devices that allow persons to be connected to the data.

Smartphones will be soon obsolete devices, all the connection possibilities will be available through other kind of devices, more natural and integrated, something like *Google Glass* and of course, *Augmented Reality* and *Mixed Reality* will be the technologies that will enhance our link with data by overlapping reality and data.

Contact lenses that works with *Augmented Reality*, are science fiction now? *Defence Advanced Research Projects Agency* (DARPA) is interested in a new wirelessly-connected contact lens recently unveiled in France. In April last year, researchers at leading French engineering *IMT Atlantique* announced the first autonomous contact lens, shown in *figure 7*, incorporating a flexible micro-battery. These contact lenses provides augmented vision assistance to users by relying visual information wirelessly.

Fig.7 - The first stand-alone contact lens with a flexible micro battery.

Source: https://www.imt-atlantique.fr.

There is another important piece of the puzzle: the security, veracity and trust in the data transactions between all the different participants. *Cloud + security* are two pieces of the game and without them, all this *Ecosystem* will never work. Data transactions should be guaranteed and all the steps should be tracked from the first step to the last one of the process thanks to *Blockchain*.

This data centric model will be complemented with *Big Data*, *Analytics* and *AI*:

- Extracting conclusions from that big amount of data acquired from *IoT* devices.

- Making possible a better maintenance thanks to the capability to predict failures or detect problems in early stages as well as the consequences of those problems.

- Learning from manpower that works in our Industries by analysing the activities in order to process all that information and be able suggest better practices by detecting bottlenecks and possible solutions.

Repetitive tasks and dangerous activities that nowadays are carried out by labour force, can be replaced or supported by robots, which means an important change for the companies and the people that works there, but this transformation is unstoppable. New jobs will be created and new profiles will be necessary but those jobs that could be replaced totally or partially with robots will disappear. People should react to this new conditions and adapt.

The implementation of robots and autonomous vehicles in the Industry will also mean the presence of new tools that will improve working conditions for current workers, but it is necessary an adaptation to all these new technologies and sometimes it will not be easy. Shipbuilding is an Industry that could take advantage by using them, but depending on the particularities of each shipyard, this technology will be more or less easy to implement and even if it is feasible, the decision should be taken with perspective, because physical robots and autonomous vehicles needs special conditions to work. A different case is the use of *RPA*, which could be easier to implement and very useful if the processes are clearly defined and can be automated.

New materials and *3D Printing* techniques will have an important role in the future of Shipbuilding as is already being demonstrated in other industries such as aeronautics and automotive but in shipbuilding there are interesting challenges, the use of *3D Printing* on board.

In the middle of this *Ecosystem* we will find a *3D Model*, created mainly with *CAD* Tools and this means that the importance of *CAD* will be even more capital than today. The interface between the *3D Model* and the rest of the *Industry 4.0* is the *Digital Twin*, the link between the reality and the virtual world, both living concurrently during the evolution of the construction and extending this world of possibilities to the entire lifecycle of the product.

CAD tools, as an important part of all this environment, should also evolve to be easily linked to these technologies, but also it is important to be adapted to the new generation of users that demands a different kind of interfaces and workflow and this will require an important effort.

This big world is now open and Shipbuilding is starting in it, but the potential is clear and to remain competitive is mandatory to study how these technologies can improve the benefits by upgrading processes, resources, workflow, cooperation between stakeholders… the tools are here, now it is necessary to study and analyse our particular case. There is no global solution for all industries, not even a global solution for a particular industry, but digitalization is on hand and it is mature enough to start implementation and be part of our strategy for the future.

6. References

[1]   A. Benayas-Ayuso and R. P. Fernández, "What should shipbuilding expect from the CAD/CAM systems of the future?," *The Naval Architect,* no. April, pp. 28-31, 2019.

[2]   "What is open source?," RedHat, [Online]. Available: https://www.redhat.com/en/topics/open-source/what-is-open-source. [Accessed 28 January 2020].

[3]   R. P. Fernandez and E. P. Cosma, "Glimpse to the future. Technological trends in the shipbuilding CAD world," in *ICASS 2019*, 2019.

[4]   "Azure Digital Twins," Microsoft Azure, [Online]. Available: https://azure.microsoft.com/en-us/services/digital-twins/. [Accessed 29 January 2020].

[5]   "How Digital Twins Simplify the IoT," Gartner, [Online]. Available: https://www.gartner.com/smarterwithgartner/how-digital-twins-simplify-the-iot/. [Accessed 29 January 2020].

[6]   S. Nakamoto, "Bitcoin: A Peer-to-Peer Electronic Cash System.," 2008. [Online]. Available: https://nakamotoinstitute.org/bitcoin/. [Accessed 28 January 2020].

[7]   E. Peter Cosma, "e-Flow - Sistema Integral Inteligente de soporte a la evacuación (1 part).," *Ingenieria Naval. No. 924. pp. 87-95.,* vol. 924, pp. 87-95, 2014.

[8]   E. Peter Cosma, "e-Flow - Sistema Integral Inteligente de soporte a la evacuación (2 part)," *Ingenieria Naval,* vol. 925, pp. 72-87, 2014.

[9]   "Google Cardboard – Google VR," Google, [Online]. Available: https://arvr.google.com/cardboard/. [Accessed 28 January 2020].

[10]   L. Cohen, P. Duboé, J. Buvat, D. Melton, A. Khadikar and H. Shah, "AR-VR-in-Operations1.pdf," 2018. [Online]. Available: https://www.capgemini.com/wp-content/uploads/2018/09/AR-VR-in-Operations1.pdf. [Accessed 28 January 2020].

[11]   "Magic Leap 1," Magic Leap, [Online]. Available: https://www.magicleap.com/. [Accessed 28 January 2020].

[12]   "Hololens 2," Microsoft, [Online]. Available: https://www.microsoft.com/en-us/hololens/hardware. [Accessed 28 January 2020].

[13]   "Glass," Google, [Online]. Available: https://www.google.com/glass/start/. [Accessed 28 January 2020].

[14]   J. A. Higgins and B. E. Tunberg Rogoza, "Hand-held controller with pressure-sensing switch for virtual-reality system". United States o America Patent US 10,180,720 B2, 1 December 2018.

[15]   M. Rouse, "Internet of things (IoT)". IOT Agenda, 2019.

[16]   C. Matt, T. Hess and A. Benlian, Digital Transformation Strategies, 2015.

[17]   T. Breur, Statistical Power Analysis and the contemporary "crisis" in social sciences, Journal of Marketing Analytics, 2016.

[18]   W. S. Marc Helmold, Progress in Performance Management: Industry Insights and Case Studies on Principles, Application Tools, and Practice, Springer, 2019.

[19]   H. Nowacki, L. E. P. D.-I. J. Dannenberg, D.-I. R. Schuster and D.-I. E. Vöge, Product Data Interfaces in CAD/CAM Applications. Symbolic Computation, Berlin: Springer, 1986.

[20] L. V. Choi and E. A. Fischer, Cybersecurity and homeland security, New York: Nova Scienc, 2005.

[21] Tiana Laurence, Introduction to Blockchain Technology, Van Haren, 2019.

[22] N. Antonopoulos and L. Gillan, Cloud Computing: Principles, Systems and Applications, Computer Comunications and Networks, Springer Science and Business Media, 2010.

[23] C. Bresnahan and R. Blum, Linux Essentials, Sybex, 2015.

[24] D. M. Mazzone, Digital or Death: Digital Transformation: The Only Choice for Business to Survive Smash and Conquer, Smashbox Consulting Inc, 2014.

[25] "Acumos AI," The Linux Foundation Projects, [Online]. Available: https://www.acumos.org/. [Accessed 28 January 2020].

[26] "TensorFlow," Google, [Online]. Available: https://www.tensorflow.org/. [Accessed 28 January 2020].

[27] "H2O Sparkling Water," H2O.ai, [Online]. Available: https://www.h2o.ai/products/h2o-sparkling-water/. [Accessed 28 January 2020].

[28] "AI Explainability 360," IBM, [Online]. Available: https://developer.ibm.com/open/projects/ai-explainability/. [Accessed 28 January 2020].

[29] "Open Robotics," ROS, [Online]. Available: https://www.openrobotics.org/. [Accessed 28 January 2020].

[30] "You've Heard Of Robots; What Are Cobots," FORBES, [Online]. Available: https://www.forbes.com/sites/cognitiveworld/2019/12/15/youve-heard-of-robots-what-are-c. [Accessed 28 January 2020].

[31] A. Pipinellis, GitHub Essentials, Packt Publishing, 2018.

[32] G. Briscoe and P. D. Wilde, "Digital Ecosystems: Evolving Service-Oriented Architectures," in *Cornell University*, 2009.

[33] M. Kozak-Holland and C. Procter, Managing Transformation Projects: Tracing Lessons from the Industrial to the Digital Revolution, Springer Nature, 2019.

Methodology of Integrated Design of the Ship Structure and Production Using the 3D Experience Platform

Davor Bolf[a,], Marko Hadjina*[a], Albert Zamarin[a], Tin Matulja[a]

a University of Rijeka, Faculty of Engineering
* Coresponding Author, hadjina@riteh.hr

Abstract

The high level of integration and efficiency of the ship structure design process with information related to the construction and outfitting of the ship is directly related to the level of shipyard competitiveness. This paper describes the methodology and procedures for integrated ship structure design and ship production technology on 3DExperience platform. The process of the ship structure modelling is described, either for producing classification documentation or for structure modelling using the classification documentation. This paper explains the level of detail in the model, as well as the complexity of modelling required to further develop the model into FEM structural models, structural and technological models intended to further elaborate and divide the ship into construction blocks. Authors outline the application of this process in the shipbuilding studies teaching, discuss the benefits and preconditions of this approach.

Key words: Shipbuilding, integrated ship structural design and production, 3DExperience, collaborative environment, education

Sažetak

Visoka i učinkovita razina integracije procesa projektiranja strukture broda sa informacijama vezanim za gradnju i opremanje broda direktno je povezana sa razinom konkurentnosti brodogradilišta. Ovim radom opisana je metodologija i procedure pri integralnom projektiranju brodske strukture i tehnologije gradnje broda na 3DExperience platformi. Opisuje se proces ranog modeliranja strukture, prije ili paralelno s izvođenjem klasifikacijske dokumentacije. U radu se obrazlaže razina detalja u modelu, kao i složenost modeliranja potrebnih za daljnju razradu modela na FEM strukturne modele, te konstrukcijske i tehnološke modele namijenjene za daljnju razradu i podjelu broda u građevne jedinice. te na razini razrade strukture u radioničku dokumentaciju. Autori prikazuju dio ovog procesa primijenjen u nastavi studija brodogradnje te diskutiraju prednosti i preduvjete ovakvog pristupa.

Ključne riječi: *Brodogradnja, integralno projektiranje strukture i gradnja broda, 3DExperience, kolaborativno okruženje, edukacija*

1. Introduction

In the current highly competitive industry, product development and production processes are becoming increasingly complex while the environment in which engineers operate has been changed [1]. This triggered the development and of advanced digital collaborative software solutions that integrate ideas, design, development and the product life cycle management (PLM) [2]. The one of the interdisciplinary, multicultural and constantly changing environment is shipbuilding industry, especially the design office, both in ship design and also in production design. The high level of integration and efficiency of the ship structure design process with information related to the construction and outfitting of the ship is directly related to the level of shipyard competitiveness. The need for fast design and rapid and accurate quality control of the product in early stages of production have triggered the implementation of such collaborative product life cycle management software not just in shipyards, but in design offices working for production. This paper describes the methodology and procedures for integrated ship structure design and ship production technology on 3DExperience platform. The process of the ship structure modelling is described, the level of detail in the model is discussed relevant to its purpose either for FEM, basic or detail, structural design or for defining construction blocks. Furthermore, the authors implemented such approach and methodology into regular class curriculum within naval architecture studies at Faculty of Engineering and the opinion about the achievements and guidelines for further application of the software in the education process is also discussed in this paper.

2. 3D Experience collaborative software platform

To support high level of integration of the ship structure design process with information related to the construction, outfitting and the complete lifecycle of the ship, the software companies today are developing the advanced collaborative platforms of integrated software solutions, in opposite to stand-alone or partial software solution integration. One such software platform is the 3D Experience [3]. It is designed to enhance collaboration and between the engineers, managers and workers and to deliver on time information to all parties involved in one project, thus enabling quick integration of the relevant information in design and production processes, as well as being improving efficiency and overall quality. The platform incorporates many products developed for different purposes such as Catia, Delmia, Enovia, Simulia and many others, each of them equipped with its special set of tools and capabilities for complete product development, production and its life cycle. 3D Experience platform can be customized to suit the need of particular industry through licensing packages which incorporate most of the tools of particular industry and educational institution.

For ship design, construction and lifecycle management Dassault systemes has prepared software solution package integrated under "Marine & Offshore Solutions" (referred as M&O in future text) [4]. The M&O is designed to follow ship lifecycle and business process by integrating 3D modelling applications (apps in future text) with Delmia and Enovia. The usage of structure design and manufacturing apps in relations to the ship life cycle is shown in Figure 1.
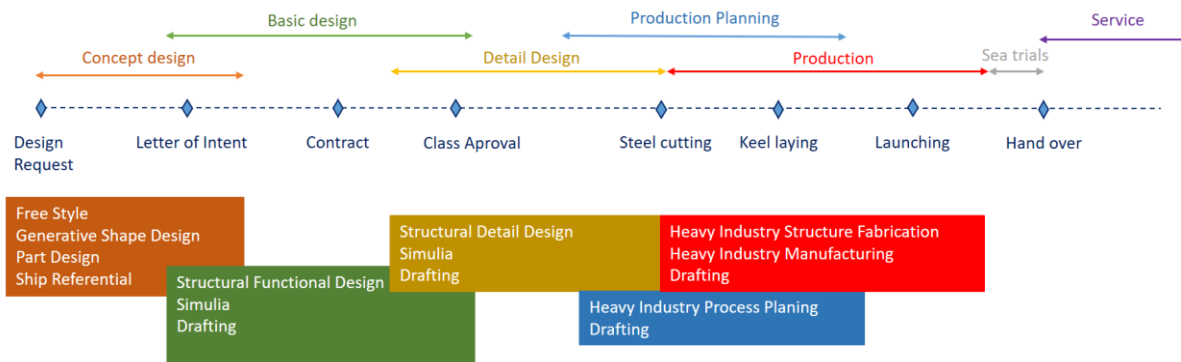
Figure 1 *Comparison of ship life cycle to most commonly used 3D Experience apps for structural design and manufacturing*

Slika 1 *Pregled najviše upotrebljavanih 3D Experience aplikacija za modeliranje strukture i tehnologiju gradnje broad u životnom ciklusu broda*

In concept design and through the basic design stage, as far as the ship structure is concerned, the most often used applications are the standard CATIA applications like "Generative Shape Design" (GSD), "Free Style Shape Design" (FS) and "Part Design" (PD). "Structural Functional Design" (SFD) and GSD apps are most used in basic design stage. Simulia is a simulation application which allows designer to verify the validity of the structural design. In this early stages of design, basic design models are divided into two types. One is the model intended for FEM analysis, containing only primary structural elements and the other model is intended for class drawings and production. The later model, usually contains more detailed structure, including secondary stiffeners and structural details (Figure 2).
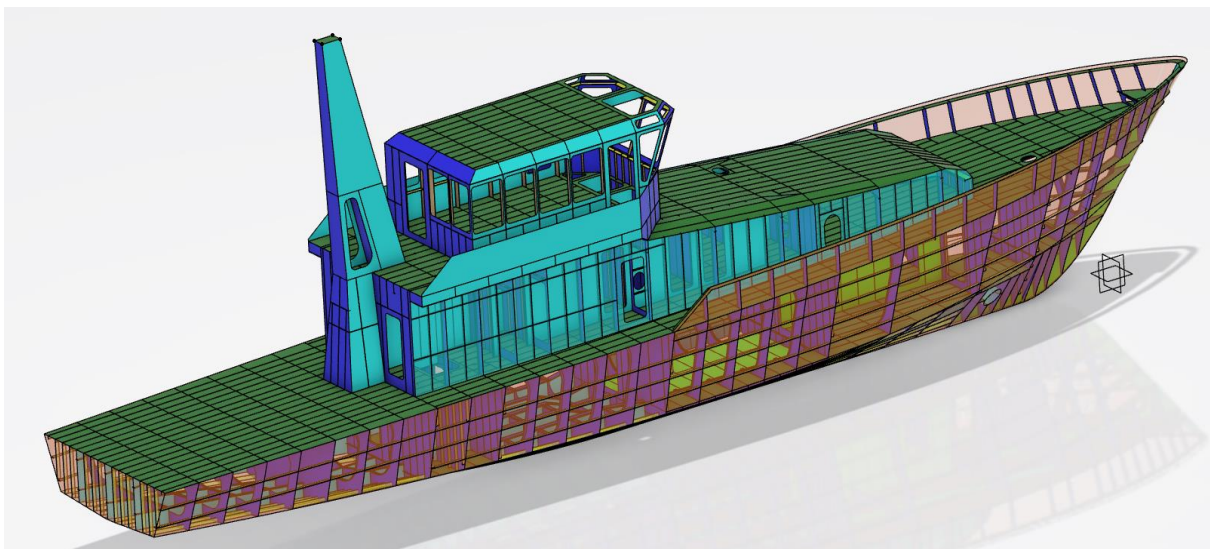
Figure 2 *Model of the ship, structure with details created using SFD app*

Figure 2 *Model broda, struktura i strukturni detalji kreirani upotrebom SFD aplikacije*

337

SFD model can be used to develop detailed production and assembly models, using "Structural Detail Design" (SDD) and semi-automated transition process which allow smooth transition from SFD to SDD. "Drafting" apps are used to extract manufacturing information and form a classification and manufacturing drawings and documentation. This app is useful in basic design stage, as well as in detail design and manufacturing stages. To achieve full functionality of drawings, generative view style (GVS) is needed. GVS can be tailored for each type of view and it is usually created according to shipyard drawing standards. The example of class drawing showing deck structure generated using GVS and drawing dress up details is shown in Figure 3.
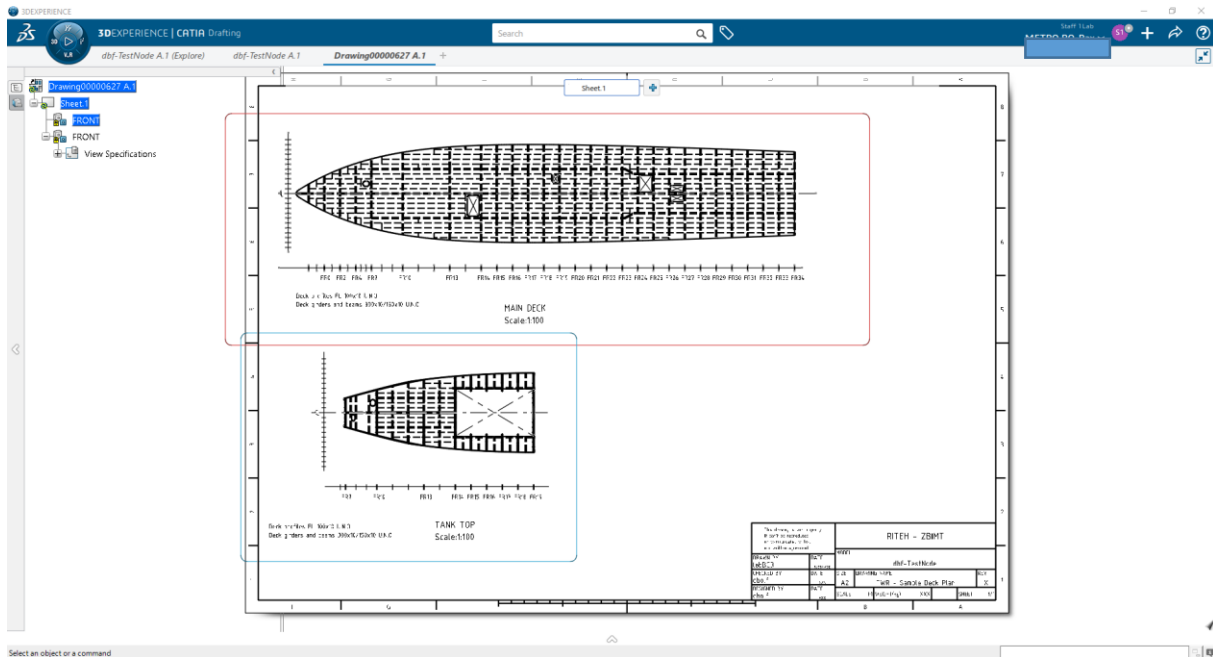
Figure 3 *Class drawing opened in "Drafting" app*

Slika 3 *Prikaz nacrta klase otvorenog u "Drafting" aplikaciji*

Combined with applications for machinery, accommodation, systems design intertwined with manufacturing and process planning apps, 3D Experience enables users to design ship by designing each system separately and build it by blocks containing multiple systems in one building unit. Using tools from different applications the model of the ship is designed, tested and prepared for the manufacturing with all necessary data, drawings and instructions, in particular making the digital twin of real product and production.

3. Case study of methodology of integrated design of the ship structure and production using the 3D Experience

In order to demonstrate and depict the methodology of structural design and manufacturing to students within Naval architecture students, 3D Experience software SFD app was used to create ship geometry. The starting position was the classification drawings and technological documentation of

the chemical tanker. The goal was to model one building block in order to present the modelling process and methodology, as well as to connect the 3D model with 2D class drawings and documentation. To achieve this, a project environment was created, using the skeleton geometry and ship reference system from chemical tanker project. The project settings, roles, skeleton geometry and SFD app were described in [5], describing the FEM analysis model and methodology of modelling for FEM analysis. However, the focus of this particular project was to present the modelling of the ship structure for class drawings and production, so the level of details presented in the 3D model needed to be much higher. In addition to ship primary structure, stiffeners, openings, slots and brackets needed to be modelled. The linear modelling sequence in 3D Experience SFD app in correlation to the principal input documentation and models are shown in Figure 4.
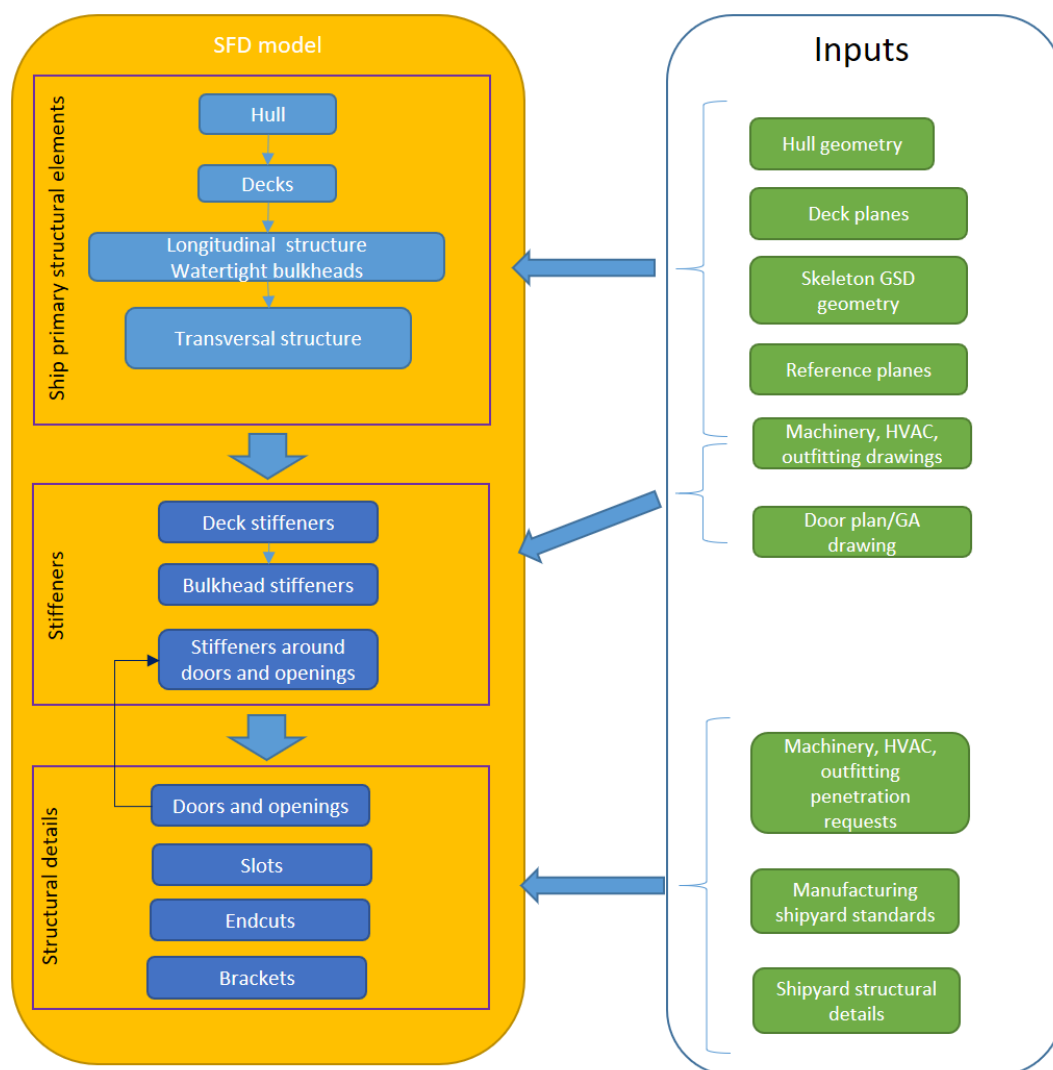
Figure 4 *Modelling sequence of ship structure using the 3D Experience SFD app*

Figure 4 *Slijed modeliranja brodske strukture upotrebom 3D Experience SFD aplikacije*

Modelling started with bottom hull plates (aka shell). Hull plates are limiting plates for almost any element below the main deck. The next stage was modelling decks and platforms, especially

decks limited by hull plates. In case study, students needed to create a model of the double bottom section, so double bottom deck was modelled second. Then the longitudinal bulkheads, watertight bulkheads and girders are modelled, following by transverse bulkheads and floors. Secondary structure needed to be modelled in the next stage. Good practice is to model the deck stiffeners prior to bulkhead stiffeners in order to limit the top limit of the bulkhead stiffeners to deck elements. Details like doors and openings are modelled in the detailing stage, adjusting the previously modelled stiffeners around the openings. Slots (openings for the stiffeners) in bulkheads, girders and beams and profile end cuts are modelled at later stages. The brackets were created at the end. Example of student work, double bottom section with details is shown in Figure 5. Slots and end cuts are symbolically presented to create model as small as possible in order to easily manipulate model in 3D environment.
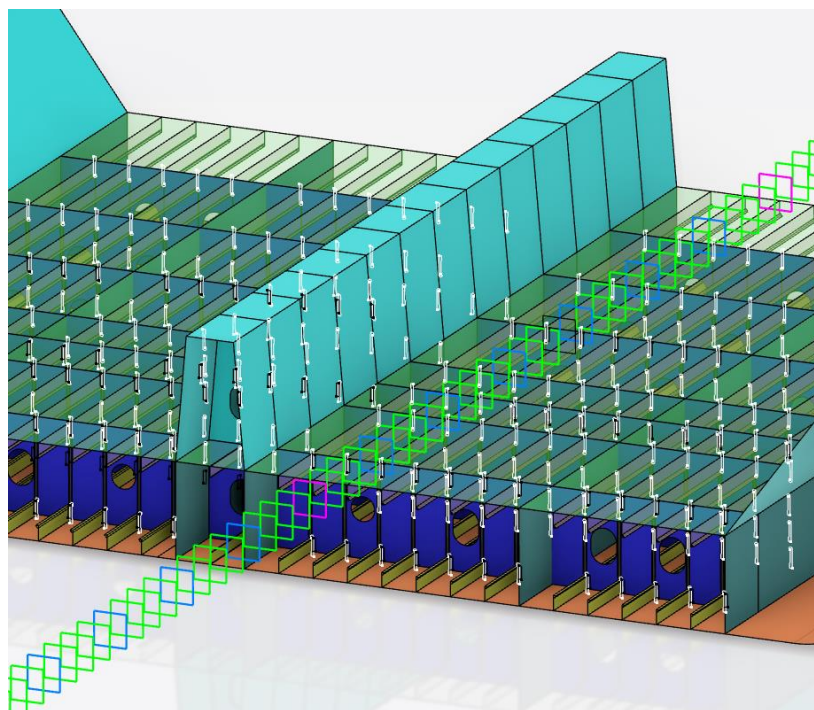
Figure 5 *Double bottom section with details modelled in 3D Experience SFD app*

Figure 5 *Sekcija dvodna s pripadnim detaljima modelirana u 3D Experience SFD aplikaciji*

To automate some of the modelling process, 3D Experience platform has several tools including "Advanced Copy" and "Advanced Connection" commands intended for faster modelling and EKL (Engineering Knowledge Language) used for scripting in 3D Experience environment. The EKL can be useful in production stage and can be used to extract data, customize models and features and create checking tools. During the student project, "Advance Copy" was used very often.

Block plan needs to be designed in early stages of the project. The block plan is a separate model, a part of the skeleton geometry set, intended for creating ship building blocks. Using the appropriate command sequence, the model created in SFD was translated into solid model with thicknesses. Most of the details created in SFD can be checked here and model can be further refined by adding structural details like user defined feature endcuts (UDF endcuts), which cannot be created in earlier

stages. The sample endcuts presented in SDD app on three different profiles can be seen in Figure 6a and sample slot in SDD app is shown in Figure 6b.
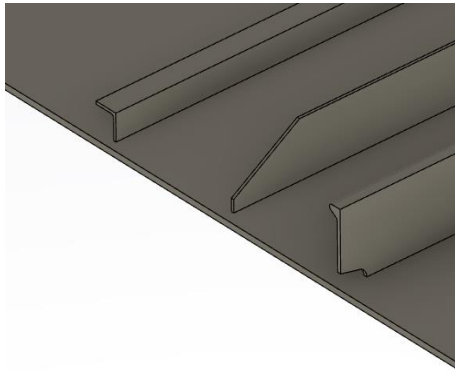
Figure 6a *SDD endcuts on 3 different profiles*

Slika 6a *SDD završetak profila na 3 različita profila*
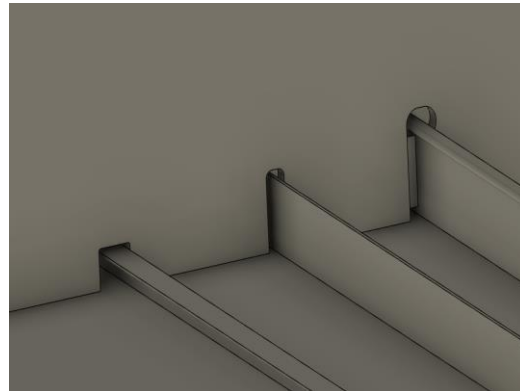
Figure 6b *SDD slots on 3 different profiles*

Slika 6b *SDD prolaz profila na 3 različita profila*

Finally, the authors would like to further elaborate the fact that this case study was actually conducted through regular naval architecture studies within University of Rijeka Faculty of Engineering. The experience from such approach was very good. The students, using such project based learning concept in group work, were starting to accommodate to a real world work environment within design offices or shipyards while also understanding the overall methodology of integrated ship design and construction as it is in a real industry environment. As for further activities, the plan is to continue to develop the preparation for manufacturing and process planning using "Delmia" module applications such as "Heavy industry process planning" and "Heavy industry manufacturing" for ship assembly design, factory layout design and manufacturing data definition to finalize the design circle by implementing the structural design, manufacturing and planning into Naval architecture studies curriculum within University of Rijeka Faculty of Engineering.

4. Conclusion

Today's highly competitive shipbuilding market demands constant improvements in shipbuilding process efficiency. One of the major challenges is to facilitate the high level of integration of the ship structure design process with information related to the construction, outfitting and the complete lifecycle of the ship using modern collaborative integrated software platforms. In this paper authors described the methodology and procedures for integrated ship structure design and ship production technology using 3D Experience platform. Such methodology was presented on case study up to the level of ship structure basic and detail design including class drawings and production drawings and information. Furthermore, the authors emphasize the need and benefits for implementation of such methodology with use of appropriate software, into education process for modern naval architecture students to be better accommodate to the needs of modern ship industry requirements.

Acknowledgements

REFERENCES

[1]   Stanić, V., Hadjina, M., Fafandjel, N. i Matulja, T. (2018). Toward shipbuilding 4.0 – an industry 4.0 changing the face of the shipbuilding industry. Brodogradnja: časopis brodogradnje i brodograđevne industrije, 69 (3), 111-128

[2]   Uran, V., Doboviček, S., Hadjina, M. i Perinić, M. (2018). AN IMPACT OF PLM SYSTEM ON COLLABORATION ACTIVITIES IN AUTOMOTIVE INDUSTRY. Proceedings: Management of Technology – Step to Sustainable Production. ITG Zagreb, 2018, 21-30

[3]   https://www.3ds.com/3dexperience

[4]   https://ifwe.3ds.com/marine-offshore

[5]   Bolf, D., Hadjina, M., Matulja, T. i Knapić, I. (2020). Implementation of Advanced Collaborative Platform for Project Based Learning in Naval Architecture Studies . Pomorski zbornik, Special edition (3), 217-226

ELEKTRO-HIDRAULIČKI UPRAVLJIVI BRODSKI DIZELSKI MOTORI NA DVOJNO GORIVO

Ivan Gospić*[a], Matko Donadić[b], Nastia Degiuli[c], Ivana Martić[c], Andrea Farkas[c]

a University of Zadar, The Maritime Department, Ulica Mihovila Pavlinovića 1, Zadar, Croatia
b *Princess Cruises*
c University of Zagreb, Faculty of Mechanical Engineering and Naval Architecture, Ivana Lučića 5, Zagreb, Croatia

* Corresponding Author, *igospic@unizd.hr*

Abstract

This paper describes the characteristic design of marine electro hydraulically controlled two-stroke and four-stroke dual-fuel engines, and emphasizes important conceptual and design specifics of the two most respectable manufacturers in the world - Wartsila and MAN. Different design solutions regarding preparation, supply and admission of fuelled gas are particularly emphasized, as well as possible conversions of the older diesel engines, normally supplied only by liquid fuel, into engines which can use both liquid and gaseous fuels. Dual-fuel marine diesel engines have many advantages and one of the most important characteristics is their operating flexibility, which along with expertly designed safety systems, allows them to be widely used on liquefied natural gas tankers, since in this case they can be successfully supplied with boil off gas generated within cargo tanks impacted by the upcoming heat load.

Key words*: electro hydraulically controlled engine; dual fuel; boil off gas; fuelled gas admission; liquefied natural gas carriers*

Sažetak

U ovom radu opisane su karakteristične projektne izvedbe brodskih elektro-hidraulički upravljivih dvotaktnih i četverotaktnih motora na dvojno gorivo, te su posebice istaknute bitne koncepcijske i konstrukcijske specifičnosti izvedbi dvaju najrespektabilnijih svjetskih proizvođača Wartsile i MAN-a. Poseban naglasak je stavljen na pripremu, dobavu i upuštanje odnosno utiskivanje plinovitog goriva, kao i na moguće konverzije postojećih dizelskih motora napajanih isključivo kapljevitim lakim i teškim gorivom u motore napajane dvojnim gorivom (kapljevitim i plinovitim). Brodske dizelske motore na dvojno gorivo karakteriziraju mnogobrojne prednosti, ponajviše njihova pogonska fleksibilnost, koja im uz vješto osmišljene sigurnosne sustave omogućuje primjenu ponajviše na tankerima ukapljenog prirodnog plina, gdje se na uspješan način napajaju plinskim otparkom generiranim nastupajućim toplinskim opterećenjem tankova tereta.

Ključne riječi: *elektro-hidraulički upravljivi motori; dvojno gorivo; plinski otparak, upuštanje plinovitog goriva; tankeri ukapljenog prirodnog plina*

1. Uvod

Već desetljećima na suvremenim trgovačkim brodovima prevladavaju dizel-motorna propulzijska postrojenja posebice ona čiju okosnicu čine dvotaktni (2T) sporokretni motori s ekstra dugim stapajem, koji su zahvaljujući razmjerno maloj brzini vrtnje izravno povezani s propelerskim vratilom, čime se uz kompaktniju izvedbu poboljšava i energetska iskoristivost ovakvih propulzijskih sustava. Srednjekretni četverotaktni motori (4T) se uglavnom koriste zajedno s mehaničkim reduktorima za propulziju RO-RO brodova, koji zbog svoje namjene iziskuju strojarnicu razmjerno manje visine, dok se brzokretni i izrazito brzokretni 4T motori (rijetko i srednjekretni) koriste za pogon električnih generatora, kako onih pomoćnih za uravnoteženje nastupajućeg električnog opterećenja broda tako i onih većih snaga kojima se uravnotežuje propulzijsko opterećenje

električnih propulzijskih sustava. Razlog navedenoj prevladavajućoj zastupljenosti dizelmotornih postrojenja leži u činjenici da su ista karakterizirana kompaktnošću, pouzdanošću i relativno visokom energetskom iskoristivošću, koja kod suvremenih sporokretnih dvotaktnih propulzijskih motora velikih snaga doseže vrijednost i do $\eta_t \approx 0.55$ [1], što ih čini izrazito konkurentnim u odnosu na plinsko i parno turbinska propulzijska postrojenja.

Ovo je izrazito bitno budući da se u novije vrijeme širom svijeta pa tako i u području brodarstava pooštravaju ekološki propisi s namjerom postizanja stalnog smanjivanja štetnih emisija u okoliš što se ponajviše postiže povećavanjem sveukupne energetske iskoristivosti brodskog energetskog sustava. U tom kontekstu je u travnju 2018. godine Međunarodna pomorska organizacija (eng. *International Maritime Organisation*, IMO) objelodanila strateški plan kojim se predviđa ukupno godišnje smanjenje emisije stakleničkih plinova do 2050. godine za najmanje 50% u odnosu na ukupnu godišnju emisiju tijekom 2008. godine [2]. Razumije se da se ovom strateškom planu može nastojati udovoljiti i povećavanjem energetske učinkovitosti cjelokupnog brodskog energetskog sustava, pa je s tim u vezi u novije vrijeme IMO uveo slijedeće propise za novogradnje: Projektni indeks energetske učinkovitosti (eng. *Energy Efficiency Design Index*, EEDI), Plan upravljanja energetskom učinkovitošću broda (eng. *Ship Energy Efficiency Management Plan*, SEEMP), te Operativni indeks energetske učinkovitosti (*Energy Efficiency Operational Index*, EEOI), koji se može primjenjivati za postojeće brodove [2].

Uzimajući u obzir, uz navedene pooštrene ekološke propise, sveprisutnu stalnu nestabilnost cijena goriva (kapljevitih i plinovitih), sve više se nameće potreba za osmišljavanjem projektnih izvedbi brodskih dizelskih motora, kojima se omogućuje fleksibilnost napajanja različitim kapljevitim (eng. *Marine Gas Oil*, MGO; eng. *Marine Diesel Oil*, MDO; eng. *Heavy Fuel Oil*, HFO) i plinovitim gorivima (eng. *Natural Gas*, NG; eng. *Petroleum Gas*, PG), uz očuvanje visoke energetske iskoristivosti i ekološki prihvatljivog izgaranja takvih goriva. Iako je primjena motora na dvojno gorivo u stacionarnim energetskim postrojenjima već desetljećima sveprisutna, ovakvi koncepcijski modeli posebice 2T sporokretnih motora svoju primjenu u brodarstvu započinju tek početkom ovog desetljeća i to prvenstveno na tankerima ukapljenog prirodnog plina (eng. *Liquified Natural Gas Carrier*, LNGC). Razlog navedenom leži u činjenici da je za razliku od četverotaktnih dizelskih motora, koji svoju primjenu u sklopu dizel-električne propulzije LNGC-a nalaze već 50-tak godina zahvaljujući razmjerno niskim tlakovima utiskivanja plina u cilindre ($5 \div 6\,\mathrm{bara}$, Ottov princip rada), primjena sporokretnih 2T motora stagnirala sve dok nisu razvijena visoko sofisticirana pouzdana rješenja napajanja istih s prirodnim plinom, odnosno plinskim otparkom iz tankova tereta (eng. *Boil Off Gas*, BOG), pri izrazito velikom tlakovima ($\approx 300\,\mathrm{bara}$, Dieselov princip rada, MAN-ovi motori [3]), odnosno dok Wartsila nije osmislila vlastitu projektnu izvedbu niskotlačnog ($10 \div 16\,\mathrm{bara}$) sustava utiskivanja generiranog plinskog otparka u dizelske 2T sporokretne motore koji rade po Ottovom principu [1]. Osim IMO ekoloških propisa, prema globalnom političkom kompromisu u svrhu zaštite okoliša, definirane su posebne zaštićene pomorske zone SECA (eng. *Sulfur Emission Control Area*) i ECA (eng. *Emission Control Area*), koje prikazuje Slika 1. za koje vrijede posebna pravila glede korištenja goriva, pa tako od 1. siječnja 2015. godine svi brodovi koji namjeravaju ući u SECA područje moraju koristiti gorivo sa sadržajem sumpora ispod 0,1% [1]. Takvi su zahtjevi proizašli uslijed uobičajenog korištenja jeftinijih brodskih teških goriva sa zamjetnim udjelom sumpora, čijim se uklanjanjem iz ovih goriva na propisanu razinu cijena istih znatno povećava. Korištenjem plinovitog goriva na brodovima, posebice generiranog plinskog otparka (kod LNGC), koji gotovo da u sebi i nema sumpora, ne samo da se zaobilazi navedeni problem već se

postiže smanjenje emisije CO_2 za 25-30%, te se smanjuje razina štetnih NOx spojeva za do 85%. Sve ovo je intenziviralo razvoj i primjenu koncepcijskih rješenja dvotaktnih sporokretnih dizelskih motora na dvojno gorivo posebice na LNGC-ima, gdje se svrsishodnim izgaranjem većeg dijela generiranog plinskog otparka uravnotežuje nastupajuće propulzijsko opterećenje tijekom navigacije, dok se razmjerno manji dio ponovno ukapljuje u relikvifikacijskom postrojenju (eng. *Reliquefication Plant*, RP) i vraća u tankove tereta ili eventualno u slučaju nužde spaljuje u incineratoru plinskog otparka (*Gas Combustion Unit*, GCU).

Posebne zaštićene zone ▢ Established Emissions Controlled Areas
Osjetljive zone čija je zaštita u razmatranju ▢ Emissions Controlled Areas under consideration
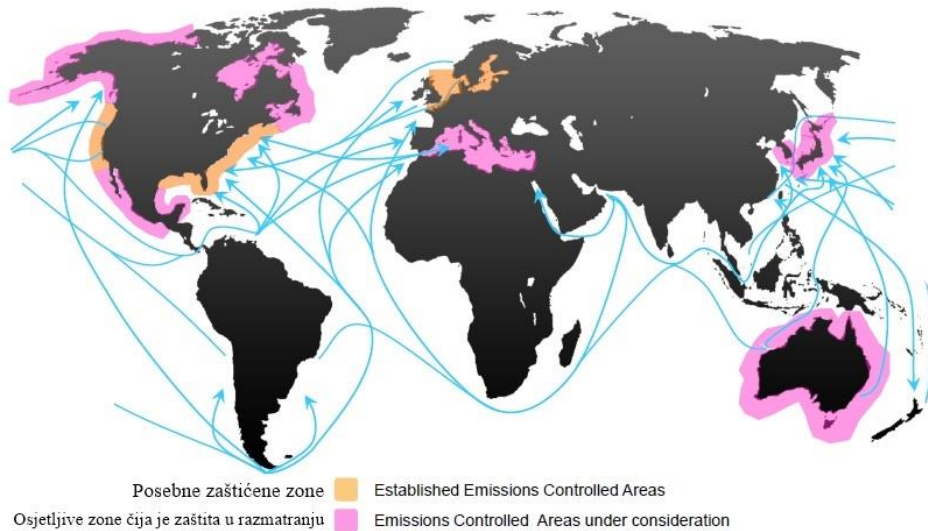
Figure 1 *Particularly ecology protected sea areas [1]*
Slika 1 Posebno ekološki štićene pomorske zone [1]

a) dizel-električna propulzija; tegljači, opskrbljivači

b) mehaničko-električna prop. kom. brodova

c) azipodna propulzija brzih plovila

d) kontaminacijski modul LNG brodskog goriva
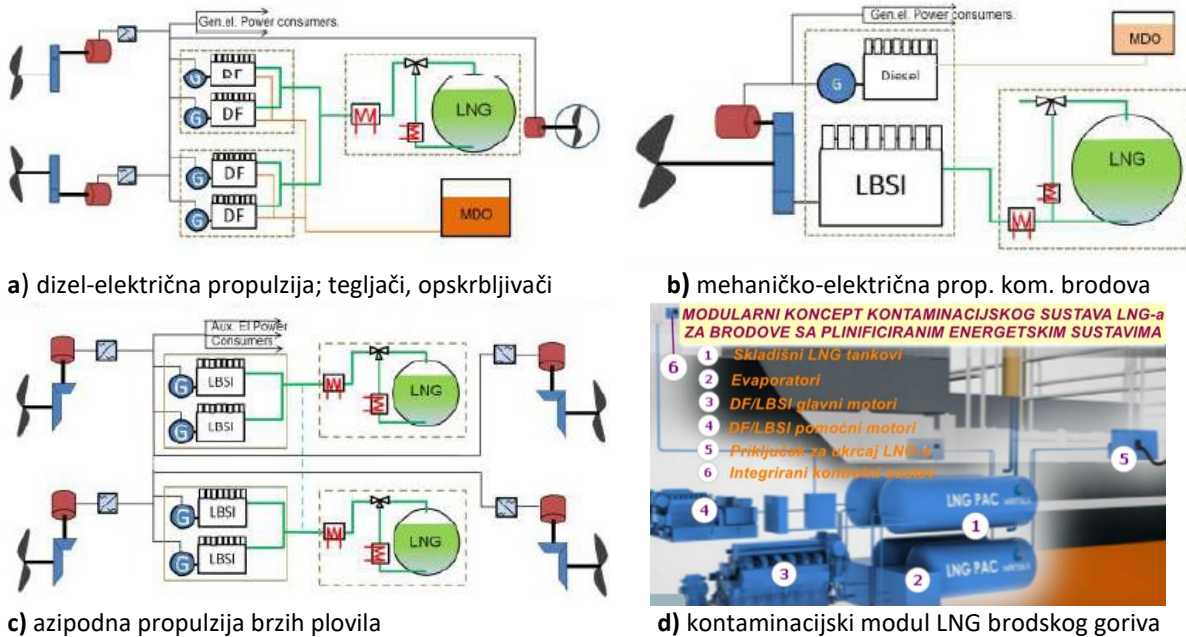
Figure 2 *Arrangements of the electric propulsion system with DF/LBSI 4T engines on the LNG fuelled ships [5]*
Slika 2 Izvedbe električnih propulzijskih sustava sa DF/LBSI 4T motorima na brodovima napajanim LNG-om [5]

Osim na LNGC-ima prirodni plin se zbog svojstvene mu čistoće i manje ekološke štetnosti sve više koristi kao glavno pogonsko gorivo u energetski učinkovitim motorima s unutrašnjim izgaranjem, koji radeći po Ottovom (plinski 4T motori) ili Otto-Dieselovom (2T i 4T na dvojno gorivo) ili Dieselovom principu (2T i 4T na dvojno gorivo) čine primarne pokretače (eng. *prime-movers*) na raznim vrstama plovila i brodova poput: trajekta (eng. *ferries*), plovila za pučinsku logistiku (eng. *offshore support vessels*), plovila obalne straže (eng. *coast guard vessels*), tankeri za prerađevine (eng. *product tankers*), kontejnerski brodovi (eng. *container ships*), itd.

Razumije se da su ovakvi *plinificirani* brodovi i plovila opremljeni osim s klasičnim skladišnim sustavom lakog i teškog goriva i sa skladišno-kontaminacijskim sustavom prirodnog plina kao glavnog pogonskog goriva. Slika 2 prikazuje tri karakteristične izvedbe električnih propulzijskih sustava, koji za proizvodnju električne snage koriste DF/LBSI 4T motore na brodovima, koji imaju vlastiti kontaminacijski sustav LNG-a kao pogonskog goriva.

2. Klasifikacija dizelskih motora na dvojno gorivo

Fundamentalni koncept napajanja motora s unutrašnjim izgaranjem dvojnim gorivom poznat je već od 1890-ih zahvaljujući provedenim eksperimentima Rudolfa Diesela tijekom njegovog istraživanja i razvijanja dizelskih motora. Upuštanjem prirodnog plina u usisni sustav dizelskog motora zamijetio je svojevrsno poboljšanje pogonskih performansi motora te su od tada motori na dvojno gorivo raspoloživi na mnogim tržištima. Njihova zastupljenost posebice je postala izražena u industrijskim postrojenjima u kojima se vršilo komprimiranje prirodnog plina već ranih tridesetih godina prošlog stoljeća. U današnje vrijeme karakterizirano nastojanjima raznih državnih i međunarodnih regulatornih tijela da se smanji emisija ekološki štetnih čimbenika poticanjem uravnoteženja barem jednog dijela nastupajućih (i rastućih) energetskih potreba korištenjem energetski obnovljivih izvora i ekološki prihvatljivijih energetskih sustava, sve su izraženija nastojanja u smjeru reduciranja potrošnje i dizelskog goriva (i drugih ekološki štetnijih fosilnih goriva). U tom kontekstu se izgaranje prirodnog plina smatra prihvatljivijim od izgaranja MGO-a, MDO-a te posebice HFO-a i u području brodarstva. Praktički stalni rast cijena dizelskog goriva uz postroženu regulatornu emisijsku politiku usmjerava projektante i konstruktore motora ka iznalaženju prikladnijih projektnih rješenja, kojima se omogućuje napajanje istih alternativnim gorivima poput prirodnog plina. Suvremeni brodski dizelski motori na dvojno gorivo su, bez obzira na njihovu taktnost i brzinu vrtnje, osposobljeni za rad u tri karakteristična operativna moda: operativni mod s plinovitim gorivom, gdje se kapljevito pilot dizelsko gorivo ubrizgava u količini dostatnoj za zapaljivanje gorive plinske smjese; operativni mod isključivo s kapljevitim gorivom (MDO i HFO); te operativni mod s varijabilnim iznosima plinovitog i kapljevitog goriva, pri čemu je minimalni iznos kapljevitog goriva predodređen nastupajućim opterećenjem motora (eng. *fuel sharing mode*). Obzirom na način upuštanja plinovitog goriva u cilindre (plinski i kombinirani operativni mod) ovi motori mogu raditi po Ottovom ili Dieselovom principu, pri čemu se kod prvo navedenih goriva plinska smjesa kod 4T motora generira tijekom usisne faze, dok kod 2T motora generiranje gorive smjese započinje na pola kompresijskog takta. Kod motora koji rade po Dieselovom principu generiranje gorive smjese započinje pred sam kraj kompresije kada se gotovo istovremeno u cilindarski prostor vrši utiskivanje (eng. *admission*) plinovitog goriva i ubrizgavanje (eng. *injection*) kapljevitog dizelskog goriva.

Brodski 4T Ottovi plinski motori (4T SI)

Pod Ottovim plinskim 4T motorima podrazumijevaju se sve one izvedbe kod kojih je jedino raspoloživo gorivo plin, koji se zapaljuje preskakanjem električne iskre (eng. *Spark Ignited*, SI), dok 4T dizelski motori na dvojno gorivo predstavljaju one projektne izvedbe, koje koriste plinovito i kapljevito dizelsko gorivo u određenom rasponu vrijednosti pri čemu se zapaljivanje istog vrši uvijek dizelskim gorivom. Slika 3, [4], prikazuje Ottov princip rada 4T motora: a) plinskih motora gdje se zapaljivanje gorive smjese vrši preskakanjem električne iskre (SI), b) motora na dvojno gorivo gdje se zapaljivanje gorive smjese vrši dizelskim pilot gorivom (eng. *Dual Fuel*, DF), te c) Dieselov princip rada kod 4T motora na dvojno gorivo (eng. *Gas Diesel*, GD).
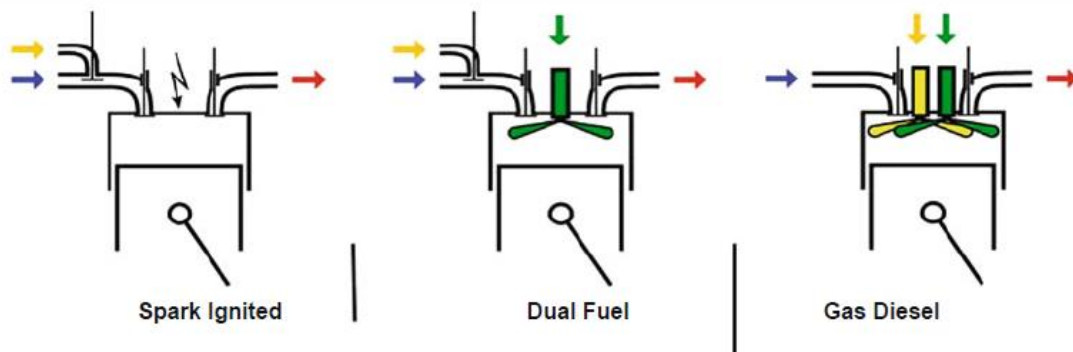
Figure 3 *Operating principle of the gas fuelled 4T engines; **left**-Otto principle for gas engines with spark ignition, **middle**-Otto principle for dual fuel engines with diesel pilot duel for ignition, **right**-Diesel principle with diesel pilot fuel for ignition [4]*

Slika 3 Principi rada 4T sa plinovitim gorivom; **lijevo**-Ottov princip s elektroničkim paljenjem , **sredina**- Ottov princip sa pilot dizelskim gorivom za paljenje, **desno**-Dieselov princip sa pilot dizelskim gorivom za paljenje [4]

Kako su 4T plinski motori u velikoj mjeri zastupljeni na plinificiranim brodovima i plovilima s električnom propulzijom ovdje će se samo nakratko izložiti njihovi operativni principi unatoč tome što sami po sebi ne spadaju u brodske dizelske motore na dvojno gorivo, koje se u ovom radu aktualizira. Pripremljeno plinovito gorivo (prirodni plin) se upušta pri razmjerno niskom tlaku ($4 \div 5 \, \text{bara}$) preko plinskih ventila u usisne ogranke, gdje se miješa s prednabijenim zrakom iza turbopuhala tijekom usisnog takta, čineći tako homogenu siromašnu gorivu smjesu, koja se pred kraj kompresije prispjevši u pretkomoru u istoj obogaćuje utiskivanjem razmjerno male količine prirodnog plina, omogućujući zapaljivanje iste preskakanjem električne iskre, Slika 4.
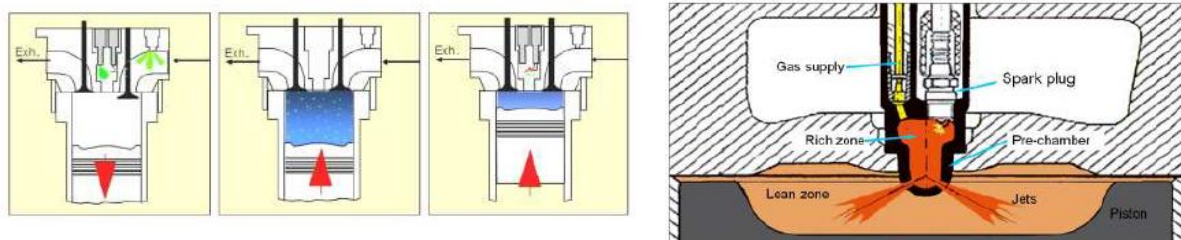
Figure 4 *Otto working principle of the gas fuelled 4T SI engines [5]*
Slika 4 Ottov radni princip 4T SI plinskog motora [5]

Zbog ovakvog načina zapaljivanja siromašne smjese karakterizirane visokim pretičkom zraka ($2 \leq \lambda \leq 2,3$), koji je omogućen SI paljenjem u pretkomori, ove motore se često naziva Ottovim plinskim motorima sa siromašnom smjesom (eng. *Lean Burn Spark Ignited*, LBSI).

U odnosu na dizelske motore iste snage, napajane sa HFO, ovi LBSI plinski motori su karakterizirani većom energetskom iskoristivošću pri višim opterećenjima te za oko 20-30% manjom emisijom stakleničkih plinova uključujući i emisiju koja proizlazi od curenja izrazito stakleničkog metana (eng. *methane slip*) zahvaljujući projektnoj izvedbi i kontroliranom izgaranju, Slika 5.
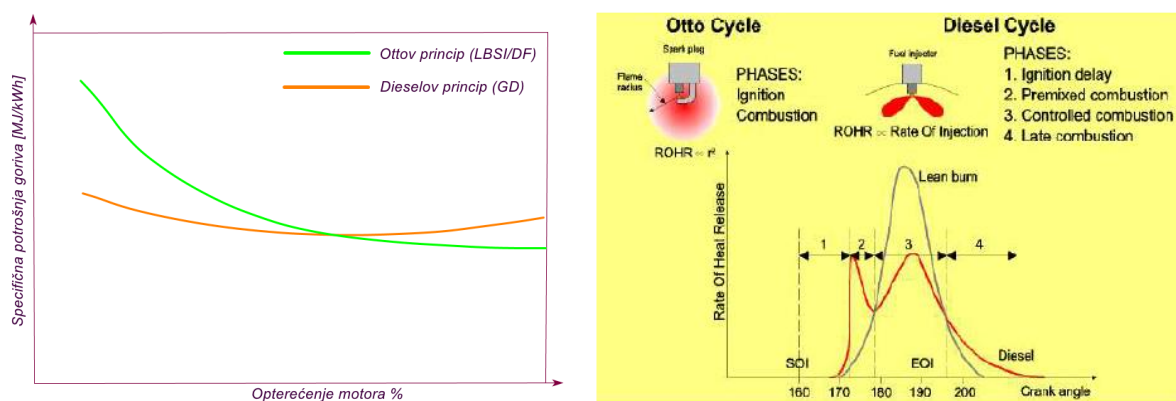
Figure 5 *Qualitative comparation of the LBSI and GD 4T engines [5]*
Slika 5 Kvalitativna usporedba LBSI i GD 4T motora [5]

3. Brodski četverotaktni dizelski motora na dvojno gorivo

DF 4T dizelski motori na dvojno gorivo (kombinirani Otto-Dieselov operativni princip)

Kod brodskih DF 4T motora sa turbonabijanjem plinovito gorivo se upušta u njihove usisne kanale pod tlakom $5 \div 6 \, \text{bara}$ te se već tijekom usisnog takta formira homogena mješavina prirodnog plina i nabijenog zraka, koja se pred sam kraj kompresijskog takta zapaljuje s dizelskim pilot gorivom (MDO) kojeg se dodaje u odgovarajućem iznosu od 0,5 do 1%, što predstavlja plinski operativni mod (eng. *Gas Mode*, GM), Slika 6a. Po potrebi se može pristupiti napajanju samo s dizelskim gorivom, čime se prelazi u dizelski operativni mod (100% dizel gorivo, eng. *Oil Mode*, OM), Slika 6b. Plinski operativni mod je provediv unutar 15-80% opterećenja motora te se na njega uvijek prelazi automatski iz dizelskog operativnog moda (MDO ili HFO) u navedenom rasponu opterećenja nakon stabilizacije izgaranja u cilindrima, što obično traje oko dvije minute, Slika 7a. Tijekom rada u dizelskom operativnom modu plinovito gorivo se ne upušta u motor, već se napajanje vrši sa MDO preko pilot brizgaljke (sa svrhom njenog hlađenja i sprečavanja onečišćenja od neizgorenog ugljika) i sa HFO preko glavne brizgaljke. Ukoliko se unutar sustava plinovitog goriva pojavi bilo kakav kvar, kao i u slučaju pada pogonskog opterećenja na 15% i manje, DF se automatski prebacuje u dizelski mod unutar tri minute. Snaga ovog motora u Ottovom operativnom modu određena je također količinom gorive smjese te je u odnosu na dizelski operativni mod manja za približno 10%.
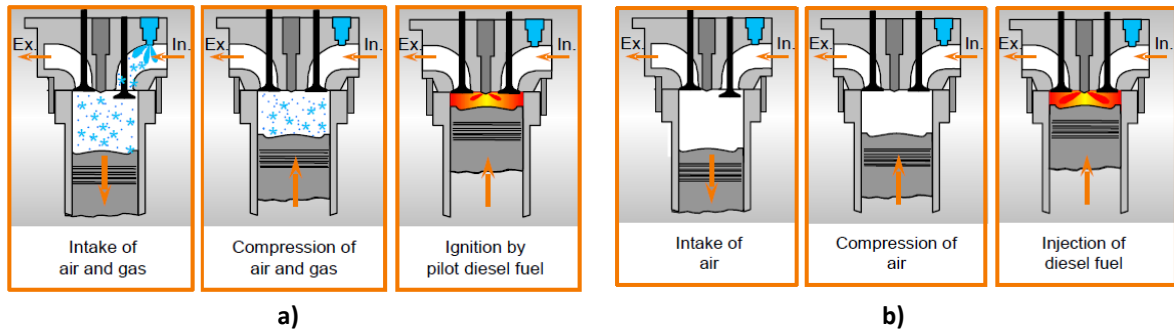
Figure 6 *Working principle of dual fuel four-stroke engines; a) Working principle of Otto dual-fuel engine with diesel pilot fuel for ignition, b) Working principle of Diesel Gas-diesel with diesel pilot fuel for ignition [6]*

Slika 6 Princip rada četverotaktnih motora na dvojno gorivo; **a)** Ottov princip rada sa pilot dizelskim gorivom za paljenje, **b)** Dieselov princip rada sa pilot gorivom za paljenje [6]

Tijekom GM moda, DF radi po Ottovom principu upuštajući smjesu prirodnog plina i zraka u cilindar, koja se potom uz kompresijski omjer svojstven dizelskim motorima komprimira na zamjetno viši tlak i na višu temperaturu. Da bi se izbjegla detonacija pred sam kraj kompresije nužno je generirati siromašnu gorivu smjesu prirodnog plina i zraka, praktički s omjerom zrak/prirodni plin oko 2,2, Slika 7b. Tako se tijekom operativnog GM karakteriziranog visokim pretičkom zraka dosižu razmjerno niže vršne temperature izgaranja, čime se ublažava disocijacija i posljedično tome smanjuje generiranje ekološki štetnih NO_x.
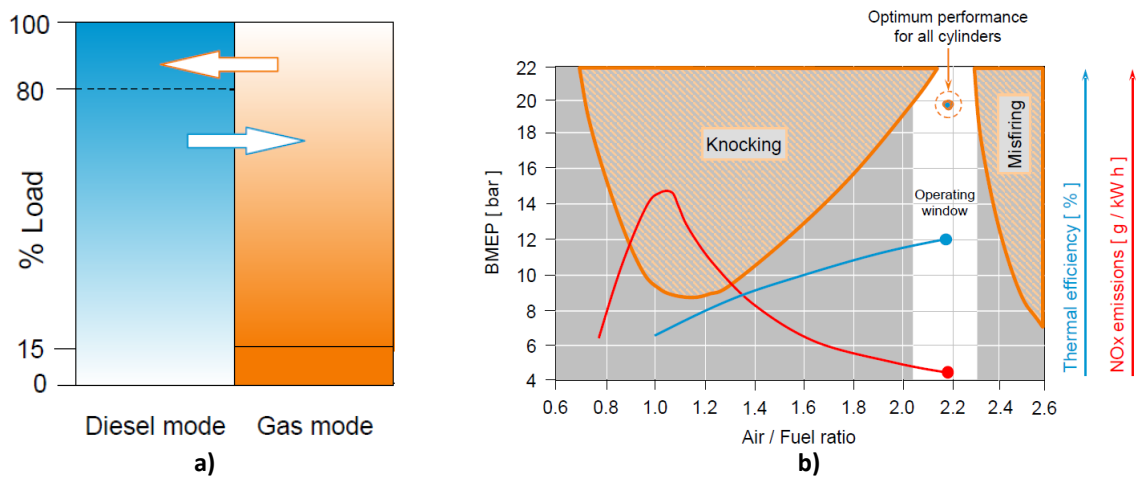
Figure 7 *a) Operating range GM and OM of DF 4T, b) Main combustion parameters versus air/fuel ratio [7]*
Slika 7 **a)** Operativni raspon GM i OM kod DF 4T, **b)** Parametri izgaranja ovisno o omjeru zrak/gorivo [7]

Na konvencionalnim brodovima čiji se propulzijski motori napajaju sa LNG-om bilo da su 4T (SI, DF i GD) ili 2T (DF i GD), Slika 8, nužno je osigurati odgovarajući kontaminacijski sustav LNG-a po uzoru na one kod LNGC-a, pa se za tu svrhu koriste prikladno izolirani tankovi LNG-a odgovarajućeg kapaciteta, bez posebnog hlađenja budući da u normalnim pogonskim uvjetima radi održavanja propisanog tlaka u spremniku sveukupno generirani otparak biva potrošen kao pogonsko gorivo unutar pripadajućeg brodskog energetskog sustava, Slika 9.

Figure 8 *Fuel gas (LNG) systems of DF 4T engines on the LNGC and on gas fuelled ships [8]*
Slika 8 Sustavi plinovitog goriva (LNG-a) DF 4T motora na LNGC i konvencionalnim brodovima [8]
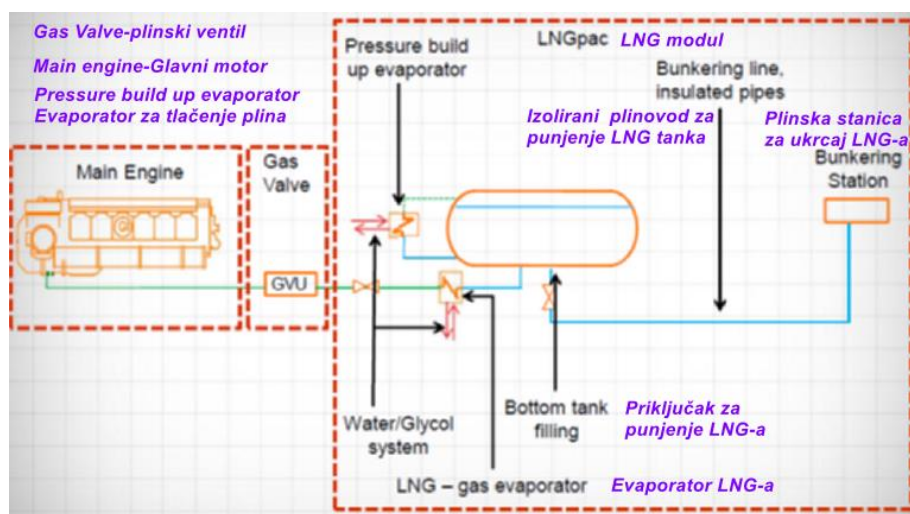
Figure 9 *Schematic of LNG contaminating system for supplying diesel engines on the gas fuelled ships [8]*
Slika 9 Shema kontaminacijskog sustava LNG-a za napajanje DF motora na konvencionalnim brodovima [8]

Često puta se u slučaju razmjerno manje potrošnje pribjegava grijanju kapljevite faze prirodnog plina kako bi ga se isparilo i vratilo u LNG tank što dovodi do željenog porasta tlaka u tanku. Tijekom uobičajenog navigacijskog opterećenja propulzijskih motora iz LNG tankova se izvlači kapljevita faza, koja se usmjerava kroz evaporator gdje se uglavnom isparava glikolom ili vodom ovisno o nastupajućim temperaturama LNG-a. U dizelskom operativnom modu DF 4T motori načelno rade kao i klasični dizelski motori na kapljevito MDO i HFO gorivo, koristeći uobičajene visokotlačne sustave ubrizgavanja sa po jednom brizgaljkom za svaki cilindar. U odnosu na brizgaljke klasičnih dizelskih motora, koje su jednokanalne s jednom iglom, brizgaljke DF 4T motora su sklopne izvedbe, dvokanalne sa dvije igle. Kroz kanal manjeg provrta podizanjem pripadajuće igle ubrizgava se pilotsko MDO gorivo tijekom plinskog operativnog moda. Kroz kanal većeg provrta dizanjem pripadajuće igle vrši se ubrizgavanje MDO ili HFO tijekom dizelskog operativnog moda, prilikom čega se također vrši i ubrizgavanje pilotskog goriva kroz kanal manjeg provrta (potreba za hlađenjem istog te anuliranja mogućeg onečišćenja sapnica od neizgorenog ugljika, i sl.), Slika 10. Za potrebe plinskog operativnog moda pripremljeni plin se upušta u usisne cilindarske kanale preko odgovarajućeg plinskog ventila i plinskih sapnica.
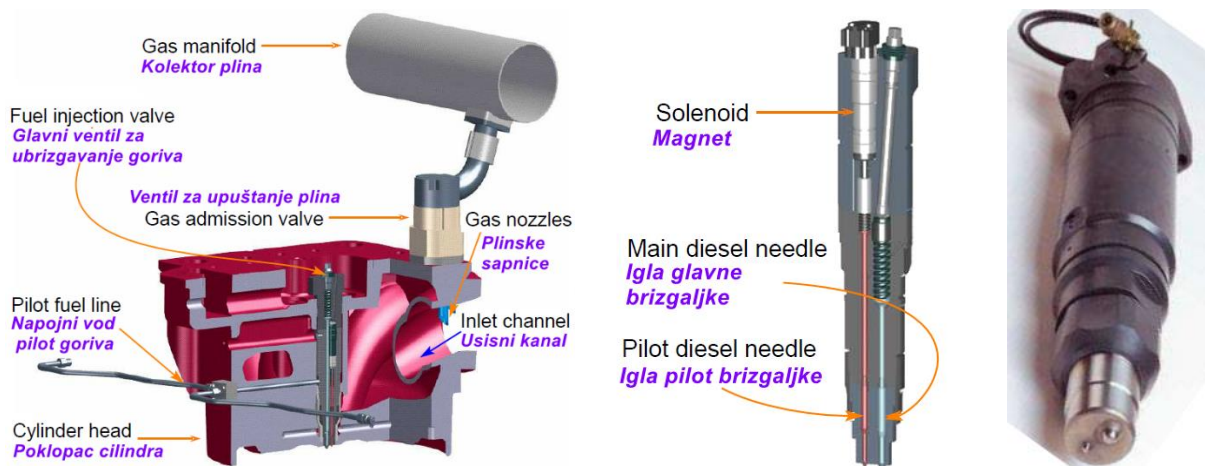
Figure 10 *Cylinder head arrangement of DF 4T engine with diesel fuel injector and gas admission valve [8]*
Slika 10 Izvedba glave DF 4T motora s elementima za ubrizgavanje MDO i HFO i upuštanje plina [8]

Suvremeni DF 4T motori na dvojno gorivo inkorporiraju elektroničko upravljanje sa svrhom poboljšavanja njihovih operativnih performansi, pa kao takvi predstavljaju provjerenu alternativu za zamjenu postojećih, jako rasprostranjenih dizelmotornih instalacija. Budući da dizelski motori zahvaljujući svojstvenoj samozapaljivosti gorive smjese bez vanjskog izvora paljenja poput električne iskre, nemaju svjećice niti sustav paljenja goriva, dizelsko pilot gorivo se koristi kao izvor zapaljivanja gorive smjese u komori izgaranja DF 4T motora na dvojno gorivo koji rade po Ottovom principu. Stoga ovi motori na dvojno gorivo, zadržavajući fundamentalne principe dizelskog pogona karakterizirane ponajprije efikasnim visokim kompresijskim omjerom, istovremeno omogućuju izgaranje jeftinijeg, čišćeg i ekološki prihvatljivijeg plinovitog goriva. Komercijalno primjenjivi DF 4T motori na dvojno gorivo, načelno se prema pogonskim specifičnostima mogu klasificirati u dvije klase: srednjekretne i umjereno brzokretne motore nazivnih brzina vrtnje do 1000 o/min karakterizirane sustavima zasebnog utiskivanja plinovitog goriva u svaki cilindar, te izrazito brzokretne sa brzinama vrtnje između 1200-1800 o/min karakteriziranih sustavom centralnog utiskivanja plinovitog goriva u usisni sustav motora.

Sustav centralnog utiskivanja plinovitog goriva

Utiskivanje plinovitog goriva u izrazito brzokretne motore (eng. *high speed*) u potpunosti je nalik primjenjivanoj metodologiji utiskivanja kod klasičnih plinskih motora, karakteriziranoj tzv. centralnim utiskivanjem plinovitog goriva (eng. *Single Point Fuel Admission*, SPFA). Uobičajeno je da se kod klasičnih plinskih, izrazito brzokretnih motora, pa tako i kod istovrsnih napajanih dvojnim gorivom, utiskivanje plinovitog goriva u usisni sustav motora vrši neposredno ispred turbopuhala, Slika 11. Plinovito gorivo se upušta u usisni sustav preko ventila kroz mješač instaliran neposredno ispred turbopuhala, po tzv. *fumigacijskom konceptu* (eng. *fumigation concept*), odnosno po konceptu centralnog uplinjavanja goriva.
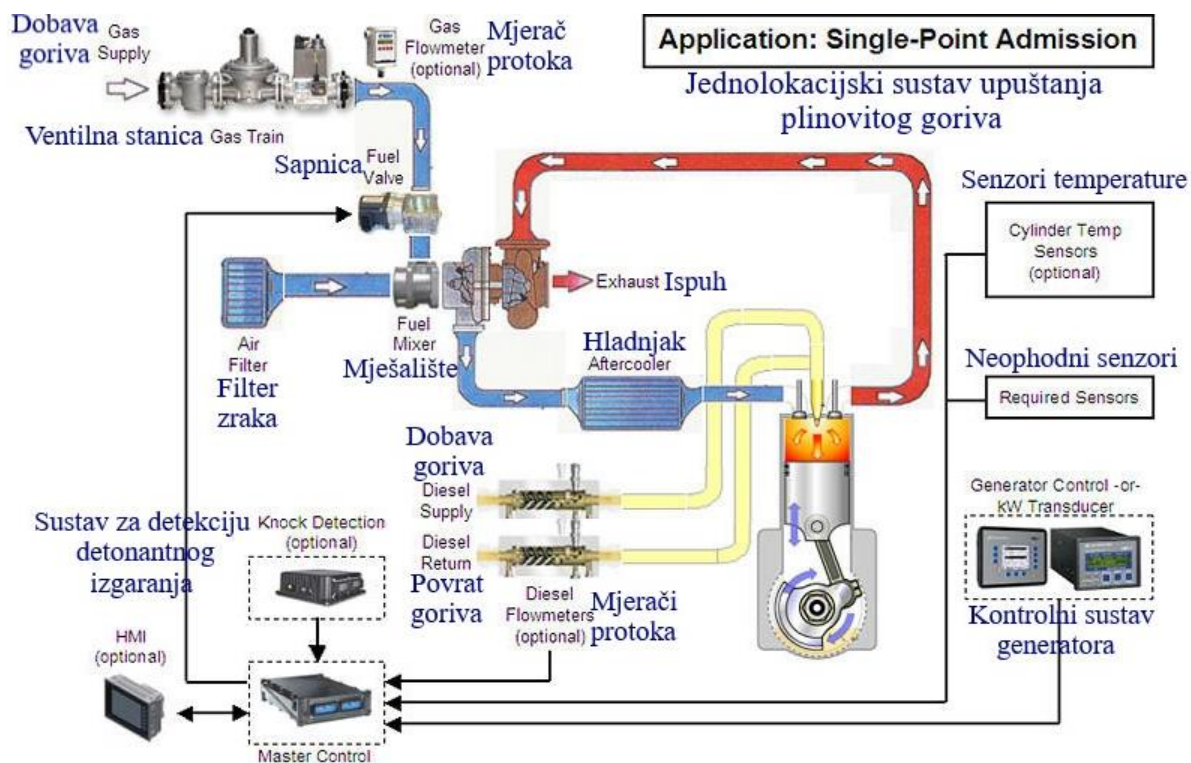
Figure 11 *Scheme of the single point gas admission fuelled system [18]*

Slika 11 Shematski prikaz centralnog upuštanja plinovitog goriva [18]

Dobavljano plinovito gorivo se filtrira neposredno ispred regulatora tlaka i zapornih ventila, pri čemu se njegov protok regulira prigušnim leptir ventilom (eng. *butterfly throttle valve*) posredstvom glavnog upravljačkog sustava, prije negoli se utisne u mješač. Upravljački sustav koristi cijeli niz senzora i pretvarača signala (eng. *transducers*) uključujući tlak plinovitog goriva, tlak i temperaturu zraka u usisnom kolektoru zraka, temeljem kojih proračunski određuje pogonski optimalni omjer dizelskog i plinovitog goriva, te potom podešava protočni regulacijski ventil plinovitog goriva u optimalni položaj. Ovom tehnikom napajanja plinovitog goriva omogućuje se zamjena dizelskog goriva s plinovitim u rasponu vrijednosti 50-70 %, a ponegdje i više.

Sustav zasebnog utiskivanja plinovitog goriva svakom cilindru

Kod srednjekretnih i umjereno brzokretnih motora plinovito gorivo se ne upušta na isti način kao kod izrazito brzokretnih motora, već se upuštanje vrši kroz zasebne ventile smještene u usisnoj grani svakog cilindra, po konceptu tzv. više pozicijskog utiskivanja (eng. *Multi Point Fuel Admission*, MPFA), Slika 12. Glavni faktor koji uvjetuje prisutnu različitost primijenjenih metodologija utiskivanja plinovitog goriva jest hodogram usisnih i ispušnih ventila, odnosno preciznije period preklapanja otvorenosti ovih ventila, koji unutar njihovog hodograma nastupa tijekom propuhivanja (ispiranja) cilindara, Slika 13. Da bi se osiguralo učinkovito propuhivanje cilindara kod Ottovih motora napajanih dvojnim gorivom, nužno je obustaviti ustrujavanje plinovitog goriva u cilindre tijekom navedenog perioda preklapanja otvorenosti ventila kako bi se onemogućilo eventualno prostrujavanje plinovitog goriva u ispušni kolektor, čija bi prisutnost u njemu bila potencijalno opasna zbog moguće pojave eksplozije. Ovaj planski

prekid napajanja plinovitim gorivom postiže se primjenom elektroničkog upravljanja prigušnim leptir ventilima plina svakog cilindra, koji su karakterizirani elektromagnetskim djelovanjem.
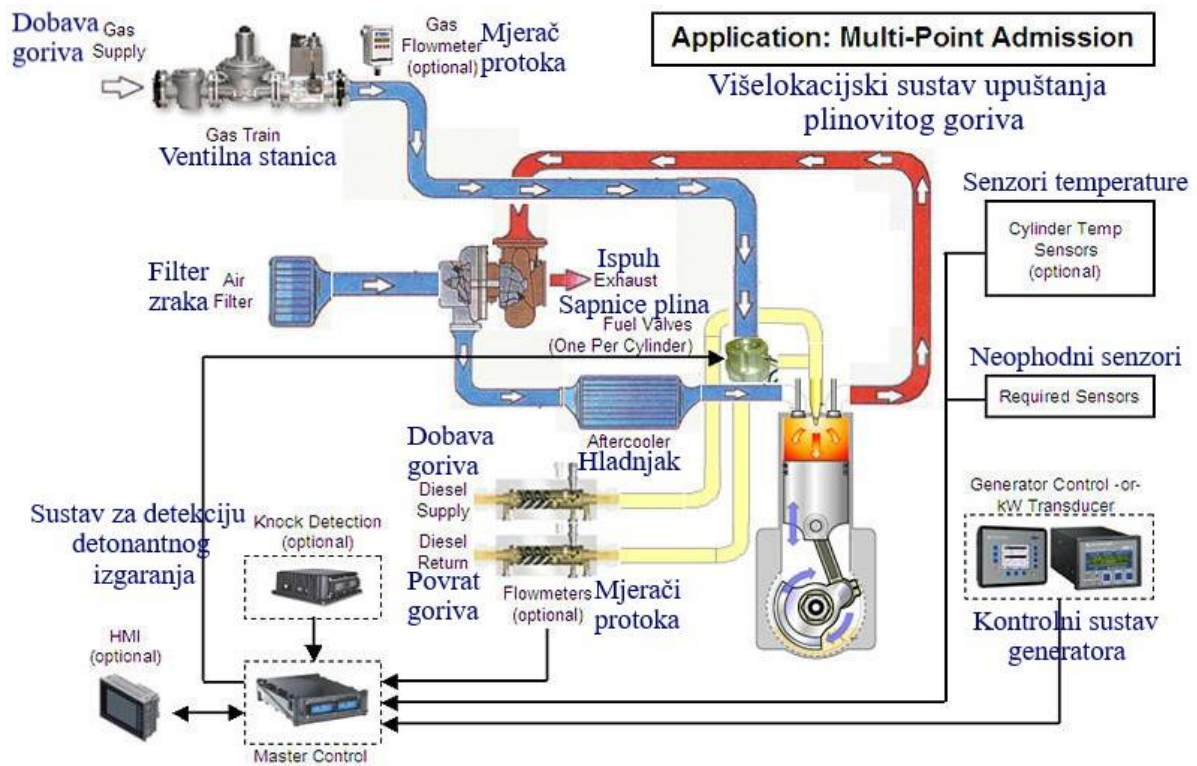
Figure 12 *Scheme of the multi point gas admission fuelled system (MPA) [18]*

Slika 12 Shematski prikaz zasebnog upuštanja plinovitog goriva cilindrima (eng. *Multi Point Admission*, MPA) [18]
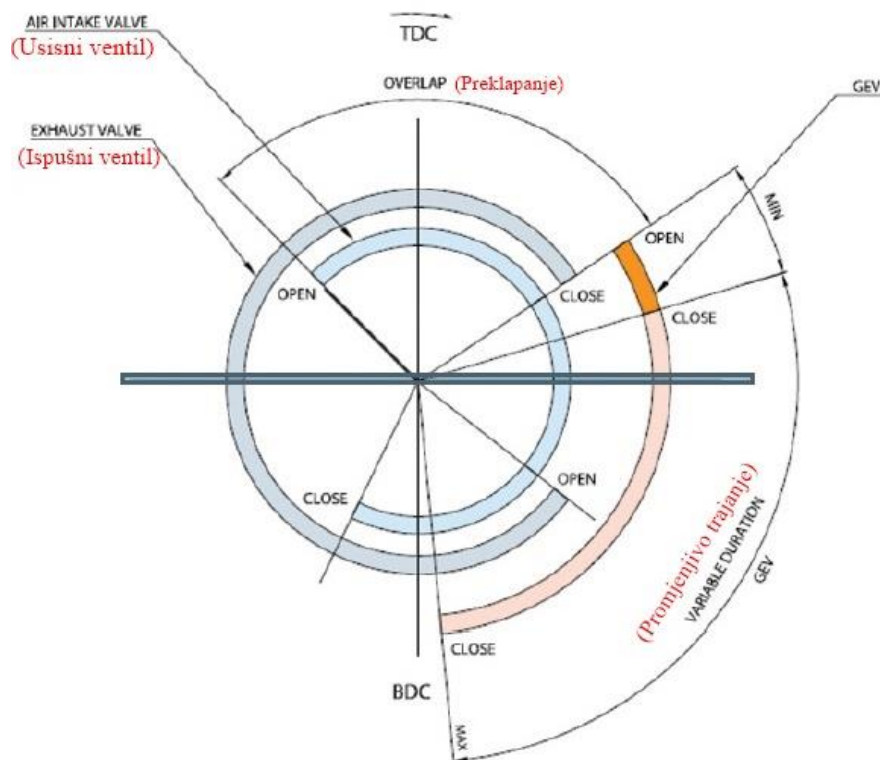
Figure 13 *Valve timing lift of the 4T DF engine [18]*

Slika 13 Hodogram ventila 4T DF motora (eng. *valve timing*) [18]

Kod izrazito brzokretnih motora na dvojno gorivo, preklopni period otvorenosti ventila je znatno kraći nego kod srednjekretnih i umjereno brzokretnih motora, tako da je kod njih moguće provesti kontinuirano napajanje plinovitog goriva. Kod srednjekretnih i umjereno brzokretnih motora elektronički se kontrolira pogon individualnih magnetskih ventila (eng. *solenoid valve*) pozicioniranih u usisnim granama pripadajućih cilindara, kao i profili i hodograma usisnih i ispušnih ventila, i hodograma ubrizgavanja dizelskog pilot goriva. Primjenom ove tehnike napajanja dvojnim gorivom obično se omogućuje zamjena dizelskog goriva sa plinovitim u iznosu od 60-80 %, a ponekad i više.

Adekvatan omjer zrak/gorivo, postiže se podešavanjem brzine vrtnje turbopuhala posredstvom elektronički kontrolirane zaklopke smještene u mimovodu ispušnih plinova oko turbine, Slika 14a. Kontrolirano napajanje plinovitim gorivom se vrši preko ventila za upuštanje plina (eng. *Gas Admission Valve*, GAV) smještenom u dobavnom kanalu nabijenog zraka tik ispred usisnog ventila u kojem se korištenjem sofisticiranog elektroničkog sustava reguliraju i tlak i količina utiskivanog plina. Time se nezavisno o otvorenosti usisnog ventila onemogućuje prostrujavanje istog u ispušni sustav, što je naročito važno tijekom perioda preklapanja otvorenosti usisnog i ispušnog ventila, Slika 14b.
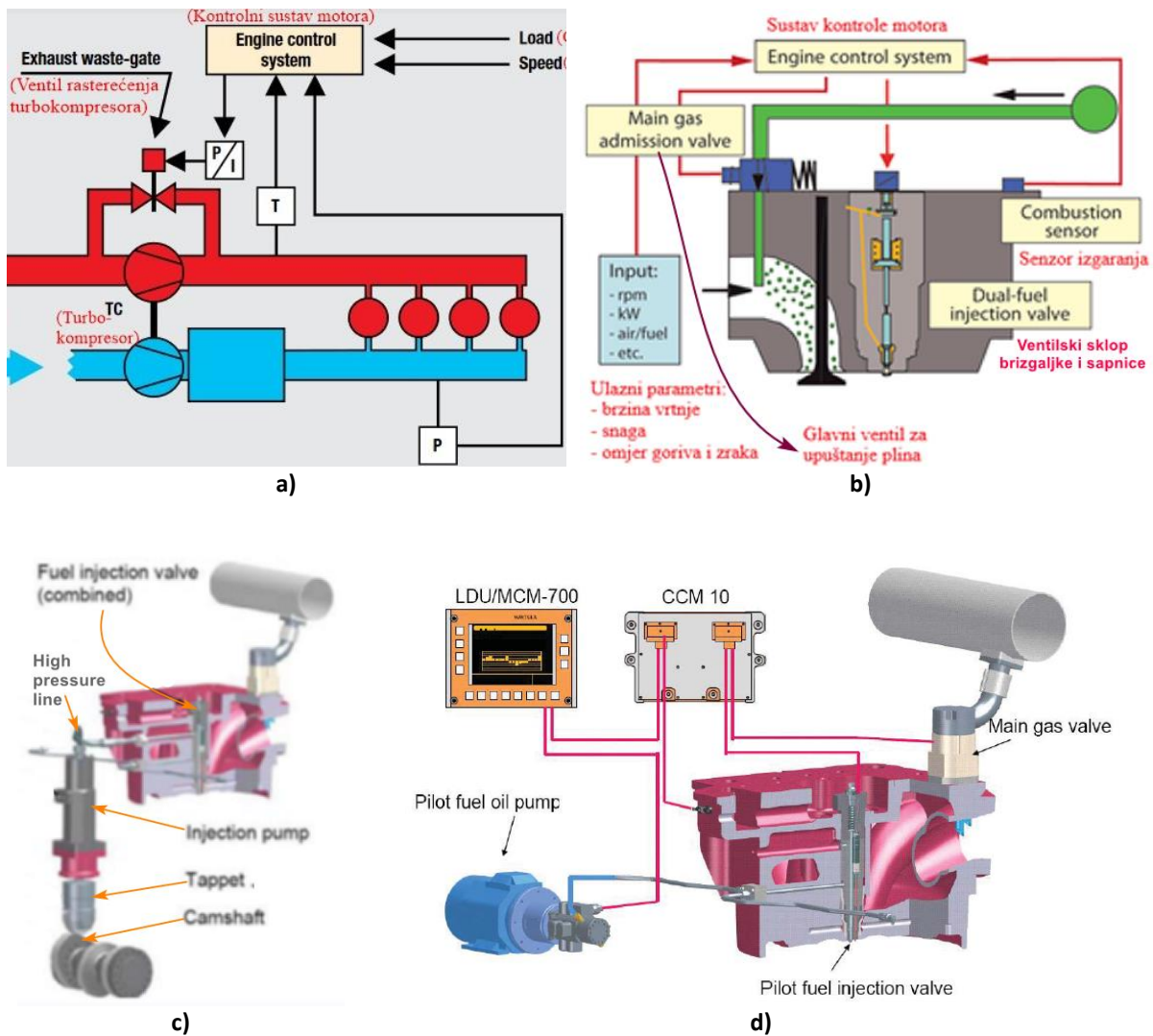
Figure 14 *a) Controlling air/fuel ratio by adjusting turbine speed, **b)** Cylinder control principle*

***c)** Classical fuel oil injection system*, ***d)** Controlling connections with cylinder head [13]*

Slika 94 a) Shematski prikaz sustava kontrole omjera goriva i zraka, **b)** Načelo upravljanja na glavi motora [13]

c) Klasični sustav za ubrizgavanja MDO/HFO, **d)** Upravljačke veze sa glavom cilindra [13]

Na sličan način se kontrolira količina glavnog i pilot dizelskog goriva, što omogućuje energetski i ekološki prihvatljivu optimizaciju pogona korištenjem ulaznih podataka poput: brzine vrtnje, opterećenja, omjera zrak/gorivo i sl.

Napajanje glavnog pogonskog goriva (MDO/HFO) vrši se klasičnim sustavom ubrizgavanja dizelskog goriva, Slika 14c, pri čemu je svaki cilindar opremljen sa jednom pumpom, koja je pogonjena bregastim vratilom i s jednom brizgaljkom, koja može biti jednokanalna ili dvokanalna kroz koju se osim glavnog pogonskog goriva ubrizgava pilot gorivo, ali iz zasebnog tzv. *common rail* sustava, Slika 15.
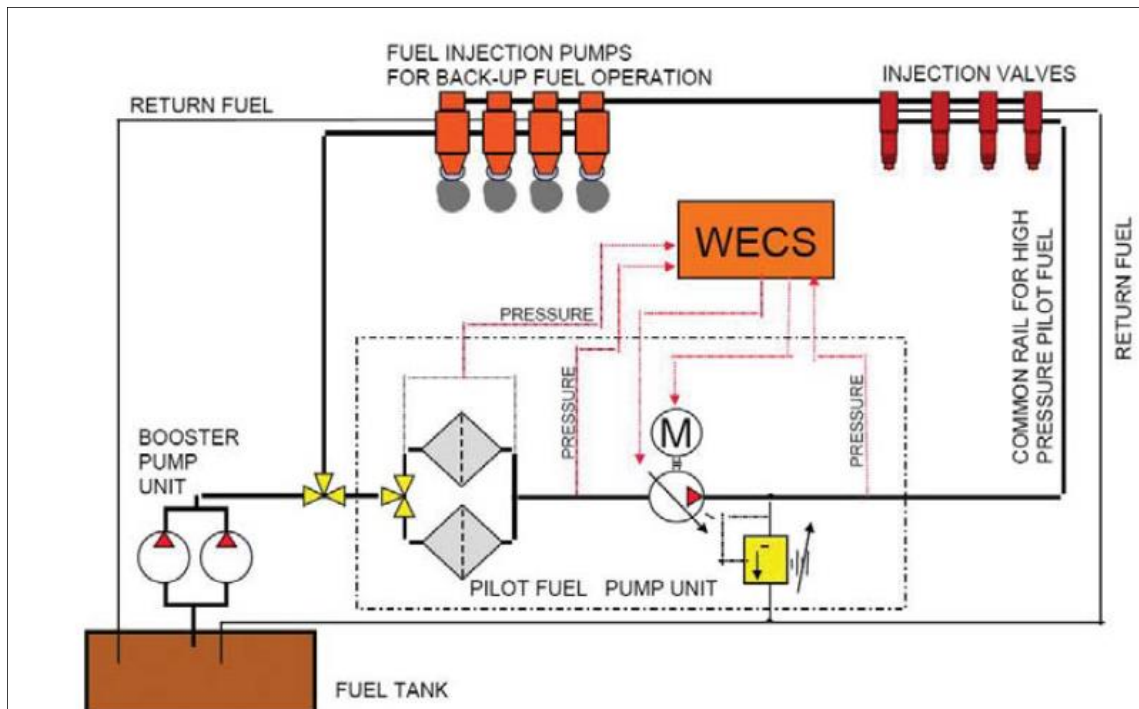
Figure 15 *Scheme of supplying and controlling of the mean and pilot fuel system [13]*

Slika 15 Shematski prikaz napajanja i kontrole u sustavu glavnog i pilotskog goriva [13]

Zasebni sustav kapljevitog pilot MDO-a uključuje radijalno klipnu pumpu promjenjive dobave, filtere goriva, regulator tlaka i zajednički vod akumulatorskog tipa (eng. *common rail*), kojim se omogućuje besprijekorna distribucija stlačenog goriva ($900 \, \text{bara}$) svakoj, elektronički kontroliranoj brizgaljci bez zamjetne fluktuacije tlaka. Elektroničkim upravljanjem pripadajućih elektromagnetskih ventila generira se optimalni hodogram ubrizgavanja pilot goriva u svaki cilindar tijekom plinskog operativnog moda motora.
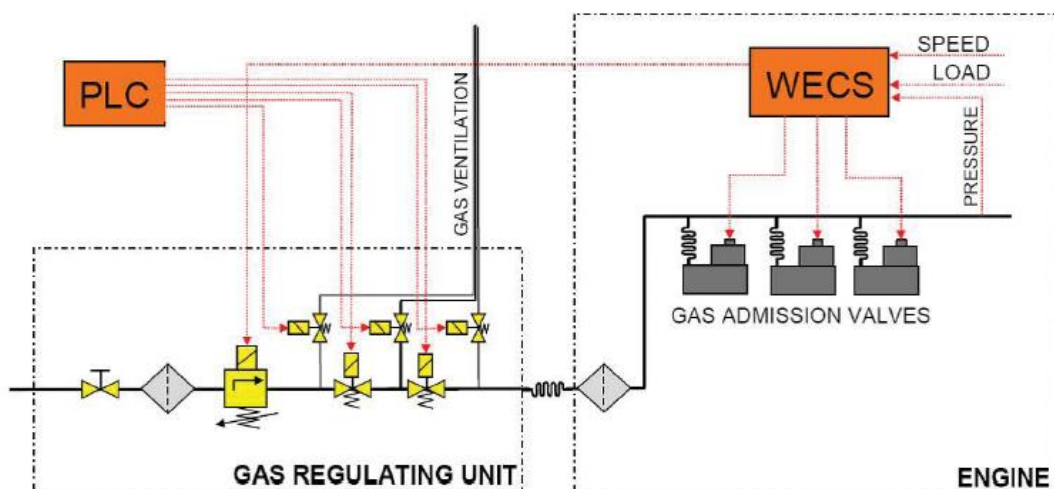
Figure 16 *Scheme of supplying and controlling of the gas fuel [13]*

356

Slika 16 Shematski prikaz napajanja i kontrole plinovitog goriva[13]

Pripadajući sustav distribucije i upuštanja plinovitog goriva prikazuje Slika 16, iz koje se vidi da isti prije upuštanja u dobavne kanale nabijenog zraka prostrujava kroz ventilsku plinsku stanicu (eng. *Gas Valve Unit*, GVU), koja sadrži filter, senzore tlaka i temperature, ventil za regulaciju tlaka, dva sigurnosna zaustavna ventila i tri daljinski kontrolirana regulacijska odušna (ventilacijska) ventila. Elektronički sustav upravljanja WECS 8000 (za Wartsiline 4T DF motore), sadrži dva glavna elektronička modula: glavni kontrolni modul MCM-700 i cilindarski kontrolni modul CCM-10, kao i mnoštvo drugih interaktivno povezanih elektroničkih modula, Slika 14d. Glavni kontrolni modul prikuplja i procesuira meritorne veličine tijekom nastupajućih operativnih uvjeta, temeljem kojih reguliranjem, hodogramom upuštanja plinovitog goriva (i hodogramom ubrizgavanja MDO/HFO u dizelskom operativnom modu) i omjerom zrak/gorivo, dovodi motor u optimalno pogonsko stanje. Ovo se postiže odašiljanjem referentnih signala, od strane glavnog kontrolnog modula prikupljenih informacija iz ostalih interaktivno povezanih kontrolnih modula, ka cilindarskom kontrolnom modulu. Propuštana količina plina u svaki cilindar regulira se sa GAV-ima koji su kontrolirani sa CCM-10, koji osim toga kontroliraju energijske unose s plinovitim gorivom i dizelskim pilot gorivom korištenjem izrazito jakih PWM signala (eng. *Pulse Width Modulation*). Svaki modul odašilje signale troputnim regulacijskim ventilima plina, kao i troputnim ventilima brizgaljki pilotskog dizel goriva, temeljem proračunatih hodograma upuštanja i ubrizgavanja ovisno o referentnim vrijednostima stečenim s glavnim kontrolnim modulom.

Brodski 4T GD motori (Dieselov operativni princip)

Kod brodskih 4T GD motora s turbonabijanjem plinovito gorivo se utiskuje u cilindre motora u komprimirani zrak pod visokim tlakom $\approx 350\,\text{bara}$ te se kao heterogena smjesa zapaljuje dizelskim pilot gorivom, kojeg se dodaje u odgovarajućem iznosu, najmanje oko 5% (*GM*), Slika 19a. Po potrebi je ostvariv dizelski operativni mod (*OM*) sa 100% kapljevitog goriva (MDO ili HFO), kao i kombinirani operativni mod (*FSM*) sa rasponom vrijednosti goriva, kapljevitog 15-80 % i plinovitog 80-15 %. U sva tri operativna moda GD projektnih izvedbi, kapljevito dizelsko gorivo se preko odgovarajućeg sustava za ubrizgavanje ubrizgava pilot brizgaljkama (GM), odnosno glavnim brizgaljkama (FSM i OM), neposredno prije utiskivanja stlačenog i pripremljenog plina, Slika 19b. Uobičajene su izvedbe sa sklopnom izvedbom brizgaljke i sapnice za unošenje kapljevitog i plinovitog goriva u komorni cilindarski prostor, Slike 17 i 18.
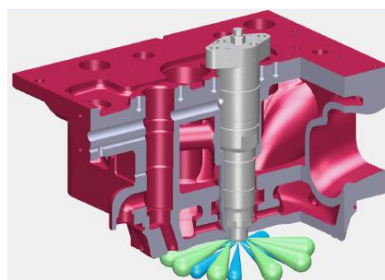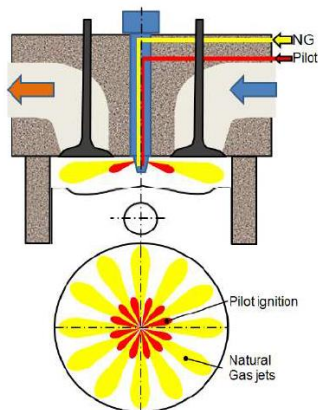
Difuzijsko izgaranje, neosjetljivost na detonaciju, praktički raspoloživi BOG ima dostatan metanski broj (MN-Methane Number)
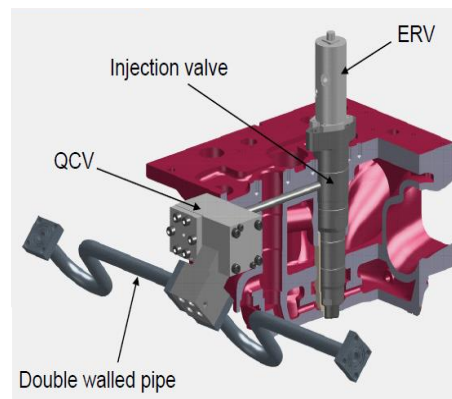
Figure 17 *Scheme of the pilot diesel oil injection and natural gas admission through common fuel element, with qualitative timing of the importation representation [6]*
Slika 17 Shematski prikaz ubrizgavanja dizelskog pilot goriva i prirodnog plina u cilindre sa prikazom kvalitativnog hodograma unosa [6]

Kod dizelskih plinskih motora plinovito gorivo se utiskuje u komprimirani zrak u cilindru motora uz istovremeno ubrizgavanje dizelskog pilot goriva potrebnog za samozapaljivanje stvorene heterogene gorive smjese.
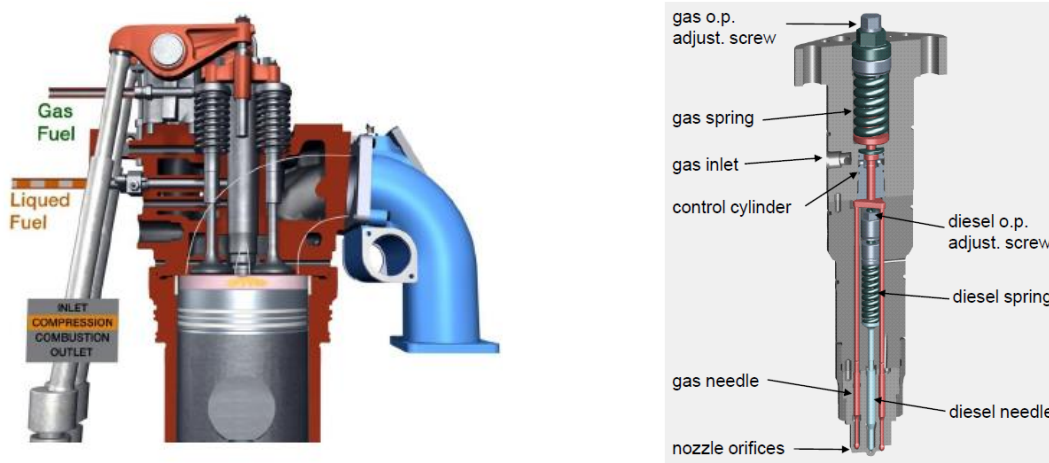
Figure 18 *Assembled design of the pilot fuel oil injector and fuel gas nozzle, from Wartsila 32GD [7]*
Slika 18 Sklopna izvedba brizgaljke dizelskog pilot goriva i sapnice plinovitog goriva, Wartsila 32GD [7]

Tlak plinovitog goriva na ulazu u cilindar mora biti veći od tlaka komprimiranog zraka u cilindru. Snaga motora je određena količinom ubrizgavanog plinovitog goriva te je zahvaljujući činjenici zadržavanja istog kompresijskog omjera kao onog kod motora napajanih dizelskim gorivom gotovo jednakog iznosa.
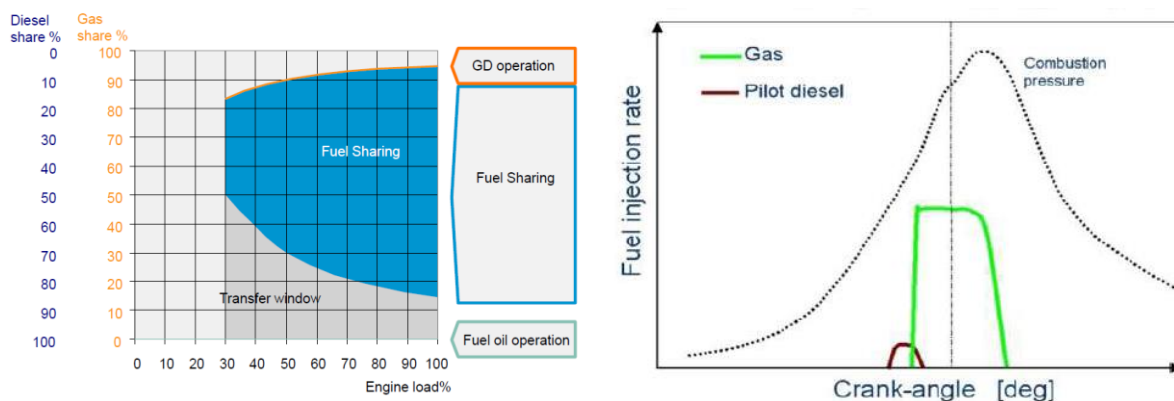
Figure 19 *Fuel supplying mods and timing of the both MDO injection and fuel gas admission, Wartsila 32GD [6]*
Slika 19 Modovi napajanja i kvalitativan prikaz profila ubrizgavanja MDO i utiskivanja plina Wartsila 32GD [6]

Sustav napajanja plinovitim gorivom čiju okosnicu čini višestupanjski visokotlačni kompresor prikazuje Slika 20. Prirodni plin se komprimira na tlak 250-350 bara, kako bi se omogućilo korektno

napajanje motora tijekom realističnih pogonskih uvjeta. Svi visokotlačni plinovodi unutar prostora strojarnice kao i na samom motoru, izvedeni su sa duplim cjevovodom pri čemu se kroz cjevovod manjeg promjera transportira plin dok je prostor kojeg formira koaksijalno postavljeni cjevovod većeg promjera iz sigurnosnih razloga provjetravan pripadajućim ventilacijskim sustavom. Isto tako iz sigurnosnih razloga taj koaksijalni otvor je kao i u njemu sadržani plinovod povezan sa sustavom inertnog plina kako bi se omogućilo inertiranje istog u slučaju detekcije eventualno propuštanog plina.

Unatoč brojnim komparativnim prednostima prema 4T DF motorima ovi motori se rijetko koriste na komercijalnim brodovima zbog izrazito visokih tlakova napajanja koji sami po sebi nameću potrebu za skupljim i tehnološki kompliciranijim sigurnosnim sustavima. U novije vrijeme radi se na intenzivnom razvoju suvremenih 4T GD motora, čime bi se omogućilo uvođenje istih na suvremene komercijalne brodove, posebice LNGC-e.
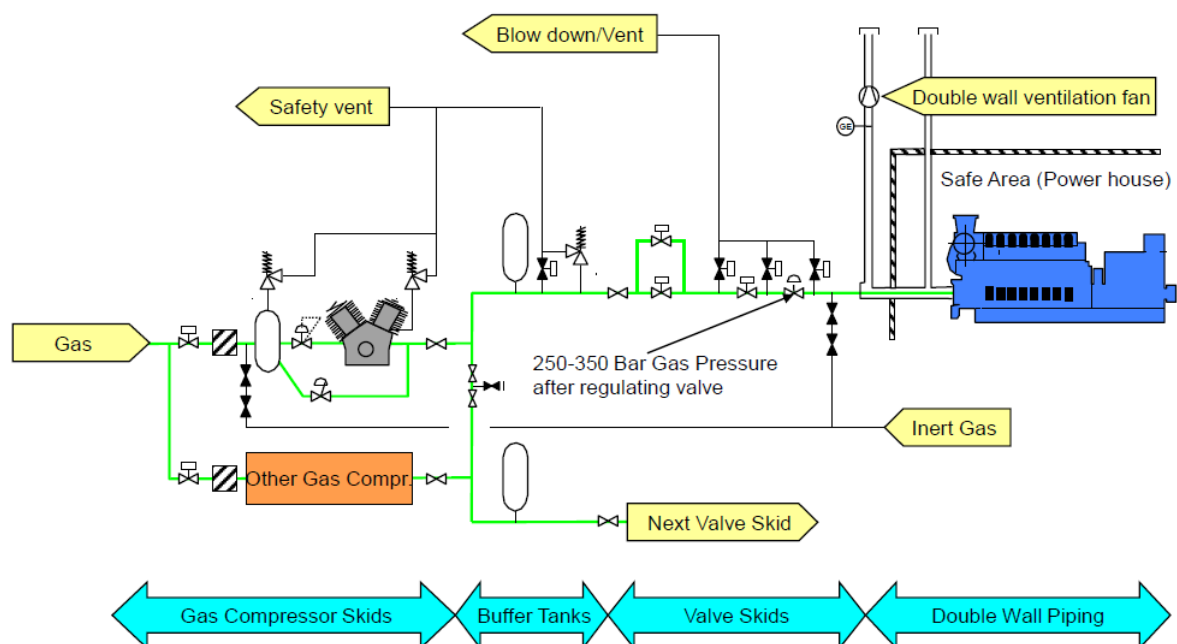
Figure 20 *Wartsila 32GD engine high pressure gas fuel system [6]*
Slika 20 Visoko-tlačni sustav plinovitog goriva Wartsila 32GD motora [6]

4. Brodski dvotaktni dizelski motori na dvojno gorivo

Kako je već prije istaknuto aktualne su dvije izvedbe brodskih 2T dizelskih motora na dvojno gorivo, one koje rade po Ottovom principu (koje se može klasificirati 2T DF motorima), kod kojih se pripremljeni prirodni plin upušta pri razmjerno niskom tlaku ($10 \div 16$ bara) otprilike na pola kompresijskog takta, te se potom nakon miješanja sa zrakom neposredno pred kraj kompresije zapaljuje dizelskim pilot gorivom u pretkomori, (Wartsilini 2T DF motori), Slika 21a, te one koji rade po Dieselovom principu (koje se može klasificirati 2T GD motorima), kod kojih se pripremljeni prirodni plin utiskuje pred kraj kompresijskog takta pri razmjerno visokim tlakovima (≈ 300 bara), te se nakon miješanja sa komprimiranim zrakom zapaljuje dizelskim pilot gorivom (MAN-ovi 2T GD motor), Slika 21b. Obzirom na postavljene IMO-ove ekološke propise (*Trier III NO$_x$ requirements*)

glede smanjenja emisije NO$_x$, 2T DF izvedbe su prihvatljive zbog svojstvene visoke redukcije dušičnih oksida, što nije slučaj sa 2T GD izvedbama koje radi reduciranja dušičnih oksida na prihvatljivu razinu moraju biti opremljeni sa SCR (eng. *Screen Catalytic Converter*) ili EGR (eng. *Exhaust Gas Recovery*) sustavima. S druge strane zahvaljujući niskotlačnom sustavu plinovitog goriva primjena 2T DF u odnosu na 2T GD smanjuje kapitalne (*CAPEX*) i operativne (*OPEX*) troškove, jer nema potrebe za instaliranjem skupocjenih i energijski zahtjevnih (razmjerno nezanemarivih pogonskih snaga), visokotlačnih plinskih sustava, bilo onih sa koji kombiniraju visokotlačne pumpe i visokotlačne evaporatore LNG-a ili onih koji koriste visokotlačne više-stupanjske stapne kompresore sa među-hlađenjem. Valja k tomu još dodati da su zahvaljujući niskom tlaku napajanja plinovitim gorivom 2T DF motori puno manje zahtjevni glede monitoringa postavljanja sigurnosnih mjera u odnosu na 2T GD motore.

a) Ottov princip rada (Wartsilini motori)   **b)** Dieselov princip rada (MAN-ovi motori)
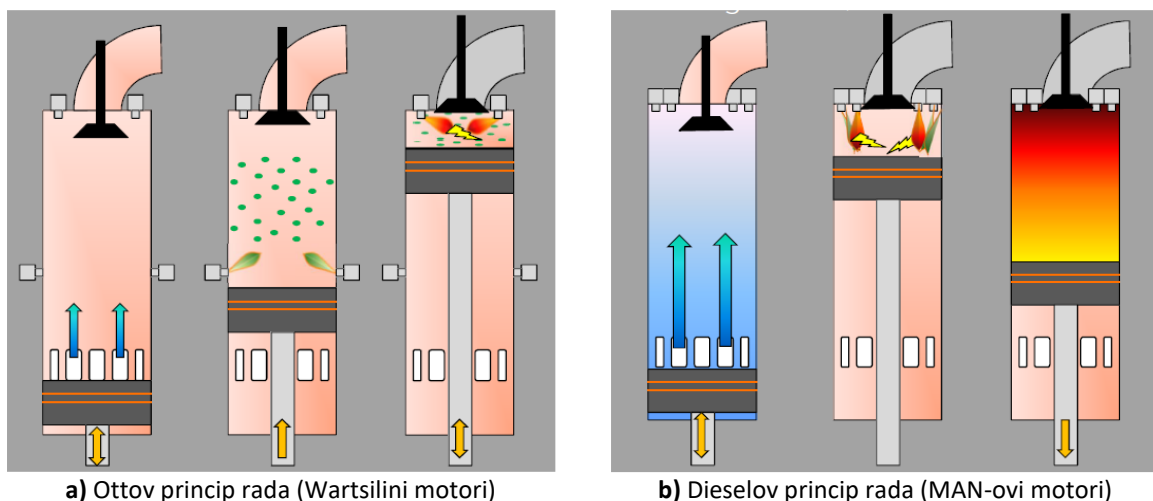
Figure 21 a) *Otto (Wartsila) and* **b)** *Diesel (MAN) working principles of the dual fuelled engines [6]*
Slika 21 a) Ottov (Wartsila) i **b)** Dieselov (MAN) radni princip 2T motora na dvojno gorivo[6]

Brodski 2T DF motori (Otto-Dieselov operativni princip)

Koncepcijske izvedbe sustava skladištenja i pripreme plinovitog goriva za 2T DF motore na LNGC-ima i konvencionalnim brodovima sa plinificiranim energetskim sustavima identične su onima za 4T DF prikazane Slikama 8 i 9, iz čega je razvidno da se zbog skladištenja LNG na tlaku bliskom atmosferskom u tankovima tereta, BOG ili prisilno isparena vrela kapljevina LNG-a u evaporatoru, moraju komprimirati na traženi tlak, koji će biti uvećan u odnosu na tlak napajanja motora za iznos pada tlaka u napojnom plinovodu prouzročenom nastupajućim aerodinamičkim otporima strujanju. Kod konvencionalnih brodova tlak skladištenja LNG-a je određen iznosom traženog tlaka napajanja, padom tlaka prostrujavanjem kroz plinovod i procijenjenim prirastom tlaka LNG-a u skladišnim tankovima zbog sveukupno nastupajućeg toplinskog opterećenja, pa u tom slučaju nema potrebe za ugradnjom kompresora i isparivača plina. Kako je uobičajeno i na LNGC-ima i na konvencionalnim brodovima sa plinificiranim energetskim sustavima napajanja s prirodnim plinom i glavnog 2T DF i pomoćnih 4T DF motora izvodi se sa zajedničkim sustavom plinovitog goriva, Slika 22 za konvencionalne brodove (kod LNGC-a se radi o gotovo identičnim sustavima). U ovoj izvedbi se vrši stlačivanje kapljevite faze LNG-a tlačnim pumpama, koja se potom prolaskom kroz evaporator potpuno isparava tako da je temperatura tako generiranog plinovitog goriva na ulasku u motore u

rasponu vrijednosti $0\,^0\mathrm{C} \le \vartheta \le 60\,^0\mathrm{C}$, dok je tlak istog ispred glavnog pogonskog 2T DF motora 16 bara, odnosno ispred 4T DF diesel-generatora 6 bara. Inače je samo napajanje 4T DF diesel generatora izvedivo samo grijanjem BOG-a iz LNG tanka, kako je to već prethodno izloženo.

Za razliku od 4T DF motora, 2T DF motori mogu raditi, osim u plinskom i dizelskom operativnom modu, i u kombiniranom plinsko-dizelskom modu (tzv. *FSM*, poput 4T GD motora) i to u rasponu sljedećih energetskih vrijednosti: plinski operativni mod, manje od 1% energije preko pilot goriva (MGO/MDO) i 99% energije preko plinovitog goriva, dizelski operativni mod 100% energije sa MGO/MDO/HFO, kombinirani plinsko-dizelski operativni mod provediv jedino u rasponu opterećenja motora od 50-100 %, i to sa 5-50% energije preko MGO/MDO/HFO i 50-95% energije preko plinovitog goriva, Slike 23 i 24. Prilikom rada u dizelskom operativnom modu (koji je inače raspoloživ uvijek osiguravajući operativnu fleksibilnost posebice u slučaju kvara unutar plinskog sustava), napajanje motora sa MDO/HFO se provodi preko glavne brizgaljke uz istovremeno reducirano napajanje sa MDO preko pilot brizgaljke (oko 0,5% sveukupne potrošnje), kako bi se omogućilo njeno hlađenje i spriječilo začepljenje njenih mlaznica. Prije prebacivanja na plinski operativni mod prelazi se s HFO na MDO napajanje.
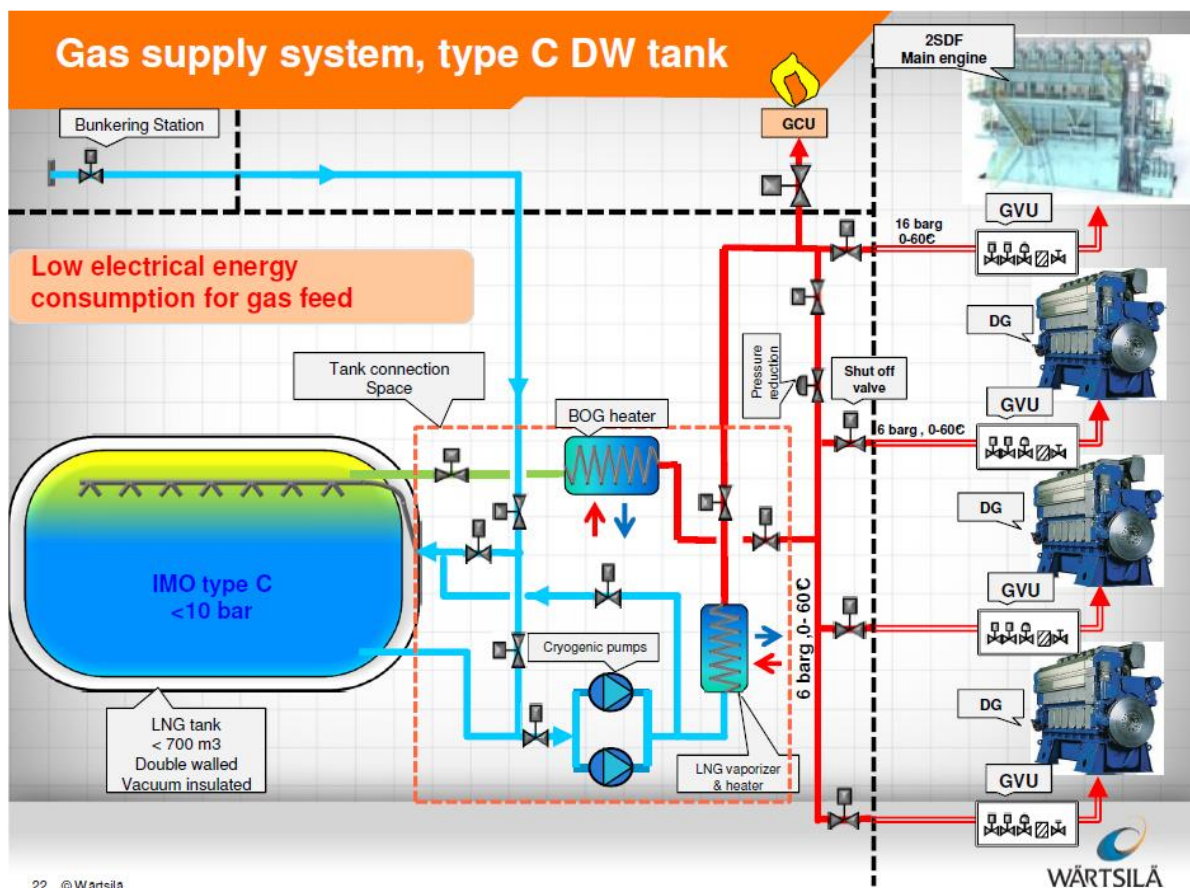
Figure 22 *Fuel gas supply system of main 2T DF engine and 4T DF gen.sets on fuelled gas ship [11]*
Slika 22 Sustav plinovitog goriva glavnog 2T DF i pomoćnih 4T DF motora na konvencionalnom brodu [11]
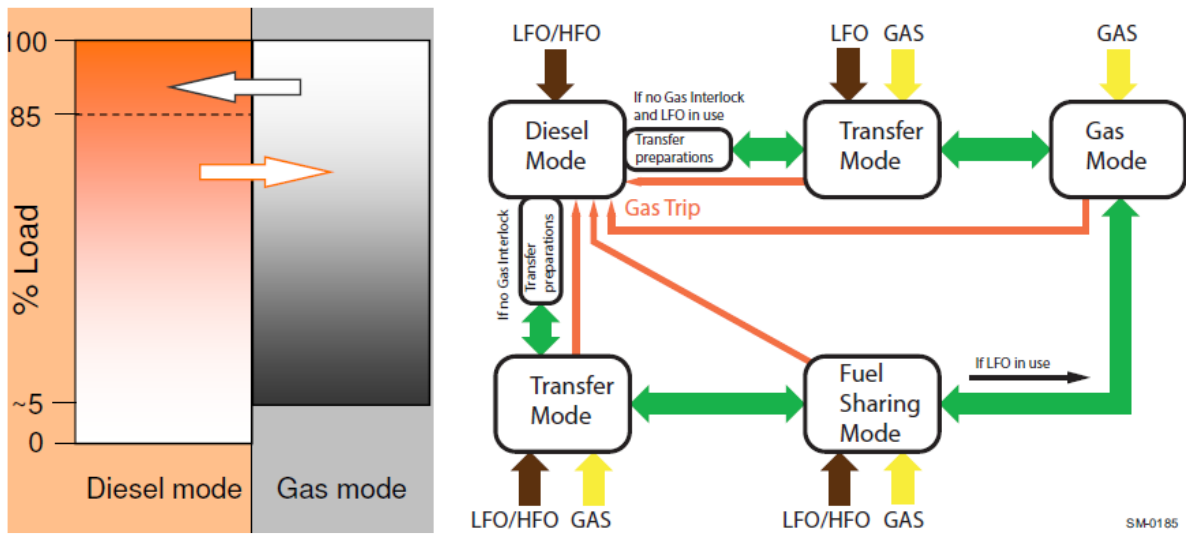
Figure 23 *Fuel gas (LNG) systems of DF 2T engines on the LNGC and on gas fuelled ships [8], [12]*
Slika 23 Sustavi plinovitog goriva DF 2T motora na LNGC i konvencionalnim brodovima za [8], [12]

FSM iziskujući najmanje 5% energije unesene kapljevitim gorivom, s mogućošću podešavanja omjera plinovitog i kapljevitog goriva (HFO/MGO/MGO), naročito je koristan pri balansiranju raspoloživog BOG-a i brzine plovidbe broda.

Prebacivanje s plinskog na dizelski mod koje traje obično 1-2 minute, moguće je ostvariti uvijek neovisno o opterećenju i brzini vrtnje motora, dok je obrnut prijelaz moguć jedino u rasponu od 10% do 80% nazivne snage motora. U plinskom modu nije moguće preopterećivanje motora, kao što je to kod dizelskog moda kojim se omogućuje kratkotrajno preopterećenje do 110% u iznimnim situacijama.
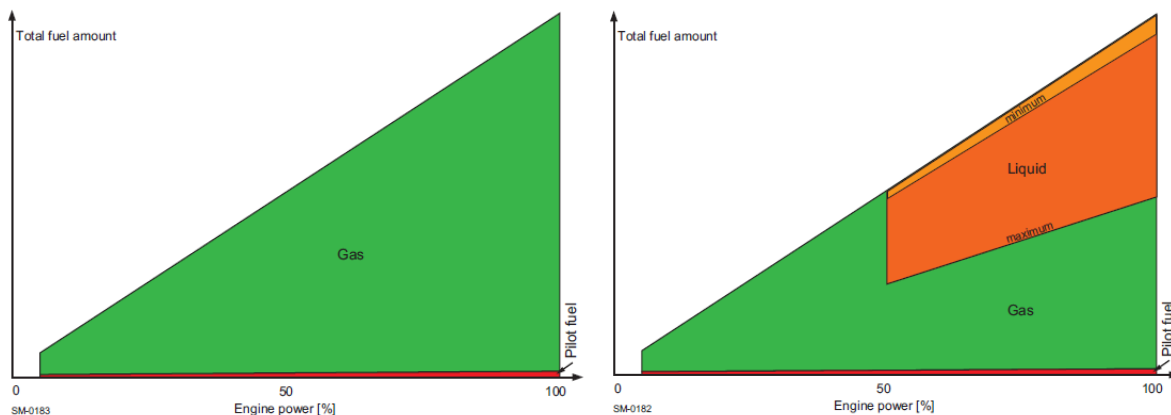
Figure 24 *Qualitative diagrams of gas and diesel fuel amounts in both gas mode and FSM [12]*
Slika 24 Kvalitativni prikaz udjela plinovitog i kapljevitog goriva tijekom plinskog i SFM [12]

Tijekom operativnog plinskog moda, prirodni plin se upušta kroz odgovarajuće ventile u svaki cilindar gdje se odmah potom miješaju sa zrakom. Plinovod je izveden s dvostrukom stjenkom, pri čemu je koaksijalni prstenasti prostor između cijevi ventiliran zahvaljujući podtlaku kojeg generira ekstrakcijski ventilator prostora GVU-a, Slika 25, a koji sadrži sve elemente kao i istovrsni u sustavima

plinovitog goriva 4T-DF motora. Tlak plinovitog goriva na ulazu u motor podesiv je unutar razmjerno uskog raspona vrijednosti koje korespondiraju nastupajućem opterećenju motora, kako bi se osigurao stabilan tlak plina u tlačno-akumulacijskoj cijevi (eng. *common rail pipe*). Navedeno se postiže posredstvom ventila za regulaciju tlaka, koji je upravljan s kontrolnim sustavom motora, pri čemu razmjerno mala količina plina zatečena između ovog ventila i motora poboljšava odzivno vrijeme sustava tijekom nastupajućih pogonskih tranzijentnosti poput fluktuirajućeg opterećenja motora. Očitanja senzora unutar GVU-a, kao i otvaranje i zatvaranje ventila, kontrolirani su elektronički ili elektro-pneumatski posredstvom kontrolnog sustava GVU-a.
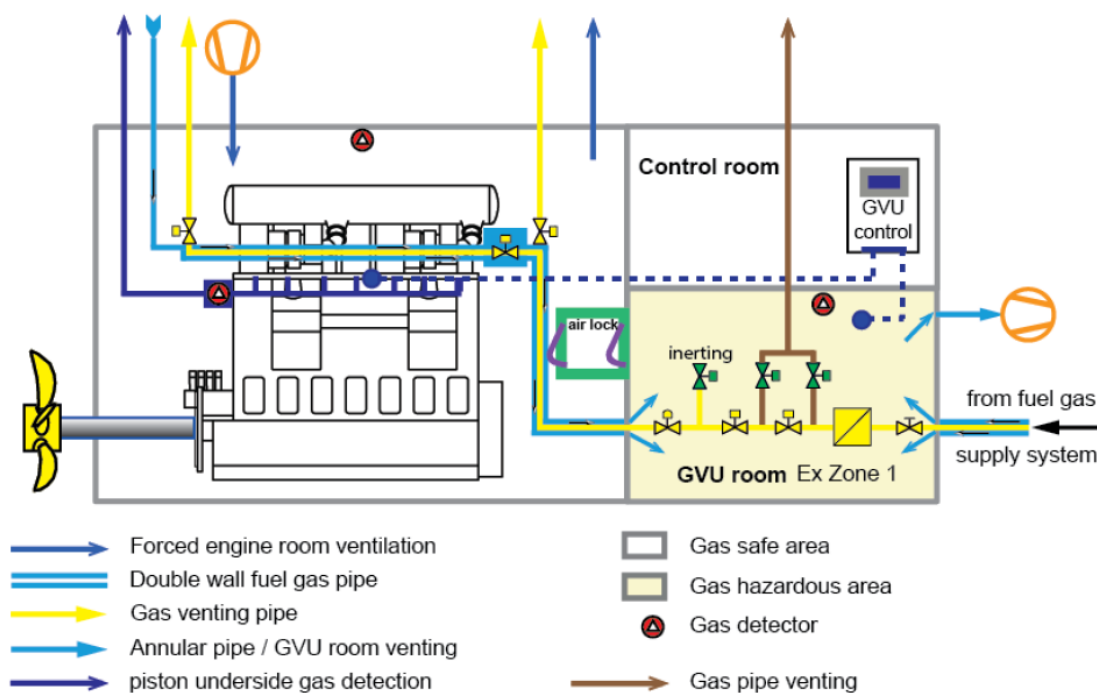
Figure 25 *Gas fuel system of DF 2T engines [16]*
Slika 25 Sustav plinovitog goriva DF 2T motora [16]

Brodski 2T GD motori na dvojno gorivo

U osnovi sustavi napajanja plinovitim gorivom GD 2T glavnih motora na LNGC mogu biti izvedeni sa visokotlačnim višestupanjskim kompresorima Slika 26, ili sa visokotlačnim pumpama u kombinaciji s evaporatorima Slika 27. Ukoliko su na brodovima instalirani 4T DF električni generatori, za potrebe njihovog napajanja se koristi prirodni plin niskog tlaka koji se oduzima iz kompresora nakon prolaska kroz drugi stupanj, Slika 26.
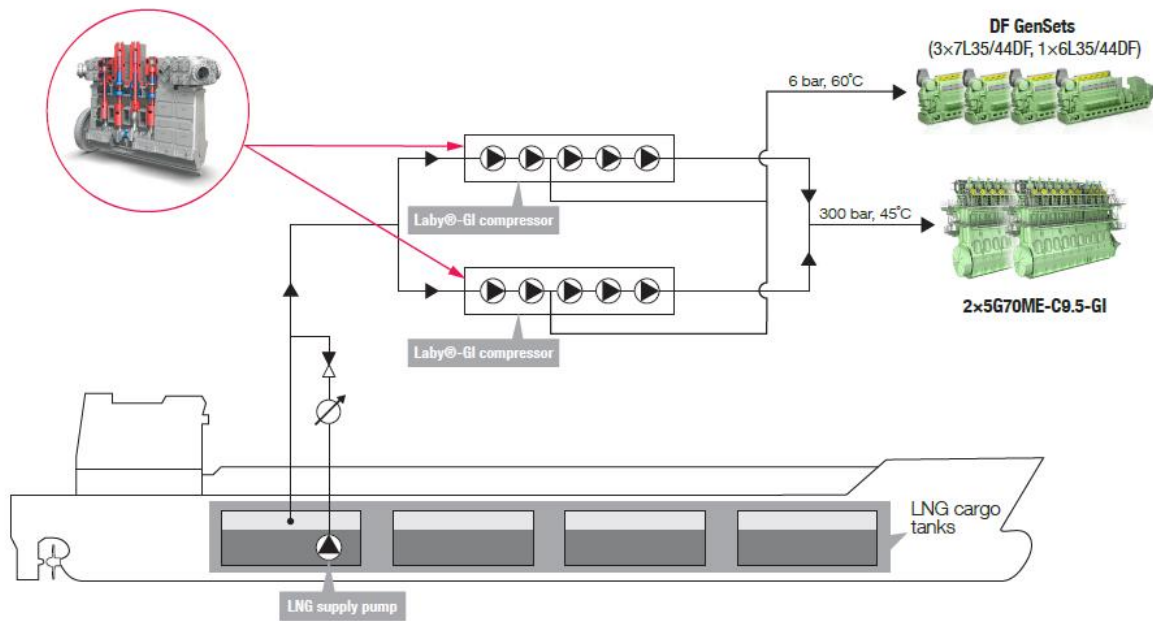
Figure 26 *Fuel gas supply systems with two multistage compressors for GD 2T main engines and DF 4T gensets on the LNGC [10]*
Slika 26 Sustav napajanja plinovitim gorivom sa dva više-stupanjska kompresora glavnih pogonskih GD 2T motora i DF 4T dizel-generatora na Qmax LNGC u [10]

Ukoliko je visokotlačni sustav plinovitog goriva za napajanje glavnog 2T GD motora izveden s visokotlačnom pumpom LNG-a i evaporatorom, napajanje 4T DF dizel-generatora se vrši preko niskotlačnih kompresora BOG-a, Slika 28.
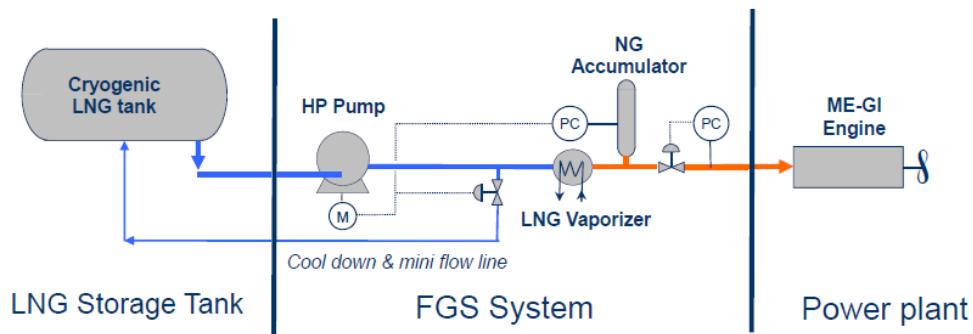
Figure 27 *Fuel gas supply systems with high-pressure pump and evaporator for GD 2T main engines [11]*
Slika 27 Sustav napajanja LNG-a sa visokotlačnom pumpom i evaporatorom glavnog GD 2T motora [11]
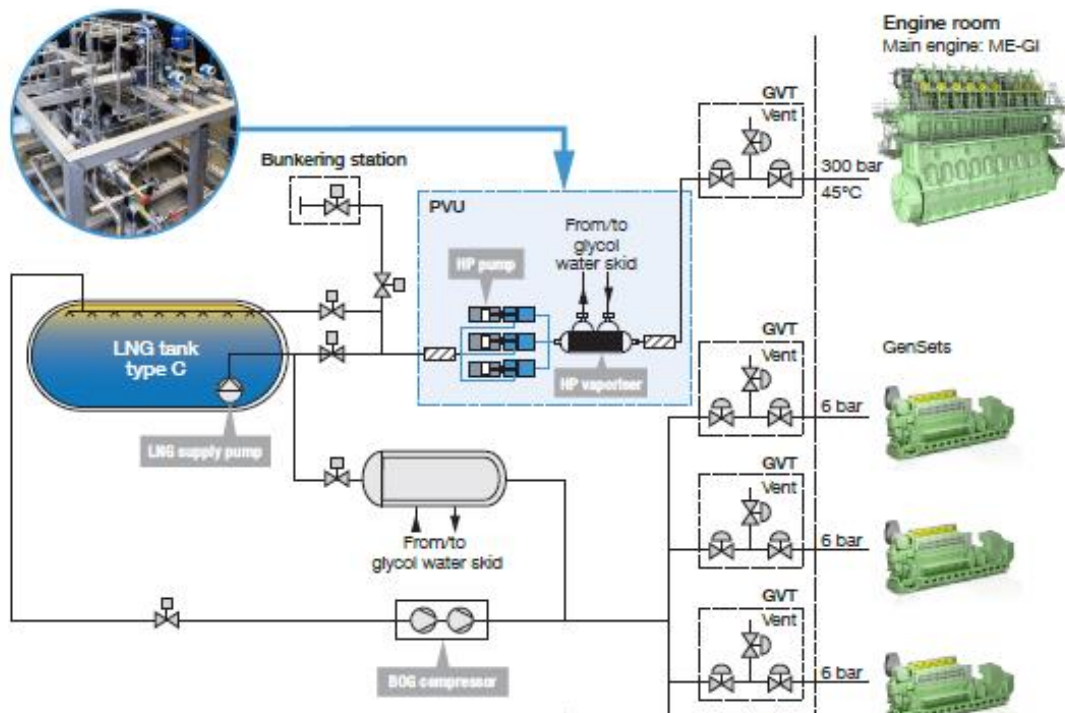
Figure 28 *Fuel gas supply system for LNG-fuelled vessels based on the pump and vaporiser unit*

for GD 2T main engines and DF 4T gen.sets [10]

Slika 28 Sustav napajanja plinovitim gorivom; sa visokotlačnim pumpama LNG-a i evaporatorom za GD 2T glavni motor i sa niskotlačnim kompresorom BOG-a za napajanje DF 4T dizel-gen. [10]

U svrhu optimizacije uvjetovane operativnim okolnostima često se odabiru rješenja koja integriraju kompresore sa pumpama i evaporatorima omogućujući pri tome parcijalno ukapljivanje (relikvifikaciju) BOG-a, Slika 29.
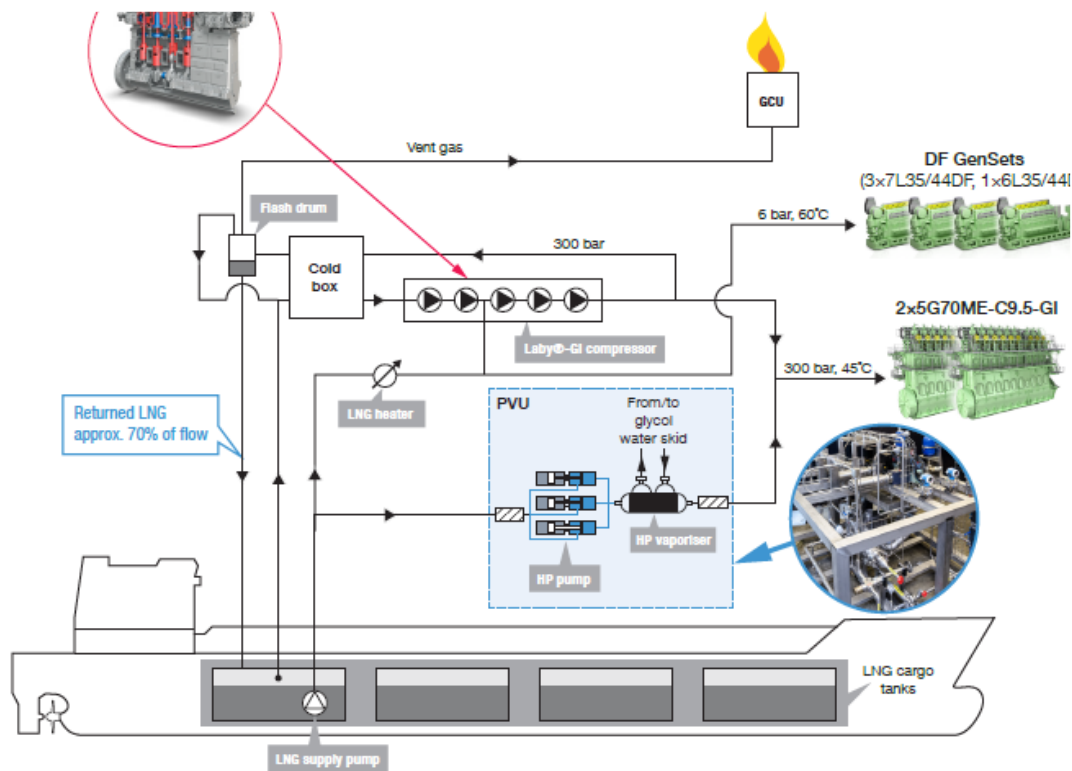
Figure 29 *Fuel gas supply system for a Qmax LNGC with partial reliquefication [10]*

Slika 29 Sustav napajanja plinovitim gorivom sa parcijalnim ukapljivanjem BOG-a na Qmax LNGC-ima [10]

Tijekom transportnog ciklusa LNGC-a ogrjevne vrijednosti BOG-a variraju od minimalno nastupajuće tijekom isplovljavanja nakrcanog broda (zbog velike prisutnosti dušika) do maksimalno nastupajuće tijekom prisilnog isparavanja kapljevite faze koja sadrži zamjetne udjele etana i propana, posebice tijekom plovidbe u balastu kada je iznos prirodno generiranog BOG-a nedostatan za napajanje 2T GD motora. Ovi motori su opremljeni s visokotlačnim sustavom (kompresorskim ili pumpno-evaporatorskim) za utiskivanje plinovitog goriva (NG), te su osposobljeni za dva operativna moda: izgaranje samo dizelskog goriva i dizelskim gorivom potpomognuto (preko pilot sustava) izgaranje plinovitog goriva varijabilne ogrjevne vrijednosti bez narušavanja termičke iskoristivosti motora. Operativni mod napajanja isključivo sa MDO/HFO svojstven je za opterećenja motora do 30%, jer tada napajanje plinovitim gorivom potpomognuto dizelskim preko pilot sustava ne osigurava stabilno izgaranje. Za sva pogonska opterećenja iznad 30% raspoloživa su dva operativna moda napajanja sa prethodno komprimiranim prirodnim plinom uz dodavanje dizelskog goriva (tzv. pilot gorivo). U tzv. operativnom modu s minimalno propisanom količinom pilot goriva, koja se kreće 5-8% ovisno o kvaliteti pilot goriva, a određuje se za 100% opterećenje motora te se održava konstantnom u rasponu opterećenja 30-100%, varijabilan je potrebni iznos plinovitog goriva te se isti u slučaju nedostatnosti BOG-a (nBOG) nadopunjuje s potrebnom količinom NG-a (pBOG), generiranom prisilnim isparavanjem LNG-a, Slika 30. Konačno, za raspone opterećenja 30-100%, operativni mod sa specificiranom količinom plinovitog goriva omogućuje istovremeno izgaranje raspoloživog BOG-a i dizelskog goriva (MDO/HFO) varijabilnog iznosa.
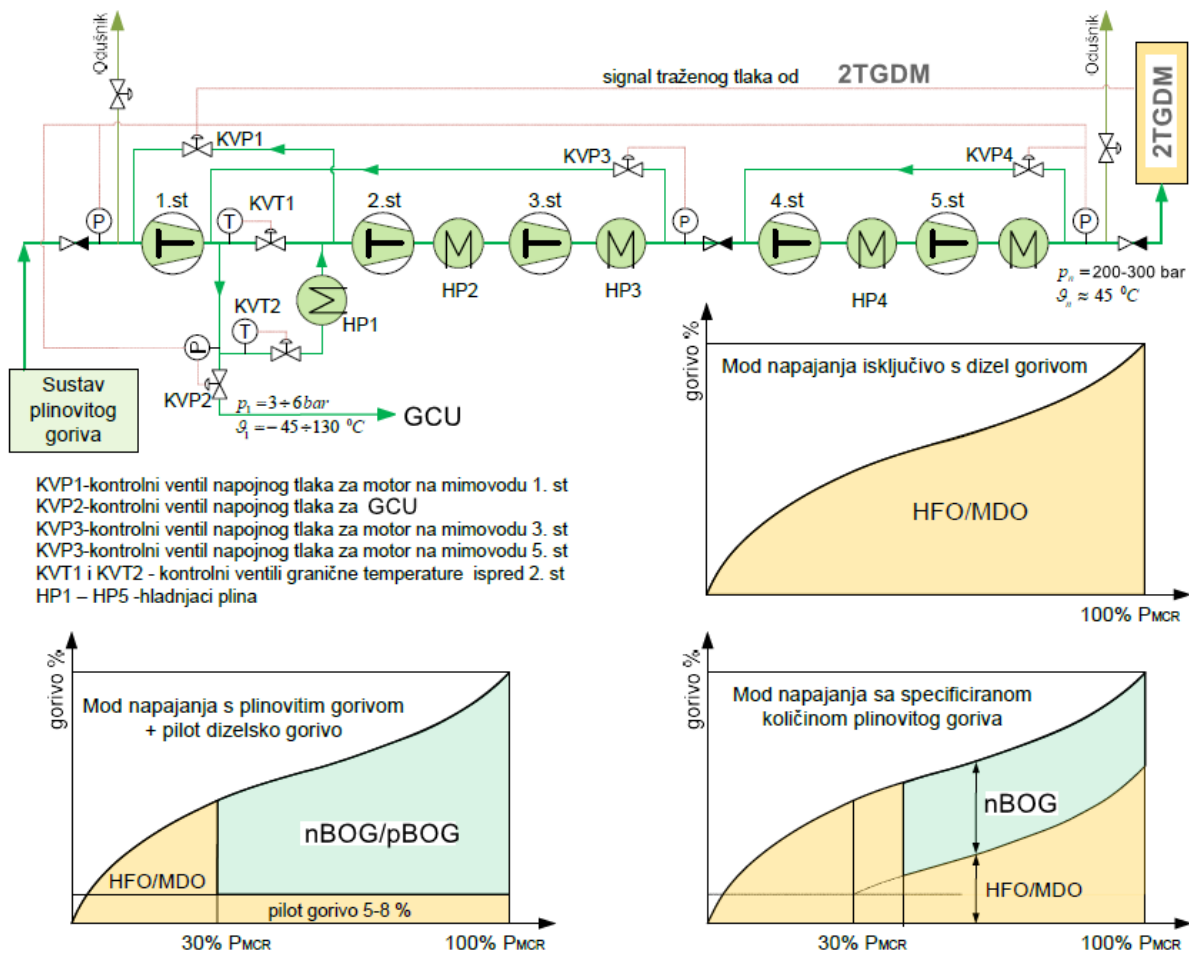
Figure 30 *System schematic of reciprocating fuel gas compressor and supply fuel modes*

Slika 30. Shematski prikaz visokotlačnog klipnog kompresora za plinovito gorivo i modovi napajanja gorivom

Za razliku od 4T DF srednjekretnih i brzokretnih motora i 2T DF gdje se plinovito gorivo utiskuje u cilindre pri razmjerno umjerenom tlaku i miješa sa zrakom, a potom zapaljuje s pilot gorivom, kod 2T GD sporokretnih motora plinovito gorivo se utiskuje u cilindre motora pri visokom tlaku (200-300 bara) i to nakon inicijalnog zapaljenja pilot goriva u modu s varijabilnim iznosom BOG-a, odnosno nakon zapaljenja varijabilnog iznosa dizelskog goriva u modu sa specificiranim iznosom nBOG-a. Budući da plinovito gorivo ne sadrži štetni sumpor, tijekom napajanja plinovitim gorivom preporučljivo je koristiti jeftinije cilindarsko ulje TBN40, te normalno tijekom napajanja isključivo teškim dizelskim gorivom prebaciti na podmazivanje s cilindarskim uljem TBN70.

Komprimiranje BOG-a kao pogonskog goriva za 2T GD motore, vrši se uporabom više-stupanjskog klipnog kompresora s izvedenim hlađenjem između karakterističnih stupnjeva (cilindara), kako to ilustrira priložena Slika 30. za 5-stupanjski klipni kompresor. Ovo visokotlačno kompresorsko postrojenje omogućuje reguliranu dobavu komprimiranog plina motoru unutar plinskom operativnom modu svojstvenog raspona opterećenja (30-100%) održavajući tlak napajanja linearno ovisnim o opterećenju motora s odgovarajućim rasponom vrijednosti od 200-300 bara. Kako je ovaj kompresorski sustav nadomjestak za LDC (eng. *Low Duty Comprresor*), istim se nakon prvostupanjske

kompresije napaja GCU (eng. *Gas Combustion Unit*), a po potrebi loženi kotao i 4T DF motori, pa se obzirom na preferiranu zalihost instaliraju po dva visokotlačna kompresorska postrojenja čija pojedinačna dobava u slučaju jednovijčane propulzije mora biti najmanje jednaka maksimalno predvidivoj količini nBOG-a, dok u slučaju dvovijčane propulzije ovaj dobavni iznos odgovara ukupnoj dobavi obaju kompresora.

2T GD sadrže elektro-hidraulički sustav upravljanja posredstvom kojeg se visokotlačnim hidrauličkim uljem po danom nalogu otvaraju sapnice plinovitog i brizgaljke kapljevitog goriva, dok se njihovo zatvaranje vrši pomoću pripadajućih opruga, Slike 31 i 32. Tako u radu sa plinovitim gorivom, ELGI ventil (eng. *Electronic Gas Injection Valve*) u točno određenom trenutku dobiva električni signal, te propušta visokotlačno hidrauličko ulje ka plinskim sapnicama, otvarajući ih kako bi se utisnula specificiran količine plina u komoru izgaranja.
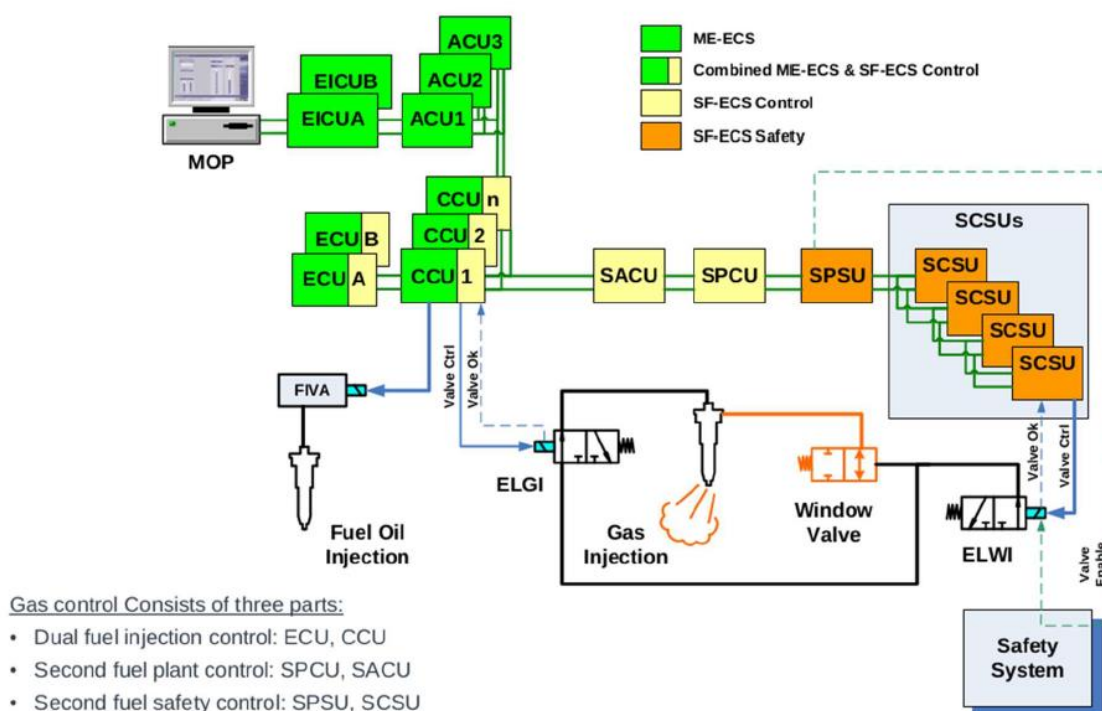
Figure 31: *Scheme of the ME-GI controlling system [17]*

Slika 31 Shematski prikaz kontrolnog sustava ME-GI motora [17]

U radu s dizelskim gorivom ovu funkciju preuzima ELFI ventil (eng. *Electronic Fuel Injection Valve*) djelujući principijelno kao ELGI ventil, pri čemu se u oba operativna moda (GM i DM) aktuiranje ovih ventila kontrolira sa cilindarskom kontrolnom jedinicom, CCU (eng. *Cylinder Control Unit*). Unutar ovog sustava naročito važnu ulogu ima kontrolni ventil plina WV (eng. *Window Valve*) za slučaj propuštanja plina kroz tijelo plinske sapnice te se pomoću njega onemogućuje nekontrolirano utiskivanje plina u komoru izgaranja, koje bi u konačnici moglo izazvati eksploziju s katastrofalnim posljedicama. U slučaju da je sapnica neispravna i da uslijed dugotrajno prisutnog visokog tlaka utiskuje previše plina u cilindar, pristupa se dreniranju plina preko pripadajućeg drenažnog ventila.
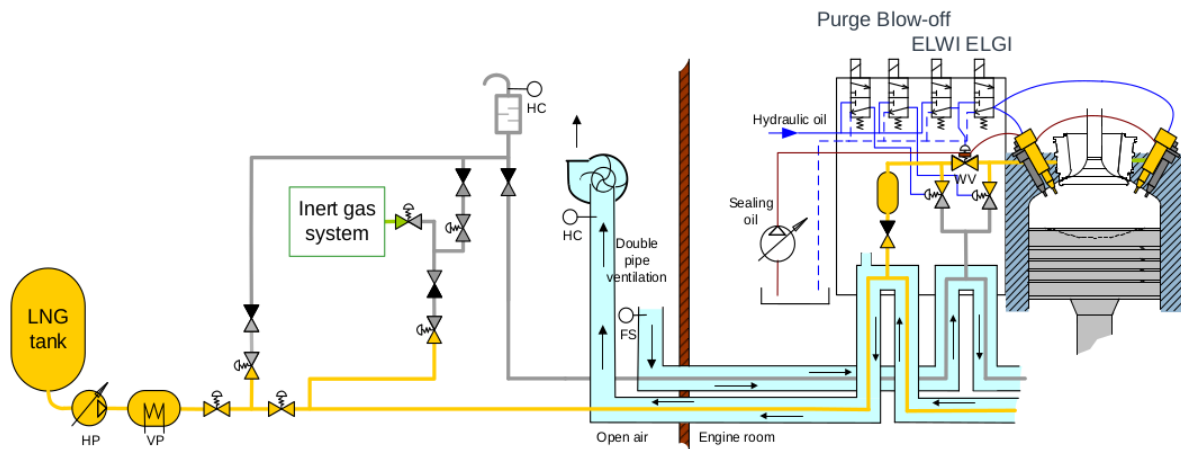
Figure 32: Scheme of the MAN ME-GI electro-hydraulically controlled system [17]

Slika 32 Shematski prikaz elektro-hidrauličkog upravljačkog sustava MAN ME-GI motora [17]

5. Zaključak

Kombiniranjem raznovrsnih izvedbi dizelskih motora na dvojno gorivo s pripadajućim sustavima skladištenja, pripreme i napajanja plinovitim gorivom ostvaruje se mogućnost za izbor optimalne projektne izvedbe brodskog energetskog sustava kako na LNGC-ima tako i na konvencionalnim brodovima zahvaljujući ponajprije iznimno visokim ekološkim standardima koje svjetska regulatorna tijela kontinuirano nameću brodarstvu i brodograđevnoj industriji. Uslijed takve nastupajuće pooštrene regulative, tijekom ovog desetljeća sve više se pristupa plinifikaciji brodskih energetskih sustava, ponajprije sa ciljem smanjenja emisije ugljičnog dioksida. S druge strane LPG tankeri, tankeri za transportiranje etilena (eng. *Ethylen Carriers*, EC) te naročito LNGC-i su tijekom navigacije izloženi neustaljenim energetskim opterećenjima, posebice propulzijskom i toplinskom čega je posljedica neujednačena količina generiranog BOG-a u uvjetima dopuštene fluktuacije tlaka u tankovima LNG-a. Stoga je iznimno važno da pripadajući energetski sustavi tih brodova ekonomično, pouzdano, sigurno i ekološki prihvatljivo participiraju u gospodarenju s tako generiranim otparkom, bilo da ga koriste kao pogonsko gorivo ili da ga, bilo u cijelosti ili djelomično relikvificiraju i vraćaju u tankove kao vrijedan komercijalni teret. Uvažavajući već odavna potvrđenu činjenicu da su dizelski motori, posebice dvotaktni sporokretni, izrazito pouzdani, kompaktni i energetski najučinkovitiji među svim toplinskim strojevima s unutrašnjim izgaranjem, pokrenuto je osmišljavanje pouzdanih, energetski učinkovitih i ekološki prihvatljivih projektnih izvedbi brodskih dvotaktnih i četverotaktnih dizelmotornih postrojenja na dvojno gorivo. Tijekom ovog desetljeća, zahvaljujući ponajviše razvoju pripadajućih sigurnosno nadzornih sustava ugrađuju se ne samo na LNGC-e nego i na ostale konvencionalne trgovačke brodove.

Učinkovitost i pouzdanost sigurnosno nadzornih sustava plinificiranih brodskih dizelmotornih postrojenja omogućena je zahvaljujući implementiranju upravljačkih sustava temeljenih na potpuno automatiziranim elektroničkim i elektro-hidrauličkim regulacijskim sustavima, kojima se između ostalog osim projektnog indeksa energetske učinkovitosti (EEDI) pospješuje i operativni indeks energetske učinkovitosti (EEOI). To je u sveukupnoj energetskoj i ekološkoj interakciji svakog broda s

prirodnim okruženjem od presudnog značaja u procesu ublažavanja nastupajućih naglih okolišnih disbalansa diljem planeta.

REFERENCES

[1]   O. Levander, *Dual Fuel Engines – Latest Developments*, Wartsila Corporation, 2011.

       Web izvor, pristupljeno 12.09.2020., URL:

       https://www.stg-online.org/onTEAM/shipefficiency/programm/PPTLevander.pdf

[2]   United Nations Publications, *Review of maritime transport 2018 (Report, United Nations),* United Nations, New York, 2018.

       Web izvor, pristupljeno 14.08.2020., URL:

       https://unctad.org/en/PublicationsLibrary/rmt2018_en.pdf

[3]   MAN Diesel&Turbo, *ME-GI Dual Fuel MAN B&W Engines,*

       Web izvor, pristupljeno 11.09.2020., URL:

       https://marine.mandieselturbo.com/docs/librariesprovider6/technical-papers/me-gi-dual-fuel-man-b-amp-w-engines433833f0bf5969569b45ff0400499204.pdf?sfvrsn=18 downloaded Jan 8 2017

[4]   Mollenhauer, K., Tschoeke, H., *Handbook of Diesel Engines,* Springer-Verlag Berlin, Heidelber 2010.

[5]   AEsoy, V., Magne Einang, P., Stenersen, D., Hennie, E., *LNG-Fuelled Engines and Fuel Systems for Medium-Speed Engines in Maritime Applications*, SAE Technical Paper 2011-01-1998, 2011

[6]   Thijssen, B., *Efficient and environmentaly friendly machinery systems for LNG carriers*, Wartsila, Finland

[7]   Thijssen, B., *Dual-Fuel Electric LNG carrier propulsion, Wartsila, Finland*

[8]   Wartsila, *The Dual Fuel Technology*, December 2015.

       Web izvor, pristupljeno 01.09.2020., URL:

       https://www.onthemosway.eu/wp-content/uploads/2015/10/5.pdf

[9]   Heinla, P., *Gas Power Plant Running on Shale Oil Retort Gas*, Wartsila, Wartsila Power Plants, 2014.Web izvor, pristupljeno 22.08.2020., URL:https://old.taltech.ee/public/p/polevkivikompetentsikeskus/Polevkivikonverents/2013/priit-heinla-2013-11-14.pdf

[10]   MAN Diesel&Turbo, *Cost-Optimized Designs of ME-GI Fuel Gas Supply Systems*

       Web izvor, pristupljeno 27.08.2020.,

       URL:https://marine.man-es.com/docs/librariesprovider6/test/cost-optimised-designs-of-me-gi-fuel-gas-supply-systems.pdf?sfvrsn=72fbeca2_6

[11]   Wettsstein, R., *The Wartsila low-speed, low-pressure, dual-fuel engine*, AJOUR Conference, ODENSE, 27/28 November 2014.

       Web izvor, pristupljeno 03.09.2020., URL:

http://www.ajourerhvervskonference.dk/imgdb/docs/Rudolf_Wettstein_2330.pdf

[12] WIN GD, RT-flex50DF, Marine Installation Manual
      Web izvor, pristupljeno 14.09.2020., URL:
      https://www.wingd.com/en/documents/rt-flex50df/engine-installation/mim/marine-
      installation-manual-(mim)/

[13] Wartsila Sea & Land Academy, Wartsila 50DF Engine Technology
      Web izvor, pristupljeno 22.03.2017, URL:
      https://cdn.wartsila.com/docs/default-source/product-files/engines/df-engine/wartsila-o-e-w-
      50df-tr.pdf?sfvrsn=6

[14] Olander, K., Dual-fuel-electric for LNGC, Wartsila, Korea, (2006)
      Web izvor, pristupljeno 04.08.2020., URL:
       http://www.google.hr/url?sa=t&rct=j&q=&esrc=s&source=web&cd=1&cad=rja&uact=
      8&ved=0CBoQFjAA&url=http%3A%2F%2Fwww.wartsila-hyundai.com%2Ffiledo

      wn%3Falias%3Dadpds%26file%3DWartsila%252B50%252BDF%252BDual%252B

      fuel%252Bengine%252Breference%252Bfor%252BLNGC%252B04%252B01%25

      2B07%252Bppt.pdf&ei=SrEuVP_BHsW9PbS7gEA&usg=AFQjCNEH5q4yyGMk4z1a

      sYb-7_4XVJJKA

[15] Stenhede, T., *Wartsila Power Plants*, KTH Royal Institute of Technology, 2006.
      Web izvor, pristupljeno 14.08.2019., URL:
      http://www.energy.kth.se/course/4a1626/ahpt2006/comb1.pdf

[16] WinGD X72DF-Marine Installation Manual
      Web izvor, pristupljeno 03.08.2020., URL:
      https://www.wingd.com/en/documents/x72df/engine-installation/mim/marine-installation-
      manual-(mim)/

[17] Christensen, P., *MAN ME-dual fuel engines*, Surveyor's day Gard/Norwegian Hull Club, Bergen,
      October 2017.
      Web izvor, pristupljeno 10.09.2020., URL:
      http://www.gard.no/Content/24305569/Dual fuel engines.pdf

[18] Martz, J., *Basics of Converting Diesels to Dual-Fuel Operation, CompressorTech two*, 2012

[19] Governor Control Systems, Inc., *Control Systems for Dual-Fuel and Bi-Fuel Engines*
      Web izvor, pristupljeno 03.04.2019., URL:
      https://www.govconsys.com/dual-fuel-and-bi-fuel-systems.htm

[20] Jääskeläinen, H., Natural Gas Engines, DieselNet
      Web izvor, pristupljeno 12.08.2020., URL:
      https://dieselnet.com/tech/engine_natural-gas.php

NON-METALLIC PIPELINES AND FITTINGS FOR SHIPS

NEMETALNI CJEVOVODI I ARMATURE NA BRODOVIMA

Žarko, Koboević*[a,], Ante, Sršen[a], Anamarija, Falkoni[a]

a Sveučilište u Dubrovniku, Pomorski odjel, Ćira Carića 4, 20000 Dubrovnik
* Corisponding Author, zarko.koboevic@unidu.hr

Abstract

The paper deals with non-metallic pipelines and fittings on ships. These include various types of pipelines and pipes such as fiberglass, then PVC pipes, b & v pipes, subor pipes. There are also composite tubes, rubber tubes and all kinds of non-metallic tubes and their fittings, seals and flanges. Each type has its own advantages and reasons why it is used in individual systems. Rubber hoses are always more flexible than plastic hoses, but their main advantage is that they have a higher abrasion resistance. It is emphasized that plastics are the material of the future and will be used more frequently. An armature is a part of a pipeline that serves to connect pipes, open, close, or adjust the desired flow values.

Key words: fiberglass; PVC pipes; composites ; rubber hoses; polymers;

Sažetak

Rad obrađuje nemetalne cjevovode i armature na brodovima. Tu spadaju razne vrste cjevovoda i cijevi poput stakloplastičnih, zatim PVC cijevi, b&v cijevi, subor cijevi. Tu su još i kompozitne cijevi, gumene cijevi i sve vrste nemetalnih cijevi i njihovih spojeva, brtvi i prirubnica. Svaka vrsta ima svoje prednosti i razloge zašto se upotrebljava u pojedinim sustavima. Gumena crijeva su uvijek nešto fleksibilnija nego plastična, ali glavna prednost im je što imaju veću otpornost na habanje. Ističe se kako su plastične mase materijal budućnosti te će učestalost njihove uporabe najvjerojatnije rasti. Armatura je dio cjevovoda koji služi spajanju cijevi, otvaranju, zatvaranju ili namještanju željenih vrijednosti protoka.

Ključne riječi: *stakloplastika; PVC cijevi; kompoziti; gumene cijevi; polimeri*

1. Uvod

Cjevovodi na brodovima koriste se za transport fluida. Neki cjevovodi se nisu znatnije mijenjali kroz duži niz godina, no ima i onih koji se redovito unapređuju. Uglavnom se radi o cjevovodima sprječavanja zagađivanja morskog okoliša te sigurnosti broda, posade, putnika ili tereta. Mnogi brodski cjevovodi se smještaju u ograničenim prostorima, pri čemu se mora voditi računa o ugradnji, praćenju rada i mogućnosti brzog i jednostavnog održavanja. Moraju biti sigurni i pouzdani u radu, a ukoliko dođe do kvara, mora biti omogućen nastavak rada barem sa smanjenim kapacitetom ili osigurano relativno brzo otklanjanje kvara. Gotovo svi brodski cjevovodi su izloženi djelovanju agresivne atmosfere (vlažnog morskog zraka) ili samih fluida, te moraju biti otporni na štetno djelovanje. Plastični materijali se sve više koriste u brodogradnji i važno je spomenuti kako su

plastične mase materijal budućnosti te će i učestalost njihove upotrebe najvjerojatnije rasti. Gumena crijeva su uvijek nešto fleksibilnija od plastičnih, ali glavna prednost im je što imaju veću otpornost na habanje, i bez problema mogu izdržati temperaturni raspon od -25° C pa do +250° C, za razliku od PVC-a gdje je temperaturni raspon od -10° C do + 60° C. I ono što je najvažnije, guma je otporna na kemikalije, posebno na sve vrste goriva, što je osnovna prednost zbog koje se i koriste kao crijeva za transport goriva u priključivanju na terminal ili neki drugi plovni obkjekt. Armatura je dio cjevovoda koji služi otvaranju, zatvaranju ili namještanju željenih vrijednosti protoka.

2. Nemetalne cijevi na brodovima

2.1. *Cijevi od stakloplastike – FRP (Fiberglass Reinforced Plastic)*

Unapređenjem tehnologije došlo je do pronalaska novih materijala za izradu cjevovoda, a sve u cilju da se izbjegne propadanje materijala. Kao rezultat istraživanja pojavili su se cjevovodi izrađeni od polimera (smole) ojačanih staklenih vlaknima koji su riješili problem korozije materijala. Ova vrsta cjevovoda izrađenih od polimera ojačanih staklenim vlaknima pruža izvrsnu otpornost na morsku vodu, različite otopine te ima iznimnu izdržljivost prema različitim vrstama kemikalija. Potrebno je istaći da ovaj materijal ima iznimna svojstva te je vrlo lagan i cjenovno je vrlo prihvatljiv. Ove osobine ga čine dosta prihvatljivim od samog čelika. Sam spomenuti materijal je napravljen i konstruiran tako da ima dugi radni vijek, tako da sam materijal može „nadživjeti" sam brod. Materijal je osmišljen i konstruiran tako da je u skladu sa svim odredbama Međunarodne pomorske organizacije, te je odobren od svih vodećih klasifikacijskih ustanova.

Za uporabu na brodu postoje dvije vrste cjevovoda izrađenih od staklenih vlakana ojačanih smolom. Postoji jedna vrsta za uporabu u spremnicima koji su izloženi velikom vanjskom tlaku i za cjevovode koji nisu izloženi visokom vanjskom tlaku. Uobičajeni promjeri ovih cijevi su od 25 mm do 900 mm. Spajanje cjevovoda izrađenih od polimera ojačanih staklenim vlaknima postiže se uporabom raznih ljepila, zatim gumenim brtvljenjem, pomoću prirubnica ili spajanjem korištenjem mehaničkih spojki. Spajanje posebnim ljepilom cjevovoda izrađenih od polimera (smole) ojačanih staklenim vlaknima se koristi do promjera od 400 mm. Za promjere cjevovoda većih od 400 mm se koriste metode spajanja pomoću gumenog brtvljenja, pomoću prirubnice ili spajanjem mehaničkim spojkama. Nisko-tlačni sustav cjevovoda se koristi u sustavima gdje je radni tlak istog do 25 Bar-a, a visoko-tlačni sustav se koristi gdje je radni tlak veći od 25 Bar-a.

Slika 101. Glavni cjevovod morske vode koji služi za hlađenje nisko-temperaturnog sustava

Fibrex je razvio standardnu liniju cijevi nazvanu IntegraLine.od staklenih vlakana s prilagodljivom otpornosti na koroziju. Ova stakloplastika je idealna za instalaciju ili zamjenu postojećih cijevi i zadovoljava mnoge primjene i zahtjeve za duži životni vijek postrojanja.

Prilagođeni cjevovodi od stakloplastike mogu zahtijevati deblje korozijske ili abrazijske barijere s različitim smolama. Također su dostupni teži strukturalni laminati i posebna staklena pojačanja koja udovoljavaju zahtjevima ugradnje i temperature.

Slika 2. Stakloplastična cijev ojačana staklenim vlaknima [3]

Smola, stakleni armaturni materijali i kompozitna konstrukcija odabrani su tako da daju postojanu otpornost na koroziju za većinu kemijskih primjena za koje se smatra da je FRP cijev prikladna. Otpornost na vremenske uvijete postiže se vanjskim premazom koji sadrži ultraljubičasti

374

stabilizator koji daje dugotrajnu otpornost. Ako se cijevi nakon mnogo godina počnu trošiti u posebno teškim okruženjima, vanjska površina može biti brušena i obložena ili obojana. Pigmentirani vanjski gel premazi se ne koriste kod IntegraLine cijevi kako bi se iskoristila prirodna prozirnost FRP cijevi. Vizualni pregled cijevi, i nakon godina službe, pouzdaniji je s "prirodnim" laminatom. Osim toga, tekući sadržaj se često može promatrati u cjevovodu. Visoka vlačna svojstva vinil esterskih smola upotrijebljenih u IntegraLine cijevima pružaju veću žilavost cijevi, što im omogućuje da se odupru pukotinama i pucanju smole prilikom podvrgavanja teškim konstrukcijskim opterećenjima. Osim otpornosti na zamor, ta otpornost također osigurava čimbenik sigurnosti od oštećenja od udaraca tijekom transporta i instalacije. IntegraLine cijev je proizvedena s vrhunskom vinil esterskom smolom otpornom na koroziju. Na sobnoj i povišenoj temperaturi, ove smole nude otpor širokom rasponu kiselina, lužina, izbjeljivača i otapala. IntegraLine cijev proizvedena je procesom namotavanja vlakana u spiralnom uzorku pod kutem od 55 stupnjeva kako bi se postigla optimalna kombinacija oblika i aksijalnih svojstava za najčešće primjene. Visoki sadržaj stakla koji proizlazi iz procesa namotavanja vlakana daje izvrsne karakteristike čvrstoće. IntegraLine cijevni priključci proizvedeni su pomoću vrlo učinkovitog laminata s kontaktnim kalupom koji se sastoji od izmjenjivih slojeva staklenog vlaknastog sloja i dvosmjernog namotavanja stakla.

Spajanje cijevi izvodi se na više načina a najčešće korišteni tip spoja je pomoću zgloba tipa Zvono i Spigot koji nudi nekoliko prednosti nad ostalim metodama. Ovo spajanje je jedno od glavnih karakteristika procesa namotavanja dvostrukog spiralnog filamenta. Zvono se dobiva tijekom proizvodnje cijevi i sastavni je dio cijevi. Glavne prednosti ove vrste spojeva su: hidrauličko brtvljenje pomoću dva elastomerna O-prstena postavljena u paralelnim utorima obrađenim na čepu. Umetanjem ključa za zaključavanje u utor kroz zvono, spoj prenosi aksijalna naprezanja duž cijevi i odupire se uzdužnim silama. S ovim spojnim sustavom može se izbjeći uporaba prostranih i skupih blokova za zabijanje ili sidrenje. Instalacija je vrlo jednostavna i brza i ne zahtjeva stručno osoblje. Zglobna krutost veća je od krutosti cijevi. To jamči vrlo stabilan spoj praktički bez ikakvih deformacija koje se mogu koristiti pri vrlo visokim tlakovima.
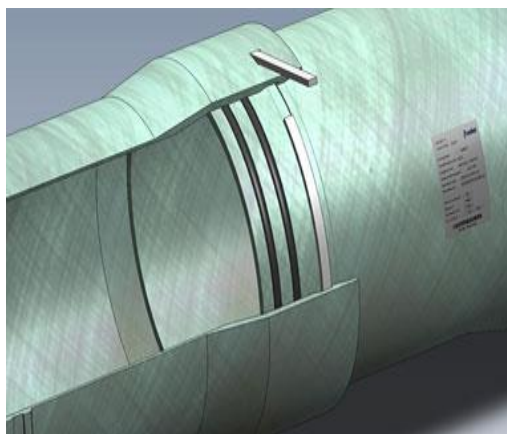
Slika 3. Dvostruki O prsteni [1]

Druge vrste spojeva koje nudi Sarplast su mehanički spoj, udubljenje zgloba i prirubnički spoj. GRP prirubnice su dostupne za zadovoljavanje standarda bušenja prema ANSI, DIN, BS, UNI, itd.

Slika 4. Prirubnice od stakloplastike [2]

Upotreba prirubnica u cjevovodima od fiberglasa omogućuje jednostavno spajanje na opremu, jednostavnu montažu i demontažu cjevovoda. Ovakve cijevi i armature, isporučuju se u brodogradilištu zajedno sa svim priborom kao što su brtve i ključevi za zaključavanje te su spremni za montažu bez potrebe za izvođenjem laminiranih ili lijepljenih spojeva u brodogradilištu.

GRP cijevni sustavi prikladni su za različite mogućnosti primjene, kao što su: cjevovodi tereta, sirova nafta, inertni plin, balast, kaljuža, kanalizacija (crne i sive vode), pitka voda.

Table 102. Prikazuje uporabu cjevovoda izrađenih od polimera (smole) ojačanih staklenim vlaknima koji se mogu koristiti u određenim prostorima na brodu

Sustavi cjevovoda	Prostor strojarnice	Drugi prostor strojarnice	Prostorija za sisaljke	Prostori za smještaj putnika	Drugi prostori na brodu	Spremnici	Spremnici goriva	Spremnici balasta	Zrako-prazni prostori	Prostori za nadzor	Paluba
			(green)					L3		(red)	
Brodski teret											
Brodski teretni cjevovodi			(red)			(green)		9			(red)
Cjevovod za pranje spremnika			(red)			(green)		9			(red)
Cjevovod za provjetravanje						(green)		9			(red)
Prirodni plin u tekućem stanju											
Cjevovodi vode			1			1	1	1	1		
Ostali cjevovodi	1	1						1	1		
Glavni cjevovodi	(green)		(red)								(red)
Opskrbni cjevovodi			(red)								
Zapaljive tekućine											
Cjevovodi tereta	(red)	(red)	(red)	(red)	(red)	3		9			(red)
Cjevovodi pogonskog goriva	(red)	(red)	(red)	(red)	(red)	3					(red)
Cjevovodi ulja za podmazivanje	(red)	(red)	(red)	(red)	(red)						(red)
Cjevovod hidrauličnog ulja	(red)	(red)	(red)	(red)	(red)						(red)
Morska voda											
Glavni cjevovod kaljuže	(red)	(red)	(red)	(red)	(red)	(green)		(green)			(red)
Protupožarni cjevovodi	(red)	(red)	(red)					(green)		(red)	
Sustav pjene za gašenje požara	(red)	(red)	(red)							(red)	
Sprinkler sustav	(red)	(red)	L3	(red)				(green)		L3	L3
Cjevovodi balasta	L3	L3	L3	L3	(red)	(green)		(green)		(red)	(red)
Cjevovodi rashladne vode	L3	L3									(red)
Cjevovodi za pranje spremnika			L3			(green)					L3
Ostali cjevovodi	(green)	(green)	(green)	(green)	(green)	(green)		(green)			(green)
Slatka voda											
Cjevovodi rashlađene vode	L3	L3								L3	L3
Cjevovodi povrata kondenzata	L3	L3	L3			(green)				(green)	(green)
Ostali cjevovodi	(green)	(green)	(green)	(green)	(green)	(green)		(green)		(green)	(green)
Sanitarni cjevovodi											
Cjevovodi odvoda sa paluba	4	4		4		(green)					(green)
Cjevovodi sanitarnih odvoda	(green)	(green)	(green)	(green)	(green)	(green)		(green)			(green)
Ostali cjevovodi	1 7	1 7	1 7	1 7	1 7					1 7	
Sondiranje / mjerenje											
Spremnici slatke i morske vode	(green)	(green)	(green)	(green)	(green)	9		(green)		(green)	(green)
Spremnici ulja i goriva	(red)	(red)	(red)	(red)	(red)	9	(green)	9			
Ostalo											
Cjevovodi zraka za upućivanje	5	5	5	5	5	(green)		(green)		5	5
Cjevovodi zraka za svakodnevu uporabu	(green)	(green)	(green)	(green)	(green)	(green)		(green)		(green)	(green)
Cjevovodi za odvod rasoline	(green)	(green)	(green)	(green)	(green)			(green)		(green)	(green)
Cjevovodi nisko-tlačne pare	(red)	(red)	8	8	8	(green)		(green)		8	8

(white)	(green)	L3	(red)
Nije primjenjiva uporaba cjevovoda od polimera (smole) ojačanih staklenim vlaknima	Dozvoljena je uporaba cjevovoda od polimera (smole) ojačanih staklenim vlaknima	Dozvoljena je uporaba cjevovoda od polimera (smole) ojačanih staklenim vlaknima po odredbama Međunarodne pomorske organizacije / razina 3	Nije dozvoljena uporaba cjevovoda od od polimera (smole) ojačanih staklenim vlaknima

Iz tablice se može zaključiti da se cjevovodi izrađeni od polimera (smole) ojačanih staklenim vlaknima najmanje koriste kod brodskih teretnih cjevovoda, cjevovoda za pranje spremnika i odušnika, te se uglavnom ovo odnosi na brodove koji prevoze rasute terete.

Cjevovodi koji su izrađeni od polimera (smole) ojačanih staklenim vlaknima najviše se koriste u sustavima slatke vode, sustavima sanitarne vode, sustava sondiranja i ostalih cjevovoda.

Slika 5. Prikazuje uporabu cjevovoda izrađenih polimera (smole) ojačanih staklenim vlaknima te se na istoj mogu vidjeti tlačni i usisni cjevovodi sisaljki morske vode na putničkom brodu

Glavni među razlozima upotrebe staklenih vlakana su visoka čvrstoća i težina, stabilnost dimenzija, dobre mehaničke osobine, jednostavnost ugradnje, smanjeni troškove instalacije, smanjeni troškovi održavanja i cjelokupna izdržljivost u ekstremnim uvjetima. Slično tome, druga prednost cijevi od fiberglasa je da ima glatku unutarnju površinu u usporedbi s tradicionalnim materijalima. Ovaj atribut, glatki unutarnji provrt, otporan je na taloženje i može stvoriti veći protok tekućine.

2.2. *PVC cijevi*

Danas se ove cijevi na brodovima koriste sve češće**. Imaju brojne prednosti, a među njima su:** ekonomija - PVC cijev je jako jeftina, raspoloživost - dostupne su u mnogim trgovačkim kućama, fleksibilnost - nisu potpuno fleksibilne ali pojedini elementi imaju veću fleksibilnost od metalnih, brza montaža, dugotrajnost, otpornost na kemikalije, crne i sive vode na brodovima i ne propadaju zbog korozivnog djelovanja fekalnih otpadnih voda.

Postoje tri osnovne vrste plastičnih cijevi:

Čvrsta zidna cijev **- s**astoje se od jednog sloja homogene matrice termoplastičnog materijala koji je spreman za upotrebu u cjevovodu.

Strukturirana zidna cijev **-** su proizvodi koji imaju optimiziran dizajn s obzirom na uporabu materijala kako bi se postigli fizički i mehanički zahtjevi za izvedbom.

Barijera cijevi **-** koristi se, na primjer, kako bi se osigurala dodatna zaštita za sadržaj koji prolazi kroz cijev (osobito pitke vode) od agresivnih kemikalija ili drugih onečišćenja.

Većina plastičnih cijevnih sustava izrađena su od termoplastičnih materijala. Metoda proizvodnje uključuje taljenje materijala, oblikovanje i hlađenje. Cijevi se normalno proizvode ekstruzijom.

Materijali PVC cijevi su:

- *ABS (akrilonitril butadien stiren) koji se* koristi za prijenos pitke vode, suspenzije i kemikalija. Ima široki temperaturni raspon, od -40 ° C do +60 ° C. Može se prilagoditi različitim primjenama mijenjanjem omjera pojedinih kemijskih komponenti. Koriste se uglavnom u industrijskim primjenama gdje su važna visoka čvrstoća i krutost udarca.

- *PVC (neomekšani polivinil klorid).* Od pedesetih godina prošlog stoljeća korištene su PVC cijevi za zamjenu korodiranih metalnih cijevi. PVC ima visoku kemijsku otpornost kroz cijeli radni temperaturni raspon, s širokim rasponom radnih tlakova. Zbog svojih dugotrajnih karakteristika čvrstoće, i ekonomičnosti, PVC sustavi čine veliki udio plastičnih cjevovodnih instalacija.

Slika 6. ABS cijevi i prirubnice [4]

- *CPVC (post klorirani polivinil klorid)* je otporan na mnoge kiseline, lužine, soli, parafinske ugljikovodike, halogene i alkohole. Nije otporan na otapala, aromate i neke klorirane ugljikovodike. Može nositi višu temperaturu tekućine od uPVC s maksimalnom radnom temperaturom koja doseže 93°C.

- PB-1 (polibutilen) se koristi u sustavima tlačnih cjevovoda za toplu i hladnu pitku vodu, predizolirane sustave daljinskog grijanja i sustave površinskog grijanja i hlađenja. Ključna svojstva su zavarljivost, otpornost na temperaturu, fleksibilnost i visoka otpornost na hidrostatski tlak.

- PP (polipropilen) PP je termoplastični polimer od polipropilena i prikladan je za uporabu s prehrambenim proizvodima, pitkom i ultra čistom vodom, kao i unutar farmaceutske i kemijske industrije. Zbog velike otpornosti udaraca u kombinaciji s

dobrom krutosti i visokom kemijskom otpornošću ovaj materijal pogodan je za primjenu u kanalizaciji.

- PE (polietilen) se već dugi niz godina uspješno koristi za sigurno prenošenje pitke vode, otpadnih voda, opasnog otpada i komprimiranih plinova. PE cijevi se izrađuju ekstruzijom u različitim dimenzijama. PE je lagan, fleksibilan i lagan za zavarivanje. Njegov glatki interijer osigurava dobre karakteristike strujanja. Ove se cijevi mogu koristiti za liniju starih cijevnih sustava kako bi se smanjilo curenje i poboljšala kvaliteta vode. Također za PE cijevni materijal, nekoliko je studija pokazalo dugogodišnji rezultat s očekivanim vijekom trajanja od više od 50 godina.

PVC ventili su oblikovani i također dolaze u mnogo vrsta: kuglasti ventili, leptir ventili, nepropusni ventili za provjeru kugle, membranski ventili.PVC nudi opciju otpornu na koroziju za različite industrijske primjene. Značajke i prednosti PVC ventila su lagan za ugradnju i maksimalna radna temperatura od 60°C. Upotreba plastičnih cijevi na brodu je za pitke vode -higijenski zahtjevi, plinove - najviši sigurnosni zahtjevi, plastične cijevi za grijanje - otpornost na temperaturu, za kanalizacije i otpadne vode- visoka kemijska otpornost.

Slika 7. Plastična cijev za inertni plin [10]

2.3. B&V cijevi

VEKA Piping & Industry BV je poznata tvrtka u VEKA grupi; ova tvrtka opskrbljuje plinovodne sustave za sve dizajne tankera s dvostrukom oplatom.
Dobro osmišljen kemijski sustav plinovoda je neophodan za okoliš i za sigurnost. Postoje mnoge mogućnosti uporabe: kemijski tankeri s jednim ili dvostrukim sustavom cjevovoda, bunker brodovi, tankovi za jestivo ulje, postrojenja za mješanje HFO i MDO, jahte.

Svi sustavi plinovoda potpuno su opremljeni prema propisima klasifikacijskih društava i zadovoljavaju najnovije sigurnosne propise.

Slika 8. VEKA cijevi na tankeru [5]

2.4. Subor cijevi

Subor Grp Pipes tvrtka je specijalizirana za proizvodnju cijevi od poliestera i armirane stakloplastike. Subor Pipe Industry And Trade Inc uložio je u novu proizvodnu liniju koja može proizvoditi GRP cijevi do 4000 mm promjera. Subor GRP novi plastični dizajn omogućio je gradnju malih, kao i izuzetno velikih promjera cijevi. Flowtite cijevi su otporne na koroziju na unutarnjoj i vanjskoj strani. Flowtite GRP cijevni sustavi mogu se naći u prijenosu pitke vode, u protupožarnoj, morskoj i desaliniziranoj vodi, u elektranama, kemijskim i industrijskim otpadom te u kanalizacijskim aplikacijama i navodnjavanju.

Amijack GRP su cijevi od poliestera, staklenih vlakana i kvarcnog pijeska proizvedene metodom centrifugalnog odljeva. Sirovinama se u određenim količinama puni rotirajući kalup kako bi se dobila slojevita kompozitna struktura s kompaktnom konstrukcijom. Sirovine se precizno mjere te dodaju u redoslijedu i skladu s dizajnom formule cijevi koja se proizvodi. Taj proces stvara vrlo kompaktnu kompozitnu strukturu, što je neophodno i vrlo važno za ugrađivanje cijevi utiskivanjem. Cijevi imaju visoku krutost prstena, a spojnice su posebno dizajnirane kako bi vanjski promjer bio sličan vanjskome promjeru cijevi. Cijevi AMIJACK isporučuju se u vanjskim promjerima između 427 mm i 2453 mm, u standardnim duljinama od 1, 2, 3 i 6 metara. Ograničenja u primjeni cijevnih sustava Flowtite gotovo i ne postoje. Koriste se podjednako za prijenos pitke vode, u protupožarnoj djelatnosti, s morskom i desaliniziranom vodom, u elektranama, u uporabi kemijskoga i industrijskog otpada, kao i u kanalizacijskim sustavima.

Slika 9. Amijack cijev [9]

Flowtite prirubnice su u različitim izvedbama i prema različitim standardima i zahtjevima. Kod spajanja dvije GRP prirubnice preko 300 mm promjera, samo jedna prirubnica ima utor brtve u lici.

Slika 10. Folwtite prirubnica [19]

Zglobovi Flowtite cijevi mogu se spojiti pomoću ojačanja staklenih vlakana i smole. Zglobovi s omotačem su česti u primjenama s aksijalnim potiskivanjem. Flowtite osigurava potrebne upute za spajanje džepnog omotača prema patentiranoj tehnologiji „butt-wrap". Važna komponenta u Flowtite cijevima je gumena brtva cijevi ili brtva između cijevi. Upotreba Flowtite cijevi na brodu: Mogu se naći u prijenosu pitke vode, u protupožarnim sustavima, sustavima morske i desalinizirane vode, prijenosu kemijskog otpada, te u kanalizacijskim aplikacijama.

2.5. Kompozitne cijevi

Kompozitni materijali (kompoziti) građeni su od međusobno čvrsto spojenih različitih materijala radi dobivanja novoga, drugačijega materijala, s fizikalnim ili kemijskim svojstvima koja nadmašuju svojstva pojedinačnih komponenata ili sa svojstvima koja te komponente same nemaju. Pritom se ne radi samo o poboljšanju preradbenih, doradnih i uporabnih svojstava (npr. povećanje specifične čvrstoće i specifičnoga modula elastičnosti, lomne žilavosti, toplinske postojanosti, otpornosti prema abraziji i puzanju), nego i transportnih, skladišnih, otpadnih, uključujući konačno i cijenu. Većina kompozita sadrži jedan materijal kao kontinuiranu fazu (matricu), a u nju su uklopljeni odvojeni dijelovi druge faze, koja najčešće ima funkciju ojačala. Postoje dva različita proizvodna procesa kompozitnih cijevi: lijevanje filamenata i rotacijsko lijevanje. Sličnosti su niti staklenih vlakana ili drugi materijali koji se mogu omotati oko ili u kalup radi stvaranja čvrstih cijevi s karakteristikama koje prevladavaju slabosti metala. Ove se niti zatim uvuku u smolu koja veže materijal za učvršćivanje u jedinstvenu cjelinu. Razlike u proizvodnim metodama su ključne za profil čvrstoće koju će imati kompozitna cijev.

Izrada kompozitnih cijevi filament winding metodom je proces prolaska niti vlakana kroz kupelj smole, a zatim ih se podvrgne napetosti na rotirajućem bubnju. Ovaj postupak je najčešći i može se koristiti za izradu kompozitne cijevi iz različitih materijala.

Slika 11. Filament winding metoda [18]

Metoda rotacionog lijevanja ili rotocast, je postupak za proizvodnju predmeta koji su šuplji, poput kompozitnih cijevi. Osnovna metoda uključuje punjenje kalupa s polimerom, grijanje alata kako bi se rastopio materijal, hlađenje i uklanjanje predmeta. Ova metoda proizvodi jaki materijal koji je estetski ugodan ali i povećane vlačne čvrstoće. Zraka i vlaga mogu se potpuno ukloniti, prevladavajući negativne osobine iz metode namotavanja vlakana.

Slika 12. Rotirajuća metoda [17]

GRV cijevi izrađene su od dvostrukog spiralnog namotaja. Glavne sirovine koje se koriste za to su staklena vlakna i vinil ester smole smola. Unutarnji sloj sastoji se od C-staklenog vela i vinilesterske smole za maksimalnu otpornost na kemikalije i na abraziju. Strukturni sloj sastoji se od smole E-stakla i vinil estera. GRV cijevi imaju bolja mehanička i kemijska svojstva u usporedbi s GRP cijevima. GRV cijevi se mogu koristiti za medij temperature do 90 º C

GRE cijevi stakleni ojačani epoksidni materijali (GRE) su alternativa cijevi od čelika koji su vrlo korisni, posebno za koroziju u agresivnim i normalnim okruženjima. Visokoučinkovita stakloplastika i epoksidna smola obrađena u diskontinuiranom procesu namotavanja vlakana je tehnologija koja se koristi u GRE cijevima GRE cijevi su prikladne i puno se koriste u cjevovodu za naftu i plin, distribuciju pitke vode, offshore aplikacije za platforme i još mnogo toga. GRE cijevi su relativno lagane, jednostavne za rukovanje i ugradnju. Toplinska vodljivost GRE cijevi je niska u usporedbi s čelikom, a time je i gubitak topline i trošak izolacije minimiziran.

Upotreba kompozitnih cijevi na brodovima je za prijevoz nafte i plina, distribuciju pitke vode, za transport kiselina, za otpadne vode.

2.6.   *Gumene cijevi*

Gumena crijeva su uvijek nešto fleksibilnija od plastičnih, ali glavna prednost im je što imaju veću otpornost na habanje, i bez problema mogu izdržati temperaturni raspon od -25° C pa do +250° C, za razliku od PVC-a gdje je temperaturni raspon od -10° C do + 60° C što je znatno manje. I ono što je najvažnije, guma je otporna na kemikalije, posebno na sve vrste goriva, što je osnovna prednost zbog koje se i koriste kao crijeva za transport goriva.

Ispušni sustav je neprestano podvrgnut velikim promjenama u temperaturi. To vrijedi osobito za mokro-ispušni sistem, gdje se voda koristi da se ohlade vrući plinovi iz motora. Gumena ili silikonska crijeva se preporučuju za ispušne sisteme, zbog svoje trajnosti, fleksibilnosti i snage. Guma je fleksibilnija, i u mogućnosti je da se proteže i smanjuje više puta. Međutim, na kraju će oslabiti i puknuti. Silikonske cijevi su znatno jače i mogu trajati šest puta duže od običnih gumenih. One su puno skuplje, ali i vrijede.

Slika 953. Gumena cijev za ispušne plinove [16]

Crijeva za gorivo morju biti jako i izdržljive. Tri vrste crijeva se obično nalaze na brodskim motorima: fleksibilna cijev (A1, A2, B1 i B2), čelične cijevi i bakrene cijevi na motorima. Crijeva se mogu provjeriti prilikom servisiranja motora, ali fleksibilne cijevi treba stalno nadzirati. Od dvije vrste, A i B, A je bolje otporna na vatru, i koristi se na pumpama za gorivo. Stoga crijevo A1 je jače i više otporno na curenje. To je također skuplje ali slično kao s ispušnim cijevima - isplati se.

CMS cijevi su cijenjene zbog svoje otpornosti na kemikalije, ulja, habanje, vrijeme i ekstremne temperature, ultraljubičasto svjetlo.

Upotreba gumenih cijevi na brodu: za ispušne plinove, za transport goriva i ulja.

Slika 14. CMS cijevi [15]

3. Diskusuja

Sa sve većim troškovima koji se pojavljuju u samoj eksploataciji broda, u ovoj diskusiji se radi o troškovima koji nastaju zbog same korozije koja oštećuje sve dijelove i pripadke broda, posebice cjevovode koji su izloženi koroziji, te zbog korozije isti su trebali biti zamjenjeni, što je značilo sve veće troškove za brodske kompanije ne samo zbog troškova zamjene cjevovoda već i zbog toga što bi brod bio bez pogona ukoliko bi se korozija pojavila i uništila glavne cjevovode brodske strojarnice. To

se može dogoditi na cjevovodu mora, rashladne vode, pare, goriva ili nekog drugog važnog medija. Potrebno je istaći da su to ogromni troškovi jer se radi o zbilja velikim komadima cjevovoda zbog kojih je ponekad potrebno izrezati oplatu da bi se ista mogla izvući kroz oplatu i istu zamjeniti s novom koju je prethodno potrebno izraditi i uklopiti na mjesto starog cjevovoda. Sve ovo već navedeno predstavlja ogromne troškove jer se brod u ovom periodu popravka ne može eksploatirati, stoga da bi se ovi problemi mogli rješiti, brodovlasnici i istraživački centri za brodogradnju su se dosjetili i riješili ovaj problem tako što su čelične cjevovode zamijenili cjevovodima od polimera ojačanih staklenim vlaknima odnosno duromerima. Na taj način uporabom novih materijala napokon se riješio problem korozije najosjetljivijih cjevovoda na brodu. U budućnosti treba uskladiti i postupke popravaka oštećenih dijelova, koji su napredovali, ali niti približno dovoljno onoliko koliko bi brodogradnja to zaista htjela postići.

Samim korištenjem ovih novih vrsta materijala brodovi postaju sve lakši i potrošak goriva će biti manji. Budućnost brodogradnje upravo se i temelji na tome, odnosno možemo istaći da je krajnji cilj brodogradnje upravo ušteda goriva koju ćemo dobiti ukoliko smanjimo težinu svake komponente ili dijela koji se ugrađuje u brod. Ukratko, možemo istaći da sama ušteda na težini pridonosi manjem potrošku goriva, ali u konačnici i smanjenoj količini ispušnih plinova kao i smanjenoj količini štetnih tvari u zraku.

4. Zaključak

Potrebno je istaći da danas kako brodogradnja tako i sve veće brodske kompanije teže smanjenju troškova kako bi se dobili što učinkovitiji brodski pogoni, te se sve više pažnje usredotočuje upravo na korištenju novih i lakših materijala u brodogradnji, jer upravo ovi novi materijali koji su navedeni u radu to i omogućavaju. Sama ušteda na težini pojedinih dijelova u brodogradnji može rezultirati povećanju brodske iskoristivosti, učinkovitosti te povećanju ekonomske isplativosti. U ovom radu obrađene su vrste nemetalnih cijevi, cjevovoda i njihovih armatura na brodovima. Počevši od cijevi od stakloplastike, njene otpornosti na koroziju, čvrstoću i ostalih prednosti koju te cijevi imaju u odnosu na metalne cijevi. Niska cijena, brza montaža i nepropusnost na većinu kemikalija samo su neke od prednosti PVC cijevi. Jednostavan dizajn pripadajućih ventila i prirubnica, za razliku od onih u metalnim cjevovodima, omogućuje bržu montažu i demontažu. Postoje još i B&V i Subbor cijevi, svaka sa svojim prednostima i kvalitetama u odnosu na onu drugu. Flowtite, nemetalne cijevi prvi su izbor mnogih inženjera širom svijeta zbog svojih niskih troškova održavanja cijevi, otpornosti na koroziju, dugog radnog vijeka. Kompozitne cijevi, zahvaljujući otpornosti na kiseline i abraziju imaju široku primjenu u transportu plinova, kiselina i još mnogo toga. Gumene cijevi zbog otpornosti na habanje i visoku temperaturu, našle su primjenu ponajviše za transport goriva i ulja na brodovima. U ovom radu objašnjene su prednosti i nedostatci svake od ovih vrsta materijala. Upravo zbog toga one su našle dobru primjenu u određenim sustavima na brodu. Ističe se da su nemetalne cijevi i cjevovodi materijali budućnosti koji će, a već negdje i jesu, polako zamjenjivati metalne cjevovode na brodu.

LITERATURA

[1]   (Cijevi od stakloplastike) http://www.fibrex.com/fiberglass-pipe, posjećeno 28.2.2019

[2]   (Primjena stakloplastike)https://endurocomposites.com/products/pipe-tank-products/pipe-fiberglass posjećeno 29.2.2019.

[3]   (Najveći proizvođač cijevi stakloplastike) http://www.sarplast.com/eng/index.php, posjećeno 1.3. 2019.

[4]   (Pvc cijev) https://www.thespruce.com/working-with-pvc-pipe-2718790, posjećeno 1.3.2019.

[5]   (B&V cijevi)http://www.vekagroup.com/en/veka_piping_industry_b_v.html, posjećeno 26.2. 2019.

[6]   (Flowtite cijevi na brodu) http://flowtite.amiantit-group.com/Technology-Materials-gaskets.aspx, posjećeno 3.3.2019.

[7]   (Primjena subor cijevi) http://subor-amiantit.eu/hr/proizvodi#primjena-prednosti, posjećeno 2.3.2019.

[8]   (Primjena plastičnih cijevi) https://www.burzanautike.com, posjećeno 2.3.2019.

[9]   (Gumene cijevi za gorivo) https://www.y-yokohama.com, posjećeno 1.3.2019.

[10]   (Cijev goriva) https://www.autopartsapi.com/eEuroparts.com/images/parts/lg_a7610e9a- 440b-4f36-a7ae-397c6d8b8558.jpg, posjećeno 1.3.2019.

[11]   (Primjena flowtite cijevi) http://www.flowtitepipe.com/wp-content/uploads/2015/02/header-3.2_standardsALT.jpg, posjećeno 3.3.2019.

[12]   (Flowtit brtve) https://www.google.hr/search?q=flowtite+gasket&rlz=1C1TEUA, posjećeno 26.2.2019.

[13]   (Pvc ventili) https://sc01.alicdn.com/kf/HTB19T1xJVXXXXXSXXXXq6xXFXXX8/DN63-pvc-ball-valve-flange-end-double.jpg_350x350.jpg, posjećeno 6.3.2019.

[14]   (Što su i kako se prave kompozitne cijevi) https://akiet.com/news/what-is-composite-pipe-and-how-is-it-made, posjećeno 6.3.2019.

[15]   (Plastične polietenske cijevi i njihova primjena) http://hr.cnkangyupipe.com, posjećeno 7.3.2019.

[16]   (Gumene cijevi za ispušne plinove) http://vulkanizacija.blogspot.com/2012/07/cijevi-za-brodske-motore.html, posjećeno 26.2.2019.

[17]   (Instalacija HSCT kompozitnih cijevi) https://akiet.com, posjećeno 9.3.2019.

[18]   (Način proizvodnje kompozitnih cijevi) https://akiet.com/news/what-is-composite-pipe-and-how-is-it-made, posjećeno 10.3.2019.

[19]   (Flowtite GRPcijevi i njihova proizvodnja) http://subor-amiantit.eu/hr/proizvodi, posjećeno 10.3.2019.

[20]   (Kompozitne cijevi) https://e-lass.eu/composites-in-the-shipping-industry, posjećeno 1.3.2019.

[21]   (Primjena kompozitnih cijevi) https://www.researchgate.net/publication/300219097_Composite_Material_Pipes_for_Transportation_of_Effluent_and_Hydrocarbon, posjećeno 28.2.2019.

[22]   (ABS plastične cijevi) https://www.plastock.co.uk/hose-pipe-and-fittings/abs-pipe-fittings, posjećeno 24.2.2019

[23]   Sršen, Ante: Nemetalni cijevovodi I armature na brodovima, završni rad, Sveučilište u Dubrovniku – Pomorski odjel, Dubrovnik, (2019.)

EXHAUST GAS CLEANING SYSTEM

Marko Buršić [a,], Kristijan Lenac [b]

a IHC Engineering Croatia, Ul. Nikola Tesle 9, 52100 Pula
b IHC Engineering Croatia, Milutina Barača 7, 5100 Rijeka
* Coresponding Author, m.bursic@royalihc.com

Abstract

Exhaust gases from ship engines contain many pollutants. Sulfur oxides (SOx) and nitrogen oxides (NOx) are particularly detrimental to the environment. As a result, various laws and regulations have been enacted to try to reduce pollution to an acceptable level. The most significant regulation is Annex VI of the MARPOL Convention. The reduction of sulfur oxide emission can be achieved in two ways. The first is the use of low sulfur fuel, the amount of which is prescribed by Annex VI of the MARPOL Convention. The second is to clean the engine exhaust gases with a scrubber system. Due to high cost of the low sulfur fuels, shipowners in many cases decide to install scrubbers on both the new and the existing ships. Installing a scrubber system on existing ships causes a lot of structural problems that need to be addressed. There are two basic types of scrubber system, dry and wet. Wet scrubbers are divided into open loop scrubbers, closed loop scrubbers and hybrids. The most commonly used NOx emission reduction system is selective catalytic reduction (SCR), in which the introduction of reducing medium (urea) into exhaust gases causes nitrogen oxides to separate into nitrogen and water.

Key words: exhaust gas; sulfur oxides; nitrogen oxides; scrubber; selective catalytic reduction

Sažetak

U ispušnim plinovima brodskih motora nalazi se mnogo štetnih tvari koje zagađuju okoliš. Posebno štetan utjecaj na okoliš imaju sumporni oksidi (SOx) i dušični oksidi (NOx). Zbog toga doneseni su razni zakoni i propisi kojima se pokušava svesti zagađenje na što prihvatljivu razinu. Najznačajniji takav propis je prilog VI MARPOL konvencije. Smanjenje emisije sumpornih oksida može se postići na dva načina. Prvi je upotrebom goriva sa niskim udjelom sumpora čija je količina propisana anexom VI MARPOL konvencije. Drugi način je pročišćavanjem ispušnih plinova motora pomoću ispirača plinova (eng. scrubber). Zbog dosta visoke cijene goriva sa niskim udjelom sumpora brodovlasnici se u dosta slučajeva odlučuju na ugradnju ispirača plinova, kako na novogradnje tako i na već postojeće brodove. Ugradnja ispirača plinova na postojeće brodove uzrokuje dosta konstrukcijskih problema koje treba riješiti. Postoje dvije osnovne vrste ispirača plinova, suhi i vlažni. Vlažni ispirači plinova se dijele na ispirače sa otvorenom petljom, zatvorenom petljom i hibride. Najčešće korišteni sistem za smanjenje emisije NOx je selektivna katalitička redukcija (SCR), kod koje se ubacivanjem reducirajućeg medija (urea) u ispušne plinove, dušični oksidi razdvajaju na dušik i vodu.

Ključne riječi: ispušni plinovi; sumporni oksidi; dušični oksidi; ispirači plinova; selektivna katalitička redukcija

1. Introduction

Exhaust emissions from marine diesel engines aminly comprise nitrogen, oxygen, carbon dioxide (CO_2) and water vapour, plus smaller quantities of nitrogen oxides, sulphur oxides, carbon monoxide, various hydrocarbons at different states of combustion and complex particular matter (PM). It is these smaller quantities together with CO_2, that are of most concern to human health and the environment. Adverse effects are experienced at local, regional and global events.

In response to these impacts the International Maritime Organization (IMO), through its Marine Environment Protection Comitee (MEPC), introduced regulations for the prevention of air pollution under Annex VI of the MARPOL Convention.

The Annex imposes a framework of mandatory limits on emissions of sulphur oxides (SO_x) and nitrogen oxides (NO_x) both globally and within designated sea areas, known as Emission Control Areas (ECAs). These are regions where neighbouring states have shown that emissions to air have particular impact on human health and the environment.

To meet reduced SO_x emission limits, ships can operate on low-sulphur residual and destilate fuels, and in the long term alternatives such as LNG (liquefied natula gas), biofuels, DME (dimethyl ether) and methanol may provide solutions. The alternative to these options are exhaust gas treatment systems (EGTS) known as SO_x scrubbers which clean the exhaust gas to reduce SO_x emissions to a level that is equivalent to the required fuel sulphur content. This offers flexibility to either operate on low-sulphur fuels or to use higher sulphur fuels.

2. Regulations

MARPOL Annex VI regulates the emissions from ships engaged in international trade and regulations 4, 13 and 14 are particulary relevant.

2.1. Regulation 4

Regulation 4 allows flag administrations to approve alternative means of compliance that are at least as effective in terms of emissions reduction as the prescribed sulphur limts. This means that a ship may operate using a fuel with a sulphur content higher than allowed by regulation 14 as long as an approved SO_x scrubber can reduce the SO_x emissions to a level that is equivalent to, or lower than, the emissions produced by compliant fuel. If a SO_x scrubber is fitted, it must be approved and verified as compliant in accordance with the IMO Exhaust Gas Cleaning Systems Guidelines (MEPC 184(59) – 2009 Guidelines for Exhaust Gas Cleaning Systems).

The Guidelines specify two testing, survey, certification and verification schemes:

- Scheme A – initial approval and certification of performance followed by in-service continuous monitoring of operating parameters plus daily spot checks of the SO_2/CO_2 emission ratio; and

- Scheme B – continuous monitoring of SO_2/CO_2 emission ration using and approved system with in-service daily spot checks of operating parameters

In either case any waswater discharged to sea must also be continuosly monitored.

2.2. Regulation 13

Regulation 13 places limits on the NO_x emissions of marine diesel engines. The limits are divided into three 'Tiers' whose applicability depends on the ship's construction date (or the date of installation of additional or non-identical replacement engines) and engine's rated speed (n). Tier I and Tier II limits were applicable to engines installed on ships constructed on or after 1 January, 2000, and 1 January, 2011 respectively.

Subject to a review of enabling technologies, Tier III limits applies to diesel engines installed on a ship constructed on or after 1 January 2016 and operating inside the North America ECA and the United States Caribbean Sea ECA, and to ships constructed on or after 1 January 2021 and operating in the North Sea ECA and Baltic Sea ECA.
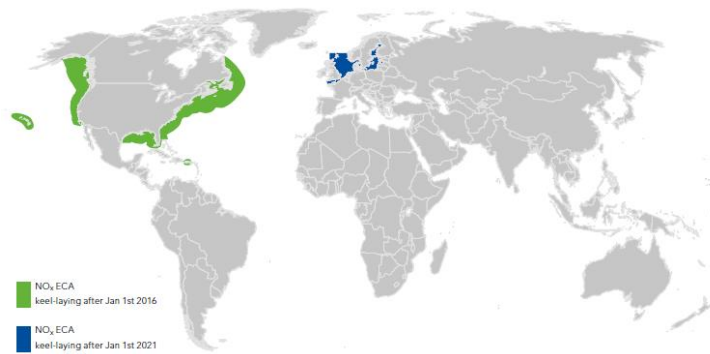
Figure 103 *MARPOL NOₓ Emission Control Areas*

2.3. Regulation 14

Regulation 14 places sulphur limits on the sulphur content of fuel to restrict SO_x and particulate matter emissions, and is applicable to all ships in service. The regulation specifies different limits for operating inside and outside an Emission Control Area for SO_x (ECA-SO_x) and these followed a stepped reduction over time, as shown in Figure 2.
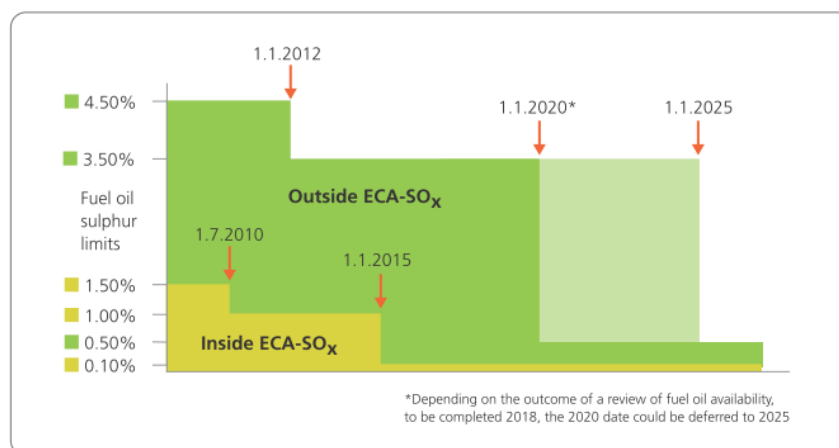
Figure 104 *The MARPOL Annex VI fuel oil sulphur limits*

As of 1 January 2020 new emission standards are enforced for fuel oil used by ships, in a regulation known as IMO 2020. The global sulphur limit (outside SECA's) dropped from an allowed 3.5% sulphur in marine fuels to 0.5%.

Table 22 Current IMO's MFO sulphur limits with enforcement dates (*Table caption style*)

Global sulphur limits	ECAs sulphur limits
4.50% m/m prior to 1 January 2012	1.50% m/m prior to 1 July 2010
3.50% m/m on and after 1 January 2012	1.50% m/m on and after 1 July 2010
0.50% m/m on and after 1 January 2020	0.10% m/m on and after 1 July 2015

The IMO has worked on ensuring consistent implementation of the 0.5% sulphur limit in its Marine Environmental Protection Committee (MEPC) and its subcommittee on Pollution Prevention and Response (PPR). This has led to the development on several regulatory and practical measures

(FONAR's, Carriage Ban, Ship Implementation Plan etc.) to enable any non-compliance to be detected, for example during port State controls (PSC's).
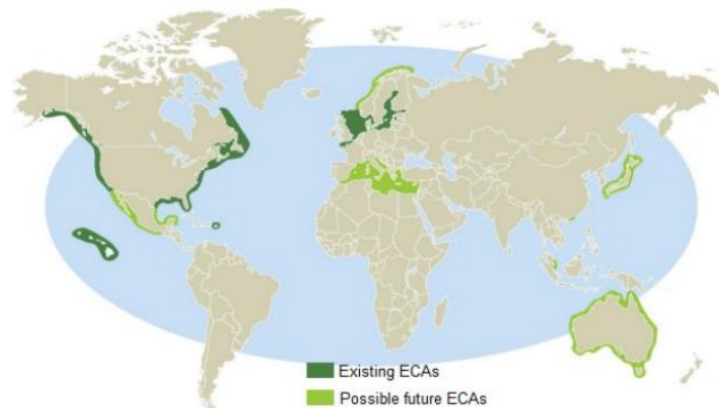
Figure 105 *Present and possible future ECA's*

3. Exhaust Gas Cleaning Systems (EGCS)

Exhaust Gas Cleaning Systems (EGCS), or 'scrubbers', are a systems designed to remove sulphur from exhaust of marine engines and boilers. Ships fitted with scrubbers are able to continue to use residual fuel with significant economic benefits for shipowners. Scrubbers are pricipally used to remove sulphur dioxide (SO_2) from the exhaust gasses but can also remove particulate matter (such as ash and heavy metals) and unburnt hydrocarbon liquids.

The exhaust is cleaned in the scrubber by mixing it thouroughly with water. The scrubber is placed between one or more engines and the exhaust gas funnel. The exhaust gas enters the scrubber through the inlet part (also reffered as jet or jetting section) where the gas is cooled and an initial SO_x and particle absorption takes place. Further cleaning is done in the outlet part also refferd as absorber. The EGCS system is equipped with exhaust bypass arrangement consisting of several bypass valves. Types of exhaust gas cleaning systems

There are four different types of EGCS available:

1. Open loop (seawater scrubber units) use untreated seawater (i.e. the natural alkalinity of the seawater) to neutralise the sulphur from exhaust gasses.
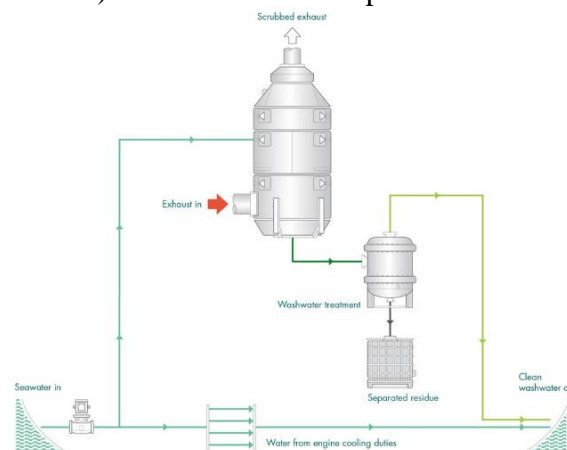
Figure 106 *Open loop EGCS*

2. Closed loop (freshwater scrubber units) are not dependent on the type of water the vessel is operating in, because when the exhaust gasses are added to freshwater in a closed loop system they are neutralised with caustic soda or magnesium oxide.
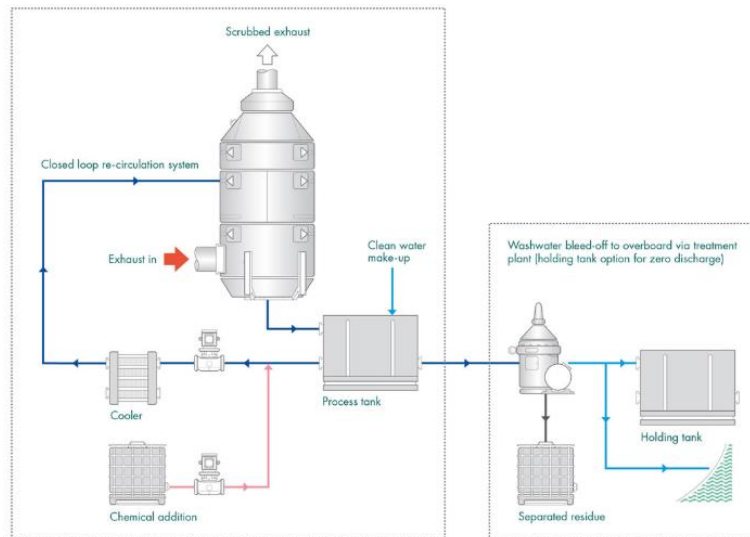
Figure 107 *Closed loop EGCS*

3. Hybrid scrubber units – allows the use of either open or closed loop.
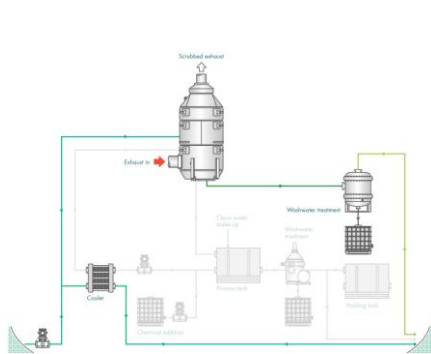
Figure 108 *Hybrid EGCS – open loop*   **Figure 109** *Hybrid EGCS – closed loop*
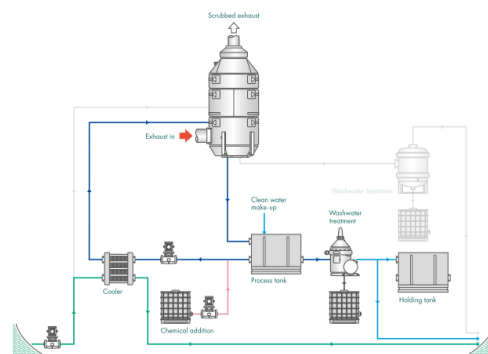
4. Dry scrubber units do not use any liquids in the process as exhaust gasses are cleaned with calcium hydroxide, commonly known as caustic lime.

The types of EGCS which will be installed on a ship are mainly under shipowners choice, depending on the routes of the vessel on which they will be installed. Currently the dominat type within the marine industry are wet scrubbers. Although dry scrubbers are simple to install and operate, their high rate of granulate consumption, which may approach 20 tonnes per day for a 20MW engine, and storage onboard of used granulate before disposal, which means considerable weight and large space requirement, makes them less common in the marine industry.

An open loop scrubber configuration has the lowest investments and operating cost, but its use may be limited by low water alcalinity or local water discharge regulations. Closed loop configuration can be used anywhere and at any time, but its operating costs are higher than the open open loop configuration. Hybrid scrubber uses both configurations: open loop operation reduces

costs whenever possible, but you can easily switch to closed loop if you need to comply with local water discharge regulations.

3.1. Exhaust gas cleaning system components

To have complete overwiev of the system components, a hybrid EGCS system will be descibed. The majority of the wet systems have following components:

- o A vessel that enables the exhaust gas stream from an engine and/or boiler to be intimately mixed with water (seawater or freshwater). For reasons of available space and access the exhaust gas cleaning units (scrubber) tend to be high up in the ship in or around the funnel area. To ensure efficient cleaning, the absorber part of the unit is partly filled with an open-structured metal packing material. The water for scrubbing is supplied through multiple pipes with sprayers, which guarantees even water distribution in all conditions.
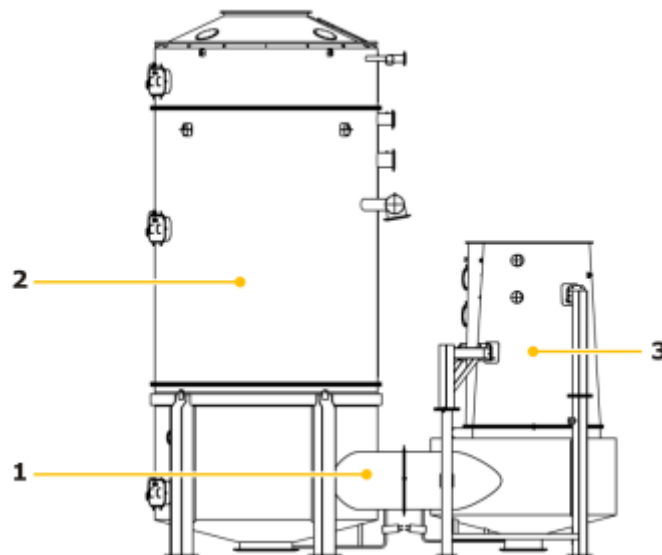
Figure 110 *Example of a scrubber: 1-ducting part, 2-absorber part (outlet), 3-jet part (inlet)*

- o Exhaust gas dampers which in most cases are divided into bypass and uptake dampers. Bypass dampers are kept open to bypass the scrubber unit. When the uptake dampers are open, the exhaust gas flow directly through the scrubber. Each engine or boiler connected to the scrubber has its own bypass and uptake damper.

Figure 111 *Exhaust gas damper*

- o Sealing air fans which supply air to exhaust gas dampers in order to create an air barrier to prevent the exhaust gas from passing through the damper once it is closed. Additionally, sealing air is used to purge the scrubber before maintenace crew needs to access it.
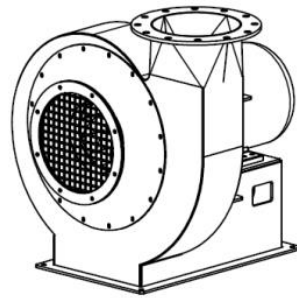
Figure 112 *Sealing air fan*

o Feed water pumps provide the flow of sea water to the scrubber unit in open loop mode. The pumps are usually located deep within the vessel and they must be powerfull enough to overcome the difference in elevation between the pump and scubber. In most cases two centrifugal pumps are used.

o Circulation pumps provide flow of recirculated water in closed loop mode. They are usually much smaller than the feed pumps and in most cases two centrifugal pumps are used.

o Circulation tank (or tanks depending on the system) are made of glass-reinforced epoxy (GRE) and polypropilene (PP) and are essential part of the closed loop or hybrid configuration. The tank allows long period of closed loop operation without water discharge. It also provides a buffer for the system, eliminating the need to constanly add or bleed of water.
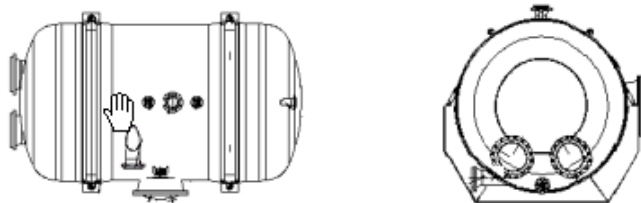
Figure 113 *Fresh water circulation tank*

o Plate heat exchanger is provided for closed loop and hybrid configuration. It ensures that the feed water is cold enough before entering the sprayers in the scrubber.

o A treatment plant to remove pollutants from the wash water after the scrubbing process. It is usually a high-speed separator that removes soot from the circulation water in closed loop, which is collected as sludge. Scubber sludge should be stored in a dedicated sludge tank and can't be burned in the ship's incinerators. It is deposited on shore.

o Monitoring equipment that monitor the quality of the cleaning process and verify if the EGC system complies with the requirements. It usually includes a data logger that records information SO_2, CO_2, pH, turbidity and so on, as well as GPS data about position, date and time. This data conforms to MEPC regulations.
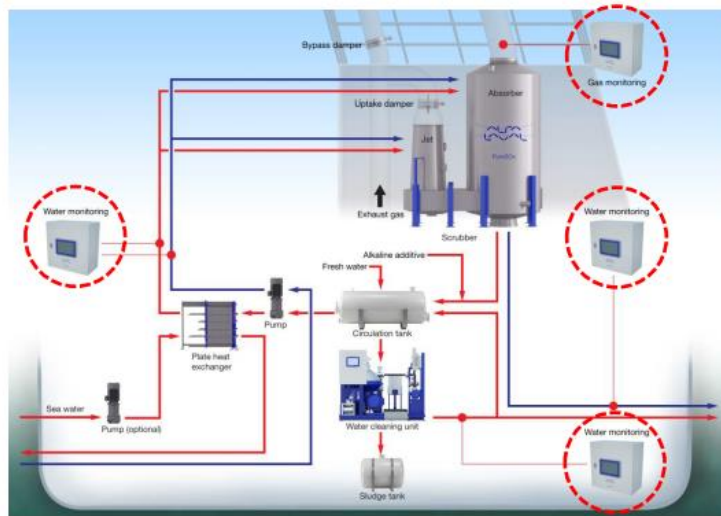
Figure 114 *Hybrid system showing water and gas analysis units*

o Various control cabinets such as Main control cabinet, Pump control cabinet, motor starters, etc…

o Consumables are required in closed loop operations. Close loop operation requires desalinated circulation water as well as dosing with an alkaline additive in the form of caustic soda or a powder like sodium carbonate. Each of these is stored in a dedicated tank. The amount of circulation water needed varies with the ambient temperature and sea water temperature. The amount of caustic soda or powder is directly determined by the engine load and the sulphur content of the fuel.

4. EGCS design and installation on ships

Before designing an EGCS, there are several information that should be assessed. This information includes number and types of engines and boilers connected to EGCS, allowable backpressure of the engines and boilers connected to the EGCS, available space for installing the EGCS, sulphur content of fuel and ships sailing routes (ambient temperature, relative humidity, alkalinity of seawater,…). All these information are interpreted by the EGCS supplier and some requirements are given. These are usually sizes of components, seawater and freshwater requirements (closed loop and hybrid system), backpressure of the scrubber, discharge water arrangement and power consumption of the system.

The biggest operation cost associated with an EGC system is the additional power requirements of the system, which is highly dependent on the cost of fuel. Other operating costs to consider include EGCS and associated equipment maintenance; increased fuel costs due to increased backpressure and power consumption; bulk reactant procurement, storage and consumption; waste management and disposal; and crew training. Open loop systems are typically less costly than closed loop systems, which are relatively similar in price to hybrid systems.

When it comes to the scrubber itself, it's important to remember that the scrubber's design affect the whole system. Not all components are placed within the ship's funnel. Different scrubber design are possible with different placements of the jet and absorber sections. Most wet SO_x

scrubbers have a split design, which means that the jet and absorber sections are physically independent one from another. A split design requires a larger space in the funnel because it has two vertical sections.

Figure 115 *Split design scrubber*

Figure 116 *Inline design*

Scrubbers can also be built with inline design, in which the absorber section is placed directly atop the jet section. This is especially appealing for vessels with difficult space constraints or stability issues, such as cruise ships and RoPax vessels. However, an inline design is also more complex. For example, careful attention must be paid to creating a safe water trap in order to protect the engine.

When designing a EGCS, for both cases a stability impact study should be carried out due to additional weight of the EGCS on the vessel. Also, a detailed general arrangement plan of the EGCS components must be performed in close cooperation with the supplier as well as the water discharge arrangements.

4.1.   EGCS materials

The choice of pipework material can significantly reduce weight and costs of the complete EGCS. Usually the EGCS supplier is responsible for almost every component except piping installed on board.

Seawater supply piping may be made of coated steel, but experience has shown that in this case it comes to rapid localised corrosion typically at welds and flanges. Instead of the glass reinforced epoxy (GRE) piping has been proved like a suitable solution.

Circulation and discharge piping are made of GRE. Wash water in wet SO_X scrubbers is highly corrosive and the scrubber components that come into contact with it should be constructed of suitable corrosion-resistant materials. GRE piping close to the scrubber must be protected from exposure to hot exhaust gases. The lighter weight and ease of assembly of non-metallic materials does however facilitate retrofit and the service life can substantially outlast metals.

Hull penetration for discharge water should be made of same material as the ship's hull and should be coated. Discharge water in Open loop can become very acidic and suitable coating should be applied.

In a closed loop or hybrid system, a zero discharge tank may be installed. When installing it on existing vessels a GRE tank with polypropylene protection layer may be good solution, instead of

having hot work for making a new tank. If the zero discharge tank will be made of steel it should be noted that it needs an epoxy protective layer or other suitable coating.

Sludge tank and sludge piping should be similar to a standard ship sludge tank. Sludge must be stored on board, landed ashore and disposed of appropriately; it is not permitted to incinerate it or discharge to the sea. If a scrubber removes 70% of the particulate matter, then approximately 500kg of sludge may be expected for every 100 tonnes (t) of residual fuel consumed by a diesel engine. This is dependent on removal rate at the scrubber and the efficiency of the washwater treatment, both in removing PM and not including excess water. Wet SO_x scrubber manufacturers typically recommend a sludge tank of around 0.5m^3 /MW of scrubbed engine power.

Usually there is no need to replace the exhaust piping. Between the engine and an EGC unit the exhaust temperature can be approximately 300°C, but after the passage through the scrubber the temperature is reduced very significantly. Due to possible backdraft from the scrubber, the inlet reducer on top of the jetting part should be made of EN.14547 (SMO254). Inlet into the jetting part may be exposed to sulphuric acid and seawater, but it is still part of the very hot exhaust system.

For closed loop and hybrid system there is need for consumable chemicals for keeping the quality of washwater. These chemicals should be stored on board. Caustic soda (NaOH) is kept stored in ship's dedicated tank which should be epoxy coated. For caustic soda piping use of Stainless Steel 304L or 316L, steel with epoxy coating, polypropylene, polyethylene, PVC or C-PVC is recommended. Since caustic soda should be heated (ideal storage temperature is 26.7^{o}C to 37°C), for exposed deck pipes use of SS piping is strongly recommended, while inboard PVC or C-PVC pipes are most convenient to be used.

For coagulant storage it is possible to use ship's dedicated steel tank, but this tank should be acid-proof or rubber coated, which is not so simple to install, especially during retrofitting. Instead an IBC container (International Bulk Container) is used, which simplifies installation and maintenance. From the IBC container to the EGCS usually plastic materials (PE, PP, PVC) are used, which are simple and cheap to install and also light weight. However, it's possible to use different materials such as fiberglass-reinforced polyester, titanium, acid-proof or rubber coated steel pipes. Coagulant pipes are relatively small in diameter which in practise means that plastic materials are more used.

4.2. *Installation of EGCS*

Installation time for an EGCS depends on the manufacturer and type of system being installed. The main consideration are size, complexity of the system and the components involved. Depending on manufacturer, the EGCS may or may not be inline. An inline unit should be installed directly in line with the silencer and exhaust gas economiser. Units that are not inline require multiple passes and often have separate bypass ducts which tend to take up more space than an inline unit.

Open loop systems have fewer components and require less tank space than a closed loop or hybrid system. Installation of open loop system can be less complicated and time consuming. Closed loop, hybrid systems and dry systems take up more space, require several tanks for storage, dosing units, separators, multiple pumps and more complex control units.

Installation of EGCS is a complex process which involves close cooperation between shipowner, shipyard and EGCS supplier. Due to its large size, the biggest problem for accommodation and installation is the scrubber unit. For retrofits the availability of space to fit the scrubber unit may be a limiting factor, although depending on design they can be fitted inside an existing or extended funnel or outside. For new builds, units can be readily accommodated at the planning stage. A wet system unit will be fitted above any exhaust boiler or exhaust gas economiser.
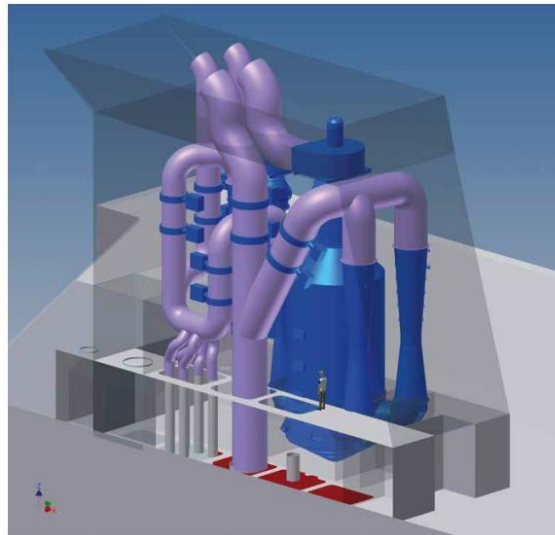
Figure 117 *Extended funnel space with a Wärtsilä-Hamworthy scrubber with two inlets*

The scrubber unit may be preassembled in one section block together with sealing air fans and damper to facilitate the installation on board. This is especially interesting for existing vessels and retrofitting the EGCS to reduce the time required for installation.

Figure 118 *Preassembled section with Alfa Laval's scrubber unit*

The scrubber unit can be installed separately, part by part, depending on transport availability. Assembling the unit must be in line with recommendations from producer.

Figure 119 *First figure example*

Figure 120 *Second figure example*

Other larger units in EGCS are the circulation tank and Water Cleaning Unit (WCU). In general, both of these units are large and require a lot of service space. The units are located below scrubber unit to facilitate the water flow from scrubber by gravitational force.

However, WCU producers suggest that its position is flexible and does not need to be in the engine room. Space may be less available on vessels with medium speed propulsion engines such as cruise and ferry when compared with cargo ships powered by slow speed engines.

WCU has a modular design and consist of three separate modules: the separator skid with a control unit and sludge pump, the feed pump skid and the coagulant dosing pump skid. As all separator units, WCU requires an overhead hoist with dedicated capacity to transport the bowl parts to a workbench for cleaning and maintenance purposes.
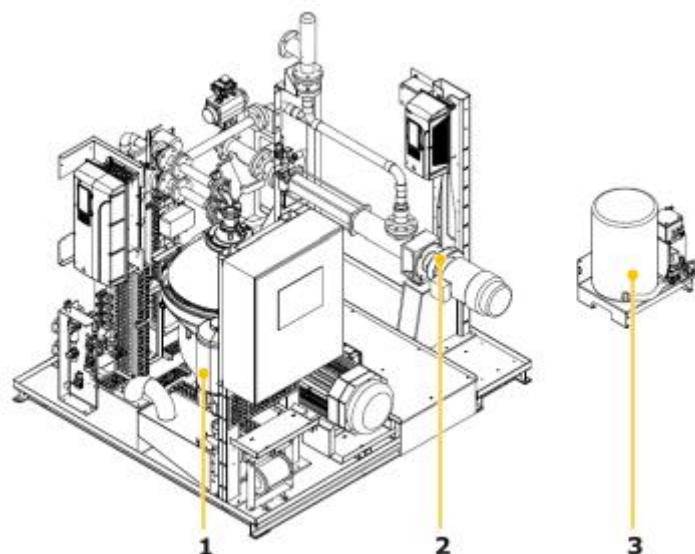
Figure 121 *Example of a Water Cleaning Unit: 1-WCU separator skid, 2-WCU feed pump skid, 3-Coagulant dosing pump skid*

399

Location of the sea water supply pumps is also one key factor when designing and installing the EGC system. In general these pumps are not self-priming and should be located below sea water level. This is usually on tank top inside engine room. Sea water suction is also an issue, especially on an existing vessel. Sea water quantity is calculated depending on the system configuration and installed power. Based on these values a sea water collector is designed. On new builds this amount of water is calculated with other consumers and one single water collector is build. For existing vessels this is not quite easy to make. In most cases additional sea water chests, enlargement of existing sea water chest or additional sea water collector might be needed.

5. NO$_x$ emission reduction system

Selective catalytic reduction is a relatively mature technology, widely used for NO$_x$ control in land-based industry and land-based transportation. SCR can reduce NOx emissions by 80-90% to below 2g/kWh. SCR systems are currently fitted to four-stroke medium-speed engines on a number of ships in service which are able to gain commercial advantage from reduced NO$_x$ emission.

The SCR system converts nitrogen oxides into nitrogen and water, by means of a reducing agent injected into the engine exhaust stream before a catalyst. Urea is the reductant typically used for marine applications. It decomposes to form ammonia in a mixing duct before adsorption onto the catalyst that facilitates the reduction process.

Typically, SCR systems are applied to four-stroke medium and high speed engines, which   have exhaust temperatures above 300°C at normal load. Slow speed crosshead engines have lower exhaust temperatures because of their higher efficiency and to date the very small number have been equipped with SCR. In an alternative design the reactor has been placed after the turbocharger and a burner used to increase the exhaust temperature to the required level.

Figure 122 *SCR arrangement – two-stroke low speed engine MAN Diesel & Turbo*

An SCR system comprises the following main components:

o   Pumping unit for transfer of urea solution from storage

o   Urea dosing unit

o   Mixing duct with urea injection point

o   Reactor housing containing replaceable catalyst blocks

o   Soot/ash cleaning system

o   NOx measurement and control cabinet
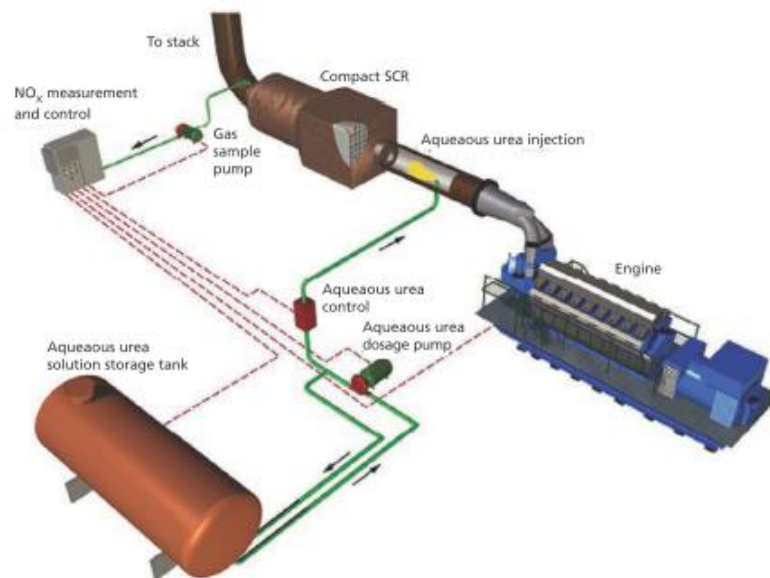
Figure 123 *Marine SCR arrangement – four-stroke medium speed engine Wärtsilä*

A pump unit transfers urea from the storage tank to the dosing unit, which regulates the flow of urea solution to the injection system based on the operation of the engine and humidity of ambient air. The humidity sensor based urea control adjustment ensures Tier 3 emission compliance in all ambient conditions. The dosing unit also controls the compressed air flow to the urea injector. The urea injector sprays the urea solution into the exhaust gas duct. After the urea injection, the exhaust gas flows through the mixing pipe to the reactor, where the NO_x reduction take place over catalyst elements. The reactor is equipped with a soot blowing system for keeping the catalyst elements clean.

For marine applications urea is used because of the hazards associated with handling ammonia, which is classed as toxic, corrosive and harmful to the environment. It is supplied in solution or can be mixed on board using bagged granules and freshwater.

The injected urea solution must be mixed thoroughly with the hot exhaust gas in a specifically designed duct before entering the reactor housing containing the catalyst. Whilst in the duct the urea combines with water from the exhaust stream and the injected solution, then decomposes to form ammonia (NH_3) and some carbon dioxide. In contact with the surface of the catalyst the NO_x components, nitric oxide (NO) and nitrogen dioxide (NO_2) react with the ammonia and oxygen from the exhaust to form nitrogen and water.

5.1.   *Installation of SCR*

As a rule of thumb, one SCR is installed per each engine and exhaust pipe. The reactor is a steel casing consisting of and inlet and outlet connection, catalyst layers, steel structure for supporting the catalyst layers and a soot blowing unit. The standard reactor is designed in a flexible way for the initial loading of catalyst layers, usually two or three, depending on the ship structure. The reactor can be installed either vertically or horizontally onboard the ship. The SCR reactor can be also integrated with silencer in order to optimise the use of space onboard.
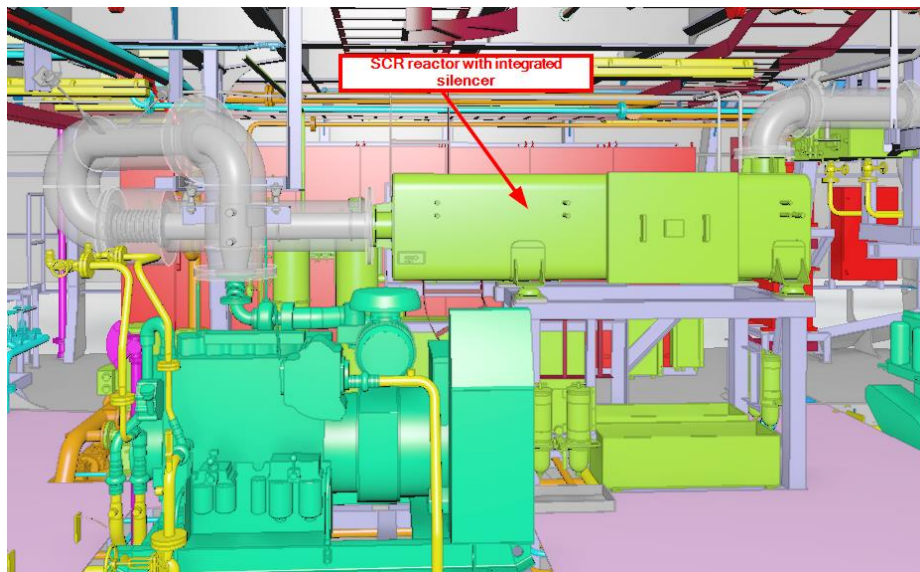
Figure 124 *SCR reactor with integrated silencer – horizontal*
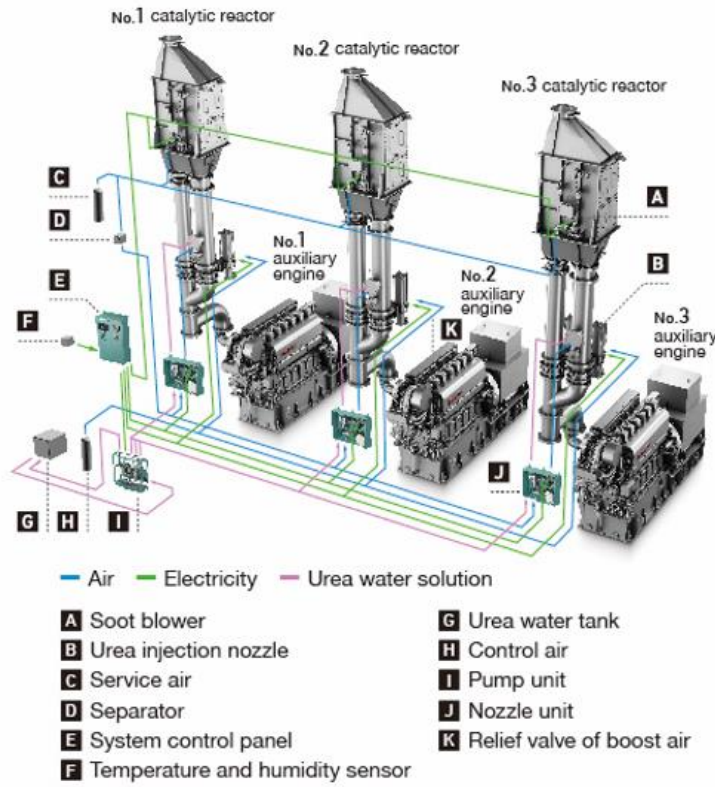
Figure 125 *SCR system overview-vertical reactor (Yanmar)*

SCR can be combined with scrubber installation in order to be compliant with the SOx regulations. In this configurations, scrubber is always installed upstream of the SCR reactor because SCR needs hot exhaust gas in order to have proper NO_x reduction.
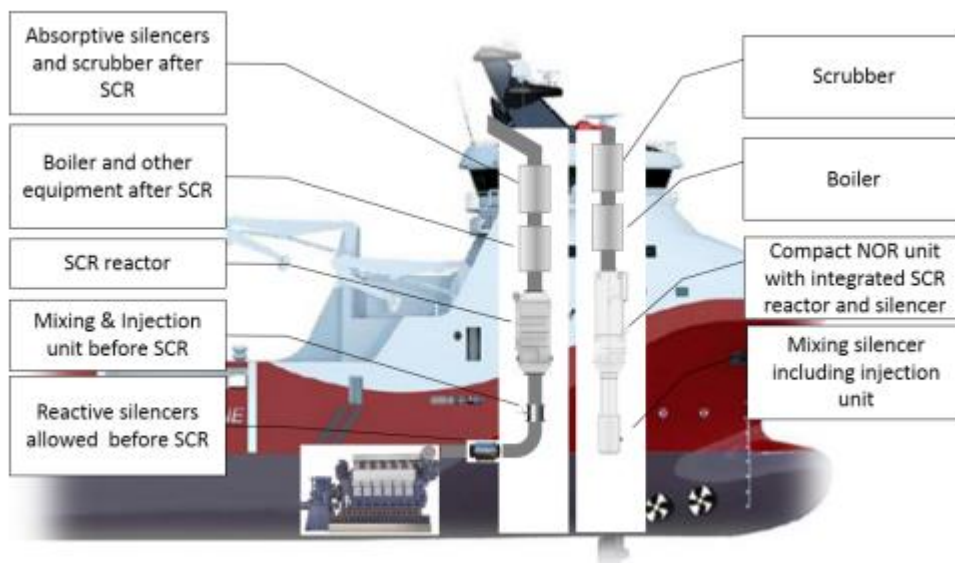
Figure 126 *SCR system with boiler and scrubber (Wärtsilä)*

6. Conclusion

MARPOL Annex VI regulations are mandatory and the global sulphur cap has come in force from 1 January 2020. The shipping industry has taken several actions in order to be compliant with these regulations. Among various SOx, NOx, and PM reduction technologies, for large marine diesel engines that are used for ocean-going vessels such as container ships, oil takers, bulk carriers and cruise ships for propulsion power rating from 2,500 to 70,000 kW EGR and SCR systems which can be applied to meet the regulations. Ships using a scrubber technology have the advantage to continue using low-cost HFO while meeting MARPOL Annex VI emission limits. However, higher backpressure, chemical consumables on board, extra power consumption, cargo loss, washwater discharge and other operational issues are to be expected.

REFERENCES

[1]   MEPC 184(59) – Guidelines for Exhaust Gas Cleaning Systems

[2]   Understanding exhaust gas treatment systems: guidance for shipowners and operators – Lloyds Register, June 2012.

[3]   OCIMF – Guide for Implementation of Sulphur Oxide Exhaust Gas Cleaning Systems – First Edition 2016

[4]   A practical guide to exhaust gas cleaning systems for the maritime industry – EGSCA Handbook 2012

[5]   Global Sulphur Cap 2020 – DNV GL 2020

[6]   Deciding your route to SO_x compliance – Alfa Laval, www.alfalaval.com

[7]   Environmental Product Guide – Wärtsilä, www.wartsila.com

[8]   Marine SCR System for Compliance with IMO NOx Tier 3 Regulations, www.yanmar.com/global/about/technology/technical_review/2018/0413_2.html

REDUCING ENVIRONMENTAL IMPACT AND FUEL COSTS BY INSTALLING A PHOTOVOLTAIC POWER PLANT ON BOARD

Vladimir Pelić [a], Tomislav Mrakovčić [*b], Vedran Medica-Viola [b], Marko Valčić [b]

a: University of Rijeka, Faculty of Maritime Studies, Studentska ulica 2, 51000 Rijeka,

b: University of Rijeka, Faculty of Engineering Vukovarska 58, 51000 Rijeka,

* Corresponding Author: tomislav.mrakovcic@riteh.hr

SUMMARY

Although maritime transport is currently the most efficient form of transport, it is facing increasingly complex challenges. International conventions and other regulations are continually imposing strict requirements that ships and their energy facilities must meet in order to reduce their negative environmental impact and increase energy efficiency. Increasing energy efficiency also contributes to market competitiveness, and is in the ship-owner's interest. Application of photovoltaic power plants on liquid cargo ships and passenger ships longer than 250 m is considered in this paper. These two ship types were chosen because their purpose and construction features do not present an obstacle to the installation of a photovoltaic power plant. The nominal power of the photovoltaic power plant on the tanker is up to 10% of the installed power of the propulsion machine, and in the passenger ship up to 10% of the total electricity requirements. In the case of tankers, in order to achieve better utilization, the possibility of "storing" energy is suggested for periods when photovoltaic system provides more electricity than needed. The surplus energy can be used for ship propulsion. By using photovoltaic power plants as a supplementary energy source, it is possible to achieve savings in fuel consumption and reduce the negative environmental impact of marine propulsion systems. The achieved results significantly depend on the area and conditions of the ship operation, and on the characteristics of the photovoltaic power plant.

Keywords: *energy efficiency, environment, photovoltaic power plants, marine plants.*

SMANJENJE UTJECAJA NA OKOLIŠ I TROŠKOVA GORIVA UGRADNJOM FOTONAPONSKE ELEKTRANE NA BRODU

Vladimir Pelić [a], Tomislav Mrakovčić [b], Vedran Medica-Viola [b], Marko Valčić [b]

a: Pomorski fakultet Sveučilišta u Rijeci, Studentska ulica 2, 51000 Rijeka,

b: Tehnički fakultet Sveučilišta u Rijeci, Vukovarska 58, 51000 Rijeka,

SAŽETAK

Premda pomorski transport predstavlja najučinkovitiji poznati oblik transporta pred njega se postavljaju sve veći izazovi. Zahtjevi koje brodovi odnosno njihova energetska postrojenja moraju ispunjavati s ciljem smanjenja negativnog utjecaja na okoliš i povećanja energetske učinkovitosti proizlaze iz međunarodnih konvencija i drugih propisa. Povećanje energetske učinkovitosti doprinosi i konkurentnosti na tržištu, te je u interesu brodovlasnika. U ovom radu razmatrati će se primjena fotonaponskih elektrana na brodovima za prijevoz tekućeg tereta i brodovima za prijevoz putnika duljine veće od 250 m. Ove dvije vrste brodova odabrane su jer njihova namjena i konstrukcijske značajke nisu smetnja ugradnji fotonaponske elektrane. Nazivna snaga fotonaponske elektrane kod tankera iznosi do 10% instalirane snage propulzijskog stroja, a kod putničkog broda do 10% od ukupnih potreba za električnom energijom. Kod tankera je radi boljeg iskorištenja predviđena mogućnost "skladištenja" energije u periodima kada se iz fotonaponskog sustava dobije više električne energije od trenutnih potreba, odnosno njeno korištenje za propulziju broda. Primjenom fotonaponskih elektrana kao dopunskog izvora energije moguće je ostvariti značajne uštede u potrošnji goriva i

smanjiti negativan utjecaja brodskih pogonskih postrojenja na okoliš. Pri tom ostvareni rezultati znatno ovise o području i uvjetima eksploatacije broda, te o značajkama fotonaponske elektrane.

Ključne riječi: *energetska učinkovitost, okoliš, fotonaponske elektrane, brodska postrojenja*

1. Introduction

Transport of goods by sea, and especially in intercontinental trade, is the most important and at the same time the most cost-effective known form of transport. The convenience of maritime transport is particularly pronounced with regard to the cost per tonne transported and the mile travelled. Although it can be said without exaggeration that the transport of goods by sea is not only energy efficient, but also an environmentally friendly form of transport, it still needs to be improved. The provisions of Annex VI of the MARPOL Convention relating to the limitation of emissions of harmful substances into the atmosphere from ships have significantly contributed to the reduction of SO_x and NO_x emissions resulting from maritime transport.

The majority of ships in maritime transport use a low-speed diesel engine as a propulsion engine primarily for its energy efficiency, durability and reliability. The use of medium-speed diesel engines in systems with electric power transmission is on the rise lately. Marine propulsion systems with electric power transmission are suitable to be upgraded with alternative sources of renewable energy. Energy systems for the direct transformation of the sunlight radiation into electricity are particularly suitable for this purpose. The use of photovoltaic (PV) cells to generate electricity began in the second half of the last century, although the PV effect was discovered much earlier. One of the first applications of PV cells (*solar cells*) was the power supply of artificial satellites. Even today it is used as an auxiliary or main source of electricity for various space research needs. Due to the complex technological process of manufacturing PV cells, their initial manufacturing cost was high, while the energy conversion efficiency was low. Thus scope of application of PV cells was exclusively limited to only special purposes. However, intensive research and the application of new materials and technologies have led not only to increased efficiency, but also to a significant cost reduction of PV cells and the systems as a whole. The development of power electronics has enabled the installation of a large number of PV cells or PV power plants in conventional power systems. This paved the way for the expansion of the application of PV systems for various purposes, from the supply of electricity to smaller facilities to PV power plants intended for the supply of settlements and cities.

Maritime has a specifically conservative attitude towards new technologies and modern technical solutions. It is therefore not surprising that the use of PV systems is mainly limited to the powering up signal buoys and lighthouses, while the use on ships is mostly reduced to auxiliary sources for charging the batteries up. Scarce examples of solar energy applications for vessel propulsion are reduced to individual cases of smaller experimental, sports or recreational vessels.

Legal restrictions prohibit vessels with internal combustion engines to be used for passenger transportation over lakes. Therefore, many boats and smaller ships designed to operate on lakes or rivers predominantly use PV systems as an additional source of electricity for propulsion in addition to the batteries.

The aim of this paper is to show that the installation of a PV power plant on a ship can help in reducing fuel consumption, and consequently reduce the negative environmental impact. It is assumed that the selected types of ships, regarding their purpose and construction features, allow

the installation of PV power plants and associated equipment without compromising the safety and functionality of the ship. The available net area for installing the PV panels on the passenger transport ship must be sufficiently large that the rated power of the installed PV power plant reaches at least 10% of the vessel's total electricity consumption. It should be noted that the energy required for the ship propulsion is not taken into account here. In the case of a liquid cargo ship (*tanker*), it is assumed that it is possible to install a PV power plant with a rated power of at least 5% of the nominal power of the propulsion machine. The passenger ship is equipped with a diesel-electric propulsion system, and the tanker is powered by a low-speed diesel engine and direct mechanical power transmission.

2. Sun as an energy source

It is well known that the Sun is the source of energy that enabled the emergence and sustainability of life on Earth. Almost all known sources (*resources*) of energy on Earth, except energy obtained by nuclear reactions, come directly or indirectly from the Sun. Although it is not in reality, the Sun is considered a *renewable* and environmentally friendly, inexhaustible source of energy. However, when considered as an energy source, Sun is a fusion nuclear reactor, in which mass is transformed into energy. Energy transformed through nuclear reactions in the Sun is emitted in the form of an electromagnetic wave into the surrounding space. It is estimated that the Sun emits $3.3 \cdot 10^{24}$ MWh of energy per year. Out of the total energy radiated by Sun, only about $1.5 \cdot 10^{15}$ MWh reaches Earth annually.

It is estimated that the temperature of the Sun's core is about 10^7 K, while the average temperature of its surface is 5760 K. The spectrum of solar radiation includes electromagnetic waves of wavelength λ of 0.12 - 10 μm, which roughly corresponds to the radiation spectrum of a black body heated to 5760 K.

If the irradiated surface (*collector or PV module*) is not placed so that the Sun's rays fall on it at right angles, then the total radiation on that surface consists of three components: *direct*, *diffuse* and *reflected* radiation. Direct solar radiation to the surface comes directly from the Sun's apparent direction. As it passes through the atmosphere, part of the Sun's radiation is scattered (*diffused*), and reaches the surface from different directions. If the irradiated surface is not perpendicular to the Sun's rays, but inclined, then the surface is irradiated also by the rays reflected from the surrounding objects. As it passes through the atmosphere, solar radiation weakens due to scattering on gas molecules (water vapour and clouds) and solid particles (dust), and due to absorption and interaction with molecules of carbon dioxide, methane, ozone and other substances. In addition, the weakening of the radiation intensity occurs due to scattering and absorption on clouds.

The radiation is not weakened due to the absorption and diffusion on its way from the Sun to the top of the Earth's atmosphere, but rays are travelling in separate directions. Therefore, the intensity of solar radiation at the very entrance to the Earth's atmosphere depends on the distance of the Earth from the Sun, which varies throughout the year. Extraterrestrial radiation is defined as the density of the energy flux of sunlight rays which are perpendicular to the exposed surface. Variations in the intensity of extraterrestrial radiation during the year do not exceed 7% relative to the minimum value. Mean value of the radiation intensity is called the *solar constant*. The standard measured value of the solar constant is $E_0 = 1353$ W/m².

While passing through the layers of the atmosphere, ozone completely absorbs ultraviolet (UV) radiation of a wavelength shorter than 0.3 μm. UV radiation in the range of 0.3 μm to 0.4 μm is

almost completely scattered. Radiation with wavelengths up to 2.5 μm in the infrared (IR) part of the spectrum is partially absorbed by water vapour. Carbon dioxide absorbs radiation of wavelengths longer than 2.5 μm. Due to scattering and absorption, the energy flux density of solar radiation reaching the Earth's surface is reduced by 25% - 50% and the electromagnetic spectrum of radiation is reduced to wavelengths from 0.3 μm to 2.5 μm.

Significant data in designing terrestrial stationary solar devices is the monthly average of daily total irradiance. These data are obtained for a specific location by systematic multiple-year measurements and data processing. If the measured data are not available, then the monthly average of the daily total irradiance of the horizontal surface is determined using empirical expressions, in which other measured climatological data are used. In this process, the insolation data is predominantly used. Insolation refers to the share of time in the day during which the solar radiation reaches the horizontal surface of the measuring device. For an accurate estimate of the amount of energy that can be obtained from the ship's solar power plant, it is necessary to obtain data on monthly averages of daily total radiation for the ship's navigation area.

3. Photovoltaic effect

The application of the photovoltaic (PV) effect is one of the most attractive ways of obtaining electricity by direct transformation from solar radiation. Becquerel in 1839 was the first to notice the phenomenon that varying brightness of the light illuminating electrodes immersed in the electrolyte causes a change in the electric current between those electrodes. The change in the conductivity of selenium with a change in light intensity was discovered in 1873 by Willoughby. Based on these and latter researches in the second half of the 19th century, Elster and Geitel developed a device to transform radiation energy into electricity (a selenium photocell), that could be used to measure light intensity. The theoretical explanation of the PV effect was given by the physicist Einstein in 1905, for which he received the Nobel Prize in Physics in 1921.

The development of PV cells takes place in parallel with the development and application of semiconductor technology. The first photocells were based on the application of selenium and copper oxide used as semiconductor materials in rectifiers. Selenium and copper-oxide were replaced by germanium and silicon as semiconductor materials in the middle of the 20th century. The first usable PV cell was manufactured out of monocrystalline silicon in 1954 by Chapin, Fulier and Pearson. This achievement marked the beginning of the accelerated development of PV cell technology.

3.1. The principle of operation of PV cells

A directly proportional dependence between the luminous flux density and the strength of the electric current in experimental investigations of the photoelectric (PV) effect was discovered by Stoletov. Subsequent experiments confirmed that the number of emitted electrons would double when the surface light intensity doubled. A theoretically plausible explanation for the PV effect was provided by Einstein who assumed that light is made up of discrete tiny particles (photons). With the help of Planck's theory of black body radiation, Einstein assumed that the energy of a photon is equal to the product of frequency and constant (Planck's constant). Taking this assumption into account, he concluded that the energy of a photon is linearly dependent on the frequency of light and not on its intensity. These assumptions, which were later also experimentally confirmed, form the basis of the

dual nature of light, which simultaneously has the properties of an electromagnetic wave and material particles. These assumptions provided a theoretical explanation of the PV effect.

The photovoltaic effect occurs when the photon has enough energy to discharge the electron of the atom that is in the boundary layer of the semiconductor material of the PV cell. The "free" electrons (*negative charge*) move towards the negative pole, and the cavities (*positive charge*) towards the positive pole of the PV cells, as shown simplified in Figure 3.1.

The energy required for an electron discharge depends on the semiconductor material. Silicon, which has four valence electrons, is often used as a base material to manufacture semiconductors. Through the process of doping phosphorus with five valence electrons or boron with three valence electrons is injected into a layer of silicon. When a doped semiconductor contains mostly free holes it is called *P-type*, and when it contains mostly free electrons it is known as *N-type*. The semiconductor materials used in PV cells are doped under precise conditions to control the concentration and regions of P- and N-type dopants. A thin surface layer is N-type region, while the rest is the P-type region.
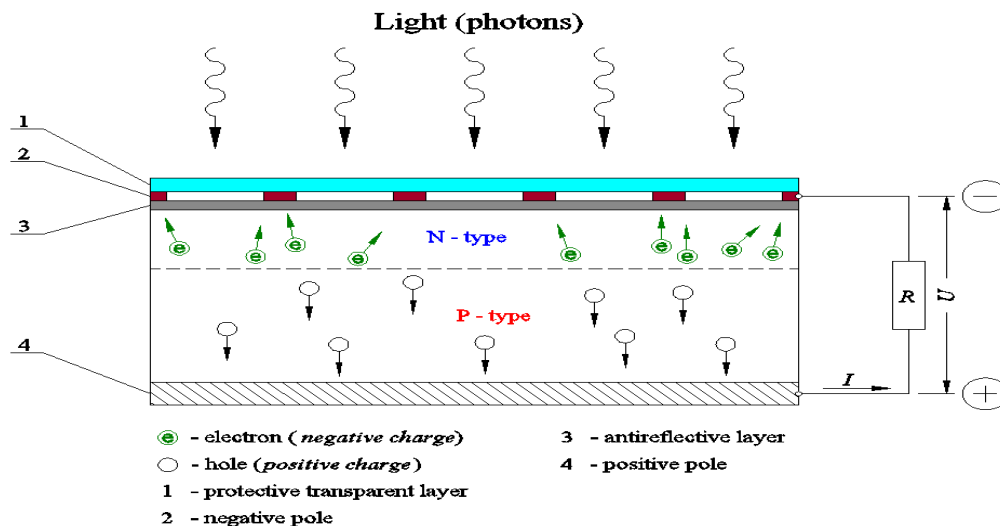
Figure 3.1. The principle of operation of the PV cell

Such silicon semiconductor board is placed with its back side in contact with the metal board, which serves as a cathode. An antireflective layer is applied on the semiconductor's front side, in order to increase the efficiency. The front contact, anode, which resembles a grid, is placed on top of the antireflective layer. The front contact does not cover more than 5% of the surface, so it has no significant effect on the absorption of solar radiation. An individual PV cell, depending on the semiconductor material used, can achieve a voltage of 0.6 to 1 V at a current density of about 15 to 30 mA/cm^2. Higher currents and voltages are obtained by parallel and series connection of PV cells. The PV panels thus obtained usually have a nominal voltage of 12 V. The power, i.e. current that the panel can produce depends primarily on the surface area of the panel. Just like PV cells, the panels can also be connected in series or in parallel, in order to achieve the required voltage and electric current.

3.2. Types of PV cells

Regarding the material structure, PV cells can be divided into: monocrystalline, polycrystalline, and amorphous (*thin* film technology). The basic material for the production of monocrystalline and polycrystalline PV cells is silicon, and in addition to silicon, other materials are used in the technology of thin film, such as: CdS / Cu_2S, CdS / CdTe, GaAlAs / GaAs, GaAs and $CuInSe_2$ (CIS). Semiconductor material and fabrication technology affect the characteristics of PV cells. Tables 3.1. and 3.2. present the features of different PV cell types.

Table 3.1. Open circuit voltage and short-circuit current for different PV cells (*source:* [1])

PV cell type	U_{oc}, V	I_{sc}, mA/cm^2
m-Si	0.65	30
p-Si	0.60	26
a-Si	0.85	15
CdS / Cu_2S	0.50	20
CdS / CdTe	0.70	15
GaAlAs / GaAs	1.00	30
GaAs	1.00	20

Table 3.2. Efficiency and expected service life for different PV cells (*source:* [2])

PV cell type	Efficiency, %	Life time, years
m-Si	15 - 18	> 30
p-Si	13 - 15	25
a-Si	5 - 7	20
$CuInSe_2$ (CIS)	9 - 11	20
CdS / CdTe	5 – 8.5	20

Table 3.1. lists the voltages at the open circuit U_{oc} and the short-circuit current density I_{sc} of different PV cell types. Table 3.2. displays data on the efficiency (degree of action) and the expected service life of PV cells. Figure 3.2. presents the share of each PV cell type in the global PV cell production.
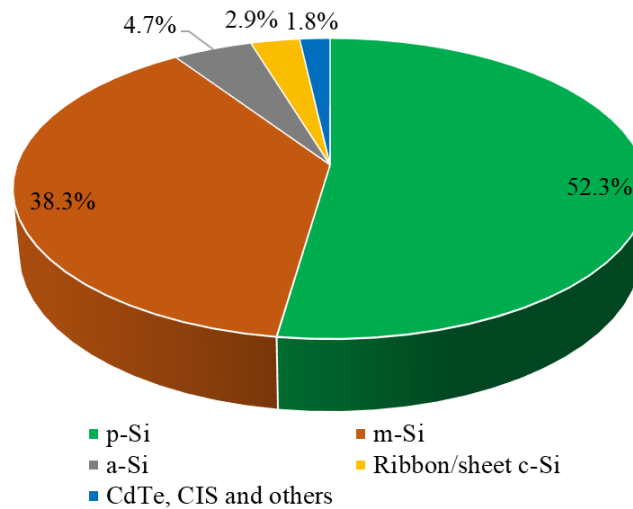
Figure 3.2. Market share of various types of PV cells in the world in 2009 (source: [2])

3.3. Efficiency of PV cells

The first PV cells had an efficiency of only 6%. Today, their efficiency generally exceeds 17%. Special PV cells with efficiency exceeding 22% are also produced. Progress in the development of PV cells, i.e. increasing their energy transformation efficiency, is presented in Figure 3.3.
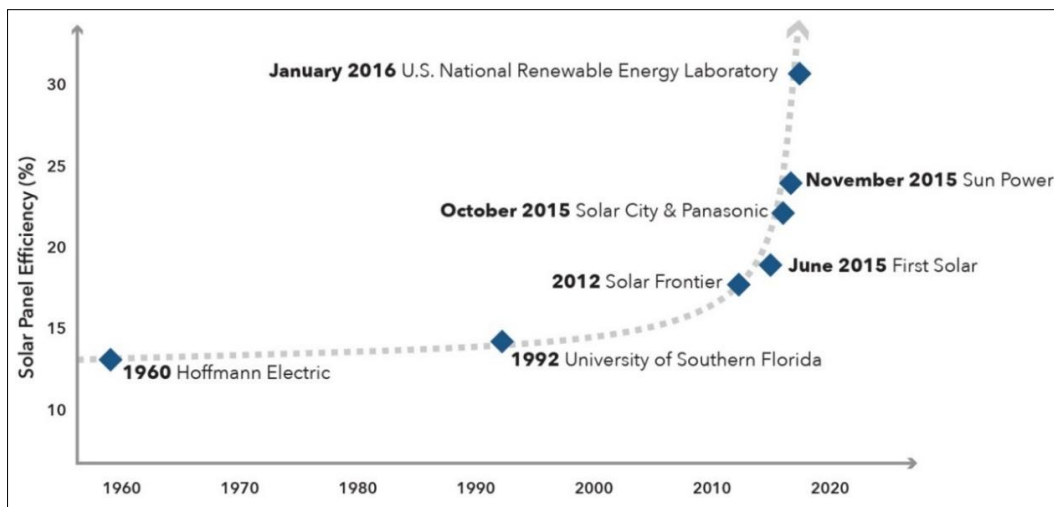
Figure 3.3. Significant gains in PV efficiency in the past 50 years (source: [3]*)*

The first silicon PV cells to appear in 1954 had an efficiency of about 6% at a cost of $10000 / W of peak power [1]. Apart from the semiconductor material and the applied manufacturing technology, the efficiency of the PV cell is also affected by temperature. According to [1], as the PV cell temperature increases, the voltage decreases by approximately 0.41% / °C, the short-circuit current increases by ~0.06% / °C, the power decreases by ~0.44% / °C. According to the same source, the consequence of the increase in temperature is a decrease in the efficiency of the PV cell by approximately 0.08% / °C. The efficiency of PV cells is significantly influenced by their age. According to the report [4], during 20 years of exploitation, PV cells lose efficiency by an average of

0.43% annually. That is, the efficiency of a PV cells after 20 years of outdoor use will be averagely 8.6% lower compared to a new PV cell.
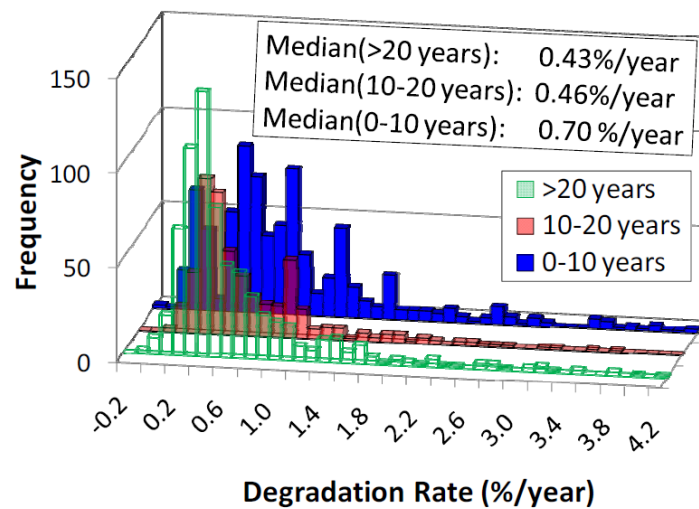
Figure 3.4. Reduction in efficiency due to "aging" of PV cells (source: [4])

Figure 3.4. displays the degradation of PV cell efficiency due to its age. The authors of the figure did an experiment on multiple PV cells. X-axis displays the average annual degradation rate over the whole exploitation time. X-axis divides all of the observed PV cells into classes with a 0.1% step of degradation rate. Y-axis displays the frequency i.e., how many observed PV cells belong to each class. For example, over 140 PV cells older than 20 years had an average annual degradation rate of 0.4% - 0.5% throughout their exploitation.

3.4. Price of PV cells and systems

Figure. 3.5. presents the trend of PV cell prices in the period from 1977 to the present. According to these data, the price of PV cells per watt of peak power has been reduced 253 times over the observed period. The reduction in the prices of PV cells, as one of the most important elements of the PV system, has significantly contributed to the reduction of the prices of the PV systems (PV power plant).

According to the data presented in the report [6], the average price of a PV system (power plant) with a power exceeding 100 kW installed during 2011 in the USA was $4.87 / W. According to the price movement forecast for large PV systems given in [7] the average price of the system in 2016 was $2.20 / W, while in 2020 the price is projected to further decrease to $1.80 / W, and in 2030 the estimated price is as low as $1.20 / W.
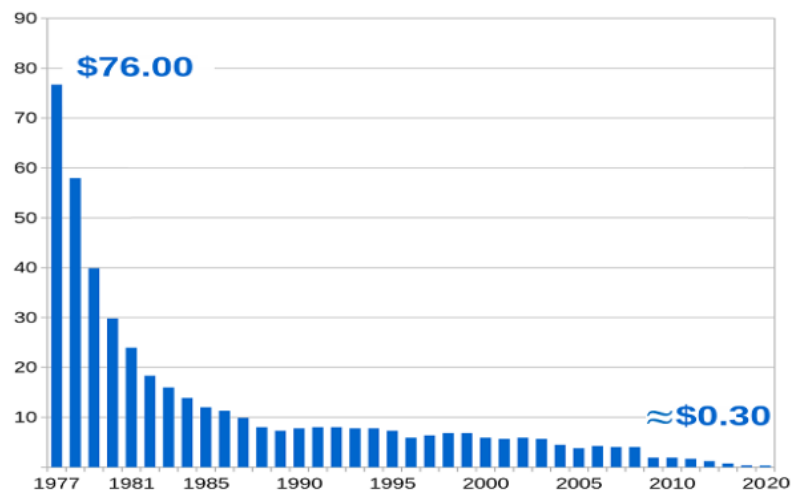
Figure 3.5. Price of PV cells per W of peak power (source: [5])

4. PV power plant on-board ship

The aim of the installation and use of the PV power plant on board is to reduce fuel consumption and emissions of harmful substances into the atmosphere that occur as a result of the operation of marine diesel engines. The following is a simplified overview of two ship power plants that use a PV power plant as an additional energy source.

Taking into account the specifics of individual types of ships with regard to their purpose, the paper considers the possibility of installing a PV power plant on a passenger ship and a liquid cargo ship (tanker). These types of ships are suitable for the installation of PV power plants because most of their floor plan surface can be used to install PV panels. In doing so, special features that are conditioned by the purpose of the ship and the conditions of operation of the ship should be taken into account.

For the purposes of the analysis, it is assumed that the length of the ship in both cases is 275 m, and the width is 45 m. It is possible to install a PV module with a total rated power of 900 kW on a ship of such dimensions. For a PV power plant of that power, a total area for the installation of PV panels of approximately 6000 m^2 is required, which implies the lowest efficiency of PV panels of 15%, i.e. the peak power of the panel is 150 W/m^2.

4.1. PV power plant on a passenger ship with diesel-electric propulsion

Connection of the PV power plant with the electric system of a passenger ship with diesel-electric propulsion is shown in Figure 4.1.

The main source of electricity for the passenger ship consists of four diesel generators with a nominal power of 11 MW. The total installed power is 44 MW, of which up to 30 MW is used for propulsion. The daily average electricity demand is approximately 4.75 MW while up to 7.75 MW is occasionally required (according to [8] for passenger ships of ~275 m in length).
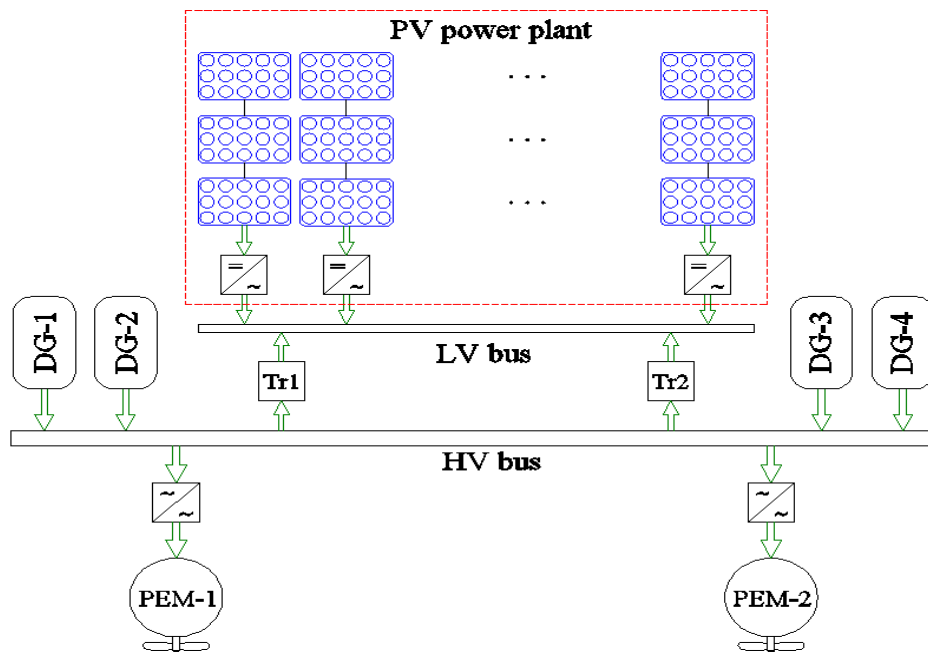
Figure 4.1. Schematic of a PV power plant on a passenger ship with diesel-electric propulsion

All the electricity obtained from the PV power plant is supplied via the converter to the main buses for power supply of low voltage consumers (LV, 440 V, 60 Hz). Propulsion motors are supplied with high voltage electricity (HV, up to 11 kV) via appropriate converters. Since the ship's needs for LV electricity in all modes of operation (navigation, stay at anchor or in port) are significantly higher than the total installed capacity of the PV power plant, it is not necessary to provide the possibility of storage of electricity.

Optimal utilization of electricity obtained from the PV power plant is achieved by means of a computer control and management system of the ship's power plant. Given the ship's low voltage electricity needs and installed power, the PV power plant can supply up to 19% of the required amount of energy.

4.2. PV power plant on a tanker with diesel engine propulsion

In Figure 4.2. the connection of the PV power plant with the power system of the liquid cargo ship is shown. A low speed two-stroke diesel engine with a maximum continuous rating of 15 MW is used for ship propulsion. The majority of electricity for all ship needs in less demanding modes of operation (stay in port, at anchor and manoeuvring) is supplied by two diesel generators (DG) with a nominal power of 2 · 0.9 MW, and by shaft generator during navigation (SG, shaft generator) with a nominal power of 1.2 MW, powered by main engine (ME). The ship's electricity needs in navigation are approximately 600 kW, while when staying in the port or anchorage they are usually lower and do not exceed 450 kW. Centrifugal pumps powered by steam turbines are used for cargo unloading, without a significant increase in electricity needs. The greatest needs for electricity are during manoeuvring (short-time operation of winches and bow thruster) when both diesel generators are used in parallel primarily for safety reasons.
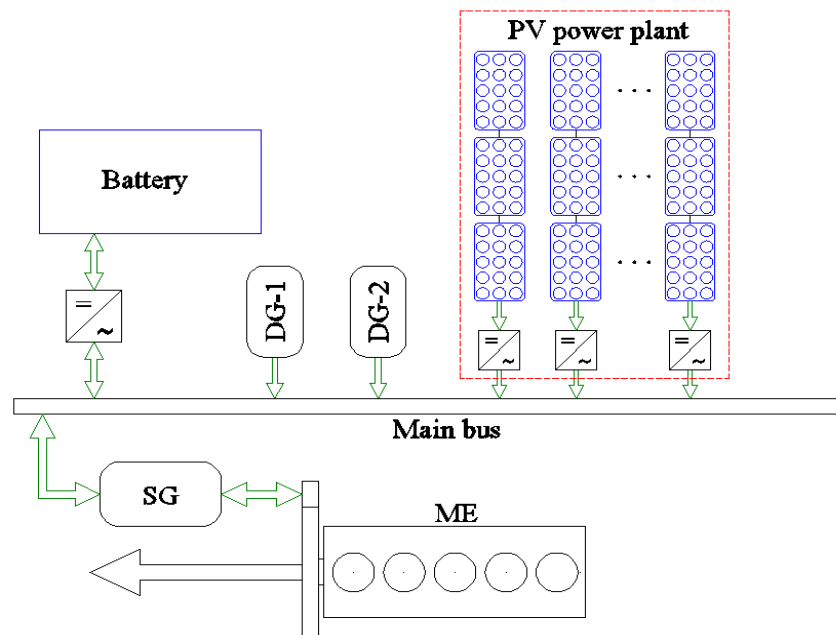
Figure 4.2. Schematic of a PV power plant on a tanker with diesel engine propulsion

Depending on the time of day and year, as well as atmospheric conditions, there are three cases:

- "night" (PV power plant does not provide electricity),
- "daily-1" (PV power plant provides less electricity than ship needs),
- "daily-2" (PV power plant provides more electricity than ship needs).

In night mode, all electricity is produced by DG or SG. In the daily regime, when the amount of electricity obtained from the PV power plant is less than required, the difference is compensated from DG or SG. In the case that the amount of electricity is greater than the current needs of the ship, the excess is stored in the battery or used for propulsion of the ship. When excess energy is used for propulsion in navigation, then the SG works as an electric motor. Optimal and safe operation in all these modes is provided by a computer-controlled control system of the ship's power plant.

4.3. Cost-effectiveness estimation of PV power plant installation

The assessment of the cost-effectiveness of the installation of a PV power plant on the example of a passenger ship will be carried out with the following assumptions:

- the ship carries passengers between Mediterranean ports and ports in the Gulf of Mexico throughout the year,
- all panels with PV cells are placed horizontally,
- the average total annual irradiation of the horizontal surface is 1600 kWh/m^2 (according to the data for the city of Split [1]),
- the service life of the PV system is 20 years,
- the average efficiency of PV cells is 17% for a service life of 20 years,
- total cost of installing a PV power plant on board with all the necessary devices and equipment is \$2.25 / W (25% higher price than the expected price in 2020),

- the installed power of the power plant is 900 kW (the area of the PV panel is approximately 6000 m^2),
- total daily electricity needs (except energy needed for propulsion) $114 \cdot 10^3$ kWh.

Table 4.1. Relation of required to electrical energy obtained from the ship's PV power plant

Needed electricity		Electricity from PV power plant		
Daily, kWh	Per year, kWh	Daily, kWh	Per year, kWh	Share in total needs [%]
114 000	41 610 000	4471	1 632 000	3.9

According to the data in Table 4.1., electricity from the ship's PV power plant in the assumed conditions would cover only 3.9% of electricity needs. Accordingly, the reduction of fuel consumption and emissions of harmful substances into the environment that occurs due to the operation of diesel engines would be achieved.

Estimation of the profitability of the initial investment in the PV power plant is presented in Table 4.2. To determine the price of kWh of electricity generated by a diesel generator, the average price of fuel with a sulphur content of less than 0.5% was used, which price was $554.56 / t in 2019 [9]. At the stated fuel price, with a specific fuel consumption of 200 g/kWh, the amount of $0.11 / kWh is obtained.

Table 4.2. Cost-effectiveness estimation of initial investment in marine PV power plant

PV plant installation total cost		Energy obtained from PV and savings achieved	
Installed power, W	900 000	Per year, kWh	1 632 000
Price, $/W	2.25	Price, $/kWh	0.11
Total price, $	2 025 000	Total (*per year*), $	179 520
Expected working life, years	20	Payback period, years	11.28

From the data in Tab. 4.2. it follows that a return on investment in a PV plant can be expected after 11.28 years, not taking into account maintenance costs. In the remaining operating life of the power plant, an average annual savings of $179 520 / year could be achieved. The expected payback period for the installation of a PV power plant of the same nominal power on a liquid cargo ship is longer, primarily due to a larger initial investment in a part of the electricity storage system. If this part of the system would be neglected, the total cost of installing a PV power plant would be approximately the same, but with a slight reduction in overall efficiency.

5. Conclusion

In the case of a passenger ship, all electricity obtained from the PV power plant is used immediately and it is not necessary to provide the possibility of storage. Under certain conditions, tankers may experience surplus electricity that needs to be stored and used in periods when the PV power plant does not provide enough electricity. Given the fact that the PV power plant is a source of electricity whose power is proportional to the intensity of light radiation from the Sun, it is necessary to compensate changes in the available electrical power.

The control and management system of a passenger ship power plant compensates for changes in the amount of electricity obtained from the PV power plant by adjusting the amount of

electricity provided by diesel generators. In the case of tankers, the excess electricity is stored in the battery, and the deficit is compensated by electricity from the battery and the shaft generator driven by the main engine. The described power plants are hybrid power systems in which the main energy sources are generators powered by diesel engines, and as an additional energy source is used PV power plant. The reliability, safety and efficiency of the system is ensured by a computer-controlled control and management system that optimizes the operation of the ship's power plant.

The contribution of the ship's PV power plant to the reduction of fuel consumption and consequently the emission of harmful substances is not questionable, but the cost-effectiveness depends on a number of factors. Significant impact on the assessment of cost-effectiveness or economic justification has the cost of:

- procurement of PV panels,
- procurement and installation of structures for fastening PV panels and other equipment
- installation of the PV power plant system,
- maintenance.

In addition to the above, the cost-effectiveness is also affected by the price of fuel, i.e., the price of kWh of electricity obtained by diesel generators, the area of navigation and operating conditions of the ship and reducing the efficiency of PV cells due to aging. Although PV systems will probably never be able to fully replace conventional ship power plants, they can already contribute to reducing the use of fossil fuels and reducing the negative impact on the environment. Previous considerations indicate that the installation of a PV power plant on board represents an environmentally and economically acceptable option for reducing the negative impact on the environment while reducing the cost of electricity production.

It is to be expected that the trend of decreasing prices of PV cells and other equipment for PV power plants will continue in the future. In addition, it is realistic to expect further improvements in the efficiency and durability of PV cells, and their adaptation to specific conditions of use on board. Prerequisites for the application of PV power plants on ships exist, but their application will still depend on oil and gas prices, further development of PV system technology, readiness of shipbuilders and shipowners to accept new technologies or environmental regulations and other impacts.

REFERENCES

[1] Kulišić, P., Vuletin, J., Zulim, I.: Sunčane ćelije, Školska knjiga, Zagreb, 1994.

[2] Kobougias, I., Tatakis, E and Prousalidis, J: PV Systems Installed in Marine Vessels: Technologies and Specifications, Advances in Power Electronics, Volume 2013, 2013.

[3] https://news.energysage.com/solar-panel-efficiency-cost-over-time / (29.04.2020.).

[4] Jordan, D., Kurtz, S.: Photovoltaic Degradation Rates - An Analytical Review, NREL/JA-5200-51664, June 2012.

[5] Arafa, A., Said, A.: A different vision for uninterruptible load using hybrid solar-grid energy, International Journal of Power Electronics and Drive System (IJPEDS) Vol. 10, No. 1, March 2019, pp. 381-387.

[6] Feldman, D., et al.: Photovoltaic (PV) Pricing Trends Historical, Recent, and Near-Term Projections, Technical Report DOE/GO-102012-3839, November 2012.

[7] Solar Photovoltaics, Volume 1: Power Sector, Issue 4/5, IRENA, June 2012.

[8] www.shipandbunker.com (30.04.2020.).

[9] Espinosa, E., Casalas-Torrens, P., Castells, M.: Hoteling Cruise Ships Power Requirements for High Voltage Shore Connection Installations, Journal of Maritime Research, Vol XIII. No. II (2016) pp 19-28.

Bi – fuel system implementation in Dredgers

Fler Peša Smirčić*

IHC Engineering Croatia d.o.o., Milutina Barača 7, 51 000 Rijeka, Croatia
* Corisponding Author, f.smircic@royalihc.com

Abstract

In today's world LNG have more and more significant role as power source. The combination of growing liquefied natural gas (LNG) supplies and new requirements for less polluting fuels in the maritime shipping industry has heightened interest in LNG as a maritime fuel.

Liquefied natural gas is a colorless and odorless liquid, which is produced by cooling natural gas below the boiling point (about –161 °C). The volume of LNG is about 1/600 of the volume in gaseous state. In ambient temperature, LNG quickly vaporizes to gaseous form.

Main reasons for using LNG are price and emission reduction.

With benefits come challenges of using LNG. From the perspective of project and design engineer's main challenges of using LNG on Dredgers is implementation itself. Main challenges are: design challenges (LNG storage needs 2–3 x more space than fuel oil storage and with that have large impact on vessel lay out), bunkering (location of bunker station, compatibility check, draining of bunker lines, arrangement of bunker station) and safety and regulations (Hazardous zones around LNG tank, engine and fuel lines, continuous ventilation in hazardous zones, no ignition sources in hazardous zones, gas detection with alarm on deck).

Key words: LNG; Dredger, Gas supply system;

Sažetak

U današnjem svijetu UPP ima sve veću i značajniju ulogu kao izvor energije. Kombinacija rastućeg broja proizvođača ukapljenog prirodnog plina i novih zahtjeva za ekološkijim gorivom u pomorskoj brodskoj industriji povećala je interes za UPP-om kao pomorskim gorivom. Ukapljeni prirodni plin je bezbojna tekućina, bez mirisa, koja nastaje hlađenjem prirodnog plina ispod točke ključanja (oko 161°C). Volumen UPP-a je oko 1/600 volumena u plinovitom stanju. Pri sobnoj temperaturi UPP brzo prelazi u plinoviti oblik.
Glavni razlozi za korištenje UPP-a su cijena i mala emisija štetnih plinova.
Uz prednosti dolaze i izazovi korištenja UPP-a. Iz perspektive projektnih i dizajn inženjera glavni izazovi korištenja UPP-a je njegova impelementacija. Glavni izazovi su: iazovi kod dizajniranja (prostor za skladištenje UPP-a je 2-3x veći od prostora za skladištenje dizelskog goriva i s tim ima veliki utjecaj na dizajn broda), ukrcaj (pozicija ukrcajne stanice, provjera kompabitilnosti, drenaža ukrcajnog cjevovoda, pozicija ukrcajne stanice) i sigurnosti i propisi (opasne zone oko UPP spremnika, cjevovod oko motora i cjevovod goriva, kontinuirana ventilacija u opasnim zonama, zabrana izvora paljenja u opasnim zonma, detekcija plina s alarmom na palubi.)

Ključne riječi: UPP; Jaružalo; Sustav za dobavu plina;

1. Introduction

In today's world LNG have more and more significant role as power source. The combination of growing liquefied natural gas (LNG) supplies and new requirements for less polluting fuels in the maritime shipping industry has heightened interest in LNG as a maritime fuel. Using LNG as primary fuel is a relatively new, the first LNG-powered vessel is a Norwegian ferry in 2000.

With benefits come challenges of using LNG. From the perspective of project and design engineer's main challenges of using LNG on Dredgers is implementation itself.

2. LNG

2.1. What is LNG

Liquefied natural gas LNG is a colorless and odorless liquid, which is produced by cooling natural gas below the boiling point (about −161 °C). The conversion of natural gas to liquid form facilitates the storage and transport. The volume of LNG is about 1/600 of the volume in gaseous state. LNG consist primarily of methane and small amounts of other hydrocarbons, and it is non-toxic.

In ambient temperature, LNG quickly vaporizes to gaseous form. Leakage of LNG may cause exposure to methane, which constitutes a risk of suffocation. Also the low temperature of the LNG poses a risk of freezing injuries in leakage or splashing situations.

In its liquid state, LNG is not explosive and cannot burn. If LNG gets into contact with warmer air, a vapor cloud will form. Natural gas has a relatively high ignition temperature and a narrow flammable range. Ignition and a consequential fire or explosion can occur only if the gas proportion in the air is within the range of 5–15%. Due to the low flame speed of burning methane in an open environment, explosions are possible only in enclosed spaces.

LNG is not corrosive, but it may cause material damage due to the low temperature. If LNG gets into contact with carbon steel, the thermal stress may lead to heavy cracking. The hull and other steel structures on the ship must be protected in leakage situations.

As LNG is considerably lighter than water, it will float if spilled on water. If a large amount of LNG is spilled on water, violent vaporization known as a rapid phase transition may occur. The large amount of energy released in the phase transition may cause a physical explosion, involving a risk of personal injury or equipment damage.

2.2. Main reasons for using LNG

Main reasons for using LNG are price and emission reduction.

2.2.1. Emission reduction

In 2008, the International Maritime Organization (IMO) announced a timeline to reduce the maximum sulfur content in vessel fuels to 0.5% by January 1, 2020. In 1973, the IMO adopted the International Convention for the Prevention of Pollution from Ships (MARPOL). Annex VI of the convention requires limits on nitrogen oxide (NOx) emissions and vessels to either use fuels containing less than 0.5% sulfur or install exhaust-cleaning systems – "scrubbers", to limit a vessels airborne emissions of sulfur oxides to an equivalent level. Compared to Heavy Fuel Oil LNG reduces: SO_x emission by 99%, NO_x emission by 85%, CO_2 emission by 25% and Particulate Matter by 99%. LNG is compliant to SO_x, NO_x and EEDI regulation and more sustainable than other emission reduction measures.
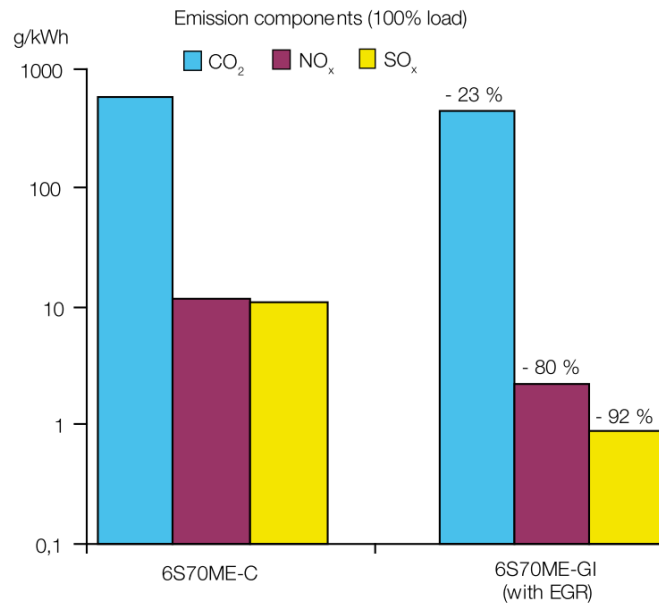
Figure 1 *MAN B&W Engine - Emission components*
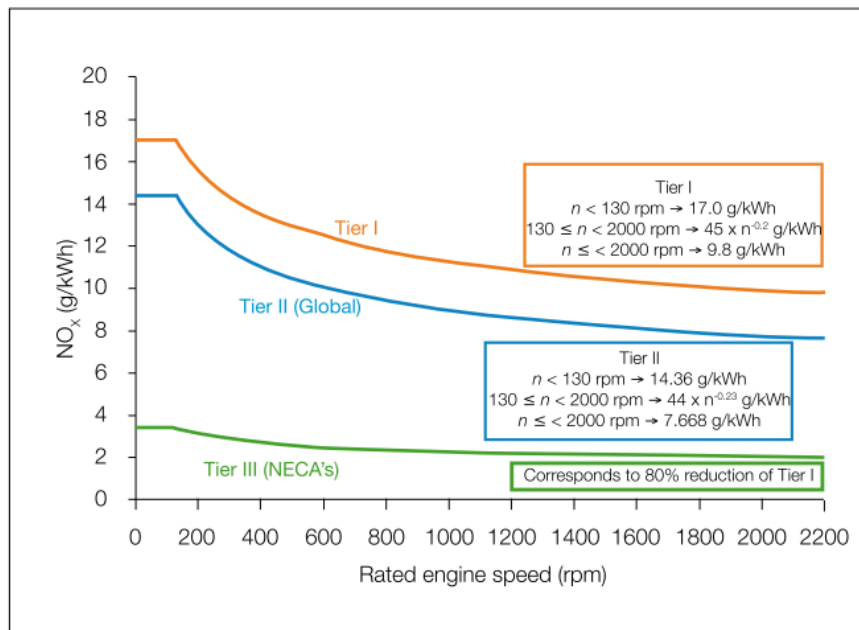
Figure 2 *IMO NO$_x$ limits*

2.2.2. Price of LNG

LNG is expected to be less costly than marine gas oil (MGO) which will be required to be used within the ECAs if no other technical measures are implemented to reduce the SOx emissions. Current low LNG prices in Europe and the USA suggest that a price – based on energy content – comparable to heavy fuel oil (HFO) seems possible, even when taking into account the small scale distribution of the LNG.
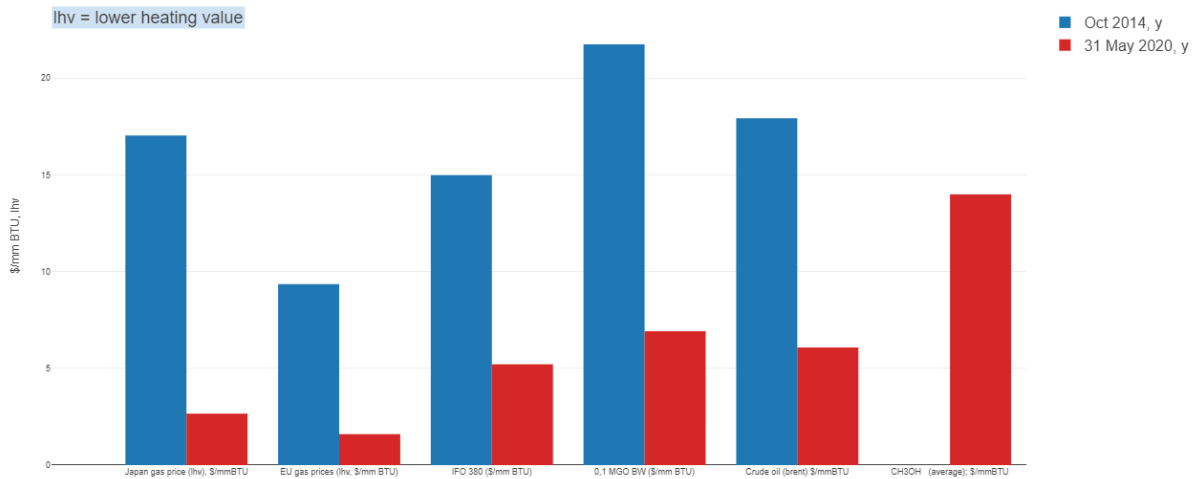
Figure 3 *Gas and Oil Prices between Oct 2014 and May 2020*

(gas: no liquefaction and distribution included)
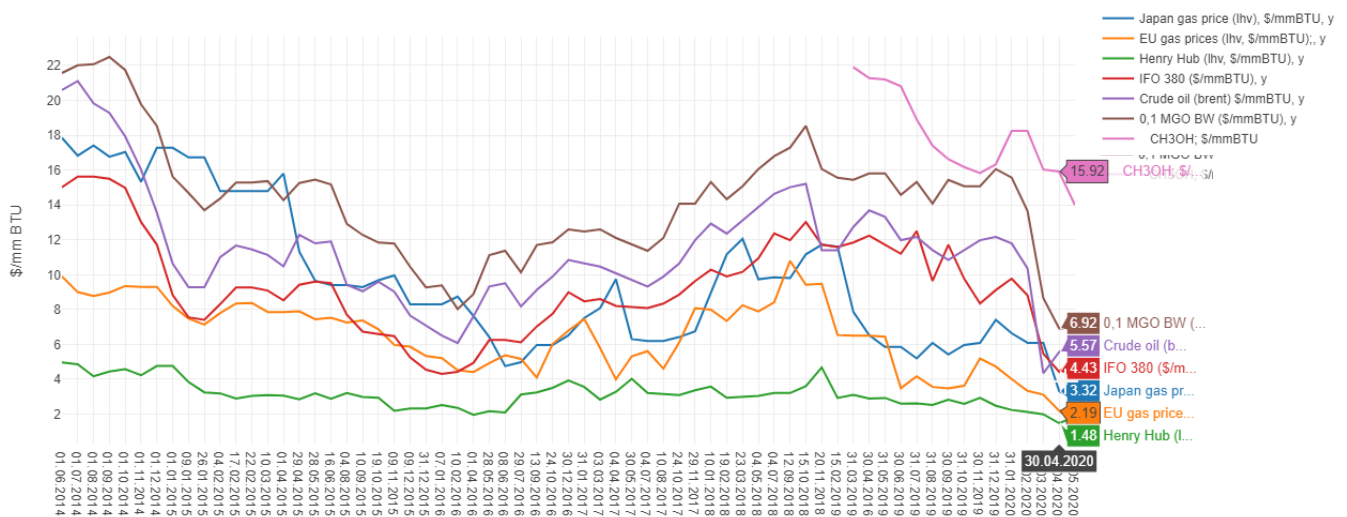
Figure 4 *Current price development*

3. Challenges of using LNG

With benefits also come challenges of using LNG. From the perspective of project and design engineer's main challenges of using LNG on Dredgers is implementation itself. Main challenges are: design challenges, bunkering and safety and regulations. For IHC most challenging project in all aspect and also regarding usage of LNG was Spartacus for DEME, Largest cutter suction dredger on the World (164m long, total power output 44180 kW, powered by 4 Wartsila 46DF and 2 Wartsila 20DF engines, which can operate on LNG, diesel fuel or heavy fuel oil). Other LNG powered ship made by IHC are Minerva and Scheldt River – first LNG-powered trailing suction hopper dredgers and Bonny River LNG-ready.

Figure 5 *Spartacus One of LNG powered ships at Royal IHC, Krimpen aan den IJssel*

3.1.   Design challenges

For all pipes class I is required stress calculation. For every pipe with design temperature of -165°C is required stress calculation. Engineer which is responsible for stress calculation need drawing of the those pipes including the watertight bulkhead / deck penetration and normal penetration where the pipes are "fixed" in the ship.

According rules (BV or other)

Stainless steel single walled pipes:

Everything with -165°C is butt weld. Any flange -165°C is welding neck RF. (7.3.6.4.1.1)

Everything with 60°C and below 50 mm diameter can be with sleeves (7.3.6.4.1.2)

Stainless steel double walled pipes -165°C is absolutely no flanges, all butt welded.

After stress calculation sometimes routing of some LNG pipes must be changed and when we have routed all pipes we need improvisation which is not always good looking. Designer and pipe designer must provide info for pipe router which pipes need stress calculation and then pipe router must take extra effort that this pipe must be separated from other system for easier future changes.

Stress calculation required new routings (red lines) of this LNG tank drain pipe.
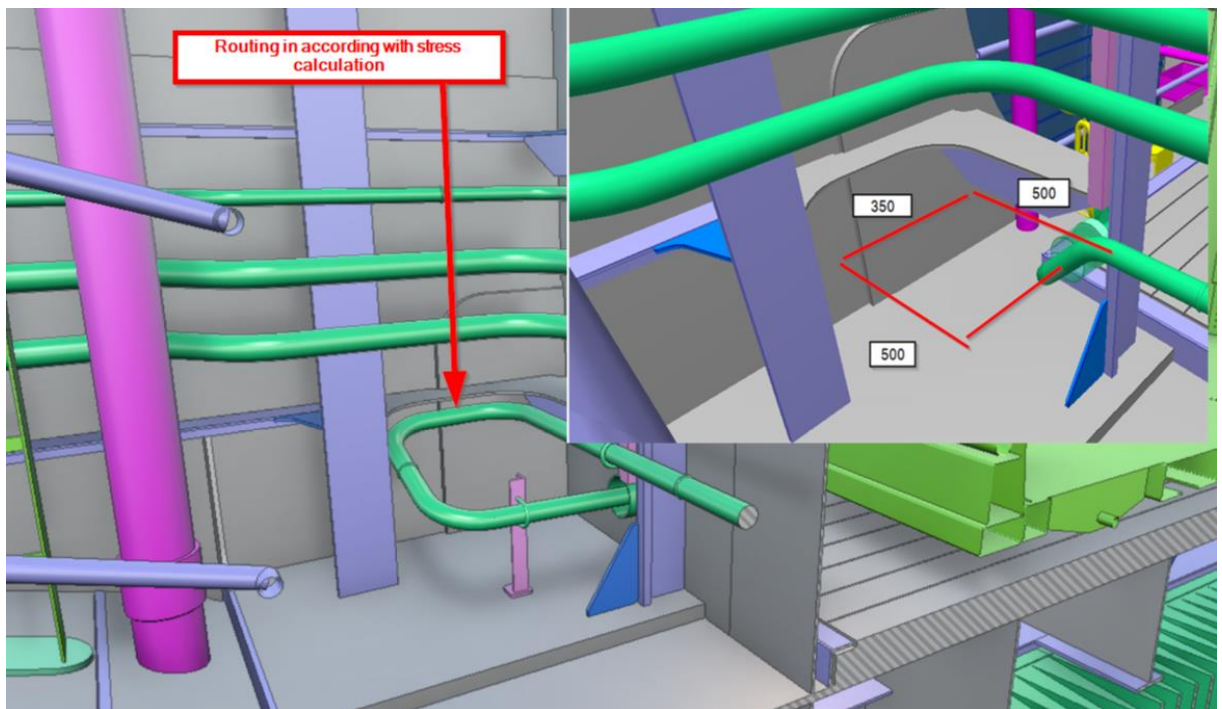
Figure 6 *Routing in accordance with stress calculation*

Supports must be placed in the model in accordance with stress calculation. In this case the bottom of the pipes is set to the L profile, not aligned along the centre of the pipe.
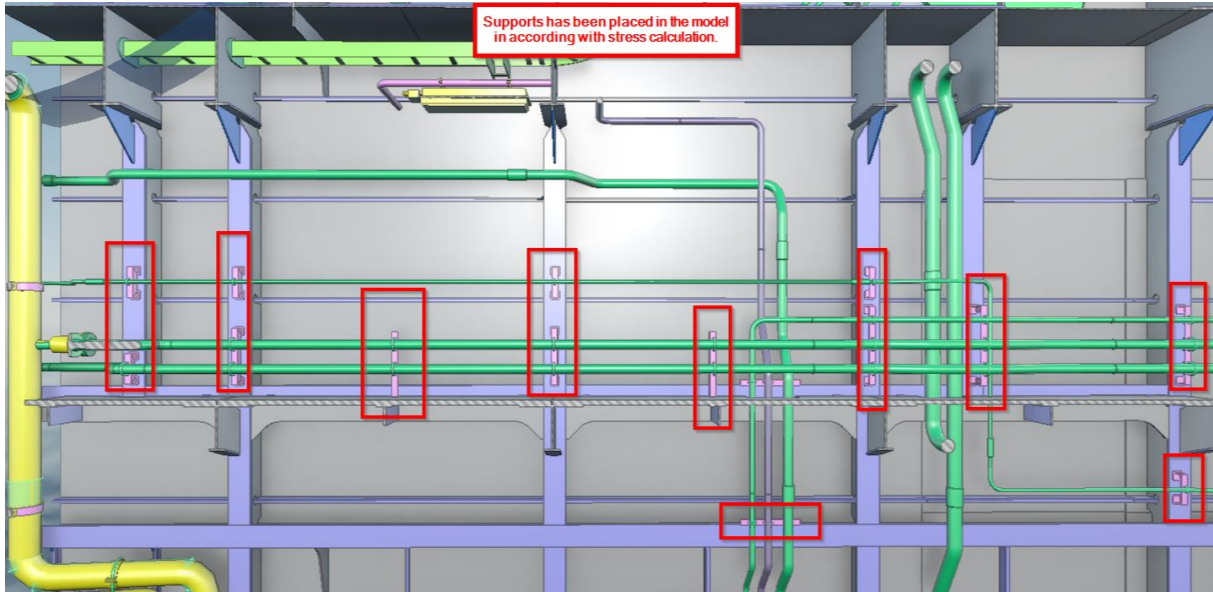
Figure 7 *Supports in accordance with stress calculation*

LNG fuel system pipes need to pass X-ray examination. For example, one project have requirements listed in figure 8.

For X-ray examination we need:
50 mm free space around pipe 4" and bigger
400 mm free space around pipe 3" and smaller
4" and bigger they can shoot with contact method
3" and smaller they have to shoot with the focus method

For welding we can do with a little less than 400, but this must be checked per weld.

Figure 8 Requirement *for X-ray examinations*

Pipes can be tack-welded in final position and taken away from ship structure for welding and X-ray examination. Only a few welds can be welded in final positions and for those welds is needed R=400 mm.
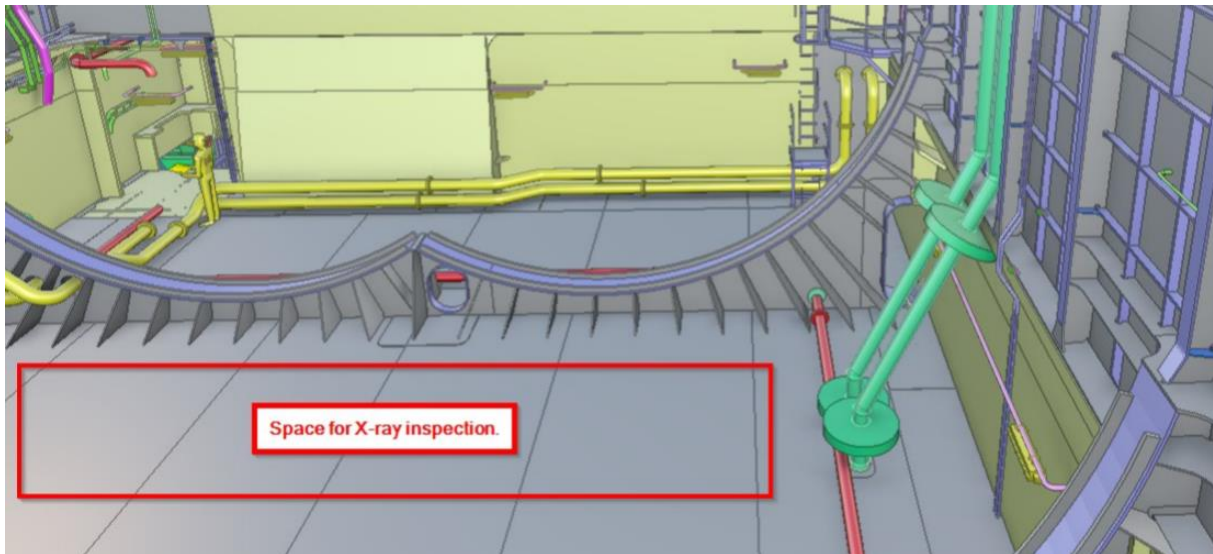
Figure 9 *X-ray examinations problems*

In next situation X-ray examination has been made out of final position. After joining of pipes and X-ray inspection pipes has been brought at final position to be prepared for last but weld connection.
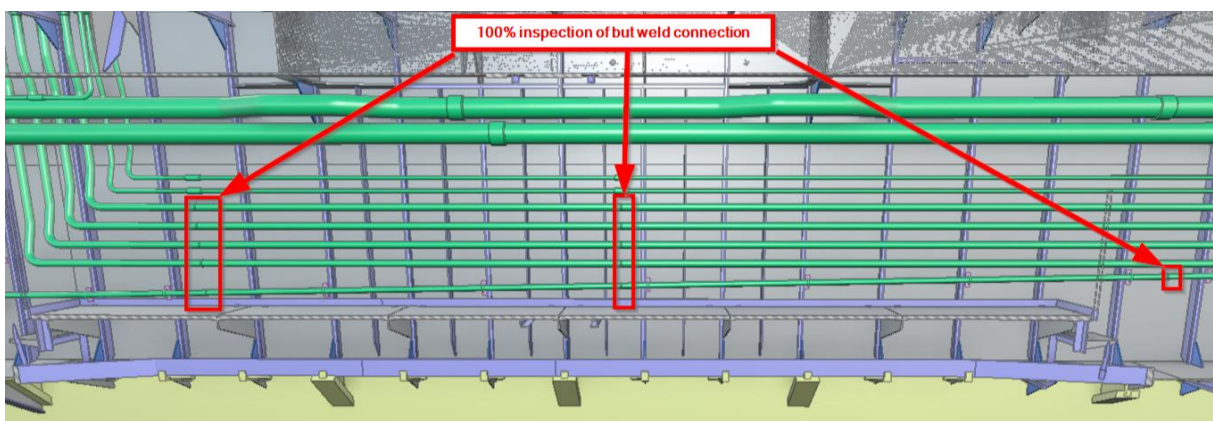
Figure 10 *X-ray examinations problems*

Additional challenges for hull designer and pipes router are pipes rules and space needed for routing.

Main principle are:

Single wall pipes:

- Used in open spaces
- Pipe to be thermally insulated

Double wall pipes:

- Used in enclosed spaces

- Annular space between the pipes to be equipped with mechanical under pressure ventilation (capacity of at least 30 air changes per hour)
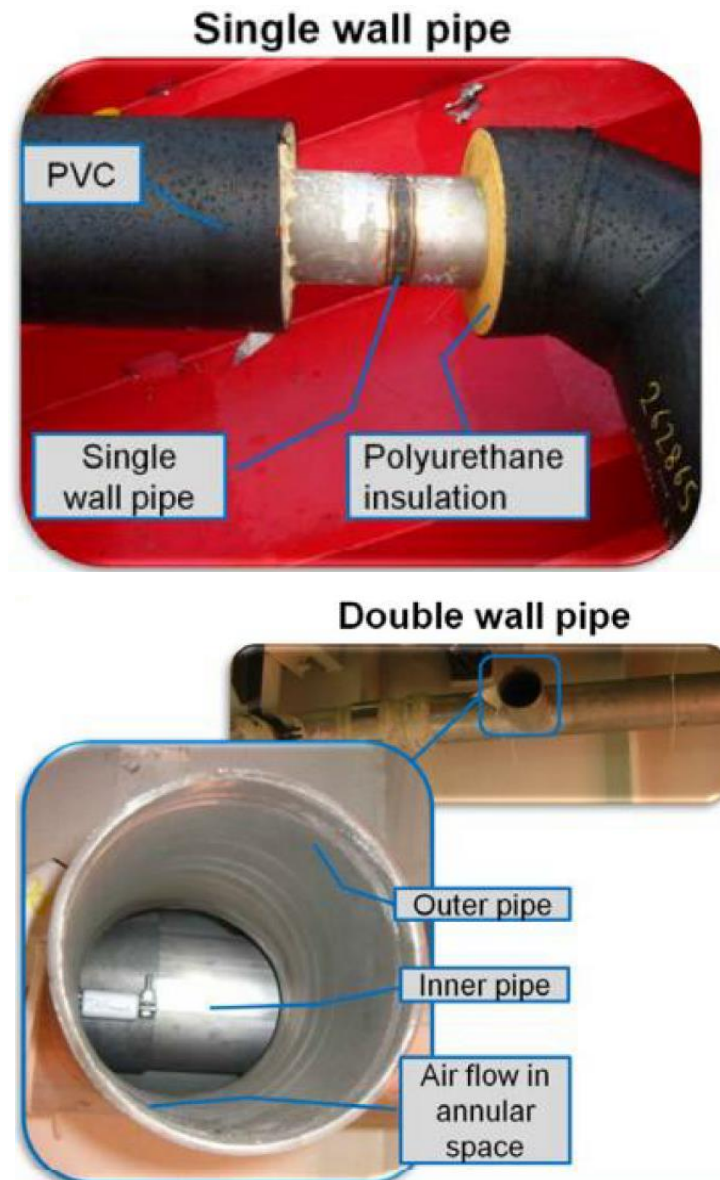
Figure 11 *Gas pipelines*

LNG storage needs 2-3 times more space than fuel oil storage and this have large impact on vessel layout. Also it must be taken in consideration tank volume vs ship autonomy vs bunkering frequency.
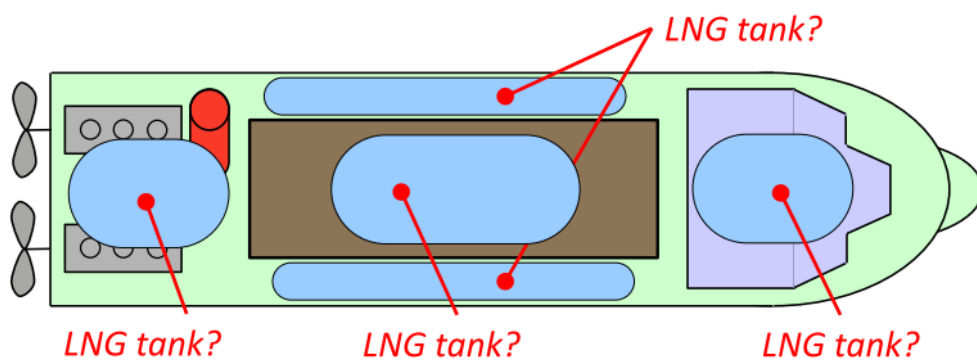
Figure 12 *Positions of LNG tank*

We have two solution for position of LNG tank and both have impact in ship design.
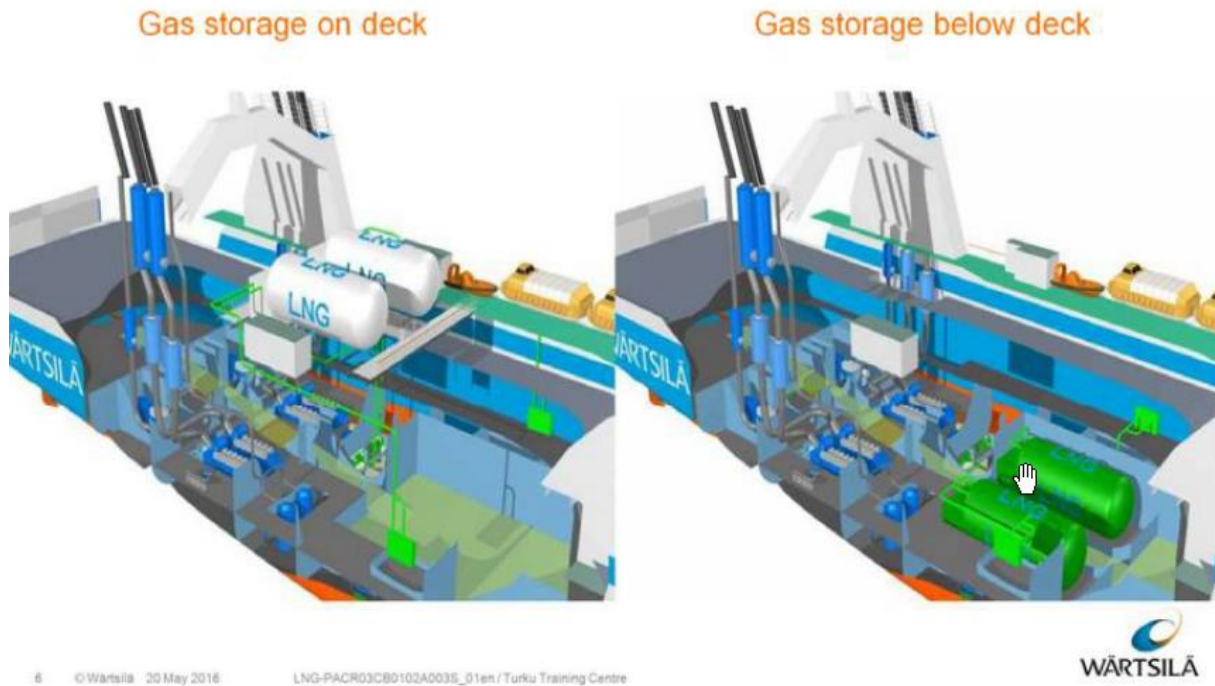
Figure 13 Two options of p*ositions of LNG tank*

For both options we have special rules and regulation to be follow – IMO IGF Code – Code of Safety for Gas-fueled Ships, which impact design of hull and pipes.

IMO IGF Code (Code of Safety for Gas-fuelled Ships)

2.8.3 Storage on open deck

■ 2.8.3.1 Both gases of compressed and the liquefied type may be accepted stored on open deck

■ 2.8.3.2 The storage tanks or in tank batteries should be located at least B/5 from the ships side. For ships other than passenger ships a tank location closer than B/5 but not less than 760 mm from the ships side may be accepted

■ 2.8.3.3 The gas storage tank or batteries and equipment should be located to assure sufficient ventilation, so as to prevent accumulation of escaped gas

■ 2.8.3.4 Tanks for liquid gas with a connection below the highest liquid level (see 2.8.1.2) should be fitted with drip trays below the tank which should be sufficient to contain the volume which could escape in the event of a pipe failure. The material of the drip tray should be stainless steel, and there should be sufficient separation or isolation so that the hull or deck structures are not exposed to unacceptable cooling, incase of liquid gas leakage

3   © Wärtsilä   20 May 2016   LNG-PACR03CB0201A0010_01en / Turku Training Centre   **WÄRTSILÄ**

IMO IGF Code (Code of Safety for Gas-fuelled Ships)

2.8.4 Storage in enclosed spaces

…in addition to 2.8.3

■ A secondary barrier of cold resistant material (stainless steel) is required

■ All connections to be installed inside a cold box made of stainless steel

■ Cold box to be ventilated and insulated

■ …More gas detectors etc.

→ It is more economical to install LNG tank in open space

4   © Wärtsilä   20 May 2016   LNG-PACR03CB0201A0010_01en / Turku Training Centre   **WÄRTSILÄ**

Figure 14 *IMO IGF code*

Structure, available space and pipe routing norms can complicate design. Engine need flexible connections but pipe designers are usually limited with space regarding structure and regarding bending radius of pipes.

In next example we have straight hose and not enough space, and designer and pipe router made compromise – bended hose.

Figure 15 *Engine and hose connection – compromise solution*

According pipe routing rules pipe should be constantly climbed and structure in some places does not allow it. In this example compromises are made. Pipe must be rearranged to go higher and structure must be changed.
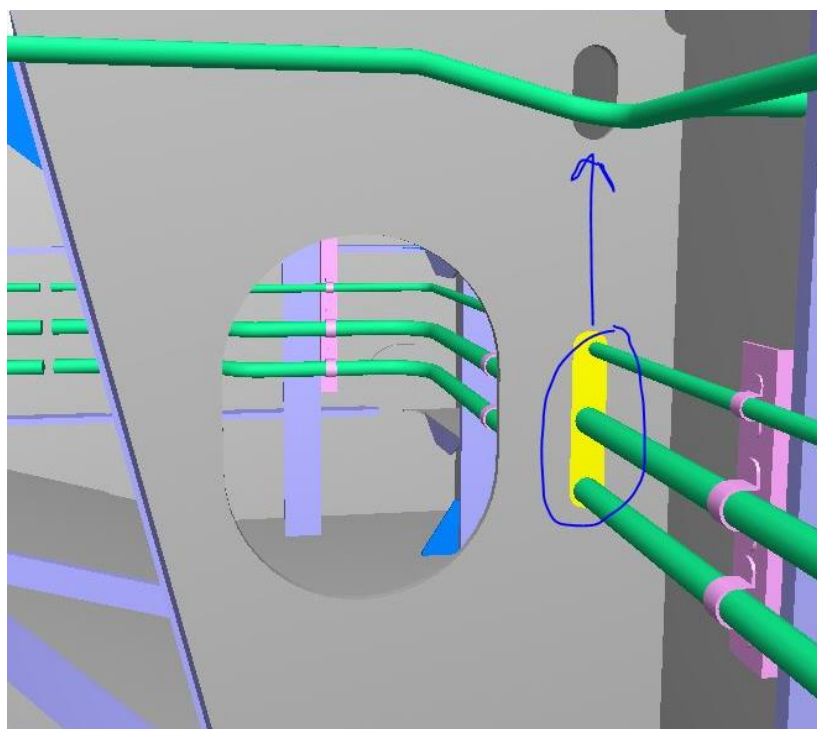
Figure 16 C*ompromise solution – pipes - structure*

In some situation problem is structure and height of pipes and router must change routing and also structure must be changed.

In this example pipes in LNG tank holding space are rearranged.
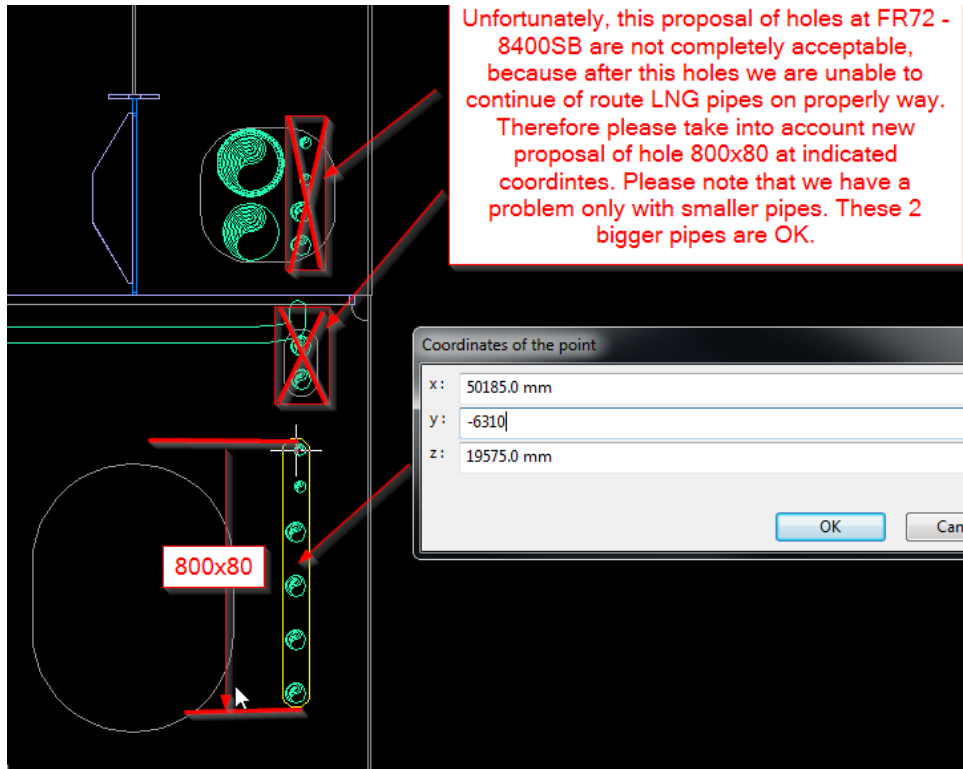
Figure 17 *Problem – pipes – holes in structure*

And final solution:
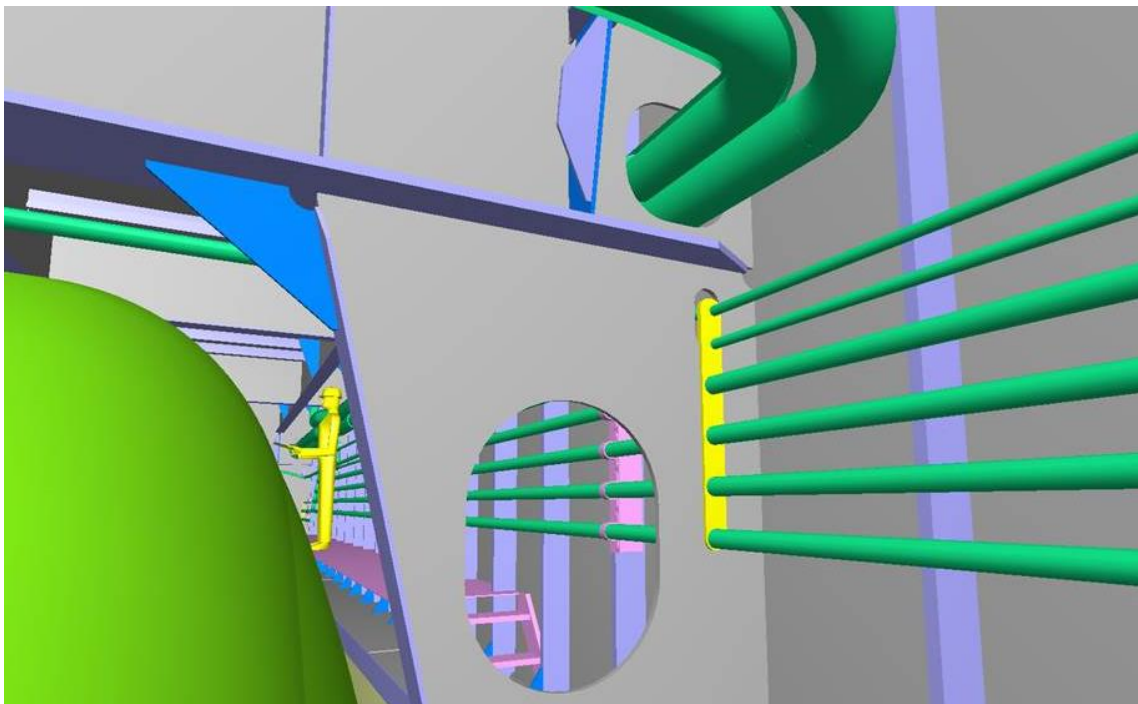
Figure 18 *Final – pipes – holes in structure*

Pipe must be routed as straight as possible often to the detriment of the structure. This require a lot of synchronized joint work of pipe router and hull designer.

In this situation new hull steel leads to problems with routing of double wall LNG pipes.
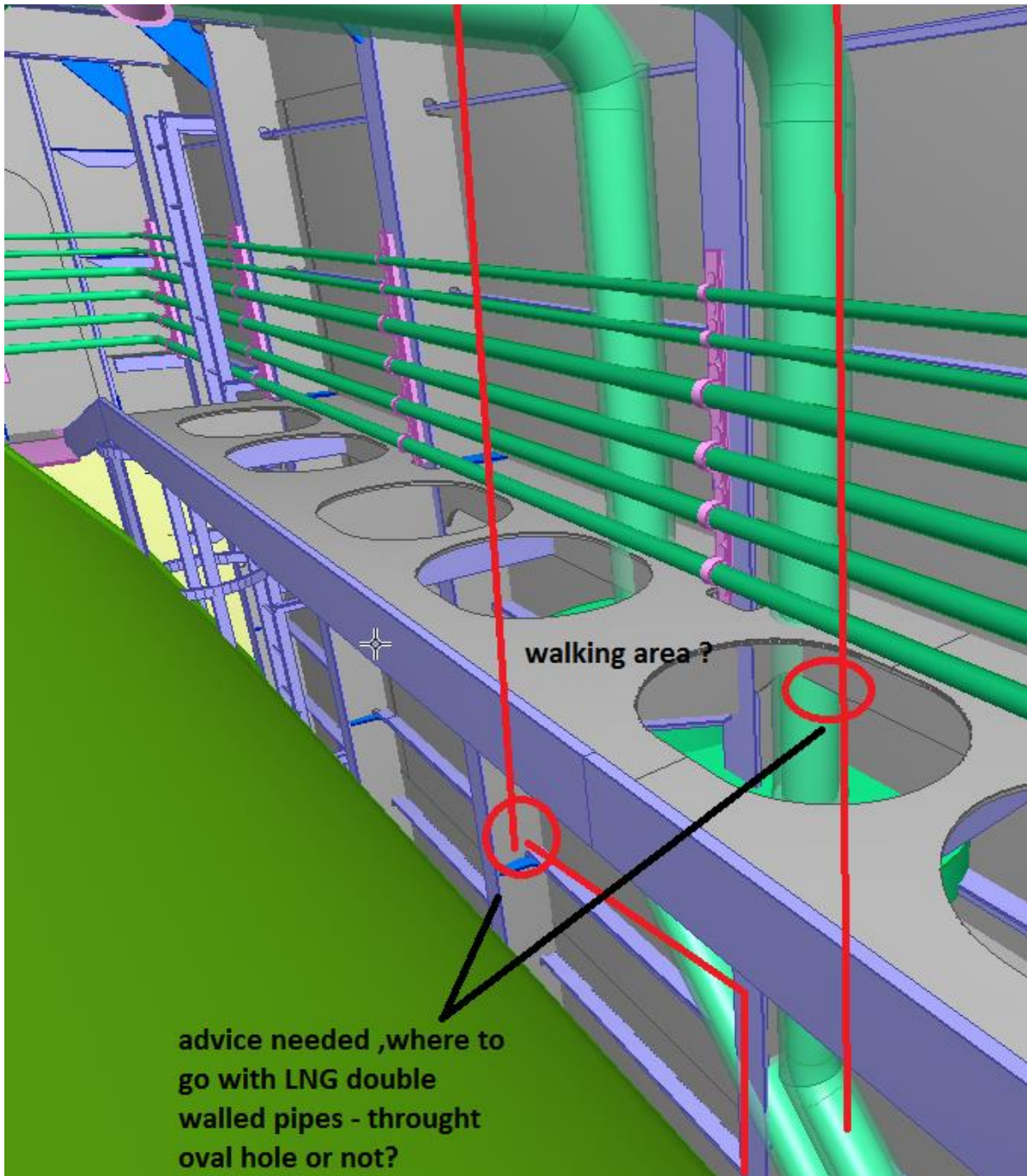
Figure 19 *Pipes routing – holes in structure*

Solution made by hull and pipe designer: pipes go through oval hole - locally will be narrow but hull designer can move the holes more to plate side so piping will be straight as possible.

LNG mast must be calculated and constructed according calculation. Calculation and construction meets strength requirements (ship gear) and stiffness requirements (natural frequencies versus sources of impact). This calculation usually includes a proposal regarding organization of the pipes.
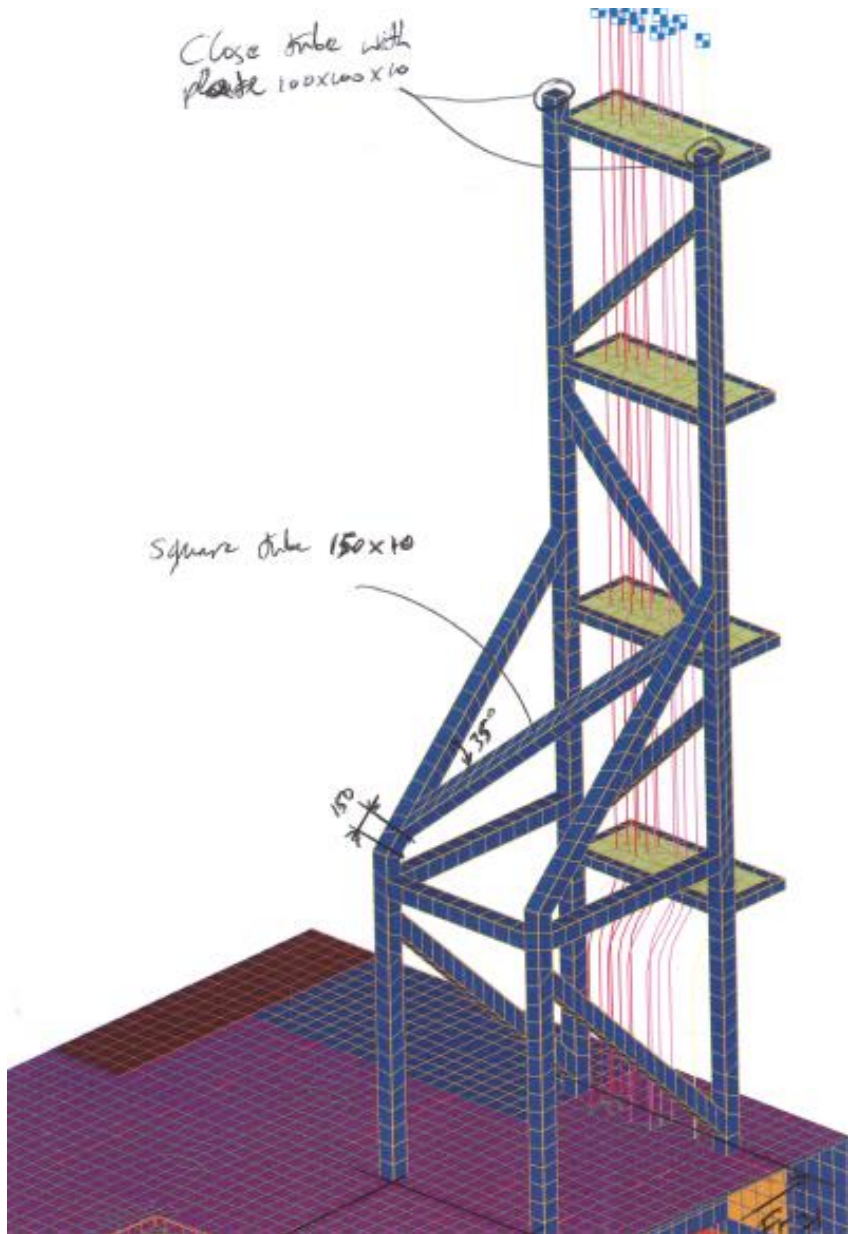
Figure 20 *LNG mast*

The Cryogenic pipe must be rinsed with nitrogen. Between the bunker station and the LNG tank, after the tank is filled with liquefied gas, there is always some gas left at the lowest point which is then blown with nitrogen. This is reason that router had to put connection at the lowest point.

3.2. Bunkering

Bunkering is also one of main challenges. First is the location of a bunker station and there we have 2 main issues: compability check and possibility of accessible position regarding draining of bunker lines. Bunker station must be of stainless steel. Drip trays shall be fitted below liquid gas bunkering connections. During bunkering operations drip tray must be constantly washed by water or drain pipe will be routed from drip tray to lowest waterline, and the stainless steel plate will be placed on the ships structure between pipe and the lowest water line to avoid LNG.
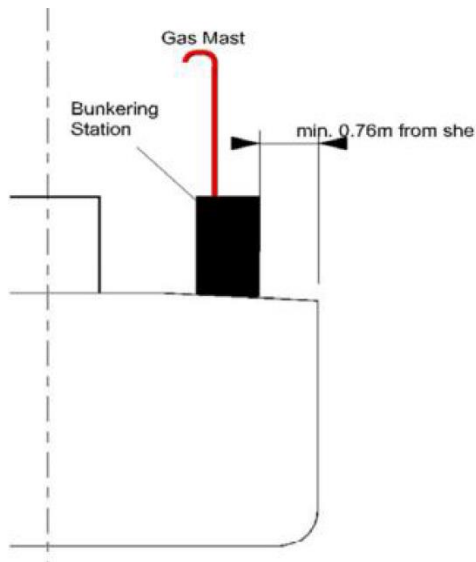
Figure 21 Position of b*unker station and real bunker station*

Figure 22 *Bunker station in operation*

Arrangement of bunker station, bunker lines dimensions and loading rates of suppliers of LNG are also big challenges.
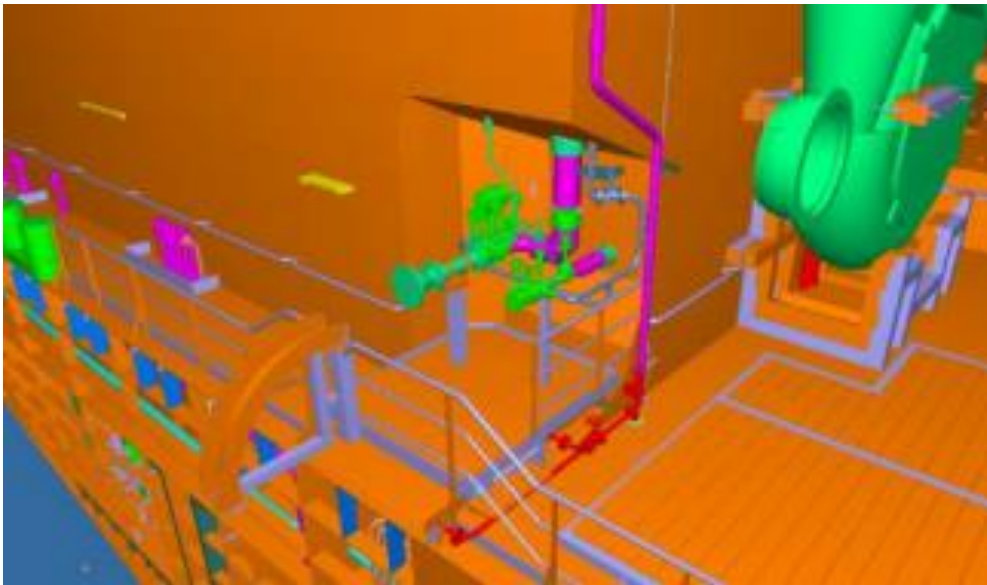
Figure 23 *Positions of LNG bunker station*

Figure 24 *As built situation of bunker station*

3.3. Safety and regulations

One special issue is safety. We must take in consideration:

- hazardous zones around LNG tank, engine and fuel lines

- continuous ventilation in hazardous zones

- no ignition sources in hazardous zones

- gas detection with alarm on deck

- hazardous zones on deck for outlets from hazardous spaces

- temporary hazardous zones around bunker station
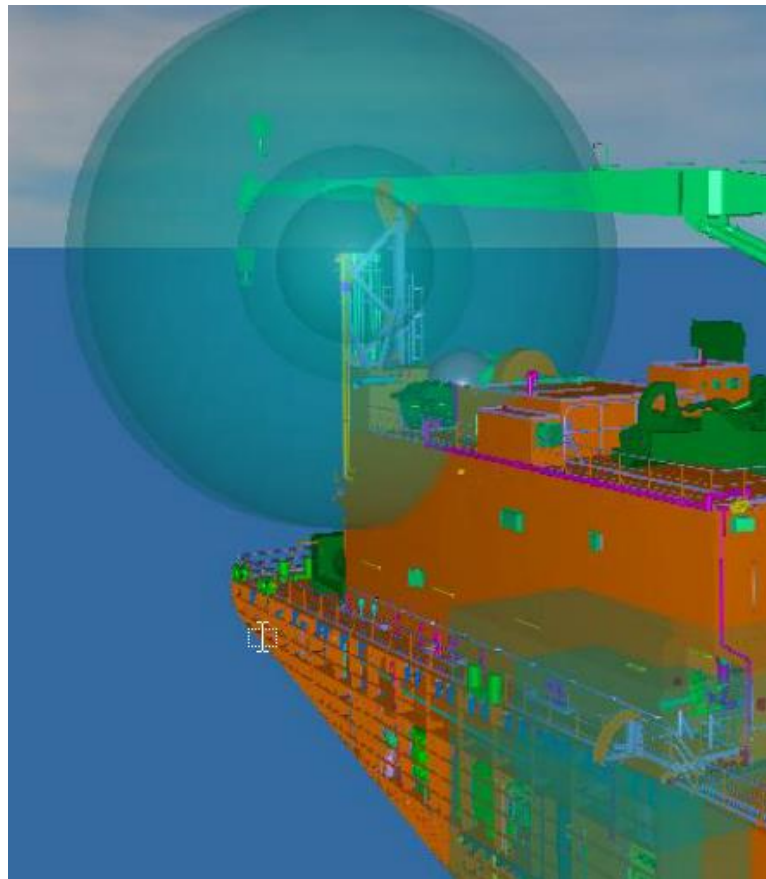
Figure 25 *Hazardous zones*

The LNGPac™ system involves hazardous areas, where explosive mixtures of gas and air may occur. The hazardous area classification must be strictly observed in all situations. The

hazardous areas must be clearly indicated by appropriate safety marking. The warning signs must not be removed.

The inside of the inner tank vessel is classified as a zone 0 hazardous area. Zone 1 classification applies to the tank connection space and the bunkering station, as well as the openings of the venting and ventilation pipes. A zone 1 hazardous area of six meters is located around the outlet of the vent mast, whereas the ventilation inlet and outlet of the tank connection space create a hazardous area of three meters in diameter. In addition, a zone 2 area of 1.5 meters surrounds the zone 1 areas.

According two possible layout we have two principle layout regarding safety and hazardous zones.
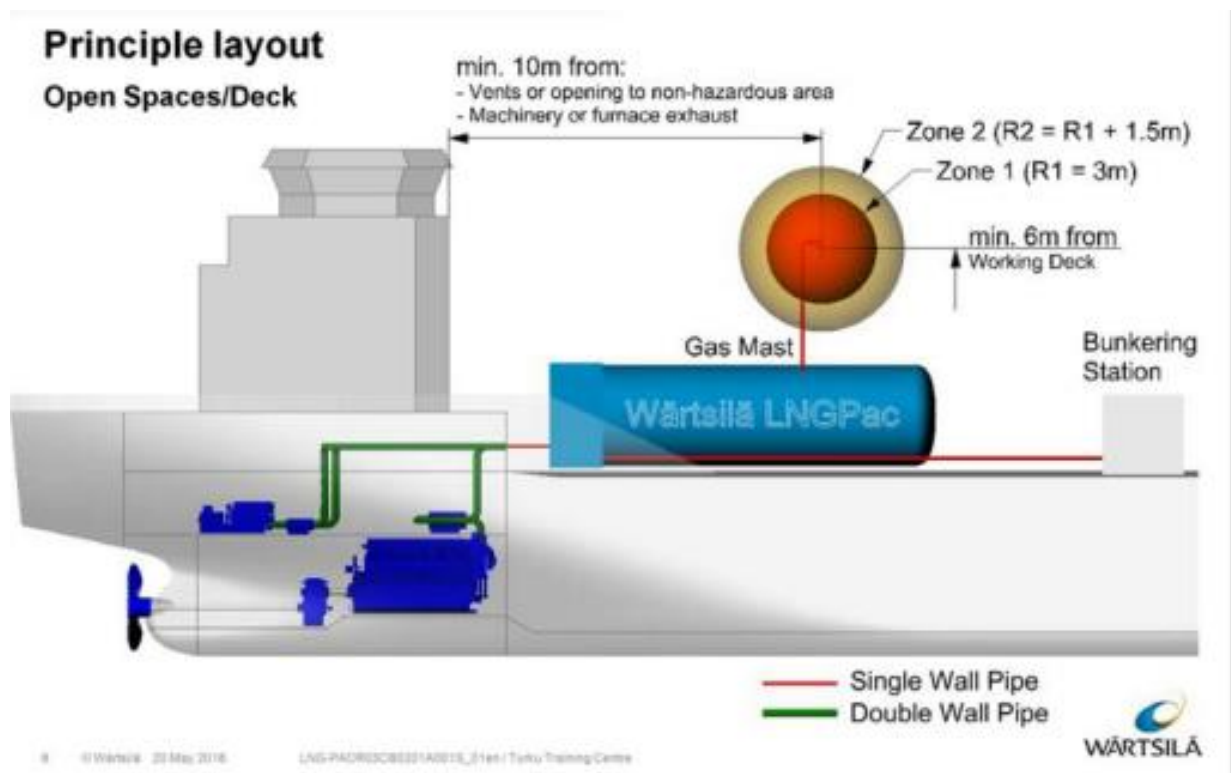
Figure 26 *Hazardous zones-LNG tank in open space*
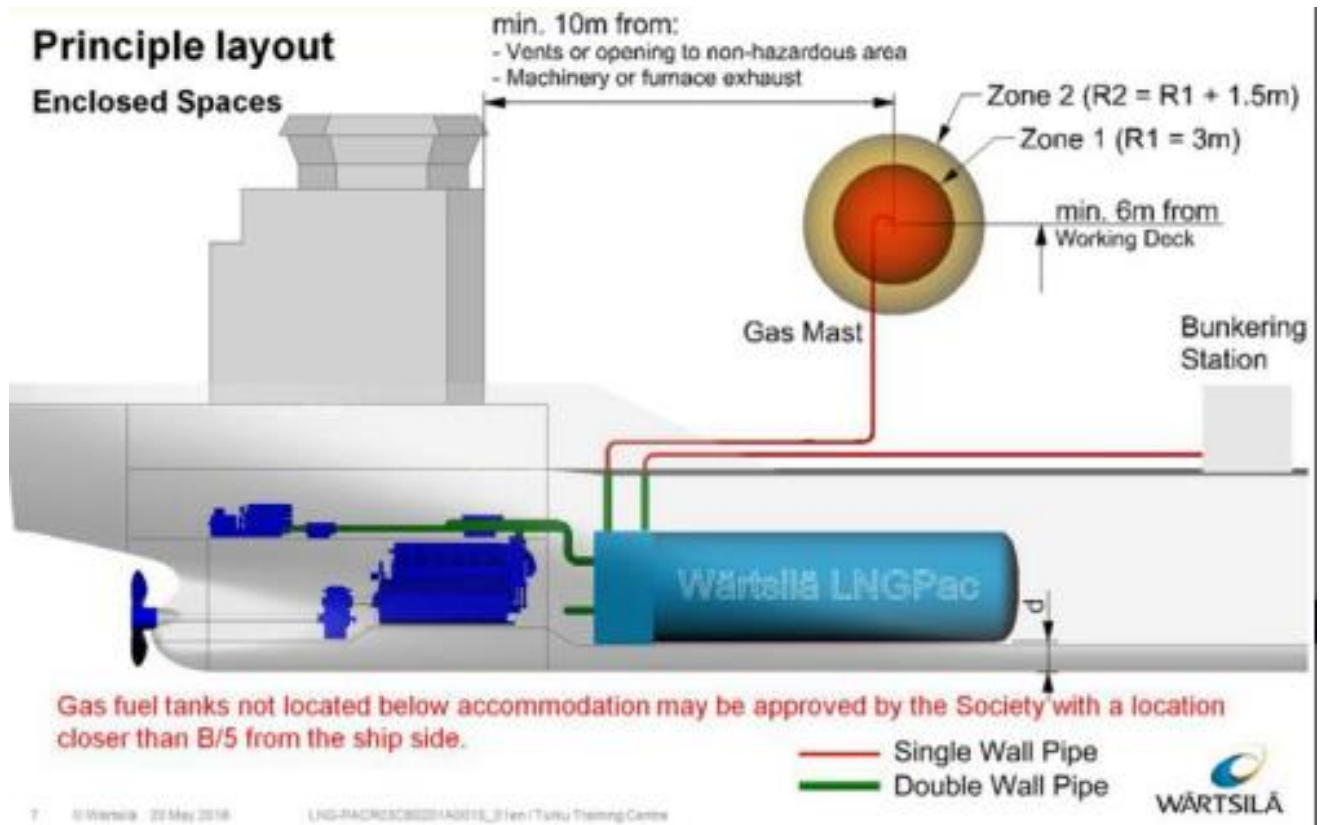
Figure 27 *Hazardous zones-LNG tank in enclosed spaces*

According SOLAS we have special rules regarding fire-safety
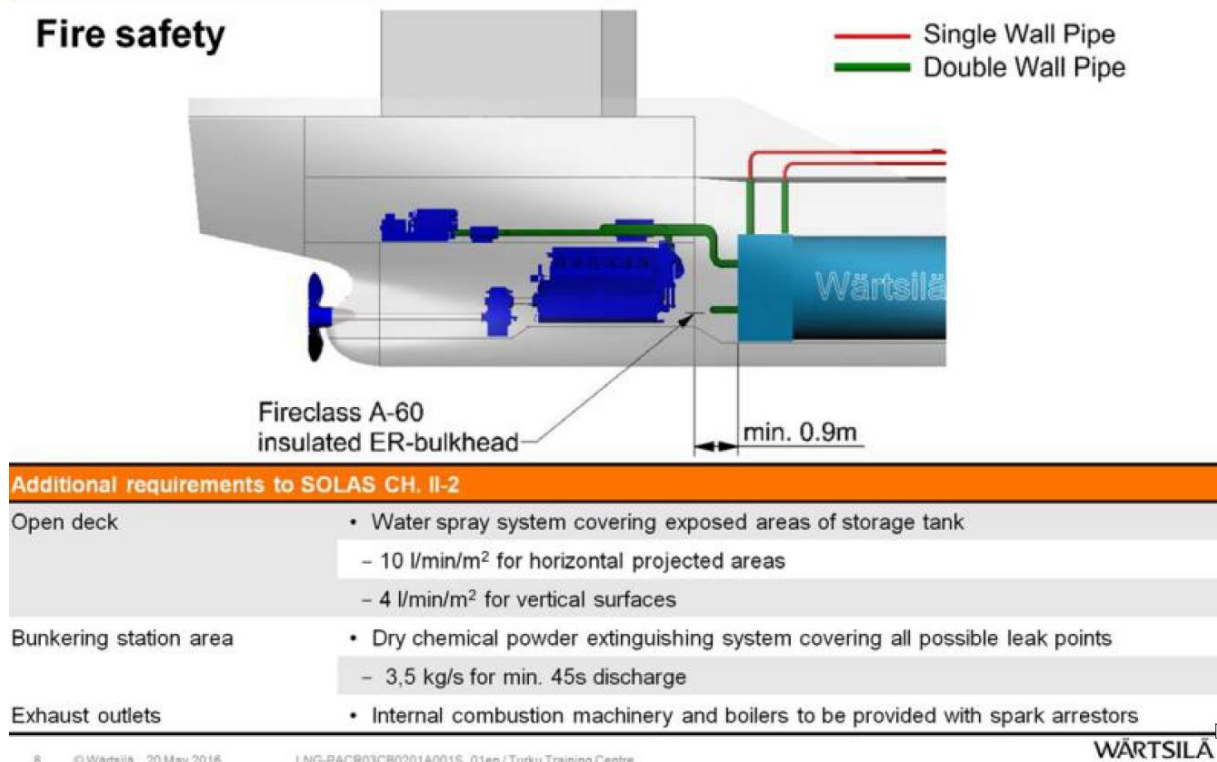
Figure 28 *Fire safety - according SOLAS*

4. Conclusion

From all the above, it can be concluded that the use of LNG on dredgers brings a lot of challenges, both in designing and constructing of the ship. Implementation of LNG on dredger requires constant collaboration between hull engineers and pipe engineers and designers to obtain optimal and secure solutions. A lot of care must be taken for the safety of the ship and the crew, but the benefits of using it in ecological and financial terms are great and will probably push LNG as a fuel even more over time.

REFERENCES

[1]   Costs and Benefits of LNG as Ship Fuel for Container Vessels, MAN Diesel & Turbo - This study was jointly performed by GL and MAN Diesel & Turbo in 2011. The work was performed by Dr. Pierre C. Sames (GL), Mr. Niels B. Clausen (MDT) and Mr. Mads Lyder Andersen (MDT).

[2]   LNG as a Maritime Fuel: Prospects and Policy – CRS Report prepared by Paul W. Parfomak, John Frittelli, Richard K. Lattanzio. Michale Ratner

[3]   LNG technology on board of vessels – IHC Jaimy de Bruine

[4]   https://www.dnvgl.com/maritime/lng/current-price-development-oil-and-gas.html

[5]   Wartsila – Instructions for Wartsila LNGPac

HYBRID AND ELECTRICAL FERRY CHARGING STATIONS WITH COMMON DC BUS

*Aleksandar, Cuculić[*a,], Ivan, Panić [a], Jasmin, Ćelić [a] Antonio, Škrobonja [a]*

a University of Rijeka, Faculty of Maritime studies, Studentska 2, 51000 Rijeka, Croatia
* cuculic@pfri.hr

Abstract

The current trend of hybridization and electrification of coastal line ferries generates increasing demands on the construction of shore connection and battery charging systems. At the same time, it is very difficult to reconcile the conflicting requirements for shore side charging power and the capacities of the existing land infrastructure. This is especially the case in smaller island towns where the largest number of such ferries dock. There, the insufficient capacity of the electrical distribution grid often requires installation of additional energy storage system or renewable energy sources. Furthermore, the characteristics of battery storage modules onboard ferries and associated charging systems are not unified, which poses a significant design problem for onshore power conversion system. In this paper the advantages of using ferry charging station with common DC bus is presented as a result of research on the project METRO - Maritime Environment-Friendly Transport Systems.

Key words: Hybrid and electrical ferry; ferry charging station; common DC bus; battery energy storage; shore connection

Sažetak

Postojeći trend hibridizacije i elektrifikacije trajekata na duž obalnim linijama generira povećane zahtjeve za konstrukcijom kopnenih priključaka i sustava za punjenje baterija. Istodobno, vrlo je teško pomiriti često oprečne zahtjeve za snagom punjenja i postojeće kapacitete kopnene distribucijske mreže. To je posebno izraženo u manjim otočkim sredinama gdje upravo ovakvi trajekti najčešće i pristaju. Nadalje, karakteristike baterijskih skladišta energije na trajektima i pripadajućih sustava punjenja često nisu unificirane što predstavlja značajan problem pri dizajniranju pretvaračkih sustava. U ovom radu prezentirane su prednosti upotrebe punionica za hibridne i električne trajekte s zajedničkom DC sabirnicom kao rezultat istraživanja na projektu METRO Maritime Environment-Friendly Transport Systems.

Ključne riječi: Hibridni i električni trajekti; punionice za trajekte; zajednička DC sabirnica; baterijska skladišta energije; kopneni priključci

5. Introduction

Block diagram of typical low voltage (LV) shore connection system according to IEC/IEEE CDV 80005-3 standard is shown in Figure 1. Requirements for distribution systems used on shore are given in IEC 60364, and ship distribution systems requirements are given in IEC 60092-101. In this paper main focus will be on shore side infrastructure.

Shore side infrastructure is supplied from local distribution grid and its main task is to transfer electrical energy to the vessel in a safe and efficient way. An equipotential bonding between the ship's hull and shore earthing electrode shall be established by the earth contacts of the plug, socket-outlet, ship connector and ship inlet. Construction of the LV equipment and operating safety procedures shall provide for the safety of personnel during the establishment of the connection of the ship supply, during all normal operations, in the event of a failure, during disconnection and when not in use.

The voltages and operating frequencies (Hz) of the ship and shore electrical systems shall match; otherwise, a frequency converter shall be utilized on shore. According to IEC/IEEE CDV 80005-

3 where ships undertake a repeated itinerary at the same ports and their dedicated berths (which is the case for ferries), other IEC voltage nominal values may be considered.[1][2]

KEYS

1. SHORE SUPPLY SYSTEM
2. SHORE-SIDE TRANSFORMER AND NEUTRAL GROUNDING RESISTOR OR/AND IT POWER SYSTEM
3. SHORE-SIDE PROTECTION RELAYING NON INTEGRATED IN SHORE-SIDE CIRCUIT-BREAKER
4. SHORE-SIDE CIRCUIT-BREAKER
5. SHORE-SIDE FEEDERS CIRCUIT-BREAKERS
6. CONTROL SHORE
7. SHORE-TO-SHIP CONNECTION AND INTERFACE EQUIPMENT

8. CONTROL SHIP
9. SHIP PROTECTION RELAYING NON INTEGRATED IN ON-BOARD SHORE CONNECTION SWITCHBOARD
10. ON-BOARD SHORE CONNECTION SWITCHBOARD
11. ON – BOARD TRANSFORMER (WHERE APPLICABLE)
12. ON-BOARD RECEIVING SWITCHBOARD

Figure 2 *Typical LV shore connection/charging system*
Slika 3 *Tipični sustav niskonaponskog kopnenog priključka*

There are two options for realizing shore to ship connection and interface equipment (key 7 in Figure 1) for energy transfer from shore to ship: conventional plug in connections (Figure 2) and wireless inductive connections (Figure 3). [3]

The key factors that will dictate the configuration of shore side infrastructure for ferry shore connection and charging system are:

- o available power from the existing distribution grid,
- o power system upgrade implementation possibility and costs,
- o power converter requirement,
- o type and location of charging station,
- o system redundancy and fault tolerance
- o possibility of using renewable power sources
- o electrical power system topology on-board ferry (ship-side).

It is very difficult to reconcile the conflicting requirements for shore side charging power and the capacities of the existing ground infrastructure. This is especially the case in smaller island towns where the largest number of such ferries dock. There, the insufficient capacity of the electrical distribution grid often requires installation of additional energy storage (ES) system or renewable energy sources. Furthermore, the characteristics of battery storage modules on board ferries and associated charging systems are not unified, which poses a significant design problem for shore connection points, meaning that in most cases a suitable power converter will be required on shore. [4]

The method of charging battery ES on ferry vessels will largely depend on the on board power system topology. For all electric ferries and ferries with DC distribution same connection point can be used for both battery charging and cold ironing, so it is logical to assume that power systems on new build vessels will be based on these topologies. It can also be expected that a large number of existing ferries that are not yet at the end of their planned lifecycle will go through a kind of "hybridization" process in order to meet increasingly stringent environmental standards. Such ships will most likely require separate connections for cold ironing and charging. Therefore, it is very important that topology of ground infrastructure is flexible enough to meet different charging requirements, or it can be easily adapted to different requirements when needed. [5]

Experience gained from exploitation of existing ferry charging stations, mostly in Norway and Sweden, has shown that on shore energy storage systems and renewable energy sources are key technologies for increasing energy efficiency and reliability of shore side power supply systems for ships. For this reason, it is also important to design shore side power infrastructure in such way to facilitate the easiest possible connection of such sources.[6]

In order to meet the above conditions, a shore connection/charging system with a common DC bus is imposes as most suitable solution for ferry shore connection and charging system at ferry terminals. In this paper, such a system is presented with special reference to the method of electrical protections and the impact on the local power grid.

6. Ferry charging station with common DC bus

Topology of shore connection/charging station with common DC bus is shown in Figure 4. There are many advantages of using the proposed topology when compared to traditional LV shore connection system fed directly from local distribution grid, of which the most significant are listed below:

o   Use of common DC bus can provide more efficient interconnection of system with different frequencies.
o   When compared to AC bus, DC bus requires less power conversion stages for connections and interconnections of equipment.
o   Parallel operation of multiple power sources is much easier on DC system because there is no need to account for frequency and phase shift during synchronization process, but only the voltage.
o   Rectifier can be placed in the same substation, together with MV/LV transformer, which reduce the length of 0.4 kV supply cables and consequently reduces possible voltage drop problems at high loads.
o   It is much easier to maintain required voltage level on DC system.
o   There is no harmonic, reactive power and skin effect issues on DC bus.
o   It is easier to design electrical protections because modern power electronic converters can almost instantaneously limit the current and power flow when required (e.g. system overload, short circuit, earth fault).
o   By using higher DC bus voltage (750-1000 V) charging current, voltage drops and copper losses are reduced compared to 0.4 kV AC distribution system.
o   Battery storage system and renewable energy sources can be connected to DC bus via simple bi-directional DC-DC converters, which also facilitates power flow management.
o   During power outages on supply distribution grid, important consumers within port facility can be supplied from battery energy storage.
o   In future, with expected rapid grow of cars, trucks and busses, it will be much easier to realize charging stations for such vehicles and increase the port revenue by selling the energy from own micro grid.
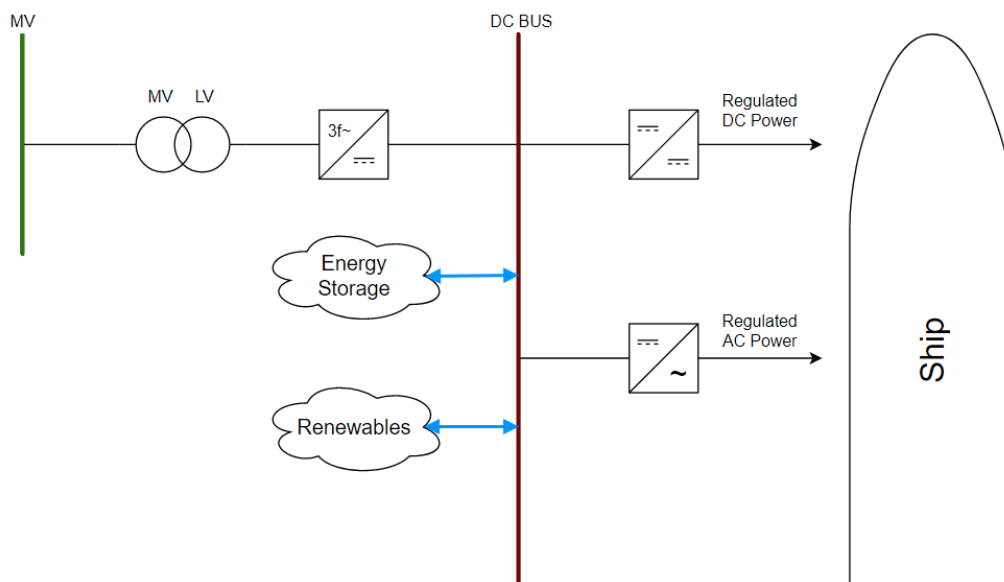
Figure 4 *Shore connection/charging system with common DC bus*
Slika 4 *Kopneni priključak/punionica s zajedničkom DC sabirnicom*

The key component in proposed charging system is rectifier system placed between LV busbar of local distribution grid and common DC bus because its operation has a direct impact both on local distribution grid power quality and DC bus voltage stability. The harmonic spectrum of the current

drawn from the grid by a nonlinear consumer depends to a large extent on the rectifier front end topology.

The comparison of three common front end topologies for rectifier systems is given in table 1. [7]

Table 1 Comparison of three most common front end topologies for rectifier systems

Tablica 6 Usporedba karakteristika tri najčešće topologije ispravljača

	Active front end (AFE)	Thyristor rectifier	Diode rectifier
Power factor	≈ 1, controlable	Varies with load (>0.94)	>0.96
THDi	< 2%	up to 12%	up to 10%
Bidirectional power flow	Yes	Yes	No
Weight and volume	80%	100%	100%
Maintenance	Complex	Less complex than AFE	Simple
DC voltage control	Controlable around rectifying voltage	Controlable from 0 to full rectyfing voltage	Can be controlled by DC-DC converter
Cost	High	Medium	Low

Although the active rectifier gives the best results in terms of harmonic distortion, it also has a number of disadvantages, primarily high installation and maintenance costs and complex design. In addition to that, for specific application the problem may be the narrow range of voltage regulation around the mean value of the rectified network voltage.

Thyristor rectifier has the ability to regulate the voltage by simply changing the firing angle of the thyristor but is much less efficient than the combination of a diode rectifier and a DC-DC converter, especially under lower load. Also, the voltage control is possible only from 0 to maximum value of rectified voltage.

Having disadvantage only in term of higher harmonic currents, the combination of front end full bridge diode rectifier (6 or 12 pulse) and DC-DC converter imposes itself as the best power supply solutions for common DC bus. If required, DC-DC converter can have insulated topology, but in most practical applications conventional buck-boost topology can be used in DC/DC stage. This may be a problem regarding the connection to the distribution network in the sense that the grid rules and regulations in Croatia requires THD <6.5% on the part of the MV network. In case of exceeding the THD limit it may be necessary to install passive harmonic filters.

7. Proposed system for common DC bus electrical protections

The interconnection of AC/DC power converter and common DC bus with LV distribution grid can only be implemented when the safe network operation is guaranteed by the use of suitable electrical protection system.

While the existing ISO standards for LV and HV shore connections define requirements and protections of standard plug in connections required for cold ironing, the standards for battery charging equipment and its integration still does not officially exist.

In order to provide safe operation of suggested charging station with common DC bus, a protection system configuration shown in Figure 5 is proposed. In case of power supply loss from distribution grid, the reconnection of DC supply must be enabled by means of auxiliary under voltage relay U<. The protective functions may be also built in AC/DC power converter control system. DC

bus connection to 0.4 kV distribution system should be done through visible lockable switch disconnector (repair and maintenance).

To ensure the safety of common DC bus, a two way transfer tripping communication line between 0.4 kV AC and DC bus interconnection protection systems must be used. Protection of DC bus consists of voltage surge arrestor and DC circuit breaker which are both included in interconnection protection system.

There should be a single earthing protection system in common DC bus which connects exposed conductive parts at 0.4 kV AC electrical equipment and DC bus equipment. Protection against electric shock on DC side is provided by means of transfer tripping from the insulation monitoring device on all the DC bus interconnection systems.
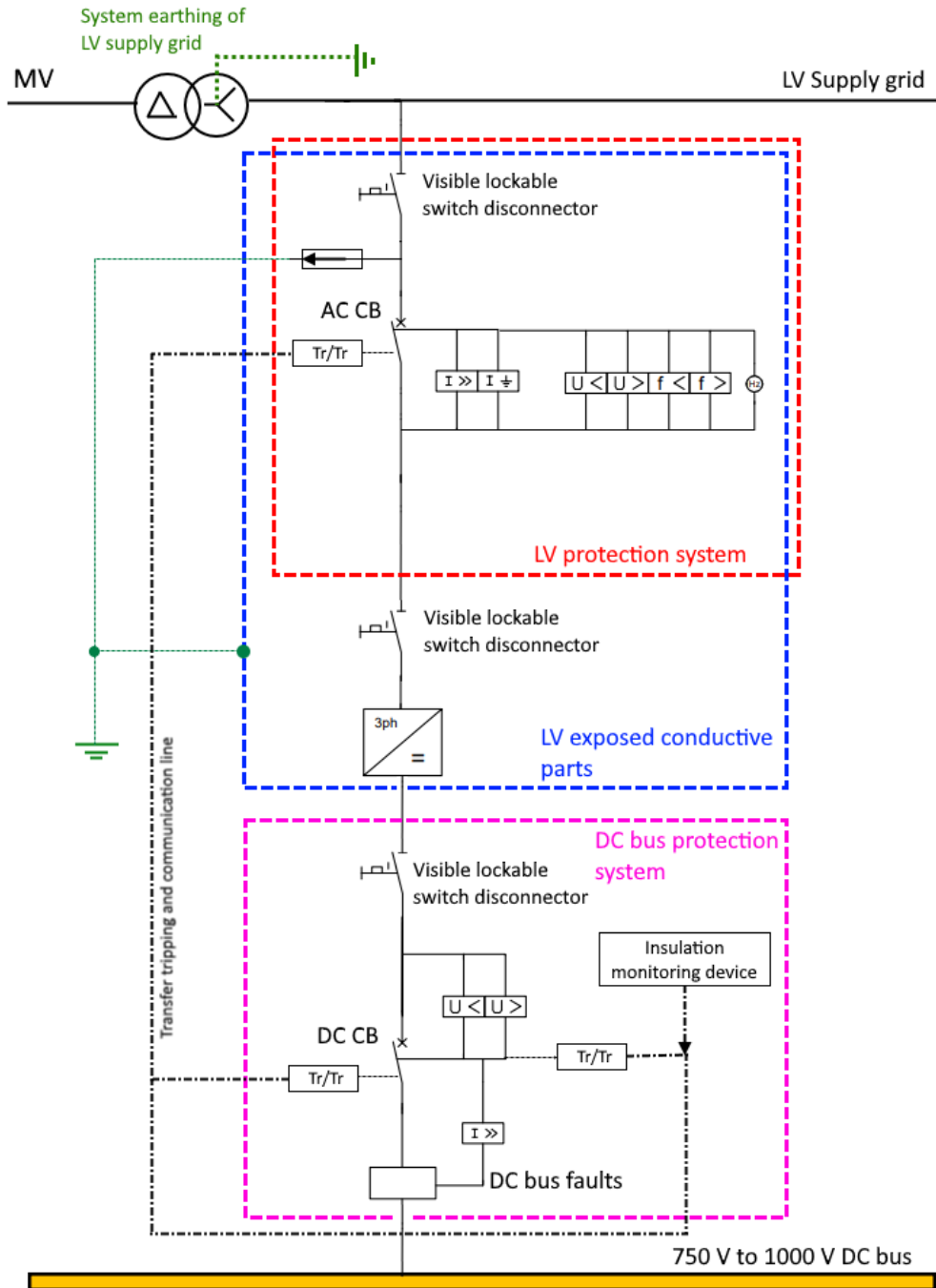
Figure 5 *Proposed electrical protection system for common DC bus*
Slika 5 *Predloženi sustav električnih zaštita za zajedničku DC sabirnicu*

8. Conclusion

Fast recharging of hybrid and electric ferry battery storage system means that the power flows through the distribution grid will be much higher and may cause overloading and under voltage problems in the surrounding local grid. Distribution grids on island and rural areas (where majority of ferry ports are located) have radial topology in most cases, which makes them more susceptible to failures and power outages that impose use of energy storage system on shore side. Furthermore, ports with insufficient capacity of the electrical distribution grid often requires installation of additional energy storage (ES) system or renewable energy sources.

Characteristics of battery storage modules onboard ferries and associated charging systems are not unified, which poses a significant design problem for shore connection points, meaning that in most cases a suitable power converter will be required on shore. In order to facilitate the easiest possible connection of such sources and provide both AC and DC power for battery charging and cold ironing, an onshore charging system with a common DC bus is selected as a best solution.

Use of common DC bus can provide more efficient interconnection of system with different frequencies. When compared to AC bus, DC bus requires less power conversion stages for connections and interconnections of equipment. With common DC bus it is easier to design electrical protections because modern power electronic converters can almost instantaneously limit the current and power flow when required (e.g. system overload, short circuit, earth fault). During power outages on supply distribution grid, important consumers within port facility can be supplied from battery energy storage. In future, with expected rapid grow of cars, trucks and busses, it will be much easier to realize charging stations for such vehicles and increase the port revenue by selling the energy from own micro grid by using suggested topology.

To ensure the safety of common DC bus a two-way transfer tripping communication line between 0.4 kV AC and DC bus interconnection protection systems should be used. There should be a single earthing protection system in common DC bus which connects exposed conductive parts at 0.4 kV AC electrical equipment and DC bus equipment. Protection against electric shock on DC side is provided by means of transfer tripping from the insulation monitoring device on all the DC bus interconnection systems.

REFERENCES

[6] IEC/IEEE DIS 80005-3 Utility connections in port — Part 3: Low Voltage Shore Connection (LVSC) Systems — General requirements.

[7] IEC/IEEE 80005-2:2016 Utility connections in port — Part 2: High and low voltage shore connection systems — Data communication for monitoring and control.

[8] Guidi, G., Suul, J.A., Jenset, F., Sofron, I. Wireless Charging for Ships. IEEE Electrification Magazine, 2017.

[9] Kumar, J. Et Al. (2020) Sizing and Allocation of Battery Energy Storage Systems in Åland Islands for Large-Scale Integration of Renewables and Electric Ferry Charging Stations, Energies 2020, 13, 317.

[10] Cuculić, A., Prenc, R., & Perović, D. (2017, January). Improving Environmental Sustainability of Ferry Transport Using Batteries and Hybrid Power Solutions. In Automation in Transportation 2017.

[11] Kumar, J. Et Al. (2019) Design and Analysis of New Harbour Grid Models to Facilitate Multiple Scenarios of Battery Charging and Onshore Supply for Modern Vessels. Energies 2019, 12, 2354.

[12] Zhang S, Sivertsen LH, Øvsthus K, Sagedal A. Study of High Power Fast Charging Station for Battery Ferry and Hybrid Ferry. In2018 21st International Conference on Electrical Machines and Systems (ICEMS) 2018 Oct 7 (pp. 2291-2295). IEEE.

THE SEA RESOURCES AND THE SUSTAINABLE FUTURE

Vedran Slapničar[a], Ivan Adum*[b], Izvor Grubišić*[b]

a University of Zagreb, Faculty of mechanical engineering and naval architecture, Ivana Lučića 5, 10 000 Zagreb, Croatia

b Boatbuilding Innovation Center, Ivana Lučića 5, 10 000 Zagreb

* Corresponding Author, vedran.slapnicar@fsb.hr

Abstract

Vast spaces, surfaces, of planet Earth, about 71 %, are covered with water. A large majority of this water surface are the oceans and seas, much lesser part in freshwater reservoirs. Some of the landlocked water surfaces, lakes, are also salted because the evaporation is larger than the freshwater influx. Human activity on seas, oceans, and lakes so far has been largely focused on transportation and fishing. Oceans, seas, lakes, and rivers are natural waterway routes suitable to accommodate large vessels, ships the most efficient and commercially most viable means of transportation. We have defined spectra of eight areas of marine technology but the focus of this paper is primarily on mariculture and marihousing. The future will demand additional food and housing we consider the sea and oceans as a natural step toward available untapped resources. The paper discusses the need and the way of interdisciplinary studies to meet all the challenges on the way. The open road for ideas and scientific mobility is most probably the best answer**.**

Key words: Sea resources; sustainable growth; areas of exploration; interdisciplinary studies

Sažetak

Velika prostranstva površine planete Zemlje prekrivena su 71% s vodom. Većinu ove vodene površine čine oceani i mora, a mnogo manji dio slatkovodne akumulacije. Neka od zatvorenih vodenih područja u što spadaju i jezera imaju bočatu vodu zbog činjenice da je isparavanje veće od priliva slatke vode. Dosad su ljudske aktivnosti na morima, oceanima i jezerima bile u velikoj mjeri fokusirane na prijevoz i ribolov. Oceani, mora, jezera i rijeke su prirodni vodeni putevi sposobni preuzeti velika plovila, brodove kao najučinkovitije i ekonomski najisplativije prijevozno sredstvo. U radu je definiran spektar od osam područja pomorskih tehnologija ali fokus ovog rada prvenstveno je u marikulturi i maristanovanju. Budućnost će zahtijevati izvore dodatne hranu i stanovanja, pa more i oceane smatramo prirodnim korakom prema dostupnim neiskorištenim resursima.U radu se razmatra potreba i način interdisciplinarnih studija kako bi se mogli efikasno suočiti s izazovima održive budućnosti koristeći morske resurse. Otvorenost idejama i znanstvena mobilnost predstavljaju najvjerojatnije najbolji odgovor.

Ključne riječi: Morski resursi; održivi razvoj; područja istraživanja; interdisciplinarne studije

1. Introduction

Water is the cradle of life on Earth and our future farm and home. In a sense, we are returning to our origins. The human population on the planet has increased dramatically, and it is in some areas quite doubtful whether the land-based resources are adequate to sustain it. The logical alternative and at hand is the water. The future is undoubtedly going to be more focused on water, on the surface, and in the deep. We are not inventing anything new, we are just listening carefully to what other people are saying and try to contribute. Let us review the spectra only, no divisions, no categorizations, identifying the 8 main areas of interest: routes-shipping, energy, food, housing, water-desalination, depth mining, and defense and research.

2. Planet Earth and Oceans

We want to widen the horizon and to introduce a synoptic view as a standard. Vast spaces, surfaces, of planet Earth, abt. 71 % to be more precise, represent seas and oceans. Besides this, some

of the landlocked water surfaces, lakes, are also salted because the evaporation is larger than the freshwater influx.

Essential principles about our ocean [1]:

1. The ocean and life in the ocean shape the features of the Earth and has a major influence on weather and climate.
2. Oceans and humans are inextricably interconnected, and ocean makes Earth habitable.
3. The ocean supports a great diversity of life and ecosystems and it is largely unexplored (less than 5% of the ocean mass has been explored).
4. The use of ocean resources has increased significantly in the last 40 years and future sustainability depends on our understanding of those resources.
5. Ocean exploration is truly interdisciplinary and requires close collaboration among biologists, chemists, climatologists, computer programmers, engineers, geologists, meteorologists, physicists, and above all a new way of thinking.
6. Desalination and mineral residue extraction (Figure 1).
7. Besides the metals nodules on sea bead such as manganese that have been detected on the seabed, one has to assume that it may be possible to start mining operations with remotely operated mining machines and do an extraction of minerals and metals from the sea solvent.
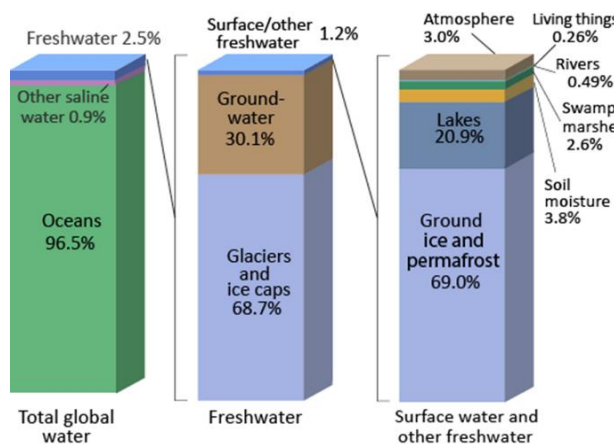
Figure 1 *World freshwater resources, [2]*
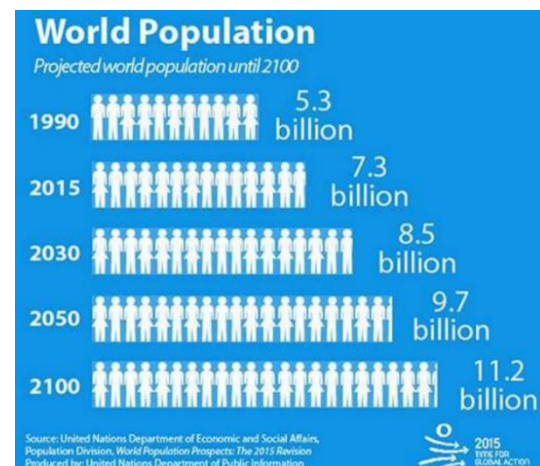
Figure 2 *Planet Earth (Source: www.un.org)*

Projected world population growth creates a demand to develop additional areas for food and housing i.e. mariculture and marihousing (Figure 2).

3. Transportation Routes and New Ship Design Shipping

Some such surfaces, albeit technically could be called lakes i.e. without direct connection with other water surfaces on the Planet, are also called seas due primarily to their size, e.g. Caspian and Aral seas. Human activity on seas, oceans, and lakes so far has been largely focused on transportation, which is rather logical, to move goods and people one has to utilize transportation routes. Oceans, seas, lakes, and rivers are natural routes, waterways are in essence roads capable of taking and accommodating large vessels, i.e. ships, the most efficient and commercially most viable means of transport (Figure 3). One estimate says that 90% of total world cargo is transported by water.

Figure 3 *Transportation routes, 158690 vessels on the map, [3]*

There is also another aspect, which should not be neglected, this ways and routes are avenues used to project power i.e. force over large distances. Human organization i.e. states have from the dawn of civilization been engaged in projecting power to take more land, control the ocean, sea, and expand commerce or simply grab other people's possessions. This is, whether we admit it or not, the main ingredient, *raison d' etre*, of our behavior so far. War and piracy have been the very foundation stones of empires.

Dry, wet, and container ships, more or less classical vessels are intended for transportation only, ship as a vehicle on sea routes. During the ship design process the variation of geometrical properties of the ship can result in the significant reduction of power required to propel vessels for the given speed, and ship lightweight. We are speaking about new ship designs with lower environmental impact (Figure 4 &5).
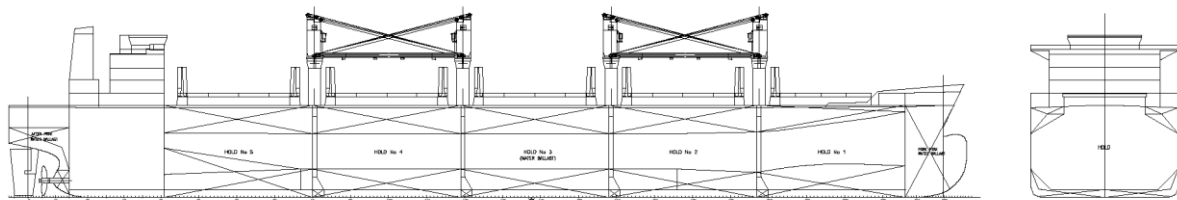
Figure 4 *Bulk carrier 63.000 dwt, CLASSIS Ship Design and Consulting*
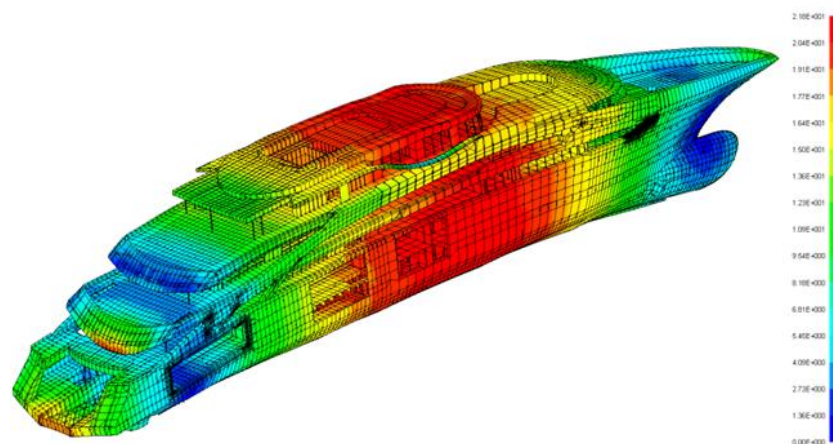
Figure 5 *Mega Yacht Structural Optimization and Analysis, UNIZAG FSB*

The Zero Emission ship (Figure 6) is a luxury cruise vessel that future customers can sail without harming the environment, as it is completely environmentally neutral and does not use any fossil fuels. The ship has fully automatic wing sails and uses solar energy and fuel cells as its power source with the possibility of usage of wind energy also.

Figure 6 *Zero-emission activity cruise vessel SWAT Hull form, Deltamarin, [4]*

4. Energy sources

According to some estimates, more than 70 % of the biomass of the planet is in the water. Humans have used this vast reservoir of food primarily to fish but also to pick up algae, albeit too a much lesser extent. Besides food and water, there are other resources in water. It has perhaps been not so much known to the so-called general public, but it is there. What is the source of energy on Earth? Sun. Prospecting and extraction go deeper and deeper, we are moving our frontiers of perception and our capabilities, the depth of our knowledge is reflexed in sea depth we are exploring. How to harness sea waves is a challenge not yet fully understood and practically applied, that goes for tides as well. How to use the potential of temperature differences on the surface and in depths, what is the minimum differential that makes it commercially viable? Should it be on an ocean-going vessel offshore or fixed installation onshore? The potential of underwater currents that

are rather strong, detected, ascertained, by submarines, can only be if proved feasible, used onboard ocean-going vessels, movable generating plants, and installations. All this technology has not to be invented, it exists and is known but in general terms only, one has to develop practical and commercially viable marine applications, solutions. That proves to be a challenge indeed. Fossil fuels are in essence sun energy stored and reused. Sun energy is also stored in water, why not extract it and use it? Why not indeed. Reusing sun energy via fossil fuels one emits carbon dioxide in the atmosphere with all the negative repercussions. The planet cannot sustain such practice, not in the long run. We have been recently exploited reusable sources of energy i.e. ones without so many negative side effects. Photosensitive panels have so far been mainly installed on land using the energy irradiation (Figure 7), why not on barges on the open sea?
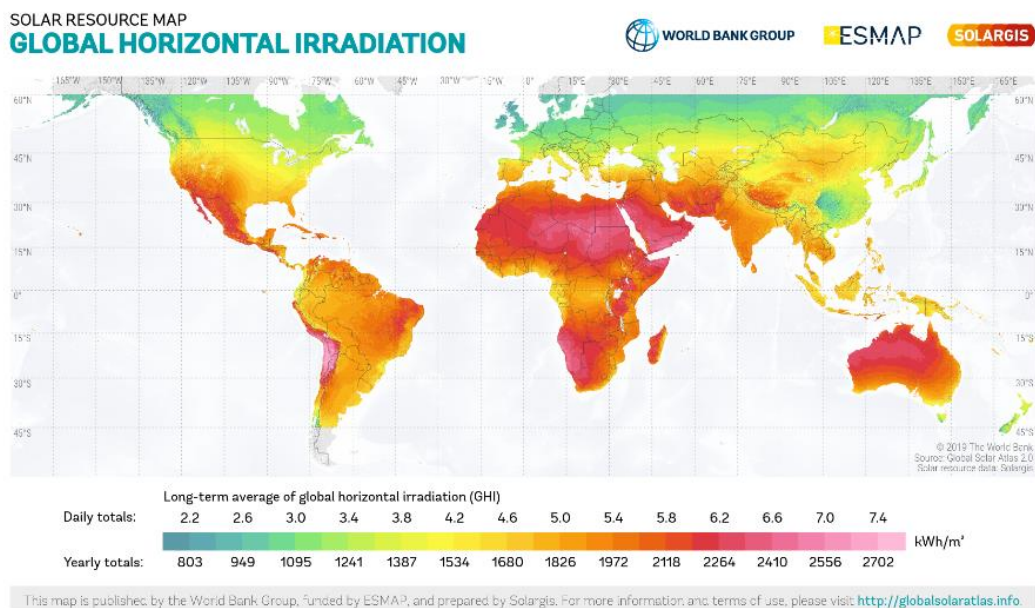
Figure 7 *Energy irradiation, [5]*

The same applies to wind farms. There are some problems due to the power transfer to the land-based grids, but they are not insurmountable. From the rather modest beginnings, extracting hydrocarbons in the Mexican gulf, one has developed rather a remarkable installation in the North Sea and offshore Africa and South America.
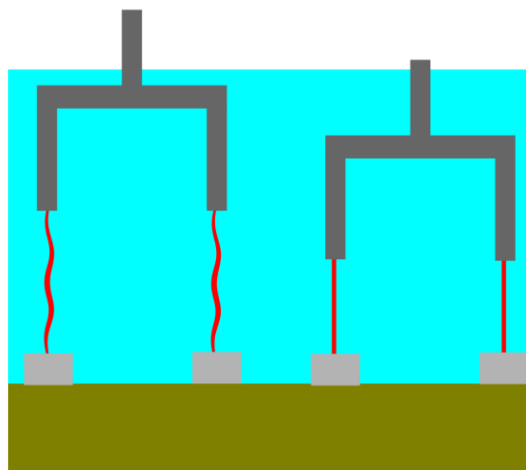
Figure 8 *Deepwater offshore tension-leg platform, [6]*

All sorts of vessel platforms and or barges are used to explore and extract hydrocarbons from the seabed (Figure 8). All sorts of vessels and or fixed installation are used to harness wind energy, wave energy, current energy, and solar energy as emitted primarily. Sea, the ocean as a reservoir or depository of sun energy. So we can ask why didn't we use these sources to do far? Because it is a more complex process than just extract hydrocarbons from the seabed. The majority shipbuilding as a confection industry of ready-made designs doesn't have satisfactory answers to the lean and sustainable ship transportation problems. So, to be capable to answer the challenges of the future it doesn't require just an additional effort of existing techniques it requires all-new ways of thinking. In Figure 9 it is shown a concept sketch and final artwork – utilizing solar, wave, and wind power to generate localized power solutions for coastal cities and as water purification plants converting seawater to fresh drinking water.

Figure 9 *Energy Island, www.mondoart.net*

5. Food and housing

Not only fish farming, but other farming also exists - vegetation. We have seen that in some countries like in Korea the dry algae are the standard product on shelves on food stores. E.g. Croatia the decade before it was almost unthinkable the so the amount and variety of sea species in the fish farming. Such systems would be used to cultivate and raise fish and other forms of marine life to help meet the nutritional needs of the world's people (Figure 10).

Figure 10 *Floating maricultural farm, [7]*

Fish farming should move to the open sea due to ecological reasons and should become self-sustainable as far as practicable. Today's systems are immersed cages served from the shore either by floating bridges or by service boats. It is a process composed of multiple steps, each step a separate one. The same goes for shell farming. Algae farming is not so much developed and is mostly sea bed harvesting. Besides ecological issues such as but not exclusively pollution the process applied is a non-continuous and non-congruent one. Ecco issues would inevitably become the deciding factor, it is highly controversial to pollute one's abode and farm. We should develop a non-invasive and sea friendly approach, we should adapt to the sea not impose on it. Same as we are now, finally, trying to live in harmony with forests and meadows.

Fishes are primarily fed by shore produced food, shells are fed by plankton indigenous sea product brought by sea currents. Tuna farms, adult fishes are caught and caged and fed up to a commercial size primarily by small pelagic fishes, sardines, and similar. One should investigate what sorts of wild fish, beside tuna, could be caught caged and fed up to the commercial size. The same applies to all sorts of mollusks including snails. Deep-sea farming suspended paternoster ropes should be possible, beside shells, snails, and mollusks, for algae as well. The substrate could be hanged on the rope in the form of sacks. Platforms as an island form composed of multi orthogonal forms or as a catamaran form, anchored to the sea bottom. Automated unmanned submersibles controlled from the island i.e. platform. The key issue would most probably be the maximal sea depth, desirable max depth of say 300 meters could be an issue due to the required length of ropes and size of the winch, min required depth abt. 150 m. Anchors in the form of boxes with retractable spikes. Winches to be electrical, a diesel-driven generator as a backup, primary source of energy solar panels, and batteries with corresponding automated regulation. Size and dimension to be suitable to house an adequate no of 20 ft containers for eventual algae processing on the spot and fish a shell packing as well. One small service catamaran to serve as tender and as a plankton catcher. The ultimate goal is to substitute shore produced food with indigenous seafood, minimum ecological, and environmental impact.

A global network of such cities in the sea can easily accommodate many millions of people and relieve the land-based population pressures (Figure 11). They can provide the inhabitants with information and serve as natural sea aquariums without artificially enclosing marine life.

Figure 11 *Ocean cities, [7]*

Floating ports and cities as a solution for sea-level rise and overpopulation

Figure 12 *Testing an innovative concept for a floating mega-island, MARIN, [8]*

By using modules such as MARIN did, floating modules, we could construct islands and forms which already exist in real nature (Figure 12). Climate changes and rising sea levels could cause as much as 150 million people in need of new living surfaces (Figure 13).

Figure 13 *Shifting shoals, George Riethof*

Conclusion

All sorts of scientific vessels, from geological to oceanographic research could service and supply data for all previously mentioned areas of interest. We need different shipbuilding or better to say marine technology and also education that is the bridge for the future. Medical researches, algae not only as a food but as a source – raw material for medicaments. The grid of Universities, Institutes, enterprises together, and authorities is an indispensable form of cooperation. We have roughly defined eight areas of marine technology. We have to start interdisciplinary studies to able to meet the challenges of the future. Much broader cooperation is needed. One has to broaden the perspective and include multi-criteria, the leader or leading designer could instead of the naval architect be a thermodynamics or geology engineer for instance, or even a marine biologist. The open road for ideas and scientific mobility is most probably the answer. The perspective should be broad but the focus should be on essential, or rather gist of the whole project. The only man with vision and determination can carry us to the other shore of the postmodern sustainable society.

REFERENCES

[1]   https://pt.slideshare.net/lorettar/essential-principles-about-our-ocean, Loretta Roberson, Assistant Professor at University of Puerto Rico, Río Piedras
[2]   https://water.usgs. gov/edu/earthwher ewater.html
[3]   https://www.marinetraffic.com, date 19.6.2018.
[4]   https://safety4sea.com/deltamarin-designers-think-different-to-envision-future-ships/
[5]   https://globalsolaratlas.info/download/world
[6]   https://en.wikipedia.org/wiki/Tension-leg_platform
[7]   https://www.thevenusproject.com/resource-based- economy/environment/cities-in-the-sea
[8]   https://www.waterforum.net/marin-test-eerste-drijvend-mega- eiland

CONCEPTUAL DESIGN OF THE SHIPYARD FOR COMPOSITE SHIPS

Josip Lasan[a], Boris Ljubenkov*[b]

a Iskra brodogradilište 1 d.o.o., Obala Jerka Šižgorića 1, 22000 Šibenik
Faculty of electrical engineering, mechanical engineering and naval architecture, Ruđera Boškovića 32, 21000 Split
* Corisponding Author, boris.ljubenkov@fesb.hr

Abstract

The paper presents design process of shipyard for composite ships. In introduction, need for investment in new nautical (production – service) center is pointed out according to increase of nautical tourism in Croatia. Ships market analysis is basis for definition of characteristic ship which is used as main product in conceptual design of the shipyard. Conceptual design of the shipyard contains elements of design spiral like arrangement of working areas, material flows, characteristic ship building dynamics, necessary number of employers and prediction of investment costs. The conclusion indicates benefits of new nautical (production – service) shipyard design.

Key words: *motor yacht; composites; conceptual design; shipyard*

Sažetak

U članku je prikazan proces projektiranja brodogradilišta za kompozitne brodove. U uvodu se naznačila potreba za osnivanjem jednog proizvodno – servisnog centra s obzirom na povećanje nautičkog turizma u Hrvatskoj. Analizom tržišta definirala se potreba za određenim tipom broda za koji se pristupilo izradi idejnog projekta brodogradilišta razradom elemenata projektne spirale. Definiran je razmještaj radnih prostora, tokovi materijala, dinamika gradnje karakterističnog broda, potreban broj djelatnika, njihovih zanimanja te procjena troškova investicije. Zaključno su navedene prednosti osnivanja brodogradilišta kompozitnih brodova.

Ključne riječi: *motorna jahta; kompoziti; idejni projekt; brodogradilište*

1. Uvod

Brodogradilište je sustav različitih djelatnosti koji omogućuju izradu projekta, izgradnju i uvođenje u rad projektom definiranih proizvodnih kapaciteta. Projekt brodogradilišta je brod, a on predstavlja proizvod koji iziskuje primjenu suvremenih tehnoloških dostignuća i kontinuirani proces modernizacije i automatizacije proizvodnih procesa.

Hrvatska, kao zemlja sa izlazom na more, ima potencijal razvoja gospodarstva kroz 4 grane, a to su ribarstvo, turizam, brodogradnja i pomorstvo. U sklopu toga je i nautički turizam koji obuhvaća 10% udjela ukupnog prihoda turizma pa se smatra granom koja je iz godine u godinu u stalnom porastu. Osnovna ponuda nautičkog turizma uključuje marine i *charter* tvrtke, a uz to svakako ide i sva prateća ponuda u koju spadaju ugostiteljski objekti ili *fitness* centri. Čak 70% europskog chartera je vezano uz Sredozemno more što doprinosi razvoju nautičkog turizma u RH. Iako se ostvaruje velika materijalna dobit ona nije razmjerna njezinom potencijalu. Specifična nautička potražnja i s njom povezana posebna nautička potrošnja vrlo se pozitivno odražava na nautičku industriju koja podrazumijeva proizvodnju brodova, proizvodnju opreme, održavanja i osposobljavanje postojećih i izgradnju novih luka (marina). Potražnja nautičara za što većim komforom i luksuznijom opremom uzrokuje da se postojeća flota brodova mora obnoviti, ali i graditi nove brodove.

Europa nastoji otvoriti novo tržište brodova s duljinom preko 50 m i kompozitnim materijalom za izradu brodske konstrukcije. Projekt se naziva *Fibreship* s kojim se nastoji riješiti problemi vezani uz gradnju brodske konstrukcije sa kompozitnim materijalima. S obzirom na novi smjer Europe kroz projekt *Fibreship*, zastupljenost kompozitnih brodova u *charter* uslugama te zahtjevom tržišta za lakim i brzim brodovima sa što većim komforom i luksuznijom opremom zahtijeva gradnju razvojno nautičkog centra koji bi u svom sklopu imao brodogradilište kompozitnih brodova. [1]

2. Analiza tržišta brodova za nautički turizam

Brod se definira kao plovni objekt namijenjen za plovidbu morem kojemu je duljina veća od 12 m i bruto tonaža veća od 15 BRT-a ili je ovlašten voziti više od 12 putnika. Brodovi duljine manje od 12 m nazivaju se brodicama.

S obzirom na široku definiciju pojma broda, brodovi za nautički turizam definiraju se kao jahte. Jahta je plovni objekt za sport i razonodu neovisno koristi li se za osobne potrebe ili gospodarsku djelatnost, a čija je duljina veća od 12 m i koja je namijenjena za dulji boravak na moru te je pored posade ovlašten prevoziti ne više od 12 putnika.

Tržištem brodova za nautički turizma dominira Sjeverna Amerika (39,1%) i Europa (29,3%). Analizom tržišta nautičkog turizma za period do 2026. godine se predviđa porast potražnje za lakim i brzim brodovima napravljenih od kompozitnih materijala. Prema *Reports Data* predviđa se porast potražnje za kompozitnim materijalima i to sa 3,63 milijardi *USD* u 2018. godini na 6,17 milijardi *USD* u 2026. [2]

Glavni proizvodi europskog tržišta brodova za nautički turizam su jedrilice i motorne jahte. Vrijednost tržišta motornih jahti 3 puta je veći od vrijednosti tržišta jedrilica. Pogoni za proizvodnju jahti za nautički turizam vodećih proizvođača europskog tržišta većinom su orijentirana na manju serijsku proizvodnju, dok je mali broj organiziran za veliku serijsku proizvodnju. Prednost manjih serija u proizvodnji je fleksibilnost tj mogućnost brže prilagodbe postojećih kapaciteta i prostora za novu seriju ili novi proizvod što treba imati na umu zbog konstantnog povećanja interesa za dužim brodovima. Analizom tržišta nautičkog turizma u Europi uočava se smanjeni broj vlasnika novih brodova, manji broj dana provedenih na moru te orijentaciju na iznajmljivanje jahti za nautički turizam (*Charter*). Obzirom da se manje osoba mlađih od 45 godina odlučuje na kupnju novog broda ciljano europsko tržište je *charter*. Trend dužine brodova prije 10-ak godina kod kupnje novih jahti za nautički turizam ili *charter* usluga je bio 13 – 17 m, dok se danas u prvi plan dovodi udobnost i prostranost pa se i sa takvim zahtjevima povećala duljina broda preko 20 m. [2]

3. Projekt karakterističnog broda

Za osnivanje karakterističnog proizvoda brodogradilišta odabire se jahta serije *Magellano*, model *Azimut Magellano 66.* [3] Linija broda kojom se opisuje karakteristični proizvod brodogradilišta je *NTUA* serija. *NTUA* serija je razvijena sredinom 90 tih godina na *National Technical Universty of Athens* od kuda dolazi i sam naziv *NTUA*. Odabrana forma karakterističnog broda je poludeplasmanska kao i forma sličnog broda *Azimut Magellano 66.* Namijenjena je brodovima za sport i opuštanje najmanje duljine 20 m, te omogućava postizanje većih brzina u poludeplasmanskom režimu plovidbe.

Karakteristični brod idejnog projekta brodogradilišta je motorna jahta sa slijedećim karakteristikama:

- Duljina preko svega; L_{OA} = 24 m
- Duljina na konstruktivnoj vodnoj liniji; L_{KVL} = 21,9 m
- Širina broda; B_{OA} = 4,4 m
- Širina na konstruktivnoj vodnoj liniji; B_{KVL} = 4,6 m
- Nosivost; Δ = 44,8 t
- Brzina krstarenja 18 nautičkih milja
- Predviđen broj putnika – 8
- Predviđen broj članova posade - 2
- Materijal za izradu broda je kompozitni materijal ojačan karbonskim vlaknima
- Svrha broda je rekreacija i užitak sa dnevnim prostorijama u nadgrađu, glavnoj i sunčanoj palubi
- Stambene zone za smještaj vlasnika, putnika i posade i strojarnica su smještene u trupu broda.

Opći plan broda prikazan je slikom 1. Detaljna analiza proizvoda što se tiče strukture i opreme koristi se u postupku razrade idejnog projekta brodogradilišta.
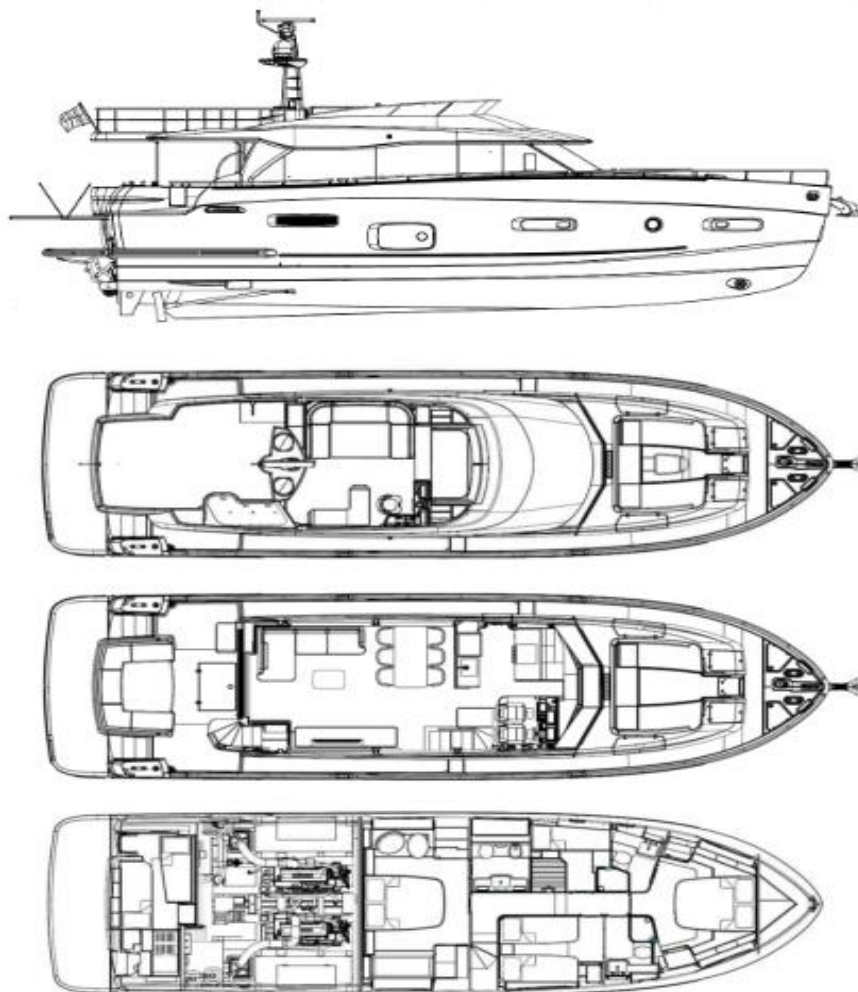
Figure 7 *Ship body plan*
Slika 8 Opći plan karaktersitičnog broda

4. Idejni projekt brodogradilišta

4.1. Projektiranje brodograđevnog procesa

Brodograđevni proces spada u grupu isprekidanih tehnoloških procesa. Karakterizira ga velik broj aktivnosti sa različitim trajanjem. Obzirom na veće dimenzije i masu, brod se dijeli na manje građevne jedinice koji se povezuju sa nizom aktivnosti opremanja građevnih jedinica ili broda u cjelini. Zbog toga je potrebno osigrati:

- Radni prostor za izradu poluproizvoda
- Prostor za skladištenje poluproizvoda
- Transportna sredstva za manipulaciju i transport do naredne radne faze.

Radne prostore je potrebno opremiti strojevima i opremom te je potrebno osigurati prohodnost transportnih putova.

Projektiranje brodograđevnog procesa je iterativni postupak koji se sastoji od elemenata prikazanih u projektnoj spirali na slici 2.
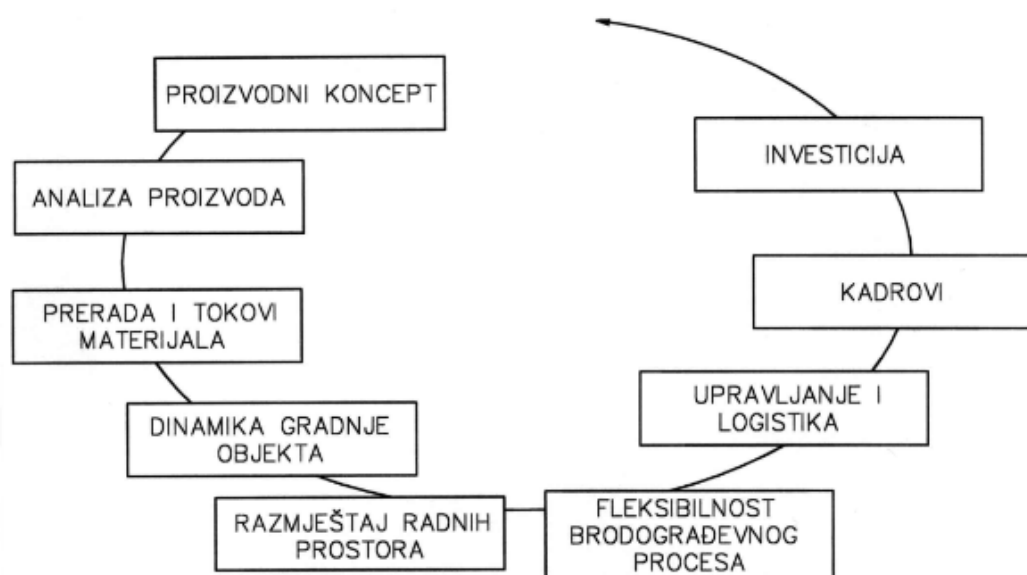
Figure 2 *Production process design spiral*
Slika 2. Projektna spirala

Svaki element projektne spirale ima svoje zahtjeve i ograničenja, a njihova međuzavisnost je složena pa se konačno rješenje traži iteracijom u nekoliko koraka. Konačni rezultat je kompromisno rješenje projekta brodograđevnog procesa u cjelini, pri čemu neće biti moguće postići najbolja rješenja pojedinačno za svaki element projekta. [4]

4.2. Proizvodni koncept

Proizvodnim konceptom definiramo građevno mjesto koje mora zadovoljiti slijedeće kriterije:

- Prometnu povezanost, kako zbog smanjivanja početnih ulaganja tako i zbog lakše povezanosti sa kooperantima i dostave radnog materijala
- Izvori energije, blizina naseljenog mjesta osigurava i blizinu električne energije i lakšu povezanost na infrastrukturu
- Radna snaga, blizina naseljenog mjesta osigurava veću mogućnost nalaženja radne snage
- Klimatski uvjeti, temperatura, vlažnost koje utječu na potrošnju energenata za nesmetano obavljanje proizvodnog procesa
- Strateški razvoj zemlje
- Potencijalni kooperanti.

Obzirom na dimenzije finalnog proizvoda i specifičnosti transporta takvog proizvoda smatra se da je najbolji izbor za osnivanje brodogradilišta lokacija u blizini morske obale. Prijedlog lokacije je prostor u Kaštel Gomilici u Splitsko – dalmatinskoj županiji, a lokacija odgovara traženim zahtjevima. [5]

Dimenzije prostora lokacije su 400 x 150 m i u blizini naseljenog mjesta, ali opet je dovoljno udaljena od njega kako proizvodni proces ne bi ometao lokalno stanovništvo. Smještaj lokacije (uz samu obalu i blizina naselja) kao i njezina prometna povezanost omogućuje manja početna ulaganja za osnivanje brodogradilišta. U neposrednoj blizini odabrane lokacije se nalazi i blizina manjeg brodogradilišta čeličnih brodova ali i zatvorena industrijska postrojenja koja osiguravaju blizinu određene infrastrukture. Budući da je lokacija u neposrednoj blizini većeg naseljenog mjesta (Split sa okolicom) osigurana je veća mogućnost pronalaska radne snage. S obzirom da se u okolici Splita pronalaze veći proizvođači kompozitnih brodova što osigurava dostupnost i stručnost radne snage. Dodatno u samoj blizini odabrane lokacije se nalaze i marine sa *charter* brodovima. To znači da brodogradilište uz mogućnost gradnje novih brodova može i pružati usluge održavanja postojeće *charter* flote.

4.3. *Prerada i tokovi materijala*

Proizvodni proces je organiziran u specijaliziranim radionicama i može se podijeliti na :

- Proces izrade konstrukcije broda
- Proces izrade elemenata brodske opreme i
- Proces opremanja i montaže broda.

Na slici 3. je prikazan shematski prikaz proizvodnog procesa brodogradilišta kompozitnih brodova. Tokovi materijala u proizvodnom procesu moraju biti pravolinijski i što kraći, a svakako treba izbjegavati povratne tokove i presijecanje dugih tokova i linija proizvodnje.

Izrada kompozitnih brodova se razlikuje od izrade čeličnih i aluminijskih brodova zbog toga jer se izrada sastoji od izrade odljevka u kalupima. Odabrani proizvod brodogradilišta dijeli se na osnovne građevne dijelove: trup broda, konstrukcija ojačanja podvodnog dijela broda, glavna paluba, nadgrađe i vodonepropusne pregrade kako je prikazano slikom 4.

Nakon izrade osnovnih građevnih dijelova izrađuju se glavni segmenti brodske konstrukcije koji se transportiraju u narednu fazu procesa a to su:

- Glavni segment trupa koji se sastoji od odljevka trupa i konstrukcije ojačanja podvodnog dijela broda
- Glavni segment palube koji se sastoji od odljevka glavne palube i uzdužnih ojačanja

- Glavni segment nadgrađa koji se sastoji od odljevka nadgrađa sa sunčanom palubom koja je ojačana sa uzdužni ojačanjima.

Izrada opreme koja se ugrađuje u segmente broda i broda kao cjeline izrađuju se u stolarskoj, elektro i mehaničkoj radionici.

Prvi radovi opremanja na izrađenim segmentima su ugradnja instalacija:

- Elektroinstalacija
- Sustava goriva, hlađenja morskom vodom, pitke vode, sive i crnih voda
- Izgradnja tankova goriva, brodske ograde.
  Navedene instalacije se pripremaju prije ugradnje na segmente broda kako bi se olakšalo i ubrzalo opremanje brodskih segmenata.

Nakon procesa laminiranja u montažno – opremu halu dopremamo tri glavna segmenta:

- Trup sa ojačanjem podvodnog dijela
- Glavna paluba ojačana sa uzdužnjacima
- Nadgrađe sa sunčanom palubom ojačanom uzdužnjacima
  Proizvodni procesi koje izvodimo u montažno – opremnoj hali su:

- Uranjeno opremanje glavnih segmenata brodske konstrukcije
- Spajanje segmenata u cjelinu i to redom:
  o Nadgrađe sa glavnom palubom
  o Nadgrađe + glavna paluba sa trupom
- Finalno opremanje broda kao cjeline.
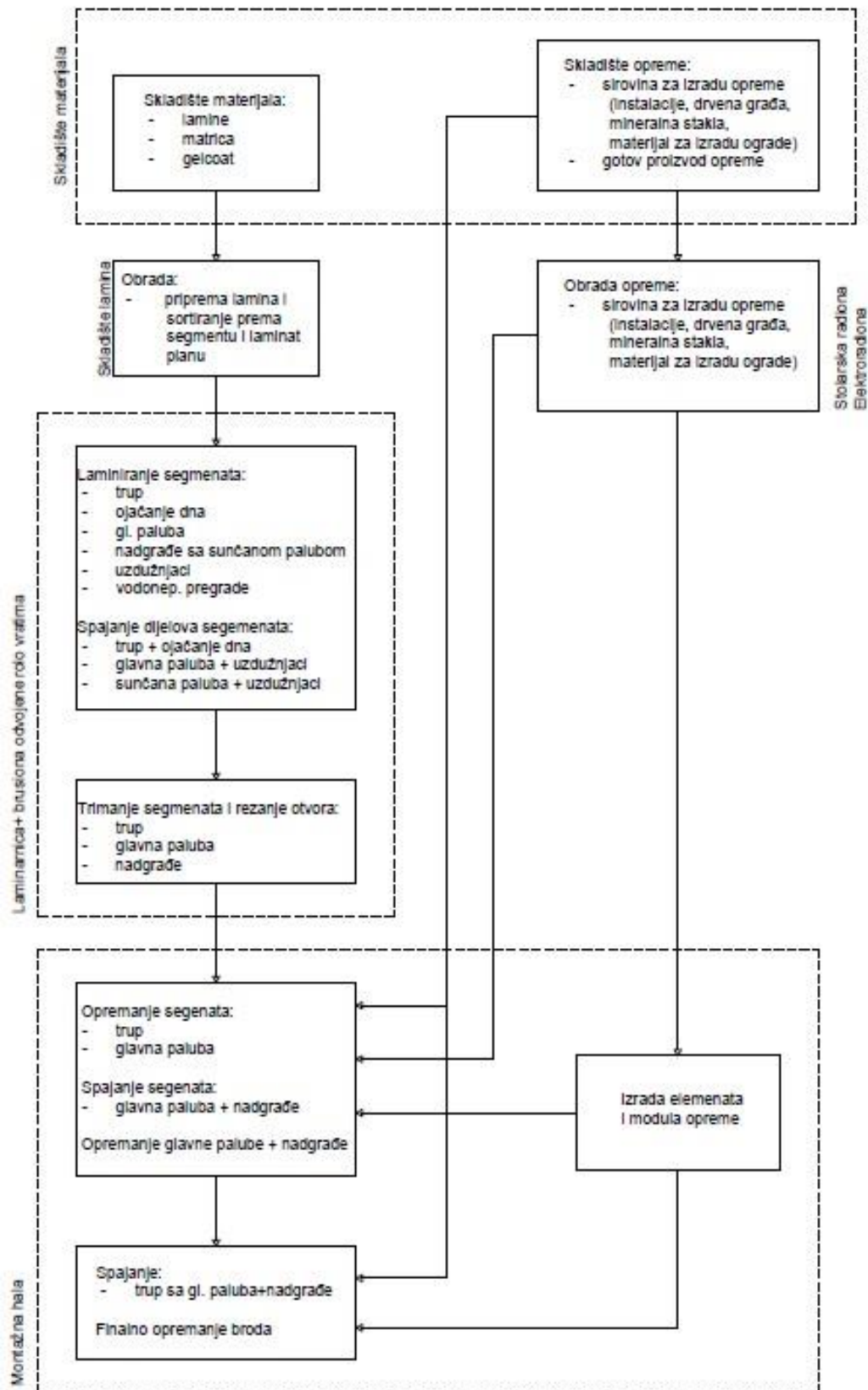
Figure 3 *Production process scheme*

Slika 3. Shema proizvodnog procesa brodogradilišta
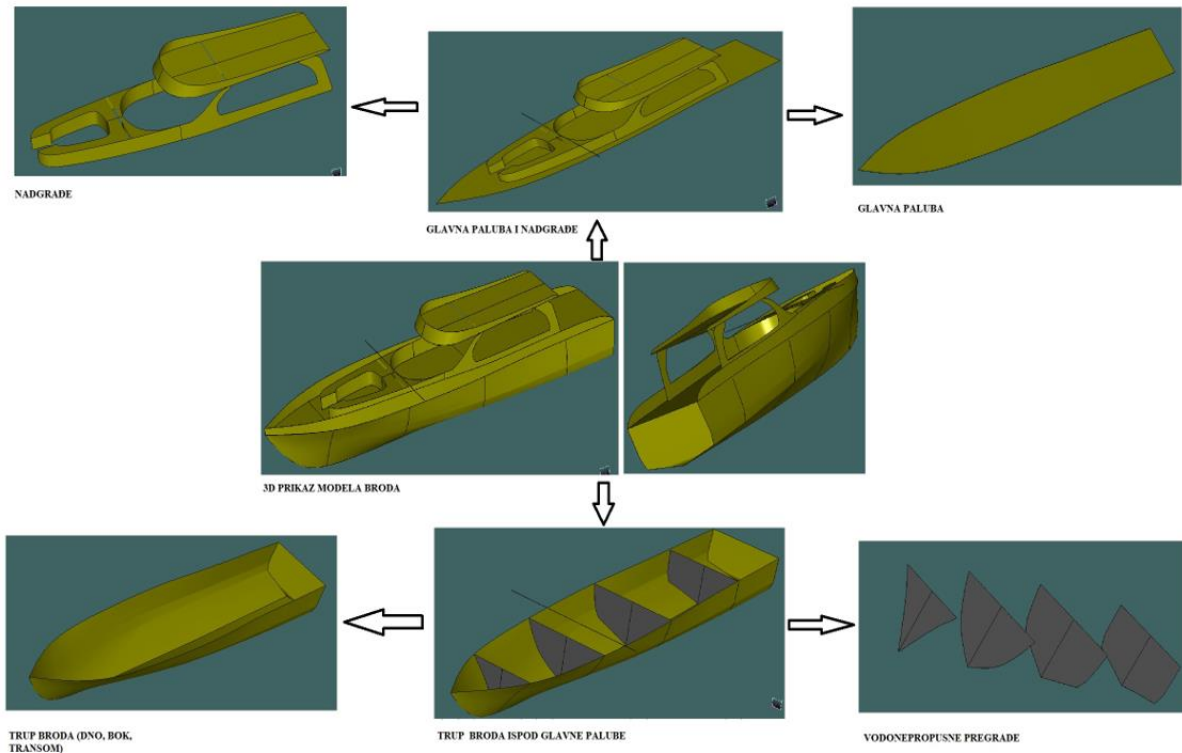
Figure 4 *Ship structure breakdown*
Slika 4. Podjela broda na osnovne građevne dijelove

4.4. *Dinamika gradnje karakterističnog broda*

Dinamika gradnje u idejnom projektu brodogradilišta definira se za karakteristični proizvod te prema prethodno definiranim tokovima prerade materijala. Podaci o potrebnom broju ljudi i vremenima za izvođenje svake faze proizvodnje su vezani za odabrani model i mogu poslužiti kao baza za seriju proizvodnje sličnog modela.

U svrhu određivanja dinamike gradnje potrebno je poznavati:

- Operacije za izvođenje svake faze radova
- Vremena izrade svih faza
- Potreban broj ljudi za njezinu realizaciju.

Prema operacijama za izvođenje svih faza radova može se odrediti potreban broj ljudi i potreban alat za izvođenje radova kao i oprema radionica. Potreban broj ljudi svake operacije određuje vrijeme trajanja operacije svih faza radova koje možemo podijeliti u 4 osnovne grupe:

- Pripremno-završno vrijeme (t_{pz}) koje je potrebno za pripremu radnog mjesta i uređenje nakon rada
- Pomoćno vrijeme (t_p) koje je potrebno za obavljanje pomoćnih poslova koji omogućuju da se izvedu tehnološke operacije izrade

- Tehnološko vrijeme (t_t) koje je potrebno za izvršavanje efektivnog rada, neovisno obavlja li se strojem ili ručno
- Dodatno vrijeme (t_d) koje služi za kompenzaciju gubitaka koje radnik ima u dan, a nije kriv za njih. [6]

Kod određivanja dinamike gradnje uzimaju se slijedeća ograničenja:
- Rad u 1. smjeni
- Izračunati radni dani su radni dani tjedna bez vikenda.

Na osnovi podataka iz razrađenih elemenata projektne spirale Analiza proizvoda i Prerada i tokovi materijala izrađene su tablice i gantogrami gradnje karakterističnog broda. Primjerom na slici 5. prikazan je gantogram izrade segmenata konstrukcije broda.
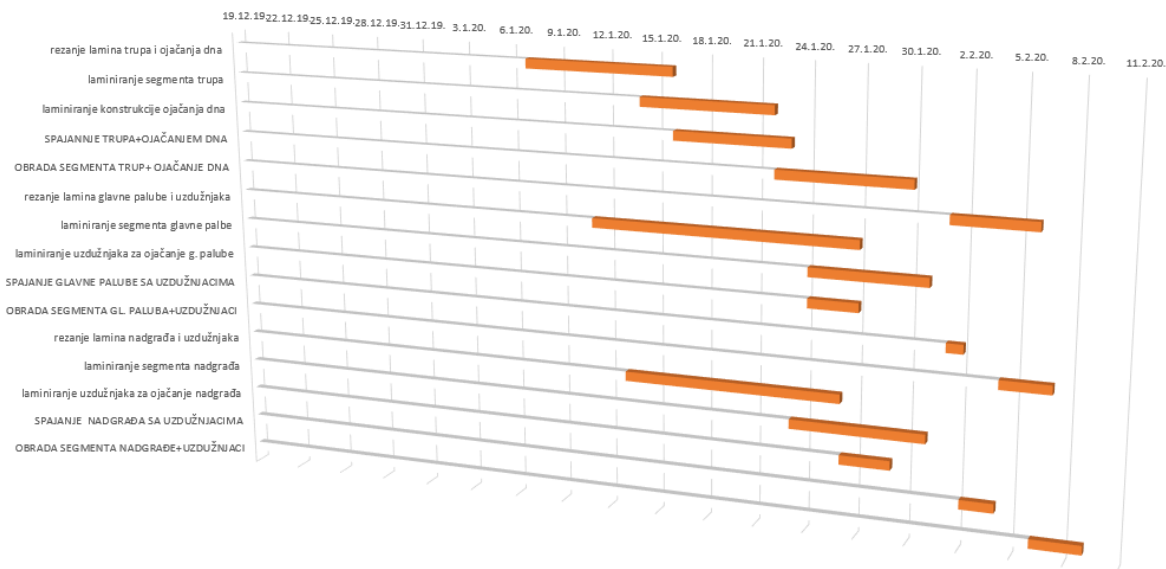
Figure 5 *Gantt chart of ship construction parts fabrication*
Slika 5. Gantogram izrade segmenata konstrukcije broda

U idejnom projektu brodogradilišta usvojeno je da je za fazu izrade segmenata kontrukcije broda treba 8 djelatnika plastičara i da za izradu segmenata konstrukcije trupa treba 34 radna dana.

Tablice i gantogrami su napravljeni i za fazu izrade opreme i za fazu montaže i opremanja trupa broda kako bi se mogao definirati godišnji kapacitet brodogradilišta. U ovim fazama potrebno je još 20 djelatnika čija struka je mehaničarska, stolarska, elektro i plastičarska.

U idejnom projektu usvaja se izrada 6 karakterističnih brodova godišnje.

4.5. Raspored radnih prostora

Prema prijedlogu lokacije brodogradilišta izvodi se razmještaj radnih prostora u cilju usvajanja tokova materijala bez povratnog hoda i presijecanja transportnih putova različitih tehnoloških faza.

Radni prostori su prilagođeni dimenzijama lokacije. Tako su radionice za izradu brodske konstrukcije izrađene sa uzdužnom podjelom u 3 lađe unutar kojih se izrađuju osnovni građevni dijelovi brodske konstrukcije za izradu glavnih segmenata broda.

Radionice za izradu opreme su odvojene od procesa izrade broda

U montažno – opremnoj hali se izvodi opremanje i spajanje broda u cjelinu. Ova radionica se nalazi u nastavku radnog prostora za izradu brodske konstrukcije kao bi se olakšao transport konstrukcije između pojedinih faza. Unutar montažno – opremne hale se nalazi prostor za skladištenje opreme koja se ugrađuje u fazama uranjenog ili finalnog opremanja broda.

Usvojenim razmještajem radnog prostora je izbjegnut povrati tok materijala i presijecanje transportnih putova različitih faza izrade brodske konstrukcije i opreme broda.

Na slici 6. prikazan je raspored radnih prostora i transportnih puteva brodogradilišta na odabranoj lokaciji.
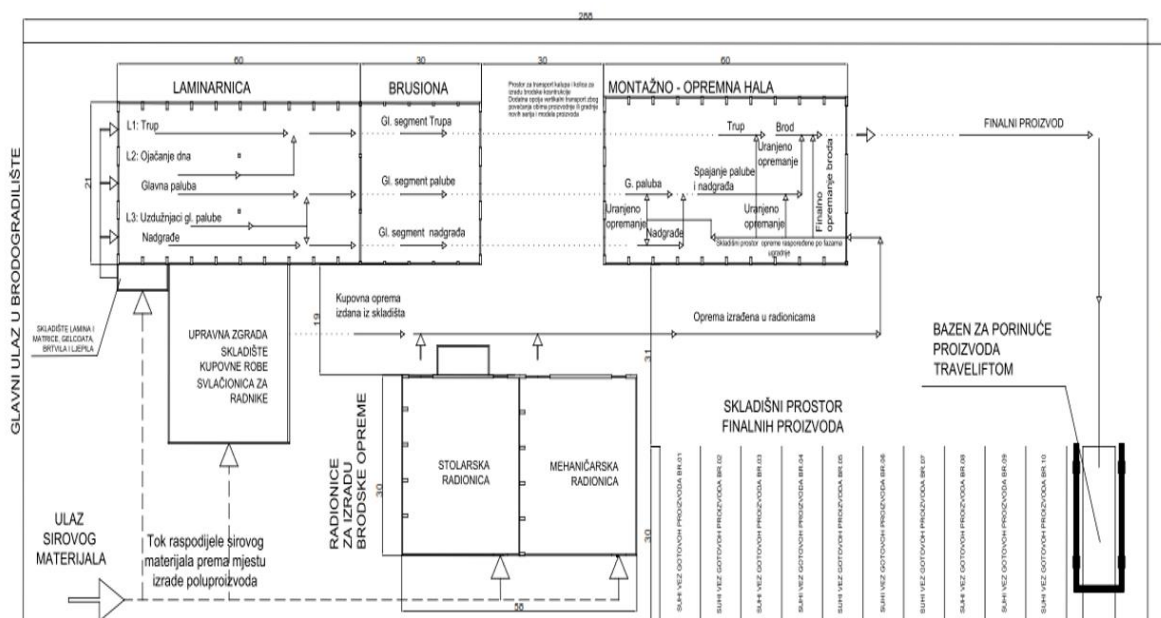
Figure 6 *Shipyard arrangement of working areas and material flows*
Slika 6. Raspored radnih prostora i tokovi materijala idejnog brodogradilišta

Idejnim projektom predviđen je prostor skladištenja gotovih proizvoda kao i prostor za porinuće traveliftom. Prostor za porinuće se može koristiti i za izvlačenje brodova koji dolaze na popravak u brodogradilište.

4.6. Investicije u idejnom projektu

Investicijske troškove idejnog brodogradilišta se sastoje od:

- Cijene zemljišta
- Građevinski radovi
- Tehnološka oprema .

Kod zemljišta važan parametar je vlasništvo, a prema toj strukturi model može biti kupnja zemljišta ili uzimanje lokacije u koncesiju na određeni period. U radu se nije razmatrao parametar vlasništva, pa se cijena nije uključivala u tablicu troškova.

Građevinski radovi uključuju:

- Betoniranje radnih prostora i transportnih putova
- Izrada i opremanje radionica i upravne zgrade
- Izgradnja bazena za porinuće broda
- Izgradnja tračnica mostnih dizalica duljine 150 m
- Provođenje energetskih instalacija.
  Tehnološka oprema uključuje sredstva rada i opremu radionica svih tehnoloških faza, a sastoji se od:

- Mostnih dizalica nosivosti 5t, raspona 27 m – 3 kom
- Mostna dizalica 75 t, raspona 30 m – 1 kom
- Transporter teških tereta Kalmar 18 – 52 t – 1 kom
- Travelift model 75BMFII nosivosti 75 t – 1 kom
- Strojevi i uređaji radionica za izradu brodske konstrukcije i opreme
- Energetska oprema brodogradilišta.

U tablici 1. su prikazane pretpostavljene vrijednosti investicijskih troškova prema gore navedenim grupama.

Table 1 Investment costs of the shipyard
Tablica 1. Investicijski troškovi idejnog brodogradilišta

OPIS TROŠKA		VRIJEDNOST
		[€]
GRAĐEVINSKI TROŠKOVI	Betoniranje radnih prostora i transportnih putova	1.000.000
	Energetske instalacije	400.000
	Tračnice mostnih dizalica dužine 150 m	150.000
	Izrada i opremanje laminarnice i brusione	3.000.000
	Izrada i opremanje montažno - opremne hale	1.000.000
	Izrada upravne zgrade	600.000
	Izgradnja bazena za porinuće finalnog proizvoda	2.000.000
TEHNOLOŠKA OPREMA	Mostna dizalica 5 t raspon 27 m, 3 kom	60.000
	Mostna dizalica -75 t raspon 30 m	200.000
	Transporter teških tereta Kalmar 75 t	200.000
	Travelift model 75BMFII nosivosti 75 t.	500.000
	Strojevi i uređaji radionica za izradu opreme i konstrukcije	2.000.000

Energetska oprema brodogradilišta	2.000.000
Kalupi za izradu segmenata brodske konstrukcije	120.000
∑ investicija [€]	**13.230.000**

5. Zaključak

Potencijal hrvatske obale sa preko 1.200 otoka te preko 5.000 km razvedene obale Hrvatskoj su osigurale vodeće mjesto kao *charter* destinacija sa preko 40% europskih rezervacija. Obzirom da se 10% hrvatskog turizma ostvaruje kroz nautički turizam u kojem Hrvatska ima veliki potencijal, kao glavna destinacija u Europi, te današnji trendovi tržišta za brodovima dužim od 20 m zbog što veće udobnosti i što veće opremljenosti broda u svrhu sporta, rekreacije i užitka stvaraju potrebu za gradnjom novih, većih i luksuznijih jahti za nautički turizam.

Analiza tržišta brodova za nautički turizam uzima u obzir i starost brodova postojeće flote. I prema tom kriteriju vidi se da mala brodogradnja ima veliki potencijal i može biti od velikog značaja za gospodarstvo Republike Hrvatske te bi se trebala smatrati strateškom gospodarskom granom.

Hrvatsko tržište brodova uz brodograditelje dijele i proizvođači opreme i materijala za gradnju broda koja je ovisan o uvozu. Čak se 90 % opreme i materijala za izradu kompozitnih brodova uvozi što doprinosi razvoju malog i srednjeg poduzetništva u funkciji razvoja nautičkog turizma i male brodogradnje.

Prema navedenom Republici Hrvatskoj nedostaju proizvodno – razvojni nautički centri koji bi mogli zadovoljiti potrebe tržišta i privući strana ulaganja. U sklopu takvog centra bi se proizvodili brodovi duljine 20 – 30 m od kompozitnog materijala i dodatno pružati usluge remonta i servisa jahti za nautički turizam.

Projektiranje brodograđevnog procesa je iterativni postupak koji se provodi u nekoliko koraka prema projektnoj spirali. Prvi krug projektne spirale predstavlja upoznavanje sa elementima spirale i postavljanje zahtjeva za osnivanjem brodogradilišta, dok se 2. ili 3. krugom ostvaruju poboljšanja s tim da je nemoguće postići maksimum svakog elementa.

Jedan od važnijih elemenata je analiza proizvoda koji je rezultat analiza tržišta brodova. Usvojeno je osnivanje motorne jahte duljine 24 m sa kompozitnim materijalom ojačan karbonskim vlaknima.

Procijenjeni troškovi granje jednog takvog brodogradilišta uključuju investicijske troškove i troškove gradnje broda te iznose 13.230.000 €. Prema usvojenom rasporedu prostora te dinamici gradnje godišnji kapacitet brodogradilišta iznosi 6 proizvedenih jedinica finalnog proizvoda na kojem je angažiran 51 zaposleni prema slijedećem rasporedu:

- 36 radnika u proizvodnji
- 15 radnika u pripremi.

Navedeni broj radnika je angažiran samo na procesu novogradnji, dok bi se uvođenjem remonta i servisa broj radnika dodatno povećao.

REFERENCES

[1]   'Engineering, production and life – cycle managment for the complete construction of large lenght fibre base', EU Horizon 2020 research and innovation programme, http://www.fibreship.eu/, 2019.

[2]   'Marine Composite Market', www.reportsanddata.com/report-detail/marine-composite-market , 2019.

[3]   'Azimut Yachts - Magellano Collection 2017 – 2018', https://www.azimutyachts.com/ , 2018.

[4]   Ljubenkov B., Mihailović M., Sladoljev Ž., Zaplatić T., Žiha K..: 'Konceptualni projekt brodogradilišta na Dunavu', Zbornik radova simpozija SORTA2010, Split/Lumbarda/Korčula, 2010.

[5]   Lasan J.: 'Idejni projekt brodogradilišta kompozitnih brodova', diplomski rad, FESB, Split, 2020.

[6]   Taboršak D.: 'Studij rada', Zagreb, 1966.

An efficient method to identify bottlenecks of the ship production process: serial lines

Viktor Ložar*, Neven Hadžić, Tihomir Opetuk, Filip Abdulaj

University of Zagreb/Faculty of Mechanical Engineering and Naval Architecture, Ivana Lučića 5, 10000Zagreb
* Corresponding Author, viktor.lozar@fsb.hr

Abstract

The ship production process involves numerous different technology treatments that are usually assembled in serial or assembly production lines affecting the shipyard's productivity level significantly. Therefore, the analysis of the production system and its design for lean production including bottlenecks identification is of great importance. An efficient method to identify bottlenecks is presented in this paper providing a shipyard's management with basic tools to meet this challenging shipyard's floor issue. The PSEToolbox software is using the semi-analytical approach to calculate the machine blockage and starvation probabilities. Useful conclusions affecting production lines' maintenance policy are presented.

Key words: Ship production; Production system engineering; Serial lines; Bottlenecks; Lean production

Sažetak
Brodograđevni proizvodni process obuhvaća velik broj različitih tehnoloških postupaka, uobičajeno objedinjenih u sklopu serijskih proizvodnig linija ili linija okrupnjavanja čija proizvodnost ima značajan utjecaj na uspješan rad cjelokupnog brodogradilišta. Stoga su analiza i projektiranje za vitku proizvodnju, uključujući identifikaciju uskih grla, iznimno važni. Ovim je radom predstavljena metoda identifikacije uskih grla kao osnovni alat i temelj razvoja vitke proizvodnje u brodogradnji. Primjenjen je polu-analitički pristup upotrebom programa PSEToolbox pomoću kojeg su određene vjerojatnosti blokade i praznog hoda strojeva. Također, prikazani su i zaključci istraživanja kako bi se omogućilo unapređenje sustava održavanja proizvodnih linija u brodogradilištu.

Ključne riječi: Brodograđevni proizvodni proces; Proizvodno inženjerstvo; Serijske linije; Uska grla; Vitka proizvodnja

1. Introduction

Analysis and design of the shipbuilding production process are almost completely omitted in the current research literature. In some cases, it is only considered as a source of constraints during the ship design phase, [1]. But there are exceptions as shown in the paper, [2]. The authors explain a control mechanism for the US Shipbuilding industry based on Markov Decision Processes. There are also affords, [3], to provide producibility information in the early stages of designing panel structures that are built in the ship hull. Some affords are made to optimate the logistic operations on a shipyard, [4], using a heuristic algorithm and virtual nodes. Developing a simulation model for shipyards is quite a problem because it requires professional skills and experience, [5].

In other industries, it is more convenient, [6], to design the manufacturing processes. Such an approach makes it possible to analyze witch machines could be switched off to achieve energy consumption without losing on manufacturing performance, [7]. There are researches and measurements about the environmental impacts of the shipyard workshops, [8]. A model for the major pollution sources identification in a shipyard was created.

Analytical models are traditionally the basic approach because their application makes it possible to identify the associated physical and mathematical basics of a problem. That is the reason why they are used as a reference scale to check the reliability of complex numerical models. However, until recently, analytic solvation of general Bernoulli production lines (arbitrary number of machines and buffer with arbitrary capacity) was unknown because of the complexity of the problem. Further, two different approaches will be mentioned: the analytical approach and the semi-analytical approach.

The analytical solution for the easiest problem of a steady response series Bernoulli production line with two machines and one buffer was published 1962. The analytical solution is solved by integral equations, [9]. However, until recently analytic solvation of general Bernoulli production lines (arbitrary number of machines and buffer with arbitrary capacity) was unknown because of the complexity of the problem.

The main reason for that is the problematical formulation of the transition matrix which is known just for a narrow band of problems, for lines with two and three machines were the probability of failure for all machines is the same. The problem is finally solved recently, [10], using the concept of a generalized transition matrix which gives the analytical solution to the problem in a simple way. The problems of the steady and transient response of a general Bernoulli production line can be solved by applying the eigenvalue problem with the assumption that the transition matrix is formulated correctly, [11]. The paper, [12], intended to develop systematic analytical methods for evaluation, analysis, and control of the system's continuous random variables.

The development of semi-analytical models was motivated by the complexity and leak of analytical formulations. In the paper, [13], the aggregation approach is used to simulate the setup time of a manufacturing line. One of the main objectives of the semi-analytical models is the relatively short processor time that makes this approach very attractive, especially in designing and optimization of the production systems. The aggregation calculation of a line production rate, [14], which is used in medium-sized systems with three to five machine lines tries to reduce energy consumption. For perishable products the demands on the machine lines are high, [15], the authors tried to explain the behavior and properties of such systems using an aggregation-based procedure. In the paper, [16], the problems of validation of the semi-analytical approach are highlighted and validation studies are based on extensive simulations. Indeed, such an approach was the only solution in the matter of complete absence of the analytical solution

2. The analytic approach

For the analytic approach, the Bernoulli line with two machines and one buffer is the simplest case. The Bernoulli random variable has a sample space of 0 and 1. This makes it easy to describe the machine state up or machine down.
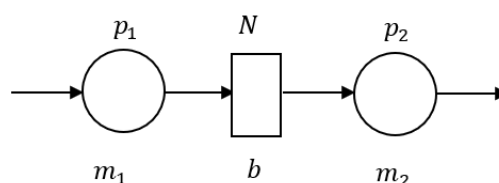
Figure 9 Two-machine Bernoulli production line, [17]
Slika 10 Bernoullieva linija sa dva stroja, [17]

The Bernoulli line needs the following conventions to be fulfilled, [17]:

- o blocked before service,
- o the first machine is never starved; the last machine is never blocked,
- o the status of the machines is determined at the beginning and the state of the buffer at the end of each time slot,
- o each machine status is determined independently from the other,
- o time-dependent failures.

2.1. State transition diagram for a system with one buffer

The state transition diagram shows all the buffer conditions of the Bernoulli production line with one buffer and two machines. The connections between each buffer condition called trajectories. Each trajectory relates to a value called transition probability which describes the probability of changing the buffer condition. The transition probability depends on the conditional probability of the machines (machine up or machine down). Each buffer condition depends on three different transition probabilities except the start and the finite status which depends on two transition probabilities (for a system with one buffer).

Such a state transition diagram can be shown in a matrix called the transition matrix, which summarizes the characteristics of the machines and the buffer. In such a matrix the sum of the three different probabilities must be one because the probability for all changes which can be achieved is one.
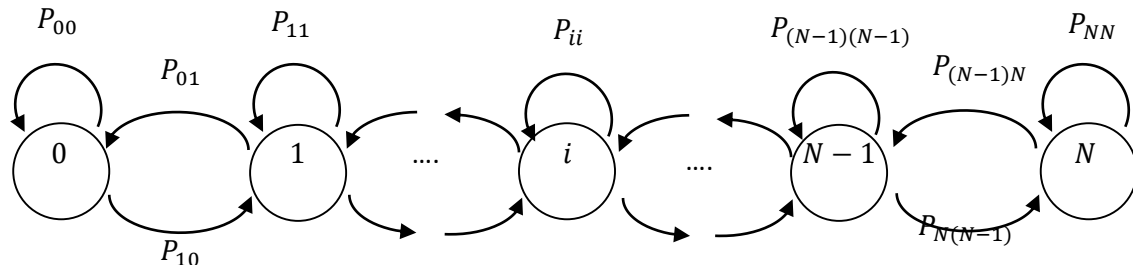
Figure 2 Transition diagram of two-machine Bernoulli production line, [17]
Slika 2 Tranzicijski dijagram Bernoullijeve linije s dva stroja, [17]

In a steady-state environment, the probability for each buffer condition will not change after a time circle n+1. In such circumstances, the transition matrix can be multiplied with the buffer conditional vector and the result will be the same buffer conditional vector. Following some mathematical operations, it is possible to define each state of the buffer conditional vector. If the buffer capacity counts 5 and the machine probabilities are different, 5 different probabilities describe the buffer occupancy.

3. The aggregation approach

The analytical approach was until 2019, [10], reserved only, for lines with two and three machines were the probability of failure for all machines was the same. The author of the book [17] claimed that it is impossible and even unnecessary to solve this multimachine and buffer problem

analytically, because of the problematical formulation of the transition matrix. That was the reason why the aggregation approach was the only way to calculate the buffer probability for lines with more than one buffer and two machines.

The aggregation approach consists of a backward aggregation, forward aggregation, and iteration of both aggregations.
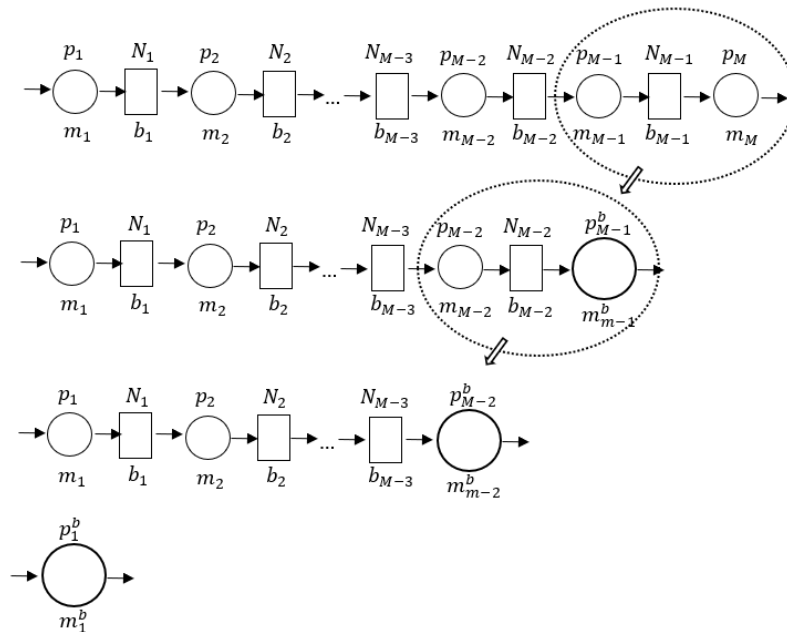
Figure 3 Backward aggregation, [17]
Slika 3 Agregacija u nazad, [17]

During the backward aggregation (see Figure 3) take the last two machines and the buffer between them and substitute this composition into a machine denoted as m_{M-1}^b, where b describes backward aggregation. The probability of this machine p_{M-1}^b is calculated as the production rate of this aggregated two machine-single buffer line. Now repeat this substitution until the whole line is aggregated into one machine p_1^b. When the backward aggregation is finished, the forward aggregation can start.
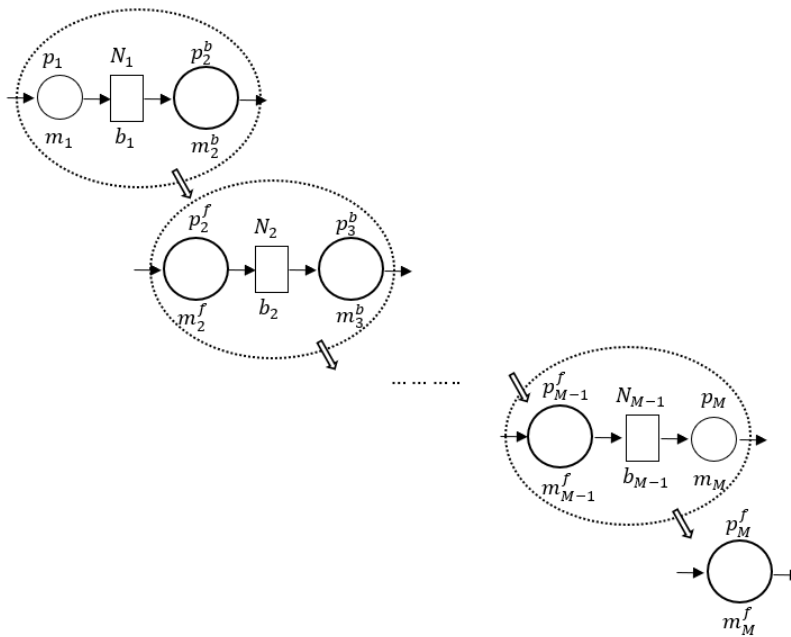
Figure 4 Forward aggregation, [17]
Slika 4 Agregacija prema naprijed, [17]

The start of the forward aggregation begins by creating the machine m_2^f which is built up of the first machine, first buffer and the aggregated rest of the line. The probability of this machine is calculated as the production rate of this aggregated two machine-single buffer line. At the end of the forward aggregation, there will be one machine, built up of the before forward-aggregated machine, the last buffer and the last machine of the line. Took the results out of the forward and backward aggregation and start with these values a new cycle of forward and backward aggregation after three to four cycles the values will not change anymore.

Using these results the following equations (1) – (5) can be used to calculate the PR Production Rate, PR, Work in Process, WIP, Blockages, BL, Starvations, ST, and the Residence time, RT.

$$PR = p_1^b = p_M^f \tag{1}$$

$$PR = p_{i+1}^b\left[1 - Q\left(p_i^f, p_{i+1}^b, N_i\right)\right]$$

$$PR = p_i^f\left[1 - Q\left(p_{i+1}^b, p_i^f, N_i\right)\right] \qquad i = 1, \dots, M-1.$$

$$WIP = \begin{cases} \dfrac{p_i^f}{p_{i+1}^b - p_i^f \alpha^{N_i}\left(p_i^f, p_{i+1}^b\right)}\left[\dfrac{1 - \alpha^{N_i}\left(p_i^f, p_{i+1}^b\right)}{1 - \alpha\left(p_i^f, p_{i+1}^b\right)} - N_i \alpha^{N_i}\left(p_i^f, p_{i+1}^b\right)\right] & \text{if } p_i^f \neq p_{i+1}^b \\ \dfrac{N_i(N_i+1)}{2\left(N_i+1-p_i^f\right)} & \text{if } p_i^f = p_{i+1}^b \end{cases} \tag{2}$$

$$BL_i = p_i Q\left(p_{i+1}^b, p_i^f, N_i\right) \qquad i = 1, \dots, M-1. \tag{3}$$

475

$$ST_i = p_i Q\left(p_{i+1}^b, p_i^f, N_i\right) \qquad\qquad i = 2, \ldots., M. \tag{4}$$

$$RT = \frac{WIP}{PR} \tag{5}$$

PR defines the average number of parts that are produced by the last machine. The WIP defines the average number of parts contained in all in process buffers. The BL defines the probability of a blocked machine. This case happens when the machine in front of the blocked one is up, the buffer in front of it is full and the machine after the blocked machine did not take an object. The ST parameter defines the probability when a machine is running out of parts. This case happens when the machine is up but the buffer in front of the machine is empty. The residence time RT can be calculated out of the WIP and PR. In some literature, it is called flow time or system cycle time.

4. Bottlenecks

The Bottleneck can be a buffer or a machine in a production line. The Bottleneck machine has not necessarily the smallest probability. The machine which has the biggest increase in the production rate during the smallest improvement is the bottleneck machine (6).

$$\frac{\partial PR}{\partial p_i} > \frac{\partial PR}{\partial p_j} \tag{6}$$

This definition is just a formal one but has no practical impact because the partial derivation is impossible to measure and to calculate, [17]. That's the reason why the definition is reformulated by the terms BL and ST.

The Bottleneck buffer is the one that has the greatest increase in the production rate during the increase of the buffer capacity by 1. This definition is also not very practical and replaced by using the BL and ST parameters.

The following arrow rule helps to define the Bottleneck machine using BL and ST: If $BL_i > ST_{i+1}$ draw an arrow from m_i to m_{i+1}; If $BL_i < ST_{i+1}$ draw an arrow from m_{i+1} to m_i. The machine in which are pointed two arrows is the Bottleneck machine. According to that rule, the buffer behind or before the Bottleneck machine is the Bottleneck buffer.

5. Illustrative example

During the shipbuilding process, there are various operations like cutting bending, welding, etc. which can be described by serial lines. The prefabrication line is a typical shipbuilding serial process. Four machines are involved in that process which ensures the flattening, drying, blasting, preserving and marking operation. Each machine has a declared capacity and an operational capacity, the ratio between these capacities describe the operational probability. The space between the machines defines the buffer capacities, see figure 5.

The PSE toolbox uses the aggregation approach to calculate the starvations, blockages and work in processes.
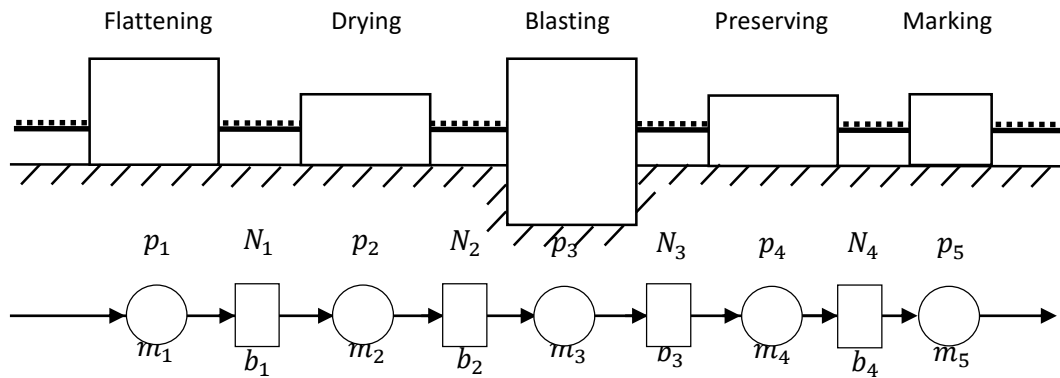
Figure 5 Plate prefabrication line and mathematical model, [10]
Slika 5 Linije predobrade limova i matematički model, [10]

Table 2 Prefabrication line – declared and operative machine capacities, [10]

Table 11 Linija predobrade – deklarirani i operativni kapaciteti strojeva, [10]

Operation	Flattening	Drying	Blasting	Preserving	Marking
Declaration[a]	2 plates/h	280 m^2/h	185 m^2/h	400 m^2/h	4 plates/h
Declared capacity, [plate/h][b]	2	3.88	2.6	5.55	4
Operative capacity, [plate/h]	1.8	3.54	2.3	4.45	3.82
Probability, p	0.9	0.912	0.885	0.801	0.955

[a] (Hadžić, Tomić, and Matić 2016)

[b] for plate dimension 12x3m

Table 2 Prefabrication line – buffer capacities, [10]

Table 2 Linija predobrade –kapaciteti skladišta, [10]

Buffer	1	2	3	4
Length, [m][a]	20	25	20	25
N[b]	1	2	1	2

[a] (Hadžić 2018).

[b] for plate dimension 12x3m
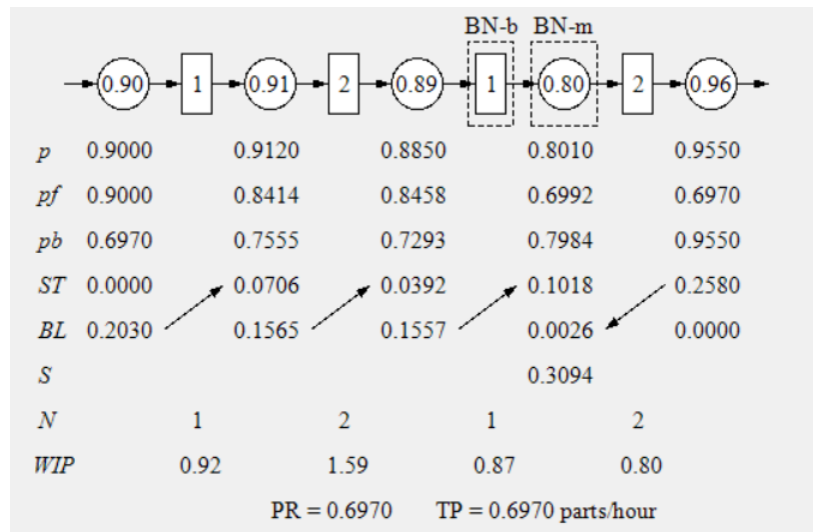
Figure 6 PSE Toolbox – calculation
Slika 6 PSE alat – proračun

In the shown example possible bottlenecks are the third buffer and the fourth machine as the analysis shows.

6. Conclusion

The identification of Bottlenecks in a production line demands strong mathematical Models as it is presented in this short review. Using such an approach makes the production process much more transparent than it is today. The planner has the opportunity to predict where the production line is week and where could be potential bottlenecks. Without knowing the behavior of a production line, it is difficult to optimize in the right direction. These are basic conditions to get a real lean production.

REFERENCES

[1] Žanić, V, Andrić, J, Hadžić, N. (2015.) Optimization procedure for liquid natural gas carrier structural design, Proceedings of the Institution of Mechanical Engineers. Part M: *Journal of Engineering for the Maritime Environment*, 229, 1; 14-35.

[2] Dong, F., Van Oyen, M. P., & Singer, D. J. (2014). Dynamic control of the N queueing network with application to shipbuilding. *International Journal of Production Research, 52*(4), 967–984.

[3] Rigterink, D., M. Collette, and D. J. Singer. (2013.) A Method for Comparing Panel Complexity to Traditional Material and Production Cost Estimating Techniques. *Ocean Engineering* 70: 61–71.

[4]   C. Wang, Y.-S. Mao, B.-Q. Hu, Z.-J. Deng, and J. G. Shin. (2016) Ship block transportation scheduling problem based on greedy algorithm. *Journal of Engineering Science and Technology Review*, vol. 9, no. 2, pp. 93–98

[5]   Myung-Gi Back, Dong-Kun Lee, Jong-Gye Shin, Jong-Hoon Woo (2016.) A study for production simulation model generation system based on data model at a shipyard. *International Journal of Naval Architecture and Ocean Engineering*, Volume 8, Issue 5, 496-510.

[6]   Wang, Z., & Gershwin, S. B. (2015). Heuristic production and sale policy for a two-product-type manufacturing system with downward substitution. *IEEE Transactions on Systems, Man, and Cybernetics: Systems, 45*(6), 929–942.

[7]   Jia, Z., Zhang, L., Arinez, J., & Xiao, G. (2016c). Performance analysis for serial production lines with Bernoulli Machines and Real-time WIP-based Machine switch-on/off control. *International Journal of Production Research, 54*(21), 6285–6301.

[8]   Wei Zhou, Jun Wang, and Xiao Zhu (2019.) Research on Environmental Assessment Model of Shipyard Workshop Based on Green Manufacturing. *Journal of Coastal Research* 94, 16-20.

[9]   Sevast'yanov BA (1962.) Influence of Storage Bin Capacity on the Average Standstill Time of Production Line, *Theory of Probability Applications*, 429-438.

[10]   Hadžić, N. (2018a) Analytical solution of the serial Bernoulli production line steady-state performance and its application in the shipbuilding process, *International Journal of Production Research*, 56, 12; 1, 14.

[11]   Hadžić N i Tomić M (2017.) Analytical solution of steady-state behaviour of Bernoulli production line with two finite buffers, *Brodogradnja/Shipbuilding*, 68(3), 85-102.

[12]   Meerkov, S. M., & Yan, C. (2016). Production lead time in serial lines: Evaluation, analysis, and control. *IEEE Transactions on Automation Science and Engineering, 13*(2), 663–675.

[13]   Zhao, C., Li, J., Huang, N., & Horst, J. (2017). Flexible lines with setups: analysis, improvement, and application. *IEEE Robotics and Automation Letters*, 2(1), 120–127.

[14]   Su, W., Xie, X., Li, J., Zheng, L., & Feng, S. C. (2017). Reducing energy consumption in serial production lines with Bernoulli reliability machines. *International Journal of Production Research, 55*(24), 7356–7379.

[15]   Naebulharam, R., & Zhang, L. (2014). Bernoulli serial lines with deteriorating product quality: Performance evaluation and system-theoretic properties. *International Journal of Production Research, 52*(5), 1479–1494.

[16]   Zhao C and Li J (2014.) Analysis and improvement of multi-product assembly systems: an application study at a furniture manufacturing plant. *International Journal of Production Research* 52(21), 6399-6413.

[17]   Li J i Meerkov SM (2009.) Production System Engineering, Springer, New York.

Advanced Methodologies for Cost-Effective, Energy Efficient and Environmentally Friendly Ship Production Process Design

Neven Hadžić*, Viktor Ložar, Tihomir Opetuk

University of Zagreb/Faculty of Mechanical Engineering and Naval Architecture, Ivana Lučića 5, 10000Zagreb
* Corresponding Author, neven.hadzic@fsb.hr

Abstract

A significant impact on the economy and the environment can be achieved if the shipbuilding production process, as the shipyard's core business, is considered as designable, changeable and adaptable. The design of a profitable manufacturing process involves the development and application of the process planning methodologies and a detailed production cost model as key tasks. The first approach requires the development of analytical and numerical procedures, while the latter involves the development of detailed and parametric models of production costs. Knowledge of the basic theoretical and practical characteristics of the process will enable the development and implementation of the green shipbuilding concept as well as the evaluation of the environmental impact of the shipbuilding industry. The basic aspects of this approach to shipbuilding are presented in more detail in this paper.

Key words: Ship production; Production system engineering; Cost-effectiveness, Energy efficiency, Environmental friendliness

Sažetak

Značajan utjecaj na gospodarstvo i okoliš može se postići ako se brodograđevni proizvodni proces, kao osnovna djelatnost brodogradilišta, razmotri kao projektabilan, promjenjiv i prilagodljiv. Projektiranje profitabilnog proizvodnog procesa podrazumijeva razvoj i primjenu metodologija planiranja procesa i detaljnog modela troškova proizvodnje kao ključnih zadataka. Prvi pristup zahtijeva razvoj analitičkih i numeričkih postupaka, dok potonji obuhvaća razvoj detaljnog i parametarskog modela proizvodnih troškova. Poznavanje temeljnih teoretskih i praktičnih karakteristika procesa omogućit će razvoj i implementaciju koncepta zelene brodogradnje kao i evaluaciju utjecaja brodograđevne djelatnosti na okoliš. Osnovni aspekti spomenutog pristupa brodogradnji prikazani su detaljnije u ovom radu.

Ključne riječi: *Brodograđevni proizvodni proces; Proizvodno inženjerstvo; Profitabilnost, Energetska efikasnost, Okolišna prihvatljivost*

1. Introduction

Major state of the art research and development efforts related to the naval architecture scientific community, as well as allocated financial resources, are traditionally focused to the enhancement of ship design methodologies considering aspects like ship hydrodynamics, structural design, ship vibrations, and marine engineering with the final goals like reduction of fuel consumption, structural reliability, marine system integrity and environmental acceptability, [1]. Unfortunately, the ship production process is usually taken for granted or is sometimes considered as a source of constraints during the ship's structural design stage, [2]. However, a significant impact on the economy and environment can be achieved if the ship production process, as the shipyards core business, is considered as designable, changeable and adoptable, [3]. Therefore, the development and application of the advanced methodologies of the ship production process including cost-effectiveness, energy efficiency, and environmental friendliness should be the main objectives of future ship production research.

2. Cost-effectiveness

The ship production process is known to be a perplexed, long-lasting and demanding production activity involved in numerous and complex space-time interactions with the final goal of generating financial benefits, [4, 5]. Both space and time attributes are distinctive as stochastic variables significantly influencing shipyard productivity, the work organization and finally competitiveness level within harsh global market demands. Moreover, the ship production process is constantly influenced by numerous daily factory floor uncertainties like raw material and equipment supply, production equipment failures, unexpected repairs and reworks, available storage and production area, available personnel, etc. It is, therefore, inevitable to apply advanced and rational management of complex space-time interactions ensuring duly and cost-effectively accomplishment of contracted appointments, [6, 7]. Otherwise, the financial benefit could be seriously jeopardized. Consequently, the shipyard's productivity level significantly influences its cost-effectiveness.

The development and implementation of production process scheduling methodologies is a critical task which, due to its extreme complexity, cannot be accomplished without the aid of software tools, [8]. This problem is in the focus of Production System Engineering (PSE). According to the existing PSE research body, mathematical modeling of production processes can be carried out using three different approaches, namely analytical, semi-analytical and numerical. Each of them differs concerning the theoretical background, modeling complexity, CPU (Central Processing Unit) costs and accuracy that should be verified using factory floor data.

Analytical models are usually considered as the most important ones, as their application enables identification of the basic physical and mathematical principles governing the problem. Consequently, the analytical approach is often used as a benchmark providing reliability of more complex numerical models. In such a context production system transitions from one to another state can be mathematically described using discrete, continuous or mixed stochastic processes, depending on the system properties. In the case of ship production, a discrete stochastic process approach can readily be applied for it is distinctive by discrete values of buffering capacities. Moreover, the modern ship production process strives towards a synchronous one with a machine downtime relatively close to the cycle time enabling in such a way the application of Bernoulli machine reliability model or the concept of Bernoulli production lines. The problem analytical approach was solved recently, [5], following a new concept of the generalized transition matrix formulation resulting in a closed-form analytical solution. Assuming the proper formulation of the transition matrix, problems of the steady-state and transient response in the case of the general Bernoulli production line can be solved quite straightforwardly as eigenvalue problem, [9].

The development of semi-analytical models was principally motivated by the problem complexity. The ground-breaking contribution in this sense was the research on asymptotic analysis techniques for the modified serial production line model, known as the aggregation procedure, [10]. Further system-theoretic properties of semi-analytical models were investigated and presented in, [11], while bottlenecks identification based on the aggregation procedure was developed in, [12]. The following research was focused on production system transient response analysis using the second largest transition matrix eigenvalue, [13]. One of the most important features attributed to semi-analytical models is the relatively low CPU cost that makes their application attractive, especially in the case of the production system design and optimization. However, a problem of the aggregation procedure validation remained open and complete research on this topic was never reported. The sole example of aggregation procedure validation using an analytical solution is

presented in, [14], only in the case of one selected system state-space point. The problem of semi-analytical models' validation is also reported in [15] and [16] where benchmark studies based on extensive simulations were presented. Indeed, in the context of analytical solution scarcity, such an approach was the only possibility.

The numerical approach to the problem remained the most preferred one. Although computationally most demanding and rather time-consuming, it attracted the attention of many researchers developing different methodologies and procedures capable of capturing most of the PSE phenomena, [17]. However, numerical investigation of the ship production process remained quite sparse with demanding observability of the output data.

Simulation of shipbuilding operation using a ProModel commercial simulator was used to evaluate the workflow scheduling and its impact on the additional project including constraints and conflicts between competing jobs, [18]. More specific ship production process analysis using Discrete Event Simulation (DES), [19], was applied in case of the shipyard metal processing facility, where difficulties regarding model input data (workshop geometry, machine properties, buffering capacities and business rules) and steep learning curve were discussed. Unfortunately, no measurable or comparable data on this topic was reported. More general and 'business style' shipyard model was formatted later using SimYard software, [8], which is evaluated repeatedly to obtain the best possible production schedule concerning total production expenses. As in the previous case, no measurable or comparable data was reported in this research. Further application of ship production process numerical analysis considered modeling of the entire workshop using program Taylor ED based on the atomized representation of the workshop layout, [6]. This research considered the deterministic response of the modeled process to a selected production program in cases of two different scenarios. DES analysis of the robotized profile cutting line was considered in [20] using eM-Plant software including bottleneck analysis and process optimization using simultaneous modifications of the crane and cutting line properties.

Further research and development of the ship production process analysis and design techniques between 2009 and 2017 were mainly driven by the large data handling approach using different kinds of data managing models like advanced planning systems, business process management, and panel block handling taking into account the uncertain operational environment, [21]. This research, although representative, has some drawbacks, i.e. the presented results cannot be easily measured and verified on the factory floor or reproduced using different software packages. Moreover, the mentioned methodologies are rather time-consuming, complex and rely on modeling performed by an experienced specialist.

Each approach to the production system modeling, i.e. analytical, semi-analytical and numerical model, requires verification using shipyard floor measurement as the most important and irreplaceable bench-mark of the production process mathematical modeling development and application. Unfortunately, none of the above-referred research papers considers this topic systematically. Presently, only the semi-analytical approach to the problem is verified using extensive simulations, [15, 16].

Besides productivity, production cost modeling is another fundamental aspect of the cost-effective production process design. Its formulation is in close relation to shipyard's floor data and daily production activities. Two fundamentally different approaches to production cost modeling can be identified in the existing literature body. The first one considers the production costs form top-

down perspective using empirical relationships between general (high level) product properties and related costs as a means to estimate a new ship cost. The second or bottom-up, approach to the problem breaks down the production project into construction units and elements to estimate costs using detailed engineering analysis of the considered production activities like cutting, welding, forming, surface protection, assembling, outfitting, etc. Consequently, the latter approach requires substantially more effort in conducting direct calculations as well as a winder and a more trustworthy data basis as compared to the top-down approach, [22, 23].

Typical applications of the top-down approach are usually related to the definition of the ship's price during initial negotiations and contract assignments. However, the real production cost may be underestimated seriously affecting the shipyard's financial benefit. On the other side, to large the estimates will potentially lower the shipyard's competitiveness level. It is, therefore, inevitable to verify them against more detailed models and shipyard's floor data, [24]. Unfortunately, the present research body provides only different formulations of the top-down approach while their verification is kept inside the chief designer's 'little black book'. The bottom-up approach to ship production cost analysis is rarely addressed in the literature. Presently the only sophisticated approach considers cost structure breakdown to work preparation, cutting, forming, welding, assembling and transport using a parametric approach to the problem while estimating the interim products' properties effects to the production costs, [25]. It does not provide means to e.g. relate energy consumption or depreciation costs with the ship construction units' properties.

3. Energy efficiency

The study on energy consumption and energy efficiency recently gained extensive research interest in the general manufacturing research community including studies focused on energy consumption monitoring, modeling and evaluation as well as production parameter optimization. Some of the governing conclusions point to relatively low-level energy consumption efficiency (even below 15%) and consequently substantial energy saving potential, [26]. A current global framework for energy-efficient manufacturing is defined by the United Nations policies for environment-friendly industry and greener industrial footprint initiative, [27]. However, a substantial effort has yet to be invested to implement the basic concepts within the real-world production processes. This is especially valid for the ship production process as one of the most energy-demanding manufacturing branches.

The research body on energy efficiency in the field of naval architecture is mainly focused on marine engineering and sustainable shipping particularly regarding efficient energy transformations of ship propulsion systems and efficient energy utilization via Energy Efficiency Design Index, [28]. On the other side, a thorough literature survey on ship production reveals that the energy-efficient concepts have not been accordingly addressed so far in the global energy nor manufacturing community, [29]. The sole example of the electricity consumption share during the ship production process is provided in [30], however, no scientific justification of the presented data was provided. Consequently, even a total energy demand and share during the ship production process are still unknown. The most significant roadmap towards the evaluation of the ship production process energy efficiency is provided in [31] following the fundamental principles of each production aspect involved.

4. Environmental friendliness

Environmental friendliness and pollution effects of the ship production process have, from a historical perspective, always been an important issue usually addressed through process development and implementation of new production technologies. Main pollutants related to the ship production process are usually classified as particles, liquids, NO_X and SO_X gasses, noise and general waste pollutants and are a consequence of processes like abrasive surface cleaning, corrosion protection, ship engine operation and production process in general, [31]. In that respect, environmental effects are relatively well regulated by different legislative frameworks stating the allowable amount of pollutant emissions, e.g. [32].

However, research on greener industrial footprint, carbon emission and implementation of green industry concepts, [27], is completely absent in the field of ship production. The sole example of green shipbuilding concept development is considered in [29]. Unfortunately, naval architecture community is mainly oriented towards the development of energy-efficient shipping, while omitting tremendous amount of research on topics like green shipbuilding, energy supply, energy management, on-grid, and off-grid system concepts, carbon emission as well as development, support and branding of green products promoted by numerous European policies, [33, 34].

5. Future research and development determinants instead of conclusion

Some of the most critical future research determinants (objectives) requiring wider recognition and financial support are:

- to develop and support competitive research groups (academics and practitioners) providing long-term ship production sustainability,
- to formulate new mathematical tools for the evaluation of the production systems,
- to evaluate the applicability of the existing evaluation methodologies,
- to develop numerical modeling methodology,
- to acquire shipyards floor data,
- to develop a bottom-up cost model, energy consumption model and evaluate the carbon footprint,
- to disseminate results and promote cost-effective and green ship production.

Hence, a concept of the generalized transition matrix should be further applied to a set of shipyard-like serial, assembly, poly-assembly, disassembly, poly-disassembly, buffer-sharing, and machine-sharing line elements: Such approach can be formulated using a new analytical tool 'Finite State Method' (FSM) implemented within ShipProLab software thus enabling its industrial application, and analysis of production system performance measures. An overall steady-state and transient behavior of the production systems should be evaluated using measures like production rate (PR), work-in-process (WIP), probability of blockage (BL) and the probability of starvation (ST) representing a backbone of the bottleneck identification, moving bottleneck analysis and design for lean production.

Along with that, a thorough validation of the aggregation procedures (semi-analytical approach) concerning the analytical solution of the problem should be conducted. To do that some of the semi-analytical models, e.g. buffer- sharing and machine-sharing, should be formulated as they cannot be exploited from the relevant literature. Validation of performance

measures, bottleneck analysis, and lean production design should be carried out systematically using FSM for different production systems complexities, number of machines and buffer capacities. From this, an important feedback can be retrieved that will be critical regarding the future development of the production system engineering and design procedures.

An application of the discrete event simulation (DES) approach should be applied for the analysis of the ship production process to verify the performance measures obtained using analytical and semi-analytical procedures. Hence, it is necessary to establish a simple and transparent DES methodology for ship production process analysis, particularly regarding the factory floor based input data evaluation and interpretation of the analysis results. The core property of the new numerical analysis methodology must be the observability of the output data. Moreover, systematic and thorough acquisition of shipyard workshops floors data, starting from the main storage and prefabrication line, over the metal processing and ship sections assembly line, up to the ship mounting and outfitting should be enabled. The acquired data could be of critical importance as input parameters for mathematical models of the ship production process as well as a benchmark for validation of the developed analytical, semi-analytical and numerical procedures.

Also, a bottom-up cost model should be developed following the fundamental engineering properties of the ship production process. The model should consider costs like personnel, consumables, depreciation and energy costs related to each production activity (prefabrication, fabrication, assembly, outfitting, transport, and material acquisition), technology operation (straightening, oxy-gas, and plasma cutting, welding, abrasive cleaning, painting, etc.) as well as to properties of ship construction units and elements (thickness, length, breadth, area, material, mass, etc.). Similar to productivity issues, the model should enable cost analysis based on the ship model in the early design stages. The model should be validated against the acquired shipyard's floor data and realistic cost structure. Such a model could be used to verify and improve the applicability of the standard top-down approaches to cost estimations during the early ship design stage.

The fundamental engineering principles of the ship production process also represent the basis for the development of the energy consumption mathematical model. The model can be developed in close relation to the bottom-up cost model. As such it could be representative of total energy demand and share analysis critical for decision making, the production policy establishment and efficient energy management. Such a model should also be validated using the acquired shipyards floor data available during the real-time production process. Finally, only a complete energy consumption model would enable the implementation of green ship production concepts, carbon footprint evaluation, rational energy policy development, and green ship branding.

REFERENCES

[1] Hadžić N. (2018) Ship production I. University of Zagreb. (In Croatian)

[2] Žanić, V, Andrić, J, Hadžić, N. (2015.) Optimization procedure for liquid natural gas carrier structural design, Proceedings of the Institution of Mechanical Engineers. Part M: *Journal of Engineering for the Maritime Environment*, 229, 1; 14-35.

[3] ElMaraghy H. (2009) Changeable and Reconfigurable Manufacturing Systems. Springer, London.

[4] Hadžić N, Tomić M, Vladimir N, Ostojić S, Senjanović I (2015) Current state and perspectives of the Croatian shipbuilding industry, Journal of Naval Architecture and Marine Engineering, 12, 33-42.

[5] Hadžić, N. (2018) Analytical solution of the serial Bernoulli production line steady-state performance and its application in the shipbuilding process, International journal of production research, 56, 12; 1, 14.

[6] Ljubenkov B, Đukić G, Kuzmanić M (2008) Simulation Methods in Shipbuilding Process Design, Journal of Mechanical Engineering 54(2), 131-139.

[7] Li J and Meerkov SM (2009) Production System Engineering, Springer, New York.

[8] Dain O, Ginsberg M, Keenan E, Pyle J, Smith T, Stoneman A, Pardoe I (2006) Stochastic shipyard simulation with Sim Yard, Proceedings of the 2006 Winter Simulation Conference, 1770-1778.

[9] Hadžić N and Tomić M (2017) Analytical solution of steady-state behaviour of Bernoulli production line with two finite buffers, Brodogradnja/Shipbuilding, 68(3), 85-102.

[10] Lim JT, Meerkov SM, Top F (1990) Homogenous, Asymptotically Reliable Serial Production Lines: Theory and Case Study, IEEE Transactions on automatic control 35(5), 524-534.

[11] Jacobs D and Meerkov SM (1995) A system-theoretic property of serial production lines: improvability, International Journal of System Science, 26(4), 755-785.

[12] Chiang SY, Kuo CT, Meerkov SM (2000) DT bottlenecks in Serial Production Lines: Theory and Application, IEEE Transactions, 16(5), 567-580.

[13] Meerkov SM and Zang L (2008) Simulation Methods in Shipbuilding Process Design, Journal of Mechanical Engineering 54, 131-139.

[14] Zhang L, Wang C, Arinez J, Biller S (2013) Transient analysis of Bernoulli serial lines: performance evaluation and system-theoretic properties, HE Transactions 45, 528-543.

[15] Li J, Meerkov SM, Zhang L (2010) Production systems engineering: Problems, solutions and applications, Annual Reviews in Control 24, 73-88.

[16] Zhao C and Li J (2014) Analysis and improvement of multi-product assembly systems: an application study at a furniture manufacturing plant, International Journal of Production Research 52(21), 6399-6413.

[17] Brandimarte P and Villa A (1995) Advanced Models for Manufacturing Systems Management, CRC Mathematical Modelling Series, London, 1995.

[18] McLean C and Shao G (2001) Simulation of shipbuilding operations, Proceedings of the 2001 Winter Simulation Conference, 870-876.

[19]   Williams DL, Finke DA, Medeiros DJ, Traband MT (2001) Discrete simulation development for a proposed shipyard steel processing facility, Proceedings of the 2001 Winter Simulation Conference, 882-887.

[20]   Hadjina M (2009) Simulation Modelling Based Methodology for Shipbuilding Process Design, Strojarstvo, 51(6), 547-553.

[21]   Wang C, Mao P, Mao Y, Shin JG (2016) Research on scheduling and optimization under certain conditions in panel block production line in shipbuilding, International Journal of naval Architecture and Ocean Engineering 8, 398-408.

[22]   Caprace JD, Rigo P., Towards a short time 'feature-based costing' for ship designs, Journal of Maritime Sciences and Technology, 2012 (17), pp. 216-230.

[23]   Deschamps L.C., Trumbule J. Chapter 10 – Cost estimating, Ship Design & Construction, Volume 1, SNAME, New Jersey, 2014.

[24]   Ross JM. A Practical Approach for Ship Construction Cost Estimating, 3rd COMPIT Conference, Siguenza, 2014.

[25]   Leal M, Gordo JM (2017) Hull's manufacturing cost structure, Brodogradnja/Shipbuilding 68(3).

[26]   Cai W, Liu F, Zhou X, Xie J (2016) Fine energy consumption allowance of workpieces in the mechanical manufacturing industry, Energy, 114, pp. 632-633.

[27]   United Nations (2010) Green Industry for a Low-Carbon Future, Vienna.

[28]   Marine Environment Protection Committee (MEPC). Standard specification for shipboard incinerators, International Maritime Organization, London, April 2014.

[29]   Hadžić, N, Kozmar H, Tomić M. (2018) Feasibility of investment in renewable energy systems for shipyards, Brodogradnja/Shipbuilding, 64, pp. 1-16.

[30]   Harish C.R., Sunil S.K. Energy Consumption and Conservation in Shipbuilding. International Journal of Innovative Research and Development, July, 2015.

[31]   Hadžić N. (2019) Ship production II. University of Zagreb. (In Croatian)

[32]   Republic of Croatia (2014) Croatian 2020 Industrial Strategy, Ministry of Economy, Zagreb.

[33]   Hadžić, N, Kozmar, H, Tomić, M. (2014) Offshore renewable energy in the Adriatic Sea with respect to the Croatian 2020 energy strategy, Renewable & sustainable energy reviews, 40, 597-607.

[34]   Hadžić, N, Tomić, M, Senjanović, I. (2014) Harmonic loading of horizontal axis tidal turbines due to non-uniform stream profile, Ocean engineering, 91, 196-207.

IMPACT OF WELDING PARAMETERS ON WELD QUALITY FOR HIGH-STRENGTH STEEL USED AT LOW TEMPERATURE

*Miroslav, Randić [*a], Duško, Pavletić [b], Igor, Bevandić [c], Dragan, Jerčić [d]*

a CROATIAN REGISTER OF SHIPPING, Branch office Rijeka, Čandekova 8b, 51000 RIJEKA
b UNIVERSITY OF RIJEKA, FACULTY OF ENGINEERING, Vukovarska 58, 51000 RIJEKA
c "DALMONT", d.o.o., Kralja Tomislava 8, 51262 KRALJEVICA
d CROATIAN REGISTER OF SHIPPING, Marasovićeva 67, 21000 SPLIT
* Corisponding Author, miroslav.randic@crs.hr

Abstract

Cracks in the welded joint can be initiated on the surface of and inside the welded joint. Cracks that are initiated on the surface of the welded joint are generally formed at the places of the highest stress concentration, especially along the edge of the seam. However, larger radii of the seam edge make surface cracks less likely. Larger seam edge radii can be reached either by subsequently machining the weld surface after welding or by properly selecting welding parameters.

In the study on the influence of welding parameters on the shape of the weld surface, especially on the size of the seam edge radius, experiments were conducted in which the influence of four welding parameters on the seam edge radius was analyzed: torch angle, number of cover passes, length of electrode stick-out and a type of a shielding gas. The experiments were performed by MAG welding process in horizontal position. The base material is high strength steel intended for use at low temperatures of type EH36. The results of the experiments conducted were analyzed by the Design of Experiments (DOE) method, and the conclusions obtained may be of use in technical practice with the aim to reduce surface cracks.

Key words: high strength steel; stress concentration; weld cracks; welding parameters

Sažetak

Pukotine se u zavarenom spoju mogu inicirati na površini i u unutrašnjosti zavarenog spoja. Pukotine koje se iniciraju na površini zavarenog spoja u pravilu nastaju na mjestima najveće koncentracije naprezanja, posebice uz rub šava. Pri tome, kod većih radijusa ruba šava manja je vjerojatnost pojave površinskih pukotina. Veći radijusi ruba šava mogu se postići naknadnom obradom površine zavara nakon zavarivanja ili odgovarajućim odabirom parametara zavarivanja.

U istraživanju utjecaja parametara zavarivanja na oblik površine zavara, posebice na veličinu radijusa ruba šava, provedeni su pokusi kod kojih je analiziran utjecaj četiri parametra zavarivanja na radijus ruba šava: broj prolaza završnog sloja, kut nagiba odnosno položaj gorionika, dužina slobodnog kraja žice, te vrsta zaštitnog plina. Pokusi su rađeni MAG postupkom zavarivanja u horizontalnom položaju. Osnovni materijal je čelik povišene čvrstoće namijenjen za rad na niskim temperaturama oznake EH36. Rezultati provedenih pokusa analizirani su metodom planiranja pokusa (DOE), a dobiveni zaključci mogu biti od koristi tehničkoj praksi u cilju smanjenja površinskih pukotina.

Ključne riječi: čelik pojačane čvrstoće; koncentracija naprezanja; pukotine u zavarima; parametri zavarivanja

1. Uvod

Od početka drugog svjetskog rata do danas zavarivanje predstavlja najčešći način spajanja metala. Mnogobrojnim postupcima zavarivanja ostvaruju se spojevi koji po svojim mehaničkim svojstvima odgovaraju osnovnom materijalu i predviđenoj namjeni. U eksploataciji su zavarene konstrukcije, pa tako i sami spojevi, često opterećeni cikličnim opterećenjima što ih čini pogodnima

za pojavu i širenje pukotina [1, 2]. Stoga su provedena i u ovom radu opisana istraživanja koja imaju za cilj smanjenje osjetljivosti sučeljnih zavarenih spojeva na pojave površinskih pukotina. Na Slici 1 prikazan je jedan takav spoj, u eksploataciji približno pet godina, na kojemu se vidi mjesto nastanka pukotina na rubu šava. Zavar se nalazi na glavnoj palubi na brodu za prijevoz naftnih derivata, odnosno na mjestu gdje se javljaju najveća vlačna naprezanja.

Figure 1 *Crack at the weld toe*
Slika 1 Pukotina na rubu šava zavarenog spoja

Iniciranju pukotina kod sučeljno zavarenih spojeva doprinosi nepravilna površina zavarenog spoja odnosno geometrijske značajke površine koje utječu na veličinu lokalnog faktora koncentracije naprezanja. U praksi postoji nekoliko načina na koji se može oblikovati površina zavara u cilju smanjenja koncentracije naprezanja. Na brodovima u izgradnji najčešće se upotrebljava metoda brušenja površine zavara [3, 4]. Međutim sve metode koje se primjenjuju nakon završenog zavarivanja iziskuju dodatne resurse, te povećavaju troškove izrade. Osnovna hipoteza u provedenom istraživanju koja su ovdje opisana je da se pravilnim odabirom parametara zavarivanja može postići geometrija zavarenog spoja sa manjom osjetljivošću na pojavu površinskih pukotina.

Više istraživača je analiziralo utjecaje raznih tehnika i parametara zavarivanja na geometriju zavarenog spoja [5, 6]. Bytyqi i suradnici analizirali su učinke jakosti struje zavarivanja na oblik zavara i utvrdili da se širina zavara povećava porastom jakosti struje zavarivanja [7]. Kasuya i Yurioka istraživali su utjecaje okolne temperature na stvaranje pukotina u zavarenom spoju [8]. Nouri i suradnici istraživali su utjecaje brzine dovođenja dodatnog materijala odnosno žice, brzine izvođenja zavarivanja odnosno brzinu gibanja električnog luka, te dužine slobodnog kraja žice na geometriju zavarivanja [9]. Tewari i suradnici proučavali su utjecaje brzine izvođenja zavarivanja i unosa topline na dubinu protaljivanja osnovnog materijala [10]. Istraživanja opisana u ovom radu temelje se na rezultatima spomenutih istraživanja te predstavljaju njihov svojevrsni nastavak.

Istraživanje je provedeno na sučeljnom V spoju čelika povišene čvrstoće pri niskim temperaturama, oznake EH36 [1, 11]. Debljina osnovnog materijala je 10 mm.

2. Provedba pokusa

Napravljeno je ukupno 24 pokusa, u kojima su metodom potpunog plana pokusa sustavno mijenjane četiri tehnike zavarivanja koje u dosadašnjim istraživanjima nisu bile sustavno istražene, a smatra se da imaju značajan utjecaj na oblik površine zavarenog spoja. U Tablici 1 prikazani su

parametri zavarivanja s odgovarajućim nivoima vrijednosti koje su mijenjane tijekom pokusa, dok je u Tablici 2 prikazan potpuni plan pokusa zavarivanja. Pokusi su, obzirom na položaj gorionika, grupirani u tri grupe, s po osam pokusa u svakoj grupi. U Tablici 1 i Tablici 2 su oznakama „-", „0" i „+" označeni nivoi odnosno vrijednosti koje su poprimale tehnike zavarivanja u određenom pokusu. Dužina uzorka, a time i zavara u pojedinom pokusu je konstantna i iznosi 150 mm.

Table 3 Welding techniques that were changed during the experiment

Tablica 1 Tehnike zavarivanja mijenjane tijekom pokusa

Tehnika zavarivanja	Nivo		
	Nizak (oznaka -)	Srednji (oznaka 0)	Viši (oznaka +)
Položaj gorionika (A)	Tehnika prema naprijed Grupa 1	Okomita tehnika Grupa 2	Tehnika prema natrag Grupa 3
Broj prolaza završnog sloja (B)	1 prolaz		3 prolaza
Dužina slobodnog kraja žice (C)	5 mm		15 mm
Vrsta zaštitnog plina (D)	82% Ar + 18% CO_2		100% CO_2

Table 2 Design of experiments

Tablica 2 Plan pokusa

Tehnika zavarivanja	Oznaka eksperimenta i grupa																							
	1-1	1-2	1-3	1-4	1-5	1-6	1-7	1-8	2-1	2-2	2-3	2-4	2-5	2-6	2-7	2-8	3-1	3-2	3-3	3-4	3-5	3-6	3-7	3-8
	Grupa 1								Grupa 2								Grupa 3							
Položaj gorionika	-	-	-	-	-	-	-	-	0	0	0	0	0	0	0	0	+	+	+	+	+	+	+	+
Broj prolaza završnog sloja	-	-	-	-	+	+	+	+	-	-	-	-	+	+	+	+	-	-	-	-	+	+	+	+
Dužina slobodnog kraja žice	-	-	+	+	-	-	+	+	-	-	+	+	-	-	+	+	-	-	+	+	-	-	+	+
Vrsta zaštitnog plina	-	+	-	+	-	+	-	+	-	+	-	+	-	+	-	+	-	+	-	+	-	+	-	+

Nakon izvršenih pokusa svi uzorci su snimljeni optičkim uređajem za beskontaktno trodimenzionalno snimanje u Centru za napredno računanje i modeliranje, Sveučilišta u Rijeci. Za snimanje je korišten ATOS (Advanced Topometric Sensor) II Triple Scan uređaj za digitalizirano mjerenje objekata. Mjerenje radijusa ruba šava rađeno je uz pomoć računalnog programa "GOM inspect" [12].

Na svakom uzorku mjerenja radijusa ruba šava su rađena u tri pojasa. Prvi pojas je određen u području od 20 do 30 mm nakon početka zavarivanja, drugi pojas je određen u sredini uzorka od 70 do 80 mm od početka zavarivanja, te je treći pojas određen u području od 120 do 130 mm od početka zavarivanja. Obzirom da je tijekom zavarivanja vršeno automatsko očitavanje parametara zavarivanja (jakost struje zavarivanja, snaga struje zavarivanja i brzina prolaza žice), utvrđeno je da su se parametri zavarivanja stabilizirali prije početnog pojasa u kojem se mjere geometrijski parametri zavarenog spoja.

Svaki pojas je širok 10 mm, a razmak između presjeka je 1 mm. Na taj način je u svakom pojasu dobiveno 11 presjeka u kojima su mjereni radijusi ruba šava zavarenog spoja.

Na svakom presjeku je određena točka u kojoj površina osnovnog materijala prelazi u nadvišenje sljemena šava. Za lijevu stranu zavara ta točka ima oznaku „TOČKA LIJEVO 02". Ova točka je na svim presjecima za sve uzorke označena na istom mjestu, odnosno na mjestu gdje započinje nadvišenje sljemena šava.

Radijus ruba šava se može definirati kao radijus kružnice koja prolazi kroz tri točke na površini zavara. U tom slučaju vrijednost radijusa ruba šava ovisi o razmaku između točaka kroz koje kružnica prolazi.

Razmak između točaka je određen 0,125 mm zato jer je utvrđeno da se najveća koncentracija naprezanja javlja u području od 0,125 mm uzduž zavarenog spoja. [13]

Obzirom da je površina zavarenog spoja nepravilnog oblika, ne postoje dva presjeka sa istim oblicima površine, stoga je za svaki presjek očitano *n* točaka, gdje broj točaka *n* za svaki presjek nije nužno isti.

„*GOM inspect*" je program koji omogućava konstruiranje kružnice kroz tri točke. Prilikom mjerenja radijusa ruba šava zavara konstruirane su kružnice kroz svake od tri označene točke na površini zavara. Obzirom da je koncentracija naprezanja najveća u području najmanjeg radijusa ruba šava, za daljnju analizu se promatra kružnica sa najmanjim radijusom. U slučaju prikazanom na slici 2 to su „TOČKA LIJEVO 02", „TOČKA LIJEVO 03" i „TOČKA LIJEVO 04", a kružnica koja prolazi kroz te tri točke je označena sa crvenom bojom.
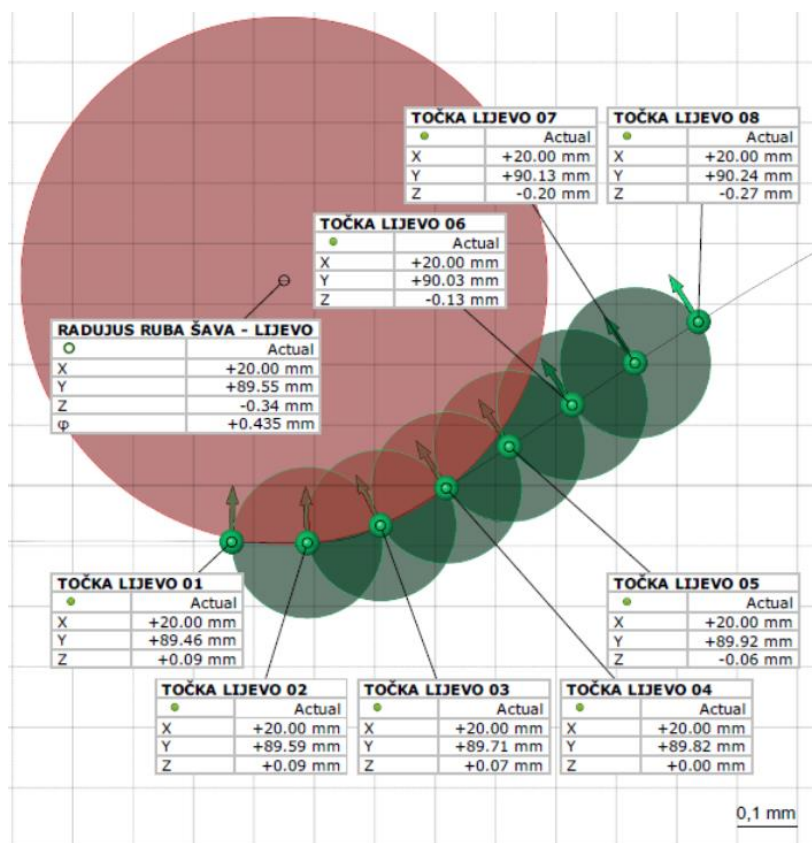
Weld toe radius in *GOM Inspect*

Slika 2 Radijus ruba šava zavara u „*GOM inspect*-u"

U Tablici 3 prikazani su najmanji radujusi izmjereni za svaki uzorak.

Table 3 Values of the smallest measured toe radii for each sample in millimetres [mm]

Table 3 Vrijednosti najmanjih izmjerenih radijusa ruba šava za svaki uzorak

Uzorak	1-1	1-2	1-3	1-4	1-5	1-6	1-7	1-8	2-1	2-2	2-3	2-4
Radijus ruba šava	0.21	0.27	0.26	0.23	0.20	0.29	0.22	0.31	0.27	0.27	0.26	0.26

Uzorak	2-5	2-6	2-7	2-8	3-1	3-2	3-3	3-4	3-5	3-6	3-7	3-8
Radijus ruba šava	0.37	0.24	0.25	0.26	0.29	0.33	0.25	0.28	0.25	0.29	0.26	0.25

2.1. *Tehnike zavarivanja*

Kao što je prije rečeno u ovom radu su analizirane četiri tehnike zavarivanja:

- Položaj gorionika
- Broj prolaza završnog sloja
- Dužina slobodnog kraja žice
- Vrsta zaštitnog plina

U nastavku nekoliko riječi o svakoj tehnici.

1.1.1 Položaj gorionika

Tijekom istraživanja pokusi su provođeni s gorionikom za zavarivanje u tri različita položaja i to *prema naprijed*, o*komito* i *prema natrag*, kako je to prikazano na Slici 3. U tehnici zavarivanja prema naprijed kut između gorionika i osnovnog materijala je manji od 90°, što rezultira manjom dubinom protaljivanja osnovnog materijala. Zavarivaču je u potpunosti vidljiv žlijeb u koji polaže zavar, no nema dobar pregled neposredno zavarenog spoja. U tehnici zavarivanja prema natrag, kut između gorionika i osnovnog materijala je veći od 90°. U ovom slučaju zavarivač u cijelosti vidi zavareni spoj, no nema neometani pogled na žlijeb. Dubina protaljivanja osnovnog materijala je u ovom slučaju

veća u odnosu na tehniku zavarivanja prema naprijed. Okomita tehnika zavarivanja predstavlja graničan slučaj prethodno spomenutih tehnika zavarivanja.
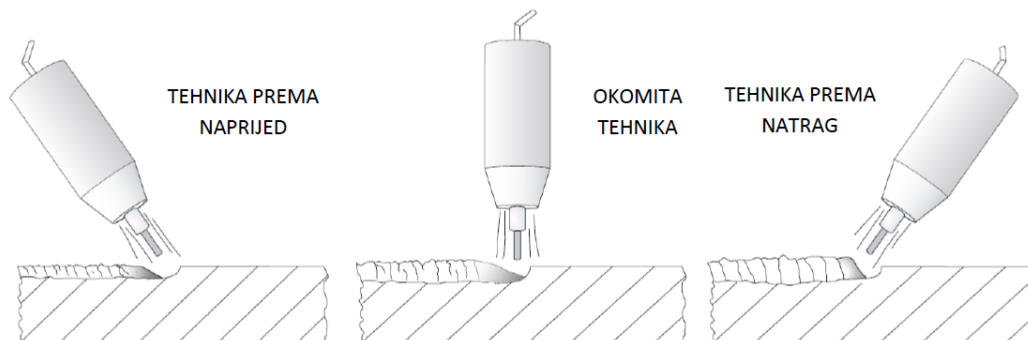
Figure 3 *Torch angle*
Slika 3 Položaj gorionika

1.1.2 Broj prolaza završnog sloja

Zavarivanje se može izvesti s manjim ili većim brojem prolaza završnog sloja. Kada se zavarivanje vrši s većim brojem prolaza završnog sloja, brzina zavarivanja je veća, pa se smanjuje toplina osnovnog materijala. Kako je cilj istraživanja analiza površine zavarenog spoja, završni slojevi kod provedenih pokusa, sukladno planu provedbe pokusa, zavareni su u jednom odnosno u tri prolaza. Broj ostalih zavara u pokusima (korijenski zavar, zavari popune) je konstantan.

1.1.3 Dužina slobodnog kraja žice

Dužina slobodnog kraja žice je duljina žice koja izlazi iz kontaktne vodilice gorionika mjereno duž žice, Slika 4. Udaljavanjem ili približavanjem gorionika od osnovnog materijala duljina slobodnog kraja žice se povećava ili smanjuje. Povećanjem duljine slobodnog kraja žice povećava se električni otpor, napon struje zavarivanja postaje veći. Obzirom da se napon održava konstantnim tijekom zavarivanja, to se automatski kompenzira smanjenjem trenutne jakosti struje. Povećavanjem duljine slobodnog kraja žice električni luk postaje nestabilan. Ova istraživanja su rađena s dvije dužine slobodnog kraja žice i to 15 mm i 5 mm.
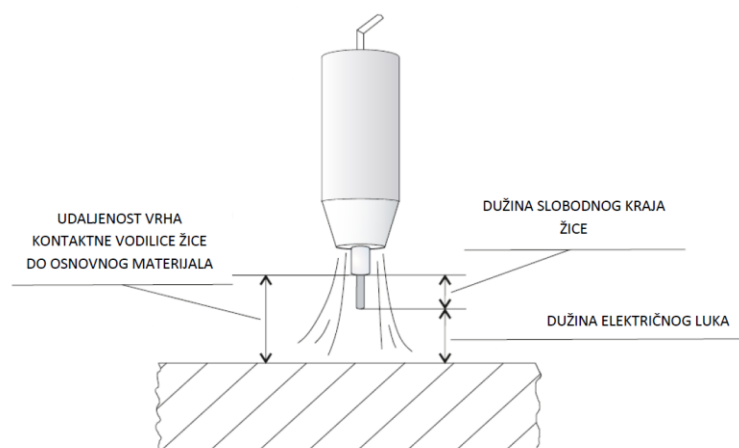
Figure 4 *Length of electrode stick-out*
Slika 4 Dužina slobodnog kraja žice

1.1.4 Vrsta zaštitnog plina

Zaštitni plinovi koji se koriste u elektrolučnom zavarivanju mogu se podijeliti u dvije glavne skupine, aktivni i inertni plinovi. Najčešće korišteni aktivni plin je ugljični dioksid CO_2, dok je argon najčešće korišteni inertni plin. Također, u određenim situacijama učestala je primjena mješavina plinova zbog ostvarivanja boljih rezultata zavarivanje u odnosu na primjenu čistih plinova. U ovom su istraživanju korištena dva zaštitna plina, tj. mješavina plinova (82% Ar + 18% CO_2) i čisti CO_2.

3. Analiza provedenih pokusa

Dobiveni rezultati analizirani su statističkim metodama [14]. Analiziran je utjecaj svake promatrane tehnike zavarivanja na geometrijski oblik površine zavarenog spoja s ciljem određivanja mjesta pojave najveće koncentracije naprezanja. Pri tome je posebno mjeren i analiziran radijus ruba šava, kao geometrijska značajka površine zavarenog spoja s najvećim utjecajem na pojavu lokalno visoke koncentracije naprezanja [15]. Izdvojene su tehnike zavarivanja u kojima se javljaju najmanji radijusi ruba šava, odnosno u kojima se javlja najviše koncentarcije naprezanja i koje treba izbjegavati tijekom postupka zavarivanja [16].

Analiza rezultata dobivenih eksperimentima i njihova interpretacija predstavljaju vrijednu podlogu za donošenje zaključaka koji mogu biti korisni u inženjerskoj praksi. Prvi korak je prepoznavanje tehnika zavarivanja i njihove interakcije, odnosno onih koje imaju značajan utjecaj na radijus ruba šava, Tablica 4. U desnom stupcu ove tablice prikazana je p-vrijednost, vrijednost na temelju koje se utvrđuje koliko su specifični podaci značajni za rezultate pokusa.

Obično se uzima 95-postotna razina značajnosti [17].

Iz Tablice 4 može se zaključiti da učinak C (dužina slobodnog kraja žice), kao i međudjelovanja AB (položaj gorionika - broj prolaza završnog sloja) i AD (položaj gorionika - vrsta zaštitnog plina) imaju značajan utjecaj na veličinu radijusa ruba šava.

Učinak D (Vrsta zaštitnog plina) je velik, međutim, s obzirom na razinu značajnosti od 95%, taj učinak nije značajan.

Table 4 Table of influence of main effects and their interactions

Table 4 Utjecaj glavnih učinaka i njihovih međudjelovanja

Glavni učinci i njihova međudjelovanja		p-vrijednost
A	Položaj gorionika	0.267
B	Broj prolaza završnog sloja	0.783
C	Dužina slobodnog kraja žice	**0.036**

D	Vrsta zaštitnog plina	0.053
AB	Položaj gorionika - Broj prolaza završnog sloja	**0.016**
AC	Položaj gorionika - Dužina slobodnog kraja žice	0.366
AD	Položaj gorionika - Vrsta zaštitnog plina	**0.027**
BC	Broj prolaza završnog sloja - Dužina slobodnog kraja žice	0.342
BD	Broj prolaza završnog sloja - Vrsta zaštitnog plina	0.247
CD	Dužina slobodnog kraja žice - Vrsta zaštitnog plina	0.882

Utjecaj glavnih učinaka prikazan je na Slici 5, a njihove međusobne interakcije prikazane su na Slici 6. Linija koja pokazuje utjecaj dužinu slobodnog kraja žice je najokomitija, to znači da je njen utjecaj na radijus ruba šava najveći i značajan. Mali radiusi ruba šava javljaju se ako se zavarivanje radi sa većim dužinama slobodnog kraja žice dodatnog materijala. Linija koja pokazuje utjecaj zaštitnog plina je vertikalna, prema Tablici 4, taj se utjecaj može smatrati velikim, ali ne i značajnim. Utjecaj broja prolaza završnog sloja je zanemariv, dok je utjecaj položaja gorionika mali. Grafikoni prikazani na Slici 6 pokazuju dvostrane interakcije pojedinih glavnih učinaka. Linije koje su paralelne među sobom predstavljaju manju interakciju. Moglo bi se primijetiti da su linije interakcije glavnih učinaka, dužina slobodnog kraja žice (C) i zaštitnog plina (D), gotovo paralelne, što znači da je njihova interakcija zanemarljiva. Grafikoni koji prikazuju interakciju položaja gorionika (A) i broja prolaza završnog sloja (B), te položaj gorionika (A) i vrsta zaštitnog plina (D) se sijeku pod velikim kutu, što znači da je njihova interakcija značajna. Ostale tri interakcije su velike, međutim nisu značajne.
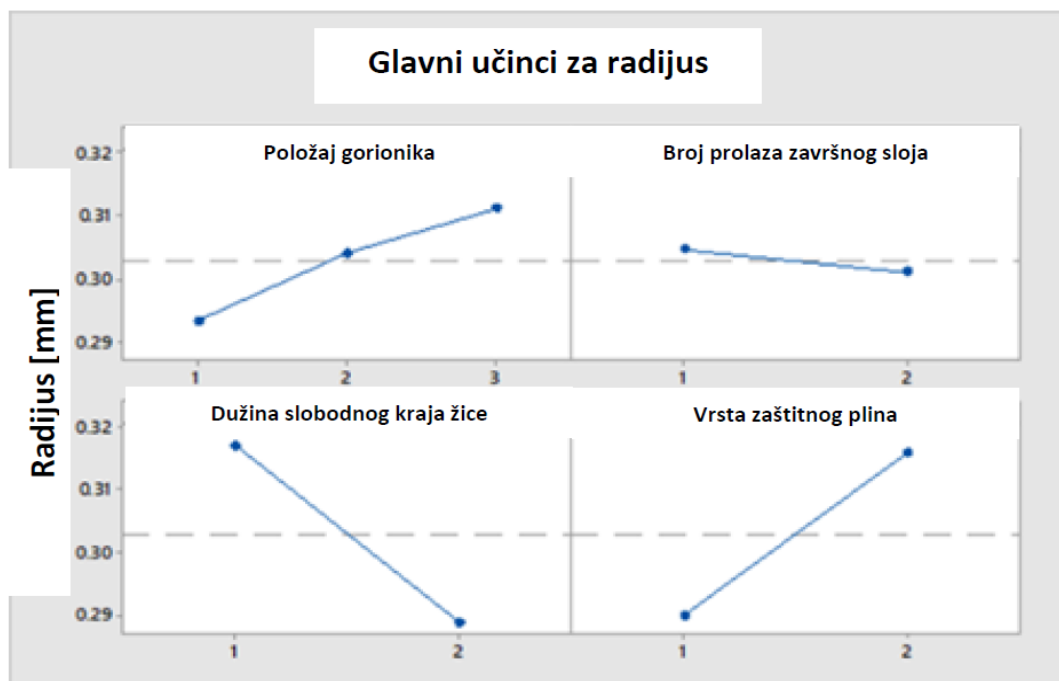
Figure 5 *Influence of main effects*

Slika 5 *Glavni učinci*
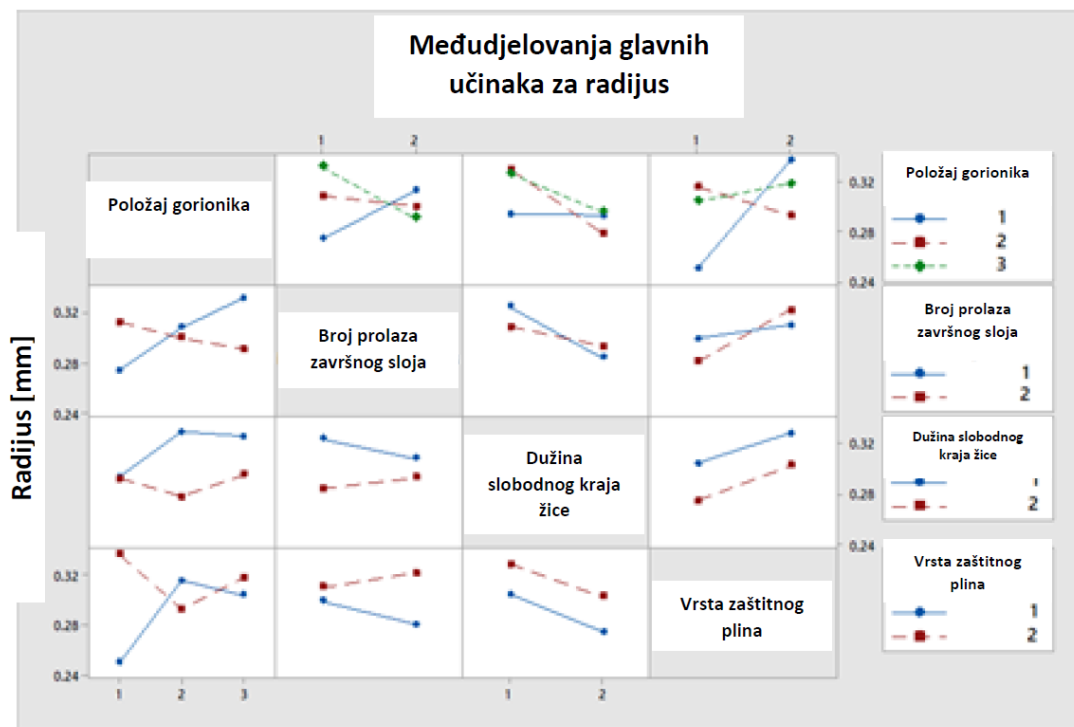
Figure 6 *Interactions of main effects*

Slika 6 *Međudjelovanja glavnih učinaka*

Konturni graf prikazan na Slici 7. prikazuje odnos radijusa ruba šava u odnosu na dužinu slobodnog kraja žice, za jedan završni prolaz zavarivanja, te za mješavinu zaštitnog plina.

Analizirajući ovaj graf može se zaključiti da se najmanji radijusi pojavljuju s duljinom slobodnog kraja žice od 15 mm i tehnikom zavarivanja naprijed. Na grafu je ova točka označena sa slovom "A". Ove tehnike zavarivanja treba izbjegavati.

U suprotnom kutu istog grafa javljaju se najveći radijusi (> 0,37 mm), označeni sa slovom "B". Dakle, prema provedenim eksperimentima, prilikom zavarivanja malom dužinom slobodnog kraja žice, tehnikom zavarivanja natrag s jednim završnim prolazom i s mješavinom zaštitnih plinova, može se očekivati najveći radijus u kojem se inicira najmanje površinskih pukotina.

496
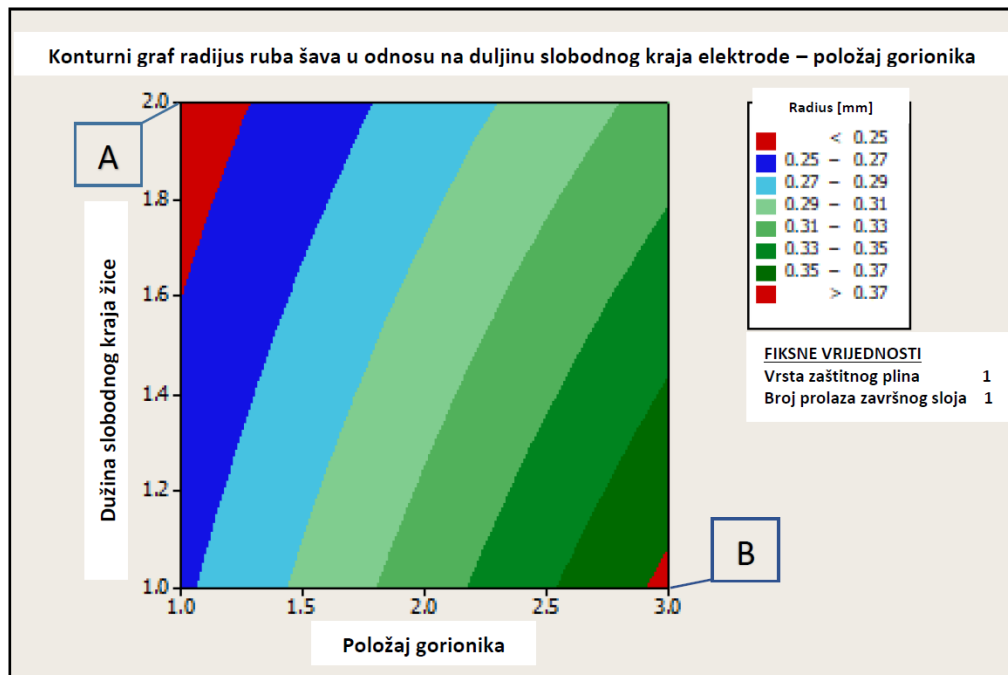
Figure 7 *T*oe radius as a function of the torch angle and the electrode stick-out
Slika 7 Radijus ruba šava u odnosu na duljinu slobodnog kraja elektrode

4. Zaključak

Ova istraživanja su obavljena sa sučeljno spojenim zavarenim spojevima. Materijal koji se je upotrebljavao je bio čelik visoke čvrstoće pri niskim temperaturama, međutim, nema razloga da se rezultati ovog istraživanje ne primijene na druge vrste čelika, ali samo za sučeljno zavarene spojeve. Ne preporuča se primjena ovih rezultata na druge materijale, poput aluminija. Rezultati tih istraživanja mogu se koristiti ako radijus ruba šava poprimi vrijednosti od 0,20 mm do 4 mm, tj. vrijednosti koje su dobivene tijekom provedenih ispitivanja. Njihova se primjena na ostalim vrijednostima radijusa ruba šava ne preporuča.

Rezultati ovih istraživanja se mogu primijeniti na najviše tri prolaza završnog sloja. S većim brojem prolaza završnog sloja površina zavara poprima drugačiji oblik, tako da se dobiveni rezultati mogu razlikovati od dobivenih u ovom istraživanju.

Analiza rezultata ovih istraživanja pokazuje da dužina slobodnog kraja žice ima značajan utjecaj na radijus ruba šava zavara. Manji radijus ruba šava zavara nastaje kada je dužina slobodnog kraja žice veća. Utjecaj zaštitnog plina je velik, mada ne i značajan, mješavinom zaštitnih plinova javljaju se manji radijusi ruba šava zavara. Kut gorionika također ima veliki utjecaj, dok broj prolaza završnog sloja ima zanemariv utjecaj na radijus ruba šava zavara.

Analizom je utvrđeno da su međudjelovanja položaja gorionika i broja prolaza završnog sloja (AB), kao i položaj gorionika i vrsta zaštitnog plina (AD) značajna. Radijus ruba šava se značajno mijenja ako se promijeni položaj gorionika i duljina slobodnog kraja žice.

Najmanji radijus ruba šava se javlja kod zavarivanja duljim slobodnim krajem žice, tehnikom zavarivanja naprijed, u jednom prolazom završnog sloja te uz zaštitu mješavinom plinova. Slijedom svega navedenoga, u cilju smanjenja rizika odnosno vjerojatnosti pojave pukotina na rubu zavarenog spoja, preporuka je izbjegavati tehnike zavarivanja čija primjena rezultira malim radijusima ruba šava.

LITERATURA

[1] Meden, G., Pavelić, A., Pavletić, D.: „Osnove zavarivanja", Tehnički fakultet, Rijeka 2000.

[2] Milićević, R. M.: „Zavarivanje", AGM knjiga, Beograd, 2011.

[3] Lechner, C., Bleicher, F., Habersohn, C., Bauer, C., Goessinger, S.: "The Use of Machine Hammer Peening Technology for Smoothening and Structuring Of Surfaces", 23rd DAAAM Symposium, Volume 23, No. 1, Beč, Austria, 2012.

[4] Haagensen, P. J., Maddox, S. J.:"IIW Recommendations on Post Weld Improvement of Steel and Aluminium Structures", The International Institute of Welding, 2001.

[5] den Ouden G, Hermans M.: "Welding technology", Delft, The Netherlands: VSSD; 2009.

[6] Jeffus L.: "Welding principles and applications", 17th ed. New York: Delmar; 2012.

[7] Bytyqi B, Osmani H, Idrizi F.. "Influence of welding parameters on seam welded quality with MAG welding", 4th International Research and Expert Conference, KVALITET 2005, Fojnica, B&H, November.

[8] Kasuya T, Yurioka N.: "Effects of ambient temperature on steel weldability", Weld Int. 1992;6(2):145–150.

[9] Nouri M, Abdollah-zadehy A, Ghaini FM.: "Effect of welding parameters on dilution and weld bead geometry in cladding", J Mater Sci Technol. 2007;23(6):817–822.

[10] Tewari SP, Gupta A, Prakash J: "Effect of welding parameters on the weldability of materials", Int J Eng Sci Technol. 2010;2:512–516.

[11] Croatian Register of Shipping, „Rules For the Classification of Ships", Part 25 – Metallic Materials, Split 2012.

[12] Randić, M., Pavletić, D., Turkalj, G.: „The Measurement of Weld Surface Geometry", XVII simpozij International Maritime Association of the Mediteranean, Lisabon, 2017.

[13] Lawrence, F. V., Ho, N., Mazumdar, P. K.: „Predicting the Fatigue Resistance of Welds", Ann. Rev. Mater. Sci., Vol. 11, 1981. str. 401 – 425.

[14] Hinkelmann K, Kempthorne O.: "Design and analyses of experiments", Vol. 1, 2nd ed. New Jersey: Wiley & Sons; 2008.

[15] Rowlands H, Antony J.: "Application of design of experiments to a spot welding process". Assembly Autom. 2003;23(3):273–279.

[16] Randić, M., Pavletić, D., Turkalj, G.: „Multiparametric investigation of welding techniques on toe radius of high strength steel at low-temperature levels using 3D-scanning techniques", Metals, Volume 9, Issue 12, Basel. Švicarska, prosinac 2019.

[17] Montgomery DC, Runger GC.: "Applied statistic and probability for engineers", 3rd ed. Arizona: John Wiley & Sons; 2003.

OPTIMIZATION OF SECONDARY STEEL CONSTRUCTIONS

Darija Jurjević[a,], Arsen Sušanj[b]

a Tehinčki fakultet Rijeka, Vukovarska 58, Rijeka
b IHC Engineering Croatia, Milutina Baraća 7, Rijeka
* Corisponding Author, darija.jurjevicc@gmail.com

Abstract

Nowadays the world is rapidly changing, especially in terms of modern technology. Trying to stay relevant in today's world of supply and demand and the ever-present desire to make more money are the two main notions in every industry. Shipbuilding is no different. The formula to stay on top of the market is to guarantee a quality product, for as small a price as possible and to deliver it in the shortest amount of time. In this paper we will discuss the optimization process in the IHC Outfitting department. Our goal was to make a complete optimization of the modeling and development process in Cutter dredgers, with emphasis on the structural strength determined by vessel calculations. The optimization was executed by dividing the process in three main stages: approaching the problem, selection of the material and the production itself. With changes in all three areas, we came up with a new - better process.

Key words: optimization; secondary steel; strength;

OPTIMIZACIJA RADA OUTFITTING UREDA

Sažetak

Svijet oko nas se konstatno mijenja, pogotovo kada govorimo o modernoj tehnologiji. Glavni cilj u svakoj industriji, pa tako i u brodogradnji, je biti uspješan i konkurentan na svjetskom tržištu. Kako bi se taj cilj ostvario potrebno je jamčiti kvalitetan proizvod, za što manju cijenu i isporuku u najkraćem mogućem roku. U ovom radu pokazati ćemo optimizaciju rada Outfitting odjela IHC-a. Naš cilj bio je provesti potpunu optimizaciju procesa izrade i proizvodnje kod Cutter dredger-a, uz naglasak na očuvanje strukturalne čvrstoće zadane proračunima. Optimizacija je provedena podjelom procesa na tri glavna područja: način pristupa problemu, odabir materijala pri modeliranju i sama proizvodnja. Uz izmjene u svim navedenim područjima, došli smo novog – poboljšanog procesa konstrukcije i izrade broda.

Ključne riječi: optimizacija; temelji; čvrstoća;

1. Uvod

U svakoj industriji, pa tako i u brodogradnji teži se ka standardizaciji procesa. Cilj standardizacije je povećanje kvalitete proizvoda uz pojednostavljenje što proizvodnje što same izvedbe modeliranja. Kada govorimo o standardizaciji Outfitting odjela, možemo govoriti o nekoliko glavnih pojmova:

1. način pristupa problemu modeliranja

2. odabir materijala – vrsta profila

3. proizvodnja – montaža

Iako već funkiconalan, način rada u Outfitting uredu imao je prostora za poboljšanje te ćemo ga u ovom radu i pokazati.

2. Način pristupa problemu

Kada je riječ o izradi temelja broj mogućih rješenja je beskonačan. To ne ide u prilog standardizaciji procesa te se on treba smanjiti dovoljno da se napravi "šablona" koja će se kasnije moći dalje koristiti, ali također ostavljajući dovoljno mjesta za prilagodbe najčešće diktirane pozicijom temelja na brodu. Optimiziranje ovog dijela procesa riješili smo uvođenjem "*Check liste*" kao naputak kako izraditi model i nacrt za određeni temelj. Na njima je točno definirana putanja 3D modeliranja i izrada nacrta od trenutka kada se zadatak dobije do trenutka kada ga se šalje u proizvodnju. Time se maksimalno reducira faktor ljudske pogreške budući da se osim samog modeliranja moraju uzeti u obzir i drugi odjeli kao i informacije o opremi koje je potrebno prikupiti prije početka izrade modela.

IHC Engineering Croatia d.o.o.
Milutina Barača 7
51000 Rijeka
CROATIA

OUTFITTING - Kontrolna lista za model i nacrt

Gradnja:	No. Drw. :		Konstruktor	Revizor

	Akcije	Alati / Komentari	Destinacije	Datum kontrole
A	O&M Reporter HVD		registriran i odobren početak rada (u Reporter unijeti 5% za početak rada, 50% za gotov 3D)	
B	Broj nacrta	Provjeriti ima li model/nacrt odgovarajući broj sekcije i broj prostora u odnosu na lokaciju, usporediti sa Marsom i Reporterom	- Ukoliko model nije u Marsu ili Reporteru nije pod odgovarajućim brojem prostora ili sekcije obavijestiti voditelja - Ukoliko procijenjeni sati u Reporteru nisu dovoljni za izradu modela i nacrt obavijestiti voditelja	
C	Nacrt opreme	Uvijek koristi nacrt od proizvođača opreme	izvor: DMS, e-mail, Projektni folder...	
	MODEL			
1	Kvaliteta materijala	Kvaliteta materijala: A, AH36, D, GRP, Al...	1. Je li model napravljen od propisane kvalitete (pogledaj listu materijala) 2. HT čelik po potrebi 3. Provjeriti postoje li posebni zahtjevi za materijal	
2	Podložna plocica - debljina	Debljina podložne pločice ovisi o veličini vijka za montažu	- IHC norm 48406	
3	Stepenice	- Provjeriti jesu li su stepenice pod odgovarajučim kutem (45,50,55,60°) "DRW Stair Arrangement" - je li dobar tip stepenica (vanjske / unutarnje), - je li dobra širina stepenica, - moraju li stepenice biti galvanizirane, - je li zadovoljena visina prolaza (min 2100mm), - je li otvor u palubi odgovarajućih dimenzija, - moraju li stepenice imati "BackPlate".	- IHC norm 51302	
4	Tava, Kadica	Na krmenoj strani "tave" postaviti "Socket" za odvod - Izbušiti rupu d=50 - izmodelirati "DUMMY Socket" d=50, t=30, sa debljinom prema dolje. (za odvodnu cijev od 1")	- IHC norm C330 - upisati u nacrt "THREADED SOCKET G1x30 IHC NORM C330"	
5	Sudarna kontrola	provjera da nemamo sudar našeg modela sa okolnim modelima (opreme, trupa, cjevarije)		
	NACRT			
6	Ažuriranje pogleda	Jesu li svi pogledi ažurirani?		
7	Naslov i podnaslov	Provjeriti stil teksta	- Sav tekst mala slova	
8	Kote	Kote za pozicioniranje modela	- kotiranje podložnih pločica (u tlocrtu se kotira profil, a ne sama podložna pločica) - kotirati položaj modela u odnosu na brodsku strukturu (kotom koja je lako mjerljiva na mjestu montaže) - označiti orijentaciju debljine - profili sa skošenim krajevima trebaju biti kotirani	
9	Oznake	- pozicijski broj izvuči zasebno za svaki dio - dimenzionirati svaki rešetkasti i pločasti pokrov		
10	Mjerilo	Naznačiti u podnaslovu ako je mjerilo različito od naznačenoga u sastavnici (1:25)		
11	Generalni pogled (uzduzni ili poprecni)	Uz osnovne kote, označiti strelicom na opremi i napisati: - Ime opreme - Broj opreme - masu opreme u kg	- Odlučiti koji je pogled prihvatljivi (poprecni ili uzduzni)	
12	Izometrijski pogled	- označiti orijentaciju modela, strelicama definirati minimalno 3 strane - ukoliko model sadržava više Mars brojeva, označiti pripadnost pojedinog strelicama - crvenom punom linijom prikazati predmetni model, bijelom linijom tipa 'crta-točka-crta' prikazati susjedne modele i strukturu - označiti visinu palube, po mogućnosti pregradu ili rebro od kojeg se mjeri pozicija modela		
13	Naputak zavarivanja	NOTE: WELDING IF NOT OTHERWISE INDICATED ∠ OR ⌂3.5	- provjeri veličine zavara sa IHC normama - stavi notu na sve nacrte gdje je potrebno zavariti nehrđajući čelik - stavtti notu na sve lokacije gdje se radi o isprekidanom zavarivanju	
14	Predmontaza	- ako se temelj nalazi na više sekcija staviti u Note : i označiti sekcije u Generalnom tlocrtu	(FOUNDATION IS LOCATED ON SEVERAL SECTIONS)	
15	Podlozne plocice	- Ako se oprema spaja sa vijcima u podloznu plocicu staviti u Note:	(WELD DOUBLE PLATES AFTER MOUNTING ON EQUIPMENT)	
16	Detalj rupa	- Ako ne postoji info. o tocnoj poziciji montažnih rupa stavite u Note, :	(HOLES TO BE TAKEN OVER FROM THE EQUIPMENT)	
17	Detalji	- spoj "tave" - spoj "soketa" na "tavu" - tipovi potpornja za vanjsku ogradu - dodatni detalji ovisno o projektu		
18	Sastavnica	- Naslov - isti kao u Reporteru i DMS-u, - Podnaslov - prostorija ili paluba, za stepenice Poz. br. - broj sekcije i broj prostora - Ispuniti svoje inicijale i datum (tko zadnji radi izmjenu stavlja svoje inicijale) - Ispuniti listu materijala, navesti broj standarda za standardne dijelove	Lista materijala u tablicu ispunite pojedinačno za: - masa rešetkastog pokrova - masa stepenica, ljestvi - masa ograde - masa podložne pločice, za standardne broj komada i tip - težine ispunjavamo za sve elemente koji su iz Marsa + ukupna masa	
19	Potpora strukture	Provjeriti trebate li potporu na brodsko strukturu?	Poslati informaciju kolegama za potporu putem maila i kopiran mail staviti u folder za tu namjenu i za određenu sekciju	DA - NE
20	E-Browser	Poslati model u cadmatic (e-browser)	File -> Send to... -> Outfitting - popratite upute za slanje ukoliko je blok mjenjao lokaciju	
21	O&M Reporter HVD	Popunjen "O&M Reporter HVD"	Nacrt poslan na checking -> ispuniti progress 75%	

* Napomena za početak izrade dokumentacije.
* Napomena u ovoj boji, za izradu modela.
* Napomena u ovoj boji, za izradu nacrta.
* Check u ovoj boji popunjava konstruktor

p1eh9tkp90ae31r3p44q8k81vfe4.xlsx   1   9/3/2020

Slika 1 – *Check list example*

3. Odabir materijala – vrsta profila

Vođeni iskustvom i primjerima mnogih projekata koje smo do sada uspješno odradili, najčešće korišteni profili za izrade temelja na cutter dreadgerima su L profili dimenzija: L75x75x8, L100x100x8 te kvadratni profili dimenzija 60x60x6 i 80x80x6. Odlučili smo usporediti upravo te profile budući da su po masi ekvivalent jedni drugima (razlike su zanemarive).
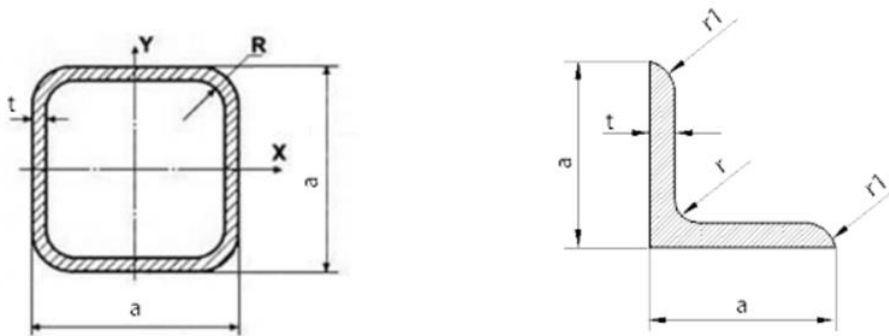
Slika 2 – *Cross sections of square tube and L profiles*

Square Tube Profiles (IHC standard)		
Size [mm]	Thk [mm]	Mass [kg/m]
40x40	2,5	2,89
40x40	4	4,39
50x50	3	4,35
60x60	3	5,29
60x60	6	9,87
70x70	4	8,15
80x80	6	13,6
80x80	8	17,5
90x90	6	15,5
100x100	6	17,4
100x100	8	22,6
100x100	10	27,4

L Profiles (IHC standard)	
Size [mm]	Mass [kg/m]
25x25x3	1,2
25x25x5	1,9
30x30x3	1,5
30x30x5	2,3
40x40x4	2,5
40x40x5	3,1
45x45x5	3,5
50x50x5	3,9
50x50x6	4,6
50x50x8	5,9
60x60x6	5,5
70x70x8	8,4

120x120	8	27,6		80x80x6		7,4
120x120	10	33,7		90x90x8		10,9
150x150	10	43,1		90x90x10		13,5
200x200	10	58,8		90x90x12		16
				100x100x8		12,2
				100x100x10		15,1
				120x120x10		18,3
				120x120x12		21,7
				150x150x12		27,5
				150x150x15		33,9
				200x200x20		60,1

Tablica 1 – *Standard available IHC profile sizes*

Primarno obraćajući pozornost na moment inercije i modul elastičnosti, nismo dobili značajne razlike:

Square Tube 60x60x6 (9.45 kg/m)				L 75x75x8 (9.03 kg/m)			
E	2,06E+11	[N/m^2]		E	2,06E+11	[N/m^2]	- modulus of elasticity
I	6,37632E-07	[m^4]		I	6,01816E-07	[m^4]	- moment of inertia
L	1	[m]		L	1	[m]	- length
ρ	8000	[kg/m^3]		ρ	8000	[kg/m^3]	- density
A	0,001296	[m^2]		A	0,001136	[m^2]	- area
g	9,81	[m/s^2]		g	9,81	[m/s^2]	- gravity

Square Tube 80x80x6 (13.2 kg/m)				L 100x100x8 (12.17 kg/m)			
E	2,06E+11	[N/m^2]		E	2,06E+11	[N/m^2]	- modulus of elasticity
I	1,63155E-06	[m^4]		I	1,48173E-06	[m^4]	- moment of inertia
L	1	[m]		L	1	[m]	- length
ρ	8000	[kg/m^3]		ρ	8000	[kg/m^3]	- density
A	0,001776	[m^2]		A	0,001536	[m^2]	- area
g	9,81	[m/s^2]		g	9,81	[m/s^2]	- gravity

Tablica 2 – *Calculations for modulus of elasticity and moment of inertia for square tube and L profiles*

U daljnjim kalkulacijama koje smo odlučili provesti, obratili smo pažnju na razlike u frekvencijama za navedene profile:

Square Tube 60x60x6 (9.45 kg/m)	
Modes	**Natural frequencies**
1	401,2724264
2	1105,290567
3	2167,587661
4	3582,789522
5	5356,270335

L 75x75x8 (9.03 kg/m)	
Modes	**Natural frequencies**
1	416,3892089
2	1146,929205
3	2249,24528
4	3717,760794
5	5558,052387

Square Tube 80x80x6 (13.2 kg/m)	
Modes	**Natural frequencies**
1	548,3217583
2	1510,3327
3	2961,916641
4	4895,729985
5	7319,116327

L 100x100x8 (12.17 kg/m)	
Modes	**Natural frequencies**
1	561,8827455
2	1547,685955
3	3035,170188
4	5016,810227
5	7500,13129

Tablica 3 – *Comparison of frequencies in square tube and L profiles*

Kod usporedbe frekvencija po njihovim modulima za navedene profile vidljiva je razlika koja se povećava za svaki idući modul. Kada uzmemo u obzir širi spektar profila koji je dostupan u IHC bazi profila, razlika u frekvencijama za kvadratne i L profile sličnih masa je konstantna.

Na sljedećim dijagramima dane su usporedbe mase profila u odnosu na:

1. Moment otpora
2. Moment tromosti
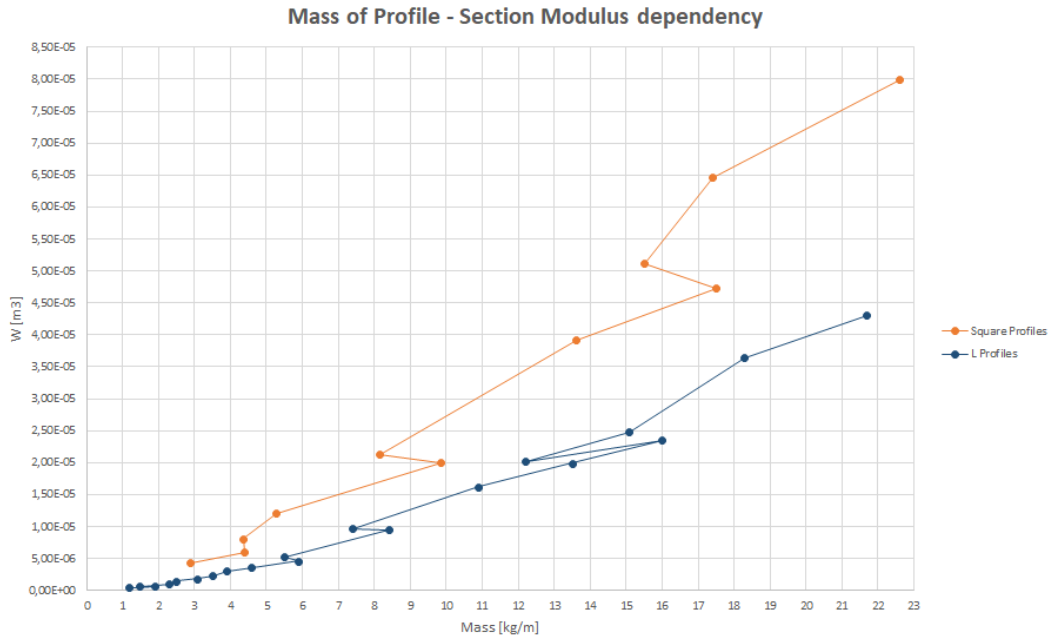
Dijagram 1 – *Mass of profile – Section Modulus depemdency*
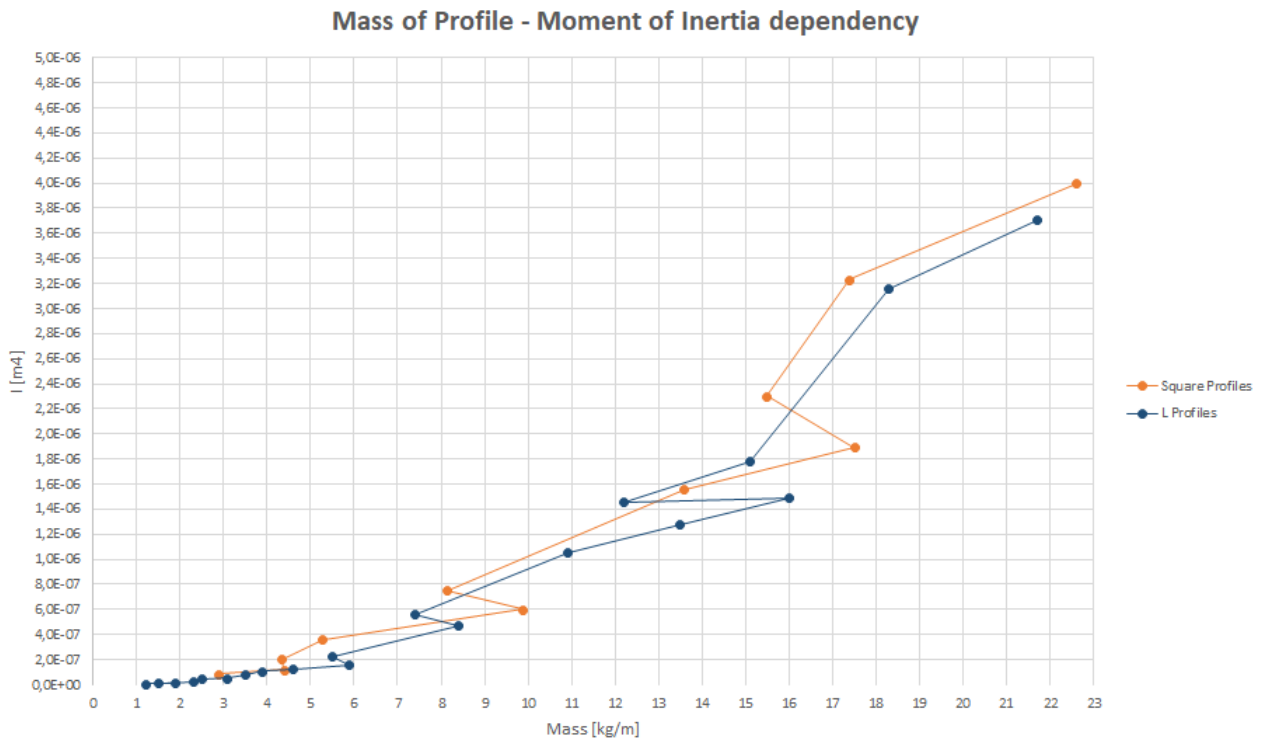
Dijagram 2 – *Mass of profile – Moment of Inertia dependency*

4. Proizvodnja

Posljednja etapa optimizacije u *outfittingu* je u proizvodnji. Još u samim početcima modeliranja osim funkcionalnosti, inženjer mora na umu imati i jednostavnost izvedbe. Kada govorimo o njoj, riječ je o nekoliko aspekata: priprema materijala, vrsta i način izvedbe kod zavarenog spoja te završne obrade (brušenje, farbanje). U ovom području prednost dajemo kvadratnim profilima. Počevši od same uštede prostora, pogotovo u prostorijama kao što je strojarnica u kojima se uvijek javlja problem njegovog nedostatka. Za skoro jednaku masu i ostale promatrane parametre koje smo razmotrili pri odabiru materijala, L profile možemo zamjeniti nešto manjim kvadratnim profilima. Kod samih spojeva profila, kvadratni spoj također ima bolju opciju zavara, kao i realizaciju vijčanog spoja – bolji prijenos vibracija i opterećenja se javlja kada se na kvadratni profil postavi double plate, nego kada imamo direktan spoj na L profilima. Kod montaže i održavanja, kvadratni spojevi imaju lakši pristup i nemaju unutarnje kuteve, što olakšava ali i ubrzava proces.

Slika 3 – *Square profile joint preperation in production*
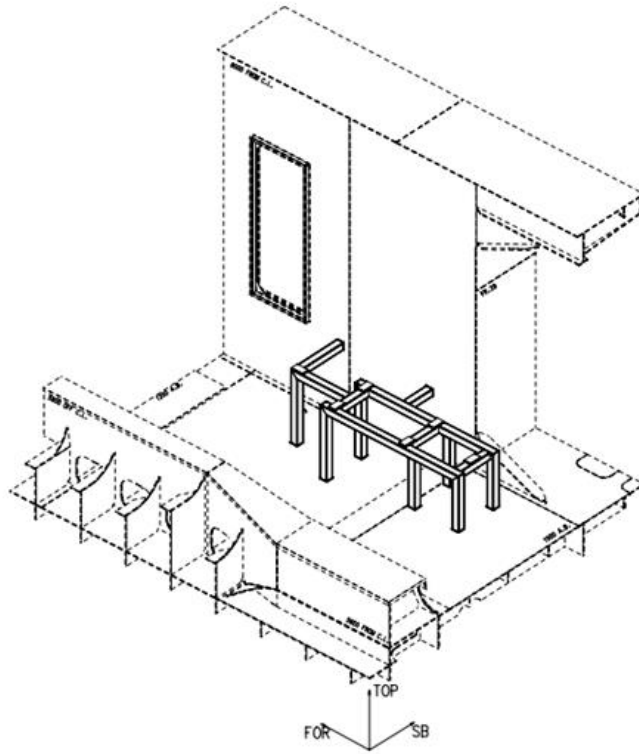
Slika 4 – *Square tube foundation – ISO view*

Slika 5 – *Square tube foundation in production*

5. Zaključak

Na kraju dana, svaki pomak ka boljem treba iskoristiti. Zbog toga i postoji proces optimizacije. Od uvođenja *Check liste,* koja je u suštini samo jedan administrativni korak u procesu, pa do izmjena standarda koje profile koristiti, sve izmjene doprinose efikasnosti sustava proizvodnje što i je krajnji cilj. Kao rezultat uvođenja izmjena dobili smo precizniji i brži protok informacija u uredu čemu je doprinjela Check lista.

Što se konstrukcijske strane tiče, uvođenjem kvadratnih profila, dobit je višestruka.

- Manje zauzeće prostora
- Lakši pristup i održavanje
- Bolji zavarni spojevi
- Veći moment otpora
- Bolje podnošenje vibracija.

Kao rezultat optimizacije dobili smo kvalitetniji proizvod i jednostavniji način rada, a upravo to je ono čemu od početka težimo.

Comparison of cable holder installation methods in pre-outfitting

Ratko Mimica*ᵃ, Tomislav Vasiljᵇ, Mate Purkićᵇ

a Brodosplit R&D ltd., Put Supavla 21/B, 21000 Split, Croatia
b Brodosplit JSC, Put Supavla 21/B, 21000 Split, Croatia
* Corisponding Author, ratko.mimica@brodosplit.hr

Abstract

Previously theorized methodologies of for cable holder installations were compared in this work, along with revision of normative for that process. Qualitative assessment was given for factors which were not considered in previous researches. Further activities were suggested based on new results and additional factors.

Key words: *Stud welding; Secondary cable holders*

Sažetak

U ovom radu uspoređene su prethodno teoretizirane metodologije postavljanja elektrotrasa te su revidirane dosadašnje norme postavljanja. Dat je kvalitativan osvrt na dodatne faktore koji nisu uzeti u obzir prethodnim istraživanjima. Na osnovu novih rezultata i dodatnih faktora predložene su daljnje radnje.

Ključne riječi: *Zavarivanje svornjaka; Sekundarne elektrotrase*

1. Uvod

Postupak postavljanja elektrotrasa opisan je u inicijalnom radu[1]. Uspostavljeno je da tada korišteni postupak postavljanja uključuje dosta međukoraka i resursa u vidu ljudi i vremena, te je u radu teoretiziran prelazak na alternativne metode postavljanja. Od navedenih alternativnih metoda, kao najbrža i najjednostavnija je ocjenjena metoda postavljanja predfabriciranih elektronosača postupkom elektrolučnog zavarivanja svornjaka(DA- Drawn Arc,ili „Nelson" postupak). Izvedena je osnovna prezentacija tehnologije[2]. Osmišljena je metoda višestrukog spajanja nosača i izvedene su osnovne projekcije uštede u slučaju zamjene trasa[3]. Izvor struje i potrebni prilkjučci su nabavljeni i testirana je inicijalna verzija metode [4]. U međuvremenu je i konvencionalna metoda postavljanja elektrotrasa doživjela određene promjene. Trenutno se koristi metodologija opisana u prethodnom radu pod „poboljšanje 1"[1], zavarivanje unaprijed izrezanih perforiranih pocinčanih komada. Ovaj rad bavi se usporedbom metodologija u stvarnim uvjetima rada, a pomoći će da se utvrde ili opovrgnu dosadašnje pretpostavke i točnije normiraju postupci postavljanja elektrotrasa. Obje situacije su razmatrane sa gledišta početka rada. Odnosno aparati i potrebna oprema su na pozicijama rada, pozicije trasa su ocrtane, uređaji su priključeni na odgovarajuće izvore.

2. Eksperimentalni dio

Alternativnom metodom („Nelson" postupak) i konvencionalnom metodom postavljeno je oko 7 i po metara trase, širine 200 mm, na postojećim sekcijama nov. 487, u fazi uranjenog opremanja(NPH, lođa 2). Zavarivanje je u PE(4G) položaju.

Alternativna metoda uključivala je jednog operatera, Hilbig 905i izvor struje za zavarivanje, K22 pištolj za zavarivanje sa potrebnim priključcima za HDO nosače, i HDO nosače sa odgovarajućim keramikama, dimenzije nosača su prethodno definirane u odnosu na nacrt, usuglašene i odobrene od

strane Projektnog ureda odgovornog za elektroinstalacije[5]. Montirano je 7,5 metara kontinuirane trase od kojih je 5 metara bilo na jednoj visini, 2 i po metra na promjenjivoj.

Konvencionalna metoda uključivala je montažera, pomoćnika, zavarivača, dva uređaja za REL zavarivanje(puntavanje i zavarivanje), uređaj za autogeno rezanje(brener), predfabricirane L nosače, predfabricirane perforirane pocinčane elektrotrase standardne dužine(**slika 1**). Montiran je 1 komad od 1,5 metara(4 nosača) i dodatni komad od 6 metara(8 nosača). Taj 6 metarski komad je u zadnjem metru na promjenjivoj visini.

Figure 12 *standard zinc-plated cable tray*
Slika 13 standardizirani komad perforirane pocinčane elektrotrase.

Obje situacije su razmatrane sa gledišta početka rada. Odnosno aparati i potrebna oprema su na pozicijama rada, pozicije trasa su ocrtane, uređaji su priključeni na odgovarajuće izvore.

3. Rezultati i diskusija

3.1. Konvencionalna metoda

Pomoćnik pozicionira početni nosač na mjesto ocrtano na stropu. Montažer „punta" taj nosač sa obje strane. Nakon toga pozicionira se sljedeći nosač na istoj strani trase(**slika 2**).

Figure 2 *positioning and tack welding of cable tray*
Slika 2 Pozicioniranje i puntavanje nosača na unaprijed označena mjesta

Pomoćnik tada pozicionira i pridržava elektrotrasu dok je montažer "punta" za dva postavljena nosača. Slijedi puntavanje dodatna dva nosača na suprotnu stranu trase. Finalna aktivnost je

puntavanje ta dva nosača za strop. Razmak između nosačima je maksimalno metar i po, za duže trase ide više nosača po istim principu postavljanja. Na *slici 3* vidljivi su izgledi spoja nakon puntavanja.

a)   b)
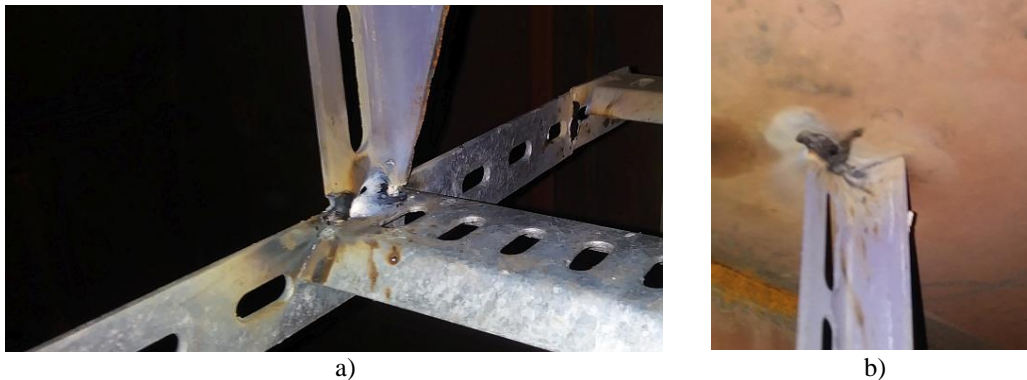
Figure 3 *joint after tack welding. a) on cable tray side; b) on hull side*
Slika 3 Izgleda spojeva nakon puntavanja. a) spoj sa trasom; b) spoj sa stropom

Na krajevima elektrotrasa se iskustveno savija put gore. Za navedeni proces potrebno je dovesti plinski gorionik("brener"), sa njim zagrijati bočne rubove na predviđenom mjestu te ih saviti za određeni iznos. Sličan postupak izvodi se ukoliko trasa mora mjenjati visinu(**slika 4**). Tada se može i odrezati dio trase kako bi se lakše savila. Iako ovakav proces podrazumjeva korištenje dodatnog uređaja, breneri i REL uređaji se uobičajeno nalaze na mjestima opremanja, zaduženi od strane montera.

Figure 4 *bending of cable tray for changing height*
Slika 4 Savijanje zbog promjene visine trase

Nakon faze pozicioniranja slijedi faza zavarivanja i brušenja. Posao je organiziran na način da pomočnik i monter postavljaju elektrotrase po sekcijama a za njima ide zavarivač sa REL uređajem i brusilicom. Vrijeme zavarivanja i brušenja nije mjereno, pretpostavka je da okvirno traje koliko i puntavanje. Detaljizirani proces prikazan je **tablicom 1** a finalni izgled spojeva **slikom 5**.

Figure 5 *joint after welding and grinding. In right bottom corner stud weld could be seen which could give insight in difference between processes*
Slika 5 Izgled spoja nakon zavarivanja i brušenja. U desnom kutu slike vidljiv je nosač ventilacije zavaren postupkom zavarivanja svornjaka koji može poslužiti za okvirnu predođbu razlike između procesa

3.2. Alternativna metoda

U prethodnim radovima pojašnjeni su detalji u vezi opreme, procesa i načina postavljanja višestrukih elektrotrasa[2],[4],[6].

Korištenjem distancera postavljanje višestrukih trasa ide kao što je predviđeno. U odnosu na već opisani postupak u ovom slučaju korišten je distancer određene dužine, taman onolike da se po njemu mogu pozicionirati idući redovi višestrukih nosača(**slika 6a**). Za različitu visinu trase koriste se različite duljine nosača. Za svaku različitu dužinu nosača potrebno je ponovo podesiti dužinu stopa na pištolju. Savijanje na krajevima ili u međuprelazima je jednostavno(**slika 6b**) i ne troši puno vremena[2]. Brušenje nakon zavarivanja nije potrebno, eventualno se odstrani keramička podloška ako nije otpala tijekom procesa.
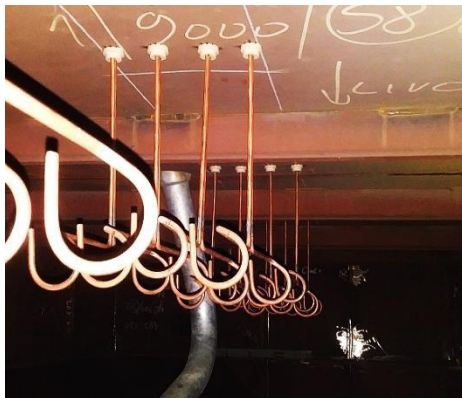
a)   b)

Figure 6 *fourfold cable tray a) general appearance and distance between holders, b) Bending of holders according to drawing*
Slika 6 četverostruka trasa: a) izgled i razmaci između nosača, b) savijanje u skladu sa nacrtom

Table 4 two method comparison on 7,5 meters sample
Table 14 Komparacija dvije metode na 7,5 metara postavljene trase

	Konvencionalna metoda	**Alternativna metoda**
Potrebni broj ljudi	3	1
Potrebne kvalifikacije	Zavarivač za PF i PE položaj	1 operater
	Monter za PF i PE položaj	
	Pomoćnik	
Potrebna oprema	2X REL aparat, Brener, L-profili, Ardic trase	Hilbig 905i, K22, HDO priključci i nosači

Izmjereno vrijeme (min):		
Puntavanje 1,5 m trase	5	-
Puntavanje 6 m trase	10	-
Savijanje kraja trase 2x	4	1
Promjena visine trase(min)	5	4
Zavarivanje*	20	3 min po redu, 13 redova = 50
Brušenje*	5	-
Ukupno za 7,5 m trase (min)	**49**	**55**
*pretpostavljene vrijednosti za konvencionalnu metodu		

Prethodnim pretpostavkama[3] predviđen je omjer 1:4 u korist alternativne metode glede brzine rada. Izmjereni omjer je ispod 1:3. Glavne razlike u odnosu na pretpostavku su vremena postavljanja višestrukih nosača. Početno je pretpostavljena brzina postavljanja od 3 nosača/min, dok je u stvarnim uvjetima brzina bila skoro dvostruko sporija. Razlog tomu je dio vremena izgubljen na pozicioniranje distancera, i dio vremena izgubljen odlaskom po nosače. Sa eventualnim pomoćnikom na raspolaganju proces bi se mogao dodatno ubrzati, uz standardno ubrzanje procesa stjecanjem potrebnog radnog iskustva i boljom organizacijom mjesta rada (normirano je vrijeme montera sa 30 godina iskustva postavljanju trasa u odnosu na tek obučenog operatera bez velikog prethodnog iskustva u postavljanju). Tako da je za očekivati povoljniji omjer od izmjerenog.

4.2.1   Dodatni faktori

Unatoč sporijem vremenu od originalno predviđenog, svejedno se potvrdilo da je proces brži, lakši i jeftiniji. Međutim, uočena su i dodatna dva faktora koja mogu utjecati na ukupnu učinkovitost procesa. Prvi od tih faktora je raspoloživost uređaja. REL uređaji i uređaji za plinsko rezanje mogu naći u više manje-svakoj sekciji u predmontaži, i imaju višestruku primjenu. Hilbig 905i je specijalizirani aparat trenutno jedini u brodogradilištu. Što sugerira zaduživanje aparata isključivo za postavljanje trasa i razduživanje istog odmah nakon postavljanja. Drugi faktor je dužina trase koja se zamjenjuje, u dosadašnjim slučajevima radilo se o nadgrađu nov 487, sa ukupno 45 metara trase koja se zamjenjuje (*tablica 2*). Od mogućih zamjena dvije trećine su manje od 7 i po metara(koliko je promatrano u radu).

Tablica 2 Dogovoreni obim zamjene po sekcijama nadgrađa na nov. 487 [5]

Table 2 agreed scope of replacement though sections nov. 487[5]

redoslijed dizanja	grupa	faza ugradnje	nacrt	Ardic			potreban broj HDO nosača				težina (kg)	vrijeme(h)
				dužina (m)	težina (kg)	vrijeme(h)	60	100	150	250		
31	527	60	60.981.527.800	13	43,84	4,29				130	20,07	0,87
36	543	60	60.981.543.800	2	6,74	0,66		20			3,09	0,13
36	534	60	60.981.534.800	1	3,37	0,33				10	1,54	0,07
33	518	60	60.981.518.800	1	3,37	0,33				10	1,54	0,07

33	518	60	60.981.518.800	12	40,46	3,96		20		100	18,53	0,80
32	523	90	-	8	26,98	2,64			80		12,35	0,53
40	512	60	60.981.512.800	3,5	11,80	1,16		4		32	5,40	0,23
39	537	60	60.981.537.800	velika visina i dosta prelaza, ne preporuča se zamjena								
32	513	60	60.981.513.800	vertikalno i na sekcijskom spoju, ne preporuča se zamjena								
32	523	60	60.981.513.800	vertikalno i na sekcijskom spoju, ne preporuča se zamjena								
26	525	60	60.981.525.800	vertikalno, ne preporuča se zamjena								
34	519	60	60.981.519.800	1,5	5,06	0,50				12	2,32	0,10
34	519	60	60.981.519.800	velika razlika u visini u odnosu na duljinu trase, ne preporuča se zamjena								
41	538	60	60.981.538.800	1,5	5,06	0,50				12	2,32	0,10
38	533	60	60.981.533.800	vertikalno, ne preporuča se zamjena								
ukupno				43,5	146,7	14,4		44	80	306	67,2	2,9

Sekcije se izrađuju jedna po jedna a to znači da bi za nastavak zamjene u ukupni proces trebali uključiti i proces zaduživanja, dopremanja, razduživanja i otpremanja stroja na dnevnoj bazi, za prosječno 40 min posla po sekciji. Opcija da uređaj bude zadužen cijelo vrijeme se ne preporučuje, jer smanjuje učinkovitost i raspoloživost uređaja, što je poseban problem kod specijaliziranih visokoučinkovitih uređaja. Kod konvencionalnog procesa potrebni uređaji već se nalaze na mjestu rada(zavarivanje širih elektrotrasa), oni nisu unikatni niti visokovrijedni, pa rad sa niskom produktivnošću ne utječe na ukupni sustav kao da se radi o visokospecijaliziranom uređaju.

Poboljšanje bi se moglo postići reorganizacijom načina rada kod opremanja sekcije. Područje rada Hilbig 905i uređaja nije ograničeno samo na postavljanje elektrotrasa, sa njim se mogu postavljati ostali električni dodaci(nosači utičnica i kutija[2]), nosači ventilacije(**slika 7**) i lakih cijevi, kao i izolacijske „canke"[4]. Hilbig 905i je, kao što je rečeno, specijalizirani uređaj, što znači da u tom području rada ne postoji bolji način obavljanja posla. Pa bi novi organizacijski cilj mogao biti maksimiziranje posla na način da se pripreme svi potrebni radovi i dodaci koji se u toj fazi opremanja mogu zavarivati sa uređajem. Tek onda da se zaduži uređaj, obavi potrebno zavarivanje i nakon toga razduži.

Figure 7 *stud welded ventilation hangers behind cable trays*
Slika 7 Ovjesi ventilacije zavareni "nelson postupkom" vidljivi iza elektrotrase

Jedan od glavnih razloga za primjenu alternativnog postupka je sigurnost na radu. Može se desiti da kod rada u naglavnom položaju dođe do pojave prskotine(obavezno je korištenje rukavica i zaštite za oči[6]). Međutim, prskotina je višestruko manje i manjih su dimenzija u odnosu na uočeno prskanje(**slika 2**) u bilo kojoj fazi korištenja REL postupka. U kasnijim fazama opremanja, zbog ugrađene opreme i obloge, prskanje predstavlja puno veći sigurnosni rizik dok u ovoj fazi uranjenog opremanja to nije toliko problematično (ostali načini pričvršćenja elemenata također rezultiraju prskotinama).

4. Zaključci

Do sad teoretizirani postupak upotrebe višestrukih HDO elektrotrasa uspoređen je na stvarnim sekcijama sa konvencionalnim načinom postavljanja. Na osnovu dobivenih mjerenja na trasi širine 200mm, duljine 7,5 metara revidirane su dosadašnje norme postavljanja.

Zabilježena prosječna brzina postavljanja HDO nosača iznosi 4 nosača u 3 min umjesto pretpostavljenih 3 nosača/min. Za četverostruku trasu izmjerena brzina iznosi oko 7,5 m/h po čovjeku umjesto predviđenih 15 m/h. Stjecanjem iskustva i boljom organizacijom rada moguće je dodatno ubrzanje procesa.

Kod zavarivanja klasičnim načinom zabilježeno je vrijeme postavljanja od 9 m/h, što je veće od originalno pretpostavljenih 3 m/h. Ali kako proces zahtjeva montažera, pomoćnika i zavarivača, brzina po čovjeku je i dalje 3 m/h.

Ispitivanjem na stvarnim sekcijama uočeni su dodatni faktori koje treba uzeti u obzir prilikom planiranja procesa. Uređaj je jedini u brodogradilištu pa je raspoloživost kritična, a predviđene dužine zamijenjenih trasa su veličine par metara. Stoga nije produktivno korištenje uređaja u ovoj fazi samo za ovu primjenu(nov. 487, ostale sekcije), jer u vremenu dok se stroj zaduži i dopremi, konvencionalnim načinom se montiraju navedeni dijelovi.

Buduću organizaciju posla bi trebalo prilagoditi na način da se maksimizira količina posla koju uređaj može obaviti u jednom zaduživanju u jednoj sekciji u jednoj fazi opremanja. To obaviti širenjem područja primjene uređaja i/ili drugačijim projektiranjem elektrotrasa.

Zabilježena veća pojava prskanja kod klasičnog načina postavljanja elektrotrasa nije toliki nedostatak u ovoj fazi opremanja(uranjeno),ali REL i slične prskajuće postupke svakako izbjegavati ili minimizirati u daljnjim fazama izgradnje broda.

REFERENCES

[1]   Ratko Mimica, Marko Tödtling, Studij rada i vremena: izrada i montaža ovjesa elektroinstalacija, *Sorta 2018*

[2]   Ratko Mimica et al., Zapisnik sa prezentacije tehnologije zavarivanja sekundarnih elektrotrasa postupkom elektrolučnog zavarivanja svornjaka, *Sorta 2018*

[3]   Ratko Mimica, Prijedlog širenja područja upotrebe predfabriciranih elektrotrasa, *interni rad*, Brodosplit R&D

[4]   Ratko Mimica, Zapisnik sa inicijalnog testiranja uređaja za zavarivanje svornjaka Hilbig 905i i komparativnog testiranja predfabriciranih nosača i izolacijskih „canki" *Sorta 2020*

[5]   Ratko Mimica, Prijedlozi izmjena trasa nadpalubnih sekcija u odnosu na redoslijed uranjenog opremanja: *interni rad*, Brodosplit R&D

[6]   Ratko Mimica, Skraćena uputstva za korištenje Hilbig 905i i K22, *interni rad*, Brodosplit R&D

Initial testing of Hilbig 905i stud welding machine with comparative tests of secondary cable holders and isolation pins

Ratko Mimica*[a], Damir Ivančić[b], Mario Livajić[c], Mladen Komšić[c], Maroje Elek[c], Vrdoljak Ivan[c]

a Brodosplit R&D ltd., Put Supavla 21/B, 21000 Split, Croatia
b Div Group ltd., Bobovica 10/A HR-10430 Samobor
c Brodosplit JSC, Put Supavla 21/B, 21000 Split, Croatia
* Coresponding Author, ratko.mimica@brodosplit.hr

Abstract

Initial testing of a portable stud welding machine acquired for Brodosplit was conducted in this work. Machine primary purpose is stud welding of secondary cable holders. To ensure that machine works properly, all required functions were tested in real work conditions. Comparative tests of prefabricated electric holder manufacturers and isolation pins were also conducted. Additional testing equipment was defined and tested. Activities needed for project continuation were suggested.

Key words: Stud welding; secondary cable holders; isolation pins

Sažetak

U ovom radu obavljeno je inicijalno ispitivanje uređaja nabavljenog za potrebe Brodosplita. Radi se o portabilnom uređaju za zavarivanje svornjaka prvenstveno namijenjenom zavarivanju nosača sekundarnih kabelskih trasa. Kako bi osigurali da je uređaj u ispravnom stanju, obavljena su testiranja potrebnih funkcija u stvarnim uvjetima rada, komparativno testiranje proizvođača predfabriciranih nosača kao i proizvođača izolacijskih pinova korištenih za postavljanje izolacije. Definirana je i testirana dodatna oprema te predložene radnje za nastavak projekta.

Ključne riječi: Zavarivanje svornjaka; Nosači sekundarnih elektrotrasa; Izolacijski pinovi;

1. Uvod

Uređaj za zavarivanje svornjaka spada u visokospecijalizirane uređaje, što znači da se na uštrb široke primjenjivosti ostvaruje izrazita produktivnost i kvaliteta spoja, samo u užem području primjene. Isplativost takvog uređaja je, osim same cijene, funkcija potencijalnog područja primjene i načina rada sa tim strojem, stoga je prije nabavke uređaja:

- istraženo glavno područje primjene[1],

- predloženo širenje područja primjene [2], [3],

- obavljena prezentacija tehnologije[4].

- analizirano širenje glavnog područja i kvantificirane potencijalne uštede[5].

Na osnovi navedenih radnji nabavljen je analizirani uređaj. Prije predaje uređaja pogonu, potrebno je ispitati osnovne postavke, postaviti parametre, definirati i osigurati potrebnu opremu, izraditi potrebna uputstva, te finalno i možda najbitnije, osmisliti način upravljanja strojem kako bi se izbjegao već evidentirani obrazac neadekvatnog odnosa prema sličnoj opremi[6].

2. Eksperimentalni dio

Ispitivanje je provedeno u prostorijama MOK-a, hala 5. Uređaj Hilbig 905i isporučen je sa uputstvima na engleskom, pištoljem za zavarivanje K22, setom priključaka za predfabricirane trase i kabelom mase. Originalna uputstva na engleskom, u papirnatom i digitalnom obliku na raspolaganju su kod službe PEN. Zavarivanje je obavljeno na konstrukciji napravljenoj od ostataka rezanja dijelova trupa nov 805, radi se o klasičnom brodskom limu. Zavarivani su predfabricirani nosači trasa dva proizvođača(E1 i E2), i izolacijski pinovi, tzv. „canke", također od dva proizvođača(C1 i C2). Kod ispitivanja zavarljivosti canki korišten je pištolj za zavarivanje SK14 sa potrebnim priključcima, za dodatnu provjeru rezultata korišten je dodatni uređaj Hilbig Elotop 502.

3. Rezultati i diskusija

Ispitivanje se može podijeliti u tri dijela: osnovne funkcije i potrebna oprema, zavarivanje predfabriciranih elektronosača, zavarivanje izolacijskih canki.

3.1. Osnovne funkcije i potrebna oprema

Prvi nedostatak je nepostojanje uputa na hrvatskom jeziku za navedeni uređaj. Dostavljen je papirnati oblik na engleskom i, nakon inzistiranja, digitalna verzija, također na engleskom. Budući da trenutni zaposlenici nemaju obvezu poznavanja engleskog postavlja se pitanje kako osigurati da se ono što je unutra napisano ispoštuje, kao garanciju dugovječnosti rada sa strojem. Iz tog razloga je napisana skraćena verzija uputstava na hrvatskom jeziku[7] te prijedlog kontrolne liste za radnika na stroju i odgovornog inženjera[8].

Nakon upoznavanja sa uputstvima uređaj je postavljen u zavarivački strujni krug. Drugi primijećeni nedostatak je kratak kabel pištolja(kabel je dvostruki: strujni i kontrolni). Originalni kabel na pištolju je oko dva metra dužine, što onemogućava široko područje rada bez pomicanja uređaja. Iako uređaj nije teško pomicati (težina samog uređaja 18kg), bilo kakvo pomicanje uređaja spada u procese koji ne dodaju vrijednost te ih je potrebno minimizirati ili, ukoliko je moguće izbaciti. Iz tog razloga PEN je naknadno isporučio dva produžna kabela za pištolj, jedan je dužine 20 metara, drugi 5 metara. 20 metarski produžni kabel je testiran i u ispravnom stanju. Problem je što je teži od samog uređaja, pa se postavlja pitanje praktičnosti i portabilnosti cijelog sustava. Taj kabel može biti na raspolaganju u posebnim uvjetima rada, za inače se sugerira korištenje kraćeg produžnog kabela.

Manji produžni kabel je testiran i u ispravnom stanju. Uređaj i ostali dijelovi zavarivačkog strujnog kruga su prikazani na **slici 1**.
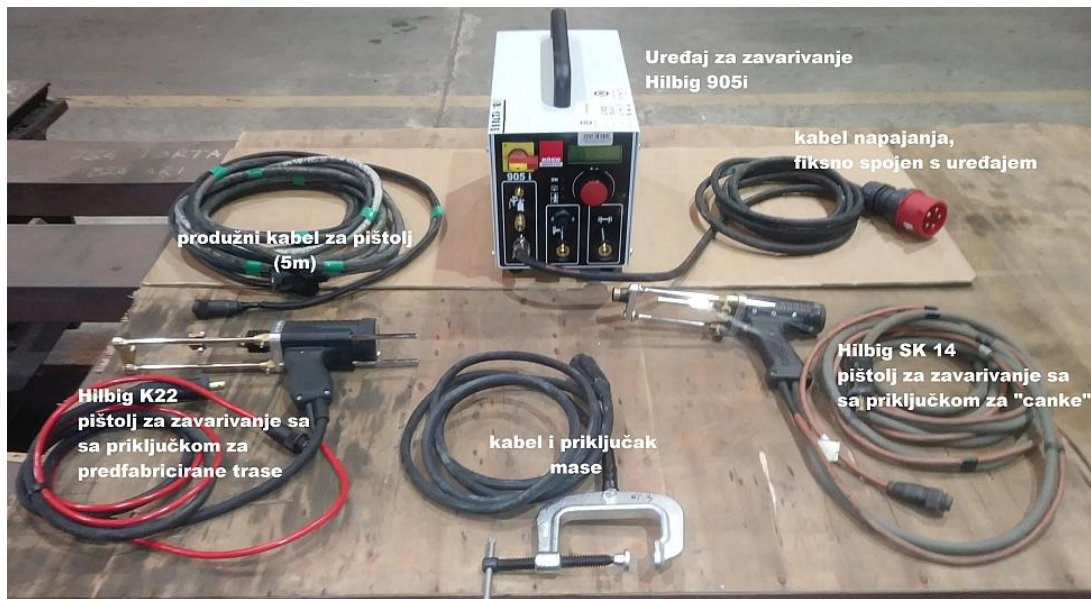
Figure 15 *complete system for welding electric cable holders and isolation pins*

Slika 16 kompletirani sustav za zavarivanje canki i predfabriciranih elektronosača.

3.2. *Zavarivanje predfabriciranih elektronosača (E1 vs. E2)*

Zadatak ovog dijela ispitivanja je dobiti ponovljive i kvalitetne rezultate. Polazišna točka su parametri sa inicijalnog ispitivanja opreme[4]. Korištene su originalne predfabricirane trase proizvođača E1(zavari 1-8) i zamjenske predfabricirane trase proizvođača E2 (ostali). Ispitane su sve duljine trase. Dubina uranjanja je održavana na oko 4.5 mm, dubina odizanja je ostavljena konstantnom na vrijednosti 2.5 mm. Varijabilni parametri i komentari pojedinih zavara prikazani su **tablicom 1**. Zavarivano je u PA i PC položaju.

Table 5 welding parameters used for electric cable holders

Table 17 Korišteni parametri zavarivanja predfabriciranih nosača

Zavar br:	Jakost struje [A]	Vrijeme trajanja [s]	HDO L= [mm]	Izgled	Komentar
1-2	550	0.55	150	Ok	Brušena podloga
3	550	0.55	150	Ok	Shop primer podloga nadalje
4	**500**	0.55	150	Ok	
5	500	**0.5**	100	Ok	
6	500	**0.45**	100		Vidljive naznake zajeda kod nedovoljnog provara
7-8	500	**0.5**	100	Ok	PC položaj zavarivanja
9	**550**	**0.55**	100	Ok	E2 proizvođač nadalje
10	**500**	**0.5**	100	Ok	

11	550	0.55	250		Izgleda nedovoljno provaren
12	600	0.55	250		Pojava prskanja izvan keramičke podloške
13	600	0.55	250		Vertikalno, pojava nesimetričnog provara
14	500	0.5	250	Ok	Smanjena nesimetričnost

Uočljiva je neravnomjernost provara, pogotovo kod zavarivanja u vertikalnom (PC) položaju(**slika 2**). 70% zavara podvrgnuto je naknadnom testu na savijanje. Unatoč neravnomjernom provaru svi uzorci su izdržali višestruke prijevoje bez pojave pukotina (**slika 3**). Slični rezultati zabilježeni su pri inicijalnom ispitivanju[4].

Trase proizvođača E2 nemaju bakreni metalni sjaj kao E1. Također, tehnološki je drugačije riješen spoj centralnog nosača, ali osim vizualno lošijeg izgleda, nije uočena procesna razlika. Dodatno je primijećeno da postoji razlika u simetričnosti u odnosu na centar nosača, nesimetričnost nije krucijalna za proces niti za izvedbu(od proizvođača je zatraženo očitovanje). Nije zabilježena razlika u rezultatima zavarivanja između E1 i E2 proizvođača.

a)   b)

Figure 18 lack of weld symmetry in PC welding position

Slika 2 Neravnomjernost provara kod zavarivanja u PC položaju
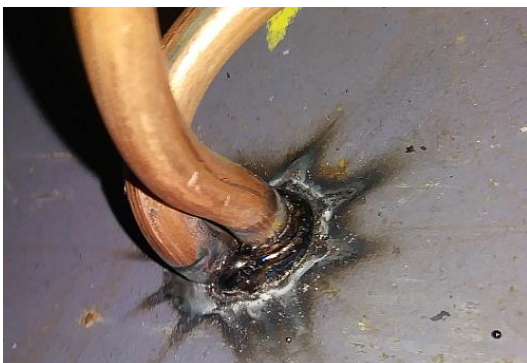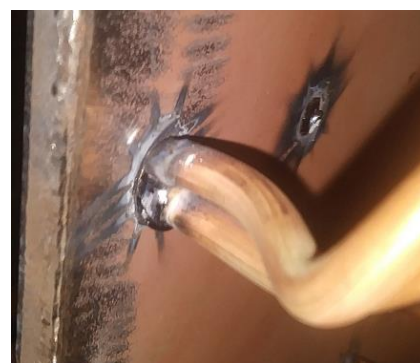
a)   b)

c)

Figure 3 multiple bending's of cable holder without cracking: a) unsymmetrical PA weld,
b) non symmetrical PC, c) symmetrical PA weld

Slika 3 Višestruki prijevoji bez pojave pukotina na: a)neravnomjerno protaljenom; b)
neravnomjernom vertikalnom i c)ravnomjerno zavarenom uzorku

Druga stavka koju je bilo potrebno testirati je praktična primjenjivost tehnologije postavljanja vise kanalnih sekundarnih trasa opisanih u prethodnom radu[5] i brodskoj proceduri SBU 900 67618 NOSAČI KABELA – HILBIG HDO[9]. Osnovna ideja je postavljanje predfabriciranih trasa umjesto klasičnih „Ardic" elektrotrasa. Kako bi se zadržali u gabaritima trase koja se zamjenjuje potrebno je predfabricirane nosače postaviti na način da su bočno minimalno udaljeni jedan od drugog.

3.2.1 Problem i rješenje problema

Prilikom postavljanja prvih višestrukih trasa uočen je problem sa ovom tehnologijom. Naime, pokušajem zavarivanja u što bližoj poziciji susjednom nosaču postoji vjerojatnost da se ta dva nosača dotaknu. Ukoliko se u tom trenutku stisne okidač na pištolju, umjesto da aktivira električni luk neophodan za zavarivanje, struja će proći kroz mjesto dodira sa susjednim nosačem.

Naravno, uvijek se može više paziti prilikom zavarivanja, ali time se znatno komplicira i odužuje ukupni proces, pogotovo u situacijama gdje je naprimjer višestruku trasu potrebno postaviti naglavno sa već postavljenim ostalim instalacijama.

Drugo rješenje bi bilo savijanje nosača nakon zavarivanja, zavarivanje idućeg nosača i onda vraćanje prvotnog u početni položaj. Međutim kao i u prvom slučaju, dodatnim procesima znatno utječemo na produktivnost procesa.

Treće rješenje je distancer između dva trenutno zavarivana nosača. Nije bitno u kojem obliku, dok zadovoljava dva kriterija:

1. Jednostavno se i brzo postavlja i skida sa nosača,
2. posjeduje izolatorska svojstva u predviđenim režimima rada uređaja.

Za testiranje je odabran odbačeni komad PVC kanalice dimenzija 60x40 mm, koji je relativno jednostavno modificirati na dužinu i oblik nosača(**slika 4**).

a)   b)

Figure 4 Two way mounting option for isolation piece

Slika 4 Mogućnost postavljanja distancera na obje strane nosača

Osim što zadovoljava postavljene uvjete kanalica je lagana, dostupna i jeftina. Postavljanje i skidanje traje ispod 3 sekunde. Sa postavljenom kanalicom na već zavareni nosač moguće je prisloniti nosač koji trenutno zavarujemo i aktivirati luk. U niti jednom pokušaju nije zabilježen kratki spoj. Treba pripaziti da je pištolj prislonjen na način da se ne blokira povrat pištolja unazad(visina odizanja). To je jednostavno ispoštovati ukoliko je kanalica okrenuta paralelno sa smjerom povrata pištolja i ukoliko se nosač ne prislanja jako tijekom okidanja.

Ovim načinom uspješno je pozicionirana dvostruka i trostruka trasa(**slika 5**), dodatak u vidu distancera je potrebno ubaciti u postojeću proceduru. Radi testiranja krajnjih mogućnosti slaganja, postavljena je deseterostruka trasa na 4 nivoa (**slika 6**). Takav način postavljanja bi bilo zanimljivo istražiti u budućnosti, ali za sada bi fokus trebao biti povratna informacija iz pogona o primjenjivosti tehnologije postavljanja kabela na ove tipove nosača.
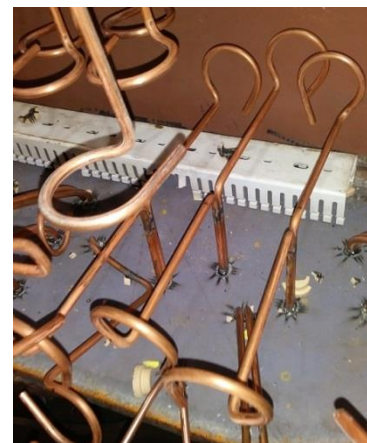
a)   b)

Figure 5 positioning of a) double , b) triple cable holder line

Slika 5 Izgled postavljene a) dvostruke, b) trostruke predfabricirane trase

Figure 6 Tenfold cable holder positioning on 4 levels. Upper level consist of 4 HDO 60 cable holders, below them are 4 HDO 150, left of them is HDO 100 and in lower right corrner HDO 250

Slika 6. Deseterostruka predfabricirana trasa na 4 nivoa. Gornja 4 nosača su HDO 60, odmah ispred(ispod) njih su 4 kom HDO 150, krajnji lijevi je HDO 100, u donjem desnom kutu je vidljiv HDO 250

3.3. *Zavarivanje izolacijskih "canki" (C1 vs. C2)*

Osim zavarivanja predfabriciranih elektrotrasa potrebno je uređaj osposobiti i za zavarivanje izolacijskih canki, ne toliko za potrebe oblaganja(Oblaganje zadužuje svoje strojeve), već zbog mogućnosti upotrebe canki kao nosača manjeg broja kabela, opisanog u istoimenom radu[3]. Stoga je potrebno utvrditi parametre i područje primjene. Iako kupljeni pištolj K22 ima mogućnost priključivanja nosača za canke, zbog jednostavnosti uporabe postupka(potrebno je demontirati postojeće nosače te montirati, centrirati i stegnuti nove. Proces ponoviti prilikom svake izmjene) preporuča se korištenje dodatnog pištolja SK14 sa već postavljenim nosačima canki(**slika 1**). Za početna ispitivanja korištene su canke dimenzija Ø3x100 mm. Dubina urona je postavljena na oko 1.5mm, visina odizanja je standardna i ne može se podešavati na SK14 pištolju. Na osnovi uputstava pokušani su osnovni parametri prikazani u **tablici 2.**

Table 2 welding parameters used for insulation pins

Table 2 Korišteni parametri zavarivanja izolacijskih canki

Zavar br:	Jakost struje [A]	Vrijeme trajanja [s]	Izgled	Komentar
1-2	300	**0.3**	-	nije ostvaren spoj, protaljeno
3	**300**	**0.125**		nije ostvaren spoj, protaljeno
4	**200**	**0.2**		nije ostvaren spoj, protaljeno
5	200	**0.15**	-	nije ostvaren spoj, protaljeno
6-7	200	**0.1**	OK	

8	**300**	**0.05**	OK	
9-35	**320**	0.05	OK*	
36-51	**250**	0.05	OK*	
52-66	**450**	**0.03**		testirano na Elotop 502, C2 samo
*ocjena vrijedi samo za jednog proizvođača				

Kod početnih zavara je ustanovljen višak energije protaljivanja, koji se manifestira izgaranjem canke i ne ostvarivanjem spoja. Idući zavari išli su u smjeru smanjenja energije zavarivanja. Od zavara 8 korišteni su postojeći iskustveni parametri radnika oblaganja koji su se pokazali uspješnima.

Tablica 2 odnosi se na parametre koji su korišteni prilikom zavarivanja C1 canki. Trenutno je u opticaju i druga verzija canki(proizvođač C2). Time se otvorila prilika za komparativni test proizvođača pod jednakim parametrima, sa dodatnom mogućnošću kontrole uz upotrebu zasebnog izvora struje (**slika 7**):
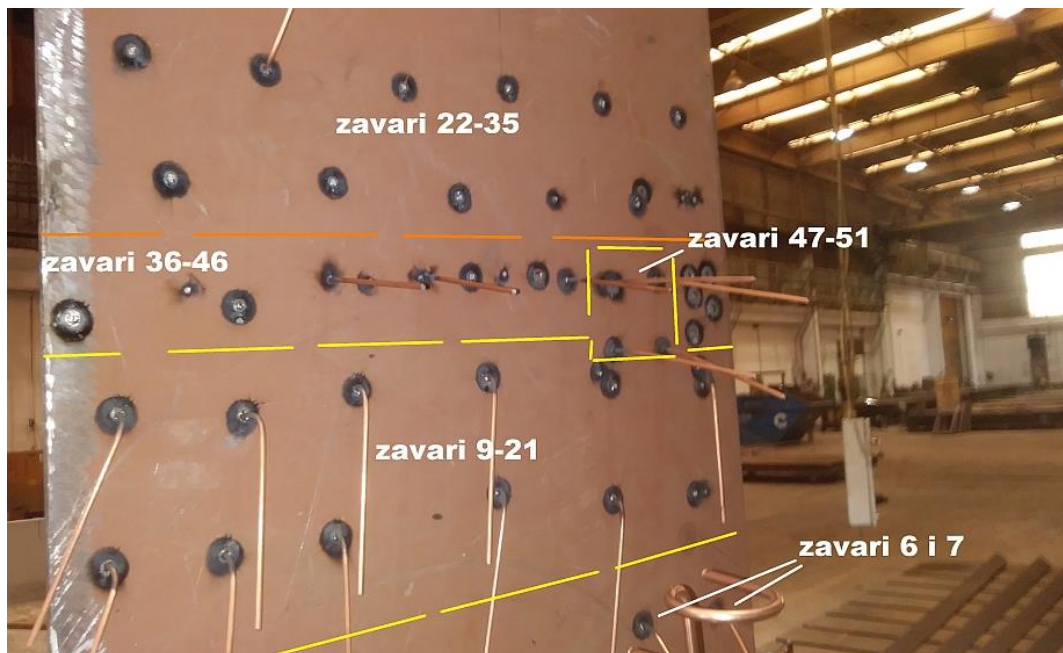
Figure 7 *comparative test results of isolation pins*

Slika 7 rezultati komparativnog testiranja izolacijskih canki.

- Zavari 9-21 su obavljeni sa C1 cankama, od 12 canki dvije su pukle kod višestrukog savijanja.
- Zavari 22-35 su obavljeni sa C2 cankama, po istim parametrima, rezultati suprotni, jedna u redu, ostale slomljene prije prvog punog previjanja.
- Zavari 36-46, C2 canke, pokušana promjena parametara, od 10 pokušaja niti jedna nije izdržala višestruke prijevoje.
- Zavari 47-51, korištene C1 canke za iste parametre, sve 4 canke izdržale višestruka previjanja.

– Zavari 52-66, korišten dodatni stroj Hilbig Elotop 502, procesni parametri(kojima se inače zavaruju C1 canke u pogonu) i C2 canke. Nije ostvaren kvalitetan spoj. Od 15 canki samo tri su ostale nakon pokušaja previjanja

Primijećeno je da su C1 canke manje osjetljive na promjene parametara, (uspješni zavari ostvareni su sa više različitih parametara, *Tablica 2*), dok je kod C2 canki vrlo mala razlika između struje koja je u potpunosti protali i ne ostvari spoj, u odnosu na struju koja neće prouzročiti dovoljno protaljivanja da ostvari spoj.

Kako je evidentno da nije do parametara, do materijala na koji zavarujemo, do pištolja niti do izvora struje, razlozi za ovakvu lošu zavarljivost C2 canki bi mogli biti u materijalu. Iz tog razloga je napravljena kemijska analiza od strane BIS Laboratorija[10], rezultati analize su u **tablici 3**.

Table 3 chemical composition of tested pins

Table 3 kemijski sastav ispitivanih canki

Uzorak:	C	Si	Mn	P	S	Cr	Ni
C1	0,068	0,22	0,35	-	0,011	-	-
C2	0,065	0,23	0,29	-	0,025	-	-

Osim manjeg postotka ugljika(što bi trebalo biti pogodnije za zavarljivost) bitna razlika je u postotcima mangana i sumpora. Sumpor je nečistoća i općenito ga treba biti što manje. Mangan po nekim istraživanjima[11] može voditi manjoj osjetljivosti ka stvaranju pukotina te finozrnatijoj strukturi protaljenog dijela materijala(bolja žilavost). Druga istraživanja navode[12] da za potrebe zavarivanja omjer mangana i sumpora trebao biti 10:1(što je skoro slučaj kod C2, kod C1 je puno manji) ali isto tako navode da količina ispod 0.30%Mn(C2 canke) može voditi porozitetu i pucanju u protaljenom dijelu.

4. Zaključci

U ovom radu obavljena su testiranja uređaja za zavarivanje svornjaka nabavljenog za potrebe Brodosplita. Uređaj Hilbig 905i je testiran u stvarnim uvjetima rada, sa namjenom postavljanja predfabriciranih nosača elektrotrasa i postavljanja izolacijskih canki. Uređaj radi kako je predviđeno.

Osim uređaja, testirani su: pištolj Hilbig K22 sa priključkom za elektrotrase; pištolj Hilbig SK 14 sa priključkom za canke; priključak mase; dvostruki produžni kabeli za pištolj duljine 5 i 20 m. Kabel od 5 m se preporuča koristiti uz pištolj K22. Kabel dužine 20 m zbog glomaznosti koristiti samo u posebnim prilikama. Sva testirana oprema radi kako je predviđeno.

Ispitani su parametri za zavarivanje predfabriciranih trasa. Zamijećena je pojava nesimetričnosti zavara, pogotovo u vertikalnom(PC) položaju. Unatoč nesimetričnosti svi testirani zavari su izdržali višestruka previjanja.

Testirana je primjenjivost procedure SBU 900 67618 NOSAČI KABELA – HILBIG HDO. Procedura je primjenjiva uz preporuku upotrebe distancera za nosač. Ukoliko je potrebno, moguće je pozicionirati višestruke elektrotrase na više nivoa.

Napravljena je komparativna analiza dvaju proizvođača predfabriciranih elektrotrasa: E1 i E2. Rezultati su pokazali da, osim vizualnih, nema procesnih razlika između njih.

Napravljena je komparativna analiza dvaju proizvođača izolacijskih canki: C1 i C2. Rezultati su pokazali da C2 canke imaju izrazito lošu zavarljivost u testiranim uvjetima. Ispitivanjem su izolirani svi faktori osim materijala canke. Kemijskom analizom je ustanovljen manjak mangana uz veći postotak sumpora u C2 cankama, što može biti razlog loše zavarljivosti.

5. Daljnje radnje

U radu je testirana tehnologija u fazi pričvršćivanja nosača. Prije širenja područja primjene neophodna je potvrda pogona da sve funkcionira kako je predviđeno u fazi postavljanja kabela na višestruke trase.

Kako bi se osigurala dugovječnost rada potrebno je educirati zaposlenike o pravilnom radu sa uređajem i njegovom održavanju. U tu svrhu originalna uputstva su prevedena na hrvatski jezik(skraćena verzija).

Sadašnji sustav upravljanja uređajima za zavarivanje nije adekvatan za praćenje rada ovog stroja. Predložena je check-lista za radnika i odgovornog inženjera/brigadira.

Ispitivanjem je vrlo jednostavno postavljena deseterostruka trasa na 4 nivoa. Jednostavnost i prilagodljivost ovakvog sustava postavljanja elektrotrasa bi svakako trebalo razmotriti u fazi projektiranja budućih novogradnji.

REFERENCES

[1]   Ratko Mimica, Marko Tödtling. Studij rada i vremena: izrada i montaža ovjesa elektroinstalacija, *Sorta 2018*
[2]   Ratko Mimica, Srđan Stefanović. Zamjena dosadašnje tehnologije zavarivanja Nelson ekvivalentima– područje primjene, standardi i primjeri iz prakse, *Sorta 2018*
[3]   Ratko Mimica, Mogućnosti uporabe „canki" kao sekundarnih elektrotrasa za manji broj kabela, *interni rad*, Brodosplit R&D
[4]   Ratko Mimica *et al*., Zapisnik sa prezentacije tehnologije zavarivanja sekundarnih elektrotrasa postupkom elektrolučnog zavarivanja svornjaka *Sorta 2018*
[5]   Ratko Mimica, Prijedlog širenja područja upotrebe predfabriciranih elektrotrasa, *interni rad*, Brodosplit R&D
[6]   Ratko Mimica, Korištenje starih i uvođenje novih tehnologija (problem orbital TIG i aparata za zavarivanje svornjaka), *interni rad*, Brodosplit R&D
[7]   Ratko Mimica, Skraćena uputstva za korištenje Hilbig 905i i K22, *interni rad*, Brodosplit R&D
[8]   Ratko Mimica, Prijedlog checkliste odgovornosti stroja Hilbig 905i, *interni rad*, Brodosplit R&D
[9]   Milardović Marina, SBU 900 67618 NOSAČI KABELA - HILBIG HDO, standardi brodogradilišta Split,
[10]   Bajlo Barbara, Ugrina Teo, IZVJEŠTAJ O ISPITIVANJU KEMIJSKOG SASTAVA MATERIJALA KEM/KS2-07/2019, Brodosplit Laboratorij
[11]   G.M.Evans, Effect of Manganese on the Microstructure and Properties of All-Weld-Metal Deposits, *supplement to welding journal* , march 1980,p *68-75*
[12]   Azom.com, The Properties and Effects of Manganese as an Alloying Element, https://www.azom.com/article.aspx?ArticleID=13027 ,july 2019.

Existing condition, testing and proces analysis of ESAB Railtrac FW 1000 welding carriage

Ratko Mimica*[a], Mladen Komšić[b],

a Brodosplit R&D ltd., Put Supavla 21/B, 21000 Split, Croatia
b Brodosplit BSO ltd., Put Supavla 21/B, 21000 Split, Croatia
* Corisponding Author, ratko.mimica@brodosplit.hr

Abstract

Set of activities which precedes implementation of new technology is described in this work. In this case, "new" technology represents already obtained, used and then forgotten machine for mechanized welding. Current condition, regarding precision and additional functions were analyzed. Usability for specific task of welding "leaflets" of Smulders project was investigated on testing samples and in real working conditions. For those conditions basic process settings were given along with suggestions for further activities.

Key words: Mechanized welding, process analysis;

Sažetak

U radu su opisani setovi aktivnosti koji prethode implementaciji nove tehnologije u pogon. U ovom slučaju ne radi se o novoj tehnologiji, već o kupljenom, korištenom, "zaboravljenom" uređaju za mehanizirano zavarivanje. Analizirano je trenutno stanje, točnost postavljenih parametara i dodatnih funkcija uređaja. Ispitana je mogućnosti uporabe Railtrac uređaja za primjenu kod zavarivanja „latica" u sklopu projekta Smulders. Ispitivanje je obavljeno na pokusnim uzorcima i u stvarnim uvjetima rada. U stvarnim uvjetima zabilježene su osnovne procesne postavke i predložene daljnje radnje.

Ključne riječi: mehanizirano zavarivanje, procesna analiza;

1. Uvod

Mehanizirano zavarivanje nudi brojne prednosti u odnosu na ručne postupke, od kojih je bitno spomenuti ponovljivost, učinkovitost i osiguranje kvalitete procesa [1]. Dodatni problem koji se javlja u današnje vrijeme je nedostatak kvalitetnog zavarivačkog kadra. U slučaju mehaniziranog zavarivanja operater ne mora nužno biti zavarivač, dovoljno je položiti kratki tečaj obuke rada strojem. Iako i u procesu opremanja mehanizirani procesi zavarivanja mogu biti od velike koristi (Nelson postupci, Orbital Tig), pravu vrijednost ovakvi uređaji mogu iskazati u procesima izrade trupa, gdje zavarivanje uniformnih dužih zavara predstavlja dominantni postupak. Trup već sad koristi određene uređaje (Panel linija, robotski gantry, miggytrac traktori) ali se i dalje velika većina spojeva izrađuje ručno. To se posebno odnosi na vertikalno zavarivanje, gdje se, iako kupljeni i testirani, ne koriste niti jedni od dostupnih uređaja.

Stoga je prvi cilj ovog rada provjeriti da razlog ne korištenja nije možda tehničke prirode, odnosno provjera tehničke dokumentacije te osnovnih i dodatnih svojstava stroja. Drugi cilj je ponuditi dodatne informacije o procesu koje bi mogle biti korisne za daljnje upravljanje ovim vrstama uređaja. Na osnovi dobivenih informacija potrebno je ispitati primjenjivost uređaja na jednom od aktivnih projekata.

2. Eksperimentalni dio

Radi se o uređaju ESAB Railtrac FW 1000 sa pripadajućom opremom: tračnicama sa magnetskim hvataljkama, kontrolne kutije i daljinskog upravljačkog panela (**Slika 1**) [2]. Oznaka W u imenu sugerira da stroj ima mogućnosti njihanja (weaving) i dodatni modul upravljanja u kontrolnoj kutiji (**Slika 2**).

| **Figure 1** *welding carriage system* | **Figure 2** *control box detail* |
| **Slika 1** prikaz cjelokupnog sustava | **Slika 2** detaljni prikaz kontrolne kutije |

Osnovni materijal je lim debljine 4 mm, kvalitete S355J2+N koji je ostao skidanjem otvora na plaštu poklopca. Korišten je dodatni materijal u obliku žice promjera 1.2 mm: Hyundai Supercored 71, klasifikacija Parametri zavarivanja držani konstantnima:

Promjer sapnice = 20 mm,

Protok plina = 18 l/min,

Udaljenost sapnice od komada= 12 mm

3. Rezultati i diskusija

3.1. Osnovne funkcije uređaja, bez paljenja luka

Prilikom rada u većim brzinama zamijećene su cikličke vibracije uređaja. Izgleda da se pojavljuju ovisno o zahvatu kotačića. Treba napomenuti da su vibracije primijećene dok je uređaj bio priključen na ventilacijski otvor tj. na relativno tanki lim. Potrebno je testirati iste parametre na većim debljinama lima ili ponoviti iste uvjete ali s drugom tračnicom, kako bi se isključila tračnica kao možebitni uzrok vibracija. Netočnost brzina gibanja je ustanovljena u gibanju odozgo prema dolje, odozdo prema gore je relativno točna (**Tablica 1**).

Table 6 measured welding speed values

Table 19 izmjerene vrijednosti postavljenih parametara

Smjer:	Postavljena vrijednost, cm/min	Izmjerena vrijednost, cm/min
gore	50	52
	60	62

	100	100
dole	50	60
	60	70
	100	120

Zavarivanje njihanjem je također ustanovljeno da funkcionira, zajedno sa dodatnim opcijama (tip weawing-a). Backfill funkcionira, isprekidani zavari funkcioniraju (zajedno sa backfill i weawing opcijom).

3.2. *Osnovni parametri zavarivanja, horizontalni položaj, navari*

Smisao ovog dijela ispitivanja je upoznavanje sa osnovnim parametrima zavarivanja u kombinaciji sa Railtrac uređajem. Uređaj je priključen na ESAB feed 30-4 dodavač žice (**Slika 3**) [3], polikabel sa ravnim gorionikom i izvor struje ESAB Mig 400t. Priključivanjem Railtrac uređaja na kontrolni dio dodavača žice ustanovljeno je da potenciometar koji regulira dobavu žice (donji desni potenciometar, **Slika 3**) na dodavaču ne funkcionira.

Figure 3 *wire system control*

Slika 3 kontrole na dodavaču žice

Figure 4 *remote control detail*

Slika 4 detaljni prikaz kontrolne kutije

Brzina dobave žice se, preko jakosti struje, kontrolira na daljinskom uređaju Railtraca (**Slika 4**). Kako na tim potenciometrima nema podjele, prilikom testiranja zabilježeni su njihovi položaji u skladu položaja kazaljki na satu. Ostali prekidači i potenciometri na dodavaču funkcioniraju kako je predviđeno. Korišteni parametri zavarivanja (uz već spomenute konstantne) su vidljivi u **Tablici 2.**

Primijećeno je uvijanje tračnica u horizontalnom položaju, budući da se centar ravnoteže nakon montaže gorionika pomiče izvan područja tračnica. Takvo savijanje je najizraženije u području između dva magnetska oslonca tračnica. Tijekom procesa zavarivanja uvijanje tračnica rezultira približavanjem gorionika radnom komadu, mijenjajući postavljene parametre. Navedeni problem se rješava uz pomoć dodatka u obliku kotačića pričvršćenog na Railtrac, kotačić se postavi na način da dodiruje površinu osnovnog materijala i učvrsti u tom položaju.

U početnim zavarima primijećena je otežana uspostava luka, pogotovo pri većim brzinama zavarivanja, protok plina povećan je na oko 18 l/min. Dodatni problem u početku zavarivanja, pri velikim brzinama i jakostima struja, je što žica u startu udari u radni komad i odigne traktor. Problem se rješava uključivanjem funkcije „creep start", koja se nalazi na dodavaču žice ESAB feed 30-4 (**Slika 3**, donji desni prekidač).

<div align="center">

Table 2 Process parameters for horizontal position

Table 2   Početni parametri navarivanja u horizontalnom položaju

</div>

Broj:	V_{zav} , cm/min	daljinski		Položaj V na dodavaču	Display dodavača		napomena
		Položaj V	Položaj A		V	A	
1	30	**7**	10	4,5			
2	30	**9**	10	4,5			
3	30	**10**	10	4,5	18,3	188	
4	30	**11:30**	10	4,5	18,3	192	
5	30	**1**	10	4,5	18,3	200	
6	30	1	10	**5,5**	22,3	196	
7	30	**10**	10	**4**	16,7	188	
8	30	10	10	**4,5**	17,3	212	
9	**45**	10	10	4,5	17,0	220	
10	**60**	10	10	4,5	17,3	184	Problemi sa uspostavom luka
11	**30**	10	10	4,5	17,5	200	Zamijećeno uvijanje tračnica
12	30	varijabilno	varijabilno	4,5	18,8	188	Testiranje potenciometara u radu
13	**35**	**11**	**11**	**5,9**	24,7	192	
14	**45**	11	11	5,9	25	180	
15	45	11	**1**	5,9	25	236	
16	**60**	11	1	**7**	32,3	268	
17	**70**	11	1	**6,5**	29,7	256	
18	**75**	11	1	**6,3**	29,3	280	Zadovoljavajući izgled

3.3. Osnovni parametri zavarivanja, horizontalni položaj, sučeoni spojevi

Jedna od razmatranih namjena Railtrac uređaja je zavarivanje jedne vrste sučeonih spojeva za povezivanje „latica" na projektu Smulders poklopci. Ne radi se o klasičnom sučeonom spoju, zavaruje se ravni lim na lim savijen pod 90° (**Slika 5**).
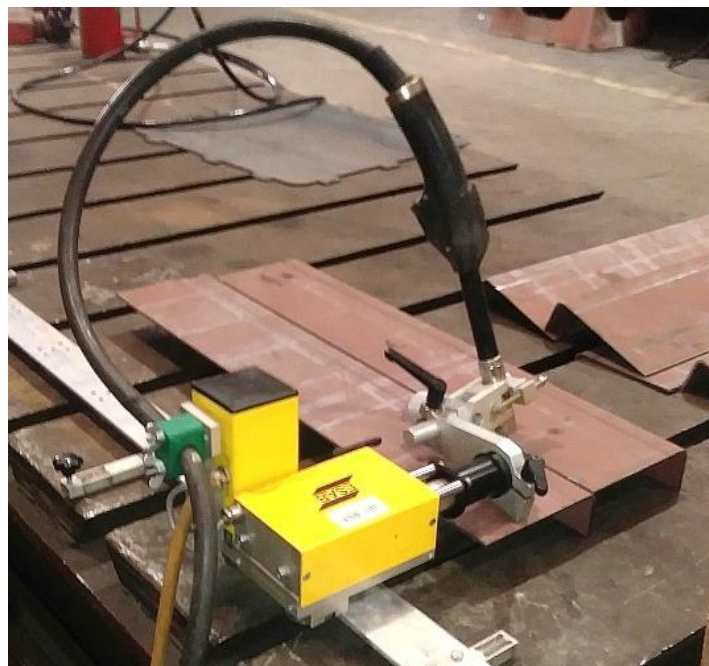
Figure 5 *Railtrac carriage,welding position and type of joint*
Slika 5 Prikaz Railtrac uređaja, pozicije zavarivanja i načina spajanja limova

Prije zavarivanja potrebno je osigurati položaj limova, tj., obaviti „puntavanje". To se može neovisnom opremom za zavarivanje a moguće je iskoristiti postojeći sustav. Railtrac se dovede do mjesta „puntavanja", gorionik sa vratom se odspoji od Railtracka, smanji se jakost struje na daljinskom upravljaču (položaj 11:00), i kratkotrajno aktivira prekidač na gorioniku. Proces ponoviti za potrebni broj „punata". Korišteni parametri zavarivanja dati su u **Tablici 3**.

Table 3 Process parameters for horizontal position
Table 3 Početni parametri zavarivanja u horizontalnom položaju

Broj:	V_{zav} [cm/min]	daljinski		Položaj V	Display dodavača		$V_{njihanja}$ [mm/s]	Amplituda [mm]	Oblik njihanja	Time delay [s]	napomena
		Položaj V	Položaj A		V	A					
19	75	11	1	6,3							Loše vođenje
20	**65**	11	1	6,3			40	3	1	0	Prevelika V_{zav}
21	65	11	1	6,3	29,3	228	60	3	1	0	protaljivanje
22	**50**	11	**12:30**	6,3	29,3	248	60	**5**	1	0	Početna zračnost 2 mm
23	**40**	11	**11:30**	6,3			60	5	1	0	Početna zračnost 4 mm
24	40	11	11:30	**5**	27,7	150	60	5	1	0	
25	40	11	12	6	27	208	**50**	5	1	0	Za bez zračnosti
26	40	11	12	**5,8**			50	**3**	**3**	**0,3**	Poboljšan depozit
27	40	11	**10:30**	5,8	24,3	180	50	3	3	0,3	Smanjeno nadvišenje
28	50	11	10:30	5,8	24,5	192	50	3	3	0,3	Početna zračnost 2 mm
29	**40**	11	10:30	5,8	24,5	185	50	3	3	0,3	Zadovoljavajući izgled

Korištenje parametara postignutih u navarivanju je moguće ukoliko imamo dobro vođenje traktora u odnosu na zavar. Ukoliko to nije slučaj, ili ukoliko dođe do pucanja „punata" ili deformacije savijanjem, postoji mogućnost da zavar skrene u jednu stranu. Na zavaru 19 vidljivo je dobro vođenje i deponiranje materijala do pola zavarene dužine, nakon toga je došlo do pucanja punata i skretanja zavara (**slika 6**). Njihanjem se rješava problem, međutim brzina zavarivanja je bila tolika da se njihanjem zavar „slagao" sa izrazito malim preklopom (**slika 7**).

Figure 6 *faulty tracking on weld no. 19*

Slika 6 loše vođenje zavara 19

Figure 7 *insufficient weaving overlap, weld 20*

Slika 7 Zavar 20, nedovoljan preklop zavara kod njihanja

Daljnji pokušaji su išli u smjeru smanjivanja brzine zavarivanja, uz varijacije jakosti struje i amplitude njihanja. Sa ovom vrstom njihanja doima se kao da je zavar (el. luk i deponirani materijal) vrlo kratko vrijeme u krajnjim dijelovima amplitude njihanja, što rezultira manjak materijala sa obje strane zavara, a protaljenu sredinu (**slika 8**). Ova pojava je izraženija što je početni razmak između osnovnog materijala veći.
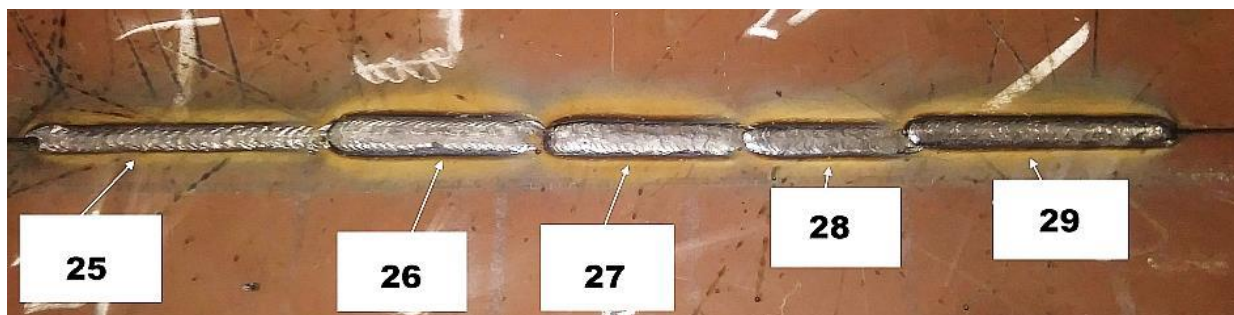
Figure 8 *weaving type and holding time comparison. Weld 25 had ziag-zag type and others interrupted weaving*

Slika 8. Razlika u načinu njihanja i vremenu zadržavanja. Zavar 25 sa cik-cak načinom i ostali sa isprekidanim njihanjem.

Daljnje poboljšanje izgleda zavara može se ostvariti podešavanjem brzine zavarivanja i jakosti struje. Dobiveni zavari izgledaju vrlo dobro, bez daljnje potrebe za brušenjem. Daljnji plan testiranja:

- Provjera parametara na stvarnoj debljini lima „latice" koje treba zavarivati su debljine 5[mm], testirani limovi su bili 4mm debljine.
- Provjera parametara u slučaju zračnosti veće od 2 mm, pronalaženje novih ukoliko stari ne odgovaraju.

3.4. Zavarivanje pripremljenih uzoraka debljine 5 mm

Uzorci su „puntani" sa donje strane, ispitivani su parametri zavarivanja kod spoja sa manjom i većom zračnosti. Kako se radi o debljem materijalu, radijus savijanja izgleda veći, što utječe na

prostor kojeg treba popuniti zavarom. Stoga je glavni fokus bio ispitivanje dodatnih podešavanja opcija njihanja na uređaju, kao što su amplituda i vrijeme zadržavanja(**Tablica 4**).

Obje opcije imaju naizgled kontradiktoran utjecaj na izgled spoja. Ustanovljeno je da smanjivanje vremena zadržavanja na krajnjim dijelovima povećava unos topline i mogućnost protaljivanja (**slika 9**), povećavanjem amplitude njihanja dobije se sličan utjecaj.

Figure 9 *difference in weaving types, zig-zag vs. interrupted weaving*
Slika 9 razlika u načinu njihanja; cik-cak u odnosu na isprekidano

Table 4 Process parameters for horizontal position
Table 4 Početni parametri navarivanja u horizontalnom položaju

Broj:	V_{zav} ,cm/min	daljinski		Položaj V	Display dodavača		$V_{njihanja}$,mm/s	Amplituda, mm	Oblik njihanja	Vremenski odmak, s	napomena
		Položaj V	Položaj A		V	A					
1	50	11	11:30	5,8	24,7	176	50	2	3	**0,5**	Bez zračnosti, uzak zavar
2	50	11	11:30	5,8			50	2	3	**0,4**	širi zavar, nedovoljno razliven
3	50	**12**	11:30	5,8			50	2	3	0,4	Bolje razlijevanje
4	50	**11**	11:30	5,8	24,7	168	50	2	3	**0,2**	Veliko nadvišenje
5	50	11	11:30	5,8			50	2	**1**	0,2	Ne funkcionira delay
6	50	11	11:30	5,8			50	2	**3**	**0,1**	Preveliki unos topline
7	50	11	11:30	5,8			50	2	3	0,3	Za bez zračnosti
8	50	11	11:30	5,8			50	**4**	3	0,3	Zračnost 2 mm, fali materijala
9	**40**	11	11:30	**6**			50	4	3	0,2	Uleknuto na većoj zračnosti
10	40	11	11:30	6			50	4	3	**0,3**	Loše vođenje
11	50	11	11:30	**6,2**			50	4	3	0,3	Za zračnost 2 mm
12	50	11	11:30	6,2	27,7	204	50	**5**	3	0,3	Zračnost 4 mm
13	**70**	11	11:30	6,2			50	5	3	0,3	
14	50	11	11:30	6,2			50	**4**	3	**0,2**	
15	50	11	11:30	**6**			50	4	3	0,2	Za zračnost 4 mm

Razlozi za to mogu se naći u samom izgledu njihanja. U slučajevima zavara 6 i 4 radi se o isprekidanom njihanju, a u slučaju zavara 5 (**Slika 9**, sredina), o klasičnom cik-cak njihanju. U slučaju isprekidanog njihanja, samo u vremenu zadržavanja u krajnjem položaju se traktor giba namještenom brzinom zavarivanja. Nakon što prođe taj interval, traktor stane dok gorionik pređe na drugu stranu zavara. Gorionik prelazi brzinom njihanja namještenom na kontroleru, ali traktor za to vrijeme stoji. Što se manji vremenski odmak (delay) postavi to će više puta u jedinici vremena traktor stati, što za posljedicu ima veći unos topline po jedinici dužine zavara. Amplituda ima sličan utjecaj, što je veća amplituda to treba duže vremena (po namještenoj brzini njihanja) da gorionik dođe iz jednog krajnjeg položaja u drugi, za to vrijeme traktor stoji.

3.5. Ispitivanje u stvarnim uvjetima rada

Sva dosadašnja ispitivanja izvršena su sa ciljem osposobljavanja uređaja za sudjelovanje u procesu zavarivanja projekta Smulders. Radi se o većem broju 6 metarskih poklopaca gdje bi automatiziranim zavarivanjem na više mjesta znatno rasteretili zavarivački kadar, poboljšali kvalitetu i ponovljivost procesa. U daljnjem radu razrađen je proces pod brojem 3 (**Slika 10**). Korišteni parametri prikazani su **Tablicom 5**.

Table 5 chosen welding parameters for horizontal position
Table 5 Početni parametri navarivanja u horizontalnom položaju

Broj:	V_{zav}, cm/	daljinski	Polož aj V	Display dodavača	V njihanj	Amp	Obli k	Vre men	napomena

		Položaj V	Položaj A		V	A					
1	50	11	11	6	29,5	185	50	5	3	0,3	
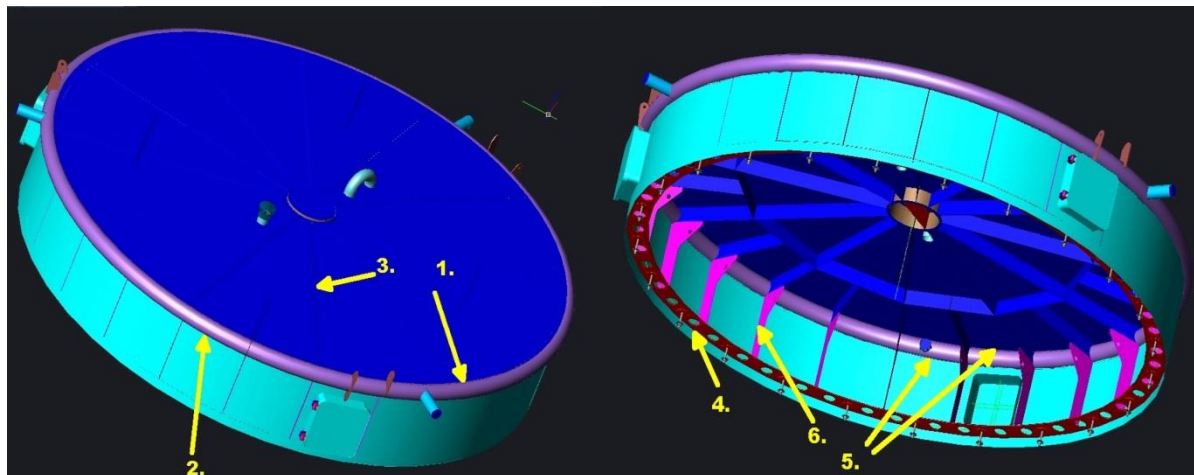
Figure 10 *3d model of wind tower cover with possible welds suitable for mechanisation*
Slika 10 3d prikaz razmatanih poklopaca i potencijalnih mogućnosti mehanizacije zavarivanja.

Postavljanje trake se odvija u skladu sa upustvima, traka se pozicionira tako da se prethodno vijci na magnetskim držačima uviju do kraja, time se magneti na toj strani odvoje od podloge što olakšava pozicioniranje trake. Udaljenost trake od ruba zavara je potrebno prekontrolirati na više mjesta (kako je udaljenost više manje jednaka, jednostavan i brz način je uzeti šablonu te dužine). Nakon potvrde udaljenosti odviti vijke dok magnetska vodilica te strane ne dotakne podlogu.

Nakon pozicioniranja trake na nju se prikači Railtrac i postavi se kotačić distancera da dodiruje podlogu. Kotačić je preporučljivo podesiti u trenutku kad je Railtrac u poziciji iznad magnetskog držača. Tijekom rada uređaja potrebno je pripaziti da se kontrolni kabeli i kabel gorionika ne zapletu, ne zapnu za vijke vodilica ili druge prepreke, te da ne prelaze preko tek zavarenog dijela. Početni zavar je ocjenjen zadovoljavajućim, iako je na drugom kraju vodilice pokazao otklon od centra zavara, spojene su obje strane sa dovoljno velikim nadvišenjem (**Slika 11**). Naknadno brušenje je ocjenjeno nepotrebnim, što nije slučaj kod ručnih zavara.

Figure 11 *first weld on wind tover cover*
Slika 11 početni zavar na poklopcu

Naknadno je pokušan zavar sa jednakim parametrima kod slučaja veće zračnosti među laticama. Otvor donje strane je bio preko 4 mm. Iako je proces započeo preko „punta" zabilježeno je protaljivanje. Dolaskom u područje manje zračnosti formirao se odgovarajući zavar (**Slika 12**).

Figure 12 *insufficient filling due to greater distances between "leaflets"*
Slika 12 Zabilježeno protaljivanje u području veće zračnosti.

Navedeni problem se može riješiti prilagodbom parametara zavarivanja, posebice smanjivanjem jakosti struje i brzine zavarivanja. Isti problem se može riješiti i smanjivanjem vremena zadržavanja, ali taj podatak nije moguće mijenjati na daljinskom uređaju tijekom procesa. Osim na jakost struje i brzinu zavarivanja, na daljinskom uređaju se može dodatno podešavati napon zavarivanja i položaj centra gorionika.

3.6. Procesna analiza

Izmjereno vrijeme zavarivanja za jednu dužinu trake (2,5 m) iznosilo je 12 min. Postavljanje trake i centriranje u odnosu na os (sa šablonom) okvirno je trajalo 5 min, a prebačaj Railtrac uređaja sa jedne na drugu traku okvirno 3 min. Mapa ukupnog promatranog procesa za zavarivanje 3 od 12 latica nalazi se u **Tablici 6.**

Table 6 Kaizen of welding 3 leaflets for Smulders project
Table 6 Kaizen procesa zavarivanja 3 latice za projekt Smulders

Ime procesa: Railtrac zavarivanje 3 latice za projekt Smulders					Diagram						
Red. broj	Korak	Trajanje (min)	Trajanje kumul.	Broj osoba	$\otimes$ oper.	$\rightarrow$ transp.	$\square$ kontr.	$\triangledown$ sklad.	Dodana vrijednost	Nedodana vrijednost potrebna	Nedodana vrijednost nepotreb.
0	spajanje uređaja	10		1		1				1	
1	postavljanje i centriranje vodilice	5	15	1		1				1	
2	postavljanje Railtrac uređaja	3	18	1		1				1	
3	zavarivanje (2,5 m)	12	30	0	1				1		
4	postavljanje i centriranje druge vodilice	5	35	1		1				1	
5	postavljanje Railtrac uređaja	3	38	1		1				1	
6	zavarivanje (2,5 m)	12	50	0	1				1		
7	postavljanje i centriranje vodilice	5	55	1		1				1	
8	postavljanje Railtrac uređaja	3	58	1		1				1	
9	zavarivanje (2,5 m)	12	70	0	1				1		
10	odspajanje uređaja	10	80	1		1				1	
			80	8	3	8	0	0	3	8	0
	UKUPNO	80			11					11	

Kako je riječ o mehaniziranom procesu samo zavarivanje ne iziskuje aktivnost operatera. On se samo mora pobrinuti da proces tokom zavarivanja ne zapne. To znači da bi se za uhodani proces postavljanje i centriranje trake moglo raditi za vrijeme rada uređaja, što je prikazano Ganttogramom na **Slici 13**.
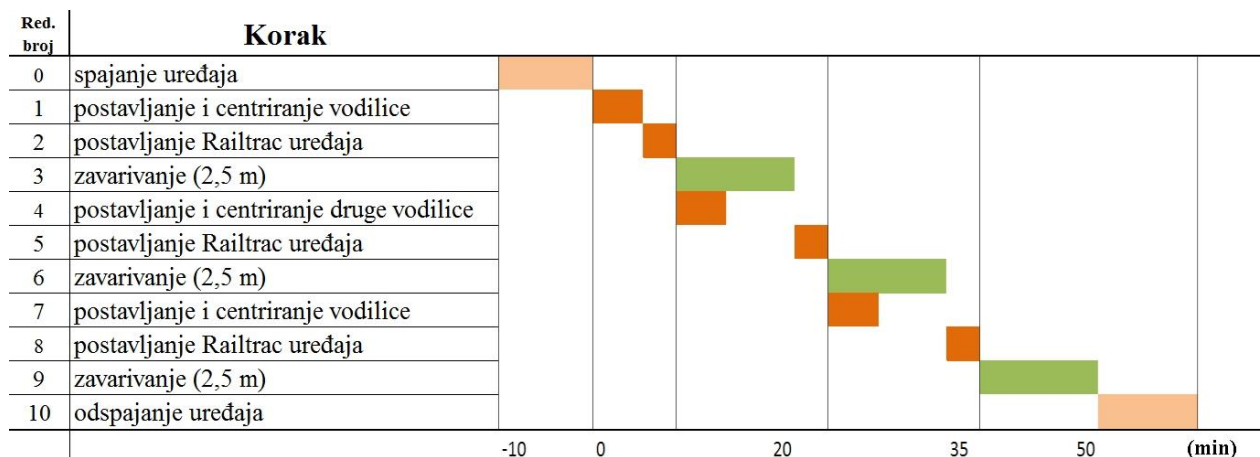
Figure 13 *Gantt chart of welding 3 leaflets for Smulders project*
Slika 13 gantogram zavarivanja tri latice za projekt Smulders

Na taj način ukupno vrijeme trajanja procesa se smanjuje za iznos vremena potrebnog za postavljanje trake, 5 min po svakoj postavljenoj traci osim prve. Osim toga bitno je primijetiti visoku učinkovitost procesa odnosno „Arc on time". El. luk gori 36 od ukupno 50 minuta trajanja osnovnog procesa, što je oko 72% za tri latice. Povećanjem broja latica arc on time raste do teoretskih 75%. Ekstrapolacijom dobivenih rezultata za zavarivanje ukupnog broja latica na jednom poklopcu bilo bi potrebno oko 3 sata. Taj podatak treba usporediti sa trenutnim normama i stvarnim trajanjima procesa zavarivanja latica.

Bitno je za napomenuti da se sa sadašnjom opremom ne može zavariti latica u potpunosti. Dužina traka Railtrac uređaja je 2,5 m, a potrebna duljina zavarivanja je preko 2,7 m. Ostatak se može zavariti ručno ili se prethodno mogu nadopuniti standardne dužine traka sa manjim dužinama (npr., pola metra). Time bi se za određeni iznos pomaknule izmjerene vrijednosti ali u korist ukupnog „arc on time" procesa.

4. Zaključci

U radu je obavljeno testiranje opreme za mehanizirano zavarivanje **EASB Railtrac FW 1000**. Oprema je već duže vremena bila u vlasništvu Brodosplita ali nije korištena. Inicijalna testiranja utvrdila su da oprema radi kao što je predviđeno, osim što u vertikalnoj poziciji, u smjeru prema dole, odstupa od namještenih vrijednosti za brzinu zavarivanja.

Testirana je osnovna funkcionalnost dodatne opreme za zavarivanje: izvor struje **ESAB Mig 400t** i dodavač žice **ESAB feed 30-4**. Pronađeni su visokoproduktivni parametri za navarivanje koji rezultiraju dobrim izgledom navara:

V_{zav}, cm/min	daljinski		Položaj V na dodavaču	Display dodavača	
	Položaj V	Položaj A		V	A
75	**11**	**1**	**6,3**	**29,3**	**280**

Navedeni parametri se ne preporučuju ukoliko linija putanje gorionika odstupa od linije zavarivanja, niti u slučaju postojanja zračnosti u spoju prije zavarivanja.

Za slučaj lošijeg vođenja ili prethodne zračnosti u spoju preporuča se korištenje njihanja, sa dodatnom opcijom zadržavanja u krajnjim položajima. Zadovoljavajući rezultati postignuti su sa sljedećim parametrima:

V_{zav}, cm/min	daljinski		Položaj V	Display dodavača		$V_{njihanja}$, mm/s	Amplituda, mm	Oblik njihanja	Vremenski odmak, s	napomena
	Položaj V	Položaj A		V	A					
50	**11**	**11:30**	**5,8**			**50**	**2**	**3**	**0,3**	Bez zračnosti
50	**11**	**11:30**	**6,2**			**50**	**4**	**3**	**0,3**	Za zračnost 2 mm
50	**11**	**11:30**	**6**			**50**	**4**	**3**	**0,2**	Za zračnost 4 mm

Uređaj je ispitan i u stvarnim uvjetima rada, na zavarivanju latica poklopaca za Smulders projekt. Dovoljno dobri rezultati postignuti su sa parametrima:

V_{zav}, cm/min	daljinski		Položaj V	Display dodavača		$V_{njihanja}$, mm/s	Amplituda, mm	Oblik njihanja	Vremenski odmak, s	napomena
	Položaj V	Položaj A		V	A					
50	**11**	**11:30**	**5,8**			**50**	**5**	**3**	**0,3**	50

U slučaju veće zračnosti preporučuje se smanjiti jakost struje i brzinu zavarivanja kako bi se omogućilo bolje nanošenje materijala.

Postavljanje trake traje oko 5 minuta, pozicionira se uz pomoć šablone i potpuno uvijenim vijcima u magnetske nosače. Nakon pozicioniranja vijci se odviju dok više nisu u kontaktu sa podlogom. Kada se proces uhoda postavljanje se može obavljati dok traje zavarivanje (naravno, u tom slučaju potrebno je imati dvije trake).

Postavljanje Railtrac uređaja traje 3 minute, zavarivanje dužine malo manje od 2,5 m traje oko 12 minuta, odnosno proces ima između 70 i 75% „arc on time". Okvirno bi se 12 latica sa ovim uređajem mogla zavariti u 3 sata.

5. Prijedlozi daljnjih radnji

Za projekt Smulders potrebno je izraditi produžetke za staze u dužini od 0,5 m, kako bi se mogla zavariti cijela potrebna dužina.

Ako se planira primjenjivati na poklopcima potrebno je ažurirati WPS, a onda i atestirati postupak.

Kratkoročno je potrebno obučiti minimalno jednog operatera za rad sa uređajem. Kvalifikacija operatera je prema normi EN 1418 ili ISO 14732.

6. Literatura

[1] – Mimica Ratko, *Orbital TIG: teoretski pregled, zatečeno stanje, daljnje smjernice, procesna analiza, vrijednosna analiza, ekonomska analiza*. Interni rad, rujan 2017.
[2] – *Railtrac FW100: instruction manual*, ESAB
[3] – *ESABFeed 30-4 M13: instruction manual*, ESAB

ADVANTAGES AND CHALLENGES OF ADDITIVE MANUFACTURING IN MARITIME INDUSTRY

Dunja Legović, Dora Vojnić
University of Rijeka, Faculty of Engineering Vukovarska 58, 51000 Rijeka,
* Corresponding Author: dlegovic@riteh.hr

SUMMARY

Additive manufacturing (e.g., 3D printing) is gaining ground in various industrial fields and everyday life. The maritime industry is not an exception. The prototype of a 3D printed full-size propeller was developed in the Netherlands and officially class-approved by Bureau Veritas in 2017. With technologies and materials that can ensure the necessary strength and precision, such manufacturing of other pieces is likely to follow.
By producing items on demand onboard or in the port, the costs of warehousing and shipping spare parts can be significantly reduced. Additive manufacturing also allows the components to be made lighter and with higher efficiency, without the additional expenses for molds required in the casting process.
A related consequence is the concern of existing suppliers caused by the lessening demand for parts. However, embracing 3D printing could allow them to expand their reach and meet the needs of more clients by selling copyrights rather than manufacturing physical items. From the present point of view, such a shift in the maritime industry is expected by 2030.

Keywords: *Additive manufacturing; 3D printing; production on demand*

PREDNOSTI I IZAZOVI ADITIVNE PROIZVODNJE U POMORSKOJ INDUSTRIJI

Dunja Legović, Dora Vojnić
Tehnički fakultet Sveučilišta u Rijeci, Vukovarska 58, 51000 Rijeka,

SAŽETAK

Aditivna proizvodnja (primjerice 3D printanje) sve je prisutnija u raznim granama industrije, kao i u svakodnevnom životu. Pomorska industrija po tom pitanju nije izuzetak. U Nizozemskoj je 2017. godine izrađen 3D print prototipa brodskog vijka u punoj veličini koji je dobio odobrenje klasifikacijskog društva Bureau Veritas. Uz razvoj tehnologija i materijala koji mogu osigurati potrebnu čvrstoću i preciznost, uskoro će se vjerojatno na sličan način proizvoditi i drugi elementi.
Troškovi skaldištenja i slanja značajno bi se smanjili ukoliko bi se zamijenski dijelovi proizvodili po potrebi, na brodu ili u luci. Također, aditivna proizvodnja dozvoljava da komponente budu lakše i gotovo bez škarta, bez dodatnih troškova za izradu kalupa za lijevanje.
Očekivana posljedica je zabrinutost postojećih proizvođača koji smatraju da će se smanjiti potražnja za dijelovima. Ipak, okretanje prema 3D printanju moglo bi im proširiti doseg i zadovoljiti potrebe većeg broja klijenata na način da prodaju autorska prava umjesto dijelova. S trenutnog stajališta, takva promjena u pomorskoj industriji mogla bi se očekivati do 2030. godine.

Ključne riječi: *aditivna proizodnja, 3D print, proizvodnja po potrebi*

1. Introduction

Additive Manufacturing (AM) is a term used to describe the technologies that add layer-upon-layer of material and build 3D objects. The process can be applied to a large range of materials: plastic, metal, concrete or even human tissue.

The initial idea goes back to 1981, when the Japanese Hideo Kodama thought of creating a three-dimensional printing, inspired by a photo-hardening polymer technology. He filed a patent for this XYZ plotter and published his research results as journal papers [1], [2]. At that point he was too far ahead of his time, as there was no interest in his publications. The invention of 3D printing is attributed to Chuck Hull of 3D Systems Corporation who, in 1984, filed his own patent for a stereolithography fabrication system. The system consisted in layers added by curing photopolymers with ultraviolet light lasers. This process originated the STL (Stereolithography) file format and the digital slicing and infill strategies, which are common to many processes today. The first commercial 3D printer, the SLA-1 was patented and released in 1986, again by Hull's company 3D Systems Corporation [3]. In 1993 MIT developed the first powder bed process using inkjet print heads. The 1990s were the decade of development of metal sintering, melting for example selective laser sintering, direct metal laser sintering, and selective laser melting. During the 2000s the various additive processes matured, and in the early 2010s the process called Fused Deposition Modeling (FDM) boomed in the scientific and hobbyist area. FDM is a rather inexpensive method, very convenient for prototyping. Its popularity was supported by the growth of companies that produce and deliver open-source 3D printers, such as Prusa [4]. When it comes to industrial purposes, the pioneers and early adopters of 3D printing purposes were aerospace and defence (A&D), starting in1989. The automotive industry followed, together with the medical and dental sector. Consumer goods were next, together with the hobby and leisure industry. The maritime industry joined in the last five years, embracing the opportunity of having 3D printers aboard ships and in ports, mostly to produce spare parts on demand. A wide range of applications happened to arise, and currently they are being explored and developed.

2. Existing 3D printing technologies

Traditionally, subtractive manufacturing processes consist in the removal of raw materials to create final products. Additive manufacturing can be seen as its opposite, since it works by building a product layer by layer.

The terminology introduced to describe the process of using a printer and CAD software to grow objects layer by layer may vary a lot. Additive manufacturing, free form fabrication, rapid prototyping, layered manufacturing and direct digital manufacturing are just a few names in common use. Most of these terms can be used interchangeably, with one exception: Rapid Prototyping (RP) refers to the production of the prototype of a new component, while Additive Manufacturing (AM) provides opportunities for both prototypes and final components. The crucial difference between those two is that RP implies that the component is created as a copy of an item that will be manufactured traditionally, using subtractive manufacturing. AM opens a world of design opportunities without the limitations of subtractive manufacturing, but usually is not meant for bulk production.

All methods have one step in common: prior to production, a 3D printable model needs to be created. This can be achieved by a computer-aided design (CAD) package, via a 3D scanner, or by a

plain digital camera and a photogrammetry software. In most cases, the 3D printed models created with CAD show relatively fewer errors than other methods, even if the errors in models can be identified and corrected before printing. CAD models can be saved in the stereolithography file format (STL), or in a more recent form, the Additive Manufacturing File format (AMF). Once completed, the STL or AMF file needs to be processed by the so-called "slicer," a software which converts the 3D model into a series of thin layers. The result is a G-code file, containing instructions tailored to a specific type of 3D printer. This G-code file gets printed with 3D printing client software, which loads the G-code, and uses it to instruct the 3D printer during the 3D printing process, depending on its type and used material.

The 3D printing technologies that are commercially available nowadays can be grouped in five categories [5], Table 1.

- Selective laser sintering (SLS)
- Fused filament fabrication (FFF)
- Stereolithography (SLA)
- Selective laser melting (SLM)
- Electron beam melting (EBM)

Table 1. *3D printing technologies*

Technology	Principle	Materials	Resolution
Selective laser sintering (SLS) Selective laser melting (SLM)	Laser beams, moving systematically, are used to melt or sinter powder material in bulk (like a laser printer)	Metal alloys Polymers	20–50 micrometers
Fused filament fabrication (FFF) or Extrusion deposition	Molten polymers or ceramics are precisely deposited (ink-jet like)	Polymers Ceramics	20–50 micrometers
Stereolithography (SLA)	A UV laser initiates photopolymerization in the liquid phase. The excess material that has not been exposed to the "activation" agent can be utilized in further projects	Polymers (resins)	20–50 micrometers
Electron beam (EBM)	Electron beams are used to melt and deposit powder material	Pure metals and alloys	20–50 micrometers

The mentioned printing principles can be applied both on a smaller scale, as well as on a larger one. "Smaller" scale refers to pieces that can fit on the top of a table, while "larger" scale refers to pieces whose dimensions may reach several meters in any direction.

An example of the latter is LSAM (pronounced L-Sam) - Large Scale Additive Manufacturing. [6]. It represents the industry leading technology for large scale 3D printing of thermoplastic polymers. LSAM machines are large, robust industrial structures built from steel plate using slot and tab construction, resulting in an order of magnitude higher strength and stiffness than typical structural steel machine construction.

LSAM machines usually have dual gantries, operating over a fixed table, and are available in configurations from 3 meters wide by 6 meters deep up to 30 meters in length. Both printing and trimming can be done on the same machine, so the slightly larger first layers can be trimmed on site.

Print heads that can print over 250 kilograms per hour are available, which means that parts of considerable size can be printed in limited time. The focus of LSAM is on producing industrial tooling, patterns, molds and production fixtures for a variety of industries including aerospace, automotive, foundry and boating.

3. 3D printing between 2015 and 2020 – expectations and reality

A study from 2015 [7] conducted within 38 German large and small companies (automotive, medical technology, infrastructure, chemical and manufacturing industries) found that companies tend to reduce inventory in stock. The focus is on the production of parts on-demand, in order to reduce storage and distribution costs. 47% of the companies claimed that they would consider replacing the traditional procurement of products and spare parts with their own production using 3D printers, 5% said they would consider using printers, but would stick to conventional production and procurement. The remaining 58% stated that they did not plan to use 3D printing at all in their work.

The survey participants were asked in which part of production they applied 3D printing then (2015) and where they believed it might be used in the following 5 years. 45% of companies (2015) used 3D printing in the prototyping phase, and 100% of companies believed that they would have used it in the next 5 years. 10% of companies chose to use 3D printing to create pilot products, and as many as 55% believed that they would have used them in the same manner within 5 years. No company then (2015) relied on 3D printing in serial production, and only 15% considered its possibility by 2020. A high 85% of companies stated that they would use 3D printing for the production of spare parts in the upcoming 5 years, while in 2015 only 10% actively did so. The important fact is that only 5% of companies stated that they would not have 3D printing in their agenda in 2020, which is a significant drop from the original 45% in 2015. The data are shown in Figure 1.
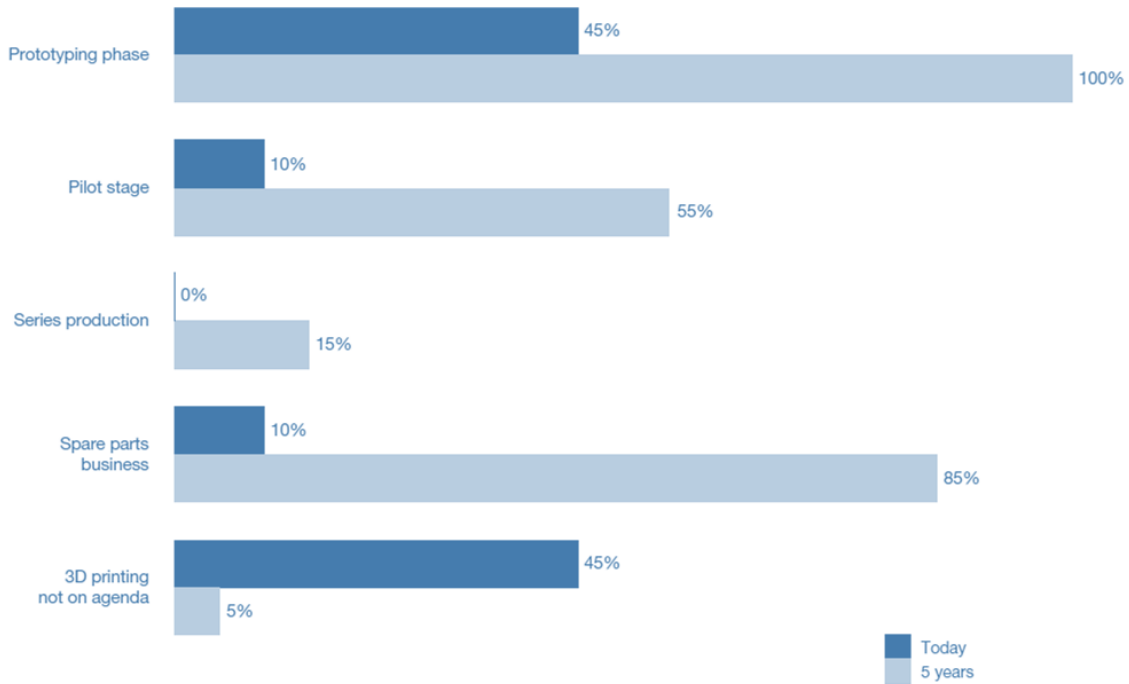
Figure 1 *Results of the 2015 Survey [7]*

As the result of further market research, two large studies by EY [8] and Ultimaker [9] were published in 2019. Both studies surveyed a significant sample of industrial companies worldwide. They included both current users and non-users of 3D printing, in order to examinate and to assess their sentiment towards the technology. Both surveys deduced that the adoption rate of 3D printing by industrial users had accelerated, but also found a lot of room for growth, which is expected to have a positive effect in the future. An interesting find by the EY's study was that 18% of the respondents were already using AM for serial production. This means that 3D printing has "crossed the chasm" of adoption, which is located at the 16% mark, according to the Technology Adoption Life Cycle model [10], as shown in Figure 2. In other words, it hit the treshold of "almost mainstream" for target groups. At this rate, the use of AM for manufacturing end-use parts is expected to be adopted by the early majority (that is 50% of all companies) by 2022. Hence, a significant increase in production volumes can be expected, and a proportional growth in the market size. For example, EY reported that out of 900 companies, 65% are already applying 3D printing and 18% are considering its application in the near future (from 24% and 12% respectively in 2016). As it happens in independent researches, Ultimaker paints a slightly different picture. Their survey found out of more than 2,500 companies, 67% of the respondents were aware of the terms '3D printing' or 'Additive Manufacturing', but only 35% were applying it—which is still a significant increase from 10% in 2014.

Technology Adoption Life Cycle
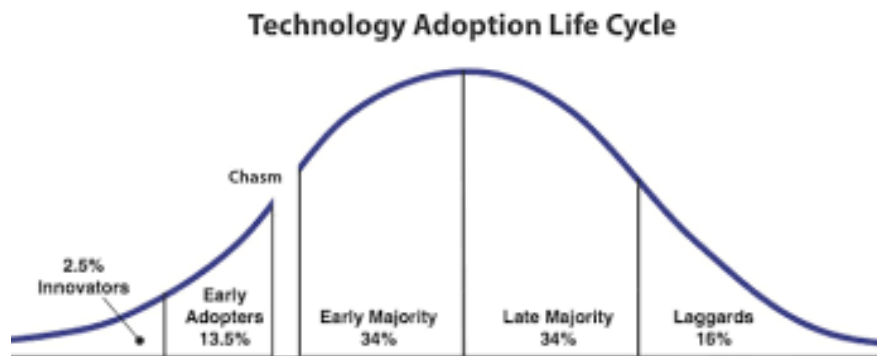
Figure 2. *Technology Adoption Life Cycle [10]*

3.1. What to expect in the future

The chart in Figure 3 summarizes data reported by ten reputable market analysts who evaluated the additive manufacturing market segment in 2019. It is based on publicly available information and it provides the estimate of the current size and future potential of the global 3D printing market [11]. In 2019, it was estimated at $12.1B on average (depending on different analysts, its range between $9.9B and $15.0B), seeing a 25% year-over-year growth since 2014. The revenue included in the estimation consists in 3D printing, software, systems, materials and services, while internal corporate investments in AM technologies are excluded. For the following five years, analysts expect the market to grow on average at 24% Compound Annual Growth Rate (CAGR), reaching $35.0B by 2024 and doubling in size approximately every three years. External variable factors must be considered, as they could lead to growth as low as 20% or as high as 28%, resulting in a market size below $24.0B or above $45.0B in 2024. Such variables depend on factors internal to the 3D printing industry, like adoption for serial production, developments in materials and systems, and reduction in total costs, to name a few. They are also related to external factors, such as customer demands and the greater economic climate.

3D Printing market forecast

Footnote:
* The historic market size was calculated by averaging the market size reported by Wohler's associates [80], EY [81], and SmarTech [82].
** The forecasted market size in the media market size reported by all market analysts.
*** The worst-case and best-case scenarios were calculated starting at ±15% of the market size in 2018 and by applying 20% and 28% CAGR respectively.
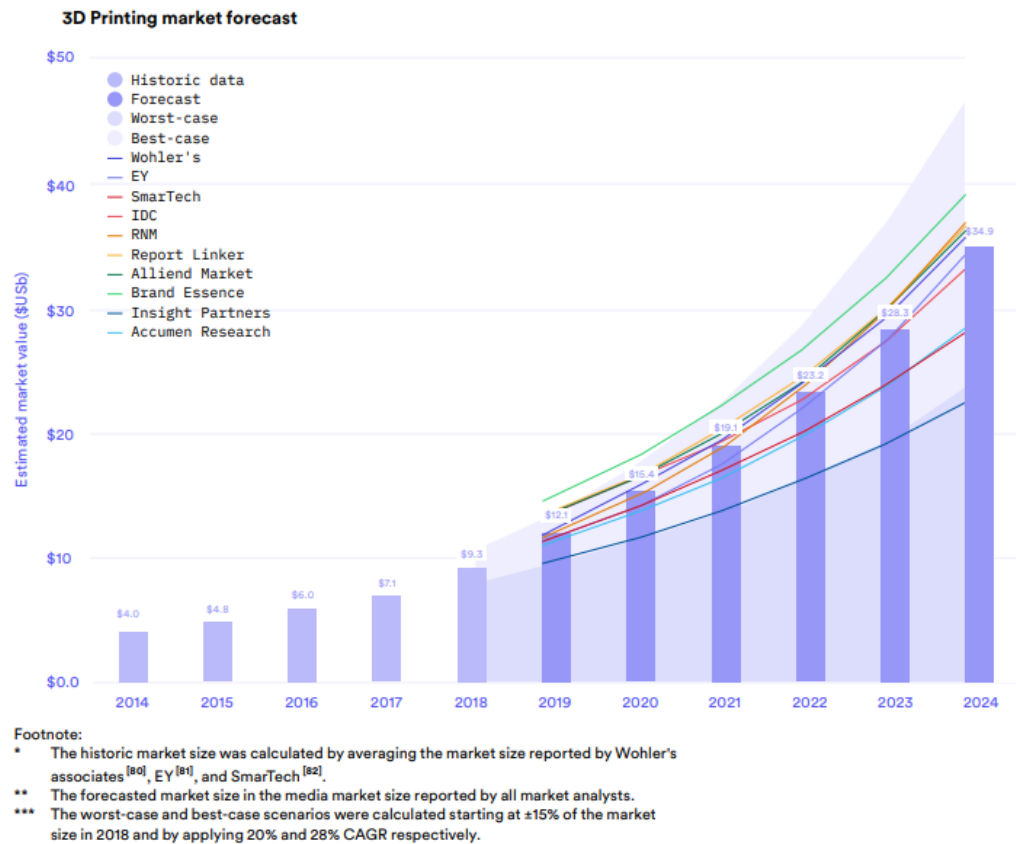
Figure 3. *3D printing market forecast until 2024 [11]*

4. Implementation of Additive Manufacturing in the Maritime industry

The advances in the adoption of AM of the maritime industry are rather recent. In 2017, at Damen Shipyard Group's headquarters in the Netherlands, the world's first 3D printed ship's propeller has been produced and class approved [12]. The so called WAAMpeller was the result of joint efforts, resources and knowledge of five companies. The triple-blade propeller design was provided by Promarin, Figure 4. The Port of Rotterdam's RAMLAB (Rotterdam Additive Manufacturing LAB) carried out fabrication using Wire Arc Additive Manufacturing (WAAM) techniques, which consisted in laying down 298 layers of Nickel Aluminum Bronze alloy. The support in software, robotics and additive manufacturing came from Autodesk's expertise. Damen provided Research and Development resources, as well as one of the Stan Tug 1606 vessels for operational testing purposes. The testing programme included bollard pull and crash stop testing in addition to speed trials. In all of the tests the WAAMpeller displayed the same behavior as a conventional casted propeller. The crash stop scenario deserves a particular mention, since it consists in going from full throttle ahead to full throttle reverse, and it represents the heaviest loading that a propeller can experience. Even under those circumstances, the same level of performance as a conventionally built propeller was achieved. Bureau Veritas' role was to verify the entire development, production and testing process. Another achievement of the RAMLAB's experts is the development and testing of spare parts convenient for 3D production, such as spacer rings, hinges, exhaust gas manifolds, turbocharger nozzle rings and turbocharger gas inlet/outlet casings.

545

In November 2019, the University of Maine revealed a boat that was fully 3D printed in one piece to demonstrate the capabilities of the LSAM technology [13]. In an industrial setting, the use of AM for spare parts and replacement components in the maritime industry is also steadily increasing, with companies like Wilhelmsen, Thyssenkrupp and Navantia leading the way.

Wilhelmsen [14] provides a combined service of 3D printing spare parts and delivery via drone. Currently, they are the only drone delivery provider authorized by the Civil Aviation Authority of Singapore (CAAS) to execute drone deliveries Beyond-Visual-Line-of-Sight (BVLOS) to vessels at anchorage. In this moment, the drones are capable of carrying a load of 5 kg over a distance of 50 km. As a future goal, F-drones' long-term ambition is to develop a larger scale drone capable of delivering 100 kg to vessels up to 100 km away. In December 2019 Wilhelmsen's Marine Products division launched an exclusive Early Adopter Program for 3D printed marine spare parts. Six maritime companies signed up to begin utilizing on-demand additive manufacturing: Berge Bulk, Carnival Maritime, Thome Ship Management, OSM Maritime Group, Executive Ship Management and Wilhelmsen Ship Management.

Thyssenkrupp is the leader in the advance of TechCenters [15]. As the first of their kind, a TechCenter was established in 2017 in Mulheim, near Thyssenkrupp's international headquarters in Essen, Germany. These facilities are set up to provide additive manufacturing production and consultancy services. A second TechCenter was opened by the company in Singapore in early 2019. In 2019 the company obtained the Approval of Manufacturer certificate, which is the first ever to be awarded by leading quality assurance and risk management firm DNV GL [16]. DNV GL's Approval of Manufacturer certificate ensures that the Thyssenkrupp TechCenter is able to produce additive manufacturing parts which are at least as reliable and productive as conventionally made parts. In particular, this refers to the 3D printing and processing of austenitic stainless steels, one of the most commonly used stainless steel grades in industry. Acceptance testing has also been cleared under the EN 10204 standard for inspection and other standards related to chemical and physical material characteristics. The production, amongst other mechanical components, includes spare parts for submarines.

Figure 4. *The WAAMpeller [12]*

Figure 5. *A probehead for taking gas samples in hot gas atmosphere, produced at the Thyssenkrupp TechCenter Additive Manufacturing [15]*

An interesting collaboration has been achieved between the Oak Ridge National Laboratory and the U.S. Navy. They have created a submarine hull prototype which consists in 6 carbon fiber

composite material sections, with a total length of 10 m. While a submarine hull of that size usually takes between $600,000 and $800,000 and around 3 to 5 months to build, the 3D printed prototype took only 4 weeks to complete, and the costs were reduced by 90%.

The year 2020 has been challenging for most industries, and some of the projects that were active in 2019 were delayed or postponed. For example, Engineers at the Rotterdam Additive Manufacturing Lab (RAMLAB) were exploring the use of additive manufacturing processes to quickly carry out repairs to damaged ships. An on-site facility was built, and it included a pair of six-axis robotic arms, capable of additively manufacturing large metal industrial parts. The idea was to reach faster fabrication by 3D printing metal components and finishing the pieces using traditional CNC milling and grinding methods within days. The progress of these activities has slowed down in 2020 due to the global pandemic.

Onboard production of spare parts seemed like a very interesting option for the maritime industry. Yet, while additive manufacturing on shore is expected to have a successful future, it is less likely that ship-borne 3D manufacturing will be as popular. Many components still require finishing by machine, thread-cutting or polishing, which are specialist skills and would require additional tools and equipment onboard. Further, mechanical components used onboard require a wide variety of different alloys for fabrication. To effectively implement shipborne 3D manufacturing, a similar range of materials would need to be kept on board, raising issues of degradation and space for storage in the correct controlled conditions. Another issue is quality control. The quality of components would still inevitably need to be verified by Manufacturers and Class, even if they are produced using OEM-approved programs and machines, as there is a risk that parts could be produced negligently or under unfavorable conditions. Taking all this into account, shoreside manufacturing, or even offshore, is likely to be a reality soon, starting with Class-approved strategically placed local workshops. By providing 3D printed spare parts on demand, the typically high supply chain costs can be reduced. Instead of going through time consuming and costly storage, shipping, customs and receiving processes, a system of unique selection, digitization, and on-site production can be embraced. With the present development, such an advancement is expected to be implemented by 2030 [17].

5. Conclusion

Additive manufacturing has been developing rapidly in the past 10 years. The maritime industry tends to be part of the late majority when it comes to adopting new technologies, especially considering the rigorous safety and structural requirements that each ship component must comply with. However, the benefits of 3D printing are becoming a part of the ship production and maintenance process. Spare parts are the fastest growing niche, as ships are always on the move and access to repair facilities or parts storage is limited to the short time vessels are docked. With the option to rely on 3D printers, whether aboard ships or in strategic ashore workshops, parts can be produced rather quickly in case of emergency. Such an approach would minimize the cost of shipping and storage. In addition to that, the various components and spare parts could be easily customized to provide a solution to the most complex situations. Another set of great advantages of 3D printing are the reduced time and costs of manufacturing compared to traditional methods. The challenge that additive manufacturing meets, in terms of on-site and on-demand production, lies mostly in quality control. Despite the standardized procedures and materials, it is not a bulk production process and each piece would require individual verification and approval. This issue

makes onboard 3D printing still just an idea and not a reality. However, the concept of sending files instead of physical products is spreading fast, and it is shifting the known ways of production and shipping towards a very different approach.

REFERENCES

[1] Kodama,H., "A Scheme for Three-Dimensional Display by Automatic Fabrication of Three-Dimensional Model," IEICE Transactions on Electronics (Japanese Edition), vol. J64-C, No. 4, pp. 237–41, April 1981

[2] Kodama, H., "Automatic method for fabricating a three-dimensional plastic model with photo-hardening polymer," Review of Scientific Instruments, Vol. 52, No. 11, pp. 1770–73, November 1981

[3] "History of 3D Printing: When Was 3D Printing Invented?". All3DP. 10 December 2018. (22.11.2019.)

[4] www.prusa3d.com (12.09.2020.)

[5] Temple, G.,"3D printing & the marine industry", OPINIONS, safety4sea.com, 25 September 2018.

[6] www.thermwood.com (11.09.2020.)

[7] Giessbauer, R.; Wuderlin, J.; Lehr, J.: "Future of spare parts is 3D: A look at the challenges and opportunities of 3D printing", Strategy&, 2017. (18.06.2020.)

[8] "3D printing: hype or game changer?"A Global EY Report 2019, EY, 2019.

[9] "3D Printing Sentiment Index", Ultimaker, 2019.

[10] Moore, G. A., "Crossing the Chasm", HarperCollins, 2014.

[11] "3D Printing trends 2020, Industry highlights and market trends", 3DHUBS, 2019.

[12] www.damen.com (10.09.2020.)

[13] composites.umaine.edu (11.09.2020.)

[14] www.wilhelmsen.com (02.09.2020.)

[15] www.thyssenkrupp.com (02.09.2020.)

[16] Spath, N. "DNV GL awards thyssenkrupp first Additive Manufacturing Approval of Manufacturer certificate", DNV GL NEWS, 26 August 2019.

[17] Hand, M. "Impact of 3D printing on shipping volumes visible from 2030: Singapore research", Seatrade Maritime News, 29 October 2019.

DESIGN AND STYLE OF SMALL CRAFTS: RELATIONSHIPS BETWEEN AESTHETIC LAYOUT AND CONSTRUCTION TYPOLOGY

Enrico Tommaso Carassale

University of Genoa, Italy
enrico.carassale@unige.it

Abstract

The compositional design of the pleasure craft is not self-referential and autonomous: apart from stylistic, sociological and fashion factors, it is strongly conditioned by the technological-constructive aspect, which sometimes becomes the foundation of the expressive code adopted therein.

In the history of modern boating, since it became a mass phenomenon, the construction method evolved in serial production has further constrained formal freedom. Nowadays, the compositional design articulates by new formal elements, respect to the past, in relation to complex mechanisms imposed by construction planning. Due to these new logics, it represent now a more complex process in the integration of the parts, being the modern boat a product increasingly characterized by the presence of serialized components. Consequently, the aesthetic approach implicitly reflects these features of constructive and productive order. The romanticism give way to a new multifaceted design vision, called to consider, right from the outline concept, multiple aspects: including the logistics of the outfitting phases, increasingly characterized by prefabrication and assembly of outsourced components. The paper in question proposes an evolutionary excursus of the design of pleasure boats, which aims to analyse and highlight the intelligibility of these effects in the aesthetic layout of the boat.

Key words: *Pleasure Boats ; Yacht Design ; Style and Aesthetics of the Boat*.

1. Introduction

In the field of yachting design, we can say the creative process at the base of a formal research, aimed at defining the shape, results by the convergence of several factors. In fact, from the compositional point of view it is reductive to identify the design of the boat solely in the shapes of the casing. Actually, the aesthetics are strongly connected with the character of the boat, meaning in this term the set of functional and performance operational characteristics of the boat, the shape is then a communication tool that transmits the possible performances of a specific model to the outside. In the design of the modern boat, aesthetics are no longer just synonymous, as in the past, with a harmonious balance in the proportions of the general parts, each of which had a specific "raison d'etre" based on essentially functionalistic criteria: now its task main seems to be oriented on emotional communication. According to the principles of modern design, expressing the contents of a product means highlighting its characteristics, emphasizing them, with a mechanism that was previously the exclusive prerogative of the visual arts and advertising. The project evolves through aesthetics in stylism; its action focuses on the materials, on the typical parts and functions that make up the entire building: the shell, the windows, the side closures, the cover, the side-hull, the bow and stern ends. This approach coincides with the massive development of the pleasure craft, that is, from the moment in which its diffusion subjects it to the rules of any serial product, subject mainly to the rules of generalization, that is, to capture the taste not of a specific ship owner but of a category as large as possible of "consumers". Nautical design today assimilates contents, methods and communicative traits typical of other sectors of industrial design. The pleasure craft is involved in general design trends; the shipyard's proposal today is no longer a simple object - a good of use - but a total offer,

which summarizes models and lifestyles: open spaces in motion to be lived in freedom, without borders or limits.

The boat becomes a place for experiences and a socialization tool, a habitable environment that conforms to the different modalities and multiple needs of modern living: in the variety of comforts and areas for common life. Hence the need for a clear aesthetic language, characterizing the external (the bodywork) [1] and internal (the habitable cell) apparatus. This initially happened for the two parts in different and discordant ways for which the pleasure boat appears to be an extremely heterogeneous and contradictory artefact.

2.   The importance of formal reference in the current design logic

The boat is now as an articulated complex, in which each part becomes the seat of specific peculiarities: the propulsive technical apparatus, the structural set, the habitable system. It is a complex coordinated with a series of internal and external parts, in which the casing also performs - in addition to the protective one - an aesthetic and communicative task, thus becoming a tool of intelligibility for the operational qualities of the object. The bodywork is the main way of communication. Its shape must "produce emotion" in reference to universally shared codes in the aesthetic field. Thus, it now becomes an expressive complex that highlights a disparate series of qualities: strength, character, stability, dynamism, marine qualities. In addition to the assets of the boat, it also summarizes stylistic features that can be associated with the particular history of the shipyard and its construction peculiarities. The aesthetic apparatus thus becomes a chronological synthesis, outlining iconographic elements that are at the same time evocative of a specific modus operandi. In the modern yacht, this representativeness extends by continuity from the exterior to the interior, the latter no longer an unrelated element but organic to the general stylistic language. Although in the past the formal dichotomy between interiors and exteriors was quite distinct, nowadays the revision of the principles of modern living, together with the new modes of nautical cruising (alternative, more sustainable and conscious), has led to new configurations of the on-board living area. The pattern of the living spaces has seen a profound transformation over time, which has led to the current continuity and connection between the spaces on board, and to their convertibility for a wide combination of housing solutions, with a view to "total liveability" which affects the shape of the superstructure. Rather than a continuous shell, the perimeter envelope now consists of multiple construction elements: sliding windows that recall the architectural concepts of curtain walls, horizontal closures that recall the verandas with tensile structures like the villas on the sea; the motor yacht progressively abandons the dynamism of forms, disregarding those compositional principles that subjected it to automotive design. We can say that the formal reference in nautical design of the last 60 years has continually changed, alternatively drawing on other Design sectors. The reasons for this change lie in the very concept of yachting: since the 1960s, it has changed from an elitist expression of the circles of sea experts linked to tradition, to a phenomenon of bourgeois customs, animated by neophytes who identify the motor boat as a status symbol. The boat becomes an element of social appeal whose value often surpasses the technical qualities of the marine vessel; therefore, aesthetic features proper of other design sectors, such as shapes, accessories, finishes and colour combinations, come together on board the boat. The accessory virtues become essential for the commercial success of the "nautical product": the pleasure boat thus combines the qualities of the marine vessel with the functionality of "terrestrial" objects becoming, by virtue of this, an unprecedented escape from everyday life. It becomes a *sports coupe*, whose function is to guarantee the same raids, beyond the limits defined by the road: a means of transgression of the rules, according to a very distant mood

compared to the sailor spirit of the yesteryear yachtsman based on attention and respect of the sea. Because of the same principle, the *boat-caravan* was born in the need for a mobile home, in the wake of the road model: the response of modern yachting to the desire to escape the limits of the house relegated to unchanging contexts. It appears as a furnished space - equipped with relaxing armchairs, deck chairs, a modular kitchen, extensible tables - very different in configuration from classic yachts. At a later stage, the "speed footprint" contaminated the flying bridge motor-yacht, through high-performance hulls and higher powers, with evident compositional implications through a new language that highlights the dynamic qualities of the craft. This approach once again reflects automotive [2] and aeronautical references, not integral –as in the past- but partial, through evocative inserts, sometimes consisting of a stylization of technical or structural components, such as engine room vents, exhaust pipes and stanchions of superstructures.

3. The design of the superstructure: the shape that conveys an effect

The project is often the synthesis of two opposing tensions: inspiration and management of the construction process: whether in the first the formal and functional components interact as a whole, in the second the project address the profitability issues and the various production phases, in order to make this construction economically justified. Therefore, the constraints related to industrialization of product - together with the development of outsourcing – deeply affect the shape of boat, since the design processes are less and less autonomous and increasingly interconnected with the several variables of the production chain. The modern project stands out for the heterogeneity of its formation, extremely dependent on the features of its components: the creative intuition, at the basis of the artisan individuality, appears to be increasingly "attenuated" by the terms of an industrialized multi-headed system. Together construction materials, serialized components have thus become relevant in the aesthetics of the boat, conditioning evermore the compositional experience. On the one hand, this resulted in general homologation of formal solutions by constructive and productive issues, typical of serialization; similarly to what happened in the automotive sector, over time the aesthetic characterization of competing models has shifted mainly from general proportions to the aesthetic solutions of the particular: namely the component become decisive (Fig.1). The iconic element, evocative of a particular conception of pleasure craft and a specific lifestyle, becomes an element of formal characterization, not extended to the whole complex but to delimited and defined parts of the perimeter envelope; in some cases it is a technical or structural part. A first example of this replacement work occurs in the USA, already in the post-ww2 period, when the design focus seems to concentrate on the optimization of the production system, through appropriate construction methodologies and compositional solutions aimed at the economy of scale. Chris Craft production was the first to develop a formal characterization of the boat body, based on the automotive imprint. In the modelling of the topside of the boat, this reference implied, beyond a mere stylistic aim, a formal synthesis compatible with the industrial rationalization process that was beginning to affect the nautical sector as well[1]. The design task had both to solve the *Venustas-Firmitas-Utilitas[2]* triad and

---

[1] The roof of the 1949 Chris Craft Sedan 23 is the result of an innovative constructive solution: it used a wooden frame with orthogonal stiffeners to create the sixth of a surface with double curvature, to which a polyvinyl fabric covering was applied. The system guaranteed weight reduction compared to traditional contemporary techniques, given the slender uprights and the large windows and the windscreen that recalled the hoods of the contemporary car model made of stamped sheet metal.

[2] Marcus Vitruvius Pollio, or just Vitruvius, established architecture as a noble and essential endeavor. In his treatise, 10 Books on Architecture (*De architectura*), Vitruvius penned the canon of classical architecture that would influence not just Romans but billions of people throughout antiquity to today.

production issues, considering the production numbers that the boating boom of the period required. This aesthetic-productive pattern of nautical design soon became a reference paradigm, exported and assimilated overseas. In Italy, Baglietto [3] and Riva [4] were the first shipyards to assume such intentions, thanks to the advice of expert managers from the American experience[3] as well: the famous *Ischia* and the *Aquarama* were in their respective typologies clear examples of an aesthetic characterization for precise references.

Figure 1 *Riva Super Aquarama. New concepts in the stylistic references of the deck*

4. Influence of the automotive style

In the 1950s, a new stylistic current tended to identify the shapes of the boat cabin with the car hood. The aesthetics of the day cruiser boat focuses on a series of details of sure appeal: the two-tone glossy bodywork, the windshield, the perimeter frames, the chromed lettering, the navigation lights, the horn, the rubbing band, the leatherette upholstery. Just like in cars!

On the other hand, stylistic innovation entailed less restrictive constructive solutions than the traditional one in wood: research was required on the development of current techniques which involved the use for some forms of plastic material, joined to the wooden parts with metal gaskets; solutions that recalled the chromed joints between the various stamped sheets of car bodies (Fig.2). The combination of different materials becomes a peculiarity of the new course of yacht construction: in this period, due to changes in production, the age index of the models presented follows the rhythms of the automotive industry, already marked by the phenomenon of "Annual model change"[4]. The

---

[3] Around 1965 Richard Ross, coming from the Chris Craft Italia plant in Fiumicino, became production manager of the Baglietto shipyard. He implemented productivity by reducing the construction time of the individual components of the boat and introducing the assembly line, with the boats moving around the shipyard for each specific stage of preparation called "just in time".

[4] Defined as "Dynamic Obsolescence", it is a principle attributed to the American designer and business executive of GM Harley Jefferson Earl (1893-1969), for which each model produced had to have a short commercial life linked to a specific aesthetic code, attributed to a specific time interval (1-2 years) annually.

stylistic influences of *Tailfin* [5] soon involved the design of the boat: it was thus that the construction type of wood declined with the increasingly widespread inserts of fiberglass parts. Inexorably, as happened in the automotive sector, obsolescence now influences nautical design, an additional reason why the construction times for wood can no longer bear the new production rhythms imposed by the logic of the market. Thus, it was that in the United States, a decade earlier than Europe, fiberglass construction became the only solution to address both formal-constructive and economic-productive constraints.[5]

Figure 2 *Chris Craft Constellation 35, 1956.*

5. The 1970s: influences of construction in marine plywood on the compositional means

The Italian and European production in the same period was still in a complete artisanal dimension, could afford construction systems to unity, and therefore still linked to the technique of wood: by virtue of this, the aesthetics of the motor yacht still took up the model American fast-commuter of the turn of the century. In Italy, as regards the production of motor cabs, the construction technology of laminated wood and plywood was still in vogue until the mid-70s, for boats up to 20 meters albeit evolved in a logic of production optimization, for commercial success that the historic national shipyards were collecting.[6] Thanks to a design revolution that -making a virtue of necessity- combined the limits of the construction system with a renewed concept of overall layout, the *Mediterranean motoryacht* [6] redefined in a single solution the aesthetic concept (self-directed from overseas influence) of the superstructure. This new concept revised the spatial distribution, the general volume and the "solids and voids" ratio of the perimeter cover. In this case, the typical

---

[5] The moulded fiberglass construction system made it possible to build shapes more similar to car bodies, with double curved surfaces with an economy of scale for large production numbers, and to make aesthetic changes to the moulds to have continuously renewed models.

[6] Baglietto Ischia, the Italian fast commuter, born from the pencil of Giorgio Barilani and the genius of Pietro Baglietto; laminated wood structure, built in more than 100 specimens between 1959 and 1967. It represented one of the first examples of medium-sized serial construction for the Italian shipbuilding industry.

constraints of marine plywood construction become opportunities for a new aesthetic characterization of the topsides: rectified and geometrized deck lines, with wedge-shaped and tapered fronts, corner fittings, sharp profiles that stop abruptly at the stern. An original language that also redesigns the volumetric proportions between hull and superstructure, that has reason to exist according to a particular construction typology. It will identify an autonomous design current, both with respect to the overseas and to the traditional local model: a style that we could define as "cutting edge". The exteriors were characterized by the evidence of technical and structural elements integrated into the superstructure, for example the raised uprights transmitted strength and safety; the inclined cut of the side windows made the profile lighter in spite of its general massive proportions. The side stood out for an inverted sheer and by the relief boxy shape of exhaust ducts, ending with a diagonal cut forward. The larboard bow, without flaring, had fuller volumes that ensured greater roominess in the forward cabins. The constructive logic by added blocks made a vertical hierarchy of the topside, characterized by the overhangs of the aft canopy and the flying bridge (Fig.3).

This formal code will leave imprints also in the modelling of the first 80s, when in the meantime the shipbuilding industry will abandon the wooden construction for the fiberglass technique. Philologically, many components that previously had a constructive function remain purely stylistic signs, thus defining a classic canon that characterize the typology. However, very soon, already in the mid-1980s, the evolution of shipbuilding aimed at the optimization of fiberglass technique methods, will mark the inexorable adoption of a new aesthetic language characterized by the "continuous casing", for which the different parts of the superstructure were no longer visibly detached and interlocking but merged into a single modelled shell [7]. The aft overhang of the flying bridge now constituted the only element of detachment.

Figure 3 *Baglietto 16,50M, by P. Caliari, 1967*

6. The fiberglass technique and the covered hull joint as an aesthetic element

However, to the detriment of total surface continuity, the fiberglass technique involves new construction constraints that reverberate on the shape of the topside: first, the hull-deck joint, a true element of break in the vertical continuity of the building (fig.4). It also represents the geometric place of the hull's maximum bulk and delimits the inversion of transverse inclination between the hull and deck mouldings [8]. This geometric-constructive constraint well highlighted by the fender bar that ends aft by an inclined line, and there the juxtaposition of the two moulded shells creates a new functional space, the stern platform. It will become a typical pattern of the modern motor yacht, as it represents an important functional connection node: between the cockpit and the tender, between the cockpit and the quay end between the cockpit and the sea.

In general, the aesthetic effect produced by this type of construction is surface plasticity: from the simpler and minimal solutions of a single deck mould, to the more articulated and complex ones of superstructures composed by several blocks. A superficial continuity in which the windows highlight the compositional language, taking up - depending on the case - the tapered and taut shapes of the architectural type or the sinuous and organic forms of zoomorphic inspiration. The construction technique thus generates a stylistic code shared by most shipyards. I.e. the diagonal upright represents an important typological and constructive element: it is an aesthetic splitting-line between the rear and the cockpit windows conferring lightness to the side; on the other hand, it constitutes a structural stiffening rib, given by the reduction of the transverse curvature radius of the edge. In models from the 90s onwards, it also identifies the junction place of two deck moldings: the lower one merged with the superstructure and the flying bridge-cockpit block. The constructive solution of the continuous shell interspersed with slender fixed windows entails limits in the interior layout; in fact, as a result the habitable cell is visually distanced from the outside: gloomy and not panoramic, with the centripetal arrangement of furnishings that follows and accentuates this oppressive isolation effect. In this way, the construction typology directly influenced the distribution choices, as well as the aesthetic choices (Fig.5).

Figure 4 *Alfamarine Cronos 83, 1985 by Arch. F. Harrauer: the topside as a continuous and tapered casing*

Figure 5 *Sunseeker Manhattan 80: example of late 90s exterior shapes based on concept of the modelled shell*

The concept of closed shell was unhinged during the first decade of 2000 when, thanks to the turnaround in the concept of motor cruising: which prefers navigation comfort to pure performance. Consequently, the concept of main-deck space changes, progressively passing from a series of functional cells to a total living space without solution of continuity. The concept of total liveability on board soon led to a reduction in the separation between interiors and exteriors. Consequently, the superstructure abandoned the concept of "closed shell", in favor of a convertible system, more open and brighter: less faired but more versatile! In addition - thanks to an expansion of on-board volumes - top speeds reduced and especially in the new types (Long range, Luxury Explorer and Trawler), the aerodynamics of the external shapes attenuated for greater consistency with the mood of the semi-displacement pace. The relationship with the environment, from a merely panoramic element, increasingly influences the distribution solutions of the new family cruisers, now merely inspired by the residential reference model [9].

The superstructure "changes its skin", becoming a heterogeneous surface aesthetically characterized by continuous windows and overlapping overhanging roofs; the main deck is now a system composed of walkable surfaces, terraces, opening windows, transformable platforms, convertible areas. According to latest trends, the large surface of windows and their lowering threshold allows greater panoramic views of interiors, as well as a physical continuity between indoor and outdoor. In addition, the sides equipped with folding surfaces provide expanded walkable surfaces, implementing the liveability of main deck, through wide bulwark balconies.

This new compositional order produces a complex element in which multiple functions interact. The design process, as well as the shapes, have to manage many technological components of the transformable machine aimed to "total liveability" of the modern motor yacht through a series of devices such as submersible stern platforms, openable balconies jutting out into the sea, automated opening systems for the roofs and side windows. The modern motor yacht increasingly characterizes as a transformable element, no longer fixed in a predefined form. By virtue of this peculiarity, the more or less serialized kinematics thus become an integral part of the project. Sliding guides, cornice elements, openable balconies, tensile structure awnings as well as constraints characterize the

aesthetics of the modern boat, which, by virtue of the new living standards, it has more and more points in common with residential architecture. The structure hides behind a technological skin, which if on the one hand allows for a formal simplicity, on the other hand, it underlies a sophisticated technology in the composition of heterogeneous materials and in the extreme precision of the combinations between components of the superstructure. Thus, the contrast between formal simplification and constructive complexity thus emerges evident in the project (fig.6).

The latest motor yacht trend seems to be oriented towards a visually minimal model, in which the roof stands out, as in the 1960s: an evident formal element, both in the lateral and longitudinal overhangs, which runs suspended over the transparency of the perimeter strip windows [10].

Figure 6 *Wally Ace 27m, 2012, by L. Bassani: forerunner of the new architectural style of motor yacht*

7.   The hull as an aesthetic complement to the superstructure

The hull, by definition, summarized the hydrodynamic, stability and seaworthiness qualities of a boat and by extension the characteristics of the freeboard (sheer, stern and bow closures), fulfilled these tasks. Moreover, in the design this part relating to the engineering field was formally distinct from the topside of the boat. Even in the period of serial production, the artefact still defines itself in two different parts, so in the logic of economies of scale, a hull could support, beyond slight adjustments, different models. With the evolution of industrialization, the hull has in fact become an integral part of the design of the topside and - as well as constituting a technical part - has become a stylistic element, secondary respect to the superstructure. The trends of modern design therefore provide for an aesthetic unification between hull and deckhouse, reducing as much as possible the parting between the two, contrary to what happened in the past. The gradual hybridization of the pleasure craft dictated by current standards has finally also affected the hull, now more "permeable" than its original function of protection and safety. This process took place gradually: at first in the management of the sheer lines, then - as mentioned- through the inclination and functional configuration of the stern, finally through the side windows, progressively extended. The hull side now integrates into the overall style: the characterizing lines there formed find continuity and complement above the waistline in the upper topside. From this point of view, the stern terminations find strict connection with the

rear superstructure, creating a coordinated complex in which the stern tail, the engine air intake[7] and the hull windows merge themselves and interact in order [11]. According to this vision, the technical parts housed along the side acquire a formal value, beyond their primary purpose. However, the element that most characterized the design unity between hull and superstructure, in an unprecedented coordination, is the opening of the surfaces of the side. These innovations are dictated by functional and aesthetic needs, such as the improvement of brightness and panoramic views for the cabins, a better rendering of the interior finishes that stand out under natural lighting, not least for the recognition from the outside of the owner stateroom in the hierarchy of the hull windows (Fig.7). This distortion of the established order, due to primary needs for the current logic of the nautical market, has led to complications in the technical design, through the introduction of new constraints (for example in the opening of portions of the side) and in juxtaposition of materials with different mechanical characteristics. Complications that were unthinkable only a few decades before. A final note we can only address to the hull whose proportions are sometimes altered and subordinated to formal rules. Sometimes properly functional elements such as the inclination of the stem and the sheer are expropriated of their original value and subject to a mere aesthetic purpose, which debases and distorts the fair relationships between engineering and architectural means, in the interaction between Strength, Utility and Beauty to express only an empty and useless stylism. The vessel should be defined as a complete project only when the different souls of the organism are correctly balanced - and mutually integrated: technical efficiency, seaworthiness, stability, safety, functionality, comfort and aesthetics. In function of a total equilibrium of all aspects of project.

8. Conclusions

Although the most performing cruise types continue to coexist on the market, such as *coupé*, *sport-fly* and *flying bridge*, the *long range* type is increasingly spreading in the different versions *trawler*, *shuttle*, and in the latest *cross-over* derivations. [12].

From a compositional point of view, the latter types have in some way created a reference model thus influencing the former as well, through: linear and continuous superstructure surfaces without visible uprights, defined by the combination of a glazed shell and the canopy-bodywork, with an increasingly strong prevalence of voids over solid. This sense of formal lightness has been made possible only thanks to the evolution of construction technology: major shipyards such as Azimut, Ferretti, Sanlorenzo and Riva have long been experimenting with hybrid construction systems that involve the use of different composite materials in the different parts of the exterior. The construction in carbon fibre, increasingly widespread for the moulded components of the topside, flanks now the fiberglass structure of the hull. What was a system used for one-off constructions, begins to have more and more diffusion also in the series production of cruising models, as in the case of the Riva 88 Folgore, the Azimut Grande, the "S" and the "Flying Bridge" series. The superstructure shell, the fly bridge shield, the radar arch, the hard top and the transom are the main parts now stratified in carbon. Its structural lightness is reflected in the formal language: now the mighty uprights that have constituted the aesthetics of the superstructure of the past decades disappear to make room for a new, more sober language - albeit with the necessary concessions to the stylistic features (historical trademarks) proper of the shipyard.

---

[7] One of the first series models with the air intake integrated in the sidewall was the Jeanneau DB 33 of the second half of the 1980s, which has a duct inserted in the moulding of the side, covered with square-shaped protective carter that echoed the general lines of the deck.

The compositional simplification is thus a metaphor for a new approach to cruising that characterizes the medium-sized motor yacht according to general trends. In the current period, the compositional vitality of the "innovative shipyards" is confirmed by the market responses to new types compared to traditional ones. The latter remain with re-editions that from the design point of view do not offer an effective formal innovation (beyond the stylistic and technological updates of the on-board components) except in typological hybridizations [16]. The Crossover phenomenon in fact represents the most innovative proposals in the reinterpretation of the motor yacht concept, according to more environmentally friendly parameters, compared to the traditional category [17]. It is no coincidence that the market for this particular sector nowadays experiences a phase of particular productive vitality in the number and variety of new models as well as in their compositional originality.

Figure 7 R*iva 88 Folgore, 2020: glazed deckhouse and formal continuity between hull and superstructure*

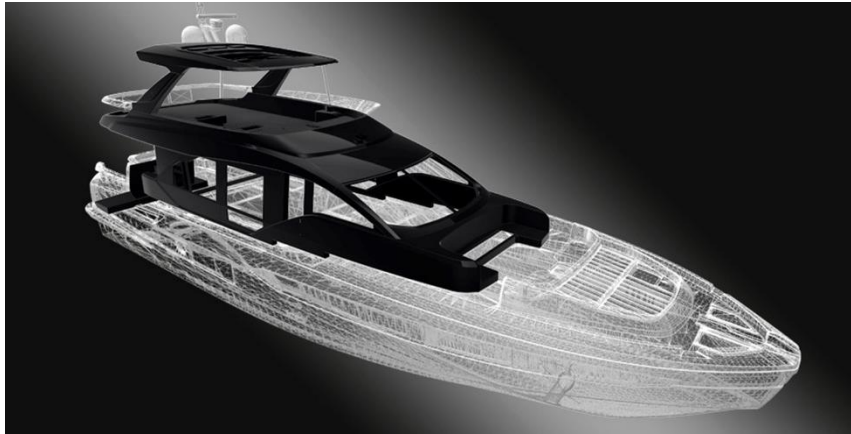**Figure 8** *Transformable systems for balcony bulwark*

Figure 9 *Azimut 78 flying bridge, 2018: superstructure in carbon fiber*

References

[1] Tumminelli P., *Boat Design,* TeNeues, NewYork, 2005.

[2] Tumminelli P., *Car Design,* TeNeues, NewYork, 2005.

[3] https://www.altomareblu.com/*nautica-pietro-baglietto*/ G.Vitale.

[4] https://motori.corriere.it/motori/cards/*cantieri-riva-storia-modelli-piu-belli-mito-aquarama-domino-super-lusso/futuro*-122-mythos.shtml

[5] https://journal.classiccars.com/2020/04/28/*50s-cars-werent-the-only-vehicles-with-fancy-fins/* L. Edsall

[6] Musio-Sale M., *Yacht Design, dal concept alla rappresentazione*, Tecniche Nuove, Milan, 2009.

[7] Carassale E., *Cronos 83, Yacth'n Italy Export Museum. Il Mediterranean Style '79_'99*, Vol.II, by Caliari P.F., Musio Sale M., Ucina, Milan 2014.

[8] https://nauticareport.it/dettnews/report/*dal-mogano-alla-vetroresina-storia-di-un-cantiere-diventato-leggenda*-6-5437

[9] Carassale E. *Evolution of the motor yacht superstructure relations between habitable plant and environmental context,* CMN 2019. Third International Conference on Nautical and Maritime Culture. 14-15 November 2019. Naples

[10] https://www.sportfair.it/2016/07/*yacht-wally-ace-conquista-leuropa*/V. Ferrandello

[11]   https://pressmare.it/*cantieri/riva/2020-09-23/il-nuovo-sport-fly-riva-88-folgore-innovativo-per-sempre*-28143

[12] Carassale E., Montecarlo76, *Yacth'n Italy Export Museum. Il Mediterranean Style '99_'15*, Vol.III, by Caliari P.F., Musio Sale M., Ucina, Milan, 2015.

[13] https://www.barcheamotore.com/*evo-r6-transformer-barche-a-motore*/

[14] https://www.boatmag.it/41199-*test-del-cranchi-settantotto-flybridge-25-metri*/ M. Darai

[15] https://www.barchemagazine.com/sanlorenzo-sx76-2/ L. Sordelli

[16] https://www.thewaymagazine.it/*luxury/sanlorenzo-lo-yacht-crossover-con-vivibilita-aumentata/*

[17]   https://www.pressmare.it/*cantieri/sanlorenzo/2020-10-02/bluegame-presenta-in-anteprima-mondiale-il-nuovo-bgx60-28324*

Images references

Figure 1 https://www.wired.com/2013/10/lamborghini-riva-aquarama/
Figure 2 https://seattle.boatshed.com/chris_craft_35_constellation-boat-254575.html
Figure 3 https://i1.wp.com/www.altomareblu.com/wp-
content/uploads/Bagliettostory_5FFC/Baglietto1650Caliari.jpg?ssl=1
Figure 4 https://www.altomareblu.com/carene-franco-harrauer/
Figure 5 https://iyc.com/yachts/manhattan-80/
Figure 6 https://www.wally.com/wallyace/wallyace27.html
Figure 7 https://www.facebook.com/rivayacht/photos/pcb.3614724051890619
Figure 8 https://www.nauticexpo.com/prod/besenzoni-spa/product-21536-518777.html
Figure 9 https://it.azimutyachts.com/azimut78.html

FESB Hydro team – Student project

*Matej Dević*a, *Duje Fržop*a, *Luka Galić*a, *Filip Raič*a, *Ante Buble*a, *Karlo Vučić*a, *Jure Bebić*a

a FESB, University of Croatia, R. Boškovića 32, 21000 Split, Croatia
* Corisponding Author, mdevic00@fesb.hr

Abstract

FESB Hydro Team is a group of young and ambitious students from the Faculty of Electrical Engineering, Mechanical Engineering and Naval Architecture in Split. It has been operating as a group since the beginning of the academic year 2018, after it was decided to spend some time on practical work at the instigation of the professors from the Department of Naval Architecture. In the period since its establishment, the group has engaged in the design and manufacture of a vessel for the international competition "Hydrocontes-X". Hydrocontest is a competition launched in 2013 at the initiative of the Hydros Foundation and the Swiss private bank Lombard Odier. The vessels are remotely controlled and powered by an electric propulsion. This type of competition brings together students from different faculties and they present themselves and their faculty by making advanced boats that must be made according to the rules of the Hydrocontest itself. The competition is conducted in three categories:

- Lightweight (load 20 kg)
- Heavyweight (load 200 kg)
- Endurance race (1h with a load of 20 kg)

This type of project, where the theoretical knowledge acquired during the study is applied, is of great importance to us as future shipbuilding engineers.

Key words: FESB; Student project; Hydrocontest-X

Sažetak

FESB Hydro Team je grupa mladih i ambicioznih studenata s Fakulteta elektrotehnike, strojarstva i brodogradnje u Splitu. Grupa djeluje od početka akademske 2018. godine, nakon što je odlučeno da će se više vremena potrošiti na praktični rad na poticaj profesora s Katedre za brodogradnju. U razdoblju od svog osnutka, grupa se bavila dizajnom i proizvodnjom plovila za međunarodno natjecanje "Hydrocontes-X". Hydrocontest je natjecanje pokrenut 2013. godine na inicijativu zaklade Hydros i švicarske privatne banke Lombard Odier. Plovila se daljinski upravljaju i pokreću električnim pogonom. Ova vrsta natjecanja okuplja studente različitih fakulteta i oni predstavljaju sebe i svoj fakultet izrađujući napredne čamce koji moraju biti izrađeni prema pravilima samog Hydrocontest-a. Natjecanje se provodi u tri kategorije:

FESB Hydro Team je grupa mladih i ambicioznih studenata Fakulteta elektrotehnike, strojarstva i brodogradnje u Splitu. Grupa djeluje od početka akademske 2018. godine, na poticaj profesora sa katedre za Brodogradnju. U periodu od osnivanja, grupa se bavila projektiranjem i izradom plovila za međunarodno natjecanje „Hydrocontes-X". Hydrocontest je natjecanje pokrenuto 2013. godine na inicijativu organizacije Hydros Foundation i Švicarske privatne banke Lombard Odier. Plovila su daljinski upravljana i pogonjena električnim propulzorom. Takva vrsta natjecanja okuplja studente različitih fakulteta te oni prezentiraju sebe i svoj fakultet izradom naprednih plovila koja moraju biti izrađena po pravilima samog Hydrocontest-a. Natjecanje se provodi u tri kategorije:

- Laka kategorija (teret 20 kg)
- Teška kategorija (teret 200 kg)
- Utrka izdržljivosti (1h sa teretom od 20 kg)

Ovakav tip projekta, gdje se primjenjuje teoretsko znanje stečeno tijekom studiranja od velike je važnosti nama kao budućim inženjerima brodogradnje.

1. Hydrocontest-X competition

Hydrocontest is a competition formed in 2013. at the initiative of Hydros Foundation and the Swiss private bank „Lombard Odier". This kind of competition gathers students from different faculties around the world to present themselves and their product that must be made according to the rules set by the Hydrocontest organisation. The aim is to build and present small remote controled vessels that are powered by an electric propulsion.

The competition is held in 3 categories:

- Lightweight (20 kg of cargo)
- Heavyweight (200 kg of cargo)
- Endurance (1 h drive with 20 kg of cargo)

Rules set by competition are as following:

1.1. Dimensions

Each boat must fit into the rectangular "dimensions box" whose inner dimensions are 2m × 2.5m × 2.5m. These dimensions must include all parts of the boat, as it will be used during racing. This must be complied with in all of the boat's geometrical configurations, if it has several configurations, including the phases during which it changes configuration, if the change takes place during racing. No part of the boat must endanger the Teams or the other boats.

1.2. Electronics

The electronics must be housed in a watertight compartment and cooled. Any boat failing to comply with the IP67 standard for the on-board electronics shall not take part in the races.

1.3. Movement

Each boat must be able to move and be manoeuvrable in forward and reverse gear.

1.4. Engine

Manufacturer: Watt & Sea POD 1'200W. Other engines are not authorised. The engine must operate in water for cooling purposes. Each Team may modify the fairing of the POD according to the following conditions:

    • Without any modification to any of the parts of the POD provided by the   Organiser, nor their position and means of fixation.

    • By the addition of any material in order to improve its hydrodynamics on the forward 50% of the POD.

Teams are reminded that it is forbidden to open the engine. The mast can be altered in any way.

Fitting of external control(s) is authorised. No intervention other than those described above shall be authorised.

1.5. *Means of propulsion*

Teams are free to choose whatever means of propulsion they wish. The Organiser will not provide any propeller to the Teams.

1.6. *Power*

The engine must be powered by a battery supplied by the Organiser. Provisional battery specifications:

- • Chemistry: Li-ion – NMC

- • Cells: Panasonic UR-18650 NSX

- • Nominal tension: 36V +

- • Nominal capacity: 7.8Ah

The innovation of this project lies in using renewable energy resources that is of crucial importance for the future of the industry. The project aims to solve problems in transport due to ecology, CO_2 emissions ect. Conceptual solutions for electric an autonomous boats are being developed, and are the key for the shipping industry in the future.

2. FESB Hydro team – about us

FESB Hydro Team is a group of young and ambitious students of Naval Architecture at the Faculty of Electrical Engineering, Mechanical Engineering and Naval Architecture in Split, Croatia.

Active as a group since 2018. and developing small efficient vessels. The team was founded at the initiative of students and professors with a goal to combine all the given theoretical knowledge and put it into use. The team consist of 13 students that are distributed into 6 groups (hydrodynamics, ship construction, ship technology, stability, programming and production).

3. Hydrodynamics

3.1. *Resistance*

Total force in the opposite direction of the boat motion is the resistance of the boat. The boat is moving through two fluids, water and air. Components of resistance are consequences of two main forces: vertical dynamic pressure and tangential stress on the surface of the frame of fluid streams. [1]

Overall resistance of the boat is determined by:

$$R_T = \ C_T \ \cdot \ \frac{1}{2} \cdot \ \rho \ \cdot v^2 \cdot S \tag{1}$$

where:

R_T - total resistance

C_T – resistance coefficient,

ρ – sea water density,

v – boat speed,

S – wetted area

The power required to overcome the resistance is called the effective power and is determined by:

$$P_E= R_T \cdot v_S \qquad (2)$$

where:

P_E – effective power, kW

R_T – total resistance, kN

Vs - boat speed, m/s

To make the hull lines plan of the boat and its 3D model respectively it was necessary to collect as much data as possible on similar boats that were competing in the previous years.

Hull modeling was done in the software package "MaxSurf Modeler". "NPL Rounded Bilge Model" form was used as a reference form, which was scaled according to the selected dimensions in terms of length, width and height. By manual adjustment of the control points the final appearance of the desired form was achieved bearing in mind the lowest possible resistance. Based on Froude's number, it was confirmed that it is a semi-displacement hull,Fn =1.23.
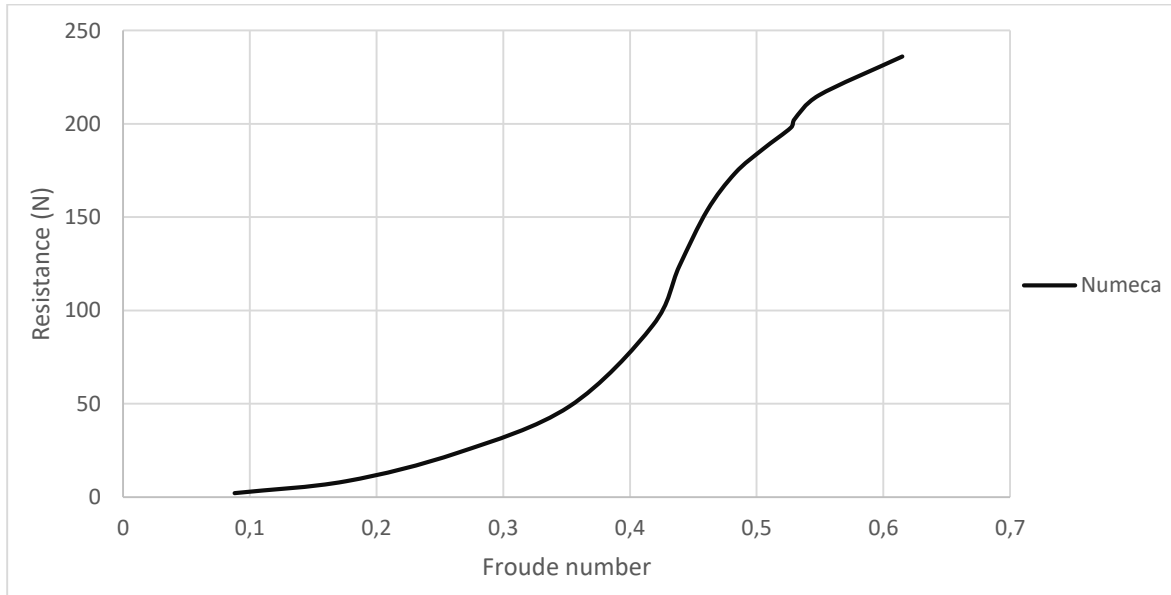

Figure 14 Graphic representation of resistance assessment

CFD was used to analyze the resistance, using the software package "Numeca Fine Marine". Numerical calculations were successfully performed and they represent a displacement of 267 kg and a draft of 0.26 m. [2]

Table 7 Graphic representation of resistance assessment using the funga method and the numeca

Speed (kts)	Resistance Numeca (N)	Resistance Fung (N)

3	29,82	15,85
4	59,08	33,6
5	135,63	86,1
5,5	185,16	138,09
6	216,02	187,72
6,5	238,23	223,7
7	255,81	248,15

The results were satisfactory, in comparison to the test run of the vessel, with minor variation that can be explained by the use of the approximate model of turbulence or the insufficient quality of network. It is also important to note that the high accuracy of the results can be affected by the experience of working with the CFD program. [3]

Using the integrated interface to visualize the results, CFView, Figures 2 and 3 show the isometric free surface and the relationship of the free surface to the wave height. Figure 2 is a representation of the free surface and "Mass fraction", a parameter through which it is shown. Mass fraction represents the ratio of air in a particular volume with values ranging from 0 to 1. Mass fraction in Figure 2 is 0,5. Figure 3 shows the wave system in the xy plane, with isoplanes representing a constant value of a certain parameter, and isolines the values at the same elevation with respect to the relevant coordinate system.
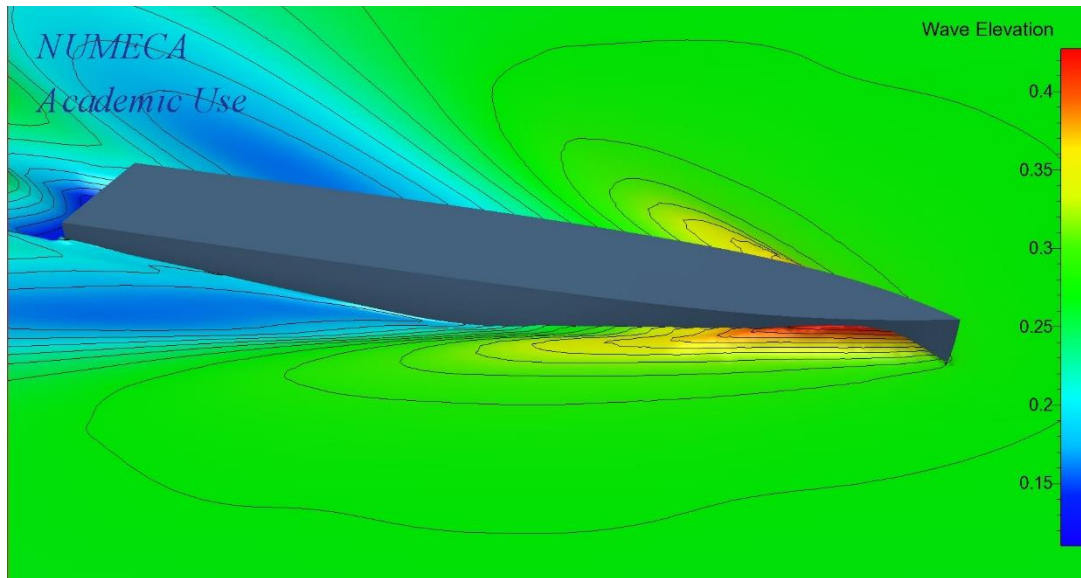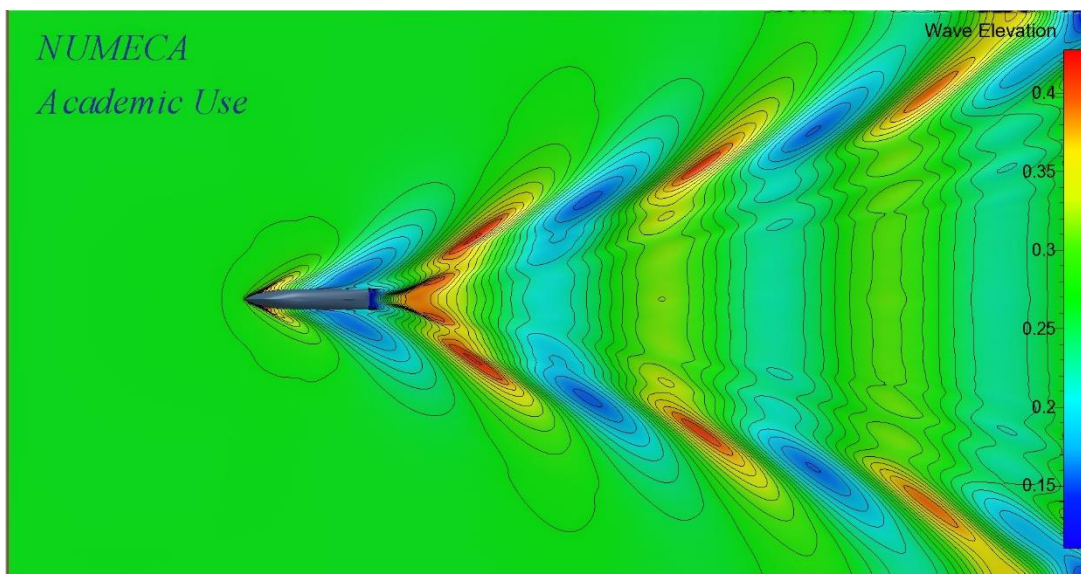

Figure 15 Isometric representation of free surface

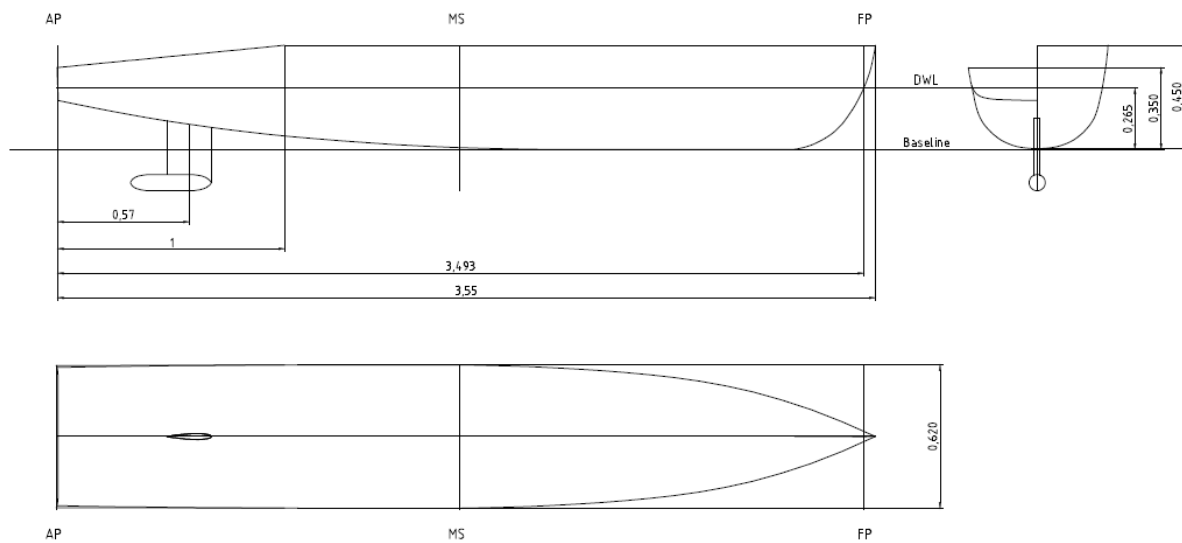
Figure 16 Free surface with wave heights

Figure 4 General arrangement

3.2. *Propulsion*

Power vs speed graph shows the engine power required for a range of boat speeds and engine speed.

By examining previous competitions, it had been noticed that the speed of progress is from 5 to 6 knots, and the diagram is made in the range from 2 to 8 knots.

The y-axis shows the required power on the brake which represents the effective power increased by the hydro-dynamic losses and the losses between the propeller and the engine. Since it is an electric motor, there are no losses between the motor and the propeller, and this value is taken to be equal to 1.
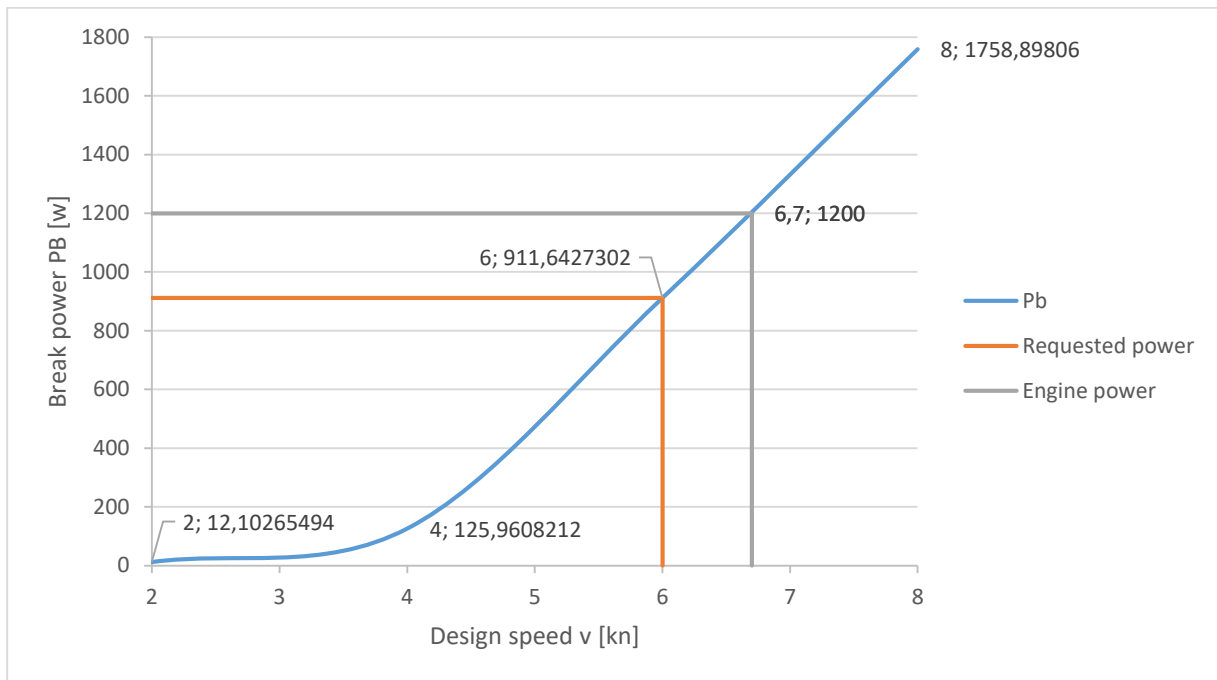
Figure 5 Power vs speed graph

As the diagram shows, the preferred speed is achieved with less engine power. The remaining difference is used in case of bad weather while driving or while maneuvering the boat.

The data required to construct the power vs speed graph as follows:

Relative rotative efficiency [4]:

$$\eta_R = 0,826 + 0,01 \cdot \frac{L}{V^{\frac{1}{3}}} + 0,02 \cdot \frac{B}{T} + 0,1 \cdot C_m = 0,826 + 0,01 \cdot \frac{3,55}{0,262^{\frac{1}{3}}} + 0,02 \cdot \frac{0,62}{0,265} + 0,1 \cdot 0,809 \qquad (3)$$
$$= 1,009$$

Hull efficiency [4]:

$$\eta_H = \frac{1 - w}{1 - t} = \frac{1 - 0,05}{1 - 0,045} = 1,005 \qquad (4)$$

Efficiency [4]:

$$\eta_0 = \frac{J * K_T}{2 * \pi * K_Q} = \frac{0,5 * 0,10533}{2 * \pi * 0,012072} = 0,694 = 69,4\% \qquad (5)$$

Effective power [4]:

$$P_E = R_t * v = 208,23 * 3,0864 = 641,97 \, W \qquad (6)$$

Thrust power [4]:

$$P_T = T * v_a = 218,08 * 2,932 = 639,36 \, W \qquad (7)$$

Delivered power [4]

$$P_D = 2 * \pi * n * Q = 2 * \pi * 24,16 * 6,05 = 920,15 \, W \qquad (8)$$

Brake engine power [4]:

$$P_B = \frac{P_E}{\eta_M \eta_R \eta_H \eta_0} = \frac{641,97}{1 * 1,009 * 1,005 * 0,694} = 911,64 \ W \tag{9}$$

According to the "power vs speed diagram", a propulsor with the best characteristics was chosen, according to which the model will be made.

The speed at the competition did not fully satisfy the design criteria.

Due to bad weather conditions in which the competition was held, the waves greatly increased the resistance, and the strength required to overcome the oncoming ones also increased.

The selected propulsor has the following parameters:

D = 0,2425 m – diameter

P = 0,1707 m – pitch

A_E/A_0 = 0,3 –expanded surface ratio

Z = 2 – number of blades

N = 1450 rmp – engine speed

The next step is to make a propulsor of the calculated parameters. Rhinoceros program was used for 3D modeling, in which a propeller model was created for the input data. Ultimately, it was decided to model only the propeller blades. The propeller hub is already made with a hole for the propeller blades.
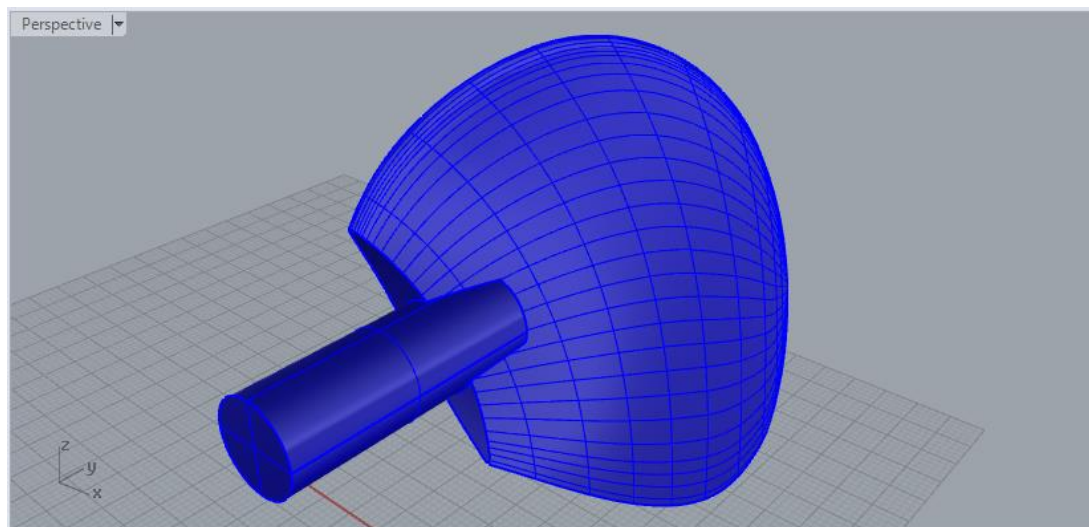

Figure 6 Propeller blade

3.3. Stability

Rules [5] that dealth directly with stability of the vessel were set as follows;

1. The vessel must be capable of returning to the inital state of equilibrium for the range of heeling angles $0° \leq \theta \leq \pm 30°$
2. The vessel must be seaworthy on waves up to 30 [cm] in height

3. The vessel must be unsinkable i.e. have enough reserve buoyancy if there is a water breach in a particular section of the vessel

It's interesting that the first rule in no way defines the means of testing the capability of the vessel to return to even keel as opposed to the previous Hydrocontest competitions. In the 2019 edition it was clearly stated that the heeling moment will be applied suddenly (dynamic heeling moment). So the 2020 rules gave leeway to narower vessel's and those with a smaller initial transverse metacentric height.
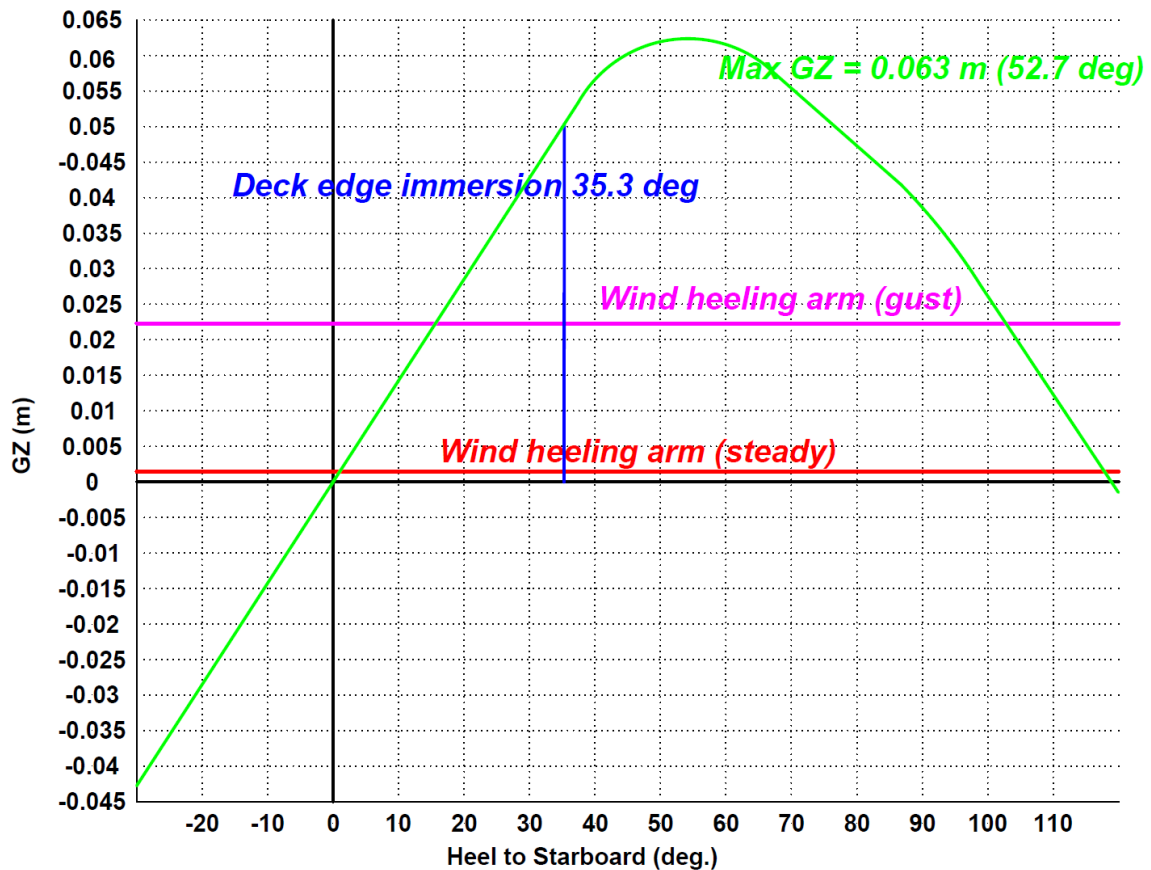

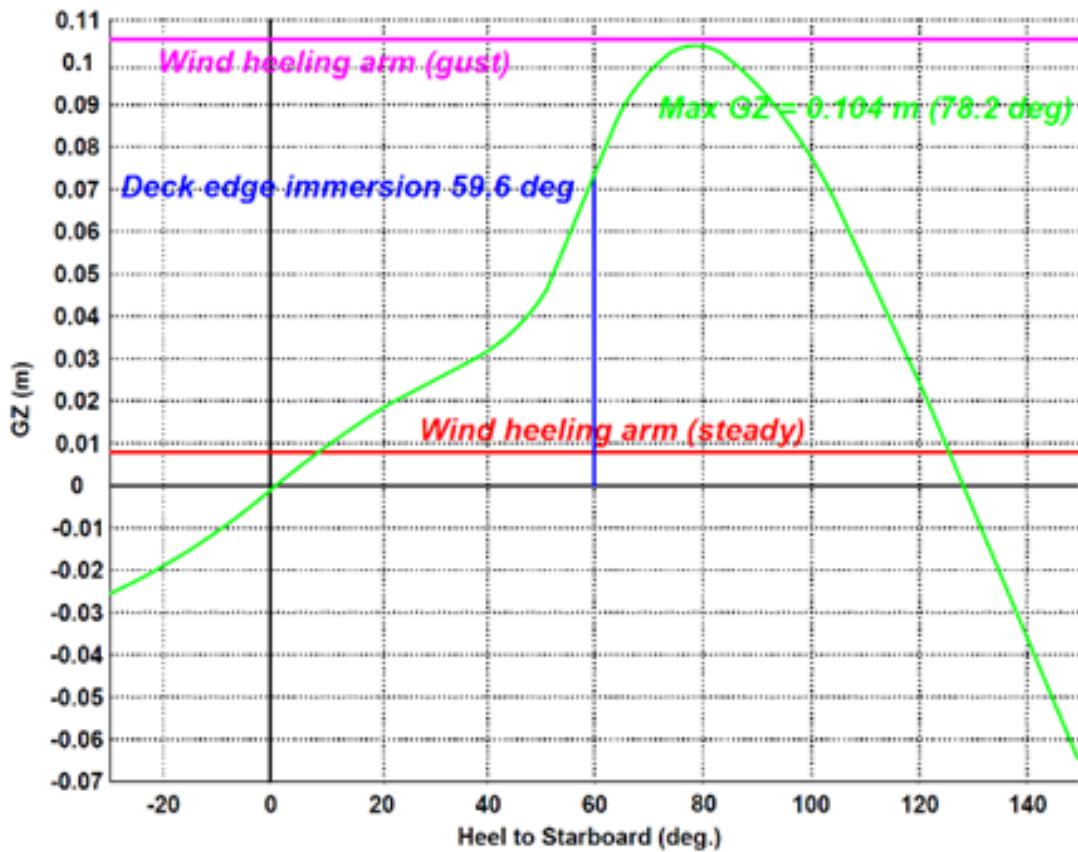**Figure 7** Righting lever diagram (Heavyweight)

Figure 8 Righting lever diagram (Lightweight)

Table 8 Comparison of characteristics

	Characteristics	Heavyweight	Lightweight	Unit
1	Range of static stability	117	127	deg.
2	Righting lever max.	0.063	0.104	m
3	Deck edge immersion angle	35.3	59.6	deg.
4	Reserve dynamic stability GUST	103	CAPSIZE	deg.
5	Angle of semi-permanent heel GUST	16.1	CAPSIZE	deg.

Analysis gave great results eventhough the goal was to make the starting conditions of the analysis as strict as possible. For the wind heeling moments modelling (gust and steady wind) extremes of the data from lake Neuchâtel, Switzerland were taken [6]. Gust ratio was calculated by doubling the highest average gust speed recorded in the last 10 years on the lake which was 15.5 knots.

$$Gust\ ratio\ = \frac{V_{GUST}^2}{V_{WIND}^2} = \frac{31^2}{8.85^2} = 12.26 \tag{10}$$

Heavyweight loadcase gave better results for the gust heeling moment which was expected as the exposed lateral surface is larger in the lightweight loadcase and therefore more wind energy can impact the vessel. Considering that it was even implied that the wind velocity gradient is constant above sea level (irrespectful of height above sea level) the results, from the stability standpoint are very good. The results from the competiton rules standpoint are too good, and a lot could have been done to hoover above the competition rules instead of being almost 100% more on the safety side.

4. Vessel construction

When dimensioning the hull structure, the main goal was to make the complete structure as light as possible and to ensure the minimum strength of the structure. It had been chosen that the hull will be built in a form of a sandwich structure. The selected matrix is vinylester infusion resin and as reinforcements in the sandwich construction were selected:

- Carbon Fiber Fabric -45/+45 400gsm

- Carbon Fiber Fabric Unidirectional 200gsm

While the chosen core material was:

- Lantor Soric XF - 4mm

The technology of making the hull and other parts of the vessel is vacuum infusion, and the mixing ratio of reinforcement and matrix for vacuum infusion is 50/50 or 50% resin to 50% carbon. The mixing ratio is important when calculating the theoretical weight of the hull and the strength of the material when calculating the load on the structure.

4.1. Design hull by direct calculation.

After the introductory analysis of the selected materials, it is necessary to perform a calculation of the structure and finally dimension the same structure. As stated, it is necessary for the construction to be as light as possible while satisfying the stability of the construction, ie the minimum strength. Finally, it was decided to use a direct construction calculation using software packages suitable for calculations - Simcenter Femap with Nastran.

4.2. Definiranje opterečenja I rubnih uvjeta

For the best possible calculation of the structure, and simulation of real conditions of use of the vessel, it is necessary to better analyze and select the loads that act on the hull during operation. The following loads are applied:

- Hydrostatic load,

- Cargo load and,

- Equipment load.

A hydrostatic pressure is applied to the hull. The pressure is modeled with an analytical field that increases the pressure linearly along the z-axis. Concentrated forces that model the tension from the 200 kilograms of cargo that a vessel must carry and approximately 20 kilograms of equipment. The forces are applied along the x-axis of a datum coordinate system. [7]

An inertia relief load is applied at the top end of the hull to bring the model into equilibrium after the loads are applied. Inertia relief is an option in NASTRAN that allows to simulate unconstrained structures in a static analysis. Inertia relief utilizes the inertia of the structure to create a state of static equilibrium, allowing the model to be solved. [8]
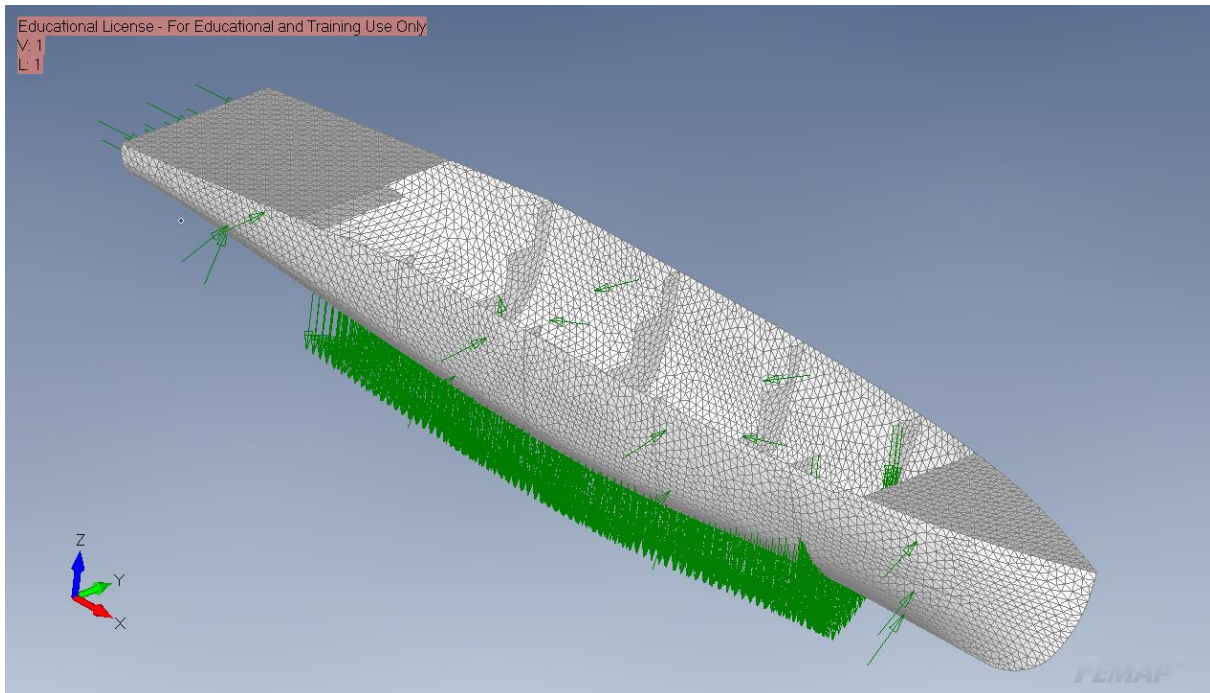
Figure 9 Hull model, loads and mesh

4.3. *Failure criteria*

The main problems that arose were the clear definition of the failure strength criteria. In a particular structural element, the loss of stability can be defined as the loss of the component's ability to carry the default load. This may be due to a lack of connection between the materials itself, although the material is still intact. Yield strength of composite materials and composite structures, due to heterogeneity, multilayer structures usually pass through a series of local yield strenght, the sum of which leads to the final structure fracture. Also the value of the longitudinal ultimate tensile strength (in the fiber direction) is much higher than the transverse ultimate tensile strength (perpendicular to the fiber direction). This is because the properties of the composite material in the longitudinal direction mainly depend on the properties of the fibers and the properties of the material in the transverse direction depend on the properties of the interlayer and on the properties of the matrix itself.

In direct calculation with Simcenter Femap with Nastran Hoffman's theory [9] was used as main failure criteria. Hoffman's theory for an orthotropic lamina in a general state of plane stress with unequal tensile and compressive strengths is given by,

$$\left(\frac{1}{X_t} - \frac{1}{X_c}\right)\sigma_1 + \left(\frac{1}{Y_t} - \frac{1}{Y_c}\right)\sigma_2 + \frac{\sigma_1^2}{X_t X_c} + \frac{\sigma_2^2}{Y_t Y_c} + \frac{\sigma_{12}^2}{S^2} + \frac{\sigma_1 \sigma_2}{X_t X_c} = 1 \qquad (11)$$

The failure index is obtained by evaluating the left-hand side of the above equation.

Where is:

X - allowable stress in 1-direction

Y - allowable stress in 2-direction

S - allowable stress in shear

Xt - allowable tensile stress in 1-direction

Xc - allowable compressive stress in 1-direction

Yt - allowable tensile stress in 2-direction

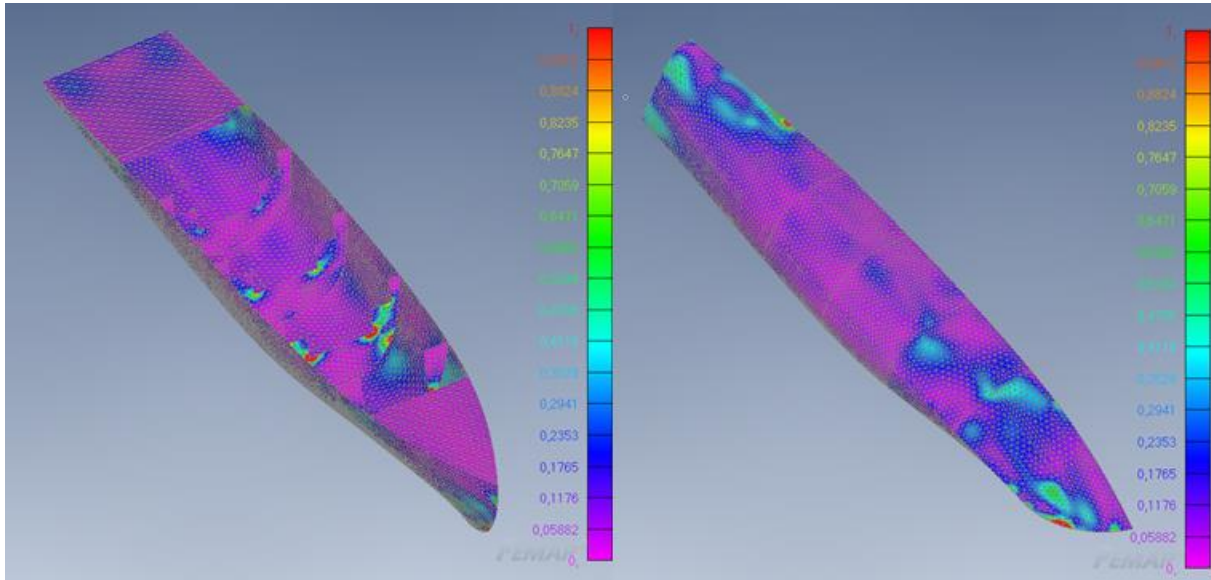Yc - allowable compressive stress in 2-direction
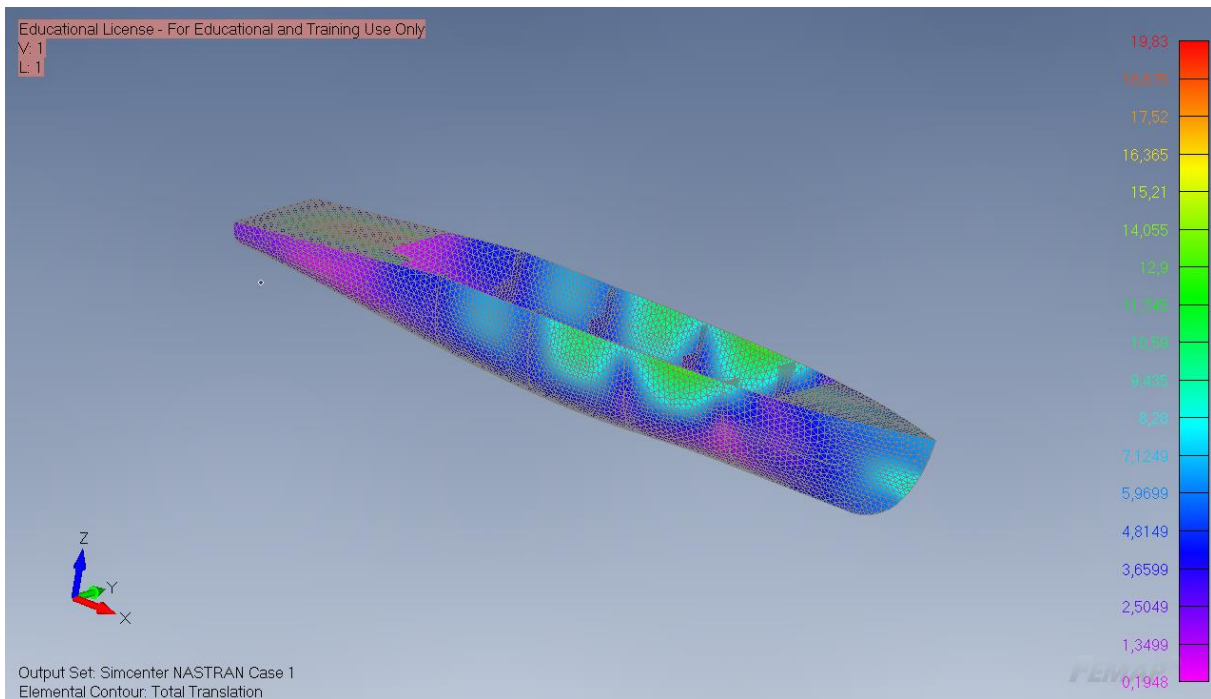

Figure 10 Hoffman laminate max failure index

Figure 171 Deformation in mm

5. Shipbuilding technology

5.1. Model surface preparation

In the first step, the surface of the male model had to be sanded with different granulations of sandpaper to get the desired shape. Sanding was done manually, from smaller to larger granulation (120, 180, 220). After sanding, it was necessary to fill in all irregularities and the holes formed during sanding with polyester putty. The sanding (180 and 220) and filling processes was alternated until we obtained the appropriate model surface. After sanding the putty, the model had to be water sanded Water sandpaper is used for manual final sanding of various wet surfaces. Sandpaper is usually in granulations of 800, 1000, 1200, 1500 and 2000.

5.2. Moulding

Wax is applied on the prepared surface and it is used as a mold release preparation. It is applied with a cotton cloth, and left to dry between applications for at least 20 minutes. While making the mold, the technique of hand lamination is used. The glass fibers needed to make the mold are cut to the appropriate dimensions. A layer of resin is applied first, then a layer of glass mat (225 g / m2) is added and this process is repeated once more. After the second layer of glass mat, the core layer "Lantor Soric XF 4 mm" is applied. After placing the core, two layers of glass mat and polyester resin are placed again.

5.3. Hull preparation

The final stage is the application of wax to the mold with ten layers, more layers of wax allow easier separation. After the wax has dried, the gelcoat is applied on the inside of the mold with a roller of 0.7-0.9 millimeters thickness. To get a good uniform thickness, it is preferable to apply it in two coats. Preparation for vacuum infusion begins with placing carbon Biax -45 / + 45 (400g / m2) along the entire length of the vessel. The second layer is carbon UDR (200g / m2) and it goes along the entire length of the vessel in the direction of the x-axis. Both sides require a layer of carbon UDR (200g / m2). This is followed by a 4mm Lantor Soric core layer. The fourth layer is carbon UDR (200g / m2), and is placed in the parts where the frames come across the x-axis. The fifth and sixth layers are carbon Biax -45 / + 45 (400g / m2). The next step is to apply the peelply, which should cover the fibers on the entire mold before applying the infusion mash. Ahead of installing the vacuum bag, it is necessary to install spiral pipes for the flow of resin and to install a connection for air extraction and resin supply. The pipes are set using T joints. The last step is to place a vacuum bag which is glued at the edges with sealing tape. [10] [11]

5.4. Vacuum infusion

It is necessary to drill holes to which the resin supply connections will come. In these places, the resin supply pipe is connected, and the end part of the pipe is placed in a resin bucket. When determining the amount of resin, it is necessary to know the area and mass of the material that will be used during the vacuum infusion. After the resin has flooded the entire mould, the excess goes through a pipeline, located in the middle of the mould, into the resin separator. The vacuum bag is removed after the reinforcements are placed. [12]

5.5. Deck and frames

Vacuum infusion process was used to make the deck and frames. The deck is made separately from the frames. Independently for the deck and for the ribs, a plate is made from which the necessary

part of the deck or frames is subsequently cut. Composite components (matrix, reinforcement and core) were determined for the construction of the vessel's deck and frames. The matrix is vinyl ester resin, the reinforcement used to make it is carbon Biax (400g / m2), and the core is Lantor Soric 4mm. The plan for laminating the deck and ribs is such that the first layer is carbon Biax -45 / + 45, then the core Lantor Soric 4mm, and the last layer is again carbon Biax -45 / + 45. After the resin has flooded the entire casting, the excess goes through the pipeline located in the middle and goes to the resin separator. When the whole plate is filled with resin, the vacuum infusion is completed. After drying the resulting plate, it is necessary to cut the deck and frames to the required dimensions. Places are provided on each plate to cut 12 small brackets. The brackets will be used as structural and deck support.

5.6. *Joining frames and hull plating*

Hull plating needs to be stiffened to take on the desired hull shape that is projected. The bulkheads are joined using polyester resin and a 404 High-Density Adhesive Filler. When assembling the frames, self-adhesive tapes are used to achieve the shape of the hull and clamps that serve as a temporary connection between the frames and the hull plating until the resin hardens and connects the hull plating to the frames. After joining the frames to the hull plating, polyurethane foam ("pur foam") is used to fill the small holes between the edge parts of the frames and the hull plating.

5.7. *Joining deck and hull plating*

PBefore joining the deck to the hull plating it is necessary to discard excess deck material and achieve the desired shape. It is also necessary to glue the brackets to the hull plating. The deck is joined to the hull by hand lamination using two layers of carbon and polyester resin. The first layer of carbon is Biax -45 / + 45 (400g / m2) and the second layer is UDR (200g / m2).

5.8. *Final stage of hull construction*

The final stage of hull construction is hull painting. Hull painting begins with the application of a primer. The primer is applied by spray. After applying the primer, next step is to apply the first coat of paint. The paint, as in the previous case, is applied by spray. The paint is applied in two coats, so it is necessary to wait up to 12 hours for the paint to dry and apply a new coat of paint again.

Figure 182 Vessel on competition

REFERENCES

[1]   Joško Dvornik - Otpor i propulzija broad

[2]   Sreenivas Jayanti – Computational Fluid Dynamics for Engineers and Scientists

[3]   NUMECA/Fine Marine: User Guide

[4]   The Propeller Handbook (Gerr, 2001)

[5]   Hydrocontest Rules; https://www.hydrocontest-x.ch/?page_id=324&lang=en (Article 11. Stability)

[6]   worldweatheronline.com

[7]   EJ Barbero: Finite element analysis of composite materials – 2007

[8]   Suresh C. Panda R. Natarajan: Finite element analysis of laminated composite plates First published: 1979

[9]   Siyuan Ma, Hassan Mahfuz: Finite element simulation of composite ship structures with fluid structure interaction 2012

[10]   Marine composites second edition 1999

[11]   Zenkert D. Sandwich structures

[12]   Shenoi RA, Wellicome JR. Composite materials in maritime structures. Volume 1 Fundametal Aspects

MJESTA ODRŽAVANJA SIMPOZIJA SORTA / PAST VENUES OF SYMPOSIUMS SORTA

1. 1974. Zagreb, Jadranbrod, Fakultet strojarstva i brodogradnje u Zagrebu, Brodarski institut, Brodogradnja

2. 1976. Zagreb, Fakultet strojarstva i brodogradnje u Zagrebu

3. 1978. Zagreb, Fakultet strojarstva i brodogradnje u Zagrebu

4. 1980. Opatija, Fakultet strojarstva i brodogradnje u Zagrebu

5. 1982. Split, Fakultet elektrotehnike, strojarstva i brodogradnje u Splitu

6. 1984. Beograd, Institut tehničkih nauka SANU

7. 1986. Pula, Brodogradilište Uljanik

8. 1988. Zagreb, Fakultet strojarstva i brodogradnje u Zagrebu

9. 1990. Dubrovnik, Fakultet strojarstva i brodogradnje u Zagrebu, Pomorski fakultet Dubrovnik

10. 1992. Opatija, Tehnički fakultet Rijeka

11. 1994. Dubrovnik Atlantska plovidba, Pomorski fakultet, Fakultet strojarstva i brodogradnje u Zagrebu

12. 1996. Zagreb, Fakultet strojarstva i brodogradnje u Zagrebu

13. 1998. Zadar, Brodogradilište Lamjana, Tankerska plovidba

14. 2000. Rijeka, Tehnički fakultet Rijeka Rijeka, Brodogradilište Viktor Lenac

15. 2002. Trogir, Brodogradilište Brodotrogir

16. 2004. Plitvička jezera, Fakultet strojarstva i brodogradnje u Zagrebu

17. 2006. Rijeka, Brodogradilište 3. maj, Tehnički fakultet Rijeka

18. 2008. Pula, Brodogradilište Uljanik

19. 2010. Lumbarda, Korčula, Fakultet elektrotehnike, strojarstva i brodogradnje u Splitu

20. 2012. Zagreb, Fakultet strojarstva i brodogradnje u Zagrebu, Brodarski institut

21. 2014. Baška, Tehnički fakultet Rijeka, Brodogradilište Viktor Lenac

22. 2016. Trogir, Fakultet strojarstva i brodogradnje u Zagrebu, Brodogradilište Brodotrogir

23. 2018. Split, Fakultet elektrotehnike, strojarstva i brodogradnje u Splitu

SORTA Standing Committee

Joško Parunov, FSB, chairman

Predrag Božanić

Marinko Brgić

Matko Bupić, Pomorski odjel Sveučilišta u Dubrovniku

Većeslav Čorić, HATZ

Nastia Degiuli, FSB

Roko Dejhalla, RITEH

Nikša Fafanđel, RITEH

Ivan Gospić, Pomorski odjel Sveučilišta u Zadru

Rajko Grubišić, FSB

Alan Klanac

Edi Kučan, 3.MAJ

Boris Ljubenkov, FESB

Šime Malenica, Bureau Veritas

Siniša Ostojić, 3.MAJ

Darko Pappo, DiV Grupa

Marta Pedišić Buča, Brodarski institut

Jasna Prpić-Oršić, RITEH

Siniša Reljić, Navis Consult

Ivo Senjanović, HAZU

Vedran Slapničar, FSB

Dragan Sorić, TSI d.o.o.

Aris Večerina, MW Business Advisors

Pero Vidan, PFST

Boris Vukušić, Udruženje male brodogradnje pri HGK

Nenad Vulić, PFST

Paul Jurišić, CRS

GOALS OF THE SYMPOSIUM SORTA 2020

SORTA 2020 is the 24th Symposium on the Theory and Practice of Shipbuilding - in memoriam prof. Leopold Sorta in the organization of the University of Rijeka - Faculty of Engineering. This 24. SORTA presents the testimony of a continuous, over 45 years lasting development of the shipbuilding profession and science on these grounds.The aim of SORTA 2020 is to promote the existing educational, scientific, research and development capacities of Croatian shipbuilding, which are ready to participate, both now and in the future, in the evolution of shipbuilding industry, STEM and progress of Croatian economy. This year's symposium coincides with a period of change for the entire shipbuilding community in Croatia and broader and furthermore, with the COVID-19 pandemic, which has challenged face-to-face meetings due to uncertainties regarding travel restrictions, physical distancing and other health related measures. To adapt to the current situation the SORTA2020 Organization Committee has transform this 24th Symposium into a fully online meeting that offered the responsible and rational possibility for scientific and professional exchanges while protecting the safety, health, and well-being of all participants.

24. simpozij Teorija i praksa brodogradnje, in memoriam prof. Leopold Sorta (Sorta 2020), održava se pod visokim pokroviteljstvom Razreda za tehničke znanosti Hrvatske akademije znanosti i umjetnosti.

The 24st symposium on Theory and Practice of Shipbuilding, in memoriam prof. Leopold Sorta (Sorta 2020), is held under the auspices of the Department of Technical Sciences of the Croatian Academy of Sciences and Arts.

Hrvatska akademija znanosti i umjetnosti

Croatian Academy of Sciences and Arts

Zrinski trg 11, HR-10000 Zagreb, Hrvatska

http://www.hazu.hr